centro de educación continua
división de estudios superiores
facultad de ingeniería, unam

A LOS ASISTENTES A LOS CURSOS DEL CENTRO DE EDUCACION CONTINUA

Las autoridades de la Facultad de Ingeniería, por conducto del Jefe del Centro de Educación Continua, otorgan una constancia de asistencia a quienes cumplan con los requisitos establecidos para cada curso. Las personas que deseen que aparezca su título profesional precediendo a su nombre en la constancia, deberán entregar copia del mismo o de su cédula a más tardar el SEGUNDO DIA de clases, en las oficinas del Centro con la señorita encargada de inscripciones.

El control de asistencia se llevará a cabo a través de la persona encargada de entregar las notas del curso. Las inasistencias serán computadas por las autoridades del Centro, con el fin de entregarle constancia solamente a los alumnos que tengan un mínimo del 80% de asistencia.

Se recomienda a los asistentes participar activamente con sus ideas y experiencias, pues los cursos que ofrece el Centro están planeados para que los profesores expongan una tesis, pero sobre todo, para que coordinen las opiniones de todos los interesados constituyendo verdaderos seminarios.

Es muy importante que todos los asistentes llenen y entreguen su hoja de inscripción al inicio del curso. Las personas comisionadas por alguna institución deberán pasar a inscribirse en las oficinas del Centro en la misma forma que los demás asistentes, entregando el oficio respectivo.

Con objeto de mejorar los servicios que el Centro de Educación Continua ofrece, al final del curso se hará una evaluación a tráves de un cuestionario diseñado para emitir juicios anónimos por parte de los asistentes.

UNIVERSIDAD NACIONAL AUTONOMA DE MEXICO
FACULTAD DE INGENIERIA
DIVISION DE ESTUDIOS SUPERIORES
CENTRO DE EDUCACION CONTINUA
DIRECTORIO GENERAL

REGISTRO DE ASISTENTES Y PROFESORES.

NOMBRE DEL CURSO: ______________________ FOLIO [ ][ ][ ][ ][ ] CLAVE ASOC [ ][ ]
1 5 6 7

[ ][ ][ ][ ][ ][※] [ ] [ ]
8 13 14 NOMBRE(S) APELLIDO PATERNO APELLIDO MATERNO 41

REG. FED. CAUS. [ ][ ][ ][ ][ ][ ][ ][ ][ ][ ] CED. PROF. [ ][ ][ ][ ][ ][ ][ ]
42 51 52 58

TEL. PARTICULAR [ ][ ][ ][ ][ ][ ][ ] TEL. OFICINA [ ][ ][ ][ ][ ][ ][ ] EXTENSION [ ][ ][ ][ ]
59 65 66 72 73 76

MARQUE CON UNA CRUZ

ASISTENTE [ ] PROFESOR [ ] [ ] [1]
77 80

[ ]
8 DOMICILIO PARTICULAR (CALLE. NUMERO Y No. INTERIOR) 41

[ ] Z.P. [ ][ ]
42 COLONIA 71 72 73

______________________ [ ][ ]
ESTADO 74 75

______________________ [ ][ ] ______________________ [ ][ ] [2]
TITULO PROFESIONAL 76 77 ESPECIALIDAD 78 79 80

[ ]
8 DOMICILIO DE OFICINA (CALLE, NUMERO Y No. INTERIOR) 41

[ ] Z.P. [ ][ ]
42 COLONIA 71 72 73

______________________ [ ][ ] [3]
ESTADO 74 75 80

ASOCIACIONES A LAS QUE PERTENECE.

______________________ [ ][ ] ______________________ [ ][ ]

______________________ [ ][ ] ______________________ [ ][ ]

DIRECTORIO DE PROFESORES DEL CURSO ANALISIS EXPERIMENTAL DE ESFUERZOS DEL 27 DE NOV. AL 8 DE DICIEMBRE, 1978.

DR. PORFIRIO BALLESTEROS BAROCIO
JEFE DE LA SECCION DE MECANICA
TEORIA Y APLICADA
D. E. S. F. I.
UNAM
TEL. 550.52.15 EXT. 4498

DR. LUIS A. FERRER ARGOITE
PROFESOR
D. E. S. F. I.
UNAM

DR. MIKLOS HETENYI
PROFESOR
UNIVERSIDAD DE STANFORD, USA.

ING. ALFONSO OLVERA LOPEZ
ESCUELA SUPERIOR DE INGENIERIA
Y ARQUITECTURA
DIRECTOR DE INGENIERIA EXPERIMENTAL
I.P.N.
TEL. 586.01.44

ING. ALFREDO OLIVARES PONCE
INVESTIGADOR
INSTITUTO DE INGENIERIA
U.N.A.M.
TEL. 548.65.60 EXT. 453

DR. SALOMON REDNER
VISHAY INTERCHNOLOGY
U.S.A.

DR. MIHIR SEN
PROFESOR
D. E. S. F. I.
U.N.A.M.

ANALISIS EXPERIMENTAL DE ESFUERZOS

Fecha	Duración	Tema	Profesor
Nov. 27	9 a 10:30 a.m.	Introducción	Dr. Miklos Hetenyi
	11 a 12:30 h	Fundamentos de Mecánica	" " "
	14 a 15:30 h	Análisis de Modelos	Dr. Luis A. Ferrer Argoite
	16 a 17:30 h	Análisis Dinámico	Dr. Mihir Sen
Nov. 28	9 a 10:30 a.m.	Fundamentos de Mecánica	Dr. Miklos Hetenyi
	11 a 12:30 h	Fotoelasticidad 2D y 3D	" " "
	14 a 14:30 h	Análisis de Modelos	Dr. Luis A. Ferrer Argoite
	16 a 17:30 h	Análisis Dinámico	Dr. Mihir Sen
Nov. 29	9 a 10:30 a.m.	Fundamentos de Mecánica	Dr. Miklos Hetenyi
	11 a 12:30 h	Fotoelasticidad 2D y 3D	Dr. Miklos Hetenyi
	14 a 15:30 h	Métodos Estadísticos	Dr. Luis A. Ferrer Argoite
	16 a 17:30 h	Método de Moire	Ing. Alfonso Olvera López
Nov. 30	9 a 10:30 h	Fundamentos de Mecánica	Dr. Miklos Hetenyi
	11 a 12:30 h	Fotoelasticidad 2D y 3D	Dr. " "
	14 a 15:30 h	Fotoelaticidad Reflectiva	Dr. Salomón Redner
	16 a 17:30 h	Método de Moire	Ing. Alfonso Olvera López

#..

Fecha	Duración	Tema	Profesor
Dic. 1°	9 a 10:30 a.m.	Strain Gages	Dr. Miklos Hetenyi
	11 a 12:30 h	Fotoelasticidad 2D y 3D	" " "
	14 a 15:30 h	Fotoelasticidad Reflectiva	Dr. Salomón Redner
	16 a 17:30 h	Método de Grid	Dr. Luis A. Ferrer Argoite
Dic. 4	9 a 12:30		Dr. Miklos Hetenyi
	17 a 18:30 h	Lacas Frágiles	Dr. Salomón Redner
	19 a 21 h	Laboratorio	Ing. Alfredo Olivares Ponce
Dic. 5	9 a 12:30 h		Dr. Miklos Hetenyi
	17 a 18:30 h	Esfuerzos Residuales	Dr. Salomón Redner
	19 a 21 h	Laboratorio	Ing. Alfredo Olivares Ponce
Dic. 6	9 a 12:30 h		Dr. Miklos Hetenyi
	17 a 18:30 h	Strain Gages	Ing. Alfredo Olivares Ponce
	19 a 21 h	Laboratorio	" " " "
Dic. 7	9 a 12:30 h		Dr. Miklos Hetenyi
	17 a 18:30 h	Strain Gages	Ing. Alfredo Olivares Ponce
	19 a 21 h	Laboratorio	Dr. Luis A. Ferrer Argoite
Dic. 8	9 a 12:30 h		Dr. Miklos Hetenyi
	17 a 18:30 h	Transductores	Ing. Alfredo Olivares Ponce
	19 a 21 h	Mesa Redonda	Todos los Profesores
		Clausura	

'edcs.

centro de educación continua
división de estudios superiores
facultad de ingeniería, unam

ANALISIS EXPERIMENTAL DE ESFUERZOS

STRAIN GAGES

NOVIEMBRE, 1978.

Palacio de Minería Calle de Tacuba 5, primer piso. México 1 D. F.

TEORIA DE LAS BANDAS EXTENSOMETRICAS

1:1 Generalidades

Con el enunciamiento por Robert Hooke en 1.678 de la ley q relaciona las tensiones y deformaciones en materiales sometidos a solicitaciones mecánicas y el posterior descubrimiento en 1.856 de Lord Kelvin referente a las variaciones que en su resistencia sufre un conductor eléctrico cuando se modifica su geometría, se establecieron los principios fundamentales de la extensometría eléctrica; si bién su nacimiento ha sido muy posterior, pudiendo decirse que fué a partir de la II guerra Mundial, cuando su aplicación empezó a vulgarizarse.

En su forma más elemental, una banda extensométrica (Strain-gage; jauge électrique d'extensometrie) está constituída (fig. 1) por un hilo metálico muy fino en forma de "parrilla" montado sobre un soporte, de tal manera, que la mayor parte de su longitud sea paralela a una dirección fija. Si deseamos conocer las deformaciones de una estructura según una dirección, pegaremos el extensímetro con sus hilos paralelos a dicha dirección y al deformarse aquella, producirá variaciones en la geometría del hilo del extensímetro que originarán una variación de su resistencia; por lo tanto disponiendo de instrumentos capaces de medir variaciones pequeñas de la resistencia original del extensímetro, podemos conocer las deformaciones mecánicas de la estructura en la que se pegó.

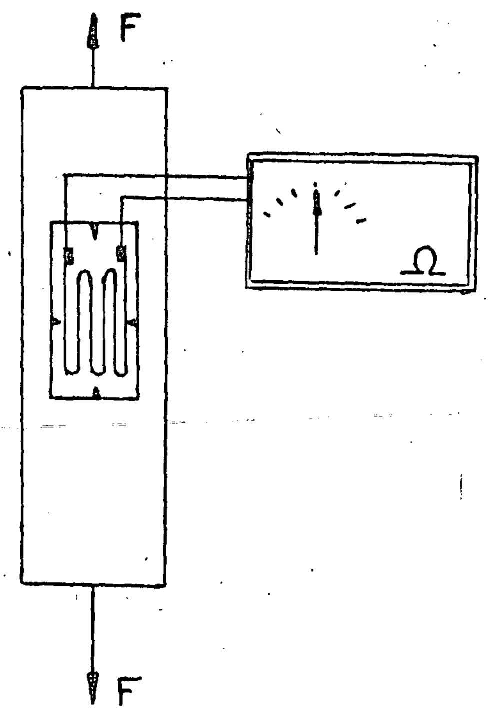

fig 1

La Resistencia de materiales nos enseña las leyes que ligan deformaciones y tensiones, siendo la extensometría la técnica que permitirá conocer el estado de tensiones de un cuerpo a partir de la medida del estado de deformaciones, sin necesidad de recurrir a ensayos destructivos, pudiendose efectuar un número ilimitado de mediciones, pués si bién el extensímetro una vez pegado es irrecuperable, sus cualidades con el tiempo perduran, dentro de los límites de utilización.

Por tanto, una banda extensométrica actua como elemento transductor, transformando la variación de una magnitud mecánica en - la de una eléctrica, facultad ésta que se aprovecha para fabricar captadores sensibles a ciertos parámetros mecánicos, pudiendo así evitarse el inconveniente de su no recuperación.

Actualmente el desarrollo de las técnicas extensométricas, ha alcanzado tal grado de perfección, que normalmente los problemas de medida de deformaciones y tensiones que puedan presentarse en ingeniería tienen solución, determinándose con exactitud la evaluación de fenómenos cuya influencia en la realización de proyectos es primordial, con la ambiciosa meta de fabricación con coeficientes de seguridad próximos a la unidad, sin perdida de garantias funcionales. Reducción de costos de fabricación, control de calidad, homologación de marcas, investigación, estudios y ensayos, mejores de fabricados, nuevos diseños, etc, etc, son logros, que incluso a corto plazo, se consiguen con equipos sencillos elementales y económicos.

1.2 PRINCIPIOS TEORICOS DEL EXTENSIMETRO OHMICO

Consideremos un extensímetro formado por un solo hilo conductor unido a una estructura, de tal forma, que las deformaciones que pueden producirse sean idénticas en ambos (fig 2).

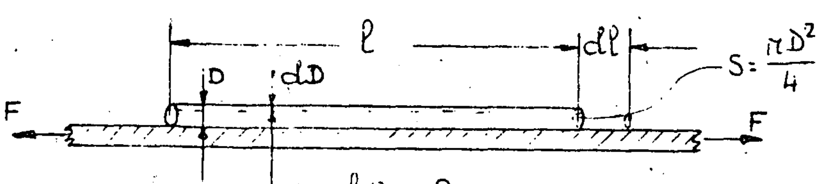

fig 2

La resistencia R del hilo tiene por valor:

$$R = \rho \frac{l}{S}$$

(ρ = resistividad)

Si el hilo sufre una deformación (alargamiento), la longitud l aumenta, la sección S disminuye y la resistividad varía dando lugar estos cambios a una variación del valor de R que podemos obtener diferenciando (1) y después deducir la relación entre la deformación elástica del hilo y la variación relativa o unitaria de resistencia, en efecto:

$$dR = \frac{S(l\,d\rho + \rho\,dl) - \rho l\,dS}{S^2} \quad \text{- - - - - - - - - -} \quad [2]$$

Dividiendo [2] por [1]

$$\frac{dR}{R} = \frac{dl}{l} + \frac{d\rho}{\rho} - \frac{dS}{S} \quad \text{- - - - - - - - - -} \quad [3]$$

Si el hilo es de forma cilíndrica:

$$S = \frac{\pi D^2}{4} \; ; \quad dS = \frac{\pi}{2} D\, dD \quad y \quad \frac{dS}{S} = \frac{2\,dD}{D}$$; sustituyendo en [3]

$$\frac{dR}{R} = \frac{dl}{l} + \frac{d\rho}{\rho} - 2\frac{dD}{D} \quad \text{- - - - - - - -} \quad [4]$$

La (4) podemos escribirla como:

$$\frac{\frac{dR}{R}}{\frac{dl}{l}} = 1 + \frac{\frac{d\rho}{\rho}}{\frac{dl}{l}} - 2\,\frac{\frac{dD}{D}}{\frac{dl}{l}}$$

pero el último término del segundo miembro, es la expresión del coeficiente de Poisson $\frac{dD}{D} : \frac{dl}{l} = -\mu$, luego sustituyendo tendemos el valor de la relación entre la variación de resistencia y la deformación unitaria.

$$\frac{\frac{dR}{R}}{\frac{dl}{l}} = 1 + \frac{\frac{d\rho}{\rho}}{\frac{dl}{l}} + 2\mu \quad \text{- - - - - - - -} \quad [5]$$

al segundo miembro de (5) se llama factor de banda o de sensibilidad K;

$$K = 1 + 2\mu + \frac{\frac{d\rho}{\rho}}{\frac{dl}{l}} \quad \text{- - - - - - - -} \quad [6]$$

Bridgaman enunció que la variación relativa de resistividad de un conductor es proporcional a la variación relativa de volúmen de dicho - conductor

$$\frac{d\rho}{\rho} = C\,\frac{dV}{V} \quad (C = \text{Constante de Bridgman}) \text{ - - - } [7]$$

Si $V = l \cdot S$ y sustituyendo [7] en [5]

$$\frac{dR}{R} = \left[(1+2\mu) + C\,(1-2\mu)\right]\frac{dl}{l} \quad \text{- - - - - - - -} \quad [8]$$

Hasta aquí, hemos considerado la sección del hilo circular, pero en las modernos b ndas impresas la sección es rectangular y la variación de resistencia $\frac{dR}{R}$, función de las deformaciones que experimenta la banda en las tres dimensiones se calculará así:

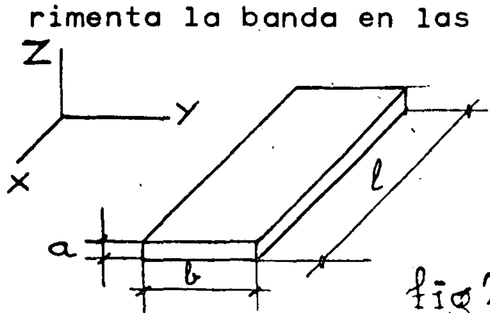

fig 2a

Siendo [redacted] (fig. 2a)

$$R = \rho\,\frac{l}{a \cdot b} \quad \text{- - - - - - - -} \quad [9]$$

y las deformaciones según los ejes X, Y, Z son:

$$\varepsilon_x = \frac{dl}{l} \quad ; \quad \varepsilon_y = \frac{db}{b} \quad , \quad \varepsilon_z = \frac{da}{a} = -\mu \frac{dl}{l} \quad \mu \frac{db}{b} \quad \mu(\varepsilon_x + \varepsilon_y)$$

diferenciando logarítmicamente la (4) tendremos

$$\frac{dR}{R} = \frac{d\rho}{\rho} + \frac{dl}{l} - \frac{da}{a} - \frac{db}{b} \quad C\frac{dV}{V} + \frac{dl}{l} - \frac{da}{a} - \frac{db}{b}$$

$$= C\left(\frac{dl}{l} + \frac{da}{a} + \frac{db}{b}\right) + \frac{dl}{l} - \frac{da}{a} - \frac{db}{b} =$$

$$= C(\varepsilon_x - \mu\varepsilon_x - \mu\varepsilon_y + \varepsilon_y) + \varepsilon_x + \mu\varepsilon_x + \mu\varepsilon_y - \varepsilon_y =$$

$$= \varepsilon_x\left[C(1-\mu) + 1 + \mu\right] + \varepsilon_y (C-1)(1-\mu)$$

y llamando

$$K_1 = C(1-\mu) + 1 + \mu$$

$$K_2 = (C-1)(1-\mu)$$

queda

$$\frac{dR}{R} = \varepsilon_x K_1 + \varepsilon_y K_2 \qquad [10]$$

La (10) nos indica que una banda extensométrica es sensible a la deformación longitudinal según la dirección de los hilos activos, pero también a la deformación transversal, siendo esto último un inconveniente que puede introducir errores. Si el valor de la constante de Bridgman se consigue que valga la unidad, $K_2=0$, pero prácticamente es muy dificil de lograr, por lo que se tiende a buscar un compromiso que haga K_2 lo menor posible y por lo menos que permita conocer el error que su presencia introduce en la medida. Veamos como se logra.

La (10) puede escribirse:

$$\frac{dR}{R} = K_1(\varepsilon_x + K_t \varepsilon_y) \qquad [10a]$$

siendo $K_t = \frac{K_2}{K_1}$ = factor de sensibilidad transversal del extensímetro. Sustituyendo:

$$\frac{dR}{R} = K_1(\varepsilon_x - K_t \mu \varepsilon_x) = K_1(1 - \mu K_t)\varepsilon_x = K\varepsilon_x \qquad [11]$$

El factor de banda dado por el fabricante es $K = K_1(1-\mu K_t)$ para $\mu = 0{,}285$

La expresión:

$$e = \frac{K_t\left(\frac{\varepsilon_y}{\varepsilon_x} + \mu\right)}{1 - \mu K_t} \times 100 \qquad [11a]$$

nos dá el error en % que sobre la medida de la deformación según ε_x introduce el factor de sensibilidad transversal. Vemos que en el caso en que la dirección de ε_x coincide con la dirección de tensiones unidireccionales (tracción o compresión simple) el error es cero, pues se cumple que $\varepsilon_y = -\mu \varepsilon_x$, (fig 2b).

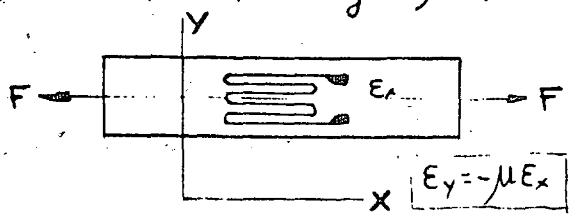

fig 2b

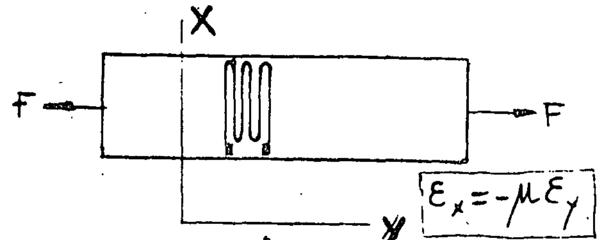

fig 2c

Según la fig. 2c vamos a medir la deformación lateral correspondiente a un estado unidireccional de tensiones, aquí por el giro dado al extensímetro, se cumple que :

$$\varepsilon_x = -\mu\, \varepsilon_y \ ; \quad \frac{\varepsilon_y}{\varepsilon_x} = -\frac{1}{\mu}$$

Si consideramos $\mu = 0{,}3$ y $K_t = 3\%$ sustituyendo en (11a), el error vale:

$$e = \frac{0{,}03\left(-\frac{1}{0{,}3}+0{,}3\right)}{1+0{,}3 \cdot 0{,}03} \times 100 = -9\%$$

El error del-9% no puede despreciarse y aún cuando en - el ejemplo se ha buscado un caso muy extremo, habrá que evaluar siempre la magnitud del error y considerar si debe o nó despreciarse.

El problema en el caso que se conozca la dirección principal de deformaciones (fig. 2b) no tiene importancia, pero como se - verá posteriormente en el caso de rosetas de dos o tres direcciones - el error por efecto de la sensibilidad lateral puede tener influencia, pués se estará siempre entre las dos posturas extremas presentadas en las fig. 2b y 2c.

1.3. OBJETO DE LAS MEDIDAS EXTENSOMETRICAS: Unidades

Los materiales empleados en la fabricación de máquinas o cualquier elemento sometido a solicitaciones externas, sufren en su estructura interna unas tensiones que deben equilibrar las cargas que soportan para que no aparezca la rotura, sobredimensionandose siempre los diseños para obtener un coeficiente de seguridad adecuado. Evidentemente el máximo conocimiento del estado de tensiones ayudará a mejorar el diseño y a reducir el coeficiente de seguridad, pero la medida directa de ten iones no siempre es posible.

Demostraremos en este capítulo, que si conocemos el estado de deformaciones en un punto, podremos calcular el estado de tensiones del mismo y determinar el valor de tensiones críticas (tensiones normales máximas o combinación, en una determinada dirección de - tensiones normales y cortantes, que puedan representar un fallo).

El estado de deformaciones se determinará a partir de las medidas, que en una, dos o tres direcciones, que se efectuen con extensímetros.

Salvo casos muy especiales, la aplicación de las bandas extensométricas será siempre en la superficie de los elementos de ensayo, por lo que solo estudiaremos el estado plano o binaxial de deformaciones y tensiones en un punto.

El concepto de deformaciones es análogo al de alargamiento unitario y lo representaremos por ε midiendose en microdeformaciones($\mu\delta$)

$$\varepsilon \cdot 10^6 = \frac{dl}{l} \cdot 10^6 = \mu\delta \text{ . . . . microdeformación (adimensional)}$$

Diversa literatura suele expresar las deformaciones en micromilimetros/milimetro o micropulgada/pulgada, creando a veces alguna confusión, en realidad es decir lo mismo de una o de otra manera, ya que se trata de la misma unidad por lo que nosotros recomendamos referirse siempre a $\mu\delta$.

El módulo de elasticidad E y las tensiones se expresarán en daN/cm^2, aunque en algunas tablas pueden aparecer estos valores en Kp/cm^2 o Kp/mm^2.

1.4 ESTADO BIAXIAL DE DEFORMACIONES

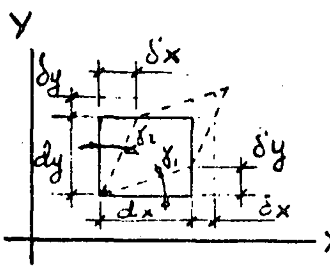

fig3

El rectángulo elemental de la fig. 3 de lados dx y dy tiene como posibles las deformaciones lineales según los ejes X e Y ya definidas y de valor:

$$\varepsilon_x = \frac{\delta x}{dx} \qquad \varepsilon_y = \frac{\delta y}{dy}$$

originadas cuando la dirección del alargamiento coincide con los ejes X e Y respectivamente y otro tipo de deformación llamada angular que aparece cuando hay un desplazamiento transversal de los lados dx y dy que motiva que la forma rectangular original se convierta en rombica. La deformación angular γ_{xy} se define como la suma de los desplazamientos transversales divididos por las longitudes originales que no le son paralelas es

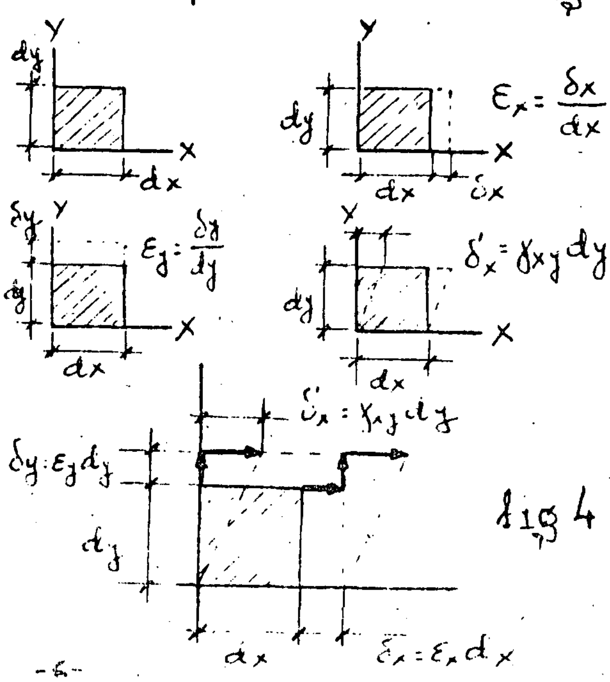

fig 4

decir:

$$\gamma_{xy} = \frac{\delta' x}{dy} + \frac{\delta' y}{dx} = tg\,\gamma_2 + tg\,\gamma_1 \simeq \gamma_1 + \gamma_2$$

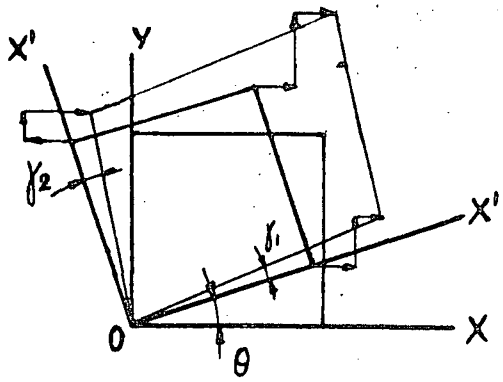

La deformación angular se considera positiva si supone una disminución del ángulo recto original por una extensión.

En un punto arbitrario (fig.4) de la superficie de una pieza cargada podemos aislar un elemento infinistesimal de material para estudiar - sus deformaciones en el plano XY y para ello aplicaremos el principio de superposición, por el cual la deformación total será la suma de las deformaciones parciales, es decir, la suma de la deformación lineal según los ejes X e Y respectivamente y la deformación angular γ_{xy}.

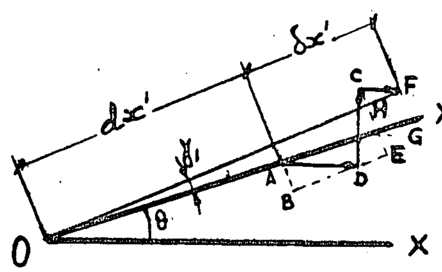

Vamos a relacionar los valores de las deformaciones según los X-Y con otro conjunto de ejes X'-Y' que forman un ángulo θ . Al ángulo θ le consideraremos positivo en sentido contrario al de las agujas del reloj.

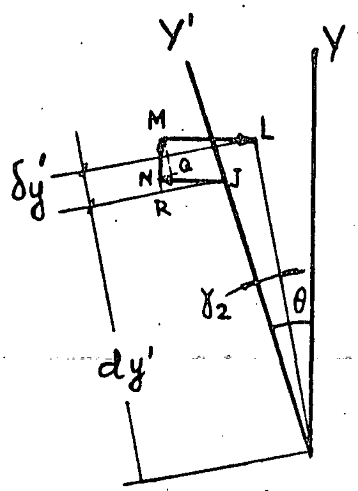

fig 5

En la fig. 5 se observa la geometría del elemento infinitesimal referido a los nuevos ejes X'-Y', el alargamiento según el eje X' será: $\varepsilon_{x'} = \dfrac{\delta x'}{dx'}$

$$\delta x' = \varepsilon_{x'}\, dx' = \overline{BD} + \overline{DE} + \overline{FH}$$

$$\overline{BD} = \varepsilon_x\, dx' \cos\theta \cos\theta = \varepsilon_x\, dx' \cos^2\theta$$

$$\overline{DE} = \varepsilon_y\, dy' \,\mathrm{sen}\,\theta \,\mathrm{sen}\,\theta = \varepsilon_y\, dy' \,\mathrm{sen}^2\theta$$

$$\overline{FH} = dx' \,\mathrm{sen}\,\theta\, \gamma_{xy} \cos\theta$$

$$\varepsilon_{x'} = \varepsilon_x \cos^2\theta + \varepsilon_y \,\mathrm{sen}^2\theta + \gamma_{xy}\,\mathrm{sen}\,\theta\cos\theta \quad \text{- - - - - - - - - -} \quad [12]$$

$$\varepsilon_{y'} = \varepsilon_x \cos^2\left(\theta+\frac{\pi}{2}\right) + \varepsilon_y \,\mathrm{sen}^2\left(\theta+\frac{\pi}{2}\right) + \gamma_{xy}\,\mathrm{sen}\left(\theta+\frac{\pi}{2}\right)\cos\left(\theta+\frac{\pi}{2}\right) \quad \text{- -} \quad [13]$$

La deformación angular viene expresada por: $\gamma_\theta = \gamma_1 + \gamma_2 = \dfrac{\overline{AI}}{dx'} + \dfrac{\overline{JK}}{dy'}$

$$\left.\begin{array}{l} \overline{AI} = -\overline{HC} + \overline{CE} - \overline{AB} \\ \overline{JK} = -\overline{RJ} + \overline{NQ} + \overline{PL} \end{array}\right\} \quad \left.\begin{array}{l} -\overline{HC} = -dx'\,\gamma_{xy}\,\mathrm{sen}^2\theta \\ \overline{CE} = \varepsilon_y\, dx'\,\mathrm{sen}\,\theta\cos\theta \\ -\overline{AB} = -\varepsilon_x\, dx'\,\mathrm{sen}\,\theta\cos\theta \end{array}\right\} \quad \begin{array}{l} -\overline{RJ} = -dy\,\varepsilon_x\,\mathrm{sen}\,\theta\cos\theta \\ \overline{NQ} = dy\,\varepsilon_y\,\mathrm{sen}\,\theta\cos\theta \\ \overline{PL} = dy\,\gamma_{xy}\cos^2\theta \end{array}$$

$$\gamma_\theta = -2\left(\varepsilon_x - \varepsilon_y\right) \operatorname{sen}\theta \cos\theta + \gamma_{xy}\left(\cos^2\theta - \operatorname{sen}^2\theta\right) \quad [14]$$

Si expresamos la (12 y (14) en función del ángulo doble podemos escribirlas

$$\varepsilon_{x'} = \frac{\varepsilon_x + \varepsilon_y}{2} + \frac{\varepsilon_x - \varepsilon_y}{2}\cos 2\theta + \frac{\gamma_{xy}}{2}\operatorname{sen} 2\theta \quad [15]$$

$$\frac{\gamma_\theta}{2} = \frac{\varepsilon_x - \varepsilon_y}{2}\operatorname{sen} 2\theta + \frac{\gamma_{xy}}{2}\cos 2\theta \quad [16]$$

Por ser funciones periódicas tendrán un máximo y un mínimo que calcularemos derivando la (15) respecto a θ e igualando a cero.

$$\frac{d\varepsilon_{x'}}{d\theta} = -2\,\frac{\varepsilon_x - \varepsilon_y}{2}\operatorname{sen} 2\theta + 2\,\frac{\gamma_{xy}}{2}\cos 2\theta = 0$$

$$\operatorname{tg} 2\,\theta_{M\cdot m} = \frac{\gamma_{xy}/2}{\frac{\varepsilon_x - \varepsilon_y}{2}} = \frac{\operatorname{sen} 2\theta}{\cos 2\theta} \quad [17]$$

de donde sustituyendo en (15) tenemos:

$$\varepsilon_{x'(M\text{-}m)} = \frac{\varepsilon_x + \varepsilon_y}{2} + \frac{1}{4\sqrt{\left(\frac{\varepsilon_x - \varepsilon_y}{2}\right)^2 + \left(\frac{\gamma_{xy}}{2}\right)^2}}\left[\left(\varepsilon_x - \varepsilon_y\right)^2 + \gamma_{xy}^2\right] =$$

$$= \frac{\varepsilon_x + \varepsilon_y}{2} \pm \sqrt{\left(\frac{\varepsilon_x - \varepsilon_y}{2}\right)^2 + \left(\frac{\gamma_{xy}}{2}\right)^2} \quad [18]$$

Los subíndices M-m indican los valores máximo y mínimo, en efecto hay dos valores de 2θ M-m que cumplen la ecuación (17) ya que $\operatorname{tg}_M 2\theta = \operatorname{tg}(2\theta + \pi)$ o sea que las direcciones de las deformaciones máxima y mínima son perpendiculares entre sí, verificándose además que la deformación angular es nula como se demuestra sustituyendo la (17) en la (16), la fig, 6 aclara lo expuesto.

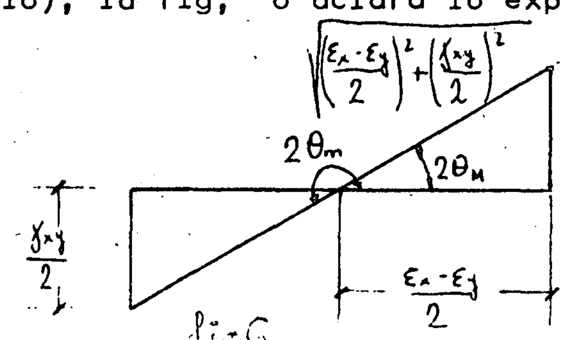

fig6

El valor máximo de la deformación angular se obtiene por el mismo procedimiento y tiene por valor:

$$\frac{\gamma_{\theta M\text{-}m}}{2} = \pm\sqrt{\left(\frac{\varepsilon_x - \varepsilon_y}{2}\right)^2 + \left(\frac{\gamma_{xy}}{2}\right)^2} \quad [19]$$

demostrándose que su dirección forma 45º con respecto a las direcciones principales.

Si el ángulo θ_M que el eje arbitrario X' forma con el eje X hacemos que sea nulo las expresiones (18) y (19) se pueden escribir:

$$\left.\begin{aligned} \varepsilon_{x'(M\cdot m)} &= \frac{\varepsilon_1 + \varepsilon_2}{2} \pm \frac{\varepsilon_1 - \varepsilon_2}{2} \\ \frac{\gamma_{M\cdot m}}{2} &= \pm\,\frac{\varepsilon_1 - \varepsilon_2}{2} \end{aligned}\right\}$$

siendo ε_1 y ε_2 las deformaciones según las direcciones principales.

Para cualquier otra dirección que forme un ángulo α respecto a las principales, las fórmulas quedarán:

$$\varepsilon_\alpha = \frac{\varepsilon_1+\varepsilon_2}{2} + \frac{\varepsilon_1-\varepsilon_2}{2}\cos 2\alpha \quad [20]$$

$$\frac{\gamma_\alpha}{2} = \frac{\varepsilon_1-\varepsilon_2}{2}\,\mathrm{sen}\,2\alpha \quad [21]$$

si llamamos:

$$d = \frac{\varepsilon_1+\varepsilon_2}{2} \quad y \quad r = \frac{\varepsilon_1-\varepsilon_2}{2}, \text{ tendremos que:}$$

$$\varepsilon_\alpha = d + r\cos 2\alpha \quad [22]$$

$$\frac{\gamma_\alpha}{2} = r\,\mathrm{sen}\,2\alpha \quad [23]$$

1.5. ESTADO BIAXIAL DE TENSIONES

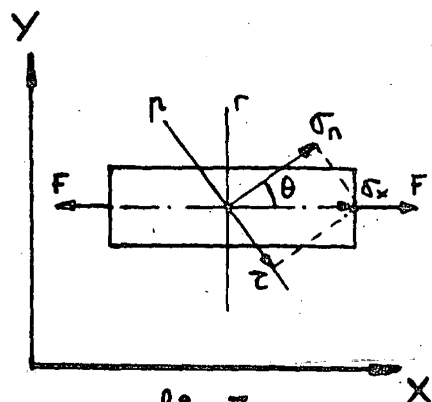

fig7

En una barra prismática sometida a una extensión pura, se llama tensión (esfuerzo o fatiga) a la fuerza que actua por unidad de superficie;

$$\sigma_x = \frac{F}{S} \; (S: \text{sección según } r\text{-}r')$$

si consideramos otra sección S' (según p'-p) cuy normal forma un ángulo θ con el eje de aplicación de fuerzas, la tensión según el eje X valdrá:

$$\sigma_x' = \frac{F}{S'} = \frac{F}{S}\cos\theta = \sigma_x\cos\theta$$

y descomponiéndola en las direcciones normal y tangencial respectivamente de p-p' tendremos que:

$$\sigma_n = \sigma_x\cos\theta\cos\theta = \sigma_x\cos^2\theta \quad [24]$$

$$\tau = \sigma_x\cos\theta\,\mathrm{sen}\,\theta = \frac{1}{2}\sigma_x\,\mathrm{sen}\,2\theta \quad [25]$$

llamándose el valor (24) tensión normal y al (25) tensión cortante.

Estudiaremos el estado biaxial de tensiones en la superficie de un cuerpo que no esté sometido a presiones exteriores; de forma análoga a como se desarrolla el caso de deformaciones, para ello aislemos un elemento infinitesimal de lados paralelos a unos eje X - Y, las acciones que actuen sobre el elemento originan mas tensiones normales y cortantes que mantienen el equilibrio del sistema. - (fig. 8).

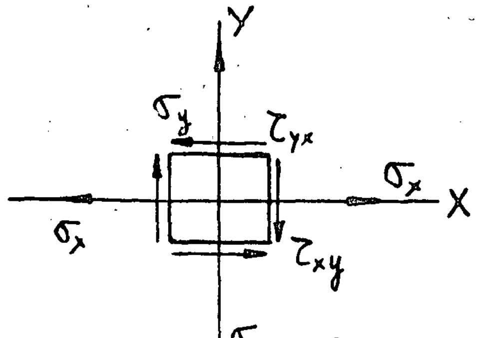

fig 8

Las tensiones normales serán positivas en caso de tracción y negativas en caso de comprensión, así mismo - las tensiones cortantes se consideran positivas cuando producen un par en sentido de las agujas del reloj y negativas en caso contrario.

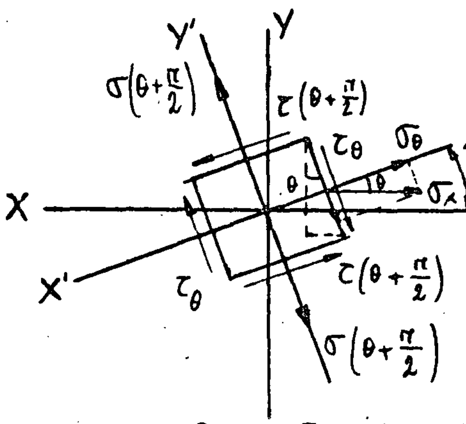

fig 9

En la fig. 9, vemos el elemento infinitesimal referenciado a unos ejes que forman un ángulo θ con los X-Y'; buscaremos el valor de las tensiones ligadas a la nueva orientación de ejes, para ello tengamos en cuenta que el equilibrio debe ser de fuerzas, en efecto:

$$\sigma_\theta S = \sigma_x S \cos\theta \cos\theta + \sigma_y S \operatorname{sen}\theta \operatorname{sen}\theta + \tau_{xy} S \cos\theta \operatorname{sen}\theta + \tau_{yx} S \operatorname{sen}\theta \cos\theta =$$
$$= \sigma_x S \cos^2\theta + \sigma_y S \operatorname{sen}^2\theta + 2\tau_{xy} S \operatorname{sen}\theta \cos\theta$$

$$\sigma_\theta = \sigma_x \cos^2\theta + \sigma_y \operatorname{sen}^2\theta + 2\tau_{xy} \operatorname{sen}\theta \cos\theta \text{ - - - - - - - } [26]$$

$$\tau_\theta = -(\sigma_x - \sigma_y) \operatorname{sen}\theta \cos\theta \operatorname{sen}\theta \cos\theta + \tau_{xy}(\cos^2\theta - \operatorname{sen}^2\theta) \text{ - - - - } [27]$$

ecuaciones que expresadas en función del ángulo doble nos dan:

$$\sigma_\theta = \frac{\sigma_x + \sigma_y}{2} + \frac{\sigma_x - \sigma_y}{2} \cos 2\theta + \tau_{xy} \operatorname{sen} 2\theta \text{ - - - - - } [28]$$

$$\tau_\theta = -\left(\frac{\sigma_x - \sigma_y}{2}\right) \operatorname{sen} 2\theta + \tau_{xy} \cos 2\theta \text{ - - - - - - - - } [29]$$

Si derivamos la (28) respecto a θ e igualamos a cero, encontraremos los valores de θ que hacen máximo y mínimo a dicha ecuación:

$$\frac{d\sigma_\theta}{d\theta} = -(\sigma_x - \sigma_y) \operatorname{sen} 2\theta + 2\tau_{xy} \cos 2\theta = 0$$

$$\operatorname{tg} 2\theta_{M \cdot m} = \frac{\operatorname{sen} 2\theta_{M \cdot m}}{\cos 2\theta_{M \cdot m}} = \frac{\tau_{xy}}{\frac{\sigma_x - \sigma_y}{2}}$$

Por consideraciones análogas a las hechas en el estudio de la deformación biaxial, se deducen que hay dos planos perpendiculares que - corresponden a las direcciones en que las tensiones normales son máxima y mínima respectivamente y en las cuales las tensiones cortantes son nulas.

$$\sigma_{M\cdot m} = \frac{\sigma_x + \sigma_y}{2} \pm \sqrt{\left(\frac{\sigma_x - \sigma_y}{2}\right)^2 + \left(\tau_{xy}\right)^2} \quad [30]$$

De la misma forma encontraremos que:

$$\tau_{M\text{-}m} = \pm \sqrt{\left(\frac{\sigma_x - \sigma_y}{2}\right)^2 + \left(\tau_{xy}\right)^2} \quad [31]$$

El valor máximo y mínimo de la tensión cortante se encuentra defasado 45º respecto a los valores principales de las tensiones normales.

Haciendo que el ángulo $\theta_M = 0$ tenemos que:

$$\sigma_{M\cdot m} = \frac{\sigma_1 + \sigma_2}{2} \pm \frac{\sigma_1 - \sigma_2}{2}$$

$$\tau_{M\text{-}m} = \pm \frac{\sigma_1 + \sigma_2}{2}$$

siendo σ_1 y σ_2 el valor de las tensiones normales máxima y mínima; las tensiones en cualquier dirección que formen un ángulo α con las principales, tienen de valor:

$$\sigma_\alpha = \frac{\sigma_1 + \sigma_2}{2} \pm \frac{\sigma_1 - \sigma_2}{2} \cos 2\alpha \quad [32]$$

$$\tau_\alpha = \frac{\sigma_1 - \sigma_2}{2} \operatorname{sen} 2\alpha \quad [32 \text{ bis}]$$

Llamando

$$\delta = \frac{\sigma_1 + \sigma_2}{2} \quad \text{y} \quad \rho = \frac{\sigma_1 - \sigma_2}{2}$$

tenemos que:

$$\sigma_\alpha = \delta + \rho \cos 2\alpha \quad [33]$$

$$\tau_\alpha = \rho \operatorname{sen} 2\alpha \quad [34]$$

1.6 RELACION ENTRE DEFORMACIONES Y TENSIONES

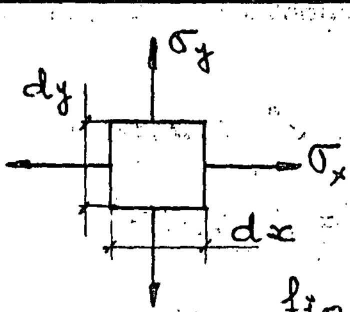

fig10

Suponemos el elemento de la fig. 10, aplicando el teorema de la superposición encontramos que;

$$\left.\begin{aligned} \varepsilon_x &= \frac{\sigma_x}{E} - \mu \frac{\sigma_y}{E} \\ \varepsilon_y &= \frac{\sigma_y}{E} - \mu \frac{\sigma_x}{E} \end{aligned}\right\}$$

$$\sigma_x = \frac{E}{1-\mu^2}\left(\varepsilon_x + \mu \varepsilon_y\right) \quad [35]$$

$$\sigma_y = \frac{E}{1-\mu^2}\left(\varepsilon_y + \mu \varepsilon_x\right) \quad [36]$$

Experimentalmente se demuestra que:

$$\gamma = \frac{\tau}{G} \qquad G = \frac{E}{2(1+\mu)} \quad [37]$$

llamándose a G coeficiente de elasticidad a cortadura.

Recordando las relaciones:

$$d = \frac{\varepsilon_1 + \varepsilon_2}{2} \qquad \delta = \frac{\sigma_1 + \sigma_2}{2}$$

$$r = \frac{\varepsilon_1 - \varepsilon_2}{2} \qquad \rho = \frac{\sigma_1 - \sigma_2}{2}$$

se deduce que:

$$\varepsilon_1 + \varepsilon_2 = \frac{\sigma_1}{E} - \mu\frac{\sigma_2}{E} + \frac{\sigma_2}{E} - \mu\frac{\sigma_1}{E} = \sigma_1 + \sigma_2 \left(\frac{1-\mu}{E}\right)$$

$$\delta = \frac{\sigma_1 + \sigma_2}{2} = \frac{\varepsilon_1 + \varepsilon_2}{2}\ \frac{E}{1-\mu} = d\ \frac{E}{1-\mu} \qquad [38]$$

$$\varepsilon_1 - \varepsilon_2 = \sigma_1 - \sigma_2\ \frac{1+\mu}{E}$$

$$\rho = \frac{\sigma_1 - \sigma_2}{2} = \frac{\varepsilon_1 - \varepsilon_2}{2}\ \frac{E}{1+\mu} = r\ \frac{E}{1+\mu} \qquad [39]$$

1.7. REPRESENTACION GRAFICA DEL ESTADO BIAXIAL DE TENSIONES Y DEFORMACIONES; CIRCULOS DE MOHR

Una de las formas más sencillas y usuales de representación del estado plano de deformaciones y tensiones es el círculo de Mohr. Recordemos que la deformación en una dirección cualquiera que forma un ángulo α respecto a las direcciones principales tiene por valor:

$$\varepsilon_\alpha = \frac{\varepsilon_1 + \varepsilon_2}{2} + \frac{\varepsilon_1 - \varepsilon_2}{2}\cos 2\alpha = d + r\cos 2\alpha$$

$$\frac{\gamma_\alpha}{2} = \frac{\varepsilon_1 - \varepsilon_2}{2}\ \text{sen}\, 2\alpha = r\ \text{sen}\, 2\alpha$$

Podemos representar prácticamente éstas ecuaciones según la fig. 11, pués se cumple que:

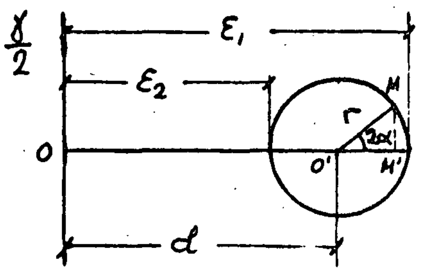

fig11

$$\varepsilon_\alpha = \overline{OM'} = d + r\cos 2\alpha$$

$$\frac{\gamma_\alpha}{2} = \overline{MM'} = r\ \text{sen}\, 2\alpha$$

Observemos que el valor máximo y el mínimo

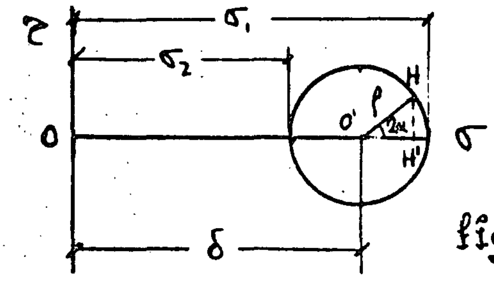

fig12

La fig. 12 nos indica el circulo de Mohr para el estado de tensiones y vemos su similitud con el de deformaciones.

$$\sigma_\alpha = \overline{OH} = \delta + \rho\cos 2\alpha$$

$$\tau_\alpha = \overline{HH'} = \rho\ \text{sen}\, 2\alpha$$

En el dominio elástico de los cuerpos isotrópicos, - existe proporcionalidad entre deformaciones y tensiones, por lo que los circulos representativos de ambos valores son concéntricos. Los coeficientes de proporcionalidad han sido deducidos en el apartado 1.6 (fig. 13).

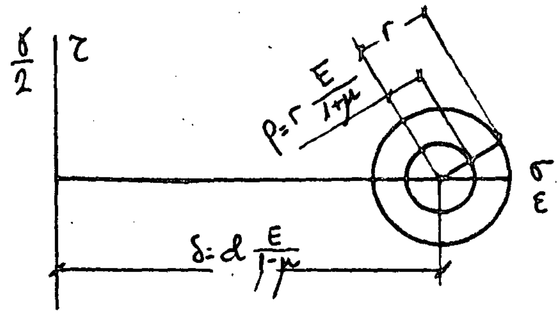

fig 13

1.8 EJEMPLOS DE APLICACION DE LOS CIRCULOS DE MOHR.

Nº 1. Sobre el elemento de la fig. 14 actuan las tensiones que se indican. Calcular analítica y gráficamente el valor y dirección de los esfuerzos principales.

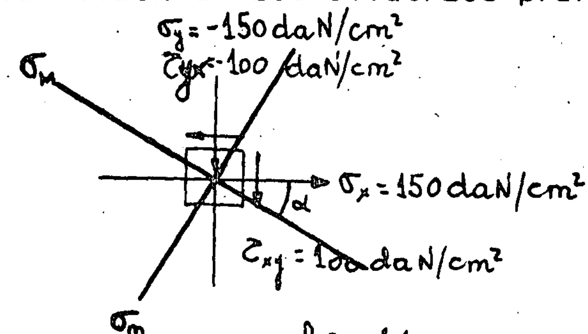

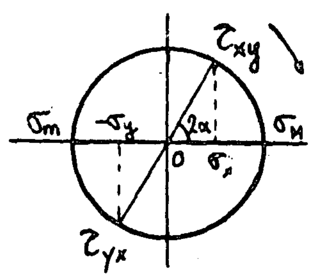

fig 14

$$\sigma_{M-m} = \frac{150+(-150)}{2} \pm \sqrt{\left(\frac{150-(-150)}{2}\right)^2 + 100^2} = \pm\ 180\ \text{daN/cm}^2$$

$$tg\ 2\alpha = \frac{100}{\frac{150-(-150)}{2}} = 0{,}66 \qquad 2\alpha = \begin{cases} 41^\circ \\ 41^\circ + 180 \end{cases} \qquad \alpha = \begin{cases} 20{,}5^\circ \\ 20{,}5^\circ + 90^\circ \end{cases}$$

Nº2 Idem al anterior. (fig 15)

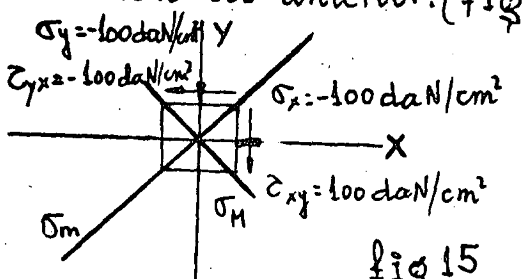

fig 15

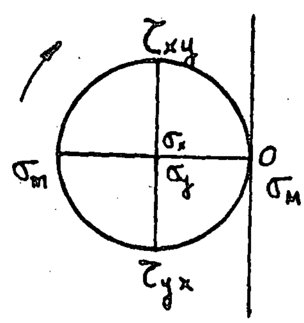

$$\delta = \frac{-100+(-100)}{2} = -100$$

$$\rho = \pm\sqrt{\left(\frac{-100-(-100)}{2}\right)^2 + 100^2} = 100$$

$$tg\ 2\alpha = \frac{100}{\frac{-100-(-100)}{2}} = -\infty$$

$$\sigma_M = \delta + \rho = -100 + 100 = 0$$

$$\sigma_m = \delta - \rho = -100 - 100 = -200$$

$$\alpha = 45^\circ$$

Casos típicos de aplicación del circulo de Mohr.

TORSION

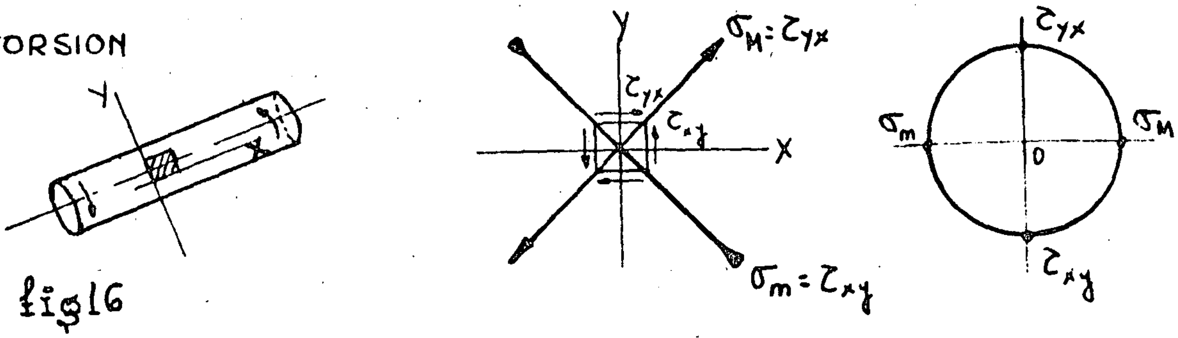

fig16

TORSION Y TRACCION

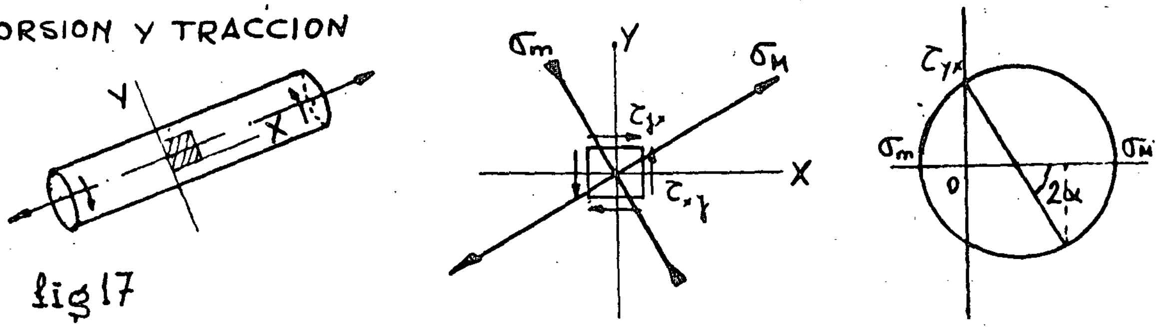

fig17

TRACCION

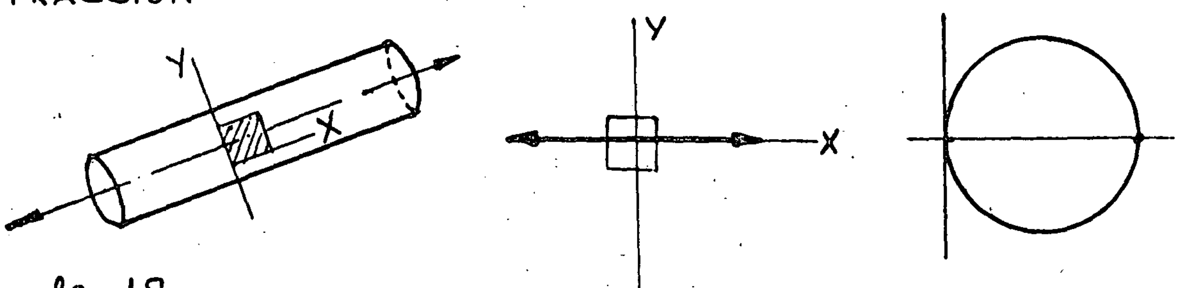

fig18

CILINDRO BAJO PRESION

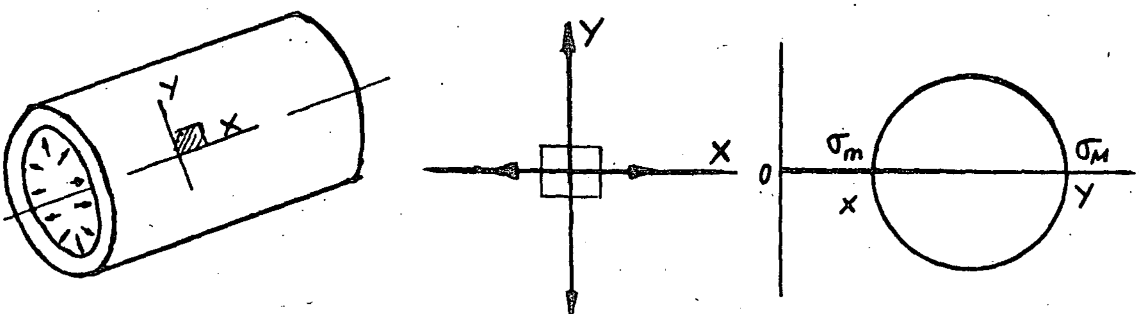

fig19

ESFERA BAJO PRESION

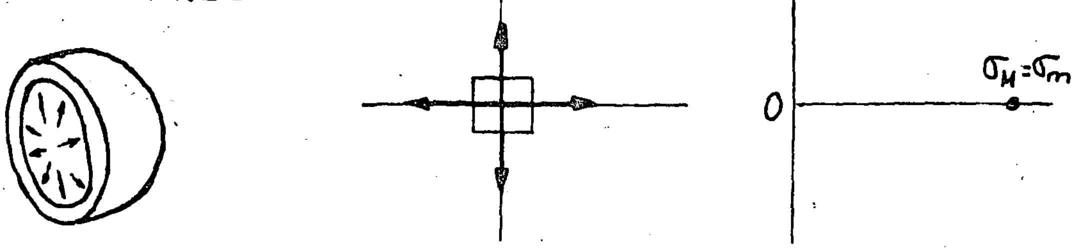

fig20

Bandas de tres direcciones o rosetas (Rectangulares)

Consideremos el valor de las deformaciones (fig. 21) en direcciones A, B y C que forman los ángulos θ_A, θ_B y θ_C respectivamente con el eje X de unos ejes arbitrarios X-Y, tendremos:

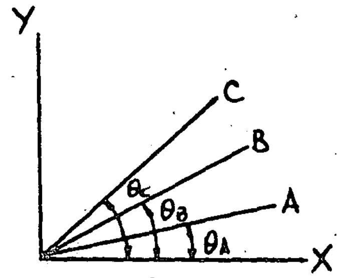

fig21

$$\varepsilon_A = \frac{\varepsilon_x+\varepsilon_y}{2} + \frac{\varepsilon_x-\varepsilon_y}{2}\cos 2\theta_A + \frac{\gamma_{xy}}{2}\operatorname{sen} 2\theta_A$$

$$\varepsilon_B = \frac{\varepsilon_x+\varepsilon_y}{2} + \frac{\varepsilon_x-\varepsilon_y}{2}\cos 2\theta_B + \frac{\gamma_{xy}}{2}\operatorname{sen} 2\theta_B$$

$$\varepsilon_C = \frac{\varepsilon_x+\varepsilon_y}{2} + \frac{\varepsilon_x-\varepsilon_y}{2}\cos 2\theta_C + \frac{\gamma_{xy}}{2}\operatorname{sen} 2\theta_C$$

Si hacemos que:

$$\theta_A = 0 \;;\quad \theta_B = \frac{\pi}{4} \;;\quad \theta_C = \frac{\pi}{2}$$ nos queda:

$$\left.\begin{aligned} \varepsilon_A &= \varepsilon_x \\ \varepsilon_B &= \frac{\varepsilon_x+\varepsilon_y}{2} + \frac{\gamma_{xy}}{2} \\ \varepsilon_C &= \varepsilon_y \end{aligned}\right\} \begin{aligned} &\varepsilon_x = \varepsilon_A \\ &\varepsilon_y = \varepsilon_C \\ &\gamma_{xy} = 2\varepsilon_B - (\varepsilon_A - \varepsilon_B) = (\varepsilon_B - \varepsilon_A) + (\varepsilon_B - \varepsilon_C) \ldots [42] \end{aligned}$$

Sustituyendo las (41 y (42) en (18) y (19) y simplificando tenemos:

$$\varepsilon_M = \frac{\varepsilon_A+\varepsilon_C}{2} + \frac{1}{\sqrt{2}}\sqrt{(\varepsilon_A-\varepsilon_B)^2 + (\varepsilon_B-\varepsilon_C)^2} \quad \text{-----} \quad [43]$$

$$\varepsilon_m = \frac{\varepsilon_A+\varepsilon_C}{2} - \frac{1}{\sqrt{2}}\sqrt{(\varepsilon_A-\varepsilon_B)^2 + (\varepsilon_B-\varepsilon_C)^2} \quad \text{-----} \quad [44]$$

$$\gamma_{M \cdot m} = \pm\sqrt{2}\,\sqrt{(\varepsilon_A-\varepsilon_B)^2 + (\varepsilon_B-\varepsilon_C)^2} \quad \text{-----} \quad [45]$$

$$\operatorname{tg} 2\theta_M = \left[\frac{(\varepsilon_B-\varepsilon_A)+(\varepsilon_B-\varepsilon_C)}{\varepsilon_A-\varepsilon_C}\right] \quad \text{-----} \quad [46]$$

El ángulo θ_M será el que forma la dirección principal máxima con la dirección A.

Los valores de las tensiones máxima y mínima

$$\sigma_{M \cdot m} = \frac{E}{2}\left[\frac{\varepsilon_A+\varepsilon_C}{1-\mu} \pm \frac{\sqrt{2}}{1+\mu}\sqrt{(\varepsilon_A-\varepsilon_B)^2 + (\varepsilon_B-\varepsilon_C)^2} \quad \text{-----} \quad [47]\right.$$

$$\tau_M = \frac{E}{\sqrt{2}\,(1+\mu)}\sqrt{(\varepsilon_A-\varepsilon_B)^2 + (\varepsilon_B-\varepsilon_C)^2} \quad \text{-----} \quad [48]$$

Las fórmulas (47) y (48) dan directamente los valores de las tensiones principales a partir de los valores de las deformaciones en las direcciones A, B y C.

Las ecuaciones anteriores corresponden a una banda extensométrica roseta rectangular como la indicada en la fig. 22.

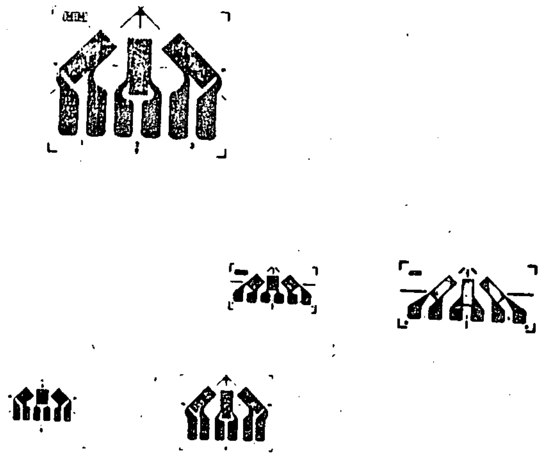

fig 22

Vamos a ver gráficamente como se determinan las deformaciones principales a partir de las deformaciones ε_A; ε_B y ε_C valiéndonos del círculo de Mohr.

Sobre el eje x (fig. 23) traslademos los valores ε_A; ε_B y ε_C. En el círculo ε_A y ε_C tienen que estar defasados 180º; por lo que el centro del mismo será $d = \frac{\varepsilon_A + \varepsilon_C}{2}$, la dirección de ε_B estará en el círculo defasada 90º; por lo que debe cumplirse la igualdad de los triángulos $\overset{\triangle}{O'BB'} = \overset{\triangle}{O'CC'}$ con lo que hemos determinado $r = \overline{CO'}$

En el círculo observamos que desde el punto A que corresponde a ε_A tenemos que correr un ángulo positivo 2α para llegar a $\varepsilon_1 = \varepsilon_M$; por lo tanto y sobre la banda roseta desplazaremos un ángulo α para la dirección de la deformación principal máxima. El ángulo α es el que forma la dirección principal máxima tomada como referencia y la dirección A, considerando como positivo el sentido contrario al giro de las agujas del reloj.

Conocido el círculo de Mohr de deformaciones fácilmente se deduce el de tensiones (ver. 1.6) de la fig. 23 se deduce:

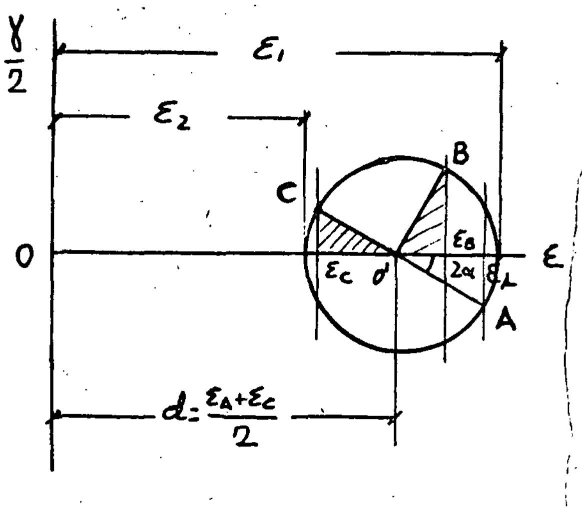

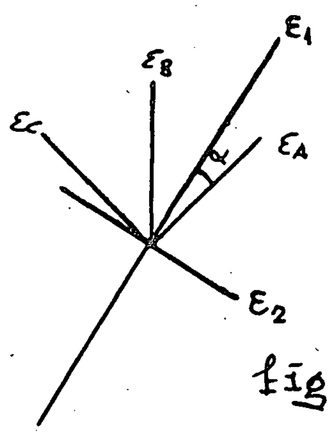

fig 23

1.10 CALCULO TABULADO PARA ROSETAS RECTANGULARES

Sean ε_A ; ε_B y ε_C las medidas de las bandas, A, B y C.

1) Cálculo de d: $d = \frac{\varepsilon_A + \varepsilon_C}{2}$ (con su signo)
2) Cálculo de r:

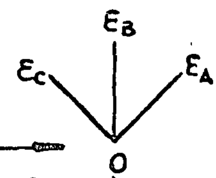

Anotar los 3 valores con su signo

Restar ($-\varepsilon_B$) a los 3 valores, se obtiene

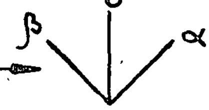

Anotar el signo que corresponda al mayor valor de α ó β en valor absoluto

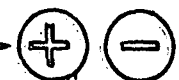

Sea, por ejemplo, α ese número. Dividir α y β por α con su signo.
Se obtiene

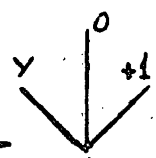

Y puede ser positivo o negativo, pero inferior a 1 en valor absoluto.
Buscar en la tabla I el valor W que corresponde a Y
Se tiene que: $r = |\alpha|\ W$ (Número positivo)
Las deformaciones principales son:

$$\varepsilon_1 = d + r$$
$$\varepsilon_2 = d - r$$

Buscar en la tabla II, el ángulo que corresponde a Y con su signo. α está comprendido entre 0 y 45º. Llevar el ángulo α en sentido externo (que se aleje de la referencia O) sobre el eje marcado con el 1.

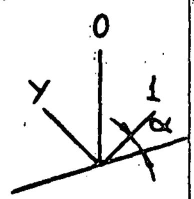

La dirección obtenida es:

Máxima si anotamos el signo +
Mínima si anotamos el signo −

TABLAS PARA EL CALCULO CON ROSETAS DE 45º

TABLA Nº 1

|y|		1	2	3	4	5	6	7	8	9
0,00	)71	71	71	71	71	71	71	71	71	71
0,01	071	71	72	72	72	72	72	72	72	72
0,02	/072	73	73	73	73	73	73	74	74	74
0,03	0,7074	74	75	75	75	75	76	76	76	76
0,04	0,7077	77	77	78	78	78	79	79	79	80
0,05	0,7080	80	81	81	81	82	82	83	83	83
0,06	0,7084	84	85	85	86	86	87	87	88	88
0,07	0,7088	89	89	90	90	91	91	92	93	93
0,08	0,7094	94	95	95	96	97	97	98	98	98
0,09	0,7099									
		00	01	02	02	03	04	04	05	06
0,10	0,7106	07	08	08	09	10	11	11	12	13
0,11	0,7114	14	15	16	17	18	18	19	20	21
0,12	0,7122	23	24	24	25	26	27	28	29	30
0,13	0,7131	31	32	33	34	35	36	37	38	39
0,14	0,7140	41	42	43	44	45	46	47	48	49
0,15	0,7150	51	52	53	54	56	57	58	59	60
0,16	0,7161	62	63	64	65	67	68	69	70	71
0,17	0,7172	74	75	76	77	78	80	81	82	83
0,18	0,7185	86	87	88	90	91	92	94	95	96
0,19	0,7198	99								
			00	01	03	04	06	07	08	10
0,20	0,7211	12	14	15	17	18	19	21	22	24
0,21	0,7225	27	28	30	31	33	34	36	37	39
0,22	0,7240	42	43	45	46	48	49	51	52	54
0,23	0,7256	57	59	61	62	64	65	67	69	70
0,24	0,7272	74	75	77	78	80	82	84	85	87
0,25	0,7289	90	92	94	96	97	99			
								01	03	04
0,26	0,7306	08	10	11	13	15	16	19	21	22
0,27	0,7324	26	28	30	32	34	36	37	39	41
0,28	0,7343	45	47	49	51	53	55	56	58	60
0,29	0,7362	64	66	68	70	72	74	76	78	80
0,30	0,7382	84	86	89	91	93	95	97	99	
										01
0,31	0,7403	05	07	09	11	14	16	18	20	22
0,32	0,7424	26	29	31	33	35	37	39	42	44
0,33	0,7446	48	51	53	55	57	60	62	64	66
0,34	0,7469	71	73	75	77	80	82	85	87	89
0,35	0,7492	94	96	99						
					01	03	05	08	10	13
0,36	0,7515	17	20	22	25	27	30	32	35	37
0,37	0,7540	42	44	47	49	52	54	57	59	62
0,38	0,7564	67	69	72	74	77	80	82	85	87
0,39	0,7590	92	95	97						
					00	03	05	08	11	13
0,40	0,7616	18	21	24	26	29	32	34	37	40
0,41	0,7642	45	48	50	53	56	58	61	64	66
0,42	0,7669	72	75	77	80	83	86	89	91	94
0,43	0,7697									
		00	03	06	08	11	14	17	20	22
0,44	0,7725	28	31	34	37	40	42	45	48	51
0,45	0,7754	57	60	63	66	69	71	74	77	80
0,46	0,7783	86	89	92	95	98				
							01	04	07	10
0,47	0,7813	16	19	22	25	28	31	34	37	40
0,48	0,7843	46	50	53	56	59	62	65	68	71
0,49	0,7874	77	80	84	87	90	93	96	99	
										03
0,50	0,7907	09	12	15	18	22	25	28	31	34
0,51	0,7937	40	44	47	50	54	57	60	63	67
0,52	0,7970	73	76	80	83	86	90	93	96	
										00
0,53	0,8003	06	09	13	16	19	23	26	29	33
0,54	0,8036	40	43	46	50	53	57	60	63	67
0,55	0,8070	73	77	80	84	87	91	94	97	
										01
0,56	0,8104	08	11	15	19	22	25	29	32	36
0,57	0,8139	43	46	50	53	57	60	64	67	71
0,58	0,8174	78	81	85	89	92	95	99		
									03	06
0,59	0,8210	14	17	21	24	28	32	35	39	43
0,60	0,8246	50	53	57	61	64	68	72	76	79
0,61	0,8283	86	90	94	97					
						01	05	09	12	1C
0,62	0,8320	24	27	31	35	39	42	46	50	54
0,63	0,8357	61	65	69	72	76	80	84	88	91
0,64	0,8395	99								

TABLA Nº 1
(continuación)

|y|	0	1	2	3	4	5	6	7	8	9
			03	07	10	14	18	22	26	30
0,65	0,8434	37	41	45	49	[illegible]	57	61	65	68
0,66	0,8472	76	80	84	[illegible]	[illegible]	[illegible]			
					[illegible]	[illegible]	[illegible]	00	04	08
0,67	0,8511	15	19	23	[illegible]	31	[illegible]	39	43	47
0,68	0,8551	55	59	63	67	71	75	79	83	87
0,69	0,8591	95	99							
				03	07	[illegible]	15	[illegible]	23	27
0,70	0,8631	35	39	43	48	[illegible]	56	[illegible]	64	68
0,71	0,8672	76	80	84	88	93	97			
								01	05	08
0,72	0,8713	17	21	26	30	34	38	42	46	51
0,73	0,8755	59	63	67	71	76	80	84	88	92
0,74	0,8796									
		01	05	09	13	18	22	26	30	35
0,75	0,8839	43	47	52	56	60	64	[illegible]	[illegible]	77
0,76	0,8881	86	90	94	99					
						03	07	11	16	20
0,77	0,8924	29	33	37	42	46	50	54	58	63
0,78	0,8968	72	76	81	85	89	94	98		
									03	07
0,79	0,9011	16	20	25	29	33	38	42	47	51
0,80	0,9055	60	64	69	73	77	82	86	91	95
0,81	0,9100	04	09	13	18	22	26	31	35	40
0,82	0,9144	49	53	58	62	67	71	76	80	85
0,83	0,9189	94	98							
				03	07	12	17	21	26	30
0,84	0,9235	39	44	48	53	57	62	67	71	76
0,85	0,9280	85	90	94	99					
						03	08	12	17	22
0,86	0,9326	31	36	40	45	49	54	59	63	68
0,87	0,9373	77	82	86	91	96				
							00	05	10	14
0,88	0,9419	24	28	33	38	43	47	52	57	61
0,89	0,9466	71	75	80	85	90	94	99		
									04	08
0,90	0,9513	18	23	27	32	37	42	46	51	56
0,91	0,9561	65	70	75	80	84	89	94	99	
										04
0,92	0,9608	13	18	23	27	32	37	42	47	52
0,93	0,9656	61	66	71	76	80	85	90	95	
										00
0,94	0,9705	09	14	19	24	29	34	39	43	48
0,95	0,9753	58	63	68	73	78	82	87	92	97
0,96	0,9802	07	12	17	22	27	31	36	41	46
0,97	0,9851	56	61	66	71	76	81	86	91	96
0,98	0,9901	05	10	15	20	25	30	35	40	45
0,99	0,9950	55	60	65	70	75	80	85	90	95
1,00	1,0000									

TABLA Nº 2

Y	0	1	2	3	4	5	6	7	8	9
— 1,0	0.0									
— 0,9	1.5	1,3	1,2	1,0	[illegible]	0,7	0,6	0,4	0,3	0,1
— 0,8	3.2	3,0	2,8	2,7	2,5	2,3	2,2	2,0	1,8	1,7
— 0,7	5.0	4,8	4,6	4,4	4,2	4,1	3,9	3,7	3,5	3,3
— 0,6	7.0	6,8	6,6	6,4	6,2	6,0	5,8	5,6	5,4	5,2
— 0,5	9.2	9,0	8,8	8,5	8,3	8,1	7,9	7,7	7,4	7,2
— 0,4	11,6	11,4	11,1	10,9	10,6	10,4	10,1	9,9	9,7	9,4
— 0,3	14,1	13,9	13,6	13,4	13,1	12,9	12,6	12,3	12,1	11,8
— 0,2	16,8	16,6	16,3	16,0	15,8	15,5	15,2	15,0	14,7	14,4
— 0,1	19,7	19,4	19,1	18,8	18,5	18,2	17,9	17,7	17,4	17,1
— 0,0	22,5	22,2	21,9	21,7	21,4	21,0	20,8	20,5	20,2	19,9
+ 0,0	22,5	22,8	23,1	23,3	23,6	24,0	24,2	24,5	24,8	25,1
+ 0,1	25,3	25,6	25,9	26,2	26,5	26,8	27,1	27,3	27,6	27,9
+ 0,2	28,2	28,4	28,7	29,0	29,2	29,5	29,8	30,0	30,3	30,6
+ 0,3	30,9	31,1	31,4	31,6	31,9	32,1	32,4	32,7	32,9	33,2
+ 0,4	33,4	33,6	33,9	34,1	34,4	34,6	34,9	35,1	35,3	35,6
+ 0,5	35,8	36,0	36,2	36,5	36,7	36,9	37,1	37,3	37,6	37,8
+ 0,6	38,0	38,2	38,4	38,6	38,8	39,0	39,2	39,4	39,6	39,8
+ 0,7	40,0	40,2	40,4	40,6	40,8	40,9	41,1	41,3	41,5	41,7
+ 0,8	41,8	42,0	42,2	42,3	42,5	42,7	42,8	43,0	43,2	43,3
+ 0,9	43,5	43,7	43,8	44,0	44,1	44,3	44,4	44,6	44,7	44,9
+ 1,0	45,0									

1.11 BANDAS DE TRES DIRECCIONES O ROSETAS (EQUIANGULARES)

Las direcciones arbitrarias de la medida de tres deformaciones en un punto podemos hacer que estén defasados 120º con lo que la banda tiene la geometría indicada en la fig. 24 y por consideraciones análogas al caso de la roseta rectangular encontramos los resultados que se indican

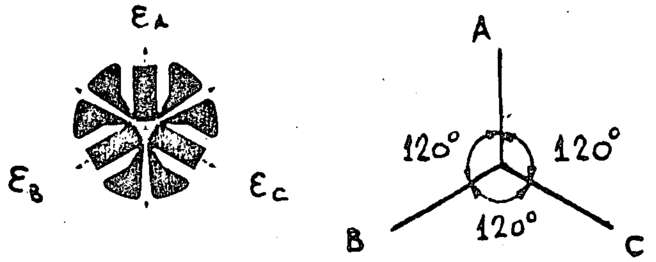

$$\sigma_{M-m} = \frac{E}{3}\left[\frac{\varepsilon_A+\varepsilon_B+\varepsilon_C}{1-\mu} \pm \frac{\sqrt{2}}{1+\mu}\sqrt{(\varepsilon_A-\varepsilon_C)^2+(\varepsilon_C-\varepsilon_B)^2+(\varepsilon_B-\varepsilon_A)^2}\right. \quad [49]$$

$$\tau = \frac{\sqrt{2}\,E}{3(1+\mu)}\sqrt{(\varepsilon_A-\varepsilon_C)^2+(\varepsilon_C-\varepsilon_B)^2+(\varepsilon_B-\varepsilon_A)^2} \quad [50]$$

$$\operatorname{tg} 2\theta = \frac{\sqrt{3}\,(\varepsilon_C-\varepsilon_B)}{2\varepsilon_A-\varepsilon_B-\varepsilon_C} \quad [51]$$

siendo θ el ángulo de la dirección principal máxima con la dirección A.

Gráficamente podemos encontrar la solución llevando sobre el eje X del diagrama de Mohr los valores de ε_A, ε_B y ε_C (fig. 25).

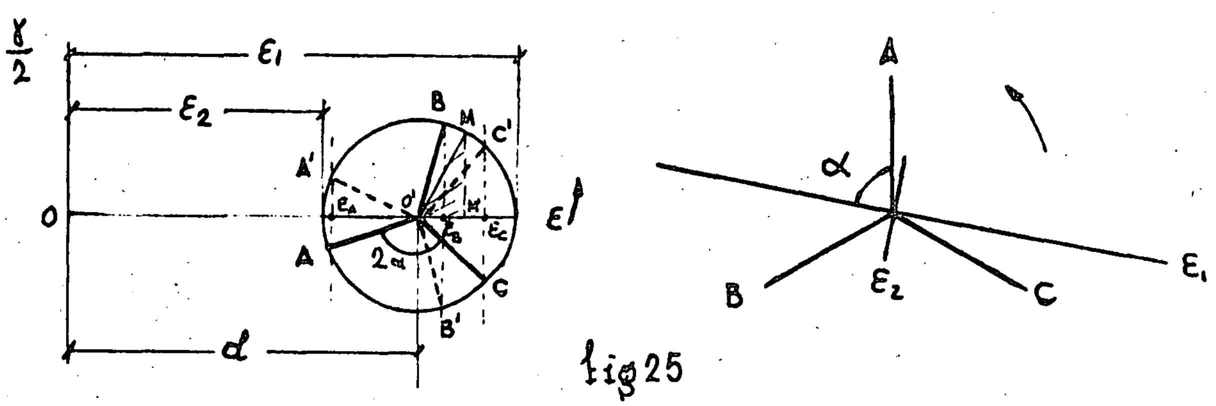

fig 25

El centro del círculo sera $d = \frac{\varepsilon_A+\varepsilon_B+\varepsilon_C}{3}$; sobre las dos proyecciones que queden a la derecha o a la izquierda del centro O; se levanta MM' perpendicular en el punto medio de las dos proyecciones y desde O' se traza una recta que forma 60º con el eje X, el punto de intersección M nos dá el radio del círculo $r = \overline{O'M}$. Aparentemente hay dos soluciones pero los puntos A'-B' y C' no guardan en el circulo el defase de 240º de acuerdo con la orientación de las -

direcciones de la banda

De la fig. 25 deducimos:

$$\left.\begin{array}{l} d = \dfrac{\varepsilon_A + \varepsilon_C + \varepsilon_B}{3} \\ \\ r = \dfrac{\varepsilon_a - d}{\cos 2\alpha} \end{array}\right\} \left.\begin{array}{l} \varepsilon_1 = d + r \\ \varepsilon_2 = d - r \end{array}\right\} \operatorname{tg} 2\alpha = \frac{\sqrt{3}\,(\varepsilon_a - \varepsilon_1)}{2\varepsilon_A - \varepsilon_B - \varepsilon_C}$$

$$\left.\begin{array}{l} \sigma_1 = \dfrac{E}{1-\mu^2}\left(\varepsilon_1 + \mu\varepsilon_2\right) \\ \\ \sigma_2 = \dfrac{E}{1-\mu^2}\left(\varepsilon_2 + \mu\varepsilon_1\right) \end{array}\right\}$$

1.12 CALCULO TABULADO PARA ROSETAS EQUIANGULARES

Sean ε_A, ε_B y ε_C las tres medidas con su signo

1) Cálculo de d: $d = \frac{\varepsilon_A + \varepsilon_B + \varepsilon_C}{3}$

2) Cálculo de r:

Anotar las tres medidas según su dirección ⟶

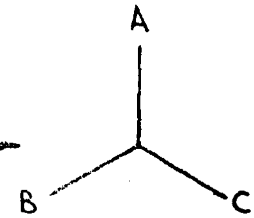

Uno al menos de los valores medios, es algebraicamente igual o menor que los otros dos. Sea por ejemplo ε_C . Se suma $(-\varepsilon_C)$ a los tres valores. Se obtiene así O y dos números positivos α y β ⟶

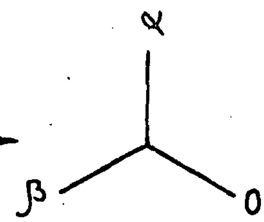

Dividimos a continuación por el número mayor α o β sea por ejemplo β ⟶

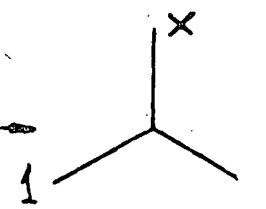

En la tabla III se obtiene un número $U=f(x)$, tal que $r = \beta \cdot U$

$\varepsilon_1 = d + r$
$\varepsilon_2 = d - r$

3) Cálculo de φ

La tabla IV dá el ángulo en función de X. Este ángulo comprendido entre O y 30º se lleva sobre el esquema de direcciones haciendo girar un ángulo φ la dirección marcada con 1 en el sentido que se aproxima a la dirección marcada con O. La dirección obtenida es la algebraicamente máxima.

TABLAS PARA
EL CALCULO CON
ROSETAS DE 120º

TABLA Nº 3

x	0	1	2	3	4	5	6	7	8	9		
0,00	0,6667	63	60	57	53	50	47	43	40	39	0,6634	0,99
0,01	34	30	27	24	20	17	13	10	07	04	01	0,98
0,02	01											
		98	95	91	88	85	82	79	75	72	0,6569	0,97
0,03	0,6569	66	63	59	56	53	50	47	44	41	37	0,96
0,04	37	34	31	28	25	22	19	16	13	09	06	0,95
0,05	06	03	00									
				97	94	91	88	85	82	79	0,6476	0,94
0,06	0,6476	73	70	67	64	61	58	55	52	49	46	0,93
0,07	46	43	40	37	34	31	28	25	22	20	17	0,92
0,08	16	14	11	08	05	02						
							99	96	94	91	0,6387	0,91
0,09	0,6388	85	82	79	76	74	71	68	65	62	60	0,90
0,10	60	57	54	51	48	46	43	40	37	35	32	0,89
0,11	32	29	26	24	21	18	16	13	10	08	04	0,88
0,12	05	02										
			99	97	94	92	89	86	84	81	0,6278	0,87
0,13	0,6278	76	73	70	68	65	63	60	58	55	52	0,86
0,14	52	50	47	45	42	40	37	35	32	30	27	0,85
0,15	27	25	22	20	17	15	12	10	07	04	02	0,84
0,16	02	00										
			98	95	93	90	88	86	83	81	0,6178	0,83
0,17	0,6178	76	74	71	69	67	64	62	60	57	55	0,82
0,18	55	53	50	48	46	44	41	39	37	34	32	0,81
0,19	32	30	28	26	23	21	19	17	14	12	10	0,80
0,20	10	08	06	04	01							
						99	97	95	93	91	0,6089	0,79
0,21	0,6089	86	84	82	80	78	76	74	72	70	68	0,78
0,22	68	66	64	62	60	58	56	54	52	50	48	0,77
0,23	48	46	44	42	40	38	36	34	32	30	28	0,76
0,24	28	26	24	22	20	19	17	15	13	11	09	0,75
0,25	09	07	05	03	02	00						
							98	96	95	93	0,5991	0,74
0,26	0,5991	89	88	86	84	82	80	79	77	75	74	0,73
0,27	74	72	70	69	67	65	64	62	60	59	57	0,72
0,28	57	55	54	52	50	49	47	46	44	42	41	0,71
0,29	41	39	38	36	35	33	32	30	28	27	25	0,70
0,30	25	24	22	21	20	18	17	15	14	13	11	0,69
0,31	10	09	08	07	05	04	02	01				
									99	98	0,5897	0,68
0,32	0,5897	96	94	93	92	90	89	88	86	85	84	0,67
0,33	64	82	81	80	79	77	76	75	74	72	71	0,66
0,34	71	70	69	68	66	65	64	63	62	60	59	0,65
0,35	59	58	57	56	55	54	53	52	51	50	48	0,64
0,36	48	47	46	45	44	43	42	41	40	39	38	0,63
0,37	38	37	36	35	34	33	32	31	30	30	29	0,62
0,38	29	28	27	26	25	24	23	22	22	21	20	0,61
0,39	20	19	18	17	17	16	15	14	13	13	12	0,60
0,40	12	11	10	10	09	08	07	07	06	05	05	0,59
0,41	05	04	03	03	02	01	01	00				
									99	99	0,5798	0,58
0,42	0,5798	97	97	96	96	95	95	94	93	93	92	0,57
0,43	92	92	91	91	90	90	89	89	88	88	87	0,56
0,44	87	87	86	86	86	85	85	84	84	83	83	0,55
0,45	83	83	82	82	82	81	81	81	80	80	80	0,54
0,46	80	79	79	79	78	78	78	78	77	77	77	0,53
0,47	77	77	77	76	76	76	76	76	75	75	75	0,52
0,48	75	75	75	75	74	74	74	74	74	74	74	0,51
0,49	74	74	74	74	74	74	74	74	74	73	0,5773	0,50
		9	8	7	6	5	4	3	2	1	0	x

TABLA Nº 4

x	0	1	2	3	4	5	6	7	8	9
0,0	0,00	0,25	0,50	0,76	1,01	1,28	1,53	1,80	2,07	2,33
0,1	2,61	2,88	3,16	3,43	3,72	3,99	4,28	4,58	4,87	5,15
0,2	5,45	5,74	6,04	6,34	6,64	6,95	7,26	7,57	7,92	8,18
0,3	8,50	8,82	9,13	9,45	9,77	10,09	10,41	10,73	11,06	11,38
0,4	11,70	12,03	12,36	12,69	13,02	13,35	13,68	14,01	14,34	14,67
0,5	15,00	15,33	15,66	15,99	16,32	16,65	16,98	17,31	17,64	17,97
0,6	18,30	18,62	18,94	19,27	19,59	19,91	20,23	20,55	20,87	21,18
0,7	21,50	21,82	22,08	22,43	22,74	23,05	23,36	23,66	23,96	24,26
0,8	24,55	24,85	25,13	25,42	25,72	26,01	26,28	26,57	26,84	27,12
0,9	27,39	27,67	27,93	28,20	28,47	28,72	28,99	29,24	29,50	29,75
1,0	30,00									

ABACO PARA EL
CALCULO DE
TENSIONES
(Para 2 medidas
según las direcciones
principales)

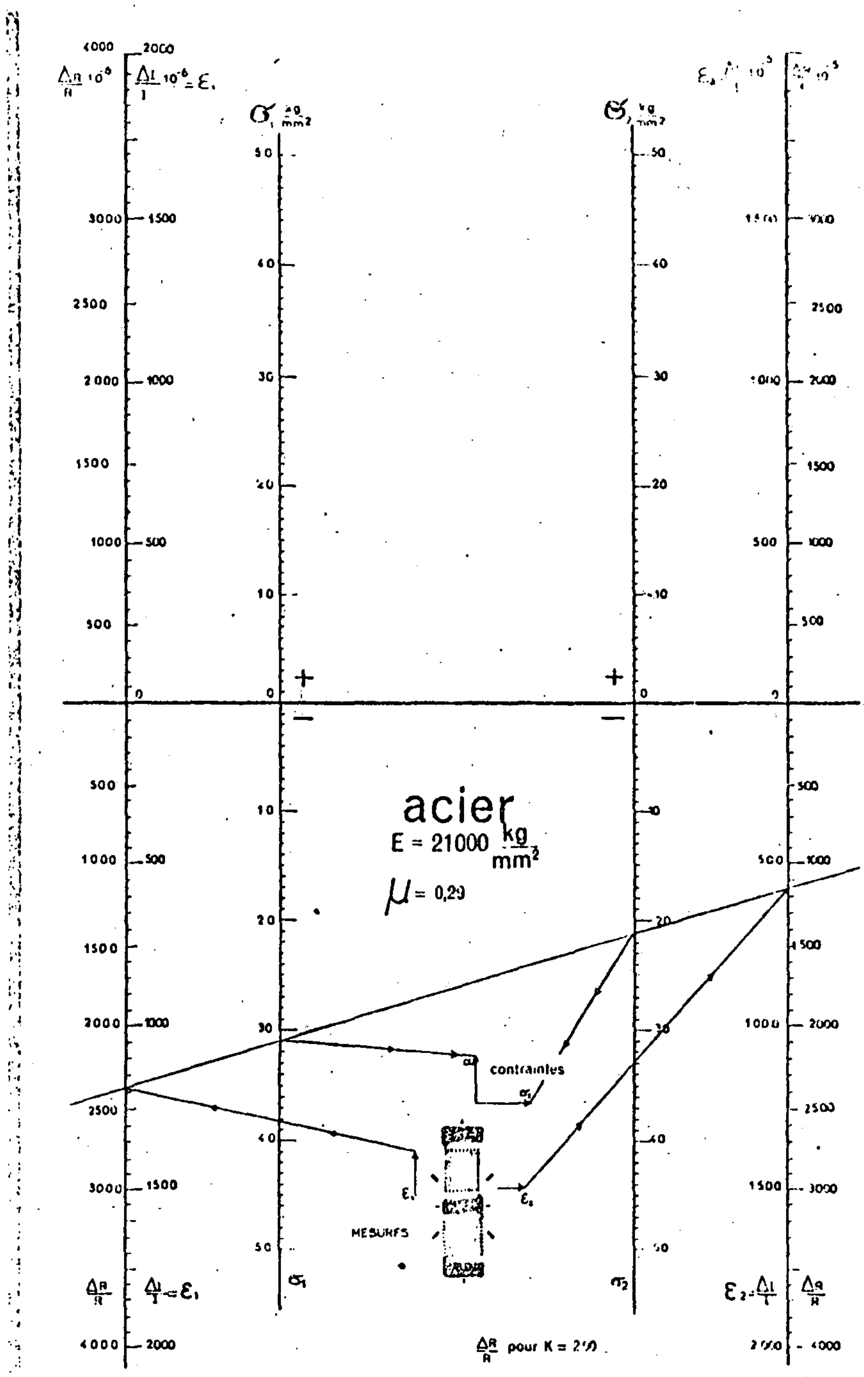

Cortesia de VISHAY MICROMESURES

1.13 ROSETA DE DOS DIRECCIONES

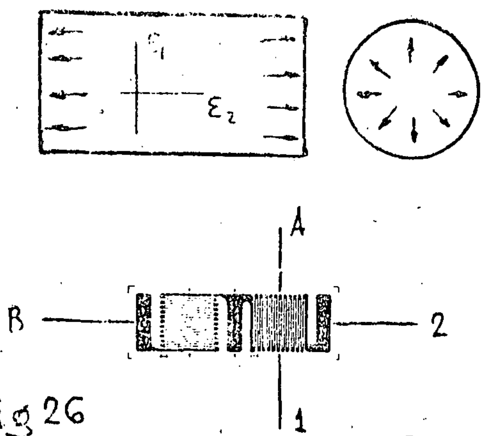

fig 26

Cuando la dirección de los ejes principales es conocida de antemano, como por ejemplo un cilindro bajo presión (fig. 26), con solo medir las deformaciones en dos direcciones perpendiculares que coincidan con las direcciones principales, será suficiente para determinar el estado de tensiones en un punto

$$\varepsilon_1 = \varepsilon_A = \varepsilon_M \; ; \quad \varepsilon_2 = \varepsilon_B = \varepsilon_m \; ; \quad \gamma_M = \varepsilon_A - \varepsilon_B$$

$$\sigma_1 = \frac{E}{1-\mu^2}\left(\varepsilon_1 + \mu\,\varepsilon_2\right) \qquad [52]$$

$$\sigma_2 = \frac{E}{1-\mu^2}\left(\varepsilon_2 + \mu\,\varepsilon_1\right) \qquad [53]$$

$$\tau = G\,\gamma = G\left(\varepsilon_1 - \varepsilon_2\right) \qquad [54]$$

Se incluyen ábacos para el cálculo rápido de tensiones a partir de las lecturas en microdeformaciones.

1.14 EXTENSIMETROS UNIDIRECCIONALES

Si se conoce la dirección principal de esfuerzos y esta es única, como en la tracción pura, la tensión es obtenida aplicando la ley de Hooke.

$$\sigma_1 = \varepsilon_1 E \qquad \varepsilon_2 = \mu\,\varepsilon_1$$

$$\sigma_2 = 0$$

1.15 CORRECCIONES DEBIDAS AL EFECTO DE LA SENSIBILIDAD TRANSVERSAL

Como vimos en el apartado 1.2 el efecto de sensibilidad transversal en el extensímetro, puede tener influencia en los resultados, sobre todo cuando se emplean bandas rosetas. A continuación se indican las correcciones que deben efectuarse sobre los valores de deformaciones principales, así como sobre la distancia del centro y radio del círculo de Mohr.

Sea ε_M ; ε_m los valores de las deformaciones principales calculados y K_t el factor de sensibilidad transversal, los ver daderos valores

$$\varepsilon'_M = \frac{1-\mu K_t}{1+K^2}\left(\varepsilon_M - K_t\,\varepsilon_m\right) \qquad [55]$$

$$\varepsilon'_m = \frac{1-\mu K_t}{1-K_t^2}\left(\varepsilon_m - K_t\,\varepsilon_M\right) \qquad [56]$$

$$d' = d\left(1-\mu K_t\right)/\left(1+K_t\right) \qquad [57]$$

$$r' = r\left(1-\mu K_t\right)/\left(1+K_t\right) \qquad [58]$$

ABACO PARA EL
CALCULO DE
TENSIONES
(Para 2 medidas
según las direcciones
principales)

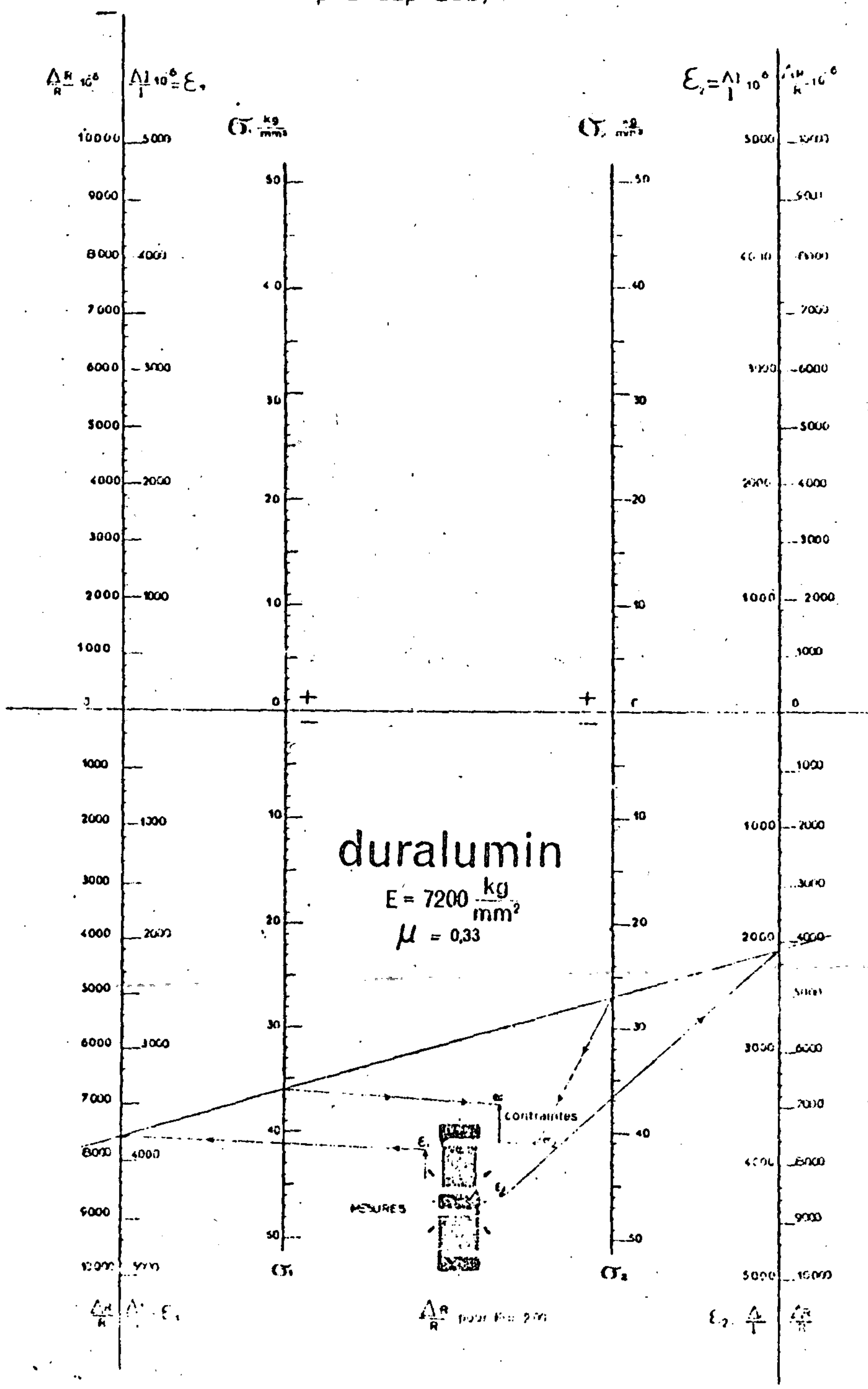

Cortesia de VISHYA MICROMESURES

PROPIEDADES DE LOS METALES DE USO MAS CORRIENTE

	Module d'Young E (1000 kg/mm²)	Coefficient de Poisson μ (s.d.)	$\frac{E}{1+\mu}$	$\frac{E}{1-\mu}$	$\frac{E}{1-\mu^2}$	σ_f	σ_0	$\sigma_0 / \sigma_.$	Masse volumique 10^3 kg/m³	Dilatation 10^{-6}/°C
Acier de Construction . . .	21,0	0,285	16,34	29,37	22,87		20 à 60	1	7,80	13
Acier 45 SC D6	22,0	0,285	17,12	30,77	23,97		145	1	7,80	13
Aciers resistants usure . .	22,0	0,29	17,06	30,99	24,[illegible]			1	7,82	25
Acier inoxydable 18-10. . .	20,3	0,29	15,74	28,59	22,16		18 à 22	1	7,95	16,5
Invar	14,1	0,29	10,93	16,60	15,39		40 à 55	1		< 0,9
Fontes grises courantes . .	9 à 12	0,29	7,0 à 9,3	12,7 à 16,9	9,8 à 1[illegible],1	7 à 9	18 à 25	3,3	7,1 à 7,2	9 à 11
Fontes grises auto	10 à 13	0,29	7,7 à 10,0	14,1 à 18,3	10,9 à 14,2	10 à 15	22 à 35	3,4	7,1 à 7,4	9 à 11
Fontes grises lingotières .	5 à 8	0,29	3,9 à 6,2	7,0 à 11,2	5,4 à 8,7		8 à 12	3,5	7,1 à 7,2	9 à 11
Fonte graphite sphéroïdal .	16 à 18	0,29	12,4 à 14,0	22,2 à 25,4	17,5 à 19,6	17 à 35	26 à 60	1,2	7,1 à 7,3	11 à 12
Fontes blanches non alliees	16 à 20	0,29	12,4 à 15,5	22,2 à 28,2	17,5 à 21,8		20 à 40	5	7,5 à 7,8	9 à 11
Fontes malléables	17 à 19	0,17	14 à 16	20,5 à 22,9	17,5 à 19,5	16 à 38	20 à 60	1	7,2 à 7,4	9 à 11
Titane	10,55	0,34	7,87	15,98	11,93	10 à 25	20 à 47	1	4,51	8,9
Alliage titane 6Al 4V	10,9	0,34	8,13	16,52	12,33					
Alliage titane 1A6V	10,5	0,34	7,83	15,91	11,88	60	90	1	4,42	8,0
Aluminium	7,05	0,34	5,26	10,68	7,98					
Alliage alu AU 4 G	7,5	0,33	5,63	11,19	8,41	12	20	1	2,8	23,5
Alliage alu AU 2 GN . . .	7,5	0,34	5,60	11,36	8,48	12	37	1	2,8	22 à 24
Alliage alu AU 5 GT	7,0	0,34	5,22	10,61	7,92	10	22 à 26	1	2,8	23
Zicral AZ8GU	7,2	0,34	5,37	10,91	8,14		55	1	2,8	23,5
Cuivre	10,0	0,33	7,51	14,92	11,22		18	1,3	8,9	17
Laiton	9,2	0,33	6,92	13,73	10,33		20	1,4	7,30	18
Bronze ordinaire	10,6	0,31	8,09	15,36	11,73		24	3	8,40	17,5
Bronze au beryllium	13	0,34	9,70	19,70	14,71		80	3	8,25	17
Beryllium	30,0	0,05	28,57	31,58	30,08	20	30	1	1,85	12,4
Magnésium	4,60	0,34	3,43	6,97	5,20				1,74	25,6
Marbre	2,6	0,3	2,00	3,71	2,80		50	15	2,8	8
Béton	1,4 à 2,1	0,3	1,1 à 1,6	2,0 à 3,0	1,5 à 2,3		30	11	1,9	14
Verre	6	0,2 à 0,3	5,0 à 4,6	7,5 à 8,6	6,2 à 6,6		3 à 8	10		
Plexiglass	0,29	0,4	0,207	0,483	0,345		8	1,2	1,8	80 à 90
Araldite	0,30	0,4	0,214	0,500	0,357		5 à 8	1,2	1,15	90 à 130

1.16 PROBLEMAS DE CALCULO EXTENSOMETRICO

Problema nº 1

Una barra de acero está sometida a una tracción pura, montándose una banda en el sentido de la tracción. Calcular las tensiones principales, si leemos $1275\,\mu\delta$ y el acero de la barra tiene $E = 21000\ Kg/mm^2$ y $\mu = 0,28$

Problema nº 2

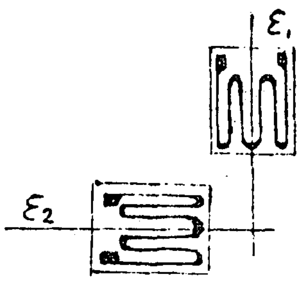

En un depósito cilindrico de aluminio ($E = 7200\ Kp/mm^2$; $\mu = 0,33$) se admite que las direcciones principales - coinciden con los ejes vertical y horizontal y en tales direcciones se montan dos bandas extensométricas - respectivamente. Las lecturas bajo carga son:

para J_1 $\quad \varepsilon_1 = 3950\,\mu\delta$

J_2 $\quad \varepsilon_2 = 2540\,\mu\delta$

Calcular las tensiones en este punto.

Problema nº 3

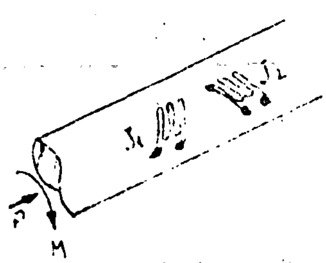

R: 40mm

En un eje cilíndrico de acero ($E = 21000\ Kp/mm^2$ $\mu = 0,28$) de 80 mm de diámetro se han montado dos bandas, J_1 y J_2 a 45º respecto a su eje. El eje no sufre flexión, pero si una compresión P y un momento de torsión M.

En el curso de una primera experiencia, se obtienen - como lecturas las siguientes:

$$\varepsilon_1 = -\varepsilon_2 = 1830\,\mu\delta$$

¿Cuales son las tensiones en el punto? ¿Cual la fuerza de compresión y el par?

En una segunda experiencia se obtiene

$$\varepsilon_1 = 2560\,\mu\delta \qquad y \qquad \varepsilon_2 = -1080\,\mu\delta$$

¿Cuales son la fuerza P y momento M?

Los problemas siguientes, se refieren al cálculo [illegible] setas, en ellos deberemos calcular:

- Direcciones principales máximas y minimas
- Deformaciones y tensiones máxima y mínima.

Problema nº 4

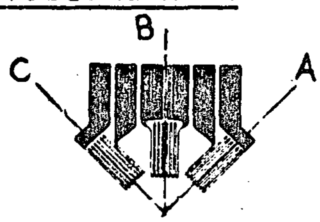

Roseta de 45º

E= 7200 Kp/mm^2 μ= 0,34

Lecturas: A = - 3790 $\mu\delta$

B = - 3220 $\mu\delta$

C = - 4750 $\mu\delta$

Problema nº 5

E= 7200 Kp/mm^2 μ= 0,34

A= + 2080 $\mu\delta$

B= - 1800 $\mu\delta$

C= - 1200 $\mu\delta$

Problema nº 6

E= 21000 Kp/ mm^2 μ= 0,29

A= + 3580 $\mu\delta$

B= + 1930 $\mu\delta$

C= + 1370 $\mu\delta$

Problema nº 7

E= 21000 Kp/mm^2 μ= 0,29

A= + 1,792 $\mu\delta$

B= 817 $\mu\delta$

C= 868 $\mu\delta$

Problema nº 8

E= 21000 Kp/mm^2 μ= 0,29

A= + 340 $\mu\delta$

B= + 520 $\mu\delta$

C= - 710 $\mu\delta$

Dar directamente las tenciones, sin pasar por deformaciones.

Problema nº 9

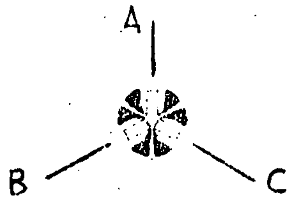

Rosetas de 120º

$E = 7200\ Kp/mm^2$ $\quad \mu = 0,34$

A= + 2400 $\mu\varepsilon$

B= + 2010 $\mu\varepsilon$

C= + 1370 $\mu\varepsilon$

Problema nº 10

$E = 7200\ Kp/mm^2$ $\quad \mu = 0,34$

A= + 4410 $\mu\varepsilon$

B= − 540 $\mu\varepsilon$

C= − 1920 $\mu\varepsilon$

Problemas nº 11

$E = 21000\ Kp/mm^2$ $\quad \mu = 0,29$

A= −120 $\mu\varepsilon$

B= +540 $\mu\varepsilon$

C= +310 $\mu\varepsilon$

Problema nº 12

$E = 7200\ Kp/mm^2$ $\quad \mu = 0,34$

A= + 1795 $\mu\varepsilon$

B= + 1803 $\mu\varepsilon$

C= + 1812 $\mu\varepsilon$

II TECNICA DE UTILIZACION DE LAS BANDAS EXTENSOMETRICAS

2.1. FABRICACION DE BANDAS EXTENSOMETRICAS

Una banda extensométrica está formada por dos elementos fundamentales que son el soporte y el conductor eléctrico sensible a las deformaciones, habiendo evolucionado grandemente la constitución y técnicas de fabricación de dichos elementos.

En un principio, se emplearon con gran difusión soportes de papel y conductores de sección circular colocados según la fig. 1, pero entre otros, presentaban los graves inconvenientes de la higroscopidad del papel, que hacía perder el aislamiento de la banda y el elevado factor de sensibilidad transversal en las partes curvas del conductor, intentándose compensar éste último efecto dando forma de zig-zag u otros diseños ingeniosos (fig 2). Actualmente una banda de calidad se fabrica sobre soportes de resinas epóxicas y por el procedimiento de fotograbado, se consiguen formas y dimensiones imposibles por los métodos clásicos (fig 3), ya que los modelos pueden hacerse a escalas muy aumentadas, constituyendo éstas las llamadas bandas de trama pelicular o de film metálico.

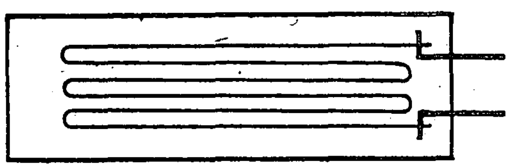

fig 1

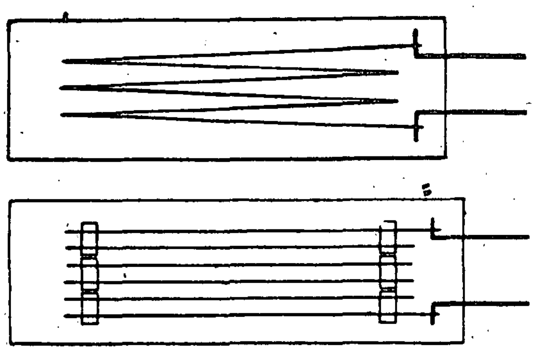

fig 2

Los principios en que se basa la extensometría, suponen que las isostáticas de la estructura bajo ensayo, pasan a través de la parte activa del extensímetro y se ha podido comprobar por fotoelasticidad, que en un extensímetro pegado a una estructura, solo en sus extremidades hay distorsión de aquellas, y nó en la zona central; por dicho motivo, dando a la banda la forma indicada en la fig. 4, conseguiremos establecer en los extremos de los conductores activos una zona de anclaje en la que se inciden los isostáticas y por su mayor sección respecto a la parte activa la variación unitaria de resistencia es menor y despreciables los coeficientes de sensibilidad transversal y longitudinal.

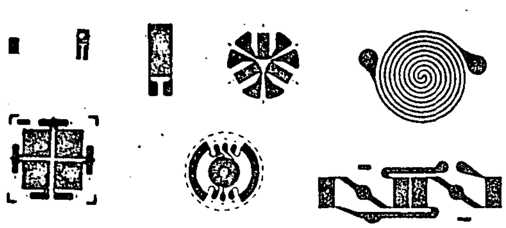

fig 3

La posibilidad de disponer de superficies adecuadas para la soldadura de los cables y la transparencia de los soportes, que permiten una colocación óptima del extensímetro, añaden ventajas a éste.

Las aleaciones del metal conductor responden a las características específicas de cada tipo, siendo a veces riguroso secreto el proceso de fabricación, en el que se incluyen técnicas sofisticadas para conseguir mejoras en la utilización de extensímetros. A título de ejemplo, en la serie CEA de la casa Vishay-Micromesures, el tratamiento dado a los extremos para soldadura de cables, hace posible que la unión soldada tenga mayor resistencia mecánica a la tracción que el cable que normalmente se utiliza, ventaja ésta que confiere seguridad a una medida extensométrica.

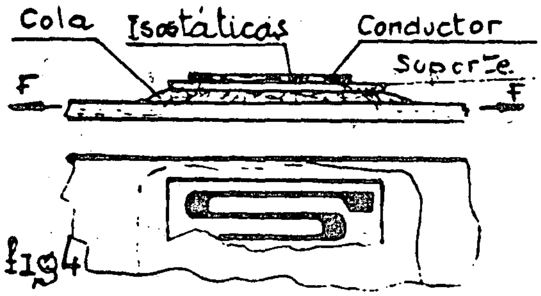

fig4

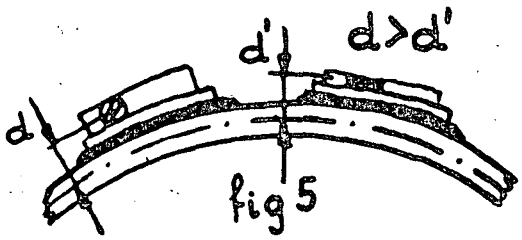

fig 5

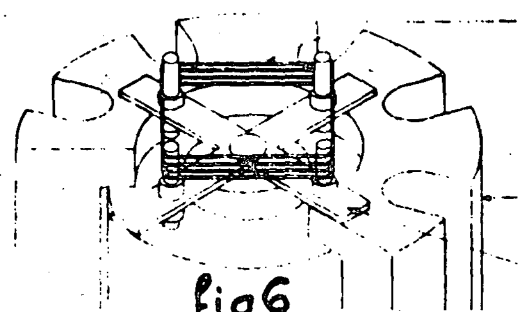
fig6

Otras ventajas de las bandas de film metálico residen, en que dado su pequeño espesor (4 micras), no introducen errores en la medida de deformaciones de secciones delgadas y se adaptan mejor sobre cualquier superficie (fig. 5).

Dejando al margen las bandas semiconductoras (de las que nos ocuparemos en otro capítulo) vemos en lo expuesto, que el verdadero sensor de las deformaciones es el conductor, siendo el soporte un medio de transición con la estructura, por lo que exige del pegado a la misma (bonded strain gauge) pero, en aplicaciones para fabricación de transductores, suele emplearse el conductor suelto montado sobre zafiros aislantes, (fig.6) que se deforma bajo estímulos mecánicos, sin necesidad del soporte propiamente dicho (unbonded - Strain-gauges).

La banda puede ser posteriormente sometida a recubrimientos y opciones tales como inclusión de hilos de salida soldados, que en determinadas aplicaciones resultan de interés.

2.2 CARACTERISTICAS TECNICAS

22.1 Valor óhmico.

El valor de la resistencia óhmica de una banda viene condicionado por motivaciones de tipo eléctrico, y hay razones para que dicho valor sea elevado de una parte o pequeño de otra, por lo que debe establecerse un compromiso entre las posturas extremas.

Motivos que aconsejan un valor elevado de resistencias:

1. Señales elevadas para debiles deformaciones, en efecto, la señal es función de la tensión de excitación, por lo que conviene que ésta sea elevada, pero para que no circule una corriente excesiva, que por efecto Joule produzca un calentamiento inadecuado, el valor óhmico será alto.

2. Evitar los errores producidos por las resistencias de contacto de los conmutadores y líneas de conexión a los instrumentos, pues siendo éstos valores pequeños su influencia será menor cuando mayor sea la resistencia de la banda.

Motivos que aconsejan valores pequeños de resistencias

1. Evitar la caída de tensión interna considerando a la banda como generador de tensión.

2. Conseguir mejor aislamiento eléctrico entre la banda y la estructura.

3. Mayor robustez, pues resistencias elevadas obligan a conductores de muy pequeña sección y por tanto frágiles.

Por lo expuesto se ha establecido como valor normal y de uso más generalizado el de 120 ohmios, siendo también muy empleados los 350 (generalmente en transductores) 600 y 1000 ohmios.

Las tolerancias de fabricación son muy estrechas 0,15% con el fín de poder equilibrar los circuitos de medida, pero no sería práctico un exceso de dicha tolerancia en límites que puedan confundirse con la variación lógica, que por efecto de montaje, sufriría la banda en su instalación. La exactitud de la medida no será afectada, por ligeras dispersiones del valor nominal.

También se construyen bandas con valores nominales que son fracciones de los indicados para los casos en que la medida requiere un circuito con dos, tres ó cuatro bandas en serie (se hacen de 30, y 60 óhmios u otros valores que no suelen ser standard).

2.2.2. FACTORES DE SENSIBILIDAD

En el estudio teórico de las bandas extensométricas (1,2) vimos que hay dos factores K1 y K2 que relacionan la variación unitaria de resistencia del conductor con la deformación que sufre en sentido longitudinal y transversal respectivamente por efecto de las solicitaciones a que esté sometido el elemento donde se instala la banda.

La variación de la resistencia es motivada por el cambio de la geometría del conductor y de la conductividad, pero si bién el primer factor afecta prácticamente igual a todos los metales, el segundo es función de la aleación empleada en la fabricación del extensímetro y es por esta razón por lo que la forma y dimensiones de la banda no influyen sobre el factor de sensibilidad.

Los constructores de bandas, utilizan procesos de fabricación que mantienen el valor del factor de sentibilidad dentro de unas tolerancias estrechas en una serie, por lo que es importante en medidas con varios extensímetros procurar que no haya dispersión en dichos valores.

Por razones de la instrumentación asociado a las medidas extensométricas, se toma como valor nominal de la sensibilidad longitudinal de las bandas el de 2 y tolerancias admitidas como muy buenas son del $\pm$ 0,5%. El factor de sensibilidad transversal se expresa en tanto por ciento del longitudinal y no debe ser superior al 1%.

El fabricante indica el valor de K obtenido en unas condiciones determinadas de temperatura y sobre medidas efectuadas con probetas de módulo de elasticidad y coeficiente de Poisson conocido, incluyendo curvas (fig. 7) donde se indica la variación del factor K respecto a variaciones de temperatura.

Para medir el factor K se utilizan balanzas de calibración basadas en producir una flexión circular a una probeta en la que se montan bandas correspondientes a una misma serie.

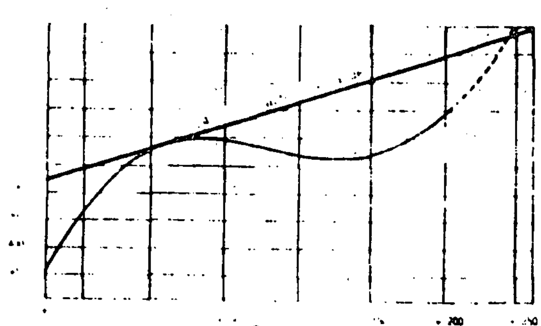

2.2.3. RESPUESTA DE TEMPERATURA

Una banda extensométrica mide todas las deformaciones que experimente el elemento sobre el que se monta, pero sabemos que las deformaciones producidas por dilataciones térmicas homogéneas no crean tensiones, por tanto (fig. 8) si consideramos una viga empotrada en un extremo sin carga alguna y hay variación de temperatura, aquella se dilatará y habrá una deformación que acusará la banda, pero por no originar tensiones, debe ser considerada como error.

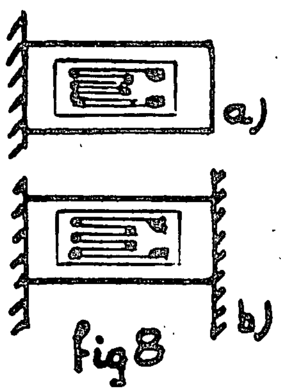

fig 8

El error por variación de temperatura se corrige, dentro de ciertos límites, fabricando el conductor de la banda con coeficientes térmico de variación de la resistividad de igual valor y signo contrario al del coeficiente de dilatación líneal del cuerpo sobre el que montan.

En efecto:

$$R_0 = \rho_0 \frac{l_0}{S} \qquad R_t = \rho_0 (1+\beta t) \frac{l_0 (1+\alpha t)}{S}$$

$$\Delta R = R_t - R_0 = \frac{1}{S}\left[\rho_0 l_0 \alpha t + l_0 \rho_0 \beta t\right] = 0$$

$$\alpha = -\beta$$

α= coeficiente dilatación lineal
β= coeficiente de variación térmico de resistividad

La relación $\alpha = -\beta$ solo es lineal dentro de unos límites de temperatura para los cuales se dice que la banda está autocompensada, los fabricantes indican la curva de respuesta en temperatura de las bandas expresadas como microdeformaciones aparentes (fig.9).

En la fig. 8a vemos que al dilatarse la viga, si la banda es autocompensada, no experimentará variación alguna en su resistencia, por el contrario (fig.8b) si la viga está empotrada en sus extremos, se originan esfuerzos de compresión cuando dilate y la banda por tener el coeficiente $-\beta$ acusará un incremento negativo en la variación unitaria de resistencia, acusando precisamente la compresión habida.

Una banda solo puede ser compensada para materiales que tengan idéntico coeficiente de dilatación. Normalmente se compensan para acero ($\alpha = 11.10^{-6}/°C$) y aluminio ($\alpha = 23.10^{-6}/°C$).

Veremos en el capítulo de técnicas de Medida, que los efectos de origen térmico pueden compensarse con disposiciones de montaje adecuados.

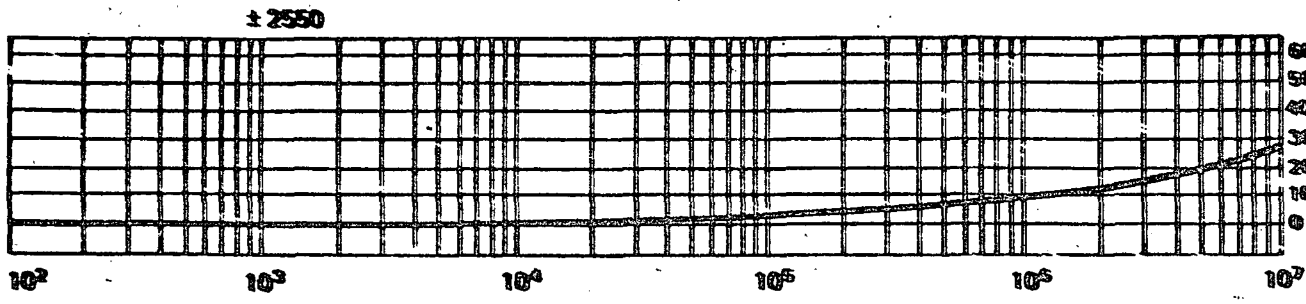

fig 10

2.2.4. LIMITES DE DEFORMACION: ESTATICA Y DINAMICA

La máxima deformación que puede soportar un extensímetro bajo carga estática se expresa en %, de la longitud de su rejilla o parte activa y depende de varios factores, entre ellos:

a) Temperatura de utilización. El valor indicado por el fabricante se refiere a temperaturas ambientes (24ºC) pero a temperaturas criogénicos, la deformación es solo una pequeña fracción de dicho valor.

b) Ductibilidad de la aleación que constituye el conductor sensible.

c) Maleabilidad del soporte de la banda y del adhesivo.

d) Forma y dimensiones del extensímetro.

e) Calidad del montaje en la extructura

Las bandas impresas de trama pelicular, admiten mayor deformación estática que las de hilo.

El fenómeno de fatiga bajo cargas alterna, presenta aspectos que influyen en las medidas y deben tenerse en cuenta pues pueden introducir errores.

El conductor metálico del extensímetro cuando se monte sobre estructuras sometidas a tensiones alternas, sufre una fatiga - cuyo efecto principal es producir una deriva del valor óhmico de la - banda, por èste motivo se ensayan las bandas sometiéndolas a ciclos de amplitud constante (±1520 $\mu\delta$; ±2250 $\mu\delta$....) observando cuando la deriva del valor óhmico representa una deformación aparente de 100 $\mu\delta$, valor éste admitido como límite (fig. 10).

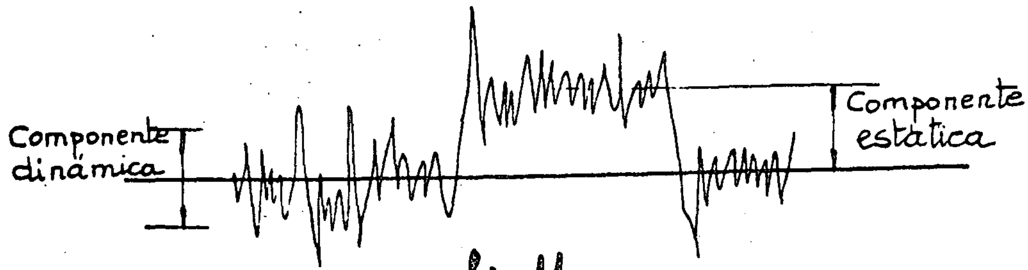

fig 11

Si en una medida dinámica queremos obtener con exactitud los valores de las componentes estáticas y dinámica (fig. 11) prestaremos especial atención en la elección del extensímetro adecuado y sobre todo se cuidará que las soldaduras de los hilos de conexión de los instrumentos a la banda sean puntuales para evitar concentración de esfuerzo en la banda y que el tamaño de la misma sea muy pequeño, ya que son los factores más influyentes para evitar llegar al límite de fatiga. En un fenómeno vibratorio la deriva no tiene gran importancia si lo que interesa conocer es solamente la amplitud de la oscilación.

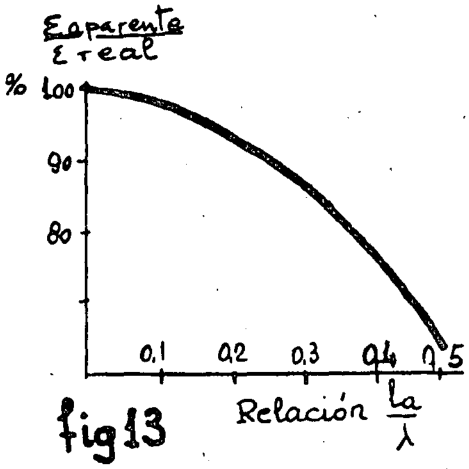

fig 13

2.2.5. LIMITE DE LA RESPUESTA EN FRECUENCIA

Una banda extensométrica por tener una longitud finita, actua como un integrador de todas las deformaciones que ocurren a lo largo de la parte activa, por esta razón si la longitud de onda del fenómeno vibratorio que se quiere medir coincide con la longitud activa de la banda (fig. 12) no acusaremos deformación alguna pues la mitad sufrirá alargamiento y la otra mitad compresión.

Las deformaciones son fenómenos que se propagan a la misma velocidad que el sonido, por tanto conocido éste valor y el de la frecuencia del fenómeno, la longitud de onda $\lambda = \frac{v}{f}$ nos indica el valor límite en el cual una banda de longitud activa $= l_a = \lambda$ no causaría deformación.

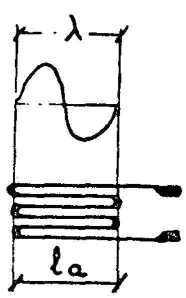

fig 12

Para evitar la anomalía anterior se admite como valor normal de l_a el 10% de λ con lo que el % de perdida de sensibilidad es prácticamente nulo (fig. 13), Se fabrican bandas con longitudes activas de 0,4 mm por lo que se pueden medir en aceros (0÷5000 m/seg) frecuencias de 10^6 Hz aunque la limitación en éste caso está en los instrumentos de medida.

Otros factores influyen en la limitación de la respuesta en frecuencia de las bandas, pues si bien la debil masa de inercia de la misma favorece el seguir fielmente un fenómeno dinámico, la elasticidad de adhesivos y soportes debe tenerse en cuenta, aunque su valoración es dificil de obtener de forma experimental, debiendo cuidarse la elección de adhesivos en medidas críticas.

2.2.6. FENOMENOS DE FLUENCIA E HISTERESIS

Supongamos que una probeta sobre la que hay montada una banda extensométrica es sometida a esfuerzos de tracción simple (fig 14), las deformaciones de la probeta son entonces transmitidas al conductor activo a través del adhesivo y del soporte, creandose unas solicitaciones de cortadura principalmente en los extremos de la banda, que deben compensarse con la fuerza antagonista que se origina en el conductor activo.

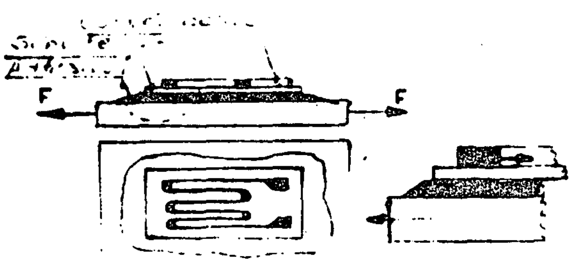

fig 14

La calidad del adhesivo y su elasticidad determinarán la magnitud de la relajación del mismo bajo las solicitaciones constantes a que esté sometido y por consiguiente que permita al conductor activo un lento retorno a su estado original. El fenómeno descrito es el de fluencia de una banda y tiene importancia considerable en medidas estáticas, no siendolo tanto en medidas dinámicas.

Por la propia naturaleza del fenómeno, se vé que la temperatura juega un papel importante en la fluencia, así como las dimensiones de la banda, participando en razón inversa al tamaño.

Es práctica muy aconsejable, someter las probetas a cargas y descargas sucesivas de magnitud lo mayor posible, antes de efectuar las medidas.

Ligado al concepto anterior puede considerarse el fenómeno de histeresis, el cual ocurre cuando queda una deformación residual después de someter a solicitaciones la probeta sobre la que está instalada la banda, siendo el principal motivo de este fenómeno que el transmita al conductor activo.

2.2.7. NIVELES OPTIMOS DE EXCITACION

La señal eléctrica que obtendremos de cualquier circuito de medida con bandas extensométricas , será proporcional a la tensión de excitación del mismo, lo cual hace presumir el empleo de niveles elevados de excitación, sin embargo hay razones para limitar dichos niveles.

La corriente eléctrica que circula por el conductor de una banda excitada, origina por efecto Joule, una elevación de temperatura al disiparse el calor producido, por cuyo motivo pueden aparecer las perturbaciones siguientes:

a) Alterar el efecto de autocompensación, cuya estabilidad es mejor con niveles bajos de excitación.

b) Modificación del estado de tensiones de la estructura bajo ensayo, al absorber ésta el calor disipado por la banda, sobre todo en materiales plásticos.

d) Derivas del cero, sobre todo en circuitos con varios bandas y en las cuales la disipación de calor no será igual y simultánea.

Los parámetros de mayor incidencia en la determinación del nivel óptimo de excitación.de una banda son:

1.- Superficie de la rejilla, cuya influencia afecta al poder de disipación de calor.

2.- Resistencia óhmica de la banda, que limita el paso de corriente.

3.- Coeficiente de conductibilidad térmica de la estructura.

4.- Tamaño de la probeta o estructura donde se monta la banda, que determina el poder de absorción de calor.

5.- Condiciones ambientales.

6.- Calidad del montaje de la banda, cuidándose de que no hayan burbujas de aire entre el soporte y la probeta.

En la tabla I se indica la potencia por cm^2 que pueden disipar las bandas según los materiales donde estén montadas y para precisiones bajas, elevadas o medias (datos cortesia de Vishay-Micromesures).

POTENCIAS RECOMENDADAS EN WATS/CM^2

PRECISION REQUERIDA

DISIPACION DE CALOR	ESTATICAS ELEVADA	ESTATICAS MEDIA	ESTATICAS BAJA	DINAMICAS ELEVADA	DINAMICAS MEDIA	DINAMICAS BAJA
Excelente. Piezas grandes de aluminio o de cobre	0,30 á 0,75	0,75 á 1,5	1,5 á 3	0,75 á 3	1,5 á 3	3 á 8
Buena. Piezas grandes de acero.	0,15 á 0,30	0,30 á 0,75	0,75 á 1,5	0,75 á 1,5	1,5 á 3	3 á 8
Media. Piezas pequeñas de acero inoxidable o titanio.	0,08 á 0,15	0,15 á 0,30	0,30 á 0,75	0,30 á 1,5	0,75 á 1,5	1,5 á 3
Mala. Plásticos, resinas epoxy.	0,01 á 0,03	0,03 á 0,08	0,08 á 0,15	0,08 á 0,15	0,15 á 0,30	0,15 á 0,75
Muy mala. Poliestireno, materiales acrílicos.	0,001 á 0,003	0,003 á 0,008	0,001 á 0,03	0,001 á 0,008	0,003 á 0,015	0,03 á 0,08

La tensión de excitación se deduce a la fórmula:

Potencia disipada: $\frac{Ve^2}{4R} = We_d$ en donde

Ve= Tensióm de excitación en Voltios

R = Resistencia nominal de la banda

La potencia por unidad de superficie es

$$\frac{W_d}{S} = W$$

Siendo S la superficie de la rejilla

Si solo disponemos de una fuente de alimentación con salida fija de tensión y esta es elevada para excitar el circuito de medida se ponen en serie unas resistencias que produzcan una caida de tensión determinada, pero sin olvidar efectuar las correcciones adecuadas por la perdida de sensibilidad que introducen las mencionadas resistencias.

2.3. PRACTICA DE MONTAJE DE BANDAS

2.3.1. Preparación de superficies

La instalación de una banda extensométrica tiene como fundamento la perfecta unión entre la banda y el cuerpo de ensayo.

Para el extensometrista cada montaje de circuitos de medida supondrá un aumento de su experiencia y una garantía de que su labor es satisfactoria, solo cuando por un exceso de confianza omite alguna de las operaciones que se indican como preceptivas, el error aparece, pero desgraciadamente no se manifiesta inutilizando la medida, sino dando como ciertos unos resultados falsos, de ahí que será criterio firme el observar toda la meticulosidad humanamente posible, con la certeza de que, si así se hace, se obtendrá resultados que justificarán el empeño puesto.

La banda puede elegirse, dentro de ciertas opciones que ofrece el fabricante, adaptada a las condiciones de utilización, pero no así la superficie donde deba instalarse, por lo que ésta última deberá ser preparada por el usuario, así como la soldadura de cables que configuran el circuito de medida.

2.5.1. Preparación de superficies

Toda superficie que debe recibir una banda se someterá generalmente a unos tratamientos mecánicos y químicos para conseguir el mayor rendimiento del adhesivo, sin que dichos tratamientos puedan suponer una modificación local de las características del cuerpo a ensayar. Dimensionalmente, se tratará una superficie doble (como mínimo) de la superficie total de la banda.

El proceso prévio será el de limpieza y desengrasado, para el que se utilizará preferentemente cloroetileno de calidad, para metales y freón para plásticos, para ello se deposita el desengrasante sobre la superficie (se facilita esta operación si viene envasado en spray) y sin dejarlo evaporar se seca con una gasa limpia y de una sola pasada, repitiendose esta operación hasta que la gasa aparezca totalmente limpia.

Conviene indicar que siempre que haya que limpiar o secar una superficie debe hacerse con una gasa limpia (no necesariamente esterilizada) o a veces con papel absorbente tipo Kleenex pero nun ca con algodones que dejarían hebras depositadas. Además la limpieza se hará en una sola pasada y jamás utilizando la misma gasa para dos pasadas sucesivas, las razones son obvias ya que si la gasa es repasada sobre la superficie, en vez de limpiar por arrastre, por efecto de estar impregnada de disolvente, la suciedad o grasa existente se disolvería más, entrando en las minusculas oclusiones que existan.

En montajes sobre metales, recordemos que al estar constituidos por cristales orientados al azar, un pulido superficial presentaría el aspecto de un espejo al quedar incluidas entre los cristales las pequeñísimas partículas arrancadas, por lo que la adhesión y cohesión en estas zonas seria muy dudosa, por tal motivo se combina el tratamiento mecánico por abrasión con un ataque por un ácido debil.

El proceso de abrasión dependerá del estado inicial de la superficie comenzando con papeles de carburo de silicio de grano 400, 200 o 150 respectivamente y que previamente se ha humedecido con el ácido, atacando en sentidos alternativos y que formen 90º entre ellos, con el fín de en cada pasada, eliminar las "crestas" que sobre el metal se van marcando; la coloración peculiar que adquiere la superficie y la desaparición de las marcas en un sentido cuando se ataque a 90º, indican que esta operación está concluida, debiendose proceder inmediatamente al secado con gasas.

Posteriormente y de inmediato, la superficie se humedece con un producto neutralizador (solución alcalina detergente) con el fín de que su pH sea adecuado para recibir el adhesivo.

En resumen haremos lo siguiente:

1º Limpieza grosera, quitar óxidos pinturas, etc, en una superficie doble que la de la banda.

2º Desengrasado absoluto y secado.

3º Abrasión progresiva combinada con ácido y secado.

4º Neutralización y secado.

Lógicamente el proceso anterior es indicado para ciertos metales, pero siempre habrá que seguir las indicaciones concretas del fabricante o de la propia experiencia.

Si se trata de superficies porosas como el caso del hormigón, habrá que impermeabilizar la zona de asentamiento de la banda, consiguiendose buenos resultados dando después de la limpieza, una capa previa de adhesivo.

En vidrio y plásticos será suficiente el empleo de freón y su limpieza con gasas.

2.3.2. Trazado de ejes de referencia

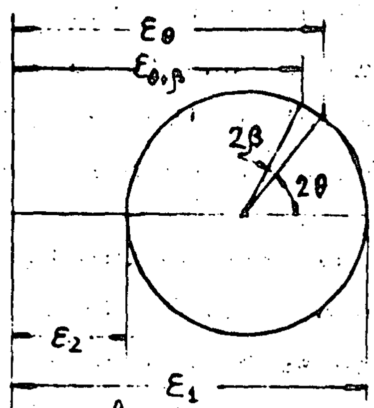

fig 15

Una mala alineación de los ejes de la banda con la dirección en la que deseamos medir las deformaciones introduce errores que son función: de la relación entre las deformaciones máximas y mínimas, del ángulo que forma la dirección en la que se desea medir y la dirección de la deformación principal máxima y del ángulo β o error de montaje de la banda (fig. 15).

Como por razones de montaje solo podemos influir sobre β, tendremos que esforzarnos en conseguir que este error sea mínimo, para ello hay que determinar sobre la superficie de asentamiento de la banda, los ejes de la dirección en que deseamos medir, pero tendremos que tener en cuenta que no podemos bajo ningún pretesto, alterar el estado de preparación de la superficie según se explicó en el apartado anterior.

Algunos montadores utilizan (nefastamente) puntas de acero de trazar, que al producir pequeñas incisiones en el material, alteran su extructura, por tanto, nosotros recomendamos siempre que sea posible no trazar sino grabar químicamente los citados ejes.

Con los instrumentos adecuados a la precisión de la medida (escuadras, goniómetros, compás, trazadores ópticos de precisión etc. etc) buscaremos unas referencias ortogonales en los límites de la zona que se ha limpiado procurando que no haya contacto de los útiles con la superficie limpia, para evitar su contaminación; situadas las referencias tracemos con un bolígrafo de punta fina o con un lapiz de grafito duro (5 ó 6) los ejes completos sobre la superficie preparada. Posteriormente, un palillo cuyo extremo lleve una bolita *zona preparada*

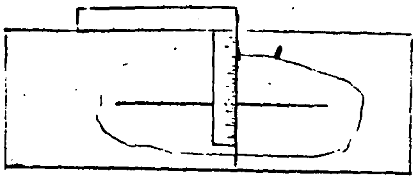

fig16

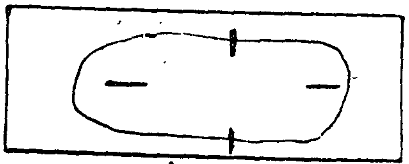

fig17

de algodón (los utilizados en Pediatría y de venta en farmacias son muy adecuados) se humedece con ácido y se pasa sobre los trazos del bolígrafo o lápiz, secando a continuación y se repite la operación pero humedeciendo un nuevo algodoncito con neutralizador; de esta forma la superficie mecánicamente no se ha modificado y sí veremos que han sido grabados los ejes de referencia, ya que la marca de grafito ha impedido la acción del ácido - sobre la propia línea y a continuación el neutralizador ha limpiado el grafito que se depositó. Este procedimiento tiene una demostrada eficacia por innumerables experiencias y es práctica su aplicación en metales.

Otra solución consiste en marcar con lápiz los ejes, pero sin que estas lleguen a cortarse dejando siempre libre la superficie - del soporte de la banda (fig. 17) pero se ve que conseguir este entraña una pericia grande y no queda exenta de problemas de contaminación de la superficie.

2.3.3. Pegado de extensímetros

El adhesivo utilizado para el pegado de bandas deberá reunir unas características adecuadas a su uso y nunca se pecará por exceso en las exigencias que en su elección hagamos. Tienen preferencia todos aquellos que solidifican por polimerización, es decir que la totalidad de los átomos que forman los componentes (normalmente dos) constituyen el sólido final, a diferencia de los pegamentos normales que solidifican por evaporación de un disolvente.

En general un buen adhesivo tendrá las siguientes características:

a) Permitir su aplicación en películas delgadas para no introducir - errores por distanciamiento de la rejilla a la superficie.

b) Ser neutro a la superficie y al soporte de la banda.

c) Transmitir los esfuerzos a la banda sin fenómenos de fluencia.

d) Técnica de aplicación facil.

e) Utilización en un márgen lo más amplio posible respecto a condiciones ambientales.

Será dificil que un solo adhesivo cumpla en grado óptimo las condiciones anteriores, pero siempre será factible establecer un compromiso para aplicaciones concretas.

Hay pegamentos de aplicación sencilla y rápida cuyo uso es de interés en piezas grandes y usos generales donde la medida se haga a temperaturas ambientales normales (20º ó 60ºC) un ejemplo de aplicación de las mismas se expone gráficamente en la fig. 18, referente al tipo M-200 de la firma Vishay-Micromesures.

Para aplicaciones que exijan una mejor precisión, como puede ser el caso de fabricación de captadores, se utilizarán adhesivos que deben someterse a un tratamiento térmico, operación que no deja de ser engorrosa. En cualquier caso, el fabricante dará normas claras de aplicación. Para usos de condiciones extremas (1000ºC) se comprende que los adhesivos se descompondrían, para ello, existen bandas encapsuladas en una vaína metálica que son fijadas por soldadura eléctrica por puntos con utensilios adecuados.

Junto con la banda, es muy práctico pegar unos soportes de terminales impresos que ayudarán a la soldadura e instalación del cableado.

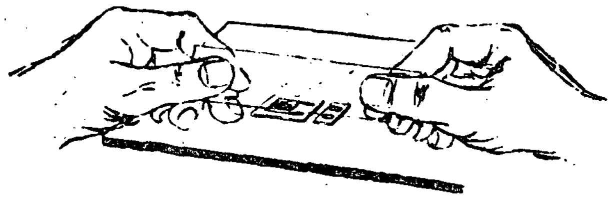

a) la banda y el terminal impreso se colocan sobre un cristal totalmente limpio y con papel transparente autoadhesivo, se cubren y se separan del cristal procurando no doblar la banda.

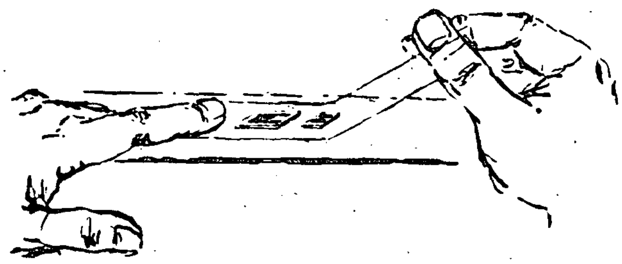

situa la cinta y banda so- el punto de medida, fijando un extremo y levantando el otro.

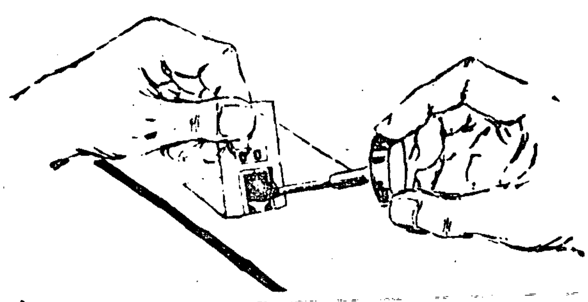

c) con el pincel del acelerador, se aplica éste sobre el reverso de la banda y terminal, procurando no contaminar la banda con adhesivo de la cinta. Dejar secar un minuto.

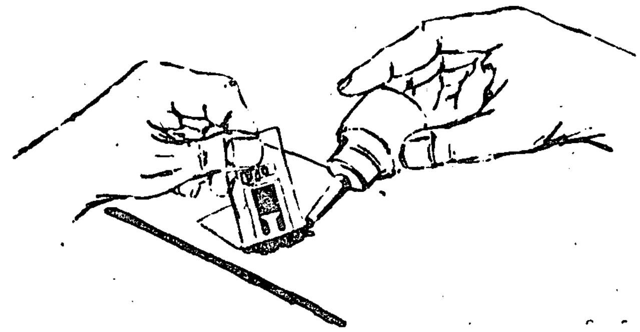

d) depositar una o dos gotas de adhesivo sobre la superficie de asentamiento.

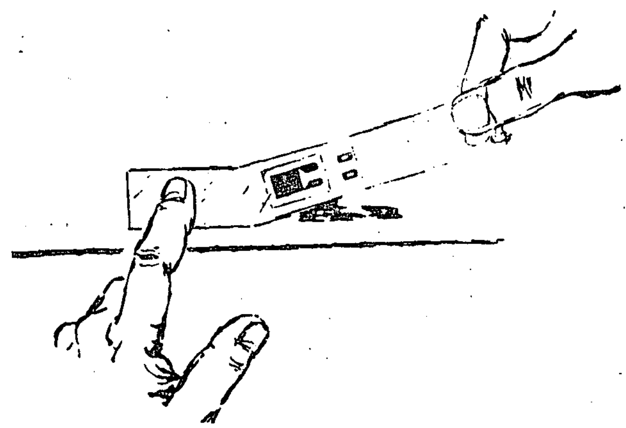

e) se va bajando la cinta y con un dedo se hace ligera presión de izquierda a derecha y evitando tocar directamente el adhesivo.

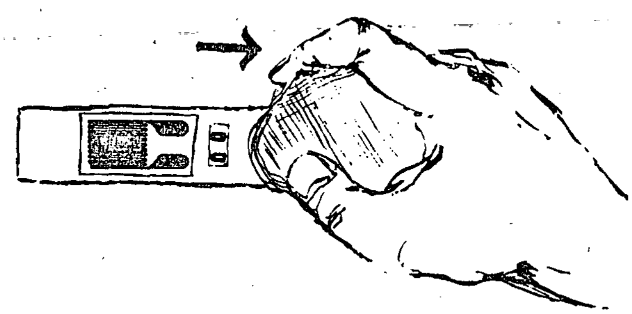

f) una gasa se pasa varias veces para evitar se formen burbujas de aire.

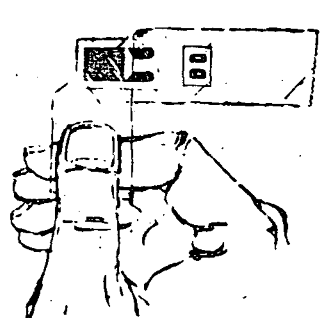

g) a los 10 minutos como mínimo se puede retirar el papel transparente que ayudó a pegar la banda como se indica.

2.3.4. Soldadura de cables

La soldadura de las bandas a los hilos de unión de los instrumentos de lectura, requieren una especial atención y el montador necesitará adquirir cierta expeciencia para dominar esta operación.

En la composición de las soldaduras se emplean aleaciones de plomo con estaño, plata o antimonio, que llevan o nó incorporada una resina y según las proporciones de dichas aleaciones resultan unas características determinadas de conductividad eléctrica, comportamiento a solicitaciones mecánicas, respuesta en temperatura etc. por todo ello no es recomendable el uso de soldaduras comúnes en aplicaciones de taller eléctrico o electrónico. Especial atención tiene el conocimiento de la temperatura de fusión que debe ser lo más inmediata superior a la que estará sometida el circuito de medida, con el fín de no tener que aportar más calor del necesario al efectuar las soldaduras.

Según el tipo de soldadura elegido será conveniente o necesario utilizar un fundente, sobre todo para hilos muy delgados, pero será totalmente imprescindible limpiar con un decapante adecuado los puntos de soldadura con el fín de eliminar los residuos de fundente y resina que podrían ocasionar corrosiones y fenómenos parásitos por efecto "pila" ya que evidentemente quedarían dos metales y un electrolito.

El soldador juega un papel muy importante, siendo recomendados aquellos de temperatura regulable; la punta del mismo nunca será cónica sino que tendrá una talla en forma de bisel. Para evitar que los cables puedan ejercer esfuerzos en la banda que pudiesen deteriorarla debe utilizarse siempre que sea posible un terminal impreso que servirá de apoyo al cable (que será de varios hilos) al que previamente se le separó un hilito y se estañó tal y como se indica en la fig. 19.

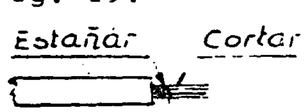

fig 19

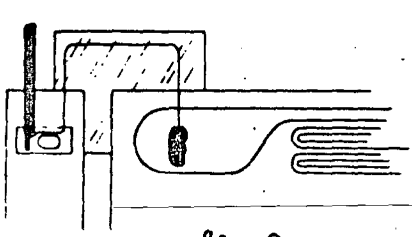

En general seguiremos el siguiente proceso:

1º Preparar el cable según la fig. 19

2º Proteger con papel autoadhesivo debil la banda, dejando al descubierto solamente los puntos de soldadura.

3º Depositar una gota de soldadura lo más pequeña posible sin aportar excesivo calor que podría desprender la banda del soporte. No debe durar esta operación más de 2 segundos, si no se consiguen el primer intento, dejar enfriar y repetir.

4º Presentar el cable ya preparado y sin aporte de soldadura, solamente manteniendo caliente y muy limpio la punta del soldador, fijar los cables a los terminales y a la banda, tal y como se indica en la fig.20.

En la banda conviene que la gota de soldadura sea lo menor posible para evitar concentración de esfuerzos, de ahí que el procedimiento explicado favorezca ésta condición al ser más fino el hilo de unión del terminal a la banda, a la vez que se consiguen dar mayor seguridad al montaje, pues un fuerte tirón del cable rompería el terminal pero no la banda.

Hemos ofrecido unas normas generales ya que el fabricante indicará en cada caso las instrucciones concretas.

2.5.5. Comprobaciones

Una vez insralada una banda deberán efectuarse diversas comprobaciones siendo preceptivas:

1º Inspección ocular. Debe hacerse con una lupa de 20 aumentos o más para confirmar que se ha situado correctamente la banda a la vez que se observará que no han quedado bolsas de aire ni "lagunas" (zonas sin adhesivos) bajo el soporte de la misma.

2º Comprobación del aislamiento. Se utilizará un megohmetro cuya tensión no exceda los 50 V, si es de válvula mejor y jamás se hará uso de los medidores de aislamiento de tipo magneto que quemarían la banda.

El aislamiento deberá ser mejor que 100 megohms, ya que un aislamiento menor, equivale a introducir un error, por colocar en paralelo con la banda otra resistencia; se puede calcular dicho error, en efecto, consideremos un aislamiento de 2 Mohms.

3º Medida del valor óhmico de la banda. Utilizar un instrumento que aprecie decimas de ohmio como mínimo; esta comprobación tiene dos objetos; el primero saber que no está rota ni cortocircuitada la rejilla y el segundo conocer la dispersión del valor nominal, sobre todo en circuitos con varias bandas para controlar desequilibrios excesivos.

2.5.6. Protecciones

Desde medidas efectuadas en laboratorio, hasta las difíciles en los conos de cohetes o cascos de barcos, encontraremos una serie de condiciones ambientales que juntamente con la duración de la medida exigirán proteger un elemento delicado con es la banda extensométrica de forma adecuada.

Las bandas, de por sí, son presentadas bajo opciones que aportan una determinada protección, así las hay encapsuladas sobre dos láminas, una inferior que constituye el soporte y otra superior de la misma naturaleza y que deja libre solo los terminales para la soldadura de cables, ésta protección evita la proyección del estaño en la soldadura y mejora enormemente el aislamiento. Otras opciones llevan unos hilos soldados, por lo que el soporte superior cubre totalmente a la banda (fig. 21).

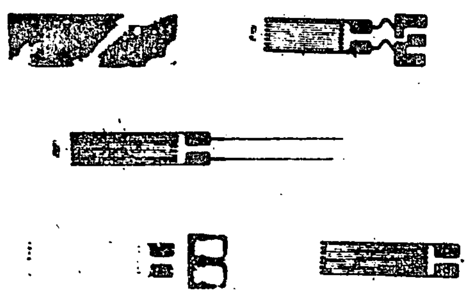

fig 21

En general la protección la consideramos bajo el aspecto de aislamiento eléctrico y de fortaleza mecánica y previamente a la instalación de la banda tendremos que conocerla, para preparar la superficie adecuadamente antes del pegado de la misma
Los criterios que debemos tener en cuenta para elegir los productos de protección estarán basados en:

a) Temperaturas extremas durante la medida, p.e. Probeta en laboratorio 22ºC $\pm$ 3ºC; estructura expuesta al sol 0-60ºC estructura de un avión en vuelo -50ºC + 120ºC.

b) Duración de las medidas, p.e. 1 hora en laboratorio; 1 año en un punto sumergido del casco de un buque.

c) Ambiente, p,e, aire seco, aire humedo, agua, aceite, chorro de agua, gases corrosivos, hidrocarburos,

No debemos olvidar antes de la aplicación de los protectores, cercionarnos de que no hay restos de adhesivo alrededor de la zona a proteger, que se limpió bien la resina fundente de las soldaprotector se adhiera, que no hay humedad, etc. en una palabra, no desdeñar ningún esfuerzo que posteriormente pueda inutilizar varias horas de laboriosos trabajos.

Una práctica muy aconsejable, siempre que sea posible, será lo de conectar provisionalmente el instrumento de lectura al circuito antes de protegerlo y sometiendo aquel a alguna solicitación, observar que el funcionamiento es lógico.

Por último, no olvidar tomar datos de posición, fotos, numeración de cables, esquemas etc. antes de la protección, ya que posteriormente sería imposible, al quedar el circuito tapado por los protectores.

La aplicación del protector la haremos siguiendo siempre las indicaciones del fabricante pero como orientación tendremos presente:

1º Extender bién el producto sobre la superficie limpia y si hay que dar varias capas, que la última cubra por completo a las anteriores. Algunos productos vienen acompañados de un componente previo, que debe aplicarse sobre la superficie con pincel y dejar secar perfectamente para luego aplicar el protector y conseguir así la mejor adhesión. Vijilar que no queden bolsas de aire.

2º Cuidar que el espesor del protector sea el adecuado, muchos protectores son blandos y fácilmente las bolitas puntuales de las soldaduras, pueden atravesar el protector con pequeñas presiones, originando contactos de masa indeseados.

3º Protección del extremo de los cables de unión a instrumentos, pues de nada sirve esmerarse en la banda si dejamos opción a que por la vaina de los cables queden huecos por donde se perdería la protección.

La fig. 22 indica un acabado tipo de protección.

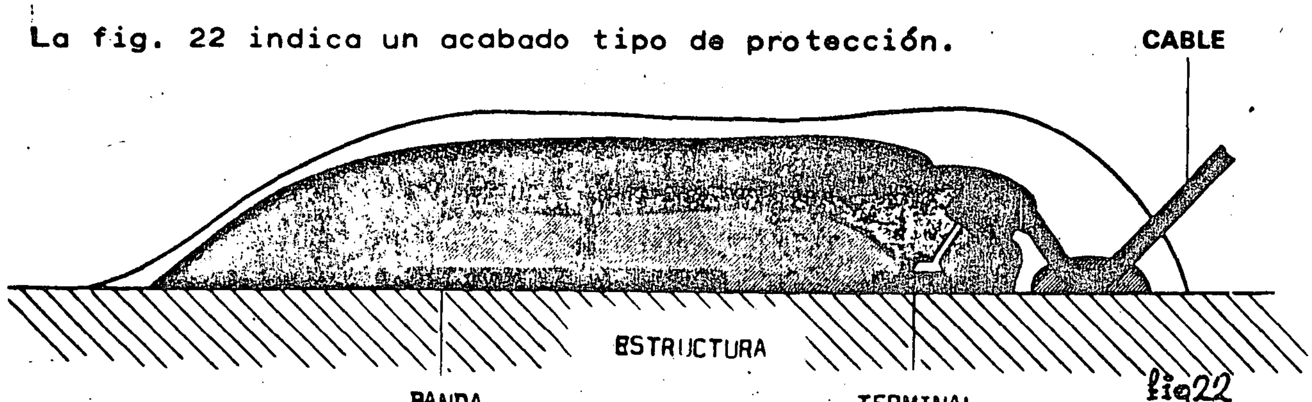

fig22

2.6.1. Indicadores de propagación de fisuras

Dos son los motivos que pueden hacer necesario el uso de estos sensores: detectar la aparición de una fisura o determinar la velocidad de propagación de la misma, en ambos casos, si bien el sensor será el mismo, variarán los instrumentos de lectura.

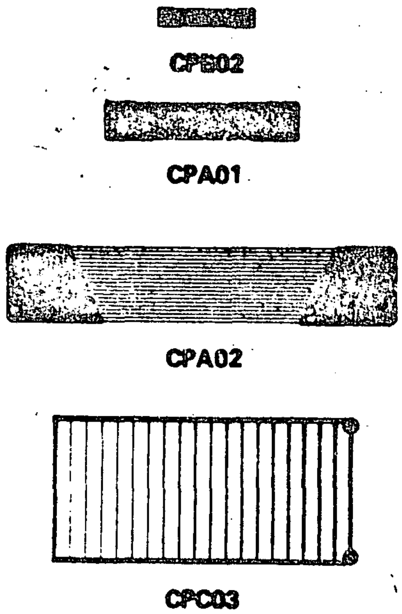

fig 23

Estos indicadores están formados por una serie de hilos en paralelo (fig. 23) montados en un soporte similar al de los extensímetros, que se pega en el punto donde se producirá la fisura, y que cuando aparezca, romperá un determinado número de conductores, deduciéndose la longitud de la fisura por medida de la resistencia con un ohmetro; si por el contrario el momento de aparición de la fisura es registrado de forma contínua por un oscilógrafo, deduciremos la velocidad con que se propaga (fig. 24).

La aleación de la que están constituidos es suficiente para soportar deformaciones superiores a ± 2000 $\mu\delta$ más de 10^8 ciclos y son montados con técnicas similares a las utilizadas en los extensímetros.

Los efectos de temperatura tienen poca influencia.

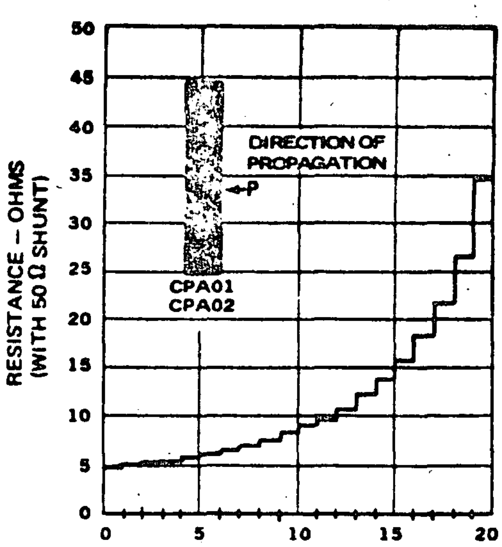

fig 24

2.6.2. Indicadores de fatiga

Al contrario que las bandas extensométricas, que miden deformaciones por variaciones instantáneas de su resistencia, los indicadores de fatiga (S/N) guardan "en memoria" todas las deformaciones experimentadas después de su instalación. La memoria aludida viene representada por una modificación permanente del valor nominal de su resistencia, que es función de la amplitud de las deformaciones y de la frecuencia con que se producen.

Las leyes de Wöhler nos dicen que:

1º En una pieza sometida a cargas alternas, la carga de rotura disminuye.

2º El número de alternancias que hay que producir para la rotura es tanto menor, cuanto mayor es la amplitud de las mismas.

3º Existe un valor de deformación máximo para el cual no se produce rotura sea cúal sea el número de ciclos con que se aplique.

En la fig. 25 se expresa gráficamente lo expuesto.

Estudios realizados por Miner, permiten afirmar que el porcentaje de vida de una pieza sometida a tensiones variables, es el mismo si aumentando la amplitud de las tensiones disminuimos su frecuencia o viceversa, siguiendo la proporción obtenida según los criterios de Wöheler.

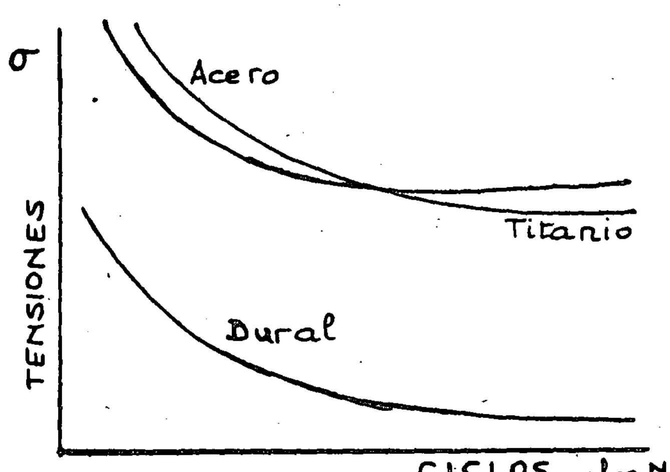

fig 25

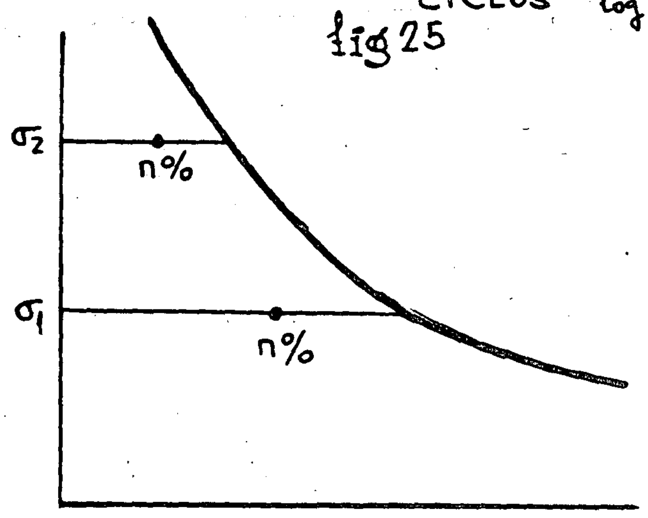

fig 26

En la fig. 26 vemos que el tanto por ciento de envejecimiento de una pieza es el mismo sometido a la tensión σ_1 y C_1, ciclos que si se somete a la tensión σ_2 y C_2 ciclos.

Se considera que las tensiones aplicadas oscilan entre un valor σ máximo y un mínimo O, si así no fuese, logicamente habrá que considerar los efectos de una componente contínua más la carga variable.

Si bién en su aspecto los indicadores de fatiga (fig. 27) son semejantes a las bandas extensométricas, la constitución de su elemento sensible es bién distinta, ya que la aleación de la rejilla persigue aumentar al máximo el efecto que en los extensímetros se trataba de eliminar; en efecto recordemos (2.2.4.) que en las bandas se establece como límite deformaciones dinámicas, aquel que produce una deriva de

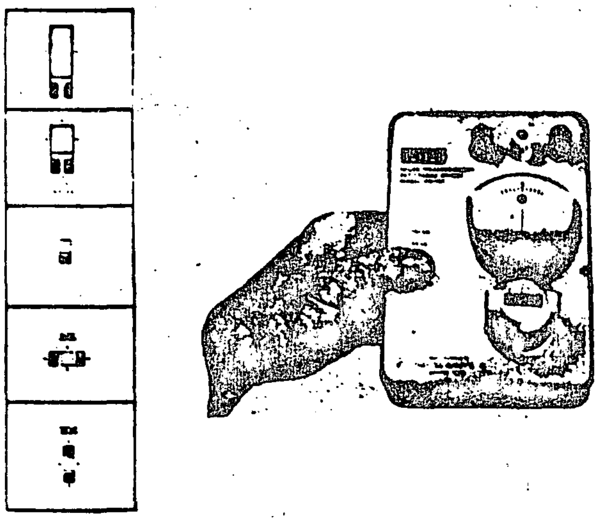

lig 27

$100 \mu\delta$, equivalente a un incremento de 0,024 ohms en una banda de 120 ohms, mientras que ahora pretendemos que estos valores sean **del** - orden de 7 a 10 ohm. Se **constituyen** en aleación **de** constantan con valor nominal de 100 ohm.

La variación de la resistencia del indicador de fatigas es producida por una distorsión de su red cristalina y por la aparición de microfisuras de la aleación de que se compone su rejilla y ha podido demostrarse experimentalmente que en algunos metales, empleados en construcción normalmente, se produce el mismo fenómeno; de ahí que estos sensores cuando son montados sobre piezas mecánicas puedan indicar con gran fidelidad el estado de envejecimiento de los materiales midiendo la desviación del valor nominal de la resistencia del sensor.

Si el envejecimiento de la aleación del sensor es distinto del material sobre el que se monta, la concordancia anterior se pierde y los resultados no tendrán valor alguno, ya que si, por ejemplo la deformación máxima capáz de desviar el valor de la resistencia del sensor, (3º ley de Wöhler) es superior a la deformación que producirá la rotura de la pieza de ensayo, el indicador de fatiga jamás acusaría desviación de su resistencia; para evitarlo se fabrican sensores multiplicadores los cuales por diversos procedimientos de fabricación se consiguen adaptar la respuesta del sensor a los materiales en que se montan (fig 28a)

La fig. 28 dá la respuesta de los sensores FWA de - Vishay-Micromesures.

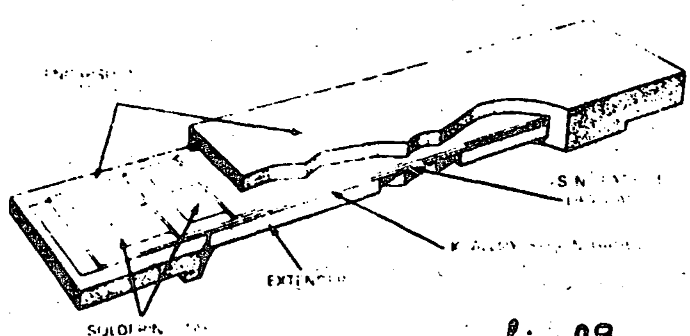

fig 28a

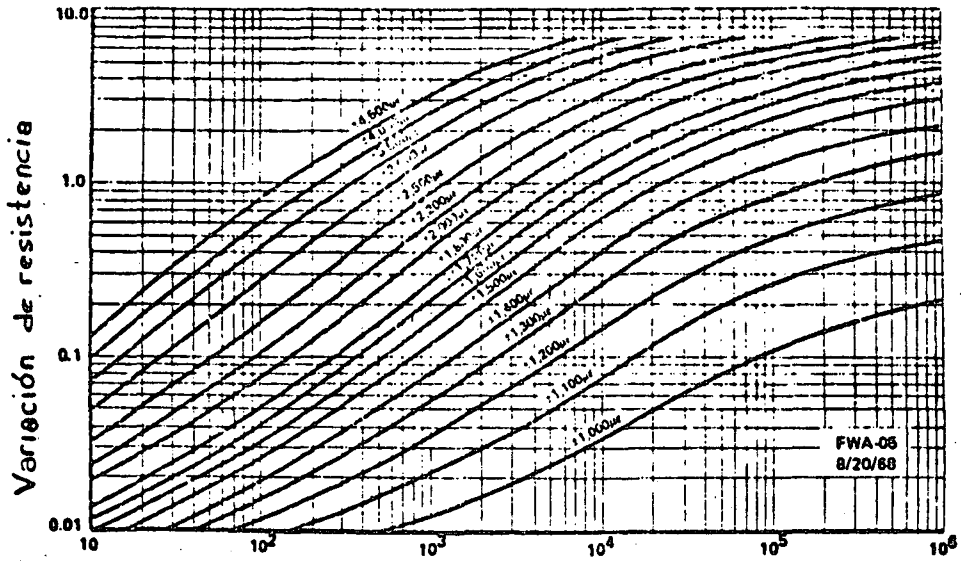

Nº de ciclos

fig28

Los indicadores de fatiga son verdaderos integradores de los efectos producidos por cargas alternas, sea cual sea su amplitud así pués, si después de 10.000 ciclos de $\pm$ 2000 $\mu\delta$ producen una desviación de la resistencia de 1,9 ohm y 100 ciclos de $\pm$ 3000 $\mu\delta$ 0,8ohm, la indicación final será de 2,7 ohm.

Al montaje de estos indicadores habrá que tener en cuenta que su eje sensible coincida con el eje de esfuerzo principal máximo, determinado previamente por cualquier procedimiento (extensométrico, fotoelasticidad, etc).

2.6.3. Sensores de temperatura

Siguiendo el mismo procedimiento de fabricación de las bandas extensométricas, pero haciendo que la aleación de la rejilla sea de niquel, se obtienen sensores cuya variación de resistencia es altamente sensible a las variaciones de temperatura siendo este fenómeno muy estable y repetitivo, de ahí que se utilice profusamente en la medida de temperaturas por contacto y utilizando las mismas técnicas de instalación que las expuestas para extensímetros. La curva ΔR-t^o (fig. 29), tiene una pendiente considerable por lo que se obtienen señales de alto nivel, pudiendose medir con gran precisión, exactitud y poder de resolución, temperaturas comprendidas entre -300 y + 500ºF.

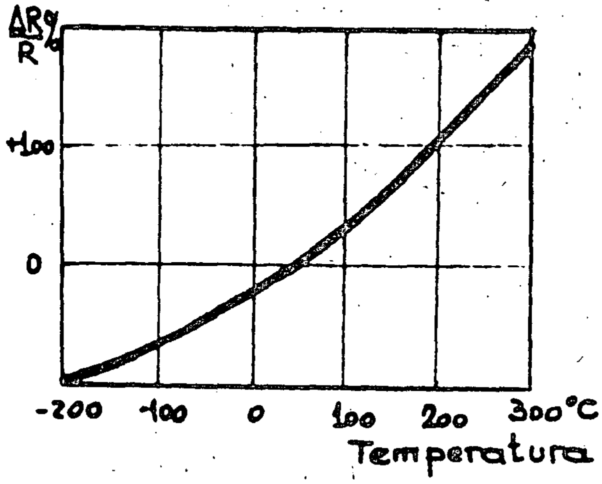

fig 29

Generalmente son fabricados para qué a la temperatura ambiente (23,9ºC su resistencia nominal sea de 50 ohm y conociendo la curva , poder conocer la temperatura midiendo por cualquier procedimiento las desviaciones de la resistencia.

Estos sensores a diferencia de los termopares que generan una f.e.m. son pasivos, necesitando de una fuente de alimentación, por eso (fig. 30) si es excitado con una fuente de intensidad constante 1mA) la lectura directa de un milivoltímetro nos valdría para conocer los Δ R directamente, no obstante como la respuesta no es lineal siempre tendríamos que tener tablas o curvas de respuesta para conocer el verdadero valor de la temperatura en ºC ó ºF. El inconveniente anterior ha sido subsanado introduciendo circuitos linealizadores en los cuales, si bién se pierde sensibilidad, la respuesta es lineal, por lo que los instrumentos de lectura pueden ir tarados directamente en escalas termométricas.

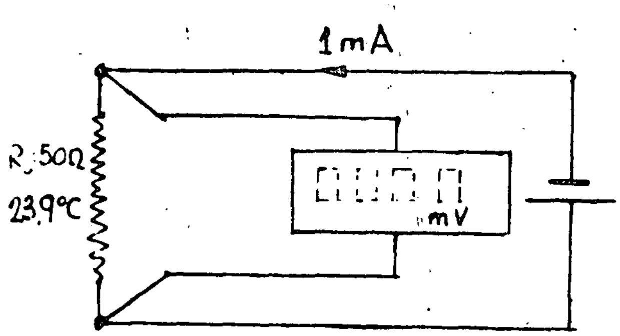

fig 30

Con el fín de utilizar para la medida de temperaturas los mismos instrumentos que para medir deformaciones, los circuitos linealizadores se calculan de tal forma que el sensor constituye una rama de un puente de Whearstone (fig. 31), de tal forma, que al leer un número entero de microdeformaciones equivalga a la variación de 1grado centígrado o Farenheit, Normalmente se fabrican redes para:

$$10\,\mu\delta \leftrightarrow 1^\circ C \leftrightarrow 1^\circ F$$

$$100\,\mu\delta \leftrightarrow 1^\circ C \leftrightarrow 1^\circ F$$

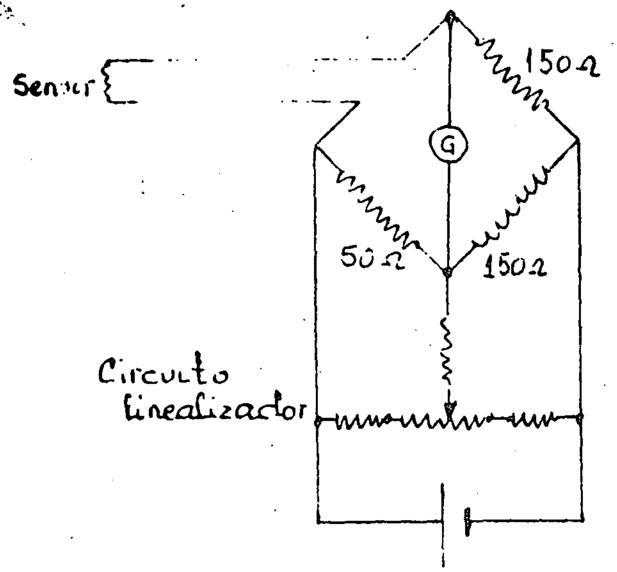

fig 31

La aleación de niquel, muy sensible a las variaciones de temperatura, obliga a utilizar fuentes de alimentación de baja d.d.p. ya que al circular corriente por el sensor el calor generado por efecto Joule introduce pequeños errores. Por otra parte, si el punto de medida está sometido a deformaciones estas las acusará el sensor, pero dado su insensibilidad a este fenómeno no tendrán gran influencia en la exactitud de la medida, de todas formas el fabricante da con los sensores las curvas de corrección por este motivo.

La longitud de los cables puede ser origen de errores por perdida de sensibilidad, pero se compensan estos efectos modificando el factor K de sensibilidad en el instrumento de lectura (esto se estudia en el próximo capítulo).

Para medida de muy bajas temperaturas (criogenia) se utilizan sensores (fig. 32) que llevan dos rejillas en serie en aleaciones de manganina nikel, con lo que se consigue linealizar circuitos desde -400ºF.

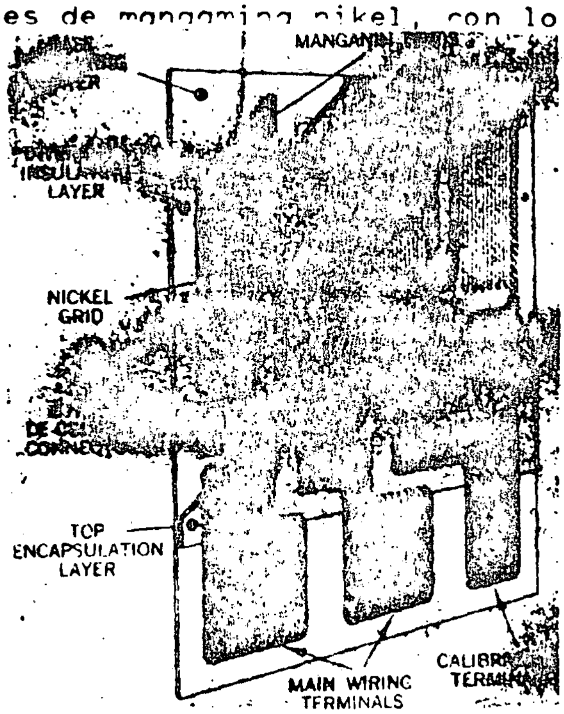

En el montaje de sensores de temperatura no habrá jamás de olvidar utilizar adhesivos soldaduras, cables protectores, etc. cuyo límite de utilización en temperatura sea superior a la que se desea medir.

2.6.4. Bandas semiconductoras

Todos los cuerpos tienen, más o menos acusada, la propiedad de sufrir variaciones en el valor de su resistividad cuando son sometidos a tensiones mecánicas, pero en los semiconductores este efecto es mucho más notable y se aprovecha por tanto, como elemento transductor para la medida de deformaciones. El fenó meno expuesto de la piezaresistividad, no debe ser confundido con el de la piezoelectricidad, que presentan los cristales de cuarzo y otros, de crear cargas eléctricas entre sus caras cuando son deformados, constituyendo elementos activos, mientras a los que aquí nos referimos son elementos pasivos, esto se necesitarán una aportación de energía esterna (alimentación) para conocer sus variaciones de resistencia.

En un semiconductor la resistividad tiene por valor $\rho = \frac{1}{eNv}$ donde N representa el número de portadores de cargas eléctricas, v su velocidad media y e, es la carga del electrón. La variación de ρ al aplicar cargas al semiconductor dependerá de la concentración específica de portadores y de la orientación cristalográfica respecto a las cargas aplicadas; si aplicamos cargas de tracción o compresión el cambio relativo de resistividad se expresa por:

$$\frac{\Delta \rho}{\rho} = \pi_\ell \, \sigma$$

llamandose a π_ℓ coeficiente de resistividad longitudinal.

Recordemos que un semiconductor es un cristal de silicio o germanio (4 electrones de valencia) al que se le añaden impurezas tipo N (arsenico, 5 electrones de valencia) o Tipo P (galio, 3 electrones de valencia) y dependiendo de la proporción de los agentes contaminantes, podrán obtenerse infinidad de elementos de muy variadas características.

El factor de sensibilidad en los extensímetros de film metálico, hemos visto que tiene de valor 2, pero si empleamos bandas cuyo elemento sensible sea un semiconductor, se pueden obtenerse valores de entre 50 y 200 y dado que dimensionalmente pueden fabricarse iguales se establecen las ventajas de:

1º Obtener niveles de señal elevados que pueden evitar una posterior amplificación.

2º Mejorar la relación señal-ruido; sin embargo su precio es mucho más elevado y su sensibilidad a la temperatura mucho más acusada que en las bandas convencionales, lo que hace que su uso quede limitado a la medida de muy pequeños valores de deformaciones y a la fabricación de captadores.

El factor de sensibilidad es definida por:

$$K = \Delta R \ldots = 1 + 2\mu + \pi_\ell E$$

siendo E= Módulo de elasticidad: μ= Coeficiente de Poisson y π_ℓ =coeficiente de resistividad longitudinal del semiconductor.

El término $\pi_\ell E$ es el equivalente al que por la constante de Bridgman se introduce en las bandas metálicas, con la salvedad de que es bastante más elevado.

La influencia de la temperatura en una banda semiconductora está intimamente ligada al número de átomos de impurezas que lleve, así para 10^{20} atomos/cm^3, el factor Ksc es constante prácticamente a las variaciones de temperatura.

$$K_{sc} = \frac{\Delta R}{R \varepsilon} = \text{Constante}$$

Si la proporción de impurezas es del orden de 10^7 atomos/cm^3 el factor de banda se verá afectado en la forma:

$$K_{sc} = \frac{T_o}{T} K_{sc(o)} + C \left(\frac{T_o}{T}\right)^2 \varepsilon$$

donde T= Temperatura absoluta; $K_{sc(o)}$ = Factor de sensibilidad a la temperatura To; C= Constante y ε =deformación.

Los diferentes niveles de contaminación de los cristales de silicio se denominan por las letras, K, L, C, D, E, F, G y H y determinan las características piezoresistivas del sémiconductor. La resistividad según tipos, oscila entre 0,001 ohm/cm y 1ohm/cm, la fig.33, resume la respuesta de las distintas clases.

Para compensar los efectos de variación de temperatura, se emplea un circuito con banda compensadora (ver tema 3) o bién el fabricante adapta el semiconductor para que dentro de ciertos límites de utilización y para determinados materiales, variaciones de temperatura no produzcan deformaciones aparentes.

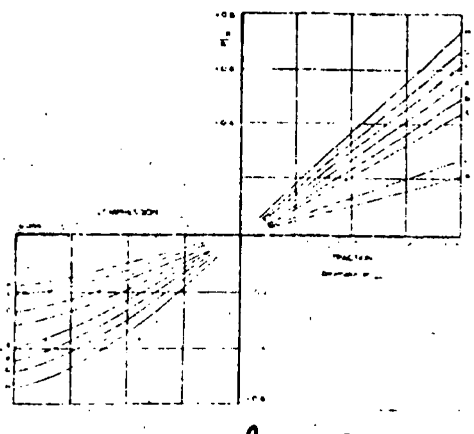

fig 33

En general las técnicas de pegado, protección, etc, serán idénticas a las de los extensímetros metálicos. Añadiremos por último que los monocristales de silicio son perfectamente elásticos, lo que hace que el fenómeno de histeresis y fluencia quede prácticamente reducido al que introdu ci el adhesiv.

2.6.5. Bandas para muy altas presiones y temperaturas

Las necesidades surgidas en la investigación de programas aeroespaciales de armamento, lineas submarinas, grandes obras de ingeniería civil, etc, donde es necesario medir deformaciones en condiciones ambientales francamente adversas, ha motivado el desarrollo de bandas especiales que pueden trabajarm bajo elevadísimas presiones y temperaturas, con excelente exactitud.

A título anecdótico señalaremos, que gracias a estas bandas especiales, se han podido medir deformaciones en el cono del fuselaje del avión cohete americano X-15. La tecnología que se expone -- corresponde a la desarrollada por la firma Microdot Inc.

El principio en que se basan es el clásico por el cual la resistencia de un conductor eléctrico varía si se somete a tensiones mecánicas, sin embargo, respecto a las bandas convencionales, se diferencian en que carecen de soporte y su parte activa la constituye un conductor en forma de U introducido en una cápsula metálica de la que está aislado por polvo o presión de óxido de manganeso (fig. 34). Se efectua su fijación al punto de medición soldando por puntos la base metálica del sensor. En la construcción del filamento se utilizan aleaciones de Niquel-Cromo para medidas hasta temperaturas de 350ºC y Platino-Tungsteno hasta 650ºC. Los hilos terminales para unión de los cables a los instrumentos de - lectura los constituyen los extremos del propio filamento y así se consigue una resistencia mecánica elevada; esta forma de terminales se realiza actuando por erosión - química sobre el hilo constitutivo del sensor de un diámetro igual al del terminal hasta que la parte activa quede al diámetro inferior adecuado.

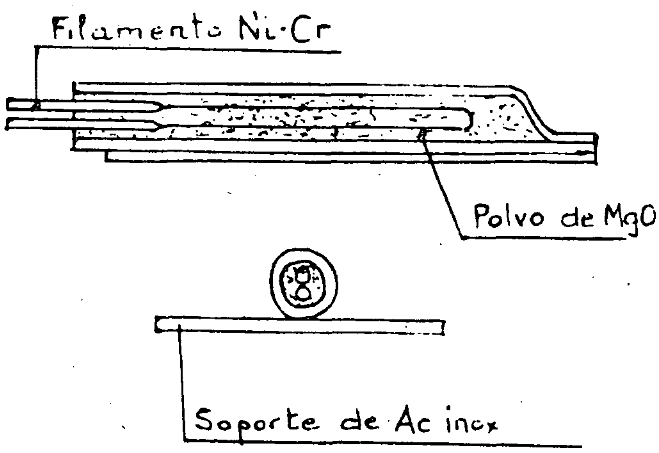

fig 34

Las aleaciones Cr-Ni del filamento se someten a tratamientos térmicos, para que la variación de resistencia debida al coeficien te térmico de resistividad, sea de la misma magnitud y signo contrario que la originada por dilatación térmica, con lo que se consigue una autocompensación en un rango de utilización que especifica el fabricante.

Si la aleación es de Pl-W, un tratamiento térmico de la misma, no ofrecerá una garantia de conseguir una buena compensación del efecto de temperatura, por estar diseñados para trabajar a elevadas temperaturas, por tal motivo, se utilizan bandas con coeficiente de sensibilidad a las deformaciones nulo y que se montan en la rama adyacente a la que se monta la banda activa en un circuito de puente Wheatstone (fig. 35); se observa que al construir la banda compensadora arrollada en espiral, la sensibilidad a la deformación mecánica es nula, y además se puede fabricar dentro de la misma cápsula de la banda activa; las ventajas que se derivan son enormes, pues se reduce el tiempo de montaje y se consigue además que los gradientes térmicos incidan con el mismo valor en ambas bandas.

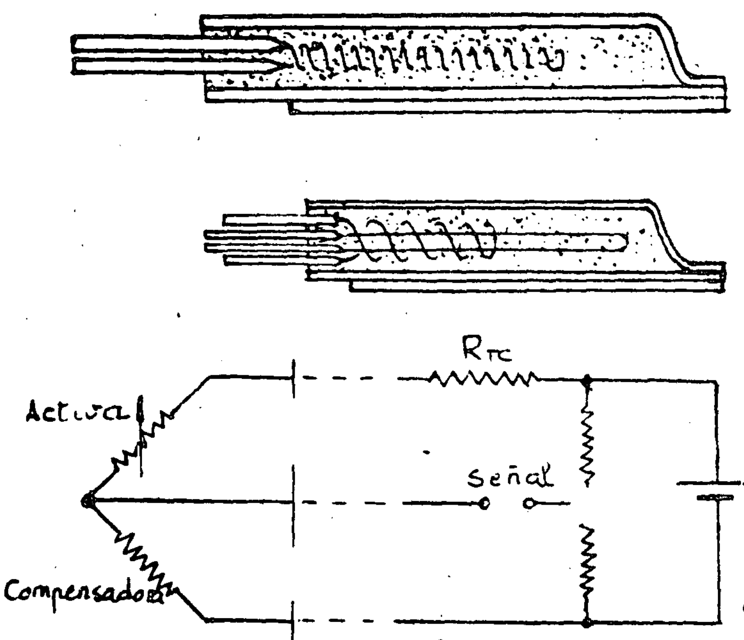

fig 35

Un pequeño inconveniente de la aleación Pl-W se debe a las diferencias que pueden haber entre el coeficiente térmico de resistividad y efecto de dilatación del material de ensayo, por eso se monta en serie una resistencia Rtc, que compensan esos errores. Siempre el fabricante incluye las especificaciones de cada tipo.

La preparación de superficies para montaje, no necesita de la meticulosidad de las bandas clasicas.

El óxido de manganeso es introducido, con suficiente compactidad, para que pueda transmitir las deformaciones de la extructura al filamento.

TEMA III

3.1. Teoría del Puente Wheatstone

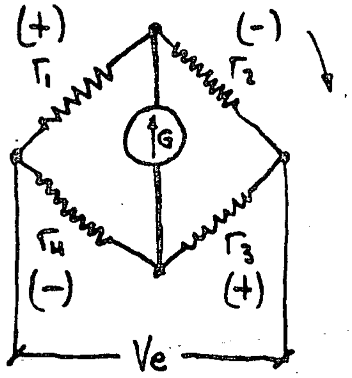

fig.1

La fig. 1 representa el esquema de un circuito en puente de Wheatstone que es el más universalmente utilizado para medidas extensométricas. Las bandas extensométricas podrán ocupar uno, dos o los cuatro brazos del puente, denominándose entonces circuitos de 1/4, 1/2, 1/1, de puente respectivamente.

Se llaman ramas activas las ocupadas por bandas que se deforman por solicitaciones mecánicas y ramas pasivas aquellas que no intervienen en la medida.

La d.d.p. Vs en la diagonal de G tiene por valor

$$V_s = V_e\left(\frac{r_1}{r_1+r_2} - \frac{r_4}{r_3+r_4}\right) \quad [1]$$

para pequeñas variaciones de r_1; r_2; r_3 y r_4 podemos derivar la [1] entonces:

$$\Delta V_s = V_e\left[\frac{\Delta r_1(r_1+r_2) - r_1(\Delta r_1+\Delta r_2)}{(r_1+r_2)^2} - \frac{\Delta r_4(r_3+r_4) - r_4(\Delta r_3+\Delta r_4)}{(r_3+r_4)^2}\right] =$$

$$= V_e\left[\frac{r_1 r_2}{(r_1+r_2)^2}\left(\frac{\Delta r_1}{r_1} - \frac{\Delta r_2}{r_2}\right) - \frac{r_3 r_4}{(r_3+r_4)^2}\left(\frac{\Delta r_4}{r_4} - \frac{\Delta r_3}{r_3}\right)\right]$$

Si el circuito está equilibrado $\frac{r_1}{r_2} = \frac{r_4}{r_3}$

$$\Delta V_s = V_e\left[\frac{r_1 r_2}{(r_1+r_2)^2}\left(\frac{\Delta r_1}{r_1} - \frac{\Delta r_2}{r_2}\right) - \frac{\frac{r_4}{r_3}}{\left(1+\frac{r_4}{r_3}\right)^2}\left(\frac{\Delta r_4}{r_4} - \frac{\Delta r_3}{r_3}\right)\right]$$

$$\Delta V_s = V_e\left[\frac{r_1 r_2}{(r_1+r_2)^2}\left(\frac{\Delta r_1}{r_1} - \frac{\Delta r_2}{r_2} + \frac{\Delta r_3}{r_3} - \frac{\Delta r_4}{r_4}\right)\right] \quad [2]$$

Si $r_1 = r_2$; $r_3 = r_4$

$$\Delta V_s = \frac{V_e}{4}\left(\frac{\Delta r_1}{r_1} - \frac{\Delta r_2}{r_2} + \frac{\Delta r_3}{r_3} - \frac{\Delta r_4}{r_4}\right) \quad [3]$$

de donde se deduce que la portación a la d, d.p. de salida V_s de dos ramas adyacentes que experimentan un Δr del mismo signo, tiene sentidos opuestos, propiedad importantísima que por algunos autores es denominado"ley de signos".

Si la expresión $\frac{\Delta r_1}{r_1} - \frac{\Delta r_2}{r_2} + \frac{\Delta r_3}{r_3} - \frac{\Delta r_4}{r_4}$, la transformamos en otra de forma $p\,\frac{\Delta r}{r}$ la [3] queda $V_s = \frac{V_e}{4}\,p\,\frac{\Delta R}{R}$ --[3a] en la que el factor de puente "p" incluirá la aportación a la señal de salida de todas y cada una de las ramas, siendo

$$p = \sum a_n b_n c_n = a_1 b_1 c_1 - a_2 b_2 c_2 + a_3 b_3 c_3 - a_4 b_4 c_4 \ldots \ldots \quad [4a]$$

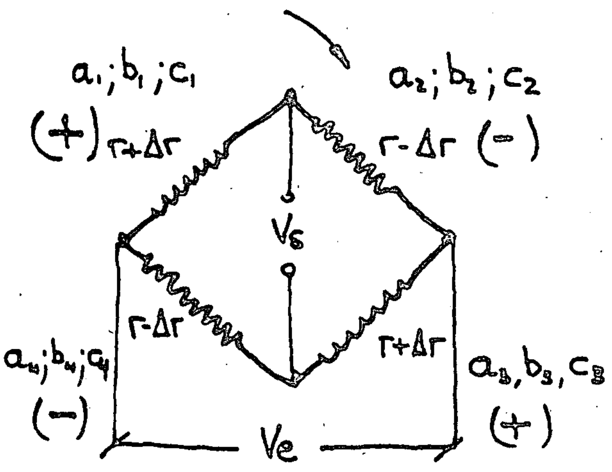

fig 2

Los subíndices indican la posición relativa de las bandas del puente, respecto a un sentido arbitrario y a cada rama le asignaremos tres coeficientes a, b,c, cuyo significado es el siguiente:

El coeficiente a es indicativo de si la rama es activa o pasiva, por lo que tiene de valor:

a= 1 para ramas activas

a= 0 para ramas pasivas

El coeficiente b indicará si una rama activa del puente sufre deformaciones por esfuerzos de tracción o de compresión, por tanto:

$b = +1$ si $\Delta r > 0$ (tracción)

$b = -1$ si $\Delta r < 0$ (compresión)

Si las ramas activas del puente no sufren deformaciones absolutas simultáneamente iguales, referiremos la deformación de cada rama al valor máximo de $\frac{\Delta R}{R}$, siendo esto expresado por el coeficiente c, que por tanto tendrá un valor comprendido

$$1 \geq c \geq 0$$

Por todo lo anterior, si consideramos el caso de la fig. 2 tendremos que:

$a_1 = a_2 = a_3 = a_4 = 1$	por ser todas las ramas activas
$b_1 = b_3 = +1$	por corresponder a esfuerzos de tracción
$b_2 = b_4 = -1$	por corresponder a esfuerzos de compresión
$c_1 = c_2 = c_3 = c_4 = 1$	por ser $\frac{\Delta R}{R}$ un valor absoluto el mismo en las cuatro ramas del puente.

por lo que:

$$p = 1.1.1 - 1.(-1)1 + 1.1.1 - 1.(-1).1 = 4 \cdot \quad V_s = \frac{V_e}{4}\,p\,\frac{\Delta R}{R} = V_e\,\frac{\Delta r}{r} \ldots \ldots \quad [5]$$

Consideremos particularmente el caso del circuito de 1/4 de puente (fig. 3a) en el se cumple:

$$\Delta V_s = V_e\left(\frac{r+\Delta r}{2r+\Delta r}-\frac{1}{2}\right) = \frac{\Delta r}{4(R+0{,}5\Delta R)} \quad \text{.....} [6]$$

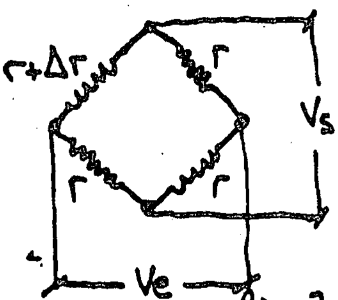

fig3a

expresión que indica la no existencia de proporcionalidad lineal entre la señal de salida y la deformación; solamente cuando ésta sea muy pequeña, se podría despreciar el termino 0,5ΔR del denominador y quedar

$$V_s = \frac{V_e}{4}\frac{\Delta R}{R} \quad \text{- - - - - - - - - - -} [7a]$$

En el circuiro de 1/2 de puente (fig. 3b) tenemos que:

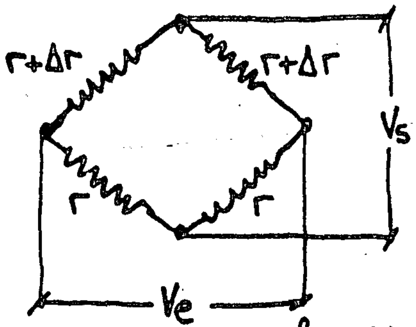

fig3b

$p = a_1b_1c_1 - a_2b_2c_2$

$a_1 = a_2 = 1$

$b_1 = 1$

$b_2 = -1$

$c_1 = c_2 = 1$

$p = 2$

$$V_s = \frac{V_e}{4}\, p\, \frac{\Delta R}{R} = \frac{V_e}{2}\frac{\Delta r}{r} \quad \text{- - - - - - - - - -} [7b]$$

que es un circuito lineal

3.1.1. Principios básicos en medidas extensométricas

Hemos visto como basándonos en el puente de Wheatstone, podemos - transformar las variaciones que la resistencia que un extensímetro experimenta cuando se deforma, en una variación de diferencia de potencial eléctrico; pero en la materialización de las medidas debe remos tener muy en cuanta ciertos principios con el fín de no cometer errores.

En primer lugar consideremos la fig. 4, en la que se representan dos circuitos de medida en 1/4 de puente que son conmutadas al instrumento de lectura a través del conmutador C_1, si la resistencia de los contactos no es constante, cada vez que conmutemos, a la variación propia de la resistencia de la banda, aña diremos la variación de la resistencia de contacto del conmutador, que introduce un error en la medida, lo que nos dice - que dentro del circuito del puente a, b, c, d no deben producirse más variaciones de resistencia que las producidas por las bandas.

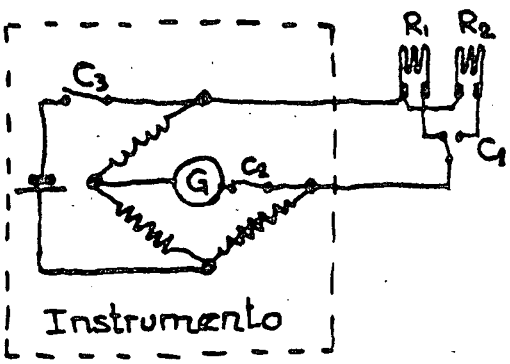

fig 4

Si existiesen otros conmutadores C_2 y C_3 que actuasen en el circuito externo del puente, no se introducirían errores, aún cuando las resistencias de contacto fluctuasen entre una y otra actuación, pues en realidad buscamos la condición de equilibrio del puente que no se ve afectada por dichas variaciones.

Por tanto en toda medida extensométrica se cuidará rigurosamente, no perturbar las ramas del puente por cambio de cables, contactos defectuosos, resistencias de conmutadores (serán de excelente calidad) etc. etc. sin embargo pequeñas perturbaciones en las diagonales no tendrán influencia.

Otra condición básica será la garantia de un perfecto aislamiento del circuito de medida, ya que defectos del aislamiento (fig. 5) suponen, bien la puesta en cortocircuito de cierta longitud activa de la banda, o bien el acoplamiento en paralelo de una resistencia de elevado valor, y en cualquiera de los casos la medida sería errónea.

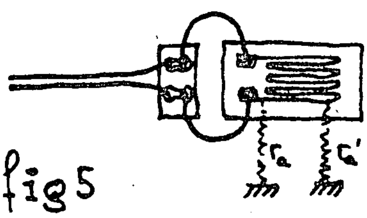

fig5

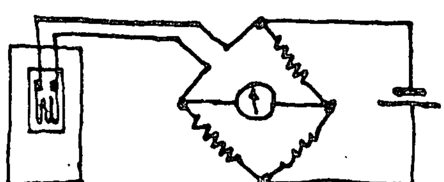

fig6a.

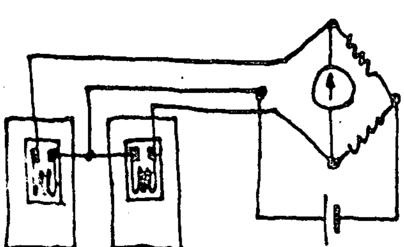

fig6b.

3.1.2. Compensación del efecto de variación de temperatura.

Los materiales sobre los que se montan las bandas sufren deformaciones por efecto de las variaciones de temperatura (tema 2 apartado 2.2.3) que no crean tensiones y que por lo tanto son origen de errores; si la banda es autocompensada, se vió que, dentro de ciertos límites de temperatura, estos errores son despreciables, no obstante, si el circuito de medida es un puente de Wheatstone, podremos corregir los errores por variación de temperatura en cualquier rango utilizando una banda pasiva o de compensación.

En la fig. 6a, la banda montada sobre probeta sufrirá deformaciones cuando hayan variaciones de temperatura, pero si (fig.6b) sobre un trocito de material idéntico al de la probeta montamos una banda compensadora, haciendo que en el puente de Wheatstone ocupe una rama adyacente respecto a la activa, ocurrirá que por variaciones de temperatura, las dos, activa y compensadora, se deformarán en la misma magnitud, pero su aportación a la señal de salida es nula por la ley de los signos y por tanto el circuito de medida solo será sensible a las solicitaciones que sufra la probeta o elemento de ensayo.

Este método presenta el inconveniente de necesitar dos bandas, pero tiene la gran ventaja de compensar los efectos de variación de temperatura en toda la gama de utilización de las bandas. Por otra parte en mediciones de varios puntos, puede emplearse una compensadora común en la mayoría de los casos; así mismo, se podrá buscar la disposición adecuada en ciertas medidas que necesitan dos o cuatro bandas activas, para que los efectos de temperatura queden compensados (Se verá con detalle en el apartado 3.1.6).

3.1.3. Configuración del cableado en diversos montajes

Sea cualquiera el instrumento de medida utilizado, las bandas se montan de forma que constituyen 1,2 o las 4 ramas de un circuito de puente de Wheatstone, incluyendose dentro del instrumento las resistencias que completen el puente según la configuración. Estudiaremos la disposición de los hilos de unión del circuito de medida a los instrumentos según las diversas configuraciones.

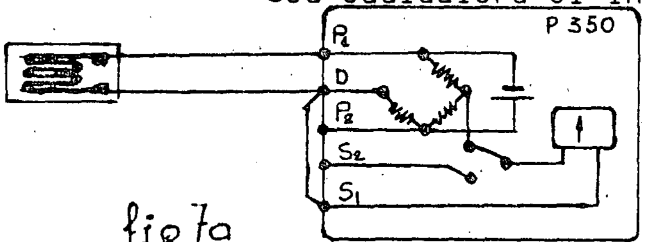

fig 7a

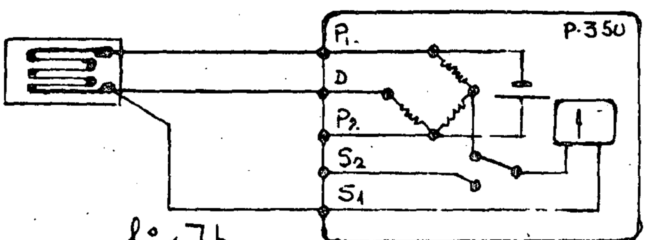

fig 7b

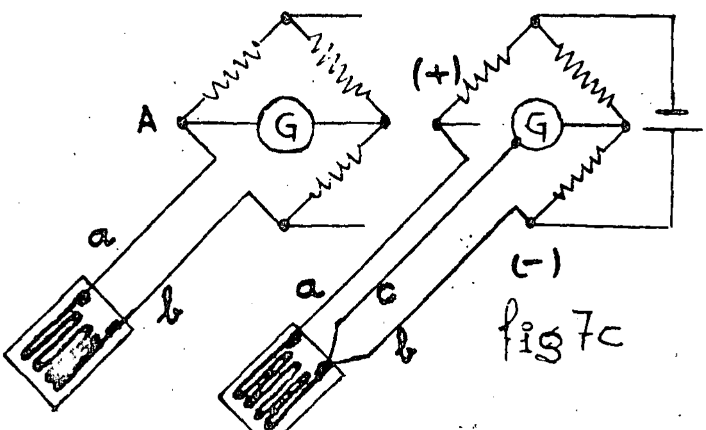

fig 7c

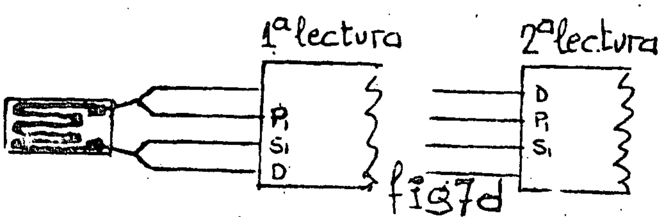

fig7d

1º Circuito de 1/4 de puente:
En el caso de medidas en las que se pueda considerar la temperatura constante, el montaje de 2 hilos de la fig. 7 se puede utilizar sin más limitaciones que los errores de linealidad, pero si la temperatura varía, aún dentro de los límites de autocompensación, (si la banda está autocompensada) nunca podremos corregir las perturbaciones que se originen en los hilos de unión, ya que éstos

no pueden autocompensarse; por ésta razón se adapta el montaje de 3 hilos (fig. 7b) en los que se consigue una simetría del circuito respecto a dos ramas adyacentes y por la ley de signos, quedan compensadas las perturbaciones en la línea.

En la fig. 7c se resume lo expuesto, viendose que el traslado del vertice A influye en que los conductores a y b actuan en una sola rama (2 hilos). El conductor c por actuar en la diagonal del puente no influye (3.1.1.) en la medida.

En medidas de gran responsabilidad, se puede utilizar el circuito de 4 hilos (fig. 7d); se harán dos medidas, conectando alternativamente los hilos según el esquema y obteniendo la media aritmética de las dos lecturas. En realidad se han efectuado dos medidas con montaje de 3 hilos para eliminar posibles asimetrías del circuito

2º Circuito de medio puente.-

El circuito de 1/2 puente es el que se ha indicado para la compensación de los efectos de temperatura. En general se utiliza cuando se quieren eliminar, efectos que actuen ramas adyacentes del puente (fig. 8). Por su simetría, las perturbaciones en la línea quedan compensadas.

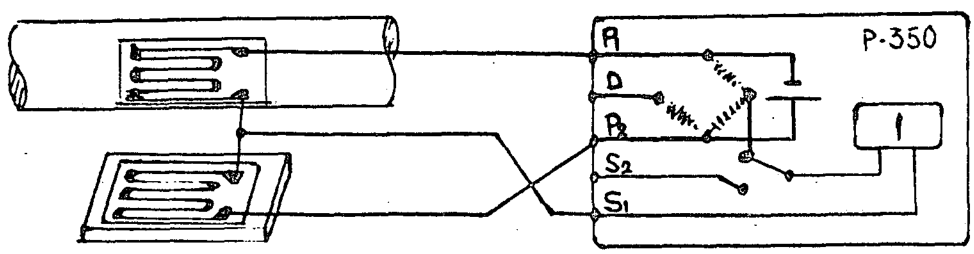

fig 8

3º Circuito de puente completo (1/1)

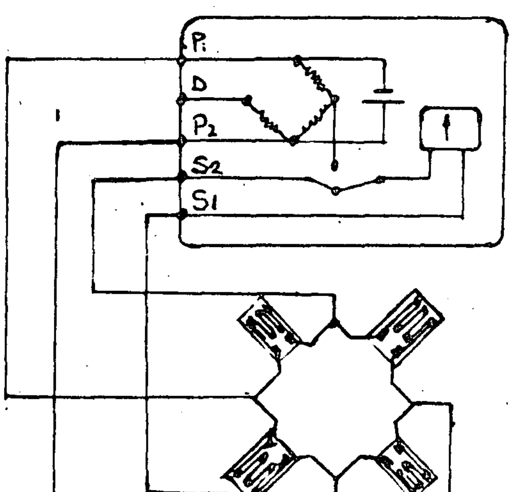

fig 9

Si utilizamos las 4 ramas como activas, obtendremos la configuración de la fig. 9, en la cual por ser un circuito simétrico se compensan los efectos parásitos que perturban por igual a la línea.

3.1.4. Perdida de sensibilidad en las líneas de transmisión

Los hilos de unión del circuito de medida extensométrico a los instrumentos de lecturas, añaden resistencias en serie a la banda, que afectan al valor del factor de banda K y suponen una perdida de sensibilidad.

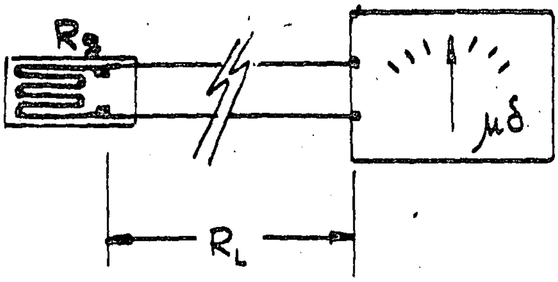

Rg. Valor óhmico nominal de la banda.

Rl= Valor óhmico de la línea de transmisión.

ΔRg. Variación del valor óhmico de la banda.

ε Alargamiento unitario

K. Factor de banda aislada

Kv Factor de banda real

fig 10

en efecto, por definición, el valor del factor de banda teórico K vale (fig. 10)

$$K = \frac{\frac{\Delta R_g}{R_g}}{\varepsilon} : \frac{\Delta R_g/R_g}{\Delta l/l} \quad . \; . \; . \qquad [7]$$

pero el factor verdadero será:

$$K_v = \frac{\frac{\Delta R_g}{R_g + R_L}}{\varepsilon} \; - \; - \; - \; - \; - \; - \qquad [7a]$$

Dado que el fabricante de bandas ignora cual será la resistencia de los hilos utilizados, habrá que introducir un factor de corrección de valor:

$$D = \frac{K_v}{K} : \frac{R_g}{R_g + R_L} \; - \; - \; - \; - \; - \qquad [8]$$

D se llama coeficiente de desensibilización y será prácticamente 1 con lineas muy cortas, pero si éstas son superiores a unos 10 metros, es aconsejable hacer la correción, para lo cual si no conocemos la resistencia del conductor deberá hallarse experimentalmente.

3.1.5. Relación entre deformación y señal de salida

El objeto principal de la Extensometría es el conocimiento del estado de deformaciones, pero en el estudio de los circuitos de medida hemos visto que las deformaciones del material donde se monta la banda, producen una variación de la resistencia de la misma y que al ser ésta parte activa de un puente de Wheatstone, origina una d.d.p. en una de sus diagonales proporcional a la deformación, es decir que será necesario establecer la relación entre el estímulo (deformación) y la respuesta (d.d.p. en el puente).

Recordando [3a]: $V_s = \frac{V_e}{4} n \frac{\Delta R}{R}$, y la [7a] $K = \frac{\Delta R/R}{\varepsilon}$

deducimos que: $$\frac{V_s}{\varepsilon} = \frac{V_e}{4} n K \; . \; - \; - \; - \; - \; - \; - \; - \; - \; - \; - \qquad [10]$$

Relación importante sobre todo cuando la lectura se efectua con instrumentos que no dan lecturas directas en microdeformaciones.

Ejemplo: El elemento de la fig. 11 está sometido a un esfuerzo de tracción simple; si medimos al aplicar la carga, a la salida del puente una V_S= 1 mV, calcular la fuerza F.

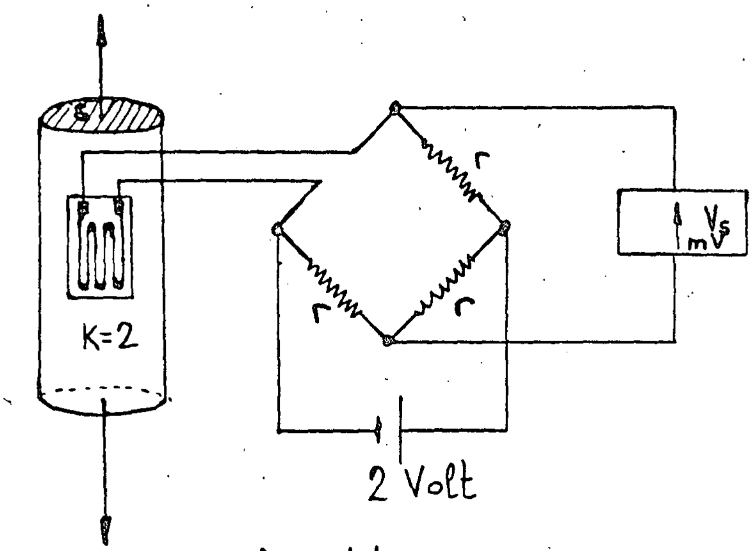

$E = 20.10^6$ N/cm²

$S = 0{,}5$ cm²

fig 11

$$V_S = \frac{V_e}{4} \, r \, K \varepsilon = \frac{2}{4} \, 2 \, \varepsilon = 1000 \, \mu V \quad (r=1)$$

$$\varepsilon = 1000 \, \mu \delta$$

$$F = \varepsilon E S = 1000 \, . \, 20 \, . \, 10^6 \, . \, 0{,}5 \, . \, 10^{-6} = \underline{\underline{10 \, KN}}$$

3.1.6. Estudio de diversos circuitos de medida

Es muy frecuente, que en el punto objeto de medida incidan esfuerzos compuestos y sin embargo, solo nos interese conocer la influencia individual de dichos esfuerzos como veremos estudiando casos particulares.

Tracción o compresión simple

Si el elemento de ensayo está sometido simultáneamente a flexión, tracción compresión y variaciones de temperatura amplias, el circuito de la fig. 12 solo será sensible a los esfuerzos de tracción ó compresión; en efecto, la variación de resistencia de cada una de las bandas es (llamando Ro= valor nominal de la banda; ΔR_T= incremento de Ro por la componente tangencial; ΔR_N= iden, normal y AR_t efecto variación de temperatura

TRACCION O COMPRESION PURA

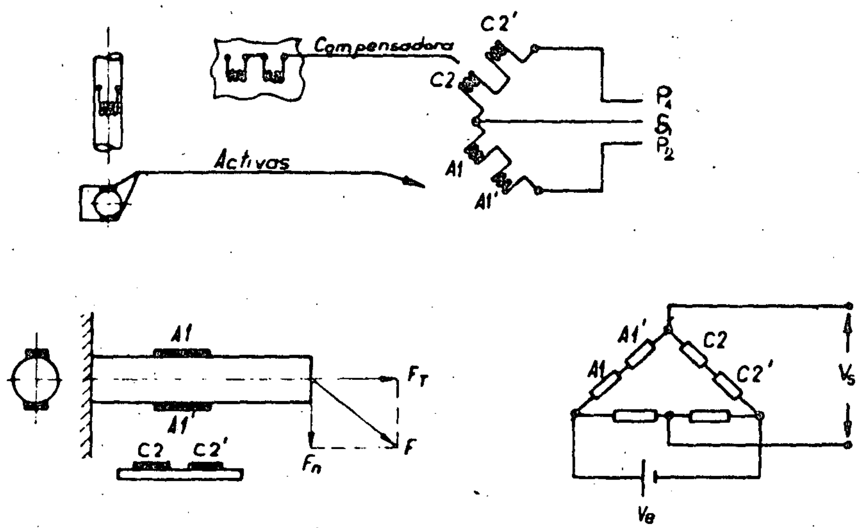

fig 12

$$R_{A1} = R_o + \Delta R_T + \Delta R_N + \Delta R_t$$

$$R_{A1} = R_o + \Delta R_T - \Delta R_N + \Delta R_t$$

$$R_{C2} = R_o + \Delta R_t$$

$$R_{C'2} = R_o + \Delta R_t$$

Si aplicamos la [3]

$$V_s = \frac{Ve}{4}\left(\frac{\Delta R_T}{2R_o} + \frac{\Delta R_N}{2R_o} + \frac{\Delta R_t}{2R_o} + \frac{\Delta R_T}{2R_o} - \frac{\Delta R_N}{2R_o} + \frac{\Delta R_t}{2R_o} - \frac{\Delta R_t}{2R_o} - \frac{\Delta R_t}{2R_o}\right) = \frac{Ve}{4}\frac{\Delta R_T}{R_o} \quad [11]$$

$$V_s = \frac{Ve}{4}\frac{\Delta R_T}{R_o} = \frac{Ve}{4} K \varepsilon_T$$

$$\varepsilon_T = \frac{\Delta l}{l} = \frac{4 V_s}{K\, Ve} \quad \text{------------} \quad [12]$$

Lo anteriormente expuesto es válido siempre que por el eje de aplicación de cargas pase un plano de simetría de la pieza, y exige el montaje de dos bandas por rama del puente, siendo aquí de aplicación el utilizar valores fraccionados (ver 2.2.1.) p.e. 60 ohms, para que la impedancia del circuito sea 120 ohm, siendo esto último preceptivo si no se montan compensadoras y se utiliza montaje de 1/4 de puente.

Flexión simple

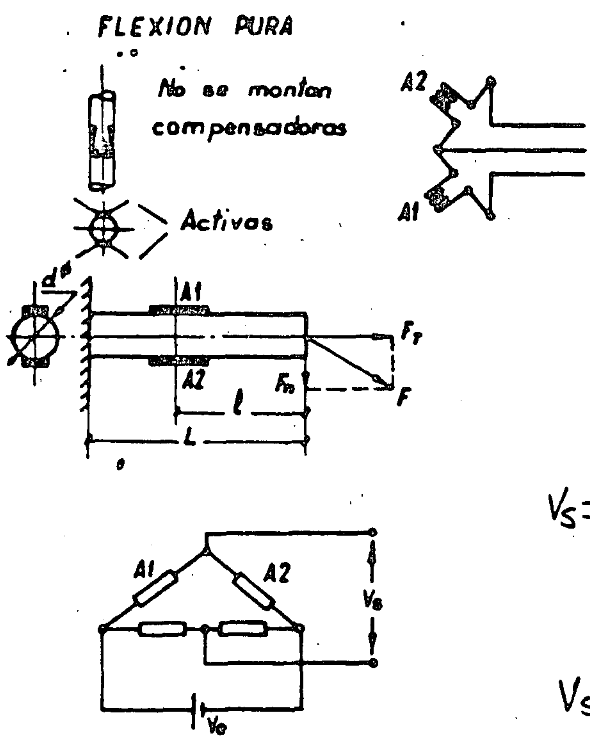

fig 13

Para medir una flexión simple (fig. 13) eliminando otras influencias, no es necesario montar bandas compensadoras, ya que el propio circuito compensa los efectos de variación de temperatura. Se cumple que:

$$R_{A1} = R_o + \Delta R_T + \Delta R_N + \Delta R_t$$

$$R_{A2} = R_o + \Delta R_T - \Delta R_N + \Delta R_t \quad \text{aplicando [3]}$$

$$V_S = \frac{V_e}{4}\left(\frac{\Delta R_T}{R_o} + \frac{\Delta R_N}{R_o} + \frac{\Delta R_t}{R_o} - \frac{\Delta R_T}{R_o} + \frac{\Delta R_N}{R_o} - \frac{\Delta R_t}{R_o}\right) =$$

$$= \frac{V_e}{2}\,\frac{\Delta R_N}{R_o} \qquad [13]$$

$$V_S = \frac{V_e}{2}\,\frac{\Delta R_N}{R_o} = \frac{V_e}{2}\,K\,\varepsilon_N$$

$$\varepsilon_N = \frac{2V_S}{V_e K} = \frac{4F_N l}{\pi E r^3} = \frac{3 l r}{L^3} f \qquad [14]$$

$$N = 0{,}56\,\frac{r}{L^2}\,\frac{E}{\rho}$$

N= frecuencia natural

f= flecha

E= Modulo elasticidad

ρ= densidad

Torsión.-

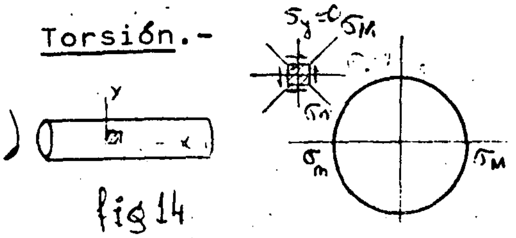

fig 14

Recordemos (fig. 14) que un eje sometido a un par de torsión experimenta sus máximas deformaciones en una dirección que forma 45º con la dirección de sus generatrias, y que dichas deformaciones son iguales y de signo contrario; por tal motivo si situamos las bandas a 45º según la fig. 15a, tenemos que:

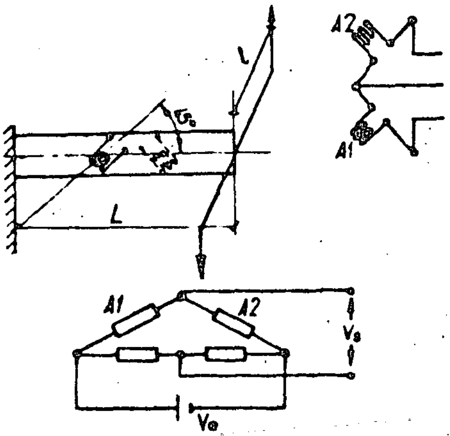

fig 15a

$$R_{A1} = R_0 + \Delta R_c + \Delta R'_T + \Delta R_t$$

$$R_{A2} = R_0 - \Delta R_c + \Delta R'_T + \Delta R_t$$

$$V_s = \frac{V_e}{4}\left(\frac{\Delta R_c}{R_0} + \frac{\Delta R_c}{R_0} + \frac{\Delta R'_T}{R_0} + \frac{\Delta R_t}{R_0} + \frac{\Delta R_c}{R_0} - \frac{\Delta R'_T}{R_0} - \frac{\Delta R_t}{R_0}\right) = \frac{V_e}{2}\,\frac{\Delta R_c}{R_0} \qquad [15]$$

Podemos considerar que: $\frac{\Delta R_c}{R_0} = K\frac{\Delta d}{d}$; $V_s = \frac{V_e}{2} K \frac{\tau}{2G}$ [16]

siendo τ el esfuerzo cortante y $G = \frac{E}{2(1+\mu)}$

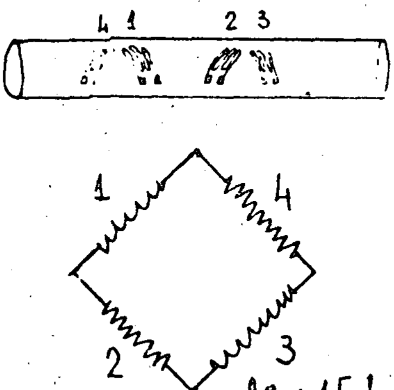

fig 15 b

En el montaje de 1/2 se eliminan los efectos de tracción y compresión - pero no la flexión, se puede demostrar que en la configuración de 1/1 de puente, el circuito de medida solo es sensible a esfuerzos producidos - por torsión (fig. 15b).

3.2. Circuitos de calibración y equilibrado

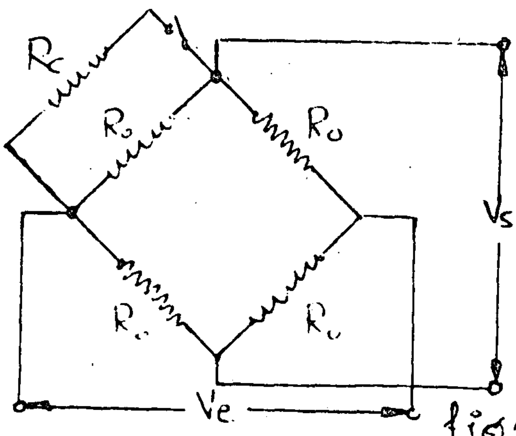

fig 16

La técnica de calibración de un puente de Wheatstone para extensometría, consiste en producir en una rama del puente, por shuntado de una resistencia, un desequilibrio igual al que se produciría al someter o determinado solicitaciones el elemento de ensayo (fig. 16).

El efecto de la resistencia de calibración R_c, es equivalente a una compresión sobre la rama que actua. Supongamos que deseamos calcular el valor de R_c para que tengamos un efecto equivalente a $500\mu\varepsilon$ en un circuito de bandas de R_o = 120 ohm, K = 2, excitado con V_e = 2 V; tenemos que:

$$\frac{\Delta R}{R} = \frac{\frac{R_c R_o}{R_c+R_o} - R_o}{R_o} = - \frac{-R_o}{R_c+R_o} \quad [17]$$

$$\varepsilon = \frac{R_o}{R_c+R_o} \, \frac{1}{K} \quad [18]$$

$$R_c = - \frac{R_o(1+\varepsilon K)}{\varepsilon K} = - 120.000 \text{ ohm} \quad [19]$$

El signo (-) indica que se trata de compresión. En la fig. 16 se supone que un solo brazo del puente es activo, en general y teniendo en cuenta el nº de brazos activos del circuito, encontramos la expresión general

$$R_c = - \frac{R_o}{N \varepsilon K} \quad [20]$$

en la que:

- Rc= Resistencia de calibración
- Ro= Valor nominal de la resistencia de una rama del puente.
- K= Factor longitudinal de sensibilidad de la banda.
- ε= Alargamiento unitario equivalente que produce Rc.
- N= Nº de brazos activos del circuito del puente.

  (El termino εK en el numerador se desprecia por ser muy pequeño).

Si el instrumento de lectura da indicaciones directas en microdeformaciones, lo explicado es suficiente, pero ocurre, sobre todo en medidas dinámicas, que tendremos que establecer una relación entre deformaciones y d.d.p. a la salida de los amplificadores que ele- van de nivel las débiles señales del puente de medida; siendo regla - práctica, buscar escalas enteras. Ejemplo.

En la fig. 17 se representa el circuito para medida de tracción simple en una barra circular de 500 mm^2 de sección, se desea que una carga 10 KN dé una indicación de 100 mV en el instrumento de lectura (1 da N/mV).

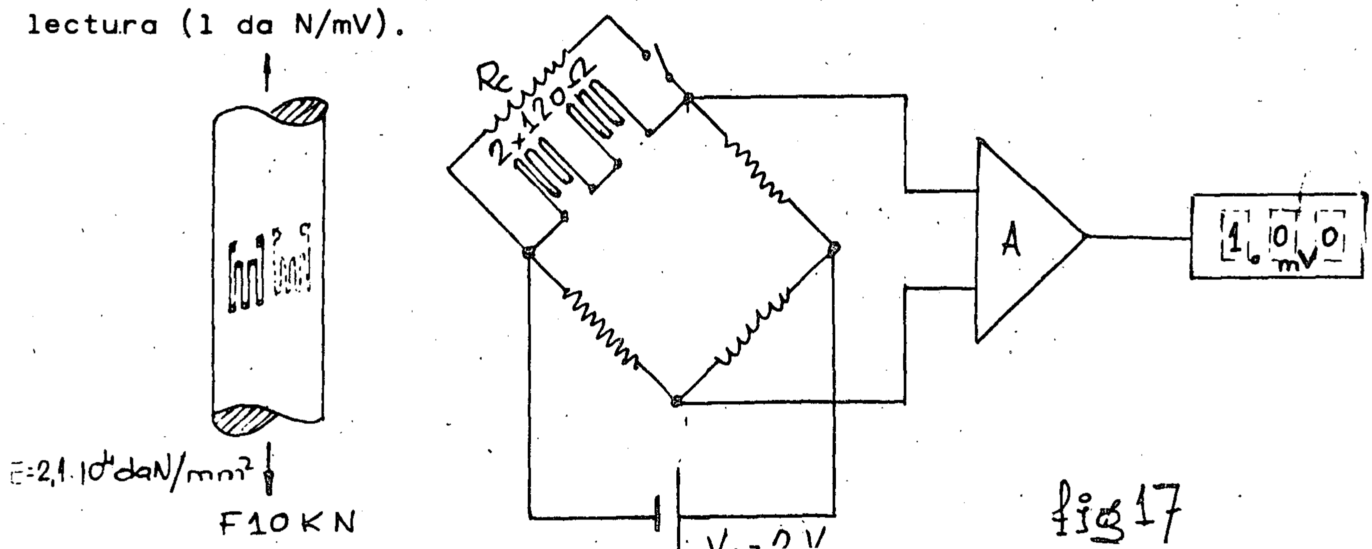

fig 17

$$\varepsilon = \frac{\sigma}{E} = \frac{\frac{F}{S}}{E} = \frac{10 \cdot 10^2 \cdot 10^6}{500 \cdot 2{,}1 \cdot 10^4} = 476 \,\mu S$$

$$V_s = \frac{V_e}{4}\,\varepsilon K = \frac{1}{2}\,476 = 238 \,\mu V$$

$$G = \frac{100\,(mV)}{0{,}238} = 420 \quad (\text{Ganancia amplificador})$$

$$R_c = \frac{2 \cdot 120}{476 \cdot 10^{-6} \cdot 2} = \underline{252\,100 \text{ ohm}}$$

Luego si colocando una Rc= 252100 ohm, ajustamos la ganancia del amplificador para leer -100 mV, tendremos el circuito preparado para leer las fuerzas F con una escala de 1 da N/mV.

Observese que se ha empleado circuito de 1/4 de puente con 2 bandas de 120 ohm en serie para eliminar efectos de flexión y torsión.

La calibración de un circuito extensométrico por shunt de una resistencia es casi universalmente aceptada, no obstante presenta el inconveniente de insertar la señal de referencia en registros dinámicos, ya que dicha señal se superpone a la componente dinámica y la suma puede salirse del rango de medida por saturación de instrumento para paliar ésto, se puede utilizar una resistencia en serie tal y como se indica en la fig. 18, asi abriendo el interruptor A dejamos sin excitación el circuito y nos marcará el cero (correspondiente a carga nula) y si a continuación cerramos B, obtendremos una señal de referencia independiente del estado de carga del circuito.

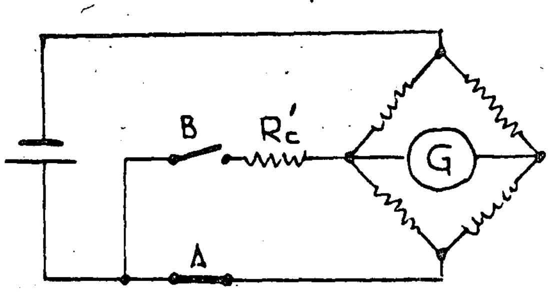

fig 18

Se demuestra que para producir la misma señal la relación entre los valores de la resistencias shunt y serie son R'c=2Rc.

Hasta aquí hemos supuesto siempre que el puente de Wheatstone estaba completamente equilibrado para cargas nulas en el circuito de medida, pero debido a las pequeñas variaciones de resistencia que se originan al montaje, (por soldaduras, variaciones de la propia resistencia de la banda al ser pegada, etc,) la señal de salida V_s tendrá un pequeño valor que conviene anular para hacer lecturas directas.

El desequilibrio inicial del puente en medidas estáticas, con instrumentos que dan lectura directa en microdeformaciones, obliga a hacer una lectura inicial estando sin carga la pieza de ensayo que será restada de las lecturas posteriores bajo carga. En el caso de medidas dinámicas, partir con un desequilibrio, equivale a introducir una componente de contínua constante.

Varios con los procedimientos que pueden utilizarse para corregir un desequilibrio inicial pero el más universal, consiste en colocar un potenciómetro de alto valor óhmico en la diagonal de alimentación del puente con el contacto móvil unido a través de una resistencia R_A al vértice intermedio tal y como se indica en la fig. 19.

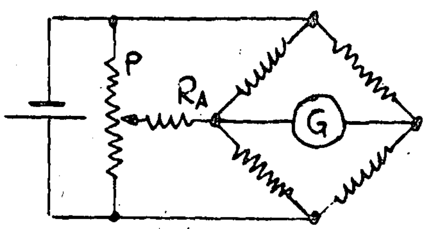

fig 19

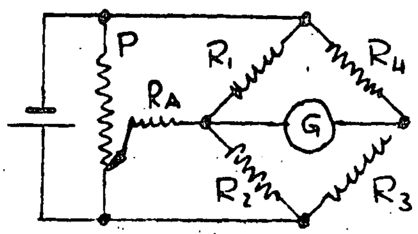

fig 20

La resistencia R_A limita el tanto por ciento de desequilibrio capáz de corregir y el potenciómetro P dá el poder de resolución de dicha ajuste. En efecto, supongamos que en el circuito de la fig. 20 queremos calcular R_A para poder corregir desequilibrios de un 2% o lo que es lo mismo suponer que:

$R_2 = R_3 = R_4 = 120$ ohm

$R_1 = 117{,}6$ ohm

La resistencia total de la rama 2 tiene que ser igual a la de la rama 1 por tanto:

$$\frac{1}{R_1} = \frac{1}{R_2} + \frac{1}{R_A} \longrightarrow \frac{1}{117{,}6} = \frac{1}{120} + \frac{1}{R_A}$$

$$R_A = \frac{R_1 . R_2}{R_2 - R_1} = \underline{5880 \text{ ohm}}$$

Para el cálculo hemos supuesto que el cursor del potenciómetro está en un extreno, por lo que si P es de valor elevado, al estar en paralelo con R, no le influye; para desequilibrios inferiores al 2% desplazando el cursor se consigue la posición en la que por G no circula corriente.

Otros procedimientos pueden consistir en añadir resistencias en serie en las ramas hasta conseguir el equilibrio, pero si bién este método es aconsejable para la construcción de captadores, no es práctico en medidas extensométricas salvo casos muy especiales.

En instrumentación para medidas dinámicas, los desequilibrios de los circuitos de medida se compensan introduciendo una contratensión en la entrada de amplificación, con lo que se consigue no desensibilizar en absoluto el circuito e incluso producir "falsos ceros" cuando las condiciones de la medida lo aconsejen (fig. 21).

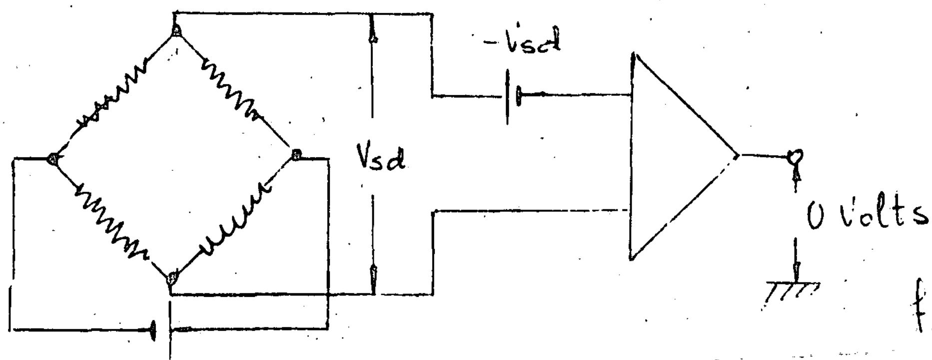

fig 21

Sea cual sea el procedimiento con el que corrijamos el desequilibrio, los componentes utilizados serán de precisión y estabilidad idéntica a la exigida al circuito de medida. El potenciómetro P será de 10 vueltas y provisto de duodial, que permitirá reestablecer las condiciones iniciales de equilibrado de manera fácil, aún cuando las condiciones originales hayan variado.

3.3. Captadores extensométricos

El conocimiento de las técnicas extensométricas abre la posibilidad de construir captadores que efectuen la transducción de cierta energía mecánica en eléctrica, pero no obstante hay que advertir que los problemas que en éste cometido se presentan, son tan complejos, que solo verdaderos especialistas serán capaces de conseguir resultados aceptables, por lo que todo lo expuesto a continuación, debe considerarse solo a título informativo, para mejor comprender el funcionamiento de estos instrumentos indispensables en un laboratorio de ensayos dinámicos.

Un captador estará formado por un dispositivo mecánico que sea sensible de forma mayoritaria a determinados parámetros fisicos (fuerza, presión, aceleración, etc) y prácticamente insensible al resto de fenómenos que incidan simultáneamente sobre él. Si sobre el elemento sensible del captador montamos bandas extensométricas, podremos medir las deformaciones de éstas relacionándolas con el parámetro que las originó, como es lógico, podremos conseguir la independencia del captador a solicitaciones no deseadas valiéndonos del adecuado diseño mecánico y de la disposición de las bandas.

La elección de los materiales que constituyen la parte mecánica del captador es de vital importancia y se tendrá muy en cuenta que el módulo de elasticidad E, sea totalmente constante en el margen de utilización y jamás sobrepasar la zona lineal de trabajo, exenta en lo posible, de fenómenos de histeresis y fluencia, siendo normativo sobrepasar en las cargas 1/10 del límite elástico. El coeficiente de dilatación tiene menos importancia una vez que las dilataciones serán homogeneas y se utilizarán bandas autocompensadas.

A título de ejemplo en la fig. 22 se ofrecen esquematicamente algunos montajes para medidas de los parámetros que se indican. Nunca habrá limite en diseñar cualquier disposición mecánica que añada mejoras para determinados fines.

Hasta aquí nos referimos a bandas extensométricas pegadas (Bonded Strain-gages) pero en captadores se utiliza generalmente otro tipo de extensímetro en el cual, el elemento sensible es un hilo sin soporte y apoyado sobre unos zafiros (unbonded strain-gages), que si bién cumple todos los principios hasta ahora expuestos, es muy distinto. En efecto, consideremos la fig. 23 en la que las bandas extensométricas tal y como las hemos concebido hasta ahora son sustituidas por hilos conductores A, B, C y D sometidos a una tensión previa; si la carcasa interna se mueve por cualquier solicitación mecánica (ej. aceleración) a derecha o izquierda respecto a la carcasa externa, los hilos A y D y los B y C sufren deformaciones de signos contrarios respectivamente. La conexión eléctrica del circuito para constituir el puente de Wheatstone se indica en la fig. 24.

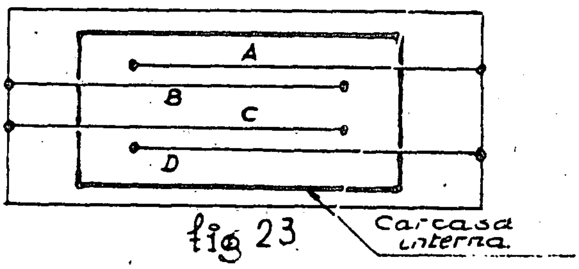

fig 23

fig24
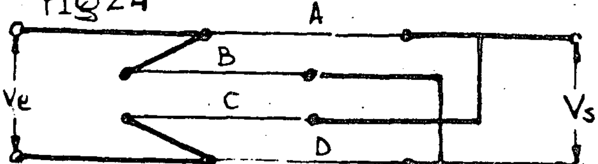

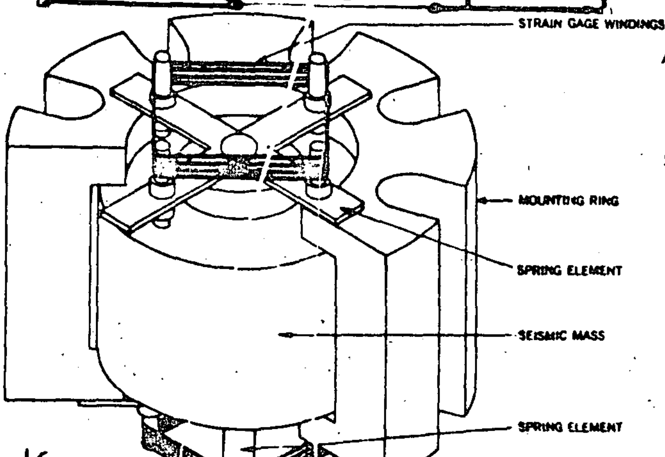

fig25

A título de ejemplo la fig. 25 indica la disposición adoptada por B&H en sus captadores de aceleración.

Desplazamiento

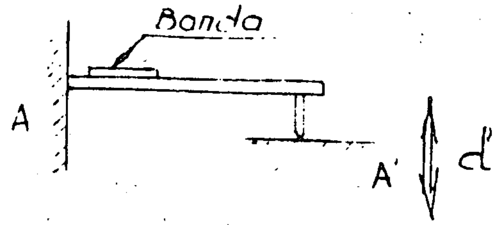

Los desplazamientos relativos entre A (fijo) y A' (móvil) producen una deformación en la lámina pro flexión, proporcional al desplazamiento d.

Fuerzas. Pesos

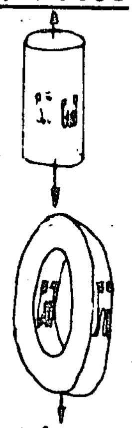

Una barra cilíndrica en tracción y/o compresión (evitar pandeo).

Anillo dinamométrico en tracción.

Aceleración-vibración

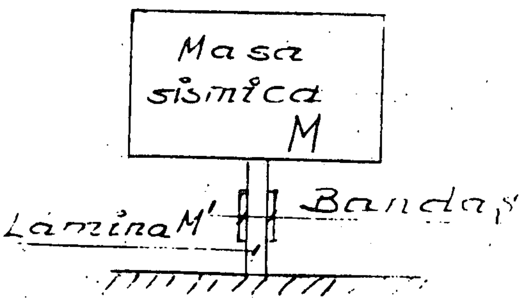

La masa sismica M es sensible a las fuerzas de aceleración y habrá proporcionalidad con la deformación que sufra a flexión la lámina M'. Sí la frecuencia propia de la lámina es superior a la del movimiento la respuesta será a la aceleración y si inferior a la velocidad del desplazamiento de M.

Presión

La membrana M se deforma si en la camara C hay variaciones de presión.

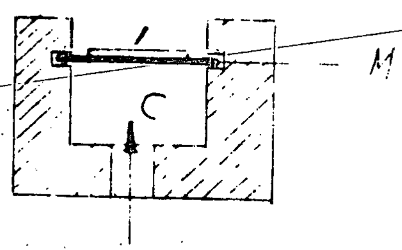

Lámina cilíndrica en flexión

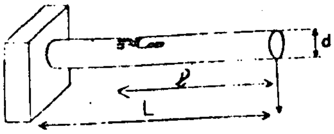

$$\varepsilon_1 = \frac{4\,F\,l}{\pi\,E\,r^3} = \frac{3\,l\,r}{L^3}\,f$$

$$\varepsilon_2 = \frac{-4\,\mu\,F\,l}{\pi\,E\,r^3} = \frac{-3\,\mu\,l\,r}{L^3}\,f$$

$$f = \frac{4\,F\,L^3}{3\,\pi\,E r^4}$$

$$N = 0{,}56\,\frac{r}{L^2}\,\frac{E}{\rho}$$

F fuerza aplicada
d = 2.r. diámetro
l brazo fuerza-banda
L brazo fuerza-encastramiento
N primera frecuencia propia
f flecha (desplazamiento de F)
ε_1 deformación longitudinal
ε_2 deformación transversal

Anillo dinamométrico

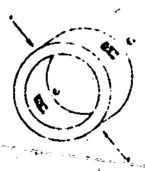

$$\varepsilon_e = \frac{3\,F\,R}{E\,a\,e^2}\left(1 - \frac{2}{\pi}\right)$$

$$\varepsilon_i = \frac{-3\,F R}{E\,a\,c^2}\left(1 - \frac{2}{\pi}\right)$$

$$f = 1{,}79\,\frac{F\,R^3}{E\,a\,e^3}$$

F fuerza aplicada
e espesor
a anchura
R radio medio
f flecha total
ε_e deformación longitudinal exterior
ε_i deformación longitudinal interior

Arbol en torsión

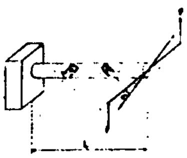

$$\varepsilon_1 = -\,\varepsilon_2 = \frac{M}{\pi\,G\,R^3} = \frac{R}{2\,L}\,\alpha$$

$$\alpha = \frac{2\,M\,L}{\pi\,G\,R^4}$$

$$\text{avec } G = \frac{E}{2\,(1+\mu)}$$

M=F l momento aplicado
L longitud total del arbol
α ángulo de giro en radiones
La distancia de las bandas no afecta
ε_1 deformación de una de las bandas
ε_2 deformación de la otra banda

FORMULAS PARA EL CALCULO DE TRANSDUCTORES

Lámina en Tracción

$$\varepsilon_1 = \frac{F}{E\,a\,e}$$

$$\varepsilon_2 = \frac{-\mu F}{E\,a\,e}$$

F fuerza aplicada
a anchura
e espesor
ε_1 deformación longitudinal
ε_2 deformación transversal

Toro circular en Tracción%compresión

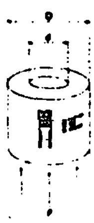

$$\varepsilon_1 = \frac{4F}{\pi E\,(D^2 - d^2)}$$

$$\varepsilon_2 = \frac{-4\mu F}{\pi E\,(D^2 - d^2)}$$

F fuerza repartida
D diámetro exterior
d diámetro interior
ε_1 deformación longitudinal
ε_2 deformación transversal

Lámina en flexión

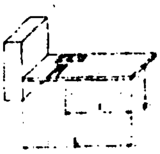

$$\varepsilon_1 = \frac{6FI}{E\,a\,e^2} = \frac{3eI}{2L^3}f$$

$$\varepsilon_2 = \frac{-6\mu FI}{E\,a\,e^2} = \frac{-3\mu eI}{2L^3}f$$

$$f = \frac{FL^3}{3EI} = \frac{4FL^3}{E\,a\,e^3}$$

$$N = 0{,}55\,\frac{1}{L^2}\quad\frac{EI}{\rho\cdot S} = 0{,}16\,\frac{e}{L^2}\quad\frac{E}{\rho}$$

F fuerza aplicada
a anchura
e espesor
I brazo fuerza-banda
L brazo fuerza-empotramiento
N primera frecuencia propia
f flecha
ε_1 deformación longitudinal
ε_2 deformación transversal

Lámina triangular en isoflexión

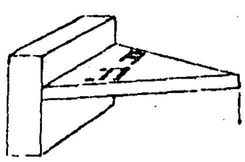

$$\varepsilon_1 = \frac{6FL}{E\,b\,e^2} = \frac{e}{L^2}f$$

$$\varepsilon_2 = \frac{-6\mu FL}{E\,b\,e^2} = \frac{-\mu e}{L^2}f$$

$$f = \frac{6FL^3}{E\,b\,e^3}$$

F fuerza aplicada (en el vértice)
b anchura base
L brazo fuerza-encastramiento (altura)
f flecha
La distancia de las bandas no afecta
ε_1 deformación longitudinal
ε_2 deformación transversal

Temperaturas extremas de compensación.- Temperaturas inferior y superior, que no deben sobrepasarse, para que, empleando la compensación, las características del captador se mantengan dentro de los límites definidos para los mismos.

Temperaturas extremas de empleo.- Temperaturas inferior y superior que, en caso de sobrepasarse, determinan la pérdida definitiva de las características del captador.

Impedancia.- Sensibilidad a fenómenos para los cuales el captador no ha sido realizado, p.e.: Sensibilidad de un acelerómetro para aceleraciones perpendiculares a su eje primario (Cross Axis Sensitivity).

Desplazamiento (Deflection).- Distancia entre las dos posiciones de un punto después de cargado, comprendido dentro de la que existe a carga nula y nominal.

Ambiente (Stamdard Test Conditions).- Conjunto de aquellos valores característicos del medio ambiente que pueden influenciar las propiedades de un captador y que deben ser definidas en la calibración.

Frecuencia natural (Natural frequency).- Frecuencia de oscilaciones libres en ausencia de cargas.

Sobrecargas eléctricas admisibles.- Potencias límites para el circuito de alimentación y que no deben sobrepasarse, bajo el riesgo:
a) De pérdida de características de captador.
b) Destrucción total del captador.

Eje primario (Primory Axis).- Eje según el cual las cargas deben ser aplicadas.

3.5. Determinación de las tensiones residuales

Introducción

Con los extensímetros ohmicos lo único que puede evaluarse son cambios de deformación. Por consiguiente, si se desea determinar el estado de deformación existente en alguna pieza es necesario poder cambiar esa deformación una cantidad medible después de que se haya pegado la banda. A continuación, interpretar adecuadamen te el cambio medido.

Las tensiones residuales determinadas por relajación son un ejemplo de este método. En él, una banda se fija a la pieza y se mide su resistencia eléctrica. Luego se perfora o corta un trozo de la pieza teniendo cuidado de que no se produzca calentamiento; y se vuelve a medir la resistencia de la banda.

Si se produce una variación correspondiente a una tracción lo que habría es una compresión y recíprocamente.

<u>Teoría. Para el caso de relación por taladro (fig.29)</u>

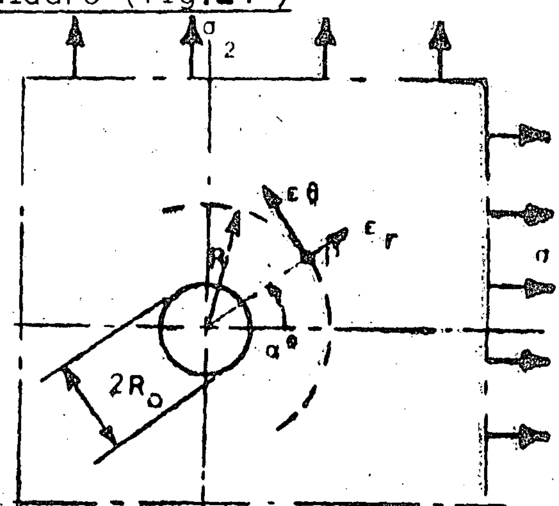

Si se hace un taladro de pequeño diámetro (2Ro) en una región con tensiones residuales, se produce una relajación de deformaciones. Las deformaciones suprimidas en el punto P a una distancia R del centro del taladro cuando solo existe la tensión σ_1 son:

$$\varepsilon_r = -\sigma_1 \frac{(1+\mu)}{2E}\left(\frac{1}{r^2} - \frac{3}{r^4}\cos 2\alpha + \frac{4}{1+\mu}\frac{1}{r^2}\cos 2\alpha\right) \rightarrow r = \frac{R}{R_o}$$

$$\varepsilon_\theta = -\sigma_1 \frac{1+\mu}{2E}\left(-\frac{1}{r^2} + \frac{3}{r^4}\cos 2\alpha - \frac{4\mu}{1+\mu}\frac{1}{r^2}\cos 2\alpha\right)$$

$$\gamma_{r\theta} = \frac{\sigma_1}{2G}\left(\frac{3}{r^4} - \frac{2}{r^2}\right) \operatorname{sen} 2\alpha$$

$$\varepsilon_r - \varepsilon_\theta = -\sigma_1 \frac{1+\mu}{2E}\left(\frac{2}{r^2} - \frac{6}{r^4}\cos 2\alpha + \frac{4}{r^2}\cos 2\alpha\right)$$

que son funciones sinusoidales de la orientación. Por ejemplo la deformación radial suprimida puede escribirse

$$\varepsilon_r = (A + B\cos 2\alpha)\sigma_1$$

Y si existen simultáneamente σ_1 y σ_2 será

$$\varepsilon_r = (A + B\cos 2\alpha)\sigma_1 + [A + B\cos 2(\alpha + 90^\circ)]\sigma_2.$$

Los coeficientes A y B pueden calcularse fácilmente a partir de las constantes μ y E E del material en cuestión y para cualquier distancia R.

También se pueden determinar experimentalmente los coeficientes A y B haciendo ensayos sin tensiones residuales sino con reales σ_1 y σ_2 conocidos, por ejemplo $\sigma_M = \sigma_1$ y $\sigma_m = 0$

Caso de la roseta (fig. 30)

Con tres bandas pegadas a una distancia R y en las direcciones a b y c a 45º pueden medirse tres deformaciones $\varepsilon_a, \varepsilon_b$ y ε_c que llevadas a la ecuación anterior (2) nos permiten despejar σ_1; σ_2 y $tg 2\beta$

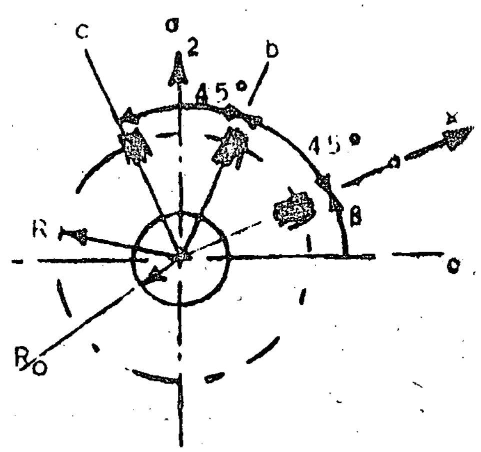

fig.30

$$\sigma_1 = \frac{(A+B\cos 2\beta)\varepsilon_a - (A-B\cos 2\beta)\varepsilon_c}{4AB\cos 2\beta}$$

$$\sigma_2 = \frac{(A+B\cos 2\beta)\varepsilon_c - (A-B\cos 2\beta)\varepsilon_a}{4AB\cos 2\beta}$$

$$tg\, 2\beta = \frac{\varepsilon_a - 2\varepsilon_b + \varepsilon_c}{\varepsilon_a - \varepsilon_c}$$

Estas expresiones son buenas si las direcciones a y c corresponden aproximadamente con las principales. En casp de que no sea así y las a y b dén las deformaciones más distintas son más satisfactorias las ecuaciones siguientes:

$$\sigma_1 = \frac{(A+B\,\mathrm{sen}\, 2\beta)\varepsilon_a - (A-B\cos 2\beta)\varepsilon_b}{2AB(\mathrm{sen}\, 2\beta + \cos 2\beta)}$$

$$\sigma_2 = \frac{(A+B\cos 2\beta)\varepsilon_b - (A-B\,\mathrm{sen}\, 2\beta)\varepsilon_a}{2AB(\mathrm{sen}\, 2\beta + \cos 2\beta)}$$

Técnicas experimentales

Como en todo lo experimental, las herramientas apropiadas, la instrumentación y la cuidadosa aplicación de los procedimientos son esenciales para obtener resultados ciertos.

Taladrado

Con brocas cilíndricas, no cónicas. La parte cortante sólo en el frente. El diámetro del cilindro se reduce a una distancia de O,16 Ø a un diámetro menor en un 12% del de la punta para dejar sitio entre la broca y el agujero para la salida de virutas.

Bandas especiales

Rosetas de bandas especialmente bién espaciadas en el círculo y con el centro de este bién definido. (fig. 31)

Puente de medida

Puente portable de baterías con potenciómetros de equilibrado.

Centrado del taladro

Soporte centrador de un microscopio sustituible por una taladradora. (fig. 32)

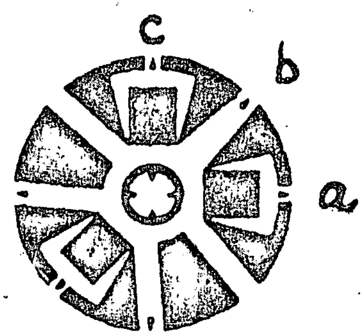

fig31

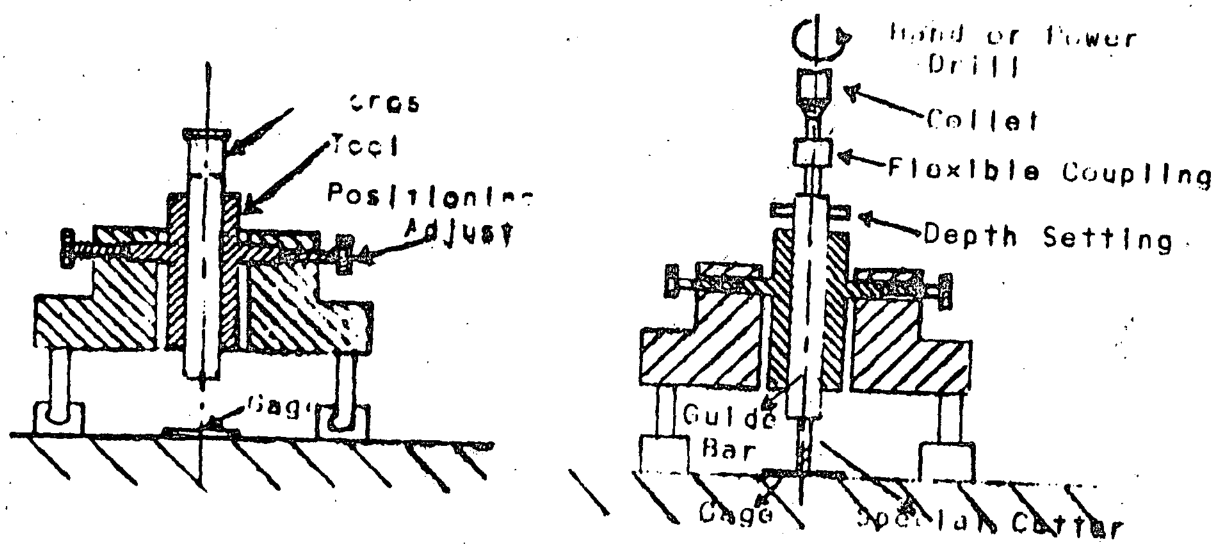

fig32

TEMA IV

4.1. Instrumentos para medidas estáticas.-

Aceptando como universal el circuito de puente de Wheatstone en medidas extensométricas, dos son los procedimientos que se pueden emplear para medir el desequilibrio que en una diagonal se produce cuando las bandas se deforman.

El "Método de oposición" introduce en la diagonal del puente (fig. 1) una tensión opuesta a la de desequilibrio, siendo el instrumento G el que controla la posición de equilibrio. Si el potenciómetro P está graduado en la escala deseada (microdeformaciones) e incluso va dotado de un indicador numérico y dispositivos de preequilibrado, podremos hacer las lecturas directas. Se comprende que para no introducir error las tensiones

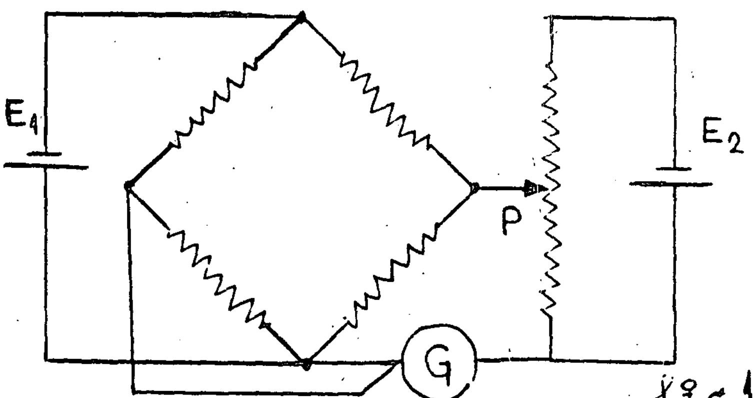

fig 1

E_1 y E_2 deben estar estabilizadas en alto grado o bién que sus variaciones sean totalmente proporcionales, pero según el esquema de la fig. 1, eso es muy dificil de conseguir, de ahí, que se utilice la disposición indicada en la fig. 2 en las que la solución si bién es satisfactoria en un aspecto, crea problemas en otros, en efecto, si alimentamos los puentes en corriente contínua, y dada su polaridad, los instrumentos nos indicarán las deformaciones producidas por esfuerzos de tracción o compresión según las desviaciones de la aguja sea en uno u otro sentido respectivamente, pero al ser excitados en corriente alterna es necesario introducir un circuito llamado detector de fase que discrimine cuando las deformaciones son de tracción o de compresión en efecto: (fig. 3)

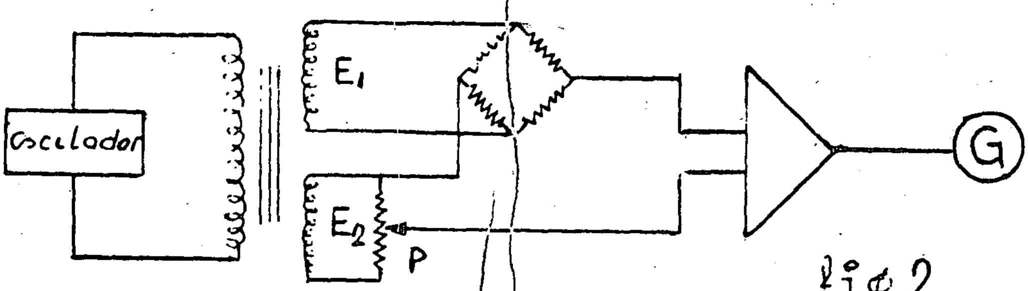

fig 2

si el puente está en equilibrio:

$$v_B - v_A = v_S = 0$$

si hay tracción en una rama:

$$v_B - v_A = v_S \text{ (Tracción)}$$

si hay compresión en una rama

$$v_B - v_A = v'_S \text{ (compresión)}$$

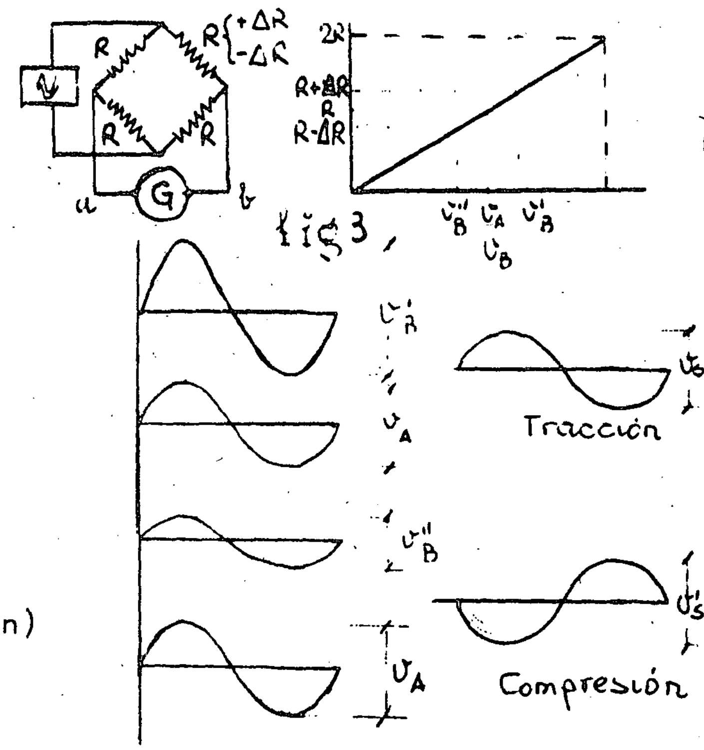

fig 3

Por otra parte, para conseguir la oposición entre las tensiones E_1 y E_2 es necesario que estén defasadas 180º y para lograrlo hay que introducir ajustes capacitivos, lo cual representa otro inconveniente; por tal motivo la casa Vishay-Micromesures, en su puente P-350, emplea como portadora una onda cuadrada, en vez de senoidal, y la oposición de fase se consigue de forma automática sin necesidad de ajustes capacitivos, ventaja que le confiere una gran aceptación por extensometristas experimentados.

En el "Método de cero" (fig. 4) el equilibrio del puente

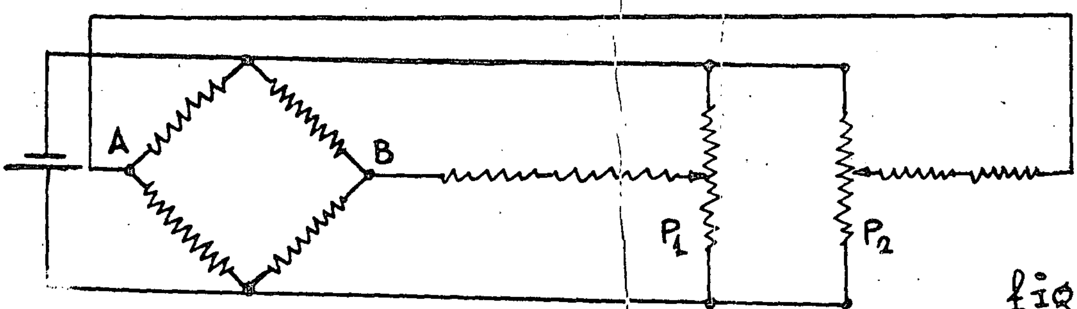

fig 4

se consigue introduciendo resistencias en las ramas del puente hasta conseguir el equilibrio inicial; los potenciómetros P_1 y P_2 se desplazan conjuntamente en sentido inverso hasta anular tensión de desequilibrio entre A y B. graduando adecuadamente los mandos de P_1 y P_2 podremos hacer lecturas directas. El mando de P_1 y P_2 puede hacerse a través de un servomecanísmo y constituir así una unidad de lectura automática.

Otro procedimiento, que actualmente está siendo cada vez mas empleado, consiste en leer directamente la señal de salida del - puente por medio de un voltímetro digital de precisión y exactitud ele vada. Este procedimiento exige a su vez que la fuente de excitación - sea muy estable (fig. 5)

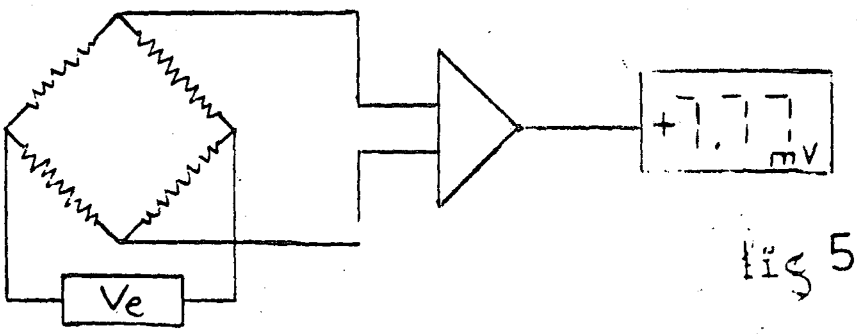

fig 5

4.1.1. Cajas de conmutación manual

Normalmente, las medidas extensométricas, habrá que efectuarlas en varios puntos, si estos son muy numerosos (se estima que superiores a 25) una unidad automática será conveniente, pero para una cantidad inferior se utilizan unidades de conmutación manual con resultados prácticos satisfactorios; ya que el mayor tiempo de lectura que será necesario emplear justifica su uso por razones meramente económicas, pues lógicamente los equipos manuales son de bajo precio.

El problema que se plantea es conmutar diversos circuitos de medida a un solo instrumento de lectura de lo que se deduce que el conmutador será de una calidad que garantice un mínimo de error en la medida (Ver 3.1.1.). Por otra parte la unidad de conmutación debe ofrecer la posibilidad de un equilibrado previo de los circuitos de medida, para que cuando ensayemos bajo carga la pieza en estudio, las lecturas puedan ser directas.

En la fig. 6 se indica la disposición adoptada por Vishay-Micromesures en su unidad S-B1 en la que se consigue una adaptación - completa de los circuitos de 1/1; 1/2 ó 1/4 de puente, asociada al instrumento P-350 o cualquier otro similar.

El potenciómetro P de equilibrado, será de precisión y de 10 vueltas para conseguir una buena resolución, si a su vez va provisto de un mando con contador numérico de vueltas (Duodial) podremos reestablecer las condiciones previas del equilibrado, aún cuando se - hubiese utilizado en otros circuitos distintos la unidad de conmutación en el curso de experiencias diversas.

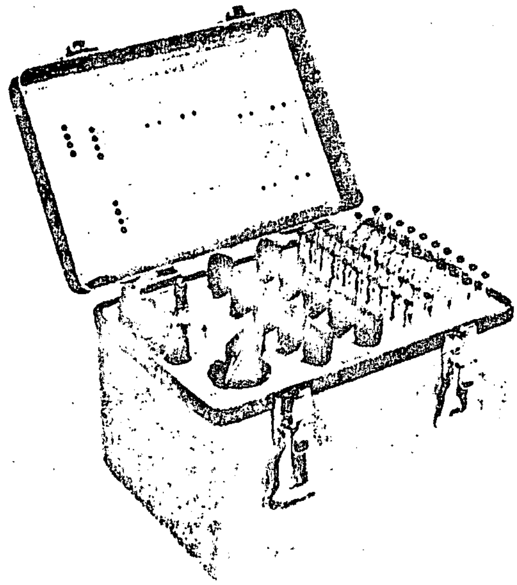

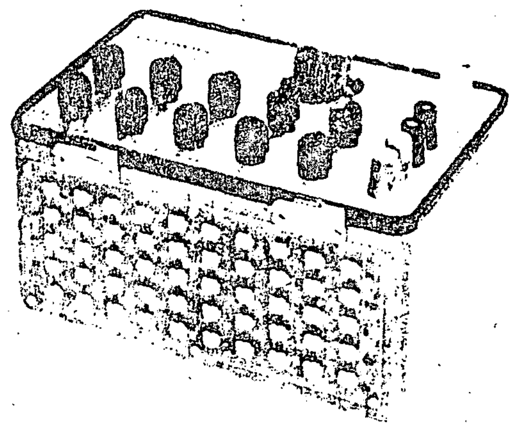

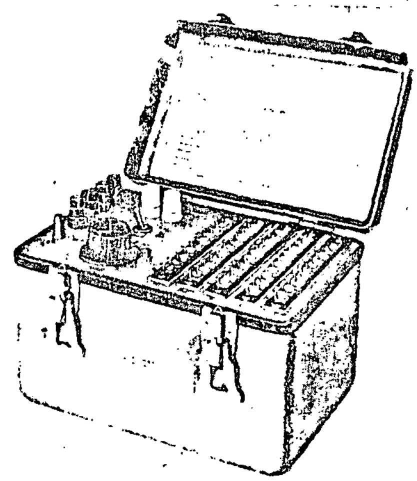

4.1.2. Instrumentos de calibración

Los instrumentos de lectura son contrastados por el fabricante en sus factorias, pero el uso y la degeneración de sus componentes con el tiempo, hace necesario una contrastación periódica de los mismos, para ello pueden seguirse varios procedimientos uno de los cuales se explicó en el apartado 3.2. y consistía en colocar resistencias en paralelo en una rama del puente, que produjesen un desequilibrio equivalente al que experimentase el mismo circuito sometido a solicitaciones concretas. Este método si bién es recomendado para calibrar los circuitos de medida no es idóneo para contrastar el instrumento de lectura, ya que nunca sabremos si al colocar la resistencia en paralelo observamos alguna anomalía, si el error es del circuito o del instrumento, por tal motivo se recomiendan dos procedimientos: 1º Simulador de deformaciones y 2º Patrón primario de deformaciones.

Simulador de deformaciones. Consiste en una caja de decadas de alta precisión y estabilidad que comprende 5 décadas que pueden obtener valores en pasos de 0,01; 0,1; 1; 10 y 100 ohm. con precisión total de ± 0,02% sobre cualquier lectura. Su estabilidad es superior a ± 50 ppm por año. A estas características responde la unidad

VE-40 de Vishay-Ellis.

Para calibrar un instrumento de lectura en extensometría, suponfremos que el simulador de deformaciones constituye la banda propiamente dicha y para ello ajustaremos un valor igual al de extensímetro p.e. 120. Efectuaremos posteriormente su conexión al instrumento en montaje de 1/4 de puente en la configuración de 3 hilos (fig. 7).

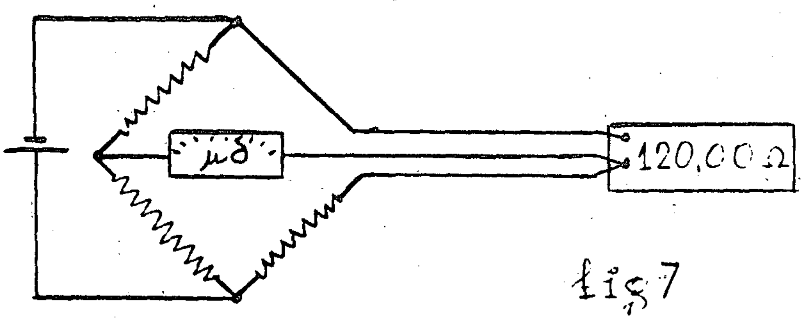

fig 7

Recordando que:

AR= K.R.

tenemos que para

$\varepsilon = 1500\,\mu\delta$ $\Delta R = 0{,}36$ ohm

$\varepsilon = 2000\,\mu\delta$ $\Delta R = 0{,}48$ "

$\varepsilon = 2500\,\mu\delta$ $\Delta R = 0{,}60$ "

Si K=2 y R= 120 ohm.

Por tanto si el instrumento de lectura está bien tarado, leemos los valores indicados de microdeformaciones, si en el simulador vamos paulatinamente fijando los valores de 120,36; 120,48 ohm etc. Tener presente que así simulamos tracciones, si disminuimos el valor 120 ohm, en la misma proporción leeríamos compresiones.

Patrón de deformaciones

Una viga de sección rectangular b.c. toma forma de arco de anillo circular, al ser sometida a flexión pura. El valor absoluto de la deformación longitudinal que sufren sus caras horizontales es $\varepsilon = \frac{6Pa}{b\,c^2 E}$ La flecha del arco de circunferencia así producido es

$$f = \frac{Pa\,b^2}{\frac{2}{3}\,b\,c^3 E}$$

La relación entre flecha y deformación es

$$\varepsilon = \frac{4c}{b^2} f$$

lo que nos dice que podemos conocer la deformación en función de la flecha y de constantes geométricas, independientemente de las cargas y del módulo de elasticidad del material.

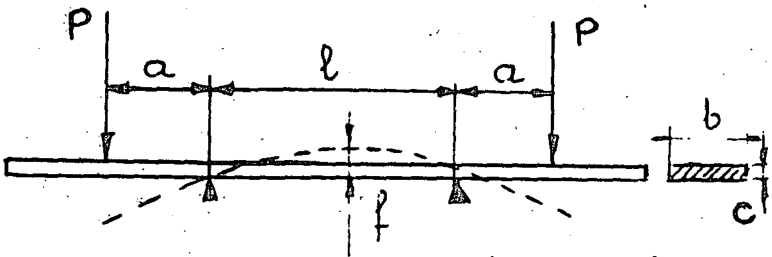

fig 8

El Patrón de Deformaciones permite fijar la flecha con lo que se puede calcular la deformación ε correspondiente. Si además se mide la deformación ε por medio de extensómetros óhmicos, se puede calcular un coeficiente de corrección para este método o comprobar sistemas extensométricos.

4.2. Sistemas automáticos de adquisición de datos.

Estos sistemas son necesarios cuando por el número de puntos de registro, el tiempo requerido para un barrido manual fuese tal que las condiciones del ensayo variasen dentro de él, y por consiguiente no fuesen datos adquiridos en igualdad condiciones los de una misma lectura; o bién cuando la magnitud y frecuencia de medidas múltiples haga tedioso y propenso a errores de anotación las lecturas manuales.

El avance tecnológico de la electrónica ha facilitado el diseño de equipos muy sofisticados, y a veces, no justifican las pequeñas ventajas que introducen el elevado precio que adquieren. Por tal motivo juzgamos oportuno describir el conjunto para aue el usuario futuro, tenga elementos de juicio para configurar el Sistema idóneo a sus necesidades, pero no entraremos en la descripción de circuitos, que se escapan del alcance de este artículo.

4.2.1. Diagrama bloque

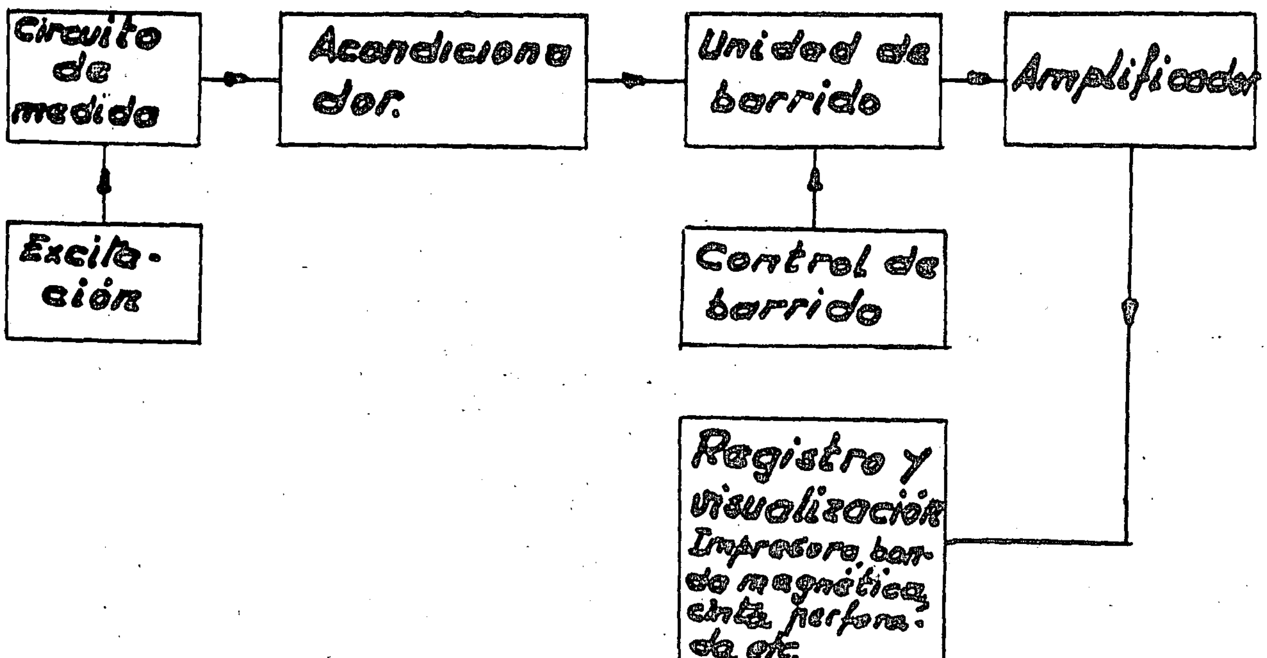

Circuito de medida.

Será cualquier circuito extensométrico, ya descrito, bién en el aspecto de bandas extensométricas, o bién bajo el concepto de captador. Generalmente podrá ser cualquier elemento transductor de energía mecánica en electrica.

Excitación.-

Por ser circuitos pasivos, tendremos que aportar energía, generalmente para excitar un circuito de puente de Wheatstone.

Acondicionador.-

Debe permitir equilibrar el circuito de medida e introducir señales de calibración.

Unidad de barrido.-

Esta unidad está destinada a conectar cada uno de los circuitos de medida a la unidad central de lectura, con una secuencia predeterminada. Sus características principales son: velocidad de conmutación; fiabilidad de los contactos, número de polos conmutados,etc.

Amplificacdor.-

Aumenta el nivel de tensión de las señales débiles que se crean en los circuitos de medida.

Control de barrido y registro.-

Lo forman circuitos electrónicos, más o menos complejos. que permiten programar las secuencias de las lecturas y de la impresión.

4.3. Sistemas analógicos de registro contínuo

Podríamos definir un sistema como el conjunto de instrumentos, debidamente acoplados, para la adquisición de datos en forma predeterminada, de las magnitudes físicas a medir.

4.3.1. Diagrama bloque

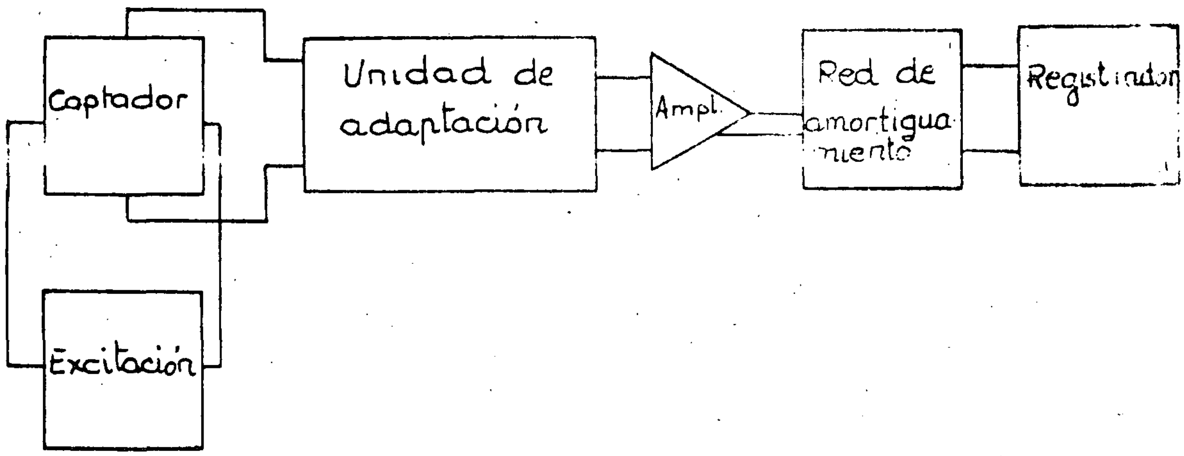

Diagrama bloque de un sistema elemental

El esquema de la figura responde a los elementos funcionales del sistema, que son:

a) Captador: Es un elemento capáz de convertir una magnitud física en eléctrica. Se basa en fenómenos resistivos, capacitivos, inductivos, piezoeléctricos, termoeléctricos, semi-conductores, etc, etc,

b) Unidad de excitación: Si el captador no autogenera su propia señal (p.e.: termopares) es necesario alimentarlo con una fuente de energía adicional.

c) Unidad de adaptación y calibración: Permite corregir y compensar los desequilibrios en los circuitos e introducirles una señal que permita la calibración de los mismos.

d) Amplificador: Las señales emitidas por los captadores pueden ser tan débiles que no sean capaces de excitar los instrumentos de lectura ó registro. Es necesario entonces el empleo de unidades intermedias que aumenten el nivel de la señal de salida.

e) Registrador ó unidades de lectura: Pueden ser cualquiera de los instrumentos clásicos destinados a registros analógicos ó digitales ó bién osciloscopios, molivoltímetros, etc,

f) Red de amortiguamiento: Sirve para adaptar las impedancias de entrada y salida de los diferentes amplificadores e instrumentos de lectura ó registro. En el caso de galvanómetros, tiene una influencia decisiva referente a la respuesta en presencia de los mismos.

4.3.2. Descripción

A Captadores

Un captador ó transductor es aquel elemento que, bajo estímulos físicos, da origen a señales eléctricas. La mayoría de los captadores proporcionan salidas analógicas en forma de d.d.p. eléctrico. Muy idealizado, podemos suponerlo tal y como se muestra esquemáticamente:

Si una viga elástica y empotrada recibe en su extremo libre un golpe, se producirá un movimiento oscilatorio amortiguado, pues bién, el transductor nos dará una d.d.p. analógica del estímulo recibido.

Los captadores los clasificaremos bajo diversos aspectos:

a) Estímulo físico, al que son sensibles: captadores de aceleraciones, vibraciones, presiones, fuerzas, desplazamientos, torsión, calor,etc

b) Principio de la transducción: Resistivos (P. de Wheatstone y potenciométricos) inductivos, piezoeléctricos, fotoeléctricos, capacitivos, semiconductores, etc.

c) Alimentación de su circuito interno: Autoexcitados, excitados, en c.c. y excitados en c.a (portadora).

Captadores más usuales son:

1º Acelerómetros.- Supongamos una masa sísmica M montada en una caja con un muelle y sistema amortiguador como el representado esquemáticamente, Si la caja es solidaria con un elemento sometido a vibraciones, se creará un movimiento relativo entre masa M y caja y entre caja y un punto fijo del espacio. Si llamamos "X" e "Y" a los desplazamientos de M respecto a caja y de caja respecto al punto fijo, respectivamente, tendremos que ante cualquier excitación aparecerá dentro de la caja una energía de valor: $dE=(x''+y'')dy$

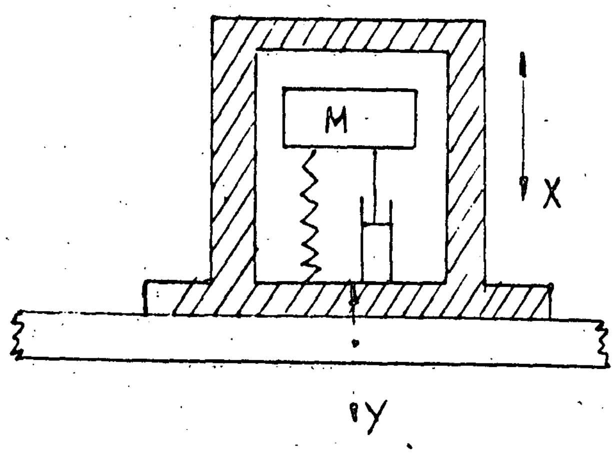

$$E = \int_0^y M(X'' + y'')\,dy = \int_0^v M(x'' + y'')\,y'\,dt \quad (1)$$

Energía que se manifiesta en tres formas: cinética, deformadora del muelle y disipada en forma de calor por el sistema amortiguador. Por tanto:

$$E = \frac{1}{2} M(x' + Y')^2 + \frac{1}{2} K x^2 + \int_0^t C\, x'^2\, dt \quad (2)$$

siendo K= característica del muelle

C= constante de amortiguamiento

Si el muelle es totalmente elástico se cumple que $\frac{K}{M} = 4\pi^2 fn^2$, y si el amortiguamiento es el ideal $\frac{S}{M} = 4\pi f_n$ de donde igualando (1) y (2), simplificando y sustituyendo, obtenemos que:

$$X'' + 4\pi f_n X' + 4\pi^2 f_n{}^2 x = -y'' \quad (3)$$

El desplazamiento "Y" varía con el tiempo y no tiene por qué ser periódico. Su armónico principal sería de la forma $y'' = Ae^{jwt}$ siendo A la amplitud y $w = 2\pi f$; de esta forma la solución de X sería: $X = Be^{jwt}$ en donde B es función compleja de w; sustituyendo en (3) queda simplificado que:

$$-B 4\pi^2 f^2 + jB\,(2\pi f) + B\,(2\pi fn)^2 = -A$$

donde los dos primeros términos pueden despreciarse si $f_n > f$ es decir, si la frecuencia natural del resorte es mayor que la frecuencia ~~cia del movimiento de la caja, entonces:~~ $\cancel{B\,(2\pi fn)^2} = -A$

$$\left.\begin{array}{l} B\,(2\pi fn)^2 = -A \\ x\,(2\pi f_n)^2 = -y'' \end{array}\right\} \; x = \frac{-y''}{(2\pi f_n)^2}$$

Vemos, por tanto, que el desplazamiento de la masa es proporcuonal a la aceleración a que se somete la caja, siempre que $f_n > f$ ($\approx f$ es el 60% de f_n)

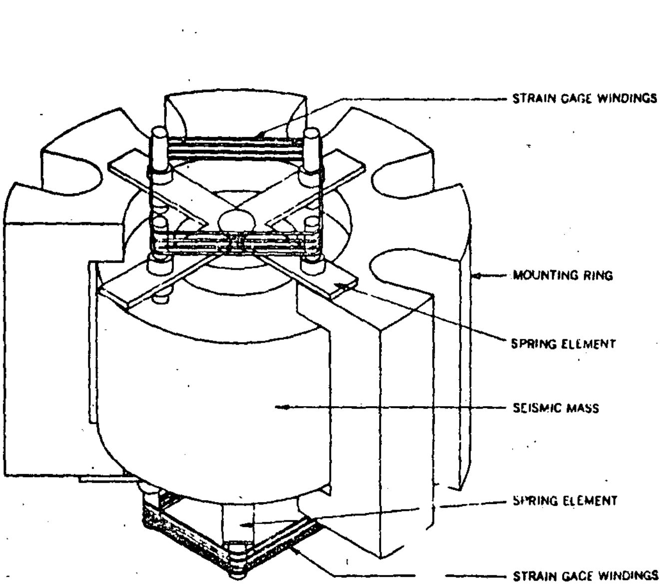

ACCELEROMETER

Si unimos la masa sísmica adecuadamente a un circuito de bandas extensométricas, tal como el mostrado en la figura, los movimientos de la masa se convertirán en deformaciones de las bandas y si éstas forman los cuatro brazos activos de un puente de Wheatstone, el desequilibrio que producen origina una d.d.p. proporcional a la aceleración a que se somete la caja.

Los acelerómetros se construyen de forma que sean sensibles en una sola dirección y con la propiedad que giros de ± 90º respecto a su posición de equilibrio equivalen a producir los mismos efectos que si se someten a una aceleración de ± 1 g, repectívamente ($g = 9{,}8\ m/seg^{-2}$).

El tipo descrito corresponde a un acelerómetro resistivo, que son más utilizados, ya que con un margen de frecuencia, relativamente amplio, permiten medir desde f = O Hz. Son, además, de muy fácil acoplo en el sistema por su baja impedancia de salida y proporcionan señales altas, no existiendo problemas de ruido ó descompensación especiales cuando haya que utilizarlos a distancias relativamente grandes.

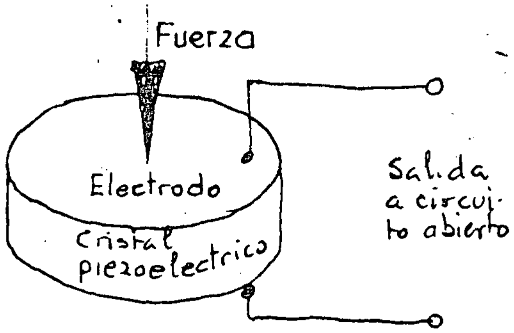

Acelerómetro piezoeléctrico.

Si a un cristal piezoeléctrico le aplicamos entre sus caras una fuerza F, se genera en las mismas una carga q, Incorporándole íntimamente una masa al cristal, tenemos un acelerómetro, en efecto: $q \quad dF = dMa$.

donde la d.d.p. V_s originada entre caras del cristal vale:

$$V_s \hat{=} \frac{q}{C} \hat{=} \frac{dF}{C} \hat{=} \frac{dMa}{C} = Ka$$

es decir, la d.d.p. V_s es proporcional a las aceleraciones que es sometida la masa M.

Los acelerómetros piezoeléctricos no necesitan alimentación, ya que son autoexcitados. Tienen una respuesta en frecuencia alta, aunque no responden bién a frecuencias próximas a O Hz. Necesitan un adaptador de impedancias para su acoplo en el sistema debido a su muy alta impedancia de salida y pueden dar problemas cuando haya que emplear cableado a distancia.

2º) Captadores de vibraciones.- Para los acelerómetros resistivos decíamos que la frecuencia del movimiento debía ser menor que la frecuencia natural del resorte, pues bién, si hacemos ahora que f fn, tendremos un captador de vibración.

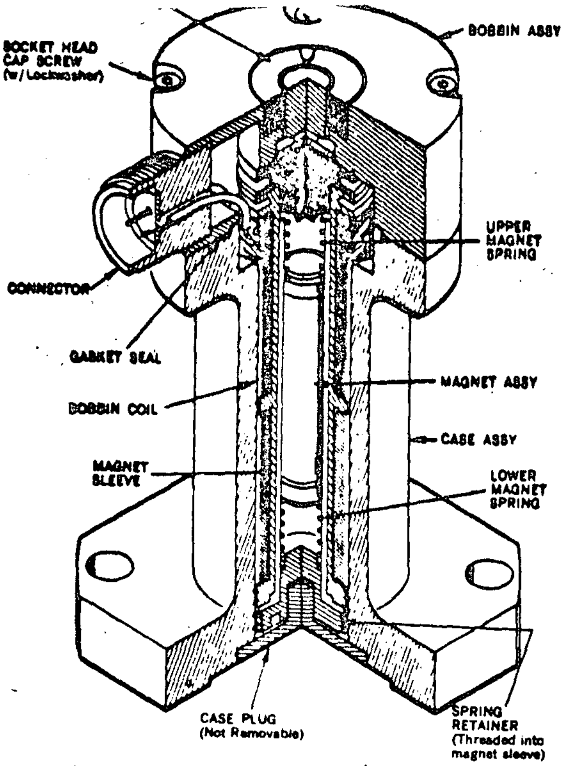

Cutaway View of Vibration Transducer

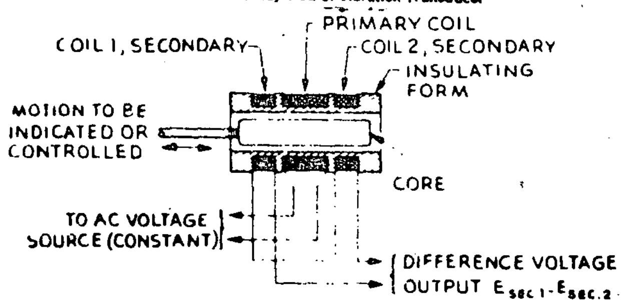

En efecto, si la caja se mueve por encima de la frecuencia de resonancia del muelle, la masa sísmica permanece "quieta" en el espacio y la corriente que se origina en las bobinas es proporcional a la velocidad de los desplazamientos de la caja.

Estos captadores tienen la ventaja de que son autoexcitados.

3º) Captadores de presión.- El fundamento es el mismo que en los acelerómetros resistivos, salvo que la masa sísmica es sustituida por un diafragma, que es el elemento sensible a las presiones.

Pueden hacerse medidas absolutas y diferenciales.

4º) Captadores basados en transformadores lineales.- Ha sido muy desarrollada la técnica del transformador diferencial lineal para su uso en transductores. Básicamente, está constituido por devanado primario y dos devanados secundarios idénticos y montados en oposición; los tres devanados constituyen la parte estática del captador y un núcleo magnético forma la parte dinámica.

Al excitar el primario con una corriente alterna constante, si el núcleo se encuentra en su posición media, no habrá d.d.p. en los terminales del secundario, pero para cualquier desplazamiento del núcleo aparecerá una d.d.p. entre terminales del secundario proporcional al desplazamiento.

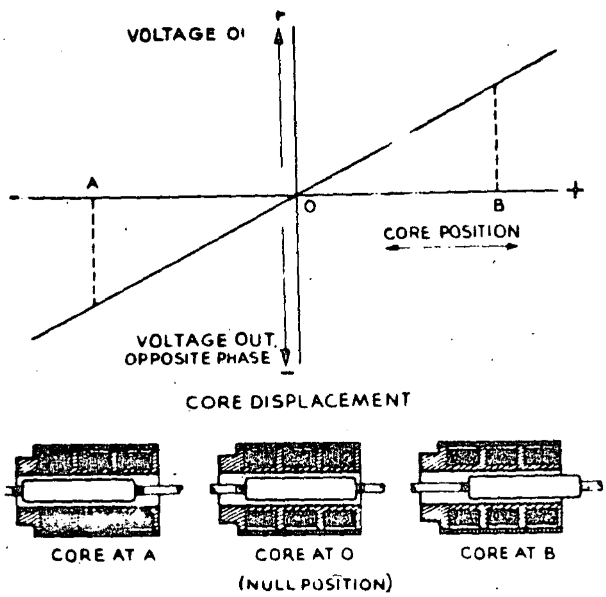

Vemos que un transductor basado en el anterior principio, puede convertir cualquier magnitud mecánica (desplazamiento, presión, fuerza, vibración, etc) en magnitud eléctrica.

Las ventajas de estos transductores son:

Salida exactamente proporcional al desplazamiento del núcleo.

Alta sensibilidad y nivel elevado a la salida.

Característica lineal de la respuesta en toda su escala.

Variación de la d.d.p, de salida desde cero, sin necesidad de equilibrar el circuito.

Estabilidad del cero.

Permiten la suma ó producto de varios desplazamientos montándolos en serie ó tandem, respectívamente,

Por el contrario, presentan el inconveniente de que necesitan demodular y filtrar la salida y de que su excitación no puede ser en corriente continua.

Para paliar el anterior inconveniente, la firma Schaevitz, ha desarrollado un modelo que puede ser excitado en c.c.; su esquema es el indicado y toda la electrónica la constituye un circuito integrado de estado sólido, de dimensiones reducidísimas, incluido dentro del propio captador. El resultado es francamente favorable.

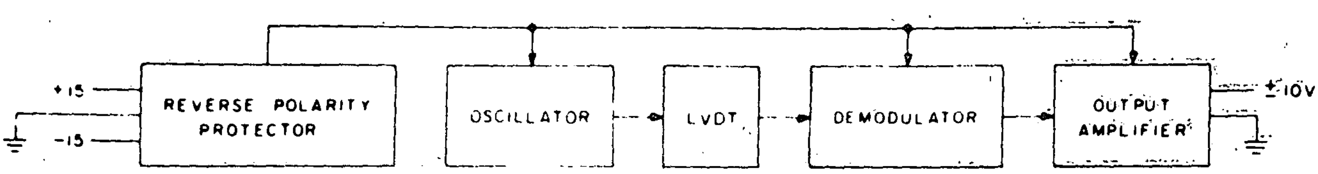

Servoacelerómetros

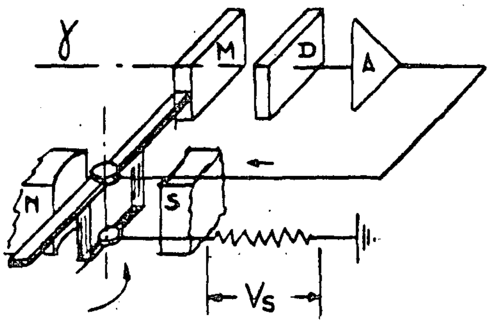

Constituyen un avance enorme en la medida de aceleraciones por las elevadas prestaciones que ofrecen. Su principio está basado en la restauración del equilibrio de una masa sismica pendular cuando éste es desplazado de su posición de reposo por una fuerza aceleradora. En efecto, de la ecuación Mr= (Momento de tensión)= I (Momento de inercia) (aceleración) deducimos que una aceleración angular aplicada al acelerómetro y actuando sobre una masa equilibrada montada en un eje giratorio, origina un par de tensión sobre dicho eje; de la misma forma, si la masa no está equilibrada (pendular) y es sometida a una aceleración lineal producirá en el eje de rotación un momento de tensión.

El fenómeno de la transducción aceleración-señal, se consigue disponiendo de un sensor de posición, capaz de detectar los movimientos de la masa sismica pendular el cual da una señal eléctrica a dichos movimientos y que es amplificada hasta conseguir el nivel adecuado para alimentar la bobina montada dentro de un campo magnético que originará el par antagonista al de torsión que creó la fuerza aceleradora. El circuito es cerrado, de ahi que la señal se obtiene como caida de tensión en R_I.

La señal de estos acelerómetros es de $\pm$ 5 VDC y en la mayoría de aplicaciones no necesitarán posterior amplificación para su registro. Son alimentados normalmente a $\pm$ 15 VDC.

B Módulos de excitación

Módulo de excitación es un elemento capáz de suministrar la energía adecuada al captador para obtener señales eléctricas propor cionales a los estímulos físicos a los que se someta. Podremos utilizar, desde una simple pila seca, hasta una sofisticada fuente de alimentación, siendo la calidad del captador y las características del sistema quienes impondrán el tipo adecuado de módulo.

Nos referiremos siempre a módulos de excitación en c.c. ya que la utilización de excitación en c.a. (portador:) cada vez está más en desuso y, cuando se utiliza, son los propios amplificadores los que llevan incorporados un oscilador que proporciona la excitación con d.d.p. de 0-10 V en frecuencias de 2 a 8 KHz, normalmente.

Un buén módulo de excitación debe suministrar una d.d.p constante; se comprende ésto, ya que cualquier variación en la d.d.p. de la excitación introducirá errores en la señal de salida del captador, que es proporcional a la excitación y a la variación del estímulo físico.

En general, la elección de un módulo de excitación se hará considerando dos aspectos:

1º) Características del captador.- Impondrán el valor de la d.d.p., intensidad de corriente y potencia; deberán considerarse los casos en que sean varios los captadores alimentados en paralelo por un solo módulo.

2º) Especificaciones propias del módulo de excitación.- Serán índice de la calidad del mismo. Deben considerarse como importantes:

Posibilidad de ajuste sobretensiones (cortocircuitos, electromagnética, térmica, electrónica, etc).

Limitador electrónico de la corriente de salida.
Reversibilidad de la polaridad.
Rizo residual de la tensión de salida.
Aislamiento de bornes de salida a masa ó tierra.
Corrientes de fugas.
Rechazo de interferencias.
Voltímetro incorporado de control.
Deriva de la salida respecto a tiempo y temperatura.
Márgenes de la temperatura de utilización.
Posibilidad de alimentación por c.a. ó por baterías.
Incorporación de acumuladores autorrecargables.
Conectores, caja de montaje, pero, etc,etc.

C. Unidades de adaptación

Una unidad de adaptación incorpora en el sistema los elementos necesarios para equilibrar el circuito de medida, es decir, para que una carga nula en el captador dé como señal de salida cero, compensando las asimetrías propias del captador, ó producidas por cables, conexionado, etc. Si los captadores son resistivos, la compensación será solo con potenciómetros, siendo necesario un ajuste capacitivo en el caso de captadores inductivos ó cuando se emplee el sistema de excitación por "onda portadora". Opcionalmente, pueden incluir un sistema de calibración y elementos pasivos (resistencias) para completar circuitos de medida de captadores, generalmente cuando se utilizan puentes de Wheatstone.

Normalmente, las especificaciones de una unidad de adaptación son referidas a circuitos con 350 ohmios y excitados con 10 V, pero no hay razón para ampliar estas especificaciones a otros valores, por ejemplo, si una unidad de adaptación permite compensar desequilibrios de $\pm$ 4 mV en un circuito de 350 ohmios con 10 V de excitación, Utilizando un circuito de 1.000 ohmios y la misma excitación, la cobertura de ajuste sería:

$$\frac{1.000}{350} \times (\pm 4) = \pm 11,4 \text{ mV.}$$

El poder de resolución debe ser del órden de 5 microvoltios para una buena unidad.

Es frecuente utilizar una resistencia fija de precisión para calibrar un circuito, conmutándola en paralelo con una rama del puente de Wheatstone. La señal así obtenida es equivalente a la que produciría el captador sometido a cierto estímulo físico. La carta que acompaña a los captadores indica el valor de la resistencia, que producirá una señal equivalente a la del captador con el 80% de su carga nominal. Con el fín de evitar la utilización de numerosas resistencias de calibración, se montan unas bornas exteriores que permiten conectar una caja de décadas y, de esta firma, seleccionar el valor adecuado para cada captador ó circuito de medida.

En medidas de Extensometría se presenta, con frecuencia, la necesidad de utilizar 1,2 ó 4 brazos activos de un circuito de puente Wheatstone. Para estos casos ó similares, las unidades de adaptación suelen llevar incorporadas las resistencias que completan los brazos pasivos del circuito, facilitando el montaje con una economía notable al disminuir el número de extendímetros por circuito de medida.

Se tendrá muy en consideración que no exista un punto común (masa), pues provocaría un cortocircuito en una rama del puente.

D Amplificadores

El amplificador es una unidad intermedia entre el circuito de medida y el registrador y su utilización será justificada por dos razones: una cuando la señal del captador sea insuficiente para excitar los instrumentos de lectura ó registro y otra en el caso de fenómenos cuya presencia sea superior a los 350 Hz, ya que los galvanómetros capaces de dar respuestas a estas frecuencias son de baja sensibilidad.

La tecnología electrónica de un amplificador para sistemas de medida ha evolucionado grandemente en los últimos años y del primitivo tipo de onda portadora (carrier), se ha pasado a las actuales de tipo diferencial, con circuitos transistorizados sencillos, estando desarrollándose actualmente técnicas más avanzadas con empleo de circuitos integrados y del amplificador operacional.

Describir circuitos electrónicos de un amplificador no es objeto de este artíiulo, pues no olvidemos que, desde el punto de vista de instrumentación, su uso, y no su constitución, es necesario conocer. Sí es preciso, sin embargo, interpretar correctamente las especificaciones que de ellos se dan, para poder elegir y utilizar siempre el modelo más idóneo para un determinado sistema.

Especificaciones de un amplificador.

Configuración (Configuration).- Indica generalmente la disposición de la entrada y salida, diciéndose que es verdaderamente "diferencial" cuando están totalmente aisladas y "single ended" cuando hay una entrada y salida común. La salida de un amplificador puede tener un punto a tierra ó estar to totalmente aislada. En este caso se dice que tiene "salidas flotantes".

Ganancia en tensión (Voltage Gain).- Normalmente será por pasos fijos (10, 20, 50, 100, 200, 500, etc) y ajuste fino entre pasos. Es importante el grado de exactitud entre pasos.

Respuesta en frecuencia (Frequency Response).- Nos indicará el % de variación de la ganancia en un determinado ancho de banda.

Tiempo de recuperación contra sobrecargas (Overload Recovery Time).- Si a un amplificador lo sometemos a una sobrecarga de 10 veces el valor final de escala, nos indicará el tiempo que transcurre desde que cesa la sobrecarga hasta que se alcanza el 90% del valor total de escala.

Linearidad (Linearity).- Idealmente, un amplificador deberá dar salidas totalmente proporcionales a las señales de entrada. El error de proporcionalidad expresado en % del valor máximo de la señal de salida lo da esta especificación.

Derivas (Drifts).-Se entiende por derivas las variaciones de la señal de salida con señal de entrada nula y puede referirse al tiempo y/ó temperatura. Las variaciones de la salida por este motivo deben mantenerse en el entorno dado en esta - especificación.

Ruido (Noise).- El ruido inherente a circuitos electrónicos (agitación térmica) limita el poder de resolución, que no podrá ser mayor que la especificación dada para ruido.

Modo común de rechazo (Common Mode Refection).- Es índice del poder de rechazar señales indeseadas. Se expresa, en dB, como la relación entre el voltaje en modo común (CMV) y la señal que dicho CMV originaría en la entrada.

$$CMR\ (dB) = 20 \log \frac{CMV}{IS}$$

Sensibilidad (Sensitivity).- Relaciona los miveles de la señal de entrada y los máximos de la señal de salida.

Máxima impedancia del circuito de medida (Máximum Source Impedance).- Es el límite superior del valor de la impedancia del circuito de medida.

Impedancia de entrada (Input Impedance).- Es la medida a la entrada del amplificador.

Impedancia de salida (Output Impedance).- Es la medida a la salida del amplificador.

Capacidad (Capability).- Máximos valores en tensión y corriente capaces de obtenerse a la salida.

Ajuste Zero Offset.- Indica la capacidad del amplificador de obtener una salida nula con las entradas conectadas a un circuito de impedancia cero.

Mínima impedancia de carga (Minimum Load Impedance).- Mínima carga que debe conectarse a la salida del amplificador para obtener la máxima salida.

Como conclusión, diremos que las especificaciones del amplificador deberán cumplir, como mínimo, las propias exigidas al sistema en conjunto. Características superiores solo producirían un encarecimiento innecesario.

E Registradores

El registrador es el instrumento que recibe las informaciones transmitidas por los captadores a través de los módulos intermedios para ser grabadas de forma que permitan el cálculo ó procesamiento de datos.

La elección del registrador, al igual que los demás componentes del sistema, estará condicionada por el parámetro a medir.

Si los fenómenos a registrar son de muy bajas frecuencias un registrador potenciométrico será suficiente. Por el contrario, si las frecuencias son de algunos herzios, tendremos que utilizar un registrador oscilográfico de haz luminoso, microfilm, placas osciloscópicas ó cinta magnética. En general, varios serán los factores que intervendrán en la elección y convendrá considerar:

Fidelidad, ó sea, distorsión que experimenta la señal en la grabación.

Valor mínimo de señal que puede ser grabado y posteriormente interpretado dentro de los límites de exactitud y precisión exigidos en la medida.

Banda de frecuencias con respuesta plana.

Número de canales simultáneos de registro.

Tratamiento posterior de la información.

En medidas dinámicas son muy utilizados los registradores oscilográficos de haz luminoso y los registradores magnéticos de cinta.

Registradores oscilográficos de haz luminoso.

La señal eléctrica procedente del captador excita un galvanómetro que refleja el haz procedente de una fuente luminosa capáz de impresionar un papel fotosensible, grabando en forma analógica la magnitud física objeto de la medida.

Cuatro son los elementos fundamentales de un oscilógrafo: mecanismo de transórte de papel, fuente luminosa de alta intensidad, sistema óptico y galvanómetros. El mecanismo de transporte de papel debe permitir varias velocidades de registro y asegurar la constancia de cada una de ellas. Una de las limitaciones de registrar fenómenos de frecuencias elevadas la impondrá la capacidad de transporte del papel para conseguir la velocidad adecuada que permita una grabación legible, con un consumo mínimo de papel.

La fuente luminosa está también intimamente ligada a la frecuencia de los fenómenos a registrar y se comprende que, para frecuencias elevadas, el tiempo de exposición del haz luminoso sobre el papel será muy breve, de ahí que la intensidad del mismo tendrá que ser grande. Se utilizan focos de lámparas de tungsteno, arco, halógenos vapor de mercurio, etc. El límite está en frecuencias de unos 25 KHz.

El sistema óptico de su oscilógrafo está formado por una serie de espejos y lentes que conducen el haz luminoso hasta el papel fotosensible, consiguiendo que la grabación sea legible. La calidad de sus componentes, su facilidad de ajuste, así como la precisión de su montaje, serán el índice de la bondad de este sistema.

El galvanómetro es el elemento fundamental de un registrador y su misión es convertir una determinada energía eléctrica en movimiento de rotación.

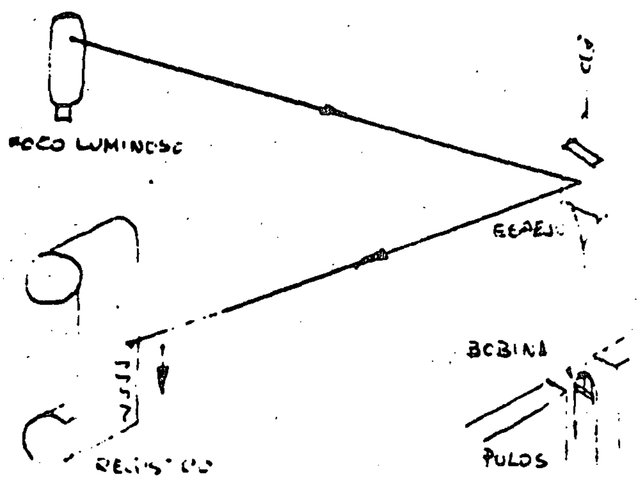

Los galvanómetros tipo D'Arsonval son los más utilizados y están constituidos por una pequeña bobina con una suspensión torsional sometida a un campo magnético constante; la suspensión es portadora de un espejo que recibe un haz de luz y lo refleja sobre papel fotosensible; el paso de una corriente por la bobina crea un campo electromagnético, cuya resultante con el campo magnético del imán permanente originará el giro de la bobina y, por tanto, el del espejo de la suspensión.

El valor T del par de torsión de la suspensión tiene por valor $T = NBi.a.\cos\phi$ siendo:

N = Número de espiras
B = Densidad de flujo
i = Corriente en la bobina
a = Ancho de la bobina
ϕ = Angulo de deflexión

La deflexión del haz luminoso es proporcional al número de espiras de la bobina e inversamente proporcional a la constante de torsión K de la suspensión; un incremento del número de espiras y un decrecimiento de la constante K, aumentará la sensibilidad, pero tambi también el periodo de la oscilación, disminuyendo, por tanto, la frecuencia natural. De aquí se deduce que un galvanómetro con amplia respuesta en frecuencia implicará sacrificio en la sensibilidad.

Un galvanómetro balístico se usa para medir la cantidad de carga desplazada por una corriente de corta duración. Supongamos (fig. a) que se cierra el interruptor e inmediatamente se abre, por G circulará una corriente de descarga que origina un giro de la suspensión. Este giro de la bobina en un campo magnético induce una f.e.m. pero, como el circuito está abierto no circula corriente por G y éste oscila indefinidamente existiendo

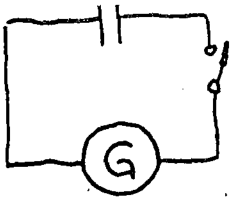

a)

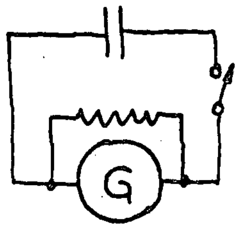

b)

como único amortiguamiento, la fricción de la suspensión.

En la(fig. b) la corriente debida a la f.e.m., inducida por el giro, se cierra por el shunt y esta corriente origina un par de torsión que se opone al movimiento producido por la descarga del condensador. El valor de la resistencia shunt limita el valor de la corriente antagonista, existiendo un valor para el cual G retorna a cero sin entrar en oscilación. Este valor de shunt se denomina resistencia externa crítica de amortiguamiento (Critical External Damping Resistance, CSDR).

Galvanómetros utilizados para frecuencias bajas necesitan el amortiguamiento indicado en el párrafo anterior. Por el contrario, para altas frecuencias el amortiguamiento se consigue introduciendo la bobina en un tubo capilar con un fluido (Silicona).

Terminología de galvanómetros

Frecuencia natural (Natural Frequency).- Es la frecuencia a la que un galvanómetro sin amortiguamiento responde con la máxima amplitud.

Sensibilidad en c.c. sin amortiguamiento (Undamped d-c- Sensitivity).- Deflexión por unidad de corriente del punto luminoso sobre un plano situado perpendicularmente a un brazo óptico determinado.

Sensibilidad en tensión (Voltage Sensitivity).- Relación de la deflexión con un determinado brazo óptico a la d.d.p. aplicada al circuito del galvanómetro, teniendo éste una resistencia interna equivalente a la resistencia de amortiguamiento.

Ejemplos

Sensibilidad de corriente $= \frac{a}{Io}$

Sensibilidad de corriente sin amortiguamiento $= \frac{a}{Ig}$

Sensibilidad de tensión $= \frac{a}{Vo}$

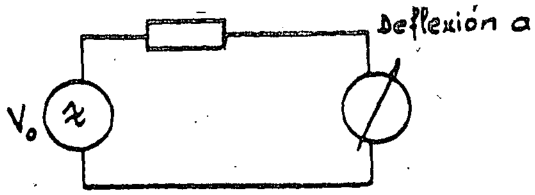

CIRCUITO DE TENSION

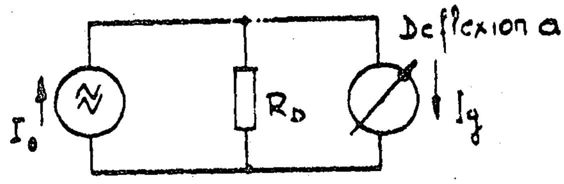

CIRCUITO DE CORRIENTE

Resistencia de amortiguamiento (Damped Resistance).- Valor de resistencia requerido para el 0,64 del amortiguamiento crítico.

Desequilibrip (Galvanometer Unbalance).- Máxima deflex.ón que se produce en un galvamómetro al someterse a una aceleración de 1 g. en cualquier plano.

Linearidad (Linearity).- Grado de concurrencia entre una posición del punto luminoso y valor teórico dividido por deflexión específica al valor total de escala, expresado en %.

Error tangenciañ (Tangential Error).- Error causado al registrar en una superficie plana, en vez de una circular de radio igual al brazo óptico.

Respuesta en frecuencia (Frequency Response).- Frecuencia a la cual la respuesta es plana.

Corriente de seguridad (Safe Current).- Máxima corriente que puede pasar permanentemente por el galvanómetro sin dañarlo.

Resistencia interna (Internal Resistance).- Resistencia interna de la suspensión y bobina media con corriente contínua.

Cálculo de redes de amortiguamiento.

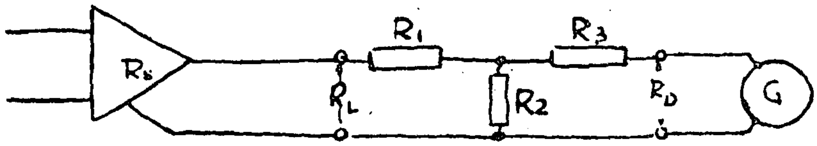

Al conectar un galvanómetro a un amplificador ó circuito de medida se presenta elproblema de acoplamiento de impedancias, ya que el amplificador tendrá un valor óptimo R_L y, a su vez, para un amortiguamiento determinado, el galvanómetro requerirá una cierta R_D. En todos los galvanómetros CEC el valor R_D indicado en sus especificaciones se refiere al 64% de su amortiguamiento crítico, equivalente a una respuesta plana hasta el 60% de su frecuencia natural.

Fijándonos en el esquema, siempre habrá unos valores R_1 - R_2 - R_3, que permitan un acoplo y las ecuaciones que establecen dichos valores son:

$$R_1 = R_L - (1-K)\ R_2$$

$$R_2 = K\ (R_g + R_D) \left[\frac{1}{1-K^2\ (R_g + R_D)/(R_L + R_S)} \right]$$

$$R_3 = \frac{(1-K)}{K}\ R_2 - R_g$$

$$R = SD/I_o$$

Donde

R_L = Optima impedancia de carga para el amplificador (

R_S = Resistencia de salida del amplificador.

R_D = Resistencia de amortiguamiento requerida por el galvanómetro.

S = Sensibilidad del galvanómetro (mA/cm).

R_g = Resistencia interna del galvanómetro

D = Deflexión deseada (cm).

I_o = Corriente de salida del amplificador para el total de escala.

K = Constante.

En galvanómetros amortiguados electromagnéticamente, el valor h = amortiguamiento total, es la suma de dos valores, uno constante, (amortiguamiento viscoso = h_v) y otro variable (amortiguamiento magnético = h_m). Las especificaciones CEC indican estos valores para cada tipo. En ellos se cumple:

$$h = h_m + h_v$$

$$\frac{h_{m1}}{h_{m2}} = \frac{R_{D1} + R_g}{R_{D2} + R_g}$$

$$R_{D2} = \frac{h_m\ (R_{D1} + R_g) - h_{m2}\ R_g}{h_{m2}}$$

Donde

h_{m1} = Componente magnética de amortiguamiento para el 64% de amortiguamiento crítico.

h_{m2} = Componente magnética de amortiguamiento para el nuevo amortiguamiento deseado.

R_{D1} = Resistencia del amortiguamiento (64%)

R_{D2} = Nueva resistencia de amortiguamienti.

Eligiendo un determinado valor de h, (CEC incluye las curvas de respuesta de un galvanómetro para diversos h), podremos uti lizar los galvanómetros como verdaderos filtros.

F REGISTRADORES ANALOGICOS DE CINTA MAGNETICA

Hace aproximadamente 30 años, Marvin Camras presentó al Navy's Bureau of Ships un instrumento que podría ser utilizado por la industria naval. Era el primer registrador en cinta magnética basado en los mismos principios que hoy se siguen utilizando.

Consideraciones teóricas

Una cinta de material ferro-magnético es el soporte de este registro. La señal eléctrica de entrada se aplica a las bobinas del circuito magnético de registro por el que pasa la cinta, el cual es sometido a una inducción proporcional al valor de entrada.

La inducción remanente forma el dato memorizado en la cinta que, al pasar por un circuito de lectura crea, por variación del flujo, una f.e.m. inducida.

Ventajas del registro magnético

Veamos primero las ventajas del registro en cinta magnética respecto a otros sistemas tradicionales, principalmente gráficos, que han hecho esta técnica indispensable en ciertos campos de aplicación y una de las más utilizadas y de más posibilidades.

1º) Permite registrar un vasto campo de frecuencias, desde c.c. hasta varios MHz.

2º) Un amplio margen dinámico ó campo de medida superior a 50 dB. Se conoce por campo de medida la razón, medida generalmente en dB, entre la máxima señal medible sin distorsión ó señal fondo de escala y la mínima señal distinguible del ruido. En otros términos, es una relación señal/ruido referida al valor fondo de escala.

Considerando la señal a medir, un campo de medida superior a 50 dB indica una resolución del orden del 0,3% del valor máximo medible.

3º) En caso de sobrecarga, los posibles desperfectos son mínimos si los comparamos con los que se pueden suceder a galvanómetros ú otros sistemas mecánicos.

4º) La información se recoge y reproduce en su forma el[illegible]. Ello permite utilizar el registrador, no solo como instru[illegible] de medida, sino también para recrear el fenómeno original, utilizando en su salida un transductor inverso al utilizado en la entrada. Esta capacidad única le hace insustituible en experiencias simuladas.

La memorización de la señal en su forma eléctrica posibilita los trabajos de adquisicón de datos en el laboratorio cuando las condiciones de medida no permitem hacerlo in situ.

5º) La cinta magnética puede borrarse y utilizarse de nuevo, lo que representa una gran economía frente a otros métodos.

6º) El fenómeno registrado puede reproducirse milea de veces, lo que asegura la obtención de la máxima información para el análisis de datos.

7º) La densidad de información obtenible en un registrador de cinta magnética no es posible con otros métodos. Cientos de canales pueden registrarse mediante técnicas de multiplexing.

8º) Otra característica, y no la menos importante, es su facilidad para varíar la base de tiempo, reproduciendo el fenómeno a distinta velocidad de la del registro.

Descripción de un registrador magnético

Con objeto de conocer alguno de los principios del diseño de estos registradores, pensados para utilización instrumental, estableceremos cuatro grupos básicos en su construcción:

1º) Electrónica de registro y reproducción, que codifica la señal, preparándola en forma adecuada para registro óptimo y la descodifica para recuperar la señal en su forma eléctrica original.

2º) Cabezas magnéticas que durante el registro convierten la señal eléctrica en diversos estados de magnetización de la cinta y durante la reproducción realiza el proceso inverso.

3º) Sistemas de arrastre cuya función es mover la cinta con la máxima suavidad y a velocidad constante. La precisión de este movimiento condiciona grandemente la calidad y coste del registrador.

4º) Cinta magnética constituida por un soporte delgado, magméticamente neutro, (plástico, poliester, generalmente) lo más resistente posible a la tracción mecánica soɔ e la que se ha depositado una suspensión de óxido férrico.

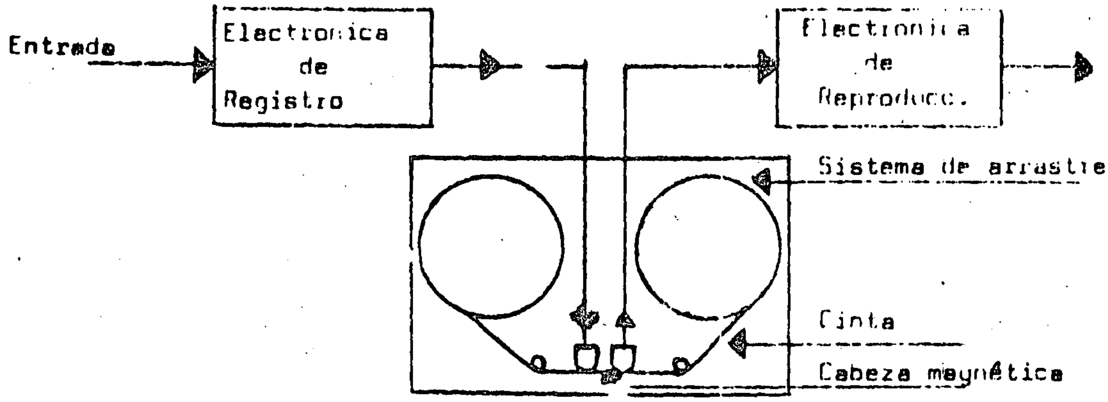

Sistema de registro en Modulación de 'recuencia

Para compensar los incc ıvenientes implícitos del registro directo; se utiliza la modulació' de la señal en frecuencia y así la inestabilidad de amplitud no prod ‹e trastornos en cuando que la información va contenida en la frecuen ɔa. La imposibilidad de registrar señales de frecuencias muy bajas no xiste, ya que señales en continua son, en realidad, representadas por recuencias más ó menos altas. En todo sistema FM, el demodulador debe ir seguido por un filtro pasabajo, cuya frecuencia de corte debe se· cerca de 1/5 de la portadora.

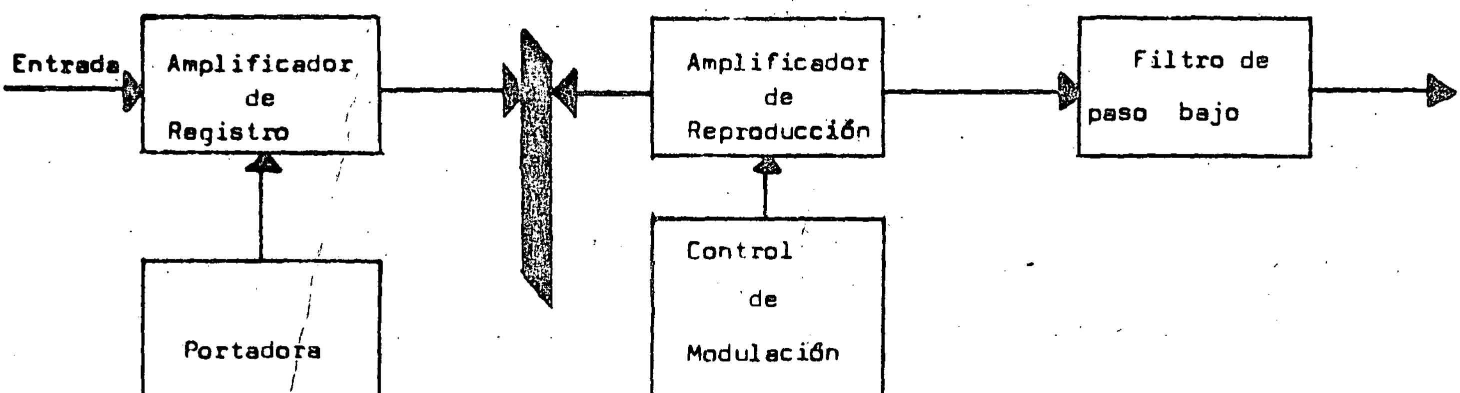

La tecnica FM lleva la señal a través de un amplificador de c.c. a un oscilador controlado por voltaje La amplitud de la señal se convierte así en una desviación de frecuencia y la frecuencia de la señal en una velocidad de desviación. Esta portadora de frecuencia ondulada se registra en la saturación. El amplificador de reproducción desmodula y filtra la señal para recoger el dato.

Una primera desventaja, inmediatamente observable, comparando los diagramas bloque, es su más compleja electrónica. Asímismo, el sistema de transporte debe ser más perfeccionado y preciso, ya que si la velocidad no es rigurosamente constante, se traduce, no en un error de la base de tiempos, sino en una modulación indeseada ó ruido. Igualmente, la respuesta de frecuencia es inferior que en el registro directo.

Sus ventajas más destacables son:

a) Posibilidad de registrar señales en continua.

b) Insensibilidad a las variaciones de amplitud, así como al ruido originado en la cinta. La relación señal/ruido es superior en algunas decenas de dB a la obtenible en el sistema directo.

Especificaciones de un registrador magnético

Respuesta en frecuencia

Viene determinada por la longitud del entrehierro de las cabezas reproductoras, la velocidad de transporte y el método de registro.

El límite superior de frecuencia lo alcanza cuando la longitud de onda registrada (velocidad cinta/frecuencia) equivale al entrehierro. Los registradores de instrumentación actuales operan a velocidades comprendidas entre 1 7/8 y 240 in/sec. Las versiones modernas pueden establecerse en dos categorías de bandas intermedia y de bandas anchas.

Relación señal-ruido

Es una indicación del margen dinámico de señales de entrada que pueden registrarse, reproducirse y separarse del ruido del sistema.

Se expresa en dB y en una función primaria de la electrónica de reproducción y del ruido de la cinta.

Distorsión armónica

Es la medida de la no linearidad del sistema. Se expresa como porcentaje de uno ó todos los armónicos respecto a la frecuencia fundamental sinusoidal.

Flutter

En los registradores de cinta de instrumentación se considera flutter como cualquier forma de variación de velocidad superior a O,2 Hz. Un cierto flutter existe siempre debido a imperfecciones en el sistema de transporte ó en el recubrimiento de la cinta. Esto produce perturbaciones en la base de tiempo e introduce ruido en el modo FM.

Se expresa en términos de %, pico a pico. Cuando se comparen especificaciones de flutter en diferentes equipos debe hacerse en el mismo ancho de banda y velocidad de cinta; normalmente a mayor velocidad, el flutter es menor.

El flutter puede reducirse significativamente acoplando un servosistema con control de alta frecuencia a un transporte de baja inercia.

Error de base de tiempos

Cuando se utilizan sistemas de banda ancha, el error de tiempo absoluto es normalmente más significativo que el error de tiempo porcentual. En tales casos, se especifica el TBE, que es la variación del flutter con el tiempo.

En la comparación de dos registradores de TBE inferior nos asegura una reducción proporcional del flutter. Un flutter a baja frecuencia produce proporcionalmente un mayor TBE.

Dynamic Skew

Se define como el error de desplazamiento de tiempo intercanales (ITDE) y es un desplazamiento variable de tiempo entre las pistas de una misma cabeza causado por tensiones no uniformes de cinta ó irregularidades en su dimensionado. Se expresa en /seg. de desplazamiento. Para que sean significativos, deben mencionarse la velocidad de cinta y el número de canales sobre los que se ha medido. Una especificación típica es $\pm$ O,25 /seg. entre pistas adyacentes de la misma cabeza a 120 ips.

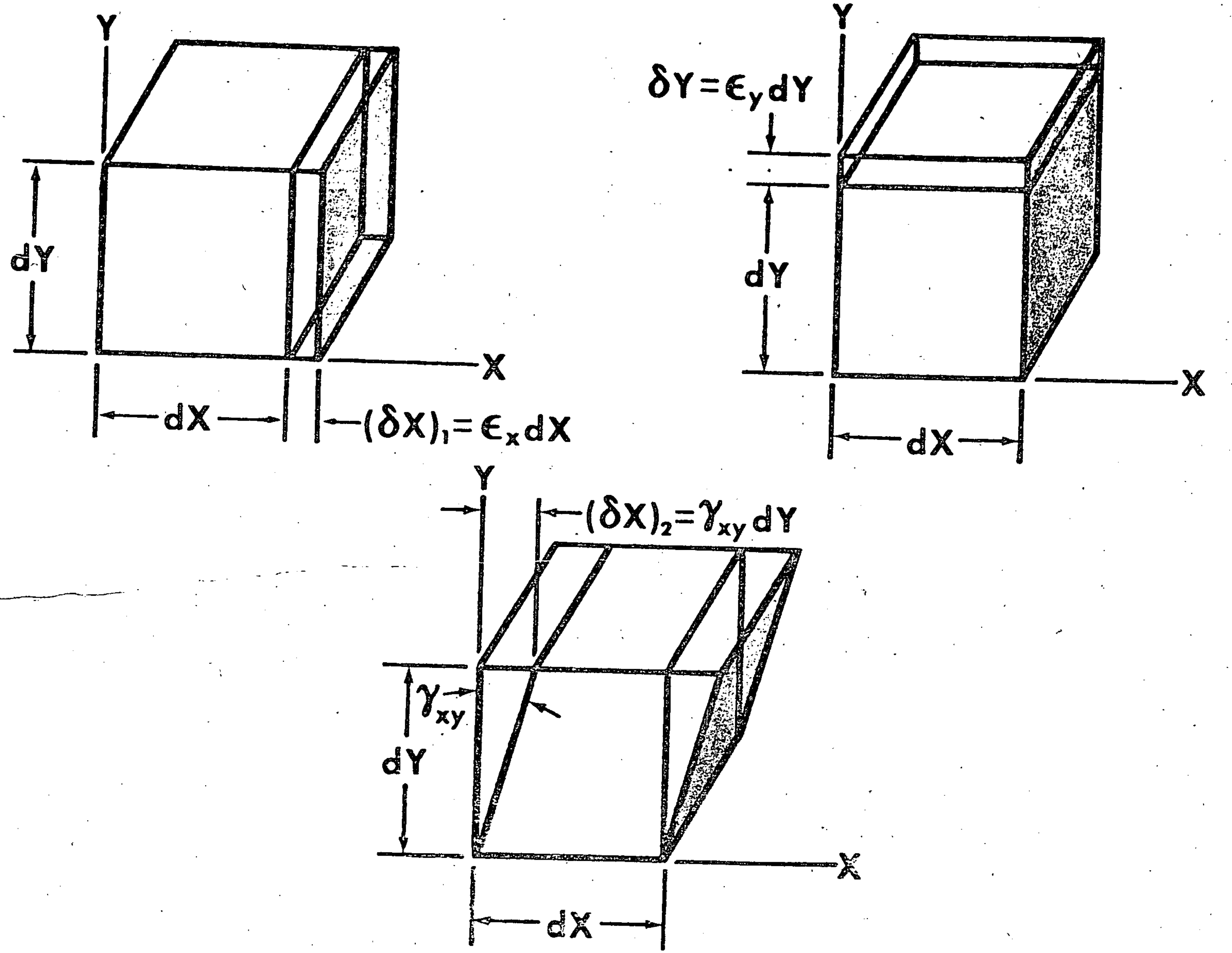
Y
dY
X
dX
$(\delta X)_1 = \epsilon_x dX$
Y
$\delta Y = \epsilon_y dY$
dY
X
dX
Y
$(\delta X)_2 = \gamma_{xy} dY$
γ_{xy}
dY
X
dX

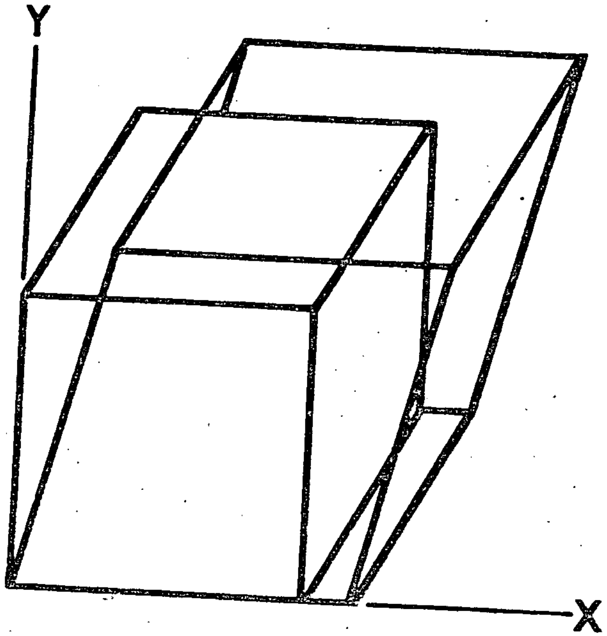
Y
X

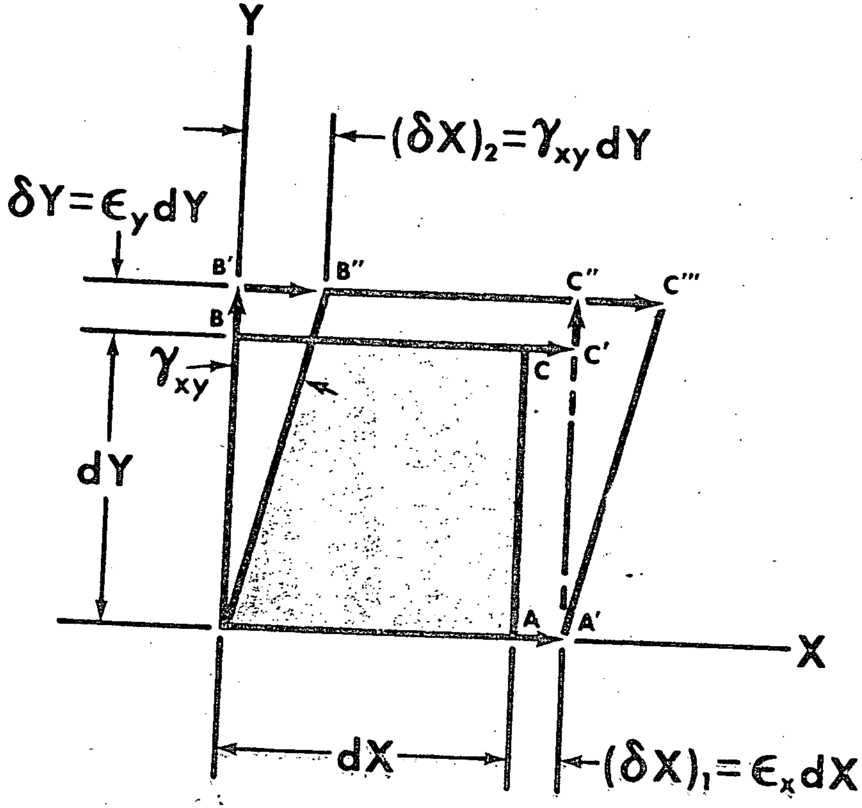
Y
$(\delta X)_2 = \gamma_{xy} dY$
$\delta Y = \epsilon_y dY$
B′
B″
C″
C‴
B
C′
C
γ_{xy}
dY
A
A′
X
dX
$(\delta X)_1 = \epsilon_x dX$

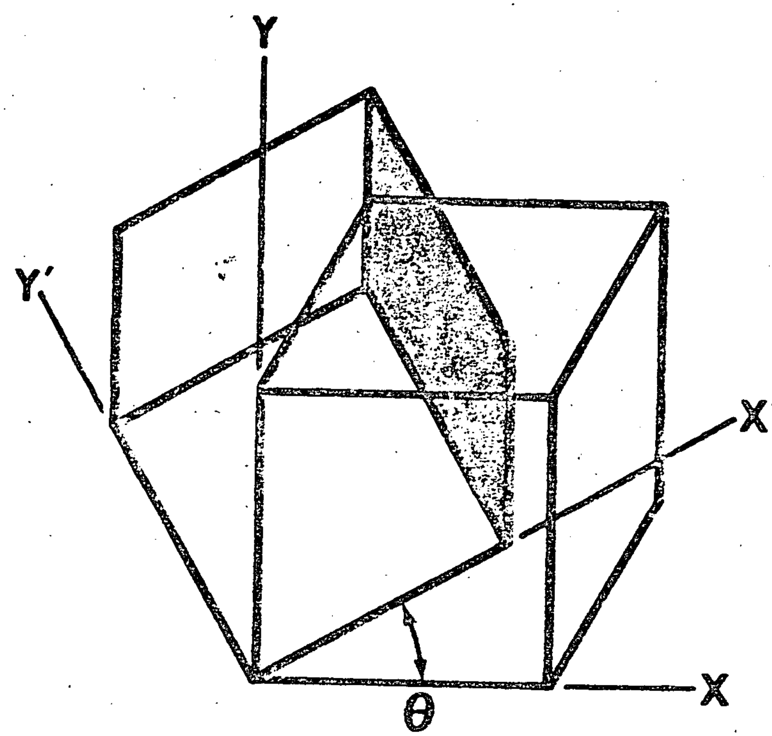
Y
Y'
X'
X
θ

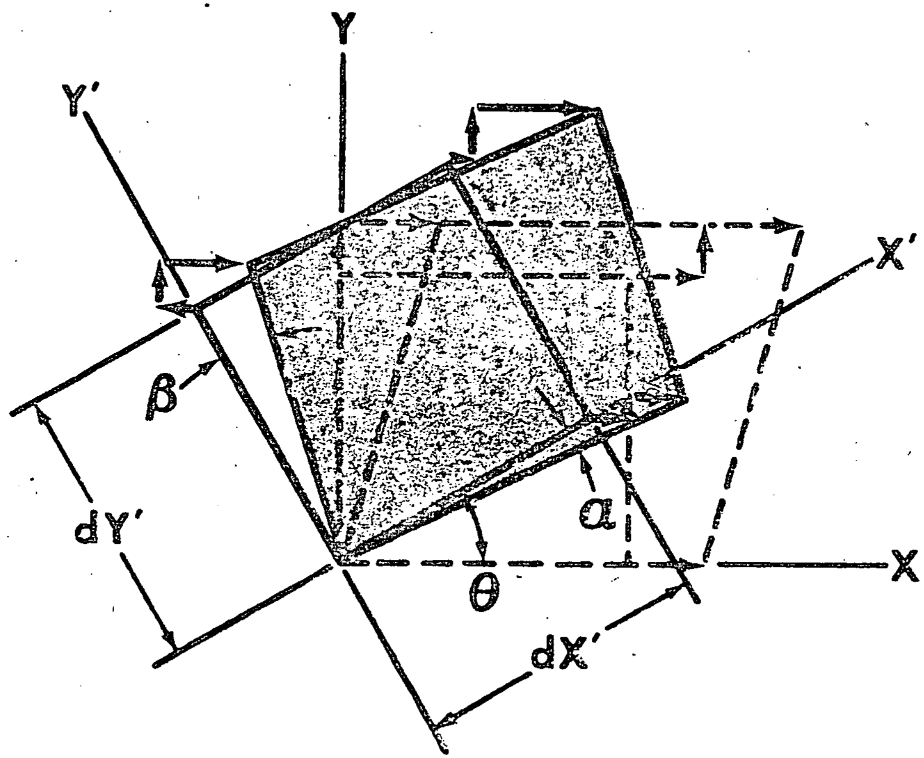
Y
Y'
X'
X
β
α
θ
dY'
dX'

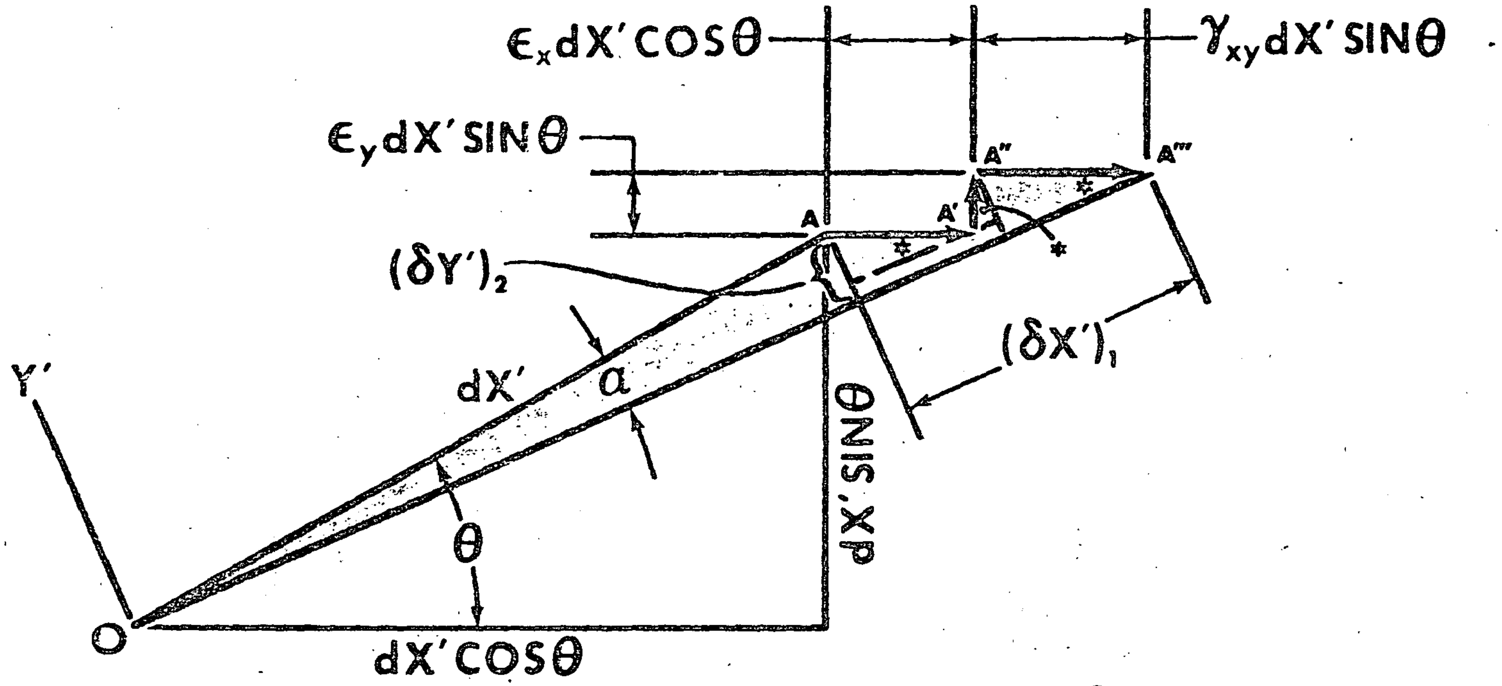

$* = \theta$ (APPROX.)

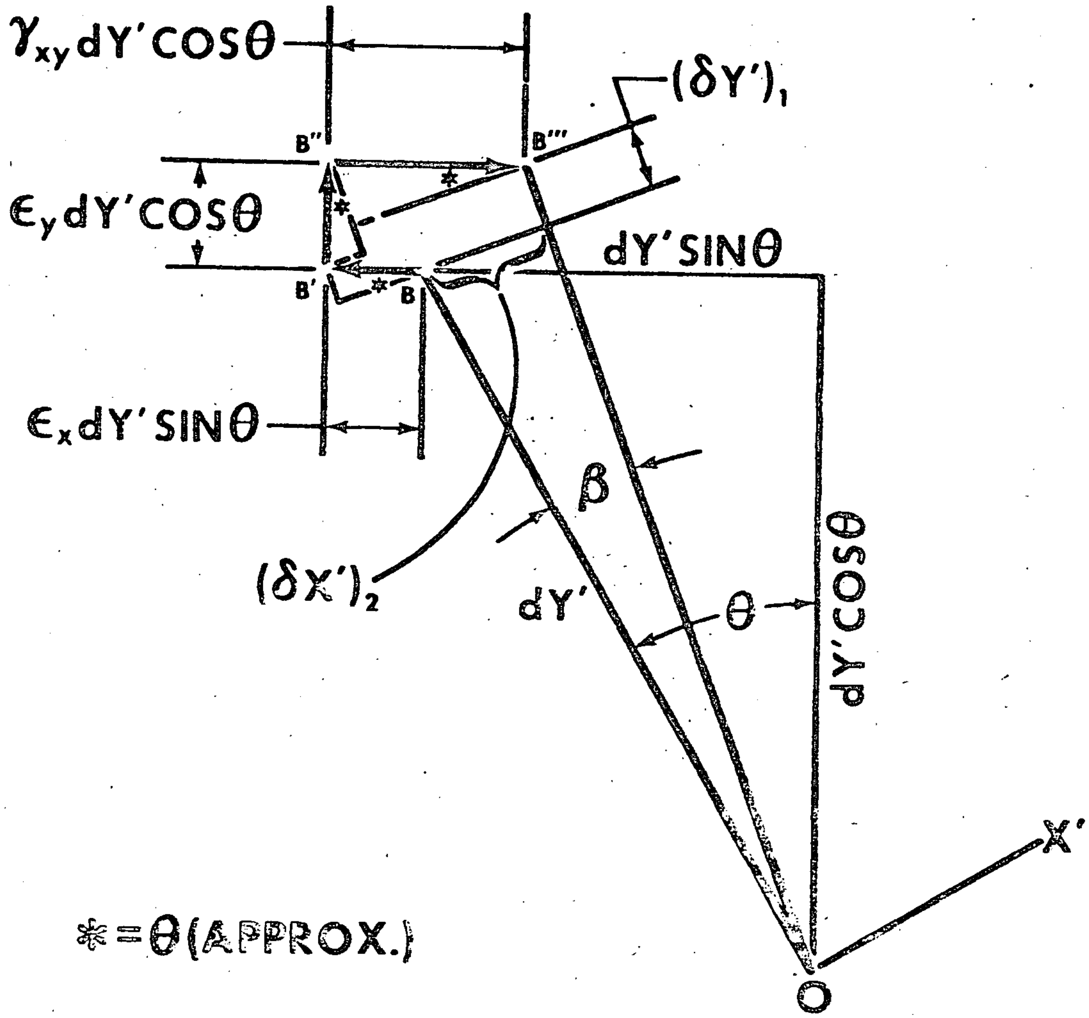
$\gamma_{xy} dY' \cos\theta$
$(\delta Y')_1$
B''
B'''
$\epsilon_y dY' \cos\theta$
$dY' \sin\theta$
B'
B
$\epsilon_x dY' \sin\theta$
β
$(\delta X')_2$
dY'
θ
$dY' \cos\theta$
X'
O
$* = \theta$ (APPROX.)

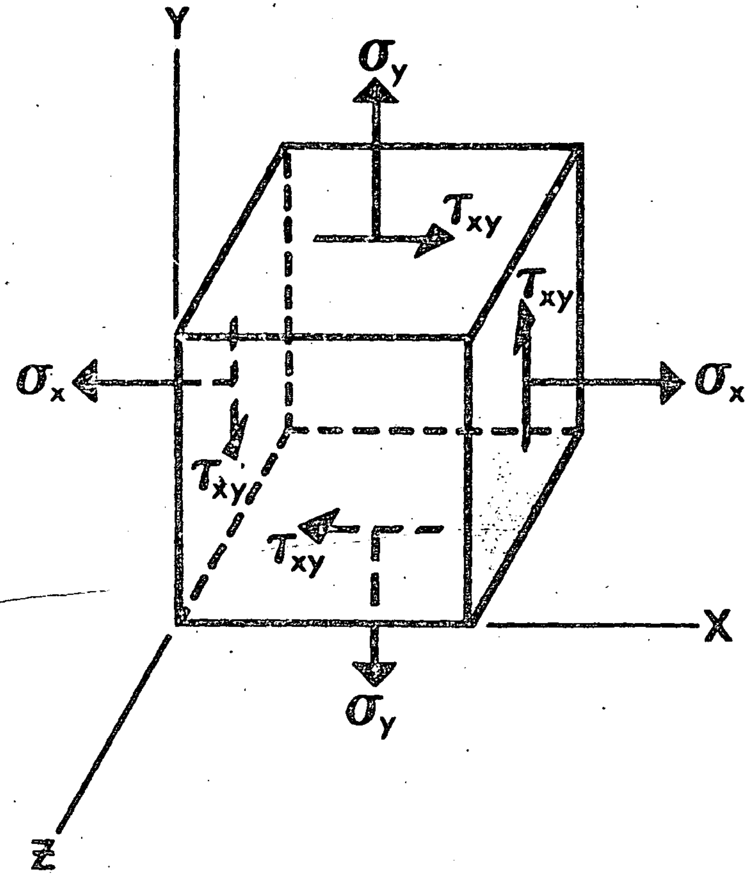
Y
σy
τxy
τxy
σx
σx
τxy
τxy
X
σy
Z

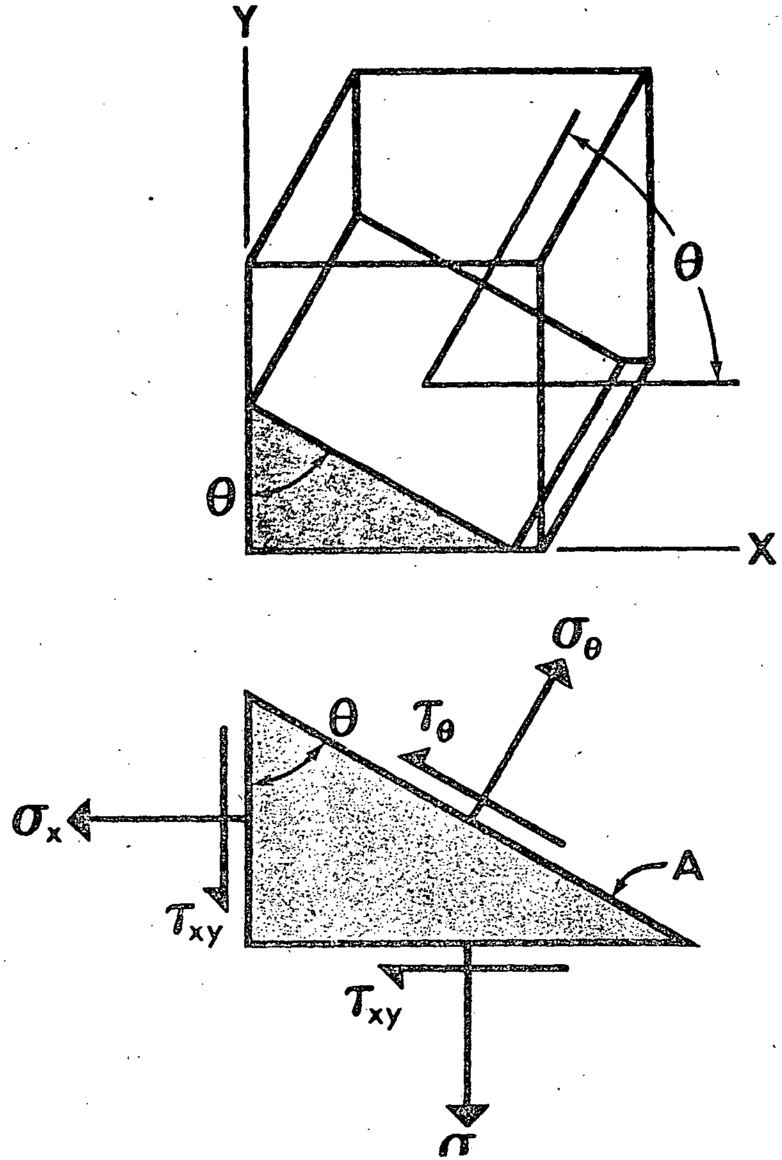
Y
θ
θ
X
σθ
θ
τθ
σx
A
τxy
τxy
σ

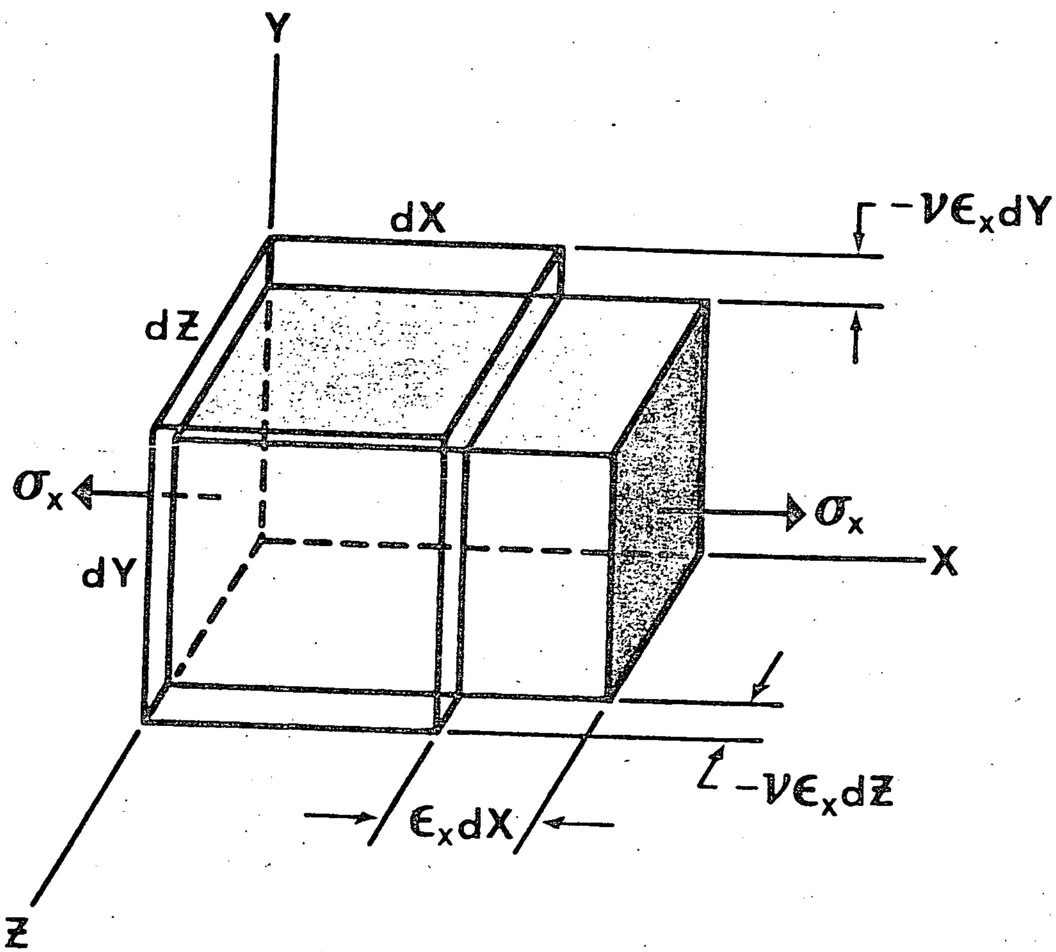
Y
dX
$-\nu\epsilon_x dY$
dZ
σ_x
σ_x
dY
X
$-\nu\epsilon_x dZ$
$\epsilon_x dX$
Z

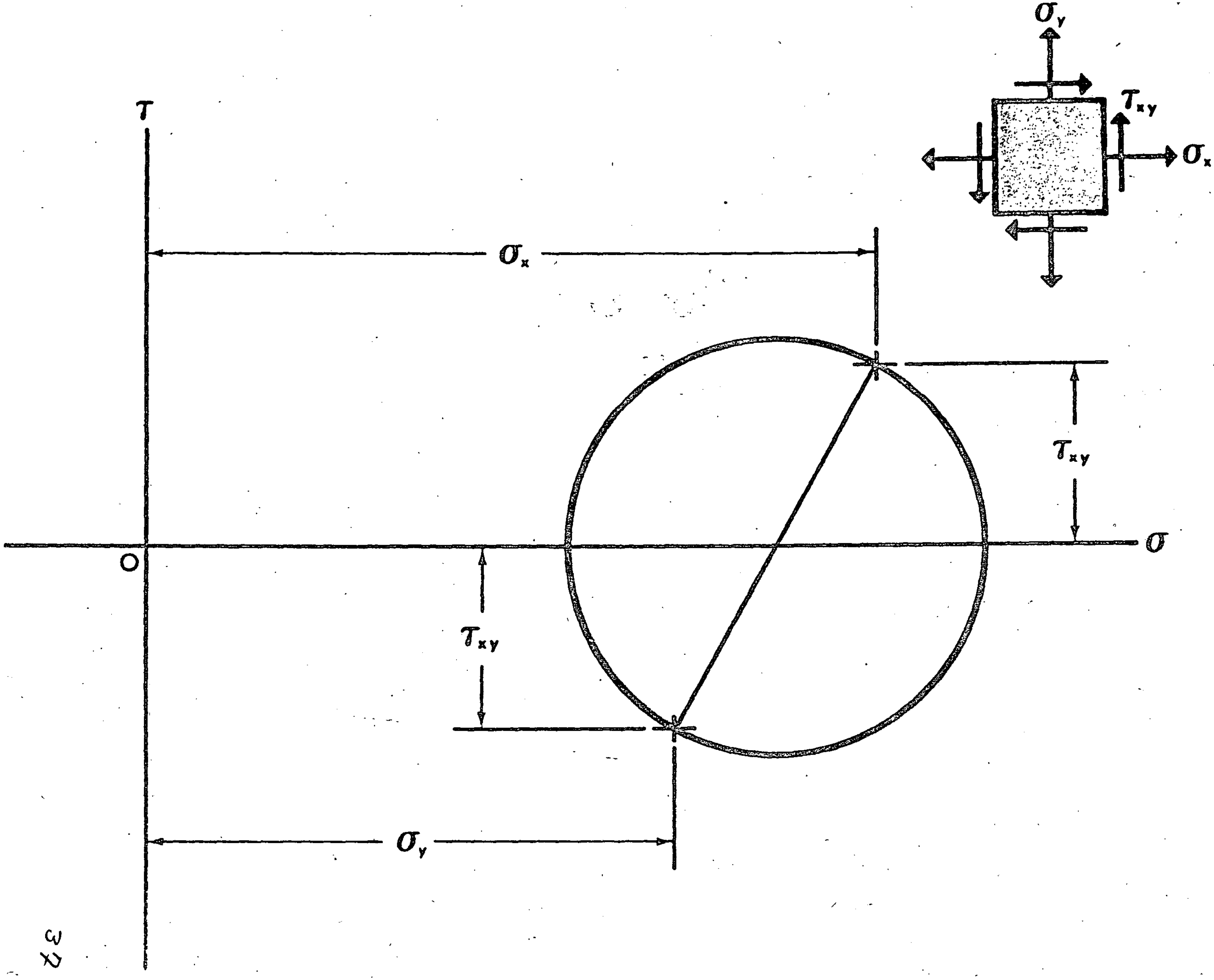
σ_y
τ_{xy}
σ_x
τ
σ_x
τ_{xy}
O
σ
τ_{xy}
σ_y

centro de educación continua
división de estudios superiores
facultad de ingeniería, unam

ANALISIS EXPERIMENTAL DE ESFUERZOS

FOTOELASTICIDAD REFLECTIVA

NOVIEMBRE, 1978.

TABLE OF CONTENTS

	Page No.
INTRODUCTION	1
SECTION 1 - DESCRIPTION AND ASSEMBLY	
1.0 Description	7
1.1 Assembly	9
SECTION 2 - MEASUREMENT OF DIRECTIONS OF PRINCIPAL STRAINS	
2.0 Introduction	10
2.1 Measurement of directions at a point	10
2.2 Measurement of directions over large areas	13
SECTION 3 - MEASUREMENTS IN NORMAL INCIDENCE - INTERPRETATION OF STRESS DISTRIBUTION	
3.0 Introduction	17
3.1 Basic data on photoelastic measurements	17
3.2 Intrepretation of photoelastic pattern - Identification of fringes	19
3.3 Measurements at a point	23
3.3.1 Tardy compensation	23
3.3.2 Operation procedure: How to measure fractional fringe orders using tardy method	24
3.3.3 Measurements in uniaxial stress field and analysis of the principal stress acting tangent to a point along a free boundary using Tardy compensation	28

Page No.

3.4 Absolute compensation - Measurements using Null Balance Method 29

3.4.1 Linear Compensator, Model 032 30

3.4.2 Uniform Field Compensator, Model 232 31

SECTION 4 - MEASUREMENTS IN OBLIQUE INCIDENCE

4.0 Introduction 35

4.1 Description of Oblique Incidence Adapter Model 033 and assembly to basic analyzer 35

4.2 Basic equations 36

4.3 Measurements 40

4.4 Use of nomograph 43

SECTION 5 - CORRECTION FACTORS

5.0 Introduction 45

5.1 Method of correction for parasitic birefringence 45

5.2 Correction factors for plane stress problems 49

5.3 Correction factors for coated plates subjected to bending 50

5.4 Correction factors due to temperature change 53

SECTION 6 - CALIBRATION OF PLASTICS

6.0 Introduction 56

6.1 Use of the Calibrator Model 010 56

6.2 Calibration of plastic using a cantilever beam 56

SECTION 7 - DESCRIPTION AND USE OF ACCESSORIES

7.0 Introduction 58

7.1 Telemicroscope Attachment Model 037 and 137 58

		Page No.
7.2	Camera Model 035 and 135	62
7.3	Camera Adapter Model 038 and Model 138 for Telemicroscope	63
7.4	Monochromator Model 036	64
7.5	Stroboscopic Light Models 034 and 134	64
7.6	Model 332 and 432 Digital Strain Readout	65

SECTION 8 - PHOTOGRAPHIC RECORDING OF FRINGE PATTERNS

8.0	General rules	67
8.1	Photography of isochromatics	68
8.2	Photography of isoclinics	69
8.3	Photographic recording through the Telemicroscope	69

SECTION 9 - REFERENCES

INTRODUCTION

Today, the use of experimental stress analysis techniques has been considerably expanded in such fields as:

- establishment of design criteria
- improvement of product reliability
- reduction of weight and cost

The necessity for these techniques has been created by current technical advances, radical designs and an increasingly competitive market.

These pressures have forced an increased work load on the engineer who by necessity is now looking for tools and methods which will help him reduce his testing time and costs as well as providing him with more data.

Photoelastic coatings, the most recent development in stress analysis techniques, has proved to be an extremely versatile yet simple tool. It is, therefore, becoming widely used both in field and laboratory testing. It combines the best features of strain gages and classical photoelasticity by providing:

- a visible picture of the surface stress distribution of the component
- stress distribution which is accurately readable at any point for both direction and magnitude

While the photoelastic model is still the only method for three-dimensional analysis, the surface coating technique eliminates the difficulties in casting complicated models yet permits the measurement of surface strains in the elastic or plastic ranges on structures, joints, weldments, etc., previously inaccessible to photoelasticity.

Polarized Light - Fundamentals

Light or luminous rays are electromagnetic vibrations similar to radio waves. An incandescent source emits radiant energy which propagates in all directions and contains a whole "spectrum" of vibrations of different frequencies or wave lengths. A portion of this spectrum is useful within limits of human perception (wave lengths between 4000 and 8000 Angstrom* units).

*Angstrom unit = 10^{-8} cm.

The vibration associated with light is perpendicular to the direction of propagation. A light source emits a train of waves containing vibrations in all perpendicular planes. However, by the introduction of a polarizing filter (P), only one component of these vibrations will be transmitted (that which is parallel to the privileged axis of the filter). Such an organized beam is called polarized light or "plane polarized" because the vibration is contained in one plane. If another polarized filter (A) is placed in its way, complete extinction of the beam can be obtained when the axes of the two filters are perpendicular to one another (See Figure 1).

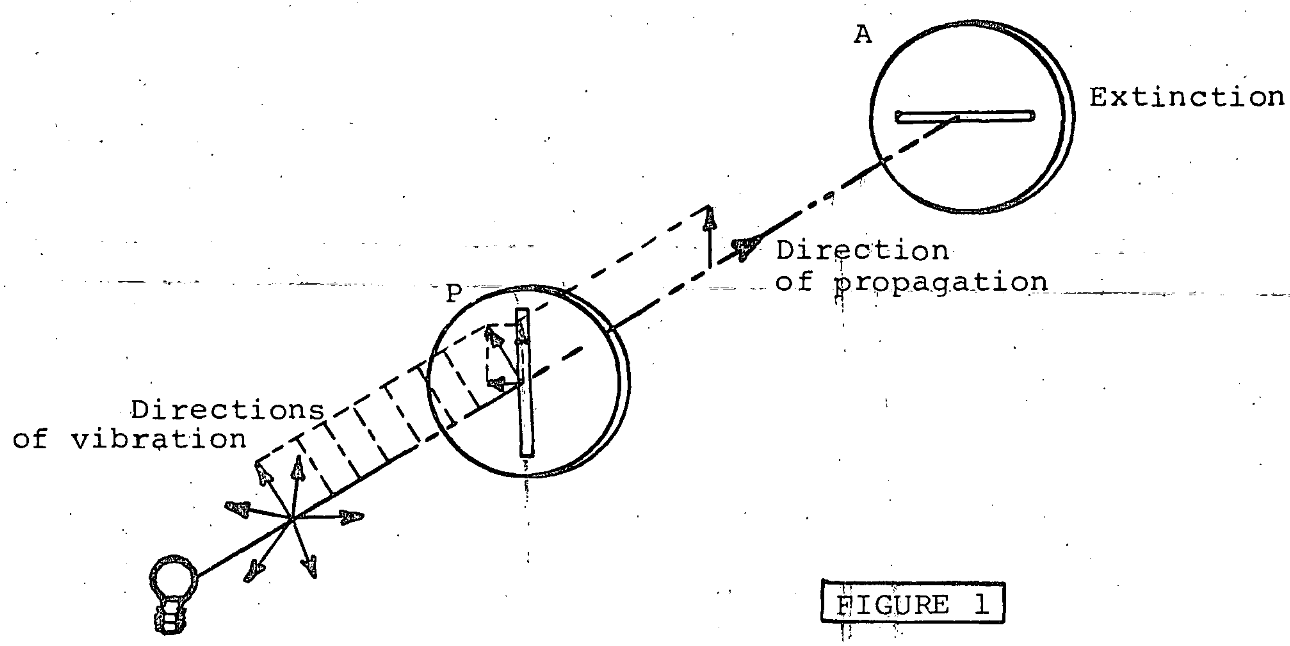

FIGURE 1

Light propagates in a vacuum or in air at a speed (C) of 3 x 10^{10} cm/sec. In other transparent bodies, the speed V is lower and the ratio C/V is called the index of refraction. In a homogenous body this index is constant regardless of the direction of propagation or plane of vibration. However, in crystals the index depends upon the orientation of vibration with respect to its axis.

Certain materials, notably plastics, behave homogenously when unstressed but become heterogenous when stressed. The change in index of refraction is a function of the stress applied similar to the resistivity and the resistance change in an electrical strain gage.

When a polarized beam (P) propagates through a transparent plastic of thickness, t, where x and y are the directions of principal strains at the point under consideration, the light vector splits and two polarized beams are propagated in planes "x" and "y". (Figure 2)

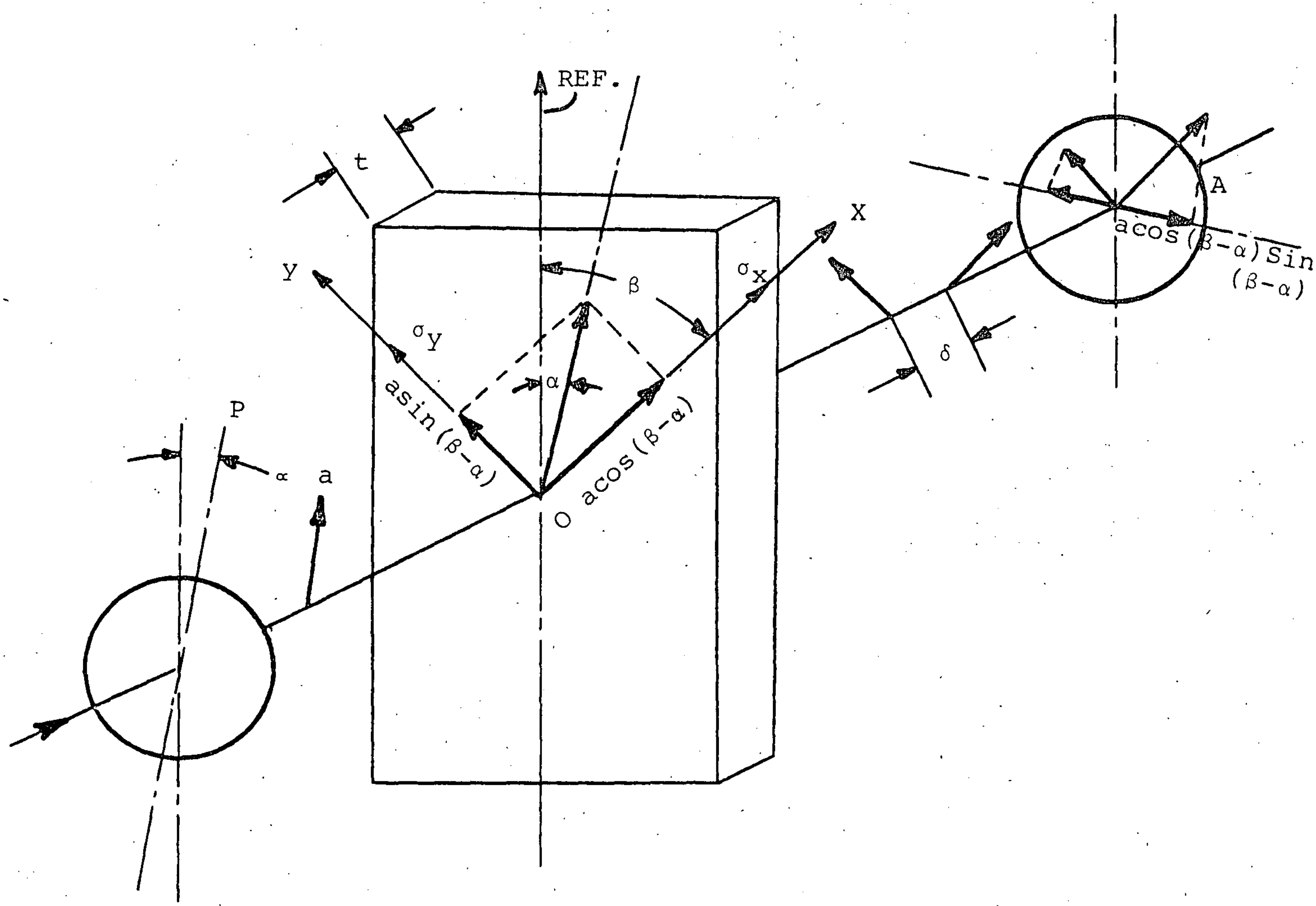

PLANE POLARISCOPE FIGURE 2

If the strain intensity along "x" and "y" is ε_x and ε_y and the speed of the light vibrating in these directions is V_x and V_y respectively, the time necessary to cross the plate for each of them will be t/V, and the relative retardation between these two beams is:

$$\delta = C\left(\frac{t}{V_x} - \frac{t}{V_y}\right) = t\,(n_x - n_y)$$

Brewster's Law established that: "The relative change in index of refraction is proportional to the difference of principal strains", or:

$$(n_x - n_y) = K\,(\varepsilon_x - \varepsilon_y)$$

The constant K is called the "strain-optical coefficient" and characterizes a physical property of the material. It is a dimensionless constant usually established by calibration and may be considered similar to the "gage factor" of resistance strain gages. Combining the expressions above, we have:

$$\delta = tK\,(\varepsilon_x - \varepsilon_y) \text{ in transmission}$$

$$\delta = 2tK(\varepsilon_x - \varepsilon_y) \text{ in reflection polariscope}$$
(light passes through the plastic twice)

Consequently, the basic relation for strain measurement using the photoelastic coating technique is:

$$\varepsilon_x - \varepsilon_y = \frac{\delta}{2tK}$$

Due to the relative retardation δ, the two waves are no longer simultaneous when emerging from the plastic. The analyzer A will transmit only one component of each of these waves (that is parallel to A) as shown on Figure 2. These waves will interfere and the resulting light intensity will be a function of:

- the retardation δ
- the angle between the analyzer and direction of principal stresses $(\beta - \alpha)$

In the case of a Plane Polariscope, the intensity of light emerging will be (Lever B on instrument set at "D" position):

$$I = a^2 \sin^2 2(\beta - \alpha) \sin^2 \frac{\pi\delta}{\lambda}$$

Adding quarter-wave plates in the path of light propagation, transforms the instrument into a <u>"Circular Polariscope"</u> (lever B on instrument set on "M" position). The emerging light intensity is now independant of the direction of principal stresses:

$$I = a^2 \ \mathrm{Sin}^2 \ \frac{\pi\delta}{\lambda} \quad \text{(See Figure 3)}$$

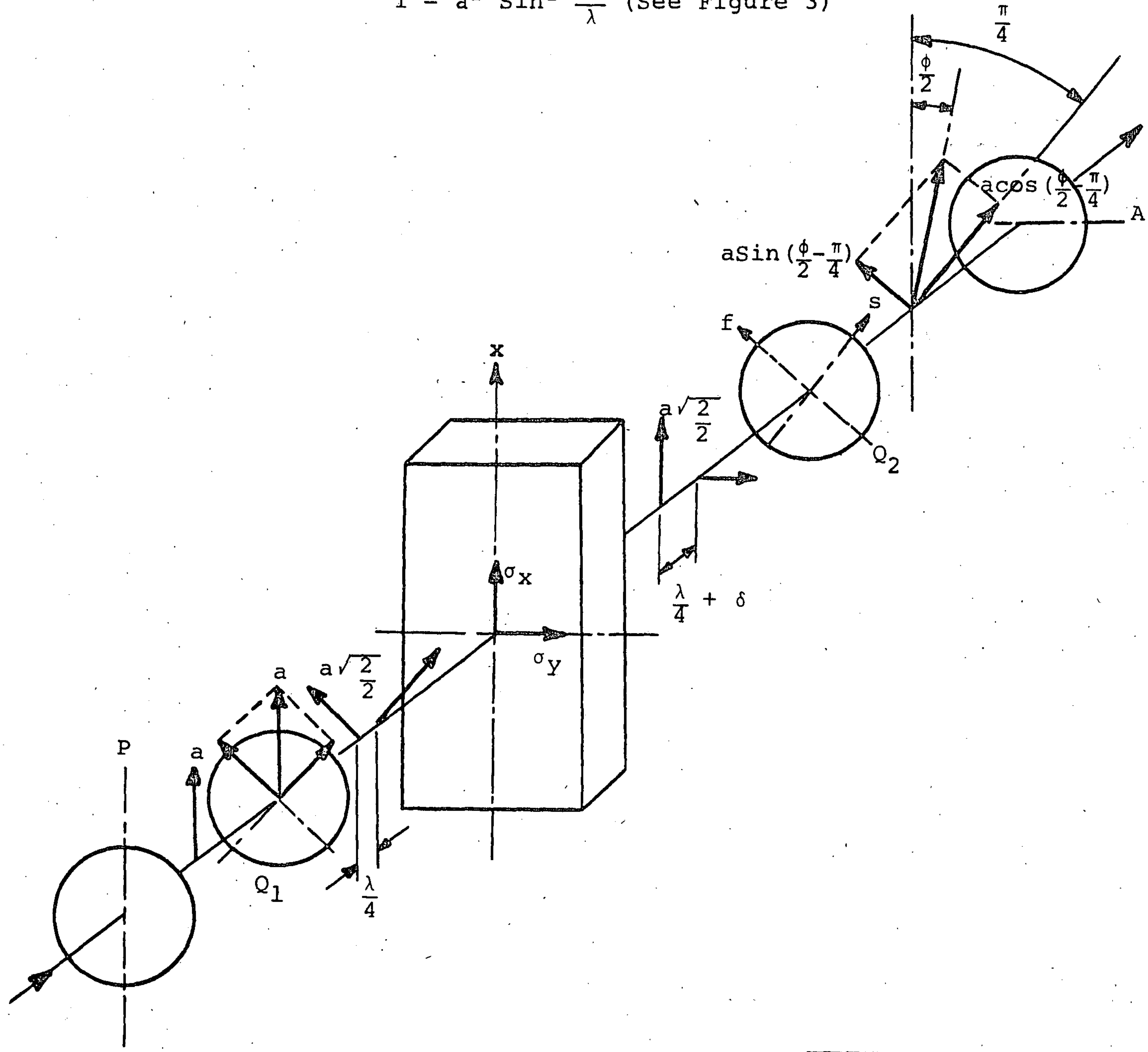

CIRCULAR POLARISCOPE

FIGURE 3

The expressions shown above basically describe the function of a polariscope.

In a "Plane Polariscope", directions of the principal stresses are measured. The light intensity becomes zero when $\beta - \alpha = 0$ (see Figure 2), or when the crossed polarizer-analyzer is parallel to the direction of principal stresses.

In the "Circular Polariscope", the light intensity becomes zero when $\delta = 0$, $\delta = 1\lambda$, $\delta = 2\lambda$ . . . . , or in general:

$$\delta = N\lambda$$

Where N is 1, 2, 3, etc.

This number N is also called fringe order and basically it expresses the size of δ. The wave length is selected:

$$\lambda = 22.7 \times 10^{-6} \text{ in.}$$

The retardation, or photoelastic signal is simply described by N. As an example, if N = 2:

$$(\delta) \text{ Retardation} = 2 \text{ fringes}$$

$$\text{or} \quad \delta = 2\lambda$$

$$\text{or} \quad \delta = 2 \times 22.7 \times 10^{-6} \text{ in.}$$

Once $\delta = N\lambda$ is known, the strains are:

$$\varepsilon_x - \varepsilon_y = \frac{\delta}{2tK} = N\frac{\lambda}{2tK} = N \times f$$

where f contains all constants and N is the result of measurements.

SECTION 1

BASIC ANALYZER

DESCRIPTION AND ASSEMBLY

1.0 DESCRIPTION

The Basic Analyzer, Model 031, consists of two ball-bearing mounted Polarizer-Quarter Wave Plate Assemblies attached to a common frame, and mechanically connected so that they rotate in unison (See Figure 4). The assembly (1) is equipped to receive the special light source (3), and the assembly (2) is provided with measurement scales. The instrument is also equipped to accept many new accessories which greatly increases the versatility of the instrument and permits any photoelastic coating task to be accurately performed.

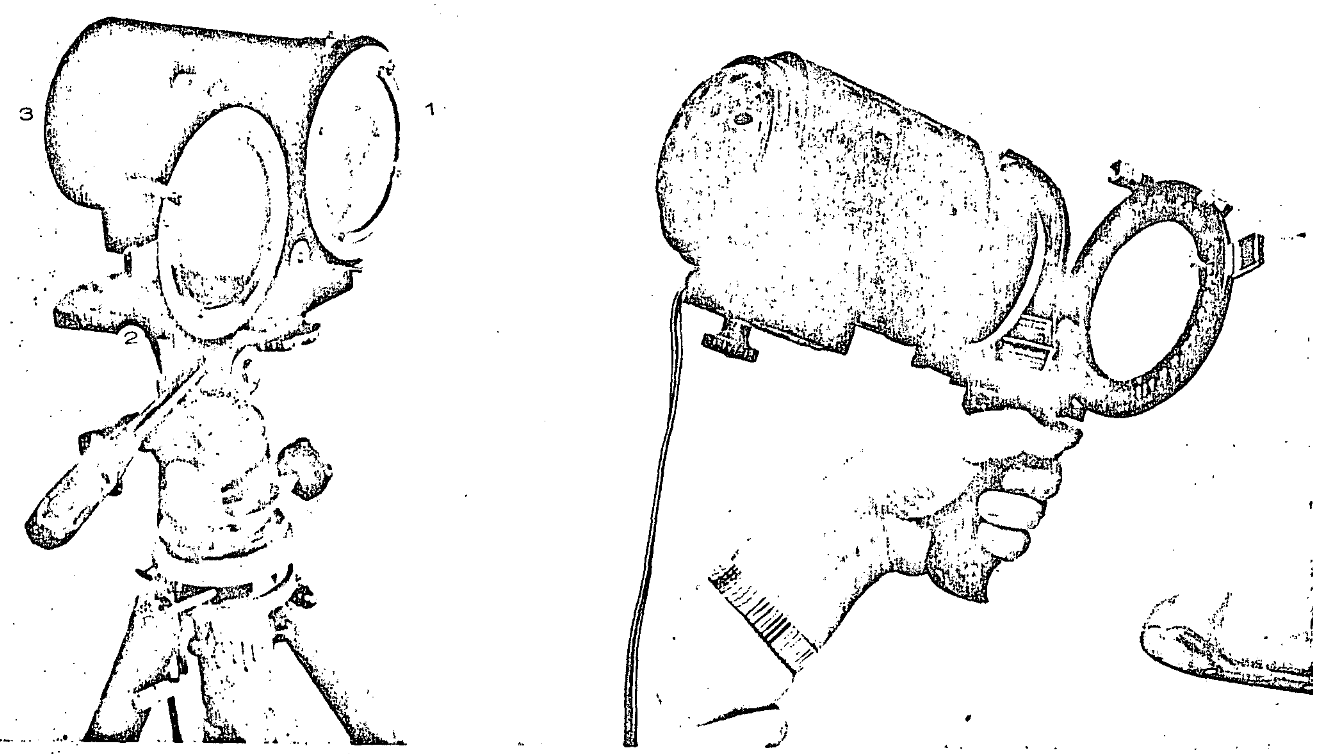

FIGURE 4

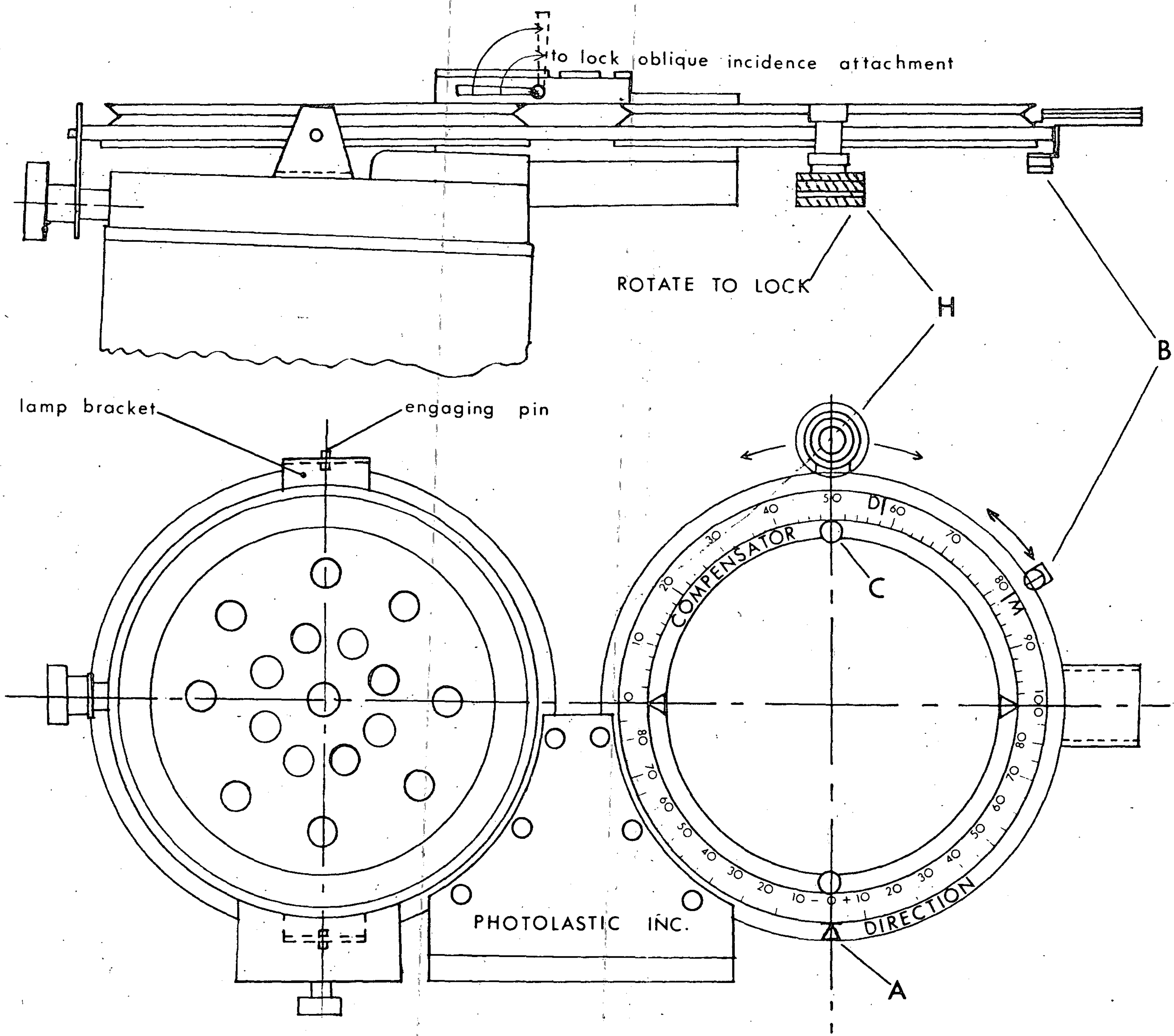
to lock oblique incidence attachment
ROTATE TO LOCK
H
B
lamp bracket
engaging pin
D
COMPENSATOR
C
M
PHOTOLASTIC INC.
DIRECTION
A

FIGURE 5

The Basic Analyzer measures three major pieces of data:

1. The directions of the principal strains or stress
2. The magnitude and sign of the tangential stress at free boundaries, or in any region of uniaxial stress condition
3. The magnitude of the difference of the principal strains or stress in bi-axial state

The instrument may be hand-held or mounted on a tripod. The hand-held feature is used to inspect areas for possible detailed analysis by quickly scanning the entire test part. The portable operation is also used when a large number of point by point measurements are to be made on a structure, and for analyzing hard-to-see areas where a tripod would be awkward. In other cases, when attention is concentrated on only a few areas, or when a laboratory test is being conducted on small parts, the instrument will usually be mounted on the tripod.

1.1 ASSEMBLY

To prepare the polariscope for operation by hand or on its tripod, proceed as follows:

1.) Remove the polariscope, light housing, and handle from the instrument case.
2.) Dust off the meter unit, using a soft tissue or cloth wet with alcohol.
3.) Mount the light housing on the meter by engaging the holes in the mounting brackets to the pins fixed to the polarizer frame. Adjust the angle to a slightly convergent position for normal incidence measurements (See Figure 5).
4.) Place the bulb in the rear position. The normal life of the lamp (type DFA TRU-FOCUS Base 150W, 120V, T12) is 15 hours.
5.) Extend the legs of the tripod to the desired length and lock them tightly if the instrument is to be used on its tripod.
6.) Mount the handles locking the tripod platform. Note: The handles are not identical; the longer one is used to control the forward tilt, the shorter to control lateral tilt.
7.) Place the analyzer directly on the tripod platform and mount in place using the 1/4"-20 thread screw provided.
8.) Attach the meter to the grip-handle for hand-held operation.

SECTION 2

MEASUREMENT OF DIRECTIONS OF PRINCIPAL STRAINS

2.0 INTRODUCTION

The principal strain directions are always measured with reference to an established line, axis, or plane. Therefore, the initial step for the determination of the direction of principal strains (or stresses) will be to select a convenient reference. In most cases, the reference direction is suggested immediately, like an axis of symmetry of the test part or structure; in other cases, a vertical or horizontal line will suffice.

2.1 MEASUREMENT OF DIRECTIONS AT A POINT

When the directions of the principal strains ε_x and ε_y are to be measured at a point, the following procedure shall be followed:

1.) Assemble the instrument, as discussed in Section 1.2.
2.) Connect the light source to a 110 volt outlet and switch the light on.
3.) Direct the light beam toward the point of interest on the part or structure being studied. The suggested distance between the instrument and the observed areas is between 1 1/2 feet and 8 feet.
4.) Orient the instrument so that one of its axis is parallel or perpendicular to the selected reference direction. Consequently, with the direction arrow reading 0°, the axes of polarization will be parallel or perpendicular to the reference.
5.) With the direction and compensation scale on the meter set at zero (Figure 5), check the unloaded part for an initial pattern which may be due to improper application of the plastic, or stresses created during the test assembly operation. If a colored pattern appears, a zero reading should be obtained before loading (Section 5, Part 5.1). In most cases, however, the plastic on the unloaded part will appear black or dark bluish, and a zero reading will not be necessary.
6.) Proceed with the loading of the part (if possible, incremental loading is recommended).

7.) Move knob "B" from "M" (magnitude) to "D" (direction) position (See Figure 5). This aligns the axes of the quarter-wave plates parallel to the direction of the polarizer and analyzer, and the meter is transformed from a "circular" to a "plane" polariscope (quarter-wave plates are optically removed from field).

8.) If measurable strains do exist, a pattern of color and black lines (or areas) will be observed. The bands of equal color (isochromatic fringes), will be discussed in measurements of magnitudes of strains (Section 3). The black lines or areas, are of primary interest to us in this discussion and they indicate:

1. Areas of zero shear strain $\varepsilon_x - \varepsilon_y = 0$ ($\delta = 0$)
2. Areas of equal direction of principal strains

Along such a black line, the direction of principal strains (or stresses) is the same as the axis of polarizer-analyzer. In order to differentiate between these two cases, loosen the lock located on handle "H", rotate the polarizer-analyzer assembly and observe any black areas or lines in the field. Upon rotation, any areas or lines that remain black and stay in a fixed position are those places where the difference of the principal strains is zero. The black lines which move as the rotation is progressing are termed "Isoclinics", and are used to determine the direction of the principal strains ε_x and ε_y. At every point on a isoclinic line, the directions of the principal strains are the same. These directions are shown by the angular position of the polarizer and analyzer (arrow "A" on Figure 5).

9.) With a grease pencil, mark a cross on the plastic coating defining the point of interest on the test part, and identify the marked point with a letter or number.

10.) By means of handle "H", rotate the polarizer-analyzer until a black line (Isoclinic) crosses over the marked point. Now, the axes of the polarizer and analyzer are parallel and perpendicular to the direction of the principal strains ε_x and ε_y at the point, and their position with respect to the selected reference is shown on the meter (Figure 6). The arrow on the meter shows the rotation in degrees of the polarizer-analyzer assembly with respect to the reference line on the part, and indicates the direction of the principal strains.

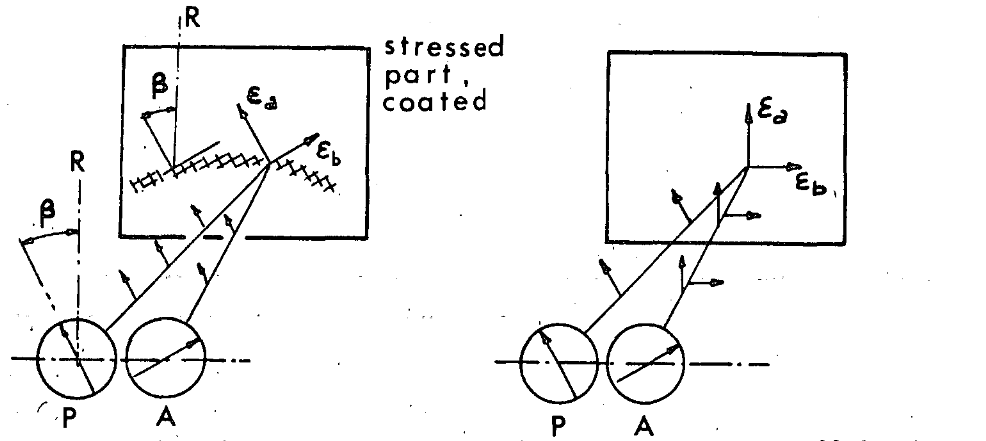

At every point where P - A are parallel to the principal stresses, a black line is observed.

When P - A are not parallel, the light is transmitted and colors are seen.

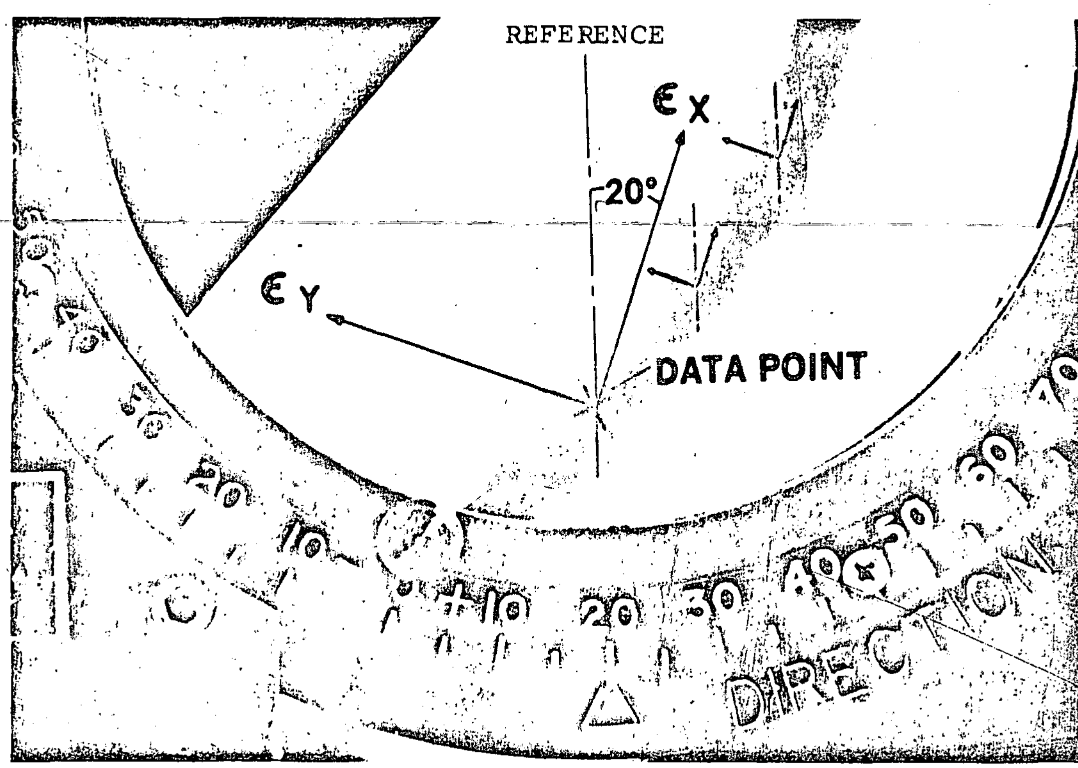

FIGURE 6

When bringing the isoclinic to the point of measurement, the polarizer-analyzer rotation may be either clockwise or counter clockwise. Therefore, in order to record the data without ambiguity, the angular rotation must be accompained with the correct sign. The clockwise rotation is considered positive and counter clockwise negative.

2.2 MEASUREMENT OF DIRECTIONS OVER LARGE AREAS

In many cases it is necessary to know the directions of the principal strains over the entire area coated, instead of at individually selected points. The initial procedure is to repeat steps 1 through 8, as previously described, for determining the principal strain directions at a point. After completing step 8, proceed as follows:

9.) By means of handle "H", rotate the polarizer-analyzer assembly to the angular positions 0°, 15°, 30°, 45°, 60°, 75°, and 90°, as indicated by arrow "A" on the meter (Figure 5). At each angular position, the black isoclinics will be observed in a different location (except for the 90° position which will be the same as that observed at 0°).

10.) With a grease pencil, trace the isoclinic lines directly on the part at each angular position, and assign to each line its corresponding direction as indicated by arrow "A" on the meter.

11.) After the isoclinics have been traced onto the plastic, transfer their positions onto onion-skin paper. The isoclinic recording can also be accomplished by photography, which is a faster and accurate technique. The photographic procedure follows:

a. Install the camera and obtain a photograph for each isoclinic at every angular position. Before taking each photograph, mark in a convenient location in the field of view, the corresponding angle for identification. Also, be careful not to alter the position of the camera from frame to frame. A color film that directly yields slides should be used.

b. Next, project the slides of the isoclinics (0°, 15°, 30°, etc.) one by one on a plain sheet of paper, and then carefully trace the isoclinics on the paper as each slide appears.

12.) Following the tracing of the family of isoclinics on paper, the isostatic flow lines can be sketched, these lines reveal the directions of the principal strains ε_x and ε_y at every location of the coated part. Figure 7 illustrates the photographs of the isoclinics in a ring subjected to diametral compression, and Figure 8 shows how these isoclinics, from a segment of the ring, were transferred on paper from which the isostatics or principal strain directions were constructed.

If the isoclinics are sharp and narrow, it means the directions of ε_x and ε_y are varying rapidly from one location to another. If the isoclinics are broad black bands or areas, the directions ε_x and ε_y are varying slowly and the boundary surrounding the whole isoclinic should be marked (not merely the center). In the case of the tensile specimen of constant cross section an isoclinic will be seen over the entire area when the axes of polarization coincide with the axes of the specimen, since the direction of ε_x is the same at every point.

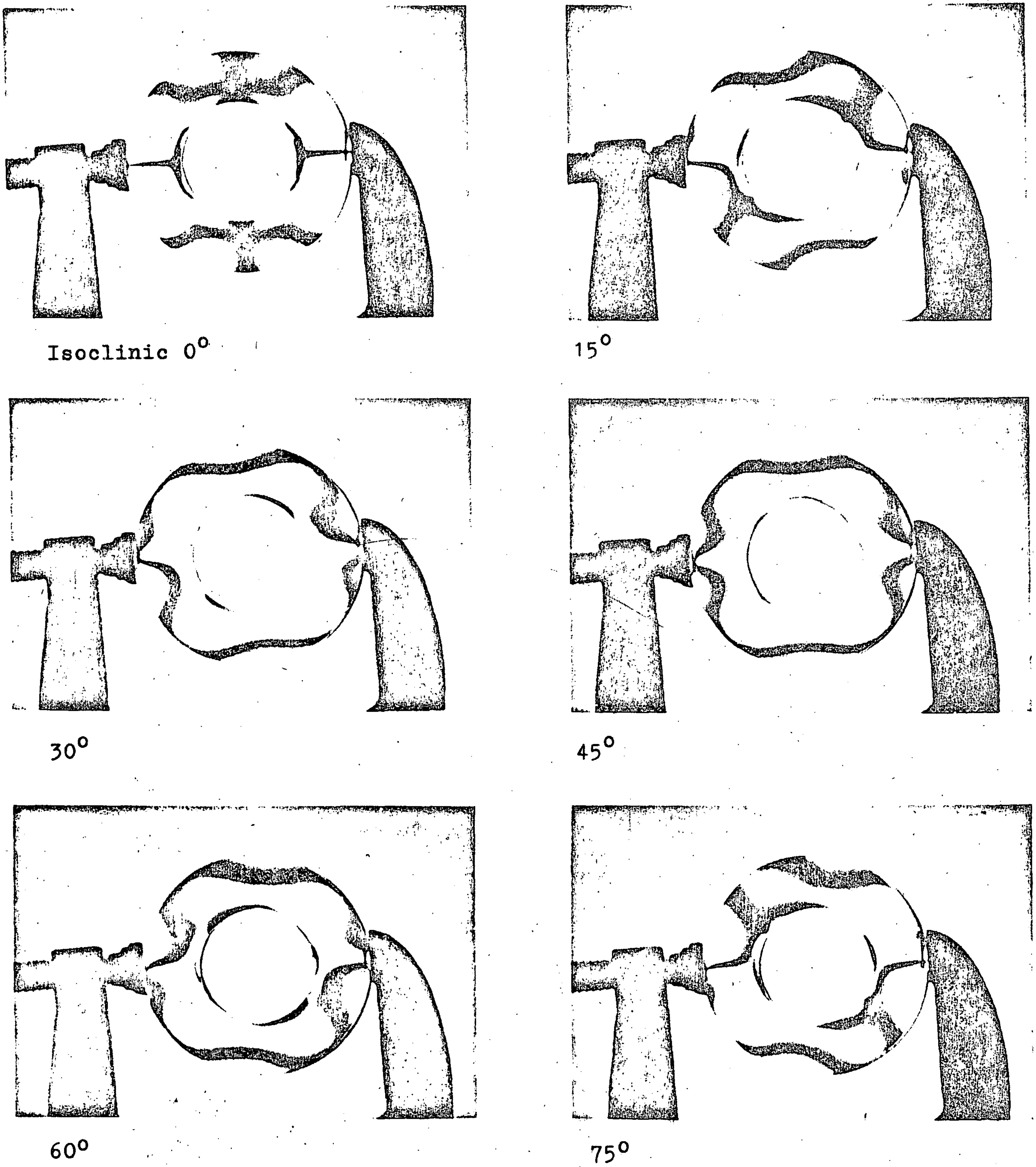

FIGURE 7

ISOCLINICS

locus of points of equal direction

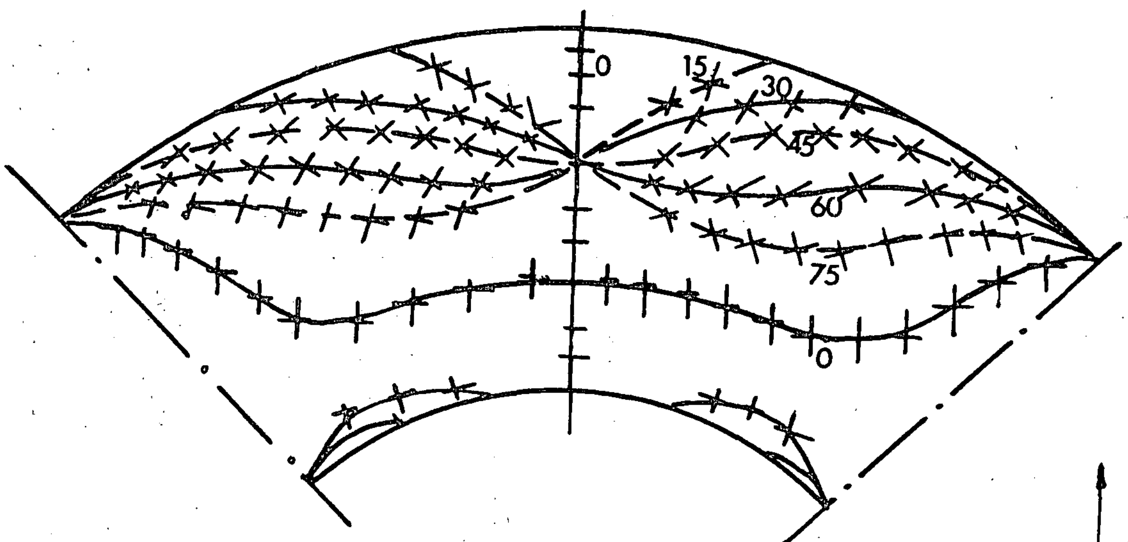

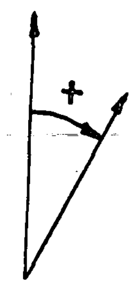

ISOSTATICS

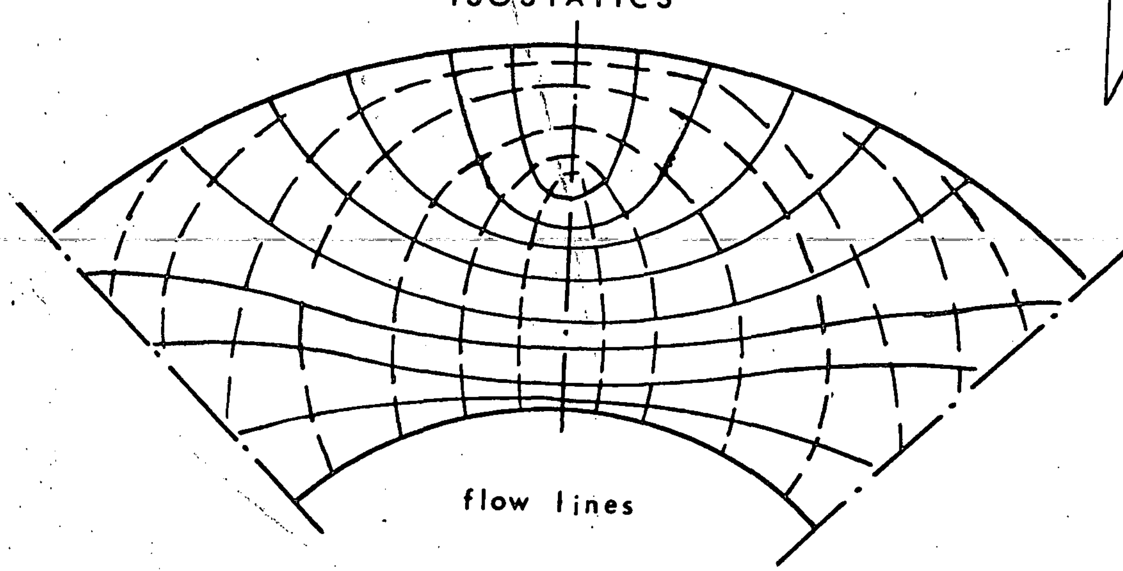

FIGURE 8

SECTION 3

MEASUREMENTS IN NORMAL INCIDENCE-INTERPRETATION OF STRESS DISTRIBUTION

3.0 INTRODUCTION

Experimental stress analysis is not always reduced to measuring the magnitude of stress. In fact, the ability to see and interpret the complete stress field is one of the important time and money saving advantages of the photoelastic coating technique. If the part being stress analyzed is being done so because of actual service failures, the display of the complete stress distribution on the part will usually offer suggestions on how to modify designs to prevent failures. Similarly, the analysis of the complete stress distribution in prototype parts could prevent potential design errors, which if not corrected, may result in expensive repairs during service operation.

The photoelastic pattern also yields valuable design information, on how to modify the part to make it lighter, and at the same time less stressed. In addition, the visual stress display shows the relative importance of various load modes applied. Often such design information is revealed not by highly stressed areas, but by low stressed areas where material could be removed. After learning how to interpret the overall stress distribution, measurement of the magnitude of the stress is then accomplished at the points of interest by the methods described herein.

3.1 BASIC DATA ON PHOTOELASTIC MEASUREMENTS

When a coated specimen is subjected to stresses, the surface strains are the same in plastic as in the coated parts:

ε_x, ε_y are principal strains in plastic (and metal)

β is the direction between ε_x and selected reference

The stresses in the part are established from strain in the elastic range by Hooke's Laws:

$$\sigma_x = \frac{E}{1-\mu^2} \quad (\varepsilon_x + \mu\varepsilon_y)$$

$$\sigma_y = \frac{E}{1-\mu^2} \quad (\varepsilon_y + \mu\varepsilon_x)$$

and

$$\sigma_x - \sigma_y = \frac{E}{1+\mu} \quad (\varepsilon_x - \varepsilon_y)$$

At every point we receive the photoelastic signal, which is the retardation between two light beams, one polarized ε_x, the other along ε_y:

$$\delta = N\lambda = 2tK \; (\varepsilon_x - \varepsilon_y)$$

where δ is the retardation (in.)
λ is the wave length (in white light $\lambda = 22.7 \times 10^{-6}$ in.)
N is called "fringe order" which we are measuring

The measured number N is then used for all the data reduction:

$$\varepsilon_x - \varepsilon_y = N \frac{\lambda}{2tK} = N \times f$$

The "fringe value" f is obtained from the plastic applied.

$$f = \frac{\lambda}{2tK} = \frac{11.35 \times 10^{-6}}{t \; K}$$

where t is the thickness of coating (inches)
K is the sensitivity of plastic, supplied by the manufacturer (for K of various plastic, see Bulletin P-1120)

The difference of principal stresses in the structure is:

$$\sigma_x - \sigma_y = (\varepsilon_x - \varepsilon_y) \frac{E}{1+\mu} = Nf \frac{E}{1+\mu}$$

Note that in NORMAL INCIDENCE measurements, the quantity measured is the DIFFERENCE OF PRINCIPAL STRESSES $\sigma_x - \sigma_y$.

In many practical applications (edges, uniaxial field, corners, long beams), one of the principal stresses is zero. In all those cases we have:

$$\sigma = N \frac{fE}{1+\mu}$$

In the case of a biaxial stress field two measurements are needed to determine the individual principal stresses σ_x and σ_y (See Section 4 on Oblique Incidence Measurements).

3.2 INTERPRETATION OF PHOTOELASTIC PATTERN-IDENTIFICATION OF FRINGES

The photoelastic pattern appears as a colorful map of lines of equal color (isochromatic lines or finges). Every equal color line represents a constant level line of N (or $\delta = N \times 22.7 \times 10^{-6}$ in.). The first logical step in analysis is to assign to those level lines their order (example N = 1, 2, 3, etc.) to identify fringe orders.

The following experiment will greatly simplify the understanding of identification of fringes:

EXPERIMENT FOR ILLUSTRATION OF PHOTOELASTIC READING AND INTERPRETATION OF STRESS DISTRIBUTION

Prepare an aluminum cantilever beam 1/8" x 1" x 10" long for analysis by coating the beam on one side with Photolastic Plastic Type PS-2 (1/8" thick). Next, clamp the beam, coated side up, to the edge of a bench or table. On the other end, hang a 5 pound weight using a wire or cable (See Figure 9). Set-up the instrument so that the polarizer-analyzer assembly is looking down on the coated beam (the handle "H" being aligned with the long axis of the beam). Now set all dials of the analyzer on zero and move knob "B" to position "M" (magnitude) setting (See Figure 5). Make sure the beam is illuminated by the light coming from the instrument.

The retardation is increasing proportional to the stress. Every time the retardation is:

$$\delta = 1,\ 2\lambda,\ 3\lambda\ .\ .\ 4 \times \lambda,$$

a particular wave disappears and the complementary color is seen. As an example, when $\delta = 25 \times 10^{-6}$ in. ($\delta = \lambda$ red), red disappears and green is observed.

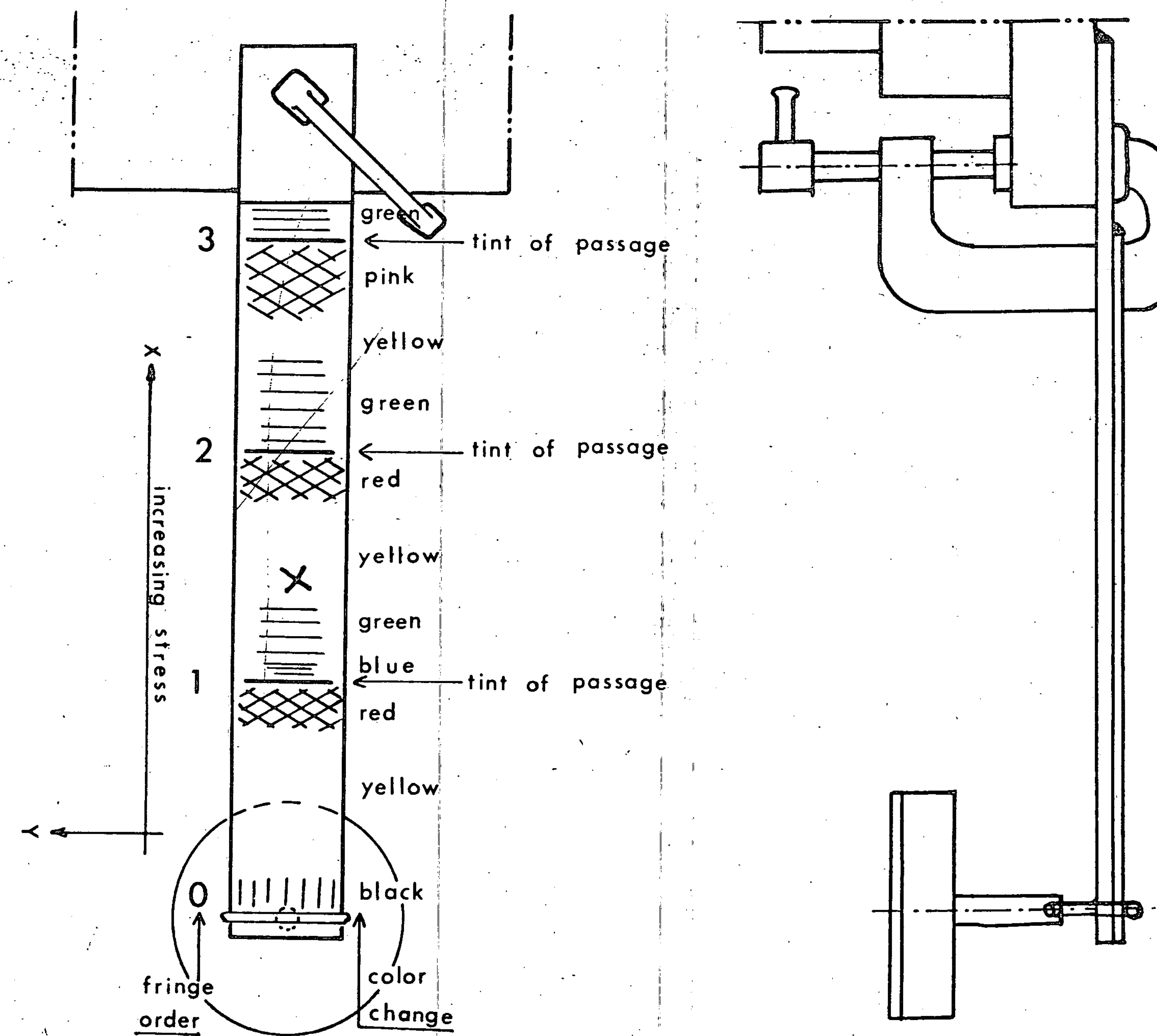
green
3
tint of passage
pink
X
yellow
green
2
tint of passage
red
increasing stress
yellow
green
blue
1
tint of passage
red
yellow
Y
0
black
fringe order
color change

FIGURE 9

The following table explains the sequence of color observed:

RETARDATION 10^{-6} IN.	COLOR OBSERVED	N
0	Black	0
12	Yellow	
18	Red	
22.7	*1st Fringe	1
25	Blue-Green	
35	Yellow	
40	Red	
45.4	*2nd Fringe	2
50	Green	
57	Yellow	
63	Red	
68.1	*3rd Fringe	3
73	Green	

Observe the colored pattern appearing on the cantilever beam and compare the color sequence to that described above and shown in Figure 9. Note how the bands of color change progressively from the loaded end of the beam (zero stress) to the clamped end (high stress). The color sequence observed is black, yellow, red, blue, yellow, red, green, yellow, red, green. The color transition from the red to the blue (1st Fringe) and from the red to green (2nd and 3rd Fringes) is sharply marked.

Now starting from the black area where $\varepsilon_x - \varepsilon_y = 0$ (loaded edge of the beam), trace a line with a grease pencil at the 1st, 2nd, and 3rd fringe locations. Note that the first fringe falls between red and blue, but in the subsequent higher order fringes, the blue color disappears and is replaced by green. Repeat the exercise several times tracing the line so that it is between the red and blue or red and green color.

The fringes are related to increasing strain as follows:

EXAMPLE: $\left.\begin{array}{l} t = .100 \\ K = .15 \end{array}\right\} f = 757\mu''/''$

Along the black fringe	N=0	$\varepsilon_x - \varepsilon_y = 0$	$\varepsilon_x - \varepsilon_y = 0$
Along the first fringe (RED-BLUE)	N=1	$\varepsilon_x - \varepsilon_y = f\mu''/''$	$\varepsilon_x - \varepsilon_y = 757\mu''/''$
Along the second fringe (1st RED-GREEN)	N=2	$\varepsilon_x - \varepsilon_y = 2f\mu''/''$	$\varepsilon_x - \varepsilon_y = 1514\mu''/''$
Along the third fringe (2nd RED-GREEN)	N=3	$\varepsilon_x - \varepsilon_y = 3f\mu''/''$	$\varepsilon_x - \varepsilon_y = 2271\mu''/''$

One can now see the significance of being able to recognize fringe orders. Once we master this first and very important step, the initial study of the overall strain distribution on a test structure is straightforward. The fringes are continuous bands (occasionally dots) ending at boundaries or making continuous loops. They do not intersect at any point. They follow in continuous sequence (if the 1st and 3rd orders are observed, the 2nd must be in between). Once one fringe is recognized (usually "0" or 1st), follow toward increasing strain level (yellow-red-green), and locate the 2nd then the 3rd, etc. Always remember the sequence for increasing strain: yellow-red-green-yellow-red-green . . . If the colors go green-red-yellow-green-red-yellow, then the strain is decreasing. In case doubt remains concerning the correct identification of the integral order fringes, use of the Models 032 and/or 232 Compensator (Section 3.4) provide a means for positive identification.

If the fringes are observed as tightly grouped loops confined to a single area (such as would be found at a notch or sometimes around holes), it means that the strain varies rapidly from one point to another resulting in a stress concentration. On the other hand, a single uniform color may cover a vary large portion of the test part, or in the case of a tensile specimen ideally aligned, the entire surface of the part will exhibit a solid color. This type of situation tells us that the strain is behaving uniformly over the entire area, neither increasing or decreasing from one point to another.

In summary, the stress distribution can easily be studied by simply being able to recognize fringes, their absolute order, and location with respect to one another on the structure or test part being analyzed.

3.3 MEASUREMENTS AT A POINT

It has been shown that in the first step of measurement one is observing the whole area and assigning to every fringe its order (N = 1, 2, 3, etc.). At every point of a fringe, N is then known and therefore:

$$\varepsilon_x - \varepsilon_y = f \times N$$

In general, the point of interest on the structure will fall between fringes, and it will be necessary to establish "fractional order" or fraction of a fringe. The technique used is called "compensation". Two basic methods are used:

1) TARDY COMPENSATION using the rotatable analyzer built into the 031 Instrument.

2) ABSOLUTE COMPENSATION or null balance, using Compensator Models 232 or 332.

3.3.1 TARDY COMPENSATION

The Tardy Compensation is a relatively fast and simple method. However, the method requires an experienced operator to be fool-proof, and if the rules that are given below are not followed exactly, serious mistakes are made. The principal of the method is shown on Figure 10.

WHEN THE POLARIZER AND ANALYZER ARE ALIGNED WITH THE DIRECTION OF PRINCIPAL STRESSES, AND THE QUARTER-WAVE PLATES ARE AT 45° ("M" POSITION), A ROTATION α OF THE ANALYZER WILL MOVE A FRINGE TO A POSITION WHERE THE FRACTIONAL ORDER IS $\frac{\alpha}{180}$ (TARDY COMPENSATION).

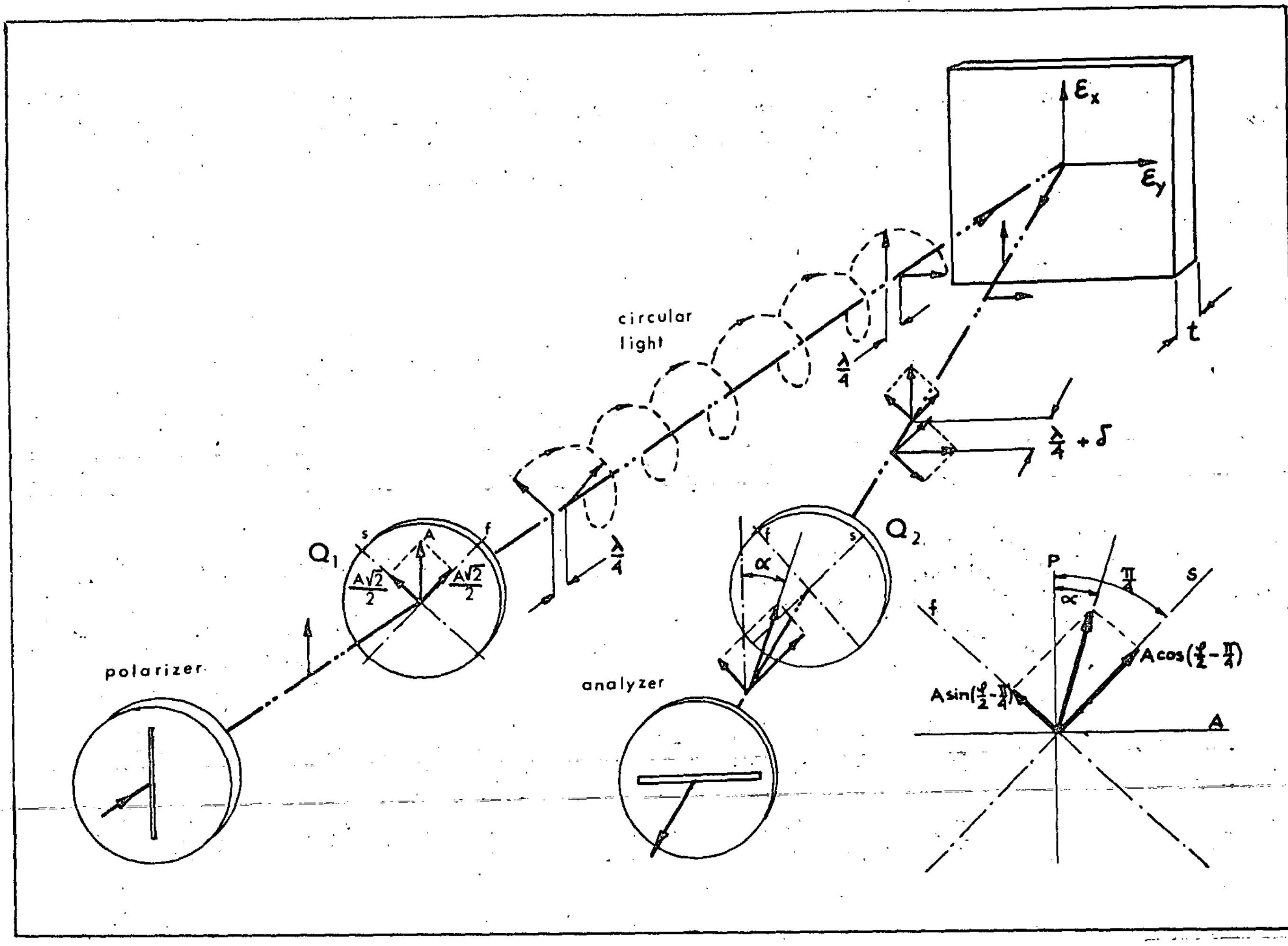

FIGURE 10

3.3.2 OPERATIONAL PROCEDURE: HOW TO MEASURE FRACTIONAL FRINGE ORDERS USING TARDY METHOD

Prepare a cantilever beam test specimen (See Section 3.2). Load the beam with a 5 pound weight, and set-up the instrument to observe the beam as described previously. This specimen will now be used to illustrate all the operational steps necessary to measure fractional fringe orders using Tardy Compensation:

1. Switch the instrument to the "D" position by means of lever "B" (Plane Polariscope set-up).

2. Unlock the knob "H" and rotate the Polarizer-Analyzer Assembly until an isoclinic comes to the point of measurement. As explained before, the isoclinic is a black line or area, and its thickness depends only on the variation of direction. In the cantilever beam experiment the isoclinic will cover the whole beam, since directions are uniform.

When step 3 is completed, the handle "H" is aligned with direction X of principal stress σ_X. The stress σ_Y is perpendicular to it. The arrow A reads the Angle β between the reference selected and direction X.

NOTE: 90° rotation of polarizer will once again bring the isoclinic to the point.

One can, therefore, choose either one of the principal stresses as direction X.

4. Once step 3 is completed, tighten the knob H. Switch the lever B to "M" position (CIRCULAR POLARISCOPE). The isoclinic fringes are now eliminated, and a colorful pattern appears. Recognize fringes and assign to every fringe its order. Trace with a grease pencil fringes 0, 1, 2, 3, etc. In many practical applications, the recognition of fringes is simple. Sometimes the Compensator Model 032 or 232 should be used, as explained later. Choose on the cantilever beam a point between fringe 1 and 2. In most cases, the point will be between n (lower order) and n + 1 (higher order). Mark the point by tracing a thin cross (+) directly on the plastic using a scriber or grease pencil.

5. Rotate the analyzer clockwise by means of knob C. The fringes will move. Observe the motion of fringes carefully. The clockwise rotation of the analyzer rotation is graduated on the scale 0 to 100. Rotate until a fringe arrives at the selected point of measurement (red on one side, green on the other side, see Figure 11). Read directly the fraction r as shown on the compensation scale (in hundreds of a fringe).

6. If lower order fringe moves to the point (fringe n), the total reading will be:

$$N = [n + \text{fraction}] = [n + r] \text{ and } N > 0$$

If higher order fringe moves to the point (fringe n + 1) the total reading will be:

$$N = -\ [(n + 1) - \text{fraction}] = -\ [n + 1 - r] \text{ and } N < 0$$

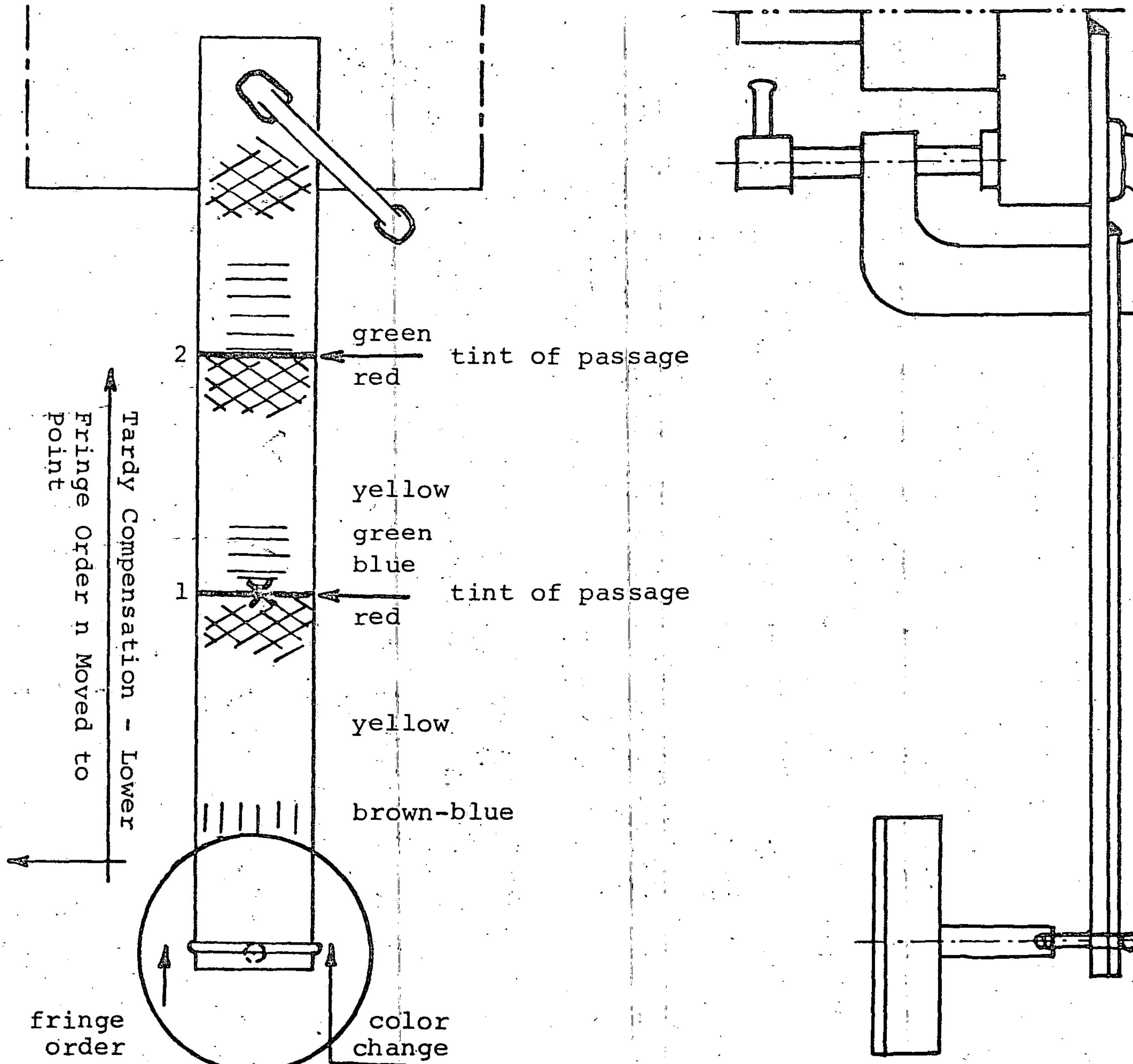
green
2
tint of passage
red
yellow
green
blue
1
tint of passage
red
yellow
brown-blue
Tardy Compensation - Lower Fringe Order n Moved to Point
fringe order
color change

FIGURE 11

In either case: $\varepsilon_x - \varepsilon_y = N \times f$

$$\sigma_x - \sigma_y = Nf \frac{E}{1+\mu}$$

(On the cantilever beam the "first" or lower order fringe n will move to the point and therefore the total reading will be N = n + r a positive number.)

NOTE:

IT IS VERY IMPORTANT TO RECOGNIZE AND UNDERSTAND THE SIGN CONVENTION USED WHEN OBTAINING NORMAL INCIDENCE MEASUREMENTS AS DESCRIBED ABOVE. THE MOST IMPORTANT POINT TO REMEMBER IS THAT ε_x IS NOT NECESSARILY THE GREATER PRINCIPAL STRAIN OR LARGER THAN ε_y.

ACCORDING TO THE SIGN CONVENTION ESTABLISHED, AFTER BRINGING AN ISOCLINIC TO THE POINT OF INTEREST, THE HANDLE "H" IS DEFINED TO BE ALIGNED WITH ε_x WITHOUT REGARD TO THE FACT THAT ε_x MAY NOT BE THE GREATER PRINCIPAL STRAIN. REMEMBER IN NORMAL INCIDENCE READINGS, WE ARE PRIMARILY CONCERNED WITH THE SIGN OF THE DIFFERENCE OF $\varepsilon_x - \varepsilon_y$, AND NOT WHETHER ε_x IS GREATER THAN ε_y OR VICE-VERSA. THE SEPARATE VALUES AND SIGN OF THE INDIVIDUAL PRINCIPAL STRAINS ε_x AND ε_y WILL BE DISCUSSED UNDER OBLIQUE INCIDENCE MEASUREMENTS IN SECTION 4.

A typical example of the sign convention used can be demonstrated with the cantilever beam. First, align the handle "H" with the long axis of the beam. Now rotate the compensator in a clockwise direction and bring the lower order fringe to the point. (With our set-up, we will observe the 1st fringe moving to the point.) Since we already know that σ_x is the longitudinal stress at the point (σ_x is tensile) and the transverse stress is zero, we will read $(\sigma_x - \sigma_y)$ or $(\sigma_x - 0)$, a positive number. Now if we rotate handle "H" 90° so that it is perpendicular to the beam, and if we again rotate the compensator clockwise, the higher order or 2nd fringe will move towards the point. In this situation, we are reading $(\sigma_x - \sigma_y)$ or $(0 - \sigma_y)$, a negative number. Obviously, both measurements have the same magnitude but opposite sign.

To summarize, the procedure for measuring the difference of the principal strains at a point by the Tardy Compensation Method follows:

1. Trace a cross at the point or identify the point by some other means, or to the direction of the stress.
2. Determine the position of fringes n and n + 1 around the point.
3. Bring a isoclinic to the point and establish ε_x as being parallel to the position of the handle "H". Read the direction β (in degrees) of ε_x to the selected reference.
4. Rotate the compensator clockwise to bring a fringe to the point and read the fraction "r" on the scale.
5. If the lower order fringe (n) moves toward the point, the total reading will be:

$$N = n + r \text{ (positive)}$$

If the higher order fringe (n + 1) moves toward the point, the total reading will be:

$$N = -[(n + 1) - r] \text{ (negative)}$$

and

$$\varepsilon_x - \varepsilon_y = N \times f$$

$$\sigma_x - \sigma_y = Nf \frac{E}{1+\mu}$$

3.3.3 MEASUREMENTS IN UNIAXIAL STRESS FIELD AND ANALYSIS OF THE PRINCIPAL STRESS ACTING TANGENT TO A POINT ALONG A FREE BOUNDARY USING TARDY COMPENSATION

The sign and magnitude of the principal stresses in uniaxial field and also at a free edge or boundary can be determined directly under normal incidence since one of the stresses acting is zero.

The procedure is as follows:

1. Bring an isoclinic to the point of interest. The handle "H" must then be parallel to the boundary at the point.
2. Move knob "B" back to the "M" position.
3. Identify fringes (n) and (n + 1) on either side of the point.

4. Rotate the compensator in a clockwise direction. If the lower fringe order (n) moves toward the point of measurement, the sign of the stress is positive and the total reading will be N = n + r. If the higher order fringe (n + 1) moves toward the point, the sign of the stress is negative and the total reading will be N = - [(n + 1) - r]. In either case, the stress will be:

$$\sigma_x = Nf \frac{E}{1+\mu} \quad \begin{pmatrix} + \text{ tension} \\ - \text{ compression} \end{pmatrix}$$

Remember, direct measurement of the individual principal stresses in biaxial state of stresses can only be obtained by the addition of oblique incidence measurements (See Section 4).

3.4 ABSOLUTE COMPENSATION - MEASUREMENTS USING NULL BALANCE METHOD

The principal of Null Balance Method is considerably simpler, than the Tardy Method. To measure a photoelastic signal at a point, we simply add to the light path an identical calibrated signal equal in size but opposite in sign (See Figure 12). By doing this, the photoelastic signal at the point is completely cancelled to read zero. This method completely eliminates the need to recognize fringes or assign orders. When the calibrated compensator adds the opposite sign equal signal, the total is zero, and BLACK is restored at the point.

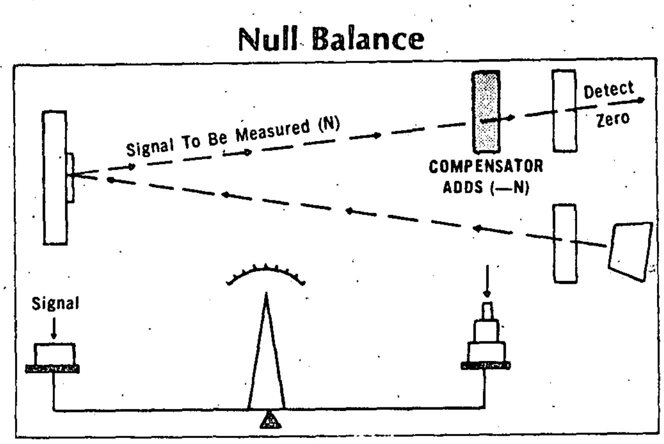

FIGURE 12

3.4.1 LINEAR COMPENSATOR, MODEL 032

The Compensator Model 032 consist of a wedge sliding in a fixed frame which is attached to the instrument as shown on Figure 13. The frame contains a window through which the part is observed. As the compensator slides in its frame, the fringes move on the specimen and numbers appear in the window. From a calibration chart (Figure 14), the signal N that the compensator adds is established. Since every point of the compensator exhibits a different N (N is varying linearly from one end to another) a "parallax" effect exists and for this reason, the linear compensator is used mostly for identification of fringes only as an auxiliary tool to the Tardy Method.

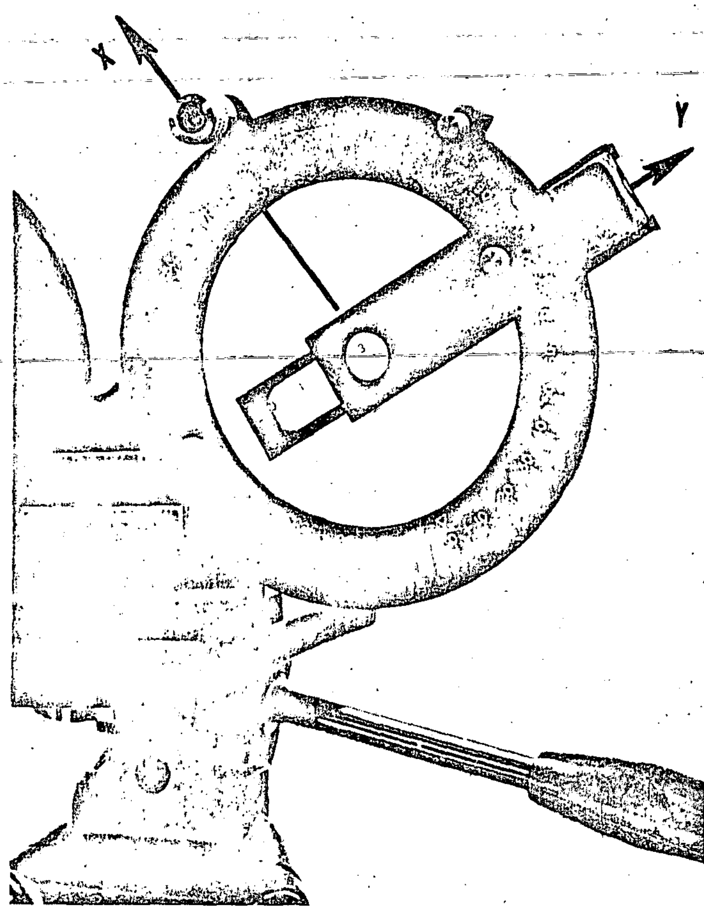

FIGURE 13

MODEL 032
LINEAR COMPENSATOR

CALIBRATION CHART

Reading on Scale	Fringe Order (N)
.50	1
1.20	2
1.90	3
2.60	4

FIGURE 14

To use the Linear Compensator for identifying an unknown fringe order at a point, proceed as follows:

1. Engage the compensator in its mount provided on the analyzer frame (See Figure 13).
2. Determine the direction of the principal strains at the point of interest as described in Section 2, Part 2.1.
3. After bringing the isoclinic to the point, lock the handle "H" in position and move the knob "B" back to the "M" (magnitude) position. Note that the handle now is aligned with **x** direction and the compensator with y direction.
4. Now observe the fringe at the point through the normal field of view. Next, observe the point through the compensator opening, and push the compensator in its slide (from right to left) until a black fringe appears at or near the point. Read the scale on the compensator and establish N from the compensator calibration chart.
5. The compensator fringes are positive. If $\sigma_x - \sigma_y$ is also positive, the compensator will add instead of subtract and no balance is possible. In this case, turn the handle "H" 90°, and repeat operation. Note that compensator will perform only when:

$$\sigma_x - \sigma_y < 0$$

3.4.2 UNIFORM FIELD COMPENSATOR, MODEL 232

The basic principal of the compensation is the same as described above, e.g. NULL BALANCE Method. The uniform field of the Model 232 Compensator eliminates parallax errors and provides better resolution than other compensation methods:

- It eliminates the need of recognizing fringes as in the TARDY Method
- It eliminates parallax errors
- It provides a numerical readout on a counter, from which the total reading N is determined, eliminating all possible mistakes of other methods.

To measure N using the Model 232 Compensator, proceed as follows:

1) Attach the compensator to the polariscope on mount provided and tighten the attachment knob (See Figure 15). Make sure the analyzer ring is set on zero on the fractional order scale.

2) Switch the lever "B" to "D" position. Release the knob "H" and rotate the polarizer-analyzer assembly until an isoclinic crosses the point where the measurement is to be made. Read the direction angle β. The handle "H" points now in x direction (σ_x) and the long axis of the compensator is in y direction.

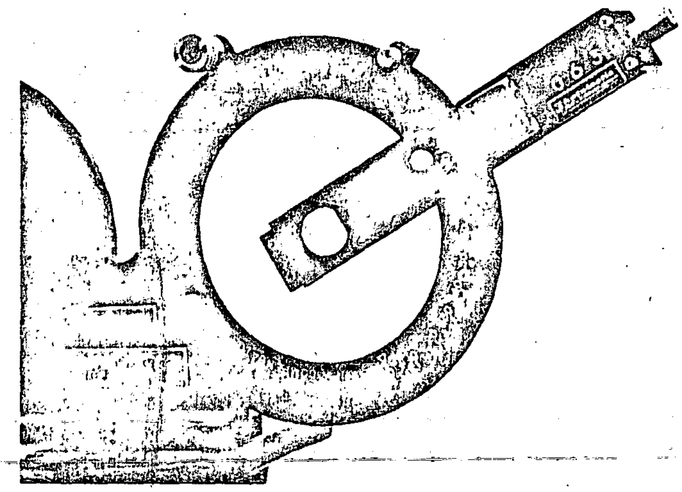

FIGURE 15

3) Switch the lever "B" back to "M" position. Isoclinics are now eliminated and colors are seen. Looking through the compensator window onto the part, observe the pattern. Turn the knob towards you, driving the compensator, and observe the fringes moving. Continue turning until a black fringe covers the point of measurement. The "Null Balance" is achieved and the N of compensator is equal and oppdsite sign to N on the specimen (See Figure 16).

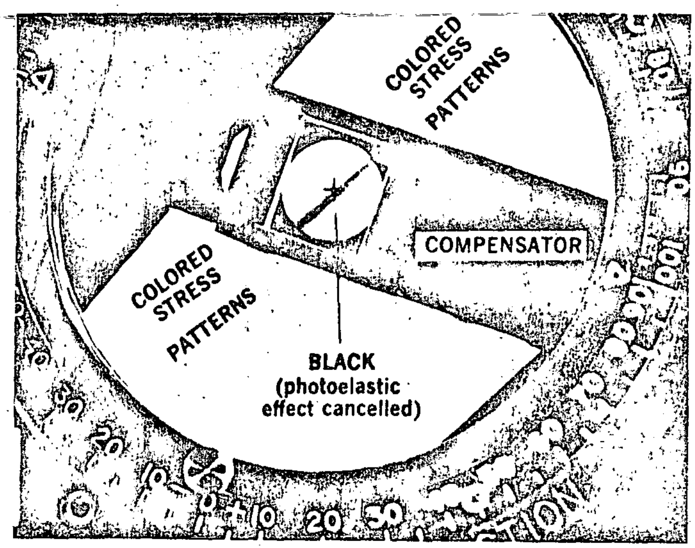

FIGURE 16

4) Read the counter. From the calibration chart read N (See Figure 17). Since the sign of compensator and part are opposite, we have:

$$(\varepsilon_x - \varepsilon_y) = - Nf$$

$$(\sigma_x - \sigma_y) = - N \frac{fE}{1+\mu}$$

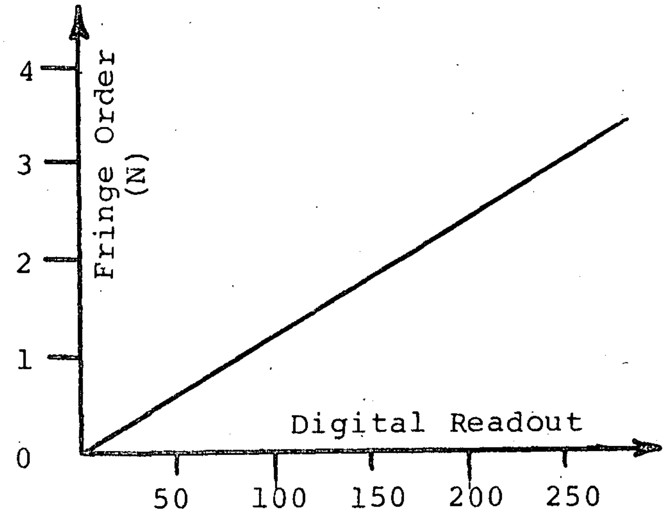

FIGURE 17

Remember that the compensator fringes are positive, and if $\varepsilon_x - \varepsilon_y$ is also positive, the compensator <u>will add</u> instead of subtract, and NULL BALANCE will <u>not be possible</u>. In this case, turn the handle "H" 90° and repeat the operation.

<u>EXAMPLE</u>: Set the cantilever beam up for analysis as previously described and align the handle "H" parallel to the long axis of the beam. In this position $\varepsilon_x - \varepsilon_y$ will be a positive number. Next, load the beam and observe the fringe pattern (at a selected point) through the normal field of view. Now, rotate the compensator knob until another fringe crosses the point. The pattern through the compensator will now be observed as one fringe order higher than that observed without the compensator. Next, rotate the handle "H" (counter-clockwise) so its position will be perpendicular to the beam ($\varepsilon_x - \varepsilon_y$ will now be a negative number). Now, by rotating the compensator knob and viewing the same point through it, a black fringe will be observed moving toward the point. Thus, in the first case, we added fringes to the initial pattern, and in the latter case, we subtracted fringes from the initial pattern.

NOTE:

1. As the counter reading is increasing, N in compensation increases.

   Looking at a point where $(\sigma_x - \sigma_y) > 0$, we will be adding N and the sequence of the colors will be:

   Yellow-Red-Green-Yellow . . . .

   Looking at a point where $\sigma_x - \sigma_y < 0$, the sequence of colors will be:

   Yellow-Green-Red-Yellow-Black

2. The resolution of the Model 232 Compensator is approximately 1/50 of a fringe (± 1 digit).
3. The 232 can also be used in conjunction with the Tardy Method to improve the resolution of the Tardy Method in difficult to read areas. In case of N < 1, set the 232 Compensator on N = 1. It will than add 1 fringe to the field and improve the resolution.

The newest compensator developed by Photolastic (Model 332) provides a direct digital readout of the strain in micro-inches per inch when the NULL BALANCE is achieved at the point of measurement (See Figure 18). This unit is also available with a printer system (Model 432) which "prints out" the Point Number (2 digits). Strain direction angle (2 digits), and the strain magnitude (4 digits).

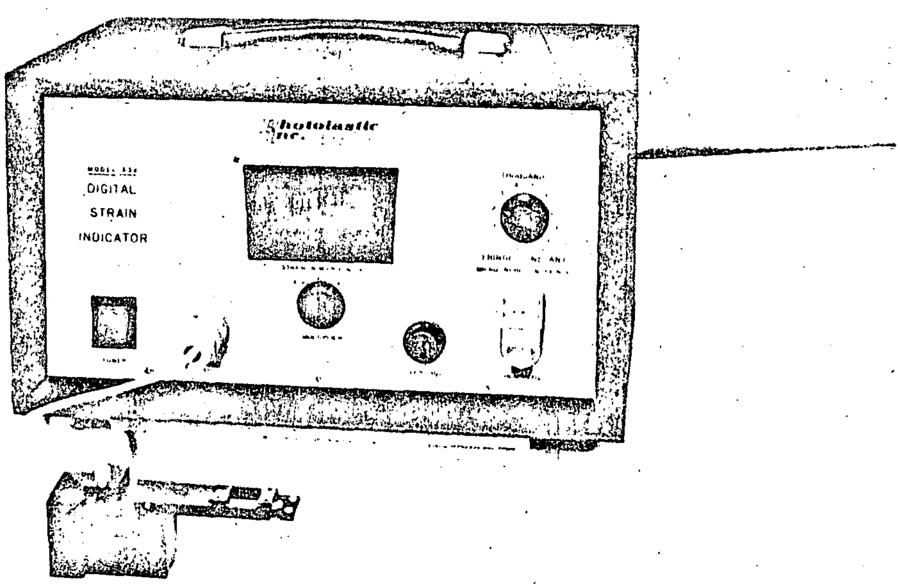

FIGURE 18

SECTION 4

MEASUREMENTS IN OBLIQUE INCIDENCE

4.0 INTRODUCTION

In the previous sections covered in this manual, it has been shown how to obtain the magnitude of the difference of principal strains and their directions with respect to some reference axis using normal incidence light.

In certain cases, however, a more complete analysis is required that necessitates separation of the two principal strains, and obtaining the individual values of each. To accomplish this a second reading is required, and that reading must be taken with oblique incidence light.

By oblique incidence, we mean that the light from the polarizer traverses the photoelastic coating at an angle and the birefringence measured depends on the secondary principal strain in the plane perpendicular to the light path. Thus, an oblique incidence reading combined with a normal incidence reading provides us with the necessary information for determining the separate values and directions of the principal strains ε_x and ε_y.

4.1 DESCRIPTION OF OBLIQUE INCIDENCE ADAPTER MODEL 033 AND ASSEMBLY TO BASIC ANALYZER

The Oblique Incidence Adapter for use with the Photolastic Analyzer has a fixed mirror angle which provides for simplified data reduction.

In addition, the unit's special design permits accessability in corners and fillets of the test part where separation of the principal strains is most desirable. The unit also telescopes for varying point to instrument distance.

It is easily attached to the analyzer by a simple locking device as shown in Figure 19.

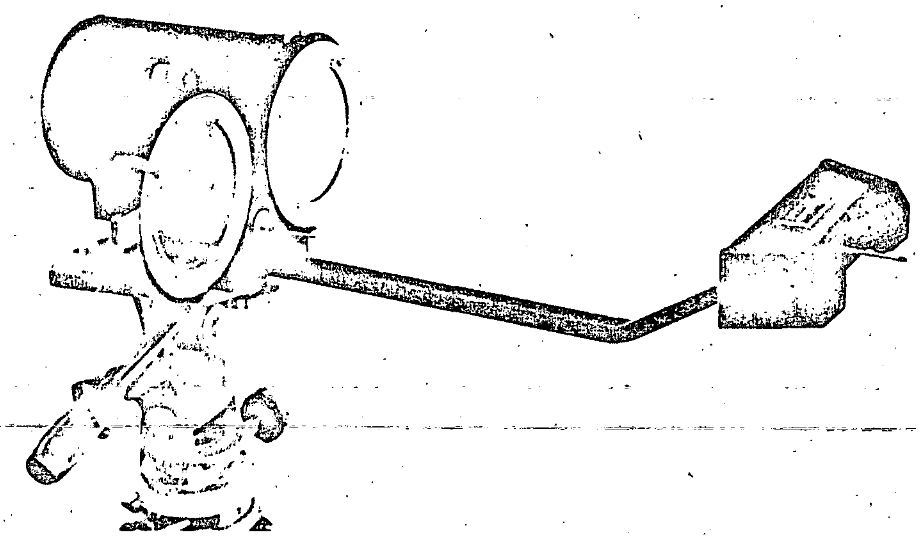

FIGURE 19

4.2 BASIC EQUATIONS

Figure 20 shows the path of light emerging from the polarizer, reflected by the oblique incidence mirror, traversing the photoelastic coating, reflected back to the mirror, and finally back to the analyzer. By referring to detail A of Figure 20, we can see that there is an angle θ between the normal of the surface of the test piece and the light ray. Thus, the measured fringe order at this point will depend on the angle θ, and on the strains existing at the point as expressed by the formula:

$$N_\theta = \frac{1}{f}\,(A\varepsilon_x - B\varepsilon_y)$$

If angle θ is small, then $A = B = 1$, and the equation reduces to that used for normal incidence measurements:

$$N_{normal} = \frac{1}{f}\,(\varepsilon_x - \varepsilon_y)$$

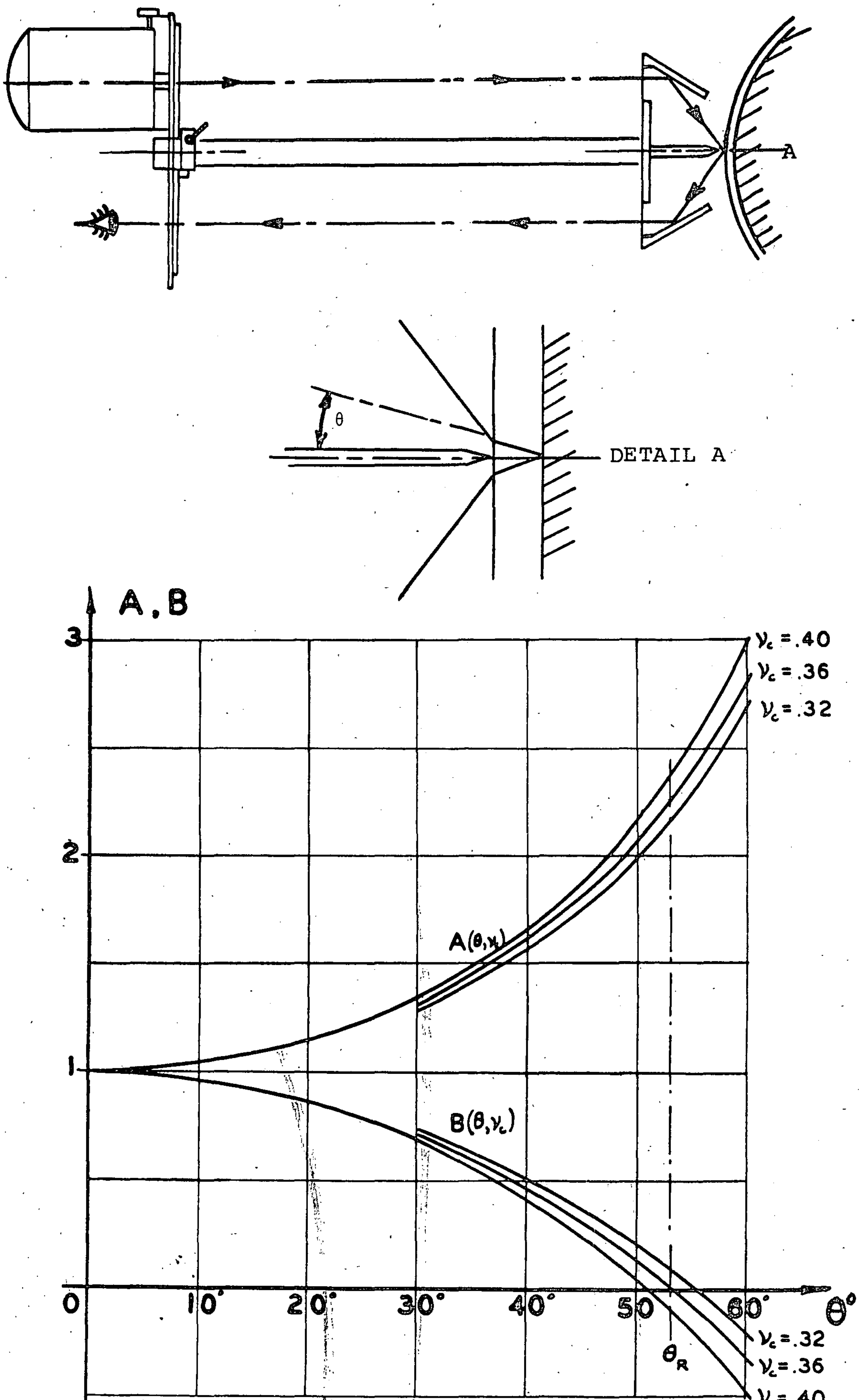
A
DETAIL A
θ
A, B
3
2
1
0
10°
20°
30°
40°
50
60°
θ°
A(θ,ν_c)
B(θ,ν_c)
θ_R
ν_c = .40
ν_c = .36
ν_c = .32
ν_c = .32
ν_c = .36
ν_c = .40

FIGURE 20

When two readings are obtained, one in normal incidence and the other in oblique incidence, the values of the two principal strains are given by:

$$\varepsilon_x = f\ (1.5\ N_\theta - N_{normal})$$

$$\varepsilon_y = f\ (1.5\ N_\theta - 2N_{normal})$$

Where the numerical values of 1, 1.5, and 2 are coefficients derived from the development of equations for oblique incidence measurements (See Technical Paper "New Oblique Incidence Method for Direct Photoelastic Measurement of Principal Strains" by S. S. Redner, "Experimental Mechanics", March 1963).

The preceeding formula utilizing the coefficients 1, 1.5 and 2 is accurate for most of the commonly used photoelastic coatings which have a Poisson's Ratio of approximately .36. However, for some plastics, such as high elongation coatings, the Poisson's Ratio will be slightly different and correction factors will have to be applied for more precise results.

For this purpose, we will rewrite the equations to read:

$$\varepsilon_x = f\ (CN_\theta - DN_{normal})$$

$$\varepsilon_y = f\ (CN_\theta - EN_{normal})$$

where C, D, and E represent the coefficients for photoelastic coatings that have a Poisson's Ratio different from most ordinary applications. Most of the available photoelastic plastics have a Poisson's Ratio between the limits of 0.34 and 0.50, and the graph shown in Figure 21, gives the numerical substitution for C, D, and E in the formula over these limits. However, as previously mentioned, under most circumstances the photoelastic coating used will more than likely have a (μ) value close to .36, and the basic equation for determing the values of ε_x and ε_y will be valid.

Once the principal strains have been determined, the principal stresses can be found by:

$$\sigma x = \frac{E}{1-\mu^2}\ (\varepsilon x + \mu \varepsilon y)$$

$$\sigma y = \frac{E}{1-\mu^2}\ (\varepsilon y + \mu \varepsilon x)$$

where E and μ are the modulus of elasticity and Poisson's Ratio of the test piece.

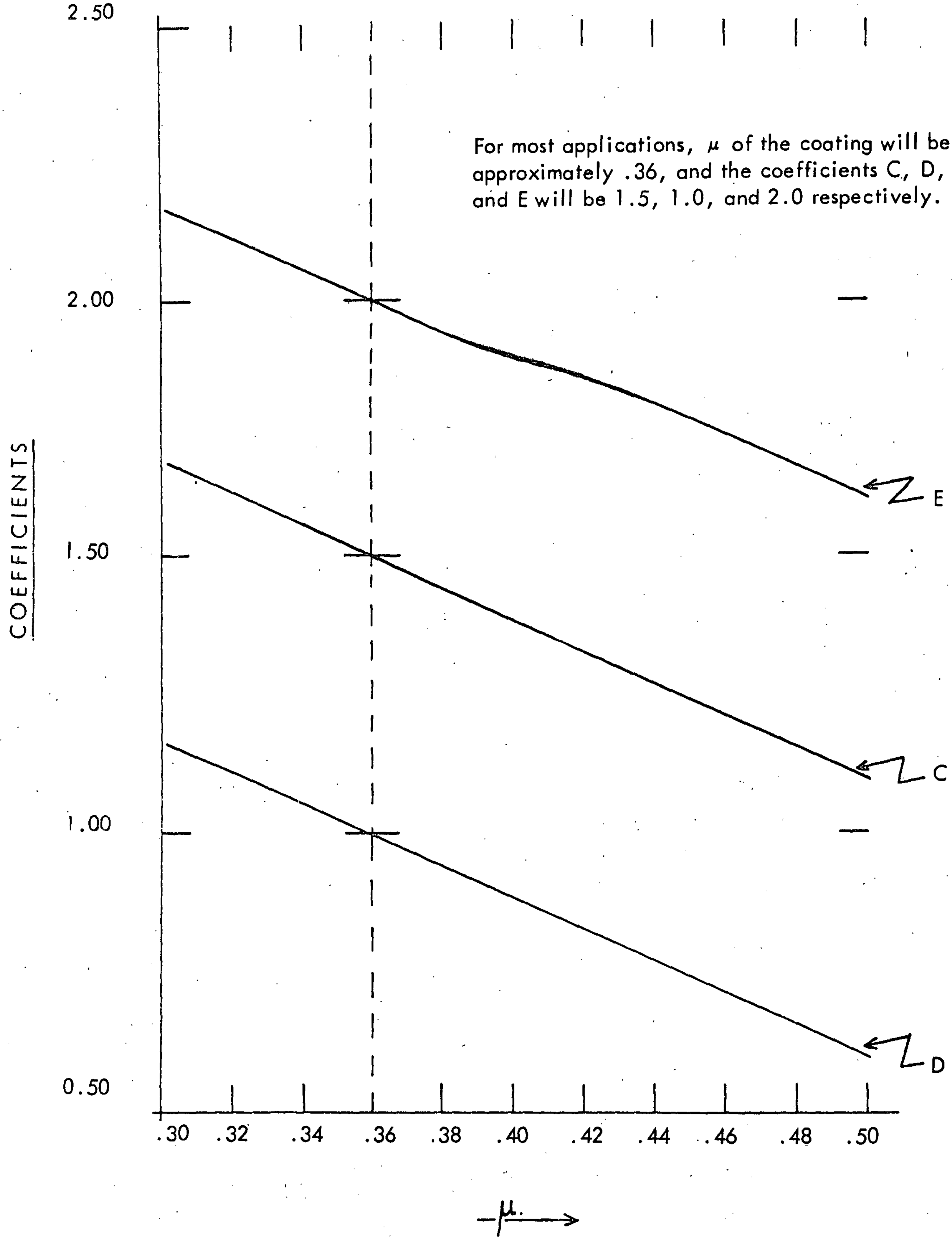

2.50
2.00
1.50
1.00
0.50
COEFFICIENTS
For most applications, μ of the coating will be approximately .36, and the coefficients C, D, and E will be 1.5, 1.0, and 2.0 respectively.
E
C
D
.30
.32
.34
.36
.38
.40
.42
.44
.46
.48
.50
μ

FIGURE 21

4.3 MEASUREMENTS

The basic difference between the technique of measurements in normal and oblique incidence is that with oblique incidence the axis of polarizer and analyzer must be maintained as follows:

1) parallel to the axis of symmetry of the mirrors of the oblique incidence adapter
2) parallel to the directions of the principal strains at the point of measurement

To satisfy the first condition, the handle "H" must always be maintained in the vertical position (direction reading on dial = 0°). The second condition, alignment of the polarizer-analyzer assembly with the directions of the principal strains, is accomplished by rotating the whole instrument in its own plane until an isoclinic appears at the point of measurement.

With the above two conditions defined, we can now proceed with making oblique incidence measurements according to the following step by step procedure:

1. Check the cleanliness of the oblique incidence adapter mirrors and attach to the basic analyzer.
2. Rotate the polarizer-analyzer assembly by means of handle "H" so that the arrow indicating direction reads 0° on the dial.
3. Switch on the light source and observe the test part in normal incidence. Mark with a grease pencil the points of interest at which oblique incidence measurements are to be made, and assign identification marks to each point.
4. Rotate knob "B" to the "D" direction position.
5. Now rotate the whole instrument in its plane until an isoclinic appears at the marked point. The axes of polarizer and analyzer will now be parallel to the direction of the principal strains at the considered point. (Note: These axes will also be identical to the axes of symmetry of the instrument.) In the case of the cantilever beam, the set-up will be as shown in Figure 22.

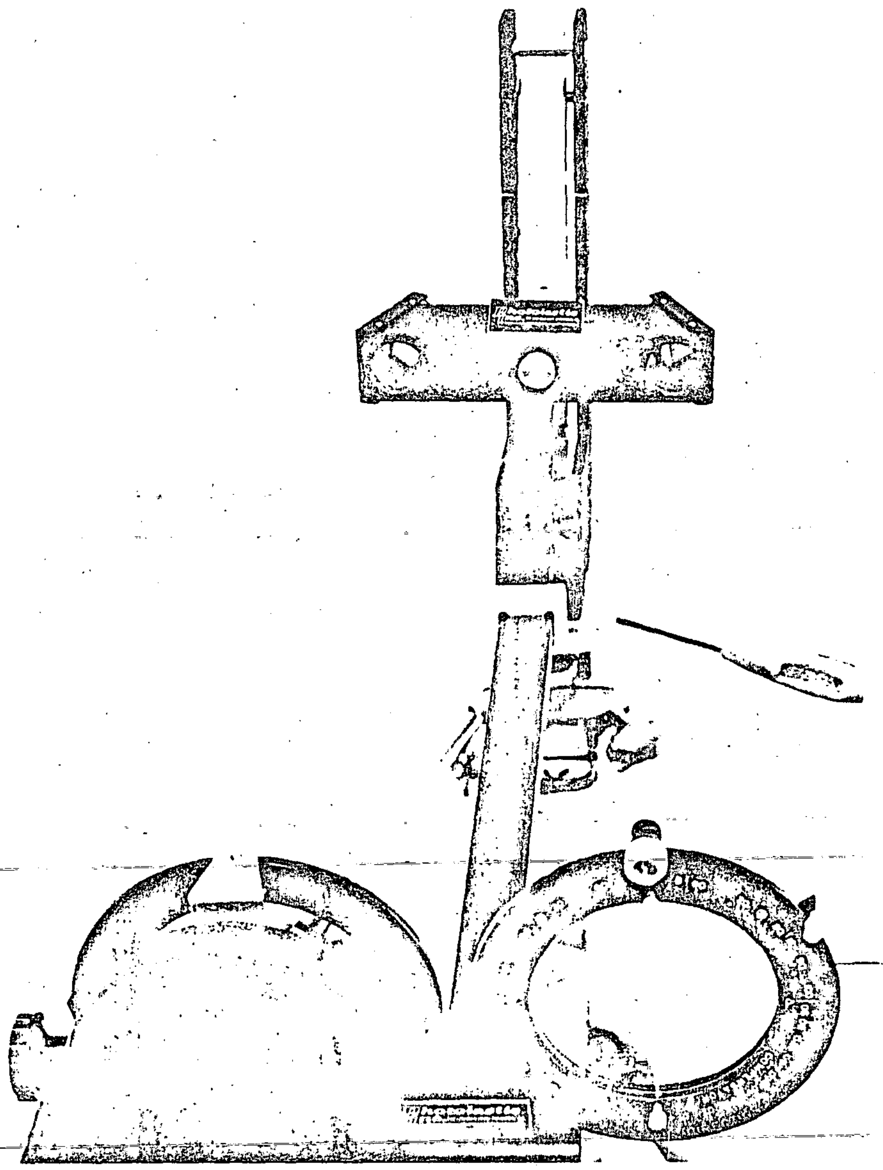

FIGURE 22

6. When step 5 has been completed, the handle "H" will be parallel to one of the principal strains (ε_x). Next rotate knob "B" back to the "M" (magnitude) position and obtain a reading in normal incidence at the selected point by either the Tardy Compensation Method or Null Balance principal as explained in Section 3.
7. Without changing the rotational position of the instrument, adjust the oblique incidence adapter so that the pointer located between and in front of the mirrors almost touches the point of measurement. Now, observe the point through the mirrors and measure the fringe order in the exact same way as for normal incidence (the same rule for determination of the sign applies).

NOTE 1:

The determination of the value N and its sign is slightly more difficult under oblique incidence since the observed area is considerably smaller. Continued practice on the cantilever beam will aid in making oblique incidence measurements on more complicated parts. The use of the digital compensator and Null Balance principle for determing N in oblique incidence is by far the most positive method to use and is strongly recommended.

8. Once the readings in normal incidence N_n and in oblique incidence N_θ have been obtained, the principal strain values can be calculated by the following formulas:

$$\varepsilon_x = f\ (1.5N_\theta - N_n)$$

$$\varepsilon_y = f\ (1.5N_\theta - 2N_n)$$

where ε_x is the strain in the direction of handle "H"
ε_y is the strain perpendicular to handle "H"
f is the fringe value expressed in micro-inches per inch per fringe

N_n and N_θ are the fringe orders measured in normal and oblique incidence.

The principal stresses can be found in the elastic range by:

$$\sigma_x = \frac{E}{1-\mu^2}\ (\varepsilon_x + \mu\varepsilon_y)$$
$$\sigma_y = \frac{E}{1-\mu^2}\ (\varepsilon_y + \mu\varepsilon_x)$$

where E and μ = modulus of elasticity and Poisson's Ratio of the test part.

For steel where $E = 30 \times 10^6$ psi, and $\mu = 0.30$, the equations reduce to:

$$\left.\begin{aligned}\sigma_x &= 66.0\ f\ (N_\theta - 0.82\ N_n)\\ \sigma_y &= 66.0\ f\ (N_\theta - 1.18\ N_n)\end{aligned}\right\}\ \text{in psi}$$

For aluminum where $E = 10 \times 10^6$ psi, and $\mu = 0.33$, the equations reduce to:

$$\left.\begin{aligned} \sigma_x &= 22.4\ f\ (N_\theta - .83\ N_n) \\ \sigma_y &= 22.4\ f\ (N_\theta - 1.17\ N_n) \end{aligned}\right\}\ \text{in psi}$$

4.4 USE OF NOMOGRAPH

A rapid numerical solution of the equations:

$$\varepsilon_x = f\ (1.5N_\theta - N_n)$$

$$\varepsilon_y = f\ (1.5N_\theta - 2N_n)$$

may be obtained by using a nomograph (Figure 23). In order to obtain the best resolution two scales are provided. Use of the nomograph simply involves drawing a straight line connecting the N_n and N_θ readings. The intersection of this line with the ε_x and ε_y scales will give a number which multiplied by the fringe value (f) gives the strains directly

Note: On the nomograph, if

$0 < N_\theta,\ N_n < 1.5$ use left scales

$1.5 < N_\theta,\ N_n < 3.5$ use right scales

$3.5 < N_\theta,\ N_n < 15$ use left scales

IMPORTANT: When using the nomograph, be careful to watch sign of N_θ and N_n whether positive or negative.

NOMOGRAPH for separation of principal STRAINS by oblique incidence method.

$$\frac{\varepsilon_x}{f} = (1.5\ N_{ox} - N_n)$$

$$\frac{\varepsilon_y}{f} = (1.5\ N_{ox} - 2N_n)$$

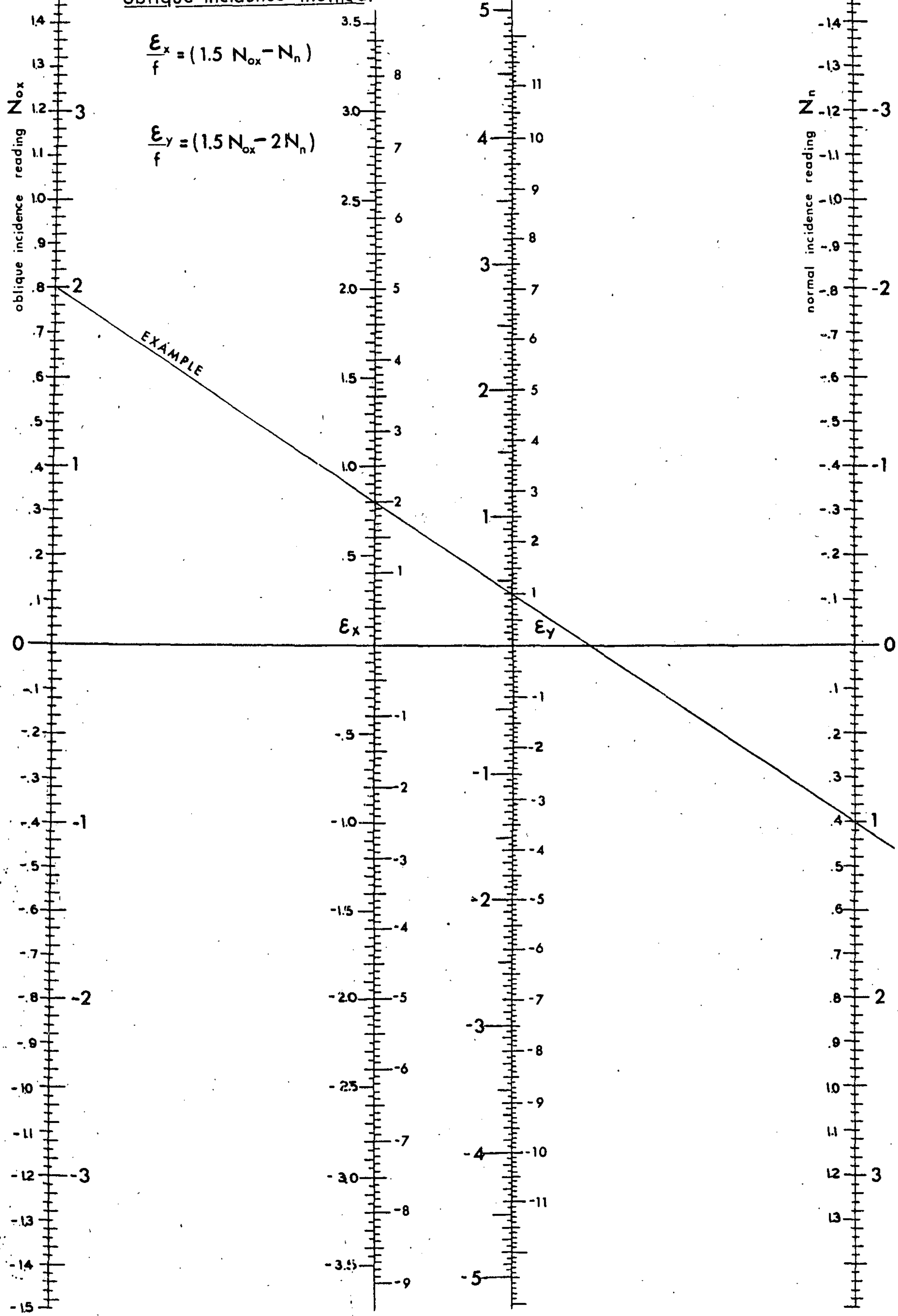

FIGURE 23

SECTION 5

CORRECTION FACTORS

5.0 INTRODUCTION

If the photoelastic coating exhibits an initial color pattern prior to loading (Parasitic Birefringence), a correction must be made in all subsequent readings taken during the test. Also, when a part is coated with a layer of photoelastic plastic and is subjected to load, the plastic coating carries a fraction of the load, and the strain on the part is thereby reduced. In most cases, the reinforcing effect of the coating on the test part is negligible. (As on structural parts like I, H, U, tubular and other beam members, thick walled parts, castings, etc.) However, in the case of plane stress problems and plates subjected to bending, a correction in the reading is required so that the experimental results can be given in terms of the uncoated part.

In other cases, when the temperature is changing during a test, a system of stresses will develop in the photoelastic coating due to the difference in the coefficient of thermal expansion between the test part and coating. If this happens, a correction factor must also be used to compensate for the effect of temperature change on the readings.

5.1 METHOD OF CORRECTION FOR PARASITIC BIREFRINGENCE

Under normal circumstances, residual birefringence in the coating can only be produced by severe mishandling of the plastic during or after application, and in such cases, it is usually more convenient to strip off the coating and apply a new one, rather than attempting to make corrections for the existing residual stresses.

It is necessary, however, to point our a few cases where residual birefringence will unavoidably occur and where readings will have to be made by applying the formulas given on page 47.

A.) RESIDUAL BIREFRINGENCE DUE TO THE TEST TEMPERATURE VARYING FROM THE BONDING TEMPERATURE.
This parasitic birefringence due to temperature will generally occur around the edges of the plastic and will extend inside the coating by as much as five times the thickness of the coating.

B.) PARASITIC BIREFRINGENCE DUE TO CONTRACTION OF THE CEMENT
Sometimes the cement is not fully polymerized; during a month or so it may continue to polymerize slightly, and therefore contract. This effect will also produce birefringence around the edges of the plastic.

C.) EDGES NOT PROTECTED AGAINST HUMIDITY
If the edges of plastic are not protected against humidity with a layer of cement, some moisture may be absorbed through the machined edges of the plastic and produce a swelling, which in turn will produce parasitic birefringence around the edges of the plastic, similar to cases (A) and (B).

For cases (A), (B), and (C), since birefringence is located around the edges of the plastic and since a free boundary is an isostatic, the procedure for correcting for parasitic birefringence consists simply of subtracting the reading under no load from the reading under load. It is assumed here that the shape of the plastic matches the free boundaries of the part.

There are cases where permanent birefringence will occur due to mishandling of the plastic or to yielding of the part after it has been coated. In these cases, the directions of principal strains of the <u>parasitic birefringence may not necessarily coincide with the directions of principal strains due to load</u>; hence, simple subtraction is not permissible. It is important to underline that <u>subtraction of the two states of stress is only permissible when the directions of the principal stresses coincide for both states of stress</u>. If they do not, the formulas outlined below must be used. In order to determine if the directions of the residual birefringence does or does not coincide with the directions under load, proceed as follows:

a) Trace or observe the isoclinics of the parasitic birefringence. (No load applied).

b) Load the part and observe the isoclinics once again. If the isoclinics under load and under no load conditions are identical (they do not move when load is applied), both states of stress (parasitic and due to load) can be subtracted one from the other. In case these isoclinics do move, use formulas (1) and (2) below:

$$(1) \qquad N_c = \sqrt{N_f^2 + N_i^2 - 2N_fN_i \cos 2(\theta_f - \theta_i)}$$

where:

N_c is the corrected fringe order due to the applied load only

N_f is the fringe order measured due to a combination of applied load and initial birefringence

N_i is the fringe order measured for no load (parasitic fringe order)

$(\theta_f - \theta_i)$ is the principal stress rotation when going from the unload to the loaded condition; it is the change in the isoclinic parameters

The angle θ of the correct isoclinic parameter due to load alone expressed by Formula (2).

$$(2) \qquad \tan 2\theta = \frac{N_f \sin 2\theta_f - N_i \sin 2\theta_i}{N_f \cos 2\theta_f - N_i \cos 2\theta_i}$$

θ is the measured angle between the major principal stress σ, and the reference direction X (see Figure 24).

When N_c is found from Formula (1), it is then multiplied by the fringe constant and the correct value of the principal strain difference is obtained.

Figure 25 shows an example of how a plot of load versus birefringence reading may look in case parasitic birefringence directions are not aligned with applied principal stress directions. To obtain correct values from such a plot, one may be justified for all practical purposes, in extrapolating the linear part of the curve. Obviously, if the magnitude of the parasitic birefringence is very high and if the misalignment is large, load-versus-reading plot will never have a linear part, and extrapolation will not be possible. In such a case the use of Formula (1) will solve the problem.

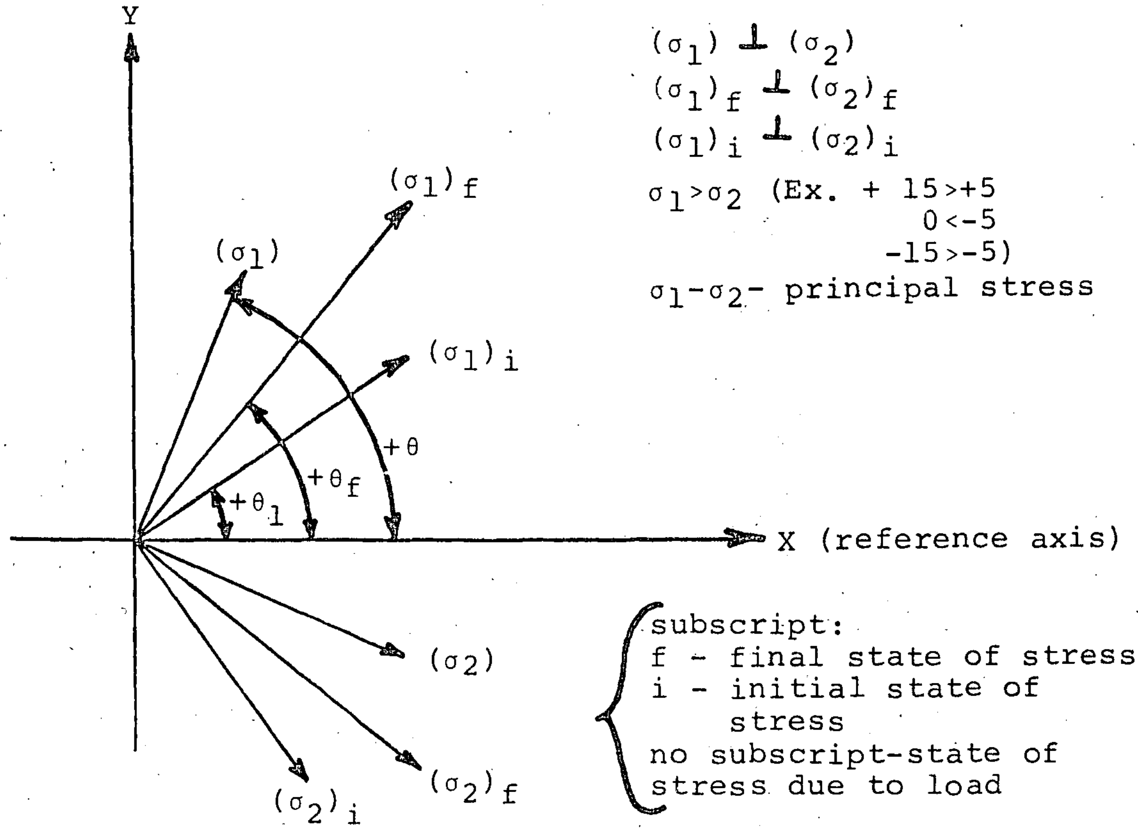

FIGURE 24

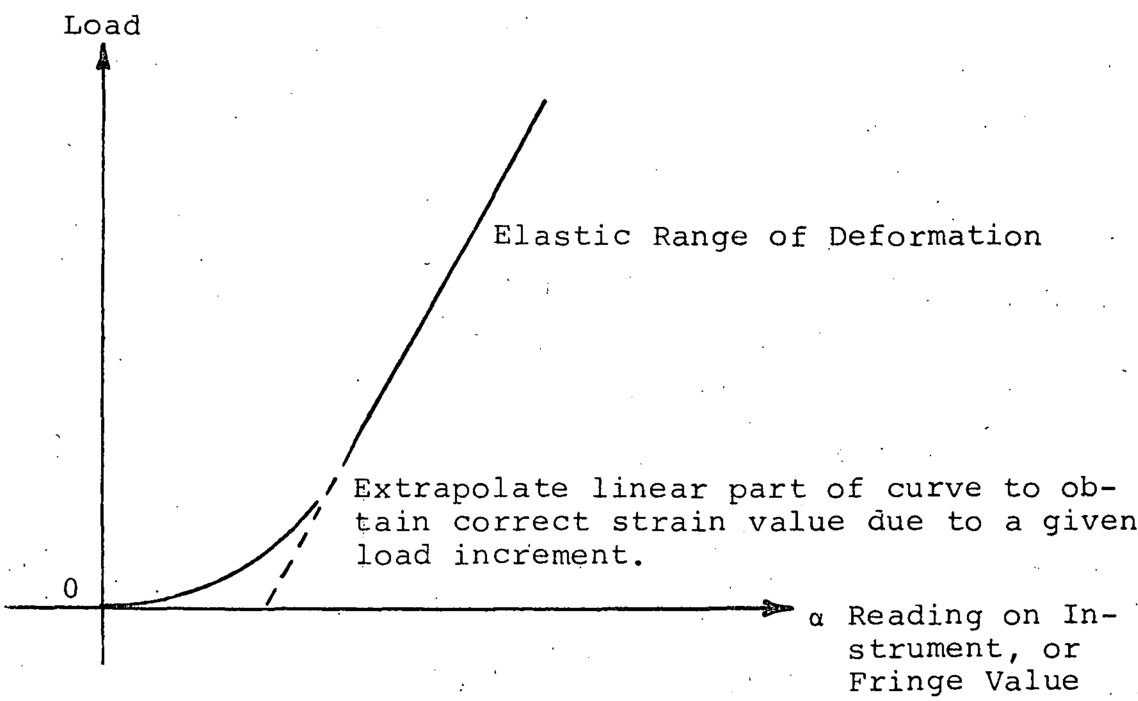

FIGURE 25

EXAMPLE: Fringe order of parasitic birefringence $N_i = 1.37$
Fringe order of birefringence measured when part is loaded $N_c = 3.42$
Change in isoclinic parameter, or $\theta_f - \theta_i$ = 15° (θ_f = 45° & θ_i = 30°)

The correct fringe order due to load is:

$$N = \sqrt{3.42^2 + 1.37^2 - 2 \times 3.42 \times 1.37 \times \cos(2 \times 15)} = 2.33$$

If the readings N_f and N_i were subtracted directly, N_c would be 2.05 and a 10% error would be introduced.

To obtain the isoclinic parameter (θ) with respect to a reference axis, X (Figure 23), Formula (2) is used: for the example cited, one would find

$$\tan 2\theta = \frac{3.42 - 1.37 \times .867}{0 - 1.37 \times .5} = -3.26$$

Remember that $\tan 2\theta = \tan (2\theta \pm 180)$. Therefore, there are two solutions for θ: $\theta_1 = -36.5°$ and $\theta_2 = +53.5°$. One of them corresponds to σ_1 and the other to $\sigma 2$.

5.2 CORRECTION FACTORS FOR PLANE STRESS PROBLEMS

In the case of plane stress problems where the bending action is negligible (such as pressure vessels, plates and panels loaded in their plane), there is some reinforcing effect although it is very small. In these situations the correction factor C_1 by which the initial readings should be divided to obtain the corrected strain value is:

$$\frac{1}{C_1} = 1 + \frac{t \text{ plastic} \times E \text{ plastic}}{t \text{ structure} \times E \text{ structure}}$$

where t = thickness of the plastic and test part
E = modulus of elasticity of the plastic and test part.

In Figure 26 the correction factor C_1 can be directly picked off the chart for various materials with respect to the thickness of the test part and the coating.

5.3 CORRECTION FACTORS FOR COATED PLATES SUBJECTED TO BENDING

When thin beams or plates are subjected to bending, the plastic coating reinforces the part and the measured strain must be corrected for this reinforcing effect. The correction factor C_2 applied must take into consideration three different effects as follows:

a) The neutral axis of the coated structure shifts.
b) The coating increases the stiffness of the plate.
c) The reading is an average strain through the coating thickness, and corresponds to the middle plane of the coating, which is located further from the neutral plane than the surface of the structure.

All of the above effects were taken into consideration when the correction factor chart (Figure 26) was constructed. Thus C_2 (correction factor for bending) can also be picked off the chart and the corrected strain reading can be obtained as follows:

Enter the ratio $\frac{\text{thickness of coating}}{\text{thickness of structure}}$ on the horizontal axis of the chart, and read the correction factor C_2 for the considered type of structure on the vertical axis.

Once the correction is known, we have:

$$\varepsilon_x - \varepsilon_y = \frac{N \times f}{C_2}$$

It is easily seen that uncorrected readings will usually be too high (C_2 larger than 1). Consequently, during the selection of the plastic, the thickness should be calculated to put C_2 in one of the following ranges: (Figure 26)

Area A: thickness of plastic small in comparison to the structure

Area B: correction C_2 reaches maximum and higher sensitivity is obtained.

CORRECTION FACTORS

C_2 — PLATES IN BENDING

C_1 — PLANE STRESS PROBLEMS

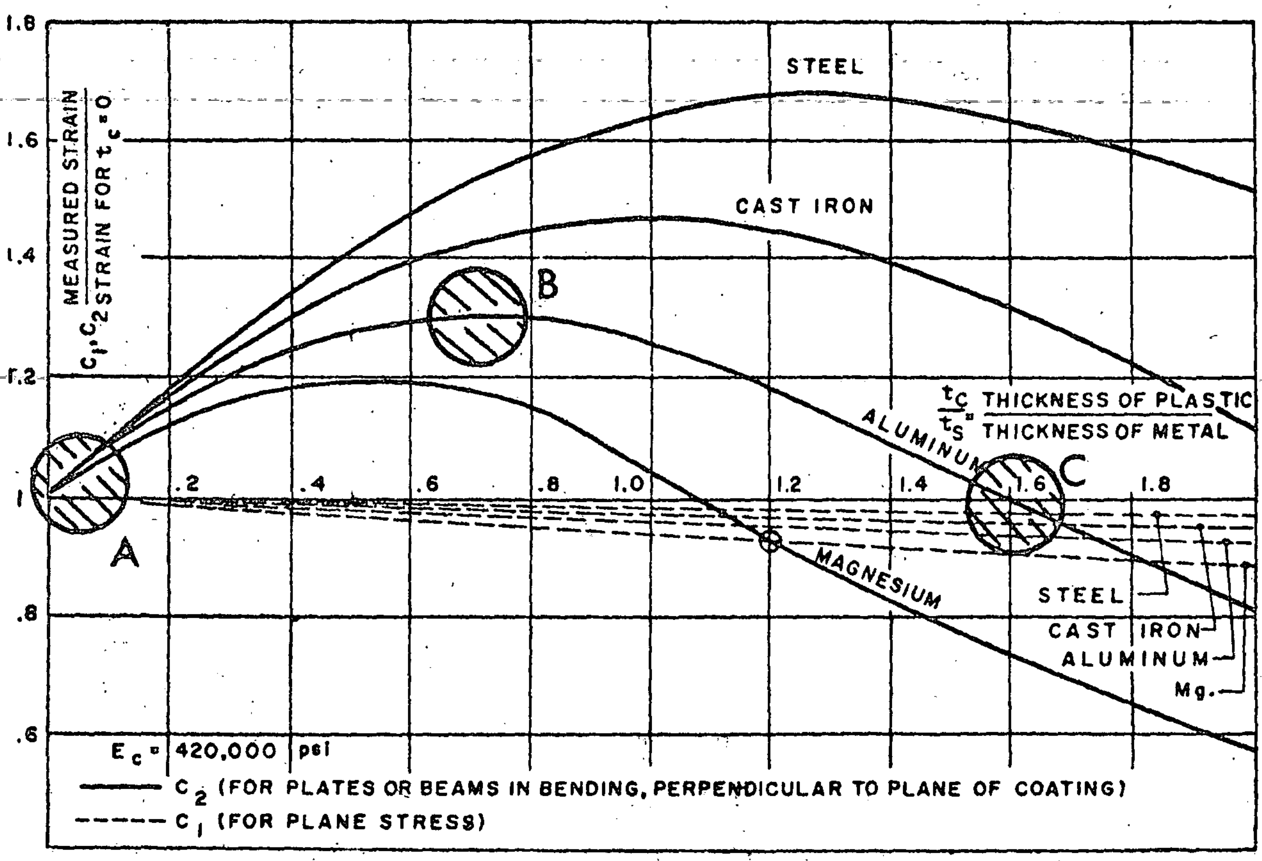

FIGURE 26

Area C: the correction factor is 1 and the selection is most useful in cases of very thin plates, and in cases where there is a combination of plane stress and bending.

Area D: where the ratio of plane stress to bending is unknown, the plastic should be selected so that the correction factor is the same for both cases.

Typical Cases

Example 1: Thin member in bending

Consider the aluminum cantilever beam described in the example of measurements 1/8" thick, 1" wide, and coated with 1/8" thick plastic.

Here: $t_{structure} = .125"$

$t_{plastic} = .125"$

and the ratio: $\frac{t_p}{t_s} = 1.0$

We read from the chart on the curve for aluminum: $C_2 = 1.25$. Suppose the reading at the point is N = 1.40 fringes and the fringe value f of the plastic is 725 μin/in/fringe. The corrected results are:

$$\varepsilon_x - \varepsilon_y = \frac{N \times f}{C} = \frac{1.40 \times 725}{1.25} = 810 \text{ μin/in}$$

Example 2: Biaxial stress field

A very large diameter cylindrical envelope forming a pressure vessel is subjected to internal pressure. The state of stress is very nearly a plane stress condition and the correction factor is then given by the dotted lines of Figure 26.

Assuming: $t_{plastic} = 0.125$

$t_{steel} = 0.625$

$$\frac{t_{plastic}}{t_{steel}} = 0.20$$

From the chart the correction factor $C_2 = 1$. Thus the reinforcing effect is negligible and can be disregarded.

Example 3

In a test the state of stress in a thin aluminum membrane is to be determined (combination of membrane stress and bending). The thickness of the plate is .060". We wish to select the plastic thickness to obtain C = 1 (no corrections to be considered).

$$t_{metal} = .060$$

For C = 1 we have for aluminum $\frac{t_p}{t_m} = 1.6$

$$t_p = t_m \times 1.6 = .096''$$

5.4 CORRECTION FACTORS DUE TO TEMPERATURE CHANGE

When the temperature is changing during a test, a system of stresses will develop in the plastic due to the difference in coefficient of linear expansions between the structure and plastic. The treatment of the thermal stress problem has been fully discussed in a recent paper*. In a practical application the following procedure is suggested:

A) In regions not located on boundaries (distance from edges of the plastic is greater than four (4) times the plastic thickness), normal incidence reading is not affected by the change of temperature, and the pattern observed is directly due to the thermal stresses to be measured.

In oblique incidence a "zero shift" will result due to change of temperature only. This "zero shift" is proportional to temperature and is given by:

$$N_{TO} = \frac{1}{f}\,\frac{1+\mu}{1-\mu}\,\frac{\sin^2\theta}{\cos\theta}\,(\alpha_s - \alpha_c)\,\Delta T = \frac{.66}{f}\,(\alpha_s - \alpha_c)\,\Delta T$$

*"Photoelastic Coating Analysis in Thermal Fields" by F. Zandman, S. Redner, and D. Post.

Where: N_{To} fringes observed, due to the change of temperature only.

μ Poisson's Ratio of plastic

$\alpha_s - \alpha_c$ Differential coefficient of thermal expansion between structure and coating.

θ Angle of oblique incidence

ΔT Change of temperature

Then, if N_{mo} is the measured fringe order in oblique incidence, the corrected value is given by:

$$N_o = N_{mo} - N_{To}$$

B) <u>On the edges</u>

The oblique incidence readings are not required on edges. In normal incidence however, fringes will appear on the edges due to a change in temperature. The most convenient procedure for analysis in this case is to prepare a dummy specimen not subjected to the same stresses in the part, but to the same changes of temperature as the investigated part, and then to take comparative readings. (Comparing the total fringe order on the coated part with that of the dummys). The same dummy specimen may also be used for oblique incidence zero shift measurements, as described above. In many cases the part itself will be used as a dummy and after the change in temperature, new "zero" readings can be obtained on the edges.

<u>Example 4:</u>

The temperature is rising from 72°F to 212°F. Using PS-2, .080" thick plastic on aluminum, what is the "zero" shift in oblique incidence?

We have: $\Delta T = 212 - 72 = 140°F$

$\alpha_s - \alpha_c = 24$ µin/in/°F

$f = 1170$ µin/in/fringe

$$N_{To} = \frac{.66}{1170} \times 24 \times 140 = 1.9 \text{ fringes}$$

The same may be established on a dummy specimen. Continuing: If N_T is due to temperature only (as established on the dummy) and N_m is the measured fringe order, the corrected result is:

$$N = N_m - N_T$$

SECTION 6

CALIBRATION OF PLASTICS

6.0 INTRODUCTION

If the K factor on a sheet of photoelastic plastic is not given by the manufacturer, or if the coating has been made from liquid plastic, it will be necessary to experimentally determine the K factor so that the fringe value f of the plastic can be computed.

6.1 USE OF THE CALIBRATOR MODEL 010

The Calibrator Model 010 is a precision instrument providing an accurate means of determining the strain-optical coefficient K, and the sensitivity of the photoelastic plastic. If used exactly in accordance with the instructions contained in Photolastic, Inc. Bulletin IB-I-100, the K factor will be measured within $\pm$ .001.

6.2 CALIBRATION OF PLASTIC USING A CANTILEVER BEAM

The cantilever beam provides a very reliable way to calibrate the plastic. Suppose an aluminum beam 1/4" thick and 1" wide is set up as described in Section 3. The small strip of plastic approximately 3" x 1" to be calibrated, is bonded to the beam, its center (point of our measurements) located 6" from the loaded end. With no load on the beam, the reading at the point is zero. After a 20 lb. weight is applied, the reading is N = 1.54 fringes. In order to establish the "f" and "k" of the plastic, first the stress on the uncoated beam is calculated:

The stress is: $$\sigma = \frac{6PL}{bh^2} = \frac{6 \times 20 \text{ lbs.} \times 6''}{1'' \times (1/4)^2} = 11,500 \text{ psi}$$

The difference of principal strains on the surface of uncoated beam is:

$$\varepsilon_x - \varepsilon_y = \frac{1 + \mu}{E} (\sigma_x - \sigma_y) = \frac{1.33}{10.3 \times 10^6} \times 11,500 = 1490 \ \mu\text{in/in}$$

In the middle plane of the plastic the strains are:

$(\varepsilon_x - \varepsilon_y)$ plastic = $(\varepsilon_x - \varepsilon_y)$ uncoated structures x C_2

from chart: (Ex: $t_p = 0.080$ $t_s = 0.250$)

$$\left(\frac{t_p}{t_s} = .32\right) \qquad C_2 = 1.21$$

and

$$(\varepsilon_x - \varepsilon_y) \text{ plastic} = 1490 \times 1.21 = 1800 \ \mu\text{in/in}$$

The fringe value $f = \dfrac{(\varepsilon_x - \varepsilon_y) \text{ plastic}}{N} = \dfrac{1800}{1.54} = 1170 \ \mu\text{in/in.}$

and the "K" factor is:

$$K = \frac{11.35}{t \times f} = \frac{11.35}{.080 \times 1170} = .122$$

SECTION 7

DESCRIPTION AND USE OF ACCESSORIES

7.0 INTRODUCTION

The Basic Photolastic Analyzer is designed to accept a wide variety of accessories available to increase its usefulness. This makes it a truly one instrument system that permits any photoelastic coating task to be accurately performed. The complete line of accessories and their description and use follows.

7.1 TELEMICROSCOPE ATTACHMENT MODEL 037 AND 137

The Telemicroscope attachment constitutes a new development for field and laboratory analysis. Taking advantage of the basic analyzer's existing optical system, it simply mounts on the tripod, and provides high magnification which allows analysis of high strain gradient areas with microscopic accuracy, and examination of a distant object. It is also desirable to use when making measurements by either the "TARDY" or "NULL BALANCE" compensation methods since the point of measurement will be greatly magnified and much easier to observe. The telemicroscope is furnished with either an F/5.6 95-205mm Zoom Lens (Model 037), or an F/3.5 43-86mm Zoom Lens (Model 137).

The telemicroscope (Model 137) is shown mounted to the Photolastic Analyzer in Figure 27. The front "zoom" lens permits observation of a relatively wide area for locating the point of interest, and then zooms to high magnification for the desired detail by projecting the image at the focal point of the rear mounted microscope.

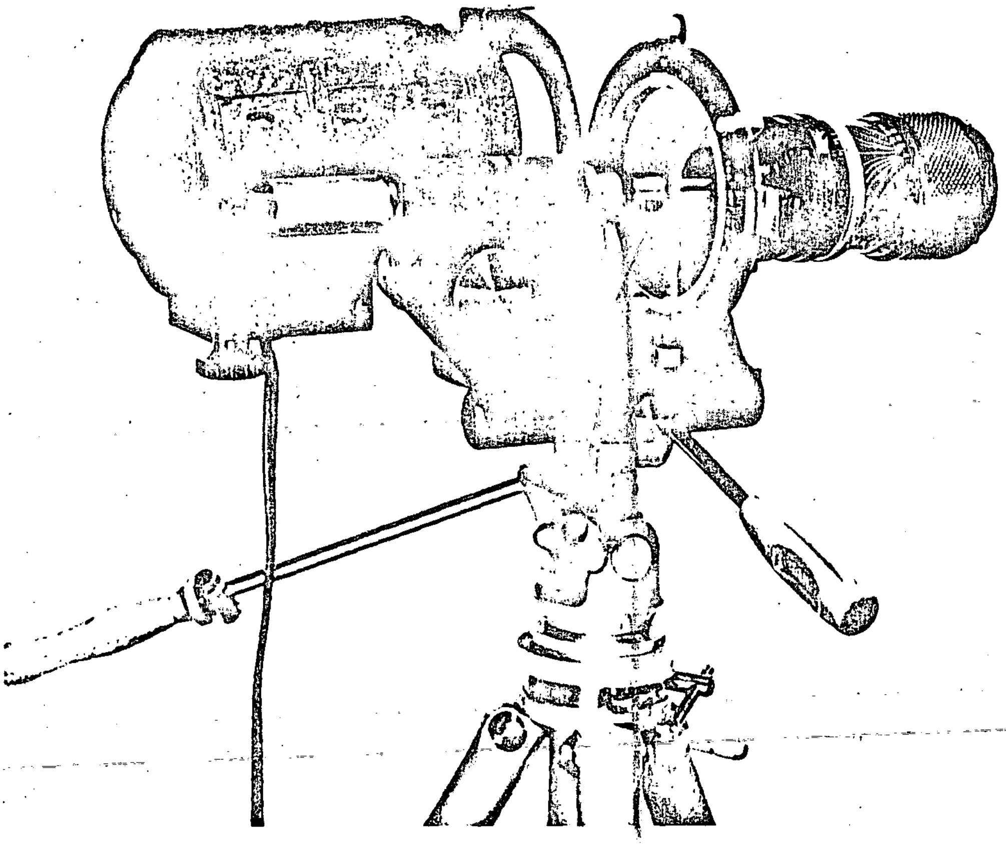

FIGURE 27

Description of the Optical System

The telemicroscope assembly consists of the following: (Refer to Figure 28)

A.) Mounting Frame - attachable to the tripod by means of the platform (A). The basic analyzer is also attached to this platform.

B.) Lens and Microscope Supports - mounted on a common axis (B), articulated in the platform (A), and allowing the telemicroscope to swing in or out of the observers field.

C.) Front Lens Adapter - allows the mounting of Nikon lenses to a 16mm movie camera.

D.) Front Lens - normally the zoom lens is installed here providing a variable focal length system of lenses. The front lens is interchangeable, and any desired lens could be installed as the front lens.

FIGURE 28

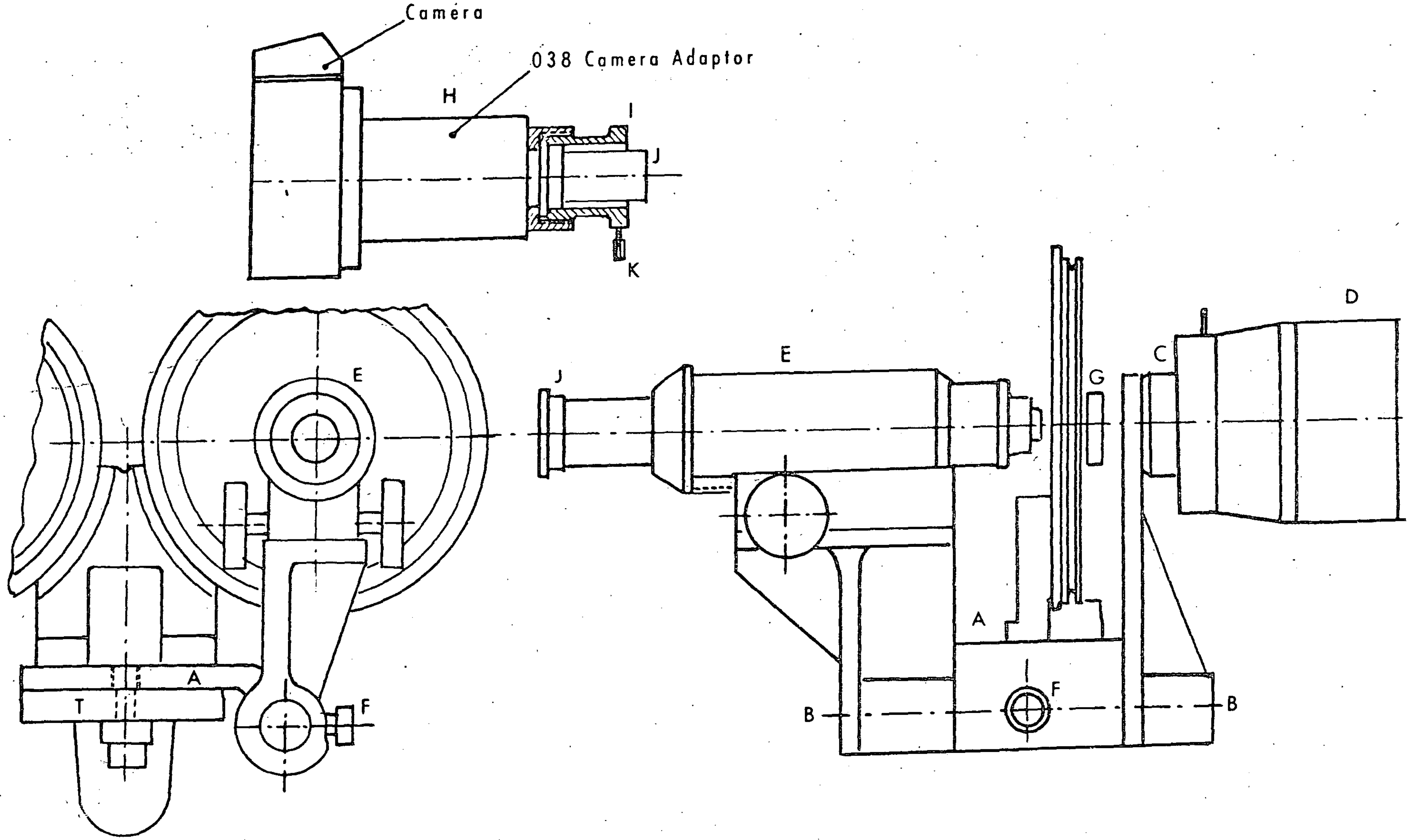

TELEMICROSCOPE SET UP.

1.) 50mm focal distance (normally supplied with the Model 035 Camera).
2.) Zoom lens of larger focal distance provided with the telemicroscope itself.

E.) Microscope - mounted on an adjustable rack to permit easy focusing. Both the objective lens and eye-piece lenses are interchangeable. Normally a 6x objective lens and a 10x eye-piece are supplied, providing a total magnification of 60x.

Assembly to the Basic Analyzer

To mount the telemicroscope to the basic analyzer, refer to Figure 28 and proceed as follows:

1.) Mount the base plate (A) to the tripod.
2.) Mount the analyzer on the base plate.
3.) Select the desired lens and mount the lens in the front lens adapter (C). This is accomplished by gently engaging the bayonnet in the mount, and then rotating the lens until the stop pin engages in the groove. (Dots on the lens and on the mount should be aligned to engage the bayonnet.)
4.) Release the stop button (F) and swing the optical system until its axis coincides with the axis of the instrument.
5.) Set the distance scale of the lens (approximately at the distance of the investigated part).
6.) Focus the microscope until a sharp image is observed. The instrument is now ready for operation.
In case the digital or linear compensator (G) is used in conjunction with the system, mount the compensator first, and then follow steps 1, 2, 3, and 4 in sequence as above.

then:

5.) Focus the microscope first on the compensator plane.
6.) Adjust the focusing ring of the front lens until a sharp image is obtained.

Selection of the Lens

For most applications only a moderate magnification is required, and the lens of maximum aperature would be selected to obtain a maximum amount of light.

The f/1.4 lens 50mm focal length is satisfactory in most cases. However, in case higher magnification is required, the zoom lens should be installed. The aperture of a high focal distance lens is smaller and for best results, the measurement should be made in dark areas or areas with a minimum amount of surrounding light.

7.2 CAMERA MODEL 035 AND 135

The camera provided with this equipment is one of the finest single lens reflex camera manufactured. It has many features and accessories that make it especially well-suited for work in the photoelastic coating field and for general industrial work. The camera is provided with a special bracket for easy mounting directly behind the basic analyzer (Figure 29).

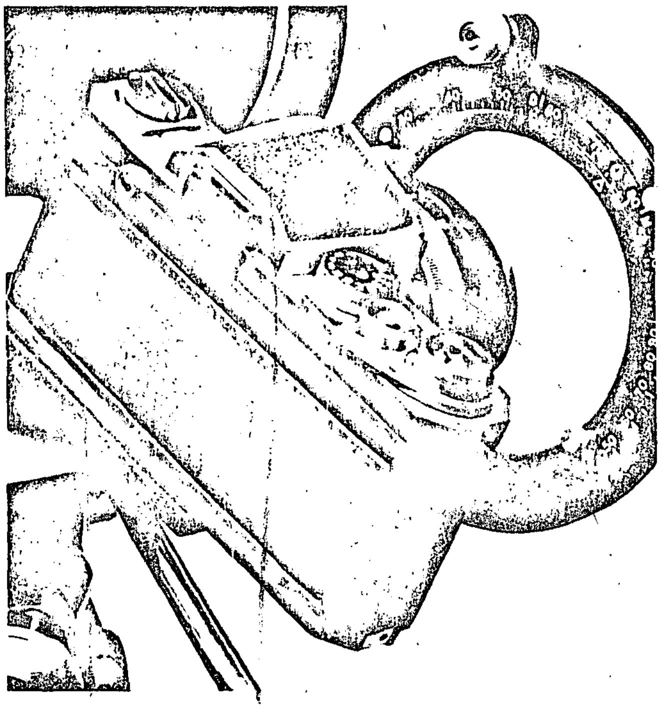

FIGURE 29

A single lens reflex unit with shutter speeds of 1 to 1/1000 second, it automatically sets the lens opening at the preset setting during exposure, but allows viewing with maximum opening. The automatic mirror swings in and out of the field during exposure. The unit is also equipped with instant action preview control, and a split image range finder with interchangeable focusing screens. The camera itself can also be fitted with a wide variety of accessories. The Model 035 comes complete with a 50mm f1.4 Auto-Nikkor Lens. In addition, the Model 135 offers a leather case, cable release, grey card set, light meter, and circular polarized analyzer filter for taking pictures when not attached to the instrument.

The general instructions for operation are enclosed with the camera. These cover:

- Loading
- Focusing
- Unloading
- Lens Setting
- Shutter Setting and Self-timer
- Changing Lenses

These instructions naturally cover the normal operation of the camera but because of its rather specialized use in the field of photoelastic coatings, specific information of photographic recording of the observed patterns is presented in Section 8 of this manual.

7.3 CAMERA ADAPTER MODEL 038 AND 138 FOR TELEMICROSCOPE

This accessory is for recording on film the observations made with the telemicroscope. Both the Model 038 and 138 Camera Adapters are self-contained units with internal lenses that attach directly to the microscope tube and camera body (in place of the camera lens). The Model 038 provides viewing through the camera while the Model 138 features a lateral eyepiece allowing observation and measurements while the camera remains attached. Normally supplied to fit the Nikon F Camera, they can also be supplied for other makes as well. Figure 28 shows how the Model 038 Camera Adapter (H) mounts to the telemicroscope. The Model 138 (Figure 30) mounts in a similar manner.

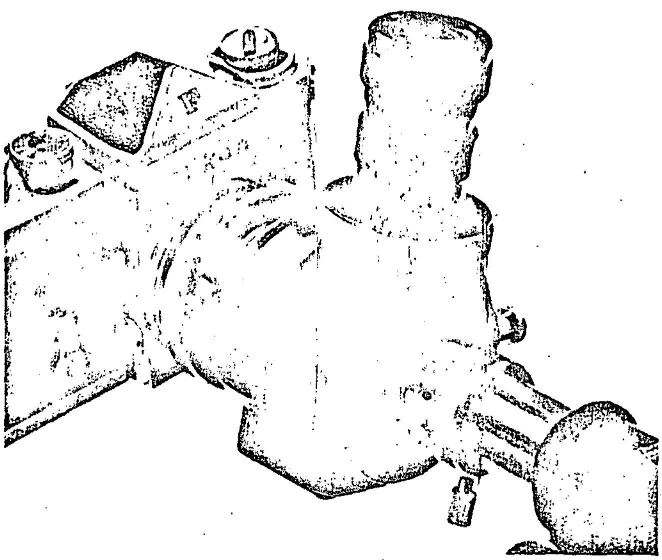

FIGURE 30

7.4 MONOCHROMATOR MODEL 036

The use of monochromatic viewing in photoelastic coatings falls into two distinct categories. These are:

1.) Black and white photography
2.) Identification of fringes when the colors washout at higher fringe orders

A truly monochromatic light source provides a very low light intensity only usable in a dark room. Semi-monochromatic lights used with standard photographic filters cause a shift in the fringe positions from color to black and white. The most efficient and economical solution is to use standard high intensity light and filter the desired band of wave lengths.

The Photolastic Monochromator is a narrow band interferential filter. It provides a band pass of 100A° at the wave length of the tint of passage producing a black fringe at every location where the tint of passage is observed in white light. It can be used in-hand or attached to the lens of the camera.

7.5 STROBOSCOPIC LIGHT MODELS 034 AND 134

When stress analysis studies under dynamic conditions (such as those found on centrigues or shakers) is required, replacement of the Basic Analyzer Light Source with a strobe accessory will provide the same sensitivity of measurement plus the advantages of a strobe light.

Both units are especially designed and manufactured for Photolastic, Inc., and they incorporate a combination of several features to increase their effectiveness in photoelastic observations. The lamps are attached to the polariscope so that its use as a portable analyzer will not be impaired (within the limits of the lamp's calbe). To maintain a light weight, the oscillator on Model 134 has its own control box separate from both lamp and power supply. This feature permits a flashing rate control up to 2C feet from the lamp.

Each model consists of lamp, power supply, and oscillator with connecting cables. Figure 31 shows how the Model 134 Strobe Light attaches to the basic analyzer. The Model 034 mounts in a similar manner. A complete set of operating instructions is supplied with each model.

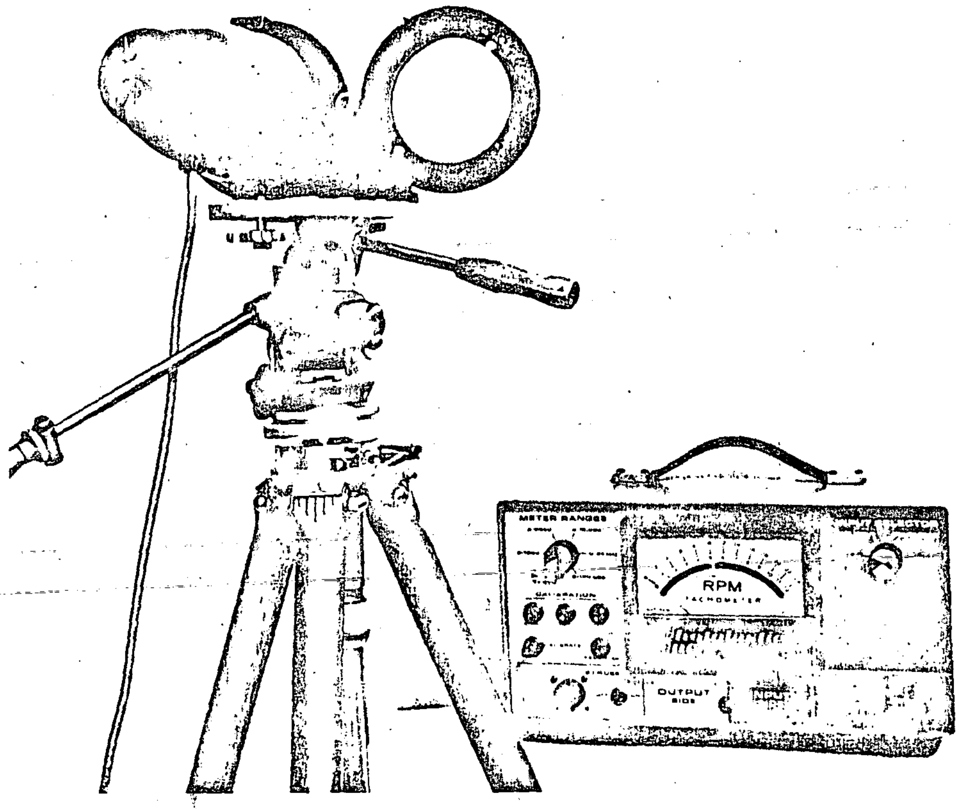

FIGURE 31

7.6 MODEL 332 and 432 DIGITAL STRAIN READOUT

Photolastic has brought automation to photoelastic stress analysis with the Model 332 or Model 432 Digital Strain Readout.

Easily attached to the basic analyzer, Model 332 (Figure 32) assures easy, fast, accurate strain measurements directly displayed-in microinches/in.-as a 4-digit readout. Model 432 provides a printout of the 4-digit strain measurement, plus a 2-digit printout of Point Number, and a 2-digit printout of the Principal Strain Direction Angle.

Because it eliminates the need to recognize fringes (or their absolute order), and the need to identify and then calculate fractional orders, it reduces human error to virtually zero. . . even with inexperienced operators.

Both Models consist of a Babinet-Soleil uniform field compensator electrically coupled to the digital strain readout.

The measuring method uses the "Null Balance" principle. Displacing the compensator wedge within the strain field adds-to the unknown quantity-an amount equal to the unknown quantity, but opposite in sign. We merely add an exact amount sufficient to achieve Zero Balance (the procedure is described in Section 3, part 3.4.2).

The electrical output from the compensator is then computed into Digital Strain Readout, displayed by the instrument.

Separate instruction manuals are available which describes in detail the set-up of electrical connections, adjustments, and operational procedure of these units.

SECTION 8

PHOTOGRAPHIC RECORDING OF FRINGE PATTERNS

8.0 GENERAL RULES

Photographic recording of the observed fringe patterns provides the simplest and most accurate method of recording data without transcription errors or forgotten details. In order to obtain satisfactory results when photographing the photoelastic patterns, the following general rules should be observed:

1.) Select the area to be photographed. The size of this area will determine the position of the camera and the proper lens. With a lens of focal length "f" the size of the area covered "L" from a distance "D" on a 35mm frame is:

$$L = \frac{D - f}{f} \times 35\text{mm}$$

If the distance D is much larger than f, the following approximation may be used:

$$L = \frac{35\text{mm}}{f\text{mm}} \times D$$

It is apparent that to cover small areas a lens of large focal distance must be used.

2.) Be sure the area of interest is well and uniformly illuminated. For overall views (test set-ups, etc.) only use several lights.

3.) Avoid parasitic reflections of windows, overhead lights, and direct reflections off polished metallic surfaces, etc.

4.) Attach the camera rigidly to the tripod. Use the cable plunger to make certain the camera does not move during the exposure.

5.) To obtain good depth of field, use as small a diaphragm opening as possible (f/22). The larger openings (f/1.4 and f/2.0) should be used only on relatively flat areas when uniform focusing can be achieved. Care should always be taken when focusing (use the split image feature of the camera on a vertical line or fringe). If no vertical reference is naturally available, make one artifically with masking tape, removing the tape before exposure.

6.) Avoid parasitic reflections and other "hot" spots that may appear in the field of view. Preferably, place the camera in a normal incidence position with respect to the part and to the illuminator, which should be slightly inclined (See Figure 33).

FIGURE 33

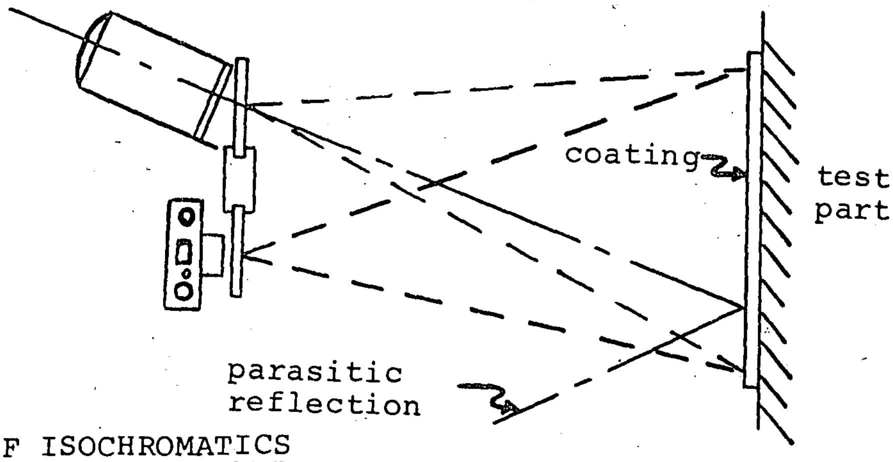

8.1 PHOTOGRAPHY OF ISOCHROMATICS

Use Ektachrome-X when slides are required, and Kodacolor-X (or the equivalent) when prints are to be made. The exposure guide (see Table I below), is based on average conditions. For best results, obtain actual lightmeter readings. The light level depends on:

- -Actual voltage on the lamp
- -Reflectivity of the cement
- -Angle of illumination
- -Distance from the light source to the part

Since most of these effects are difficult to evaluate, it is suggested to take three frames of each position adding one "underexposed" and one "overexposed".

For exposure use Table I which follows:

TABLE I

Time-Exposure Data

Distance - Analyzer to Test Part		2 ft.			4 ft.			
ASA Film Speed		20	64-80	200	20	64-80	200	3000
Diaphragm Opening f/x	f/16	2	1/2	1/4	4	1	1/2	1/30
	f/8	1/2	1/4	1/15	1	1/4	1/8	1/125
	f/4	1/8	1/30	1/60	1/4	1/15	1/30	1/500
	f/2	1/30	1/125	1/125	1/15	1/60	1/125	

8.2 PHOTOGRAPHY OF ISOCLINICS

A very convenient method of recording isoclinics is to use color transparency film such as Kodachrome-X (or equivalent). While the analyzer-polarizer assembly is rotated successively to different positions (0°, 15°, 30°, 45°, etc.), obtain photographs without changing the position of the camera. The resulting slides can then be projected later on white paper for tracing the isoclinics and isostatics.

In this case, the slides should be overexposed. This will show sharper isoclinics. When black and white film is used, the isoclinics should be recorded at a low strain level to avoid confusion with isochromatic fringes.

8.3 PHOTOGRAPHIC RECORDING THROUGH THE TELEMICROSCOPE

Photographic recording of the observed patterns viewed through the telemicroscope may be obtained by installation of the camera adapter Model 038 or 138 on the microscope.

1.) Set up the telemicroscope as for visual observation. Next, tighten all tripod handles to obtain maximum rigidity of the system.
2.) Mount the 50mm lens in the front of the telemicroscope, and focus on the area of interest.
3.) Engage the camera adapter to the camera. This adapter is mounted in exactly the same manner as the camera lens.
4.) Unscrew the eyepiece holder (I) from the camera adapter. Now introduce the eyepiece (J) in the camera adapter and tighten the eyepiece retainer back. (See Figure 28).
   Note: When the eyepiece is removed from the microscope, care should be taken to avoid any motion that would destroy the focus obtained.
5.) Now gently introduce the camera adapter (with the camera attached) to the microscope until the eyepiece hits the stop. Tighten the adapter on the microscope tube using the knob (K). The set-up is now ready to take photographs with no additional focusing required.
   Note: It is possible to check the focusing using "through-the-lens" viewing of the camera although the light intensity will be lower.

SECTION 9

REFERENCES

BIBLIOGRAPHY ON PHOTOELASTIC COATINGS

1. Experimental Stress Analysis - Principles and Methods, by G. S. Holister: Cambridge University Press 1967.

2. Handbook of Experimental Stress Analysis, by M. Hetenyi: John Wiley & Sons, Inc.

3. Stress Analysis by O. C. Zienkiewics and G. S. Holister: Published by John Wiley & Sons, Inc.

4. Designing by Photoelasticity by R. B. Heywood: Published by Chapman & Hall, 37 Esses St., London, England.

5. Photoelastic Coatings for Aerospace Measurements by S. Redner: Preprint No. 1AS64, Instrument Society of America, May 1964.

6. Structural Test Applications Utilizing Large Continuous Photoelastic Coating by R. W. McIver: SESA February 1965, Experimental Mechanics.

7. Photoelastic Coating Technique for Determining Stress Distribution in Welded Structures by Dr. F. Zandman: Welding Journal Research, Supplement May 1960.

8. Effect of Photostress Analysis on Casting Design by Dr. F. Zandman: Paper No. C41, The Society of Die Casting Engineers, September 1962.

9. Plastic Strains & Energy Density in Cracked Plates by W. W. Gerberich and J. L. Swedlow: SESA Part 1, November 1964, Part II, December 1964, Experimental Mechanics.

10. Maximum Shear Strain Measurements & Determination of Initial Yielding by the Use of the Photoelastic Coating Technique by Dr. F. Zandman: Special Technical Publication No. 289, A.S.T.M. 1960.

11. The Use of High Speed Photography & Photoelastic Coatings for the Determination of Dynamic Strains by C. A. Cole, Jr., J. F. Quinlan and Dr. F. Zandman: Paper E-10, 5th International Congress of High Speed Photography, October 1960.

12. An Investigation of the Elastic-Plastic Strain Distribution around Cracks in Various Sheet Materials by J. R. Dixon and W. Visser: International Symposium, IIT, Chicago, October 1961, Edited by M. M. Frocht.

13. Hot Engine Stresses Brought to Light by Dr. F. Zandman and H. N. Maier: Product Engineering, July 24, 1961.

14. Photoelastic Coating Analysis in Thermal Fields, by F. Zandman, S. S. Redner, and D. Post: SESA Paper, Dept. 1963.

15. Reinforcing Effects of Birefringent Coatings by Dr. F. Zandman, S. Redner, and E. I. Reigner: SESA Paper #588, 1959.

16. Accuracy of Birefringent Coating Method for Coatings Arbitrary Thickness by D. Post, Dr. F. Zandman: SESA Paper #557, 1959.

17. New Oblique Incidence Method for Direct Photoelastic Measurement of Principal Strains by S. Redner: SESA Paper, March 1963.

18. New Method for Determining Strain on the Surface of a Body with Photoelastic Coatings (Strip Method) by R. O'Ryan: SESA, August 1965, Experimental Mechanics.

centro de educación continua
división de estudios superiores
facultad de ingeniería, unam

ANALISIS EXPERIMENTAL DE ESFUERZOS

ARTICULOS TECNICOS

NOVIEMBRE, 1978.

The Transfer-grid Method, a Practical Moiré Stress-analysis Tool

Grids are applied to any part within minutes by a transfer technique which does not require any special skills. An optical instrument for moiré-fringe production, remote from the part (no contact master) is described

by Felix Zandman

ABSTRACT A practical and simple moiré stress-analysis technique is described. The grid is applied to any part by a transfer method, like a decal, not necessitating mechanical engraving or photoetching nor any special environmental care. The moiré fringes are observed remotely from the part without master contact. This is done through the use of a projection device and a master held in a plane where the projected image of the working grid is formed. Limitations of the method, as well as its applications, are discussed.

Introduction

The moiré stress-analysis technique* has been limited in its usefulness until recently, principally because of the difficulties involved in the application of grids to the test part. The only methods available were by engine ruling, photoengraving or photoetching which are very expensive and tedious, demanding high degrees of skill and consuming a considerable amount of time.

Still another difficulty was apparent in the necessity of using masters directly in contact with the active grid to produce the fringe pattern. In many instances contact is prohibited, difficult or impossible.

This paper describes a recently developed, simple and inexpensive method of grid application. It also describes an instrument for producing moiré fringes without contacting the part with a master.

Producing and Applying the Grid

During the development of this new technique, the following parameters were established and considered:

(*a*) Produce a grid which can be stored, handled, shipped and applied without producing grid distortions.

(*b*) Grid application should be permissible under normal lighting conditions by personnel familiar with usual stress-analysis techniques.

(*c*) Grid should be applicable to flat or cylindrical surfaces of any material.

(*d*) Grid and application method should be economical.

(*e*) Grid should be capable of withstanding high temperatures and extreme elongations.

To accomplish the above objectives, the following concept resulted; produce a transferrable grid or dot system of a highly reflective thin metal film which is supported by a rigid, easily stripped carrier. This was achieved by taking a stainless-steel plate of 0.005-in. thickness and covering it with a layer of nickel in such a way that the peel strength of nickel to stainless steel is very low. A layer of photoresist is then applied to the nickel and a print of the desired grid or dot system is made. After development, the areas in the unexposed portion of the image are etched. The etching process is stopped as soon as the pattern is formed.

An alternate method involves evaporating or plating nickel through a mask onto the stainless-steel backing. Material other than nickel can also be used; we have found, however, that nickel produces good results in terms of reflectivity, temperature, peel strength and process handling.

At this point, the transferrable grid on its backing plate can be stored, shipped and eventually applied

Felix Zandman is associated with Vishay Intertechnology, Inc., Malvern, Pa.

* *For those interested in a description of the principles of moiré, several excellent papers by A. J. Durelli of The Catholic University, Washington, D. C. are recommended.*

to the part without concern for distortion.

The method of applying (transferring) the grid consists of:

(*a*) Cleaning the surface to which the application is to be made. (This is similar to surface preparation used for strain gages or photoelastic coatings.)

(*b*) Applying cement to part. (A black adhesive is used for reflection techniques on opaque parts, a transparent adhesive for transmission techniques on transparent parts.)

(*c*) Application of the grid-plate sandwich to the cement-coated part, making certain that the grid is in contact with the cement. If the part is mildly curved, the plate can be made to conform to the curvature. (For sharp curvatures, the grid is first stripped off the backing plate with cellophane tape; now the tape, which is very flexible, is the carrier and it conforms more easily. This method can produce some grid distortions.)

(*d*) The cement is then allowed to cure. (Twenty-four hours at room temperature or a few hours at elevated temperatures.)

(*e*) After the cement is fully cured, the backing plate (or tape) is peeled off and the part is now ready for testing.

The sequence of grid application described above is schematically shown in Fig. 1.

Types of Grids

Employing this technique for manufacturing grids, practically any pattern can be produced such as lines, grids, dots, circles, triangles, etc. For practical production and stocking reasons, the available commercial patterns† have been limited to lines, grids or dots of 200, 500, 1,000, and 2,000 lines-per-inch density. These are normally made in 4- × 4-in. and 1 × 1-in. sizes.

In addition, individual gages made of concentric circles of 500 lines-per-radial-inch density are produced with a gage diameter of 0.2 in.

Moiré Fringes Without Master Contact

The principle of producing moiré fringes without resorting to direct contact between the master and the active grid is accomplished by projecting the image of the working grid onto a plane remote from the part and then placing a suitable master grid in the same image plane of the working grid. Moiré fringes will then be produced in the remote plane.[1, 2]

The instrument developed to accomplish this† consists of a very accurate optical system containing high-resolution, color-corrected, non-distorting lenses. The basic magnification is 1:1, thus providing the same result as two grids of the same line pitch in contact (matched grids). Magnification adjustability provides the same results as two mis-

† *Photolastic, Inc., 176 Lincoln Highway, Malvern, Pa.*

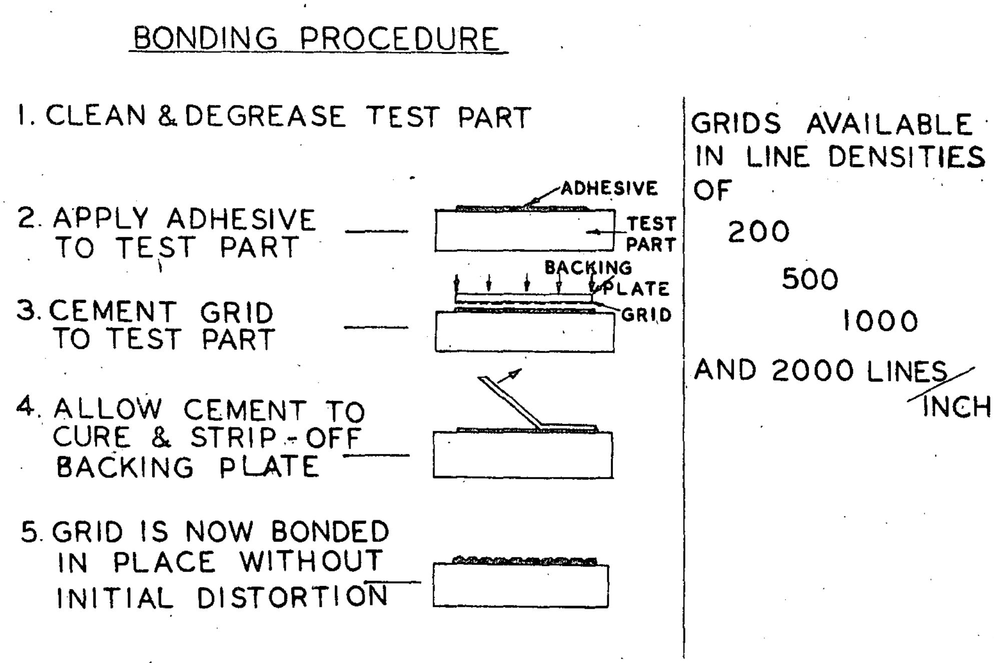

Fig. 1—Bondable moiré grids

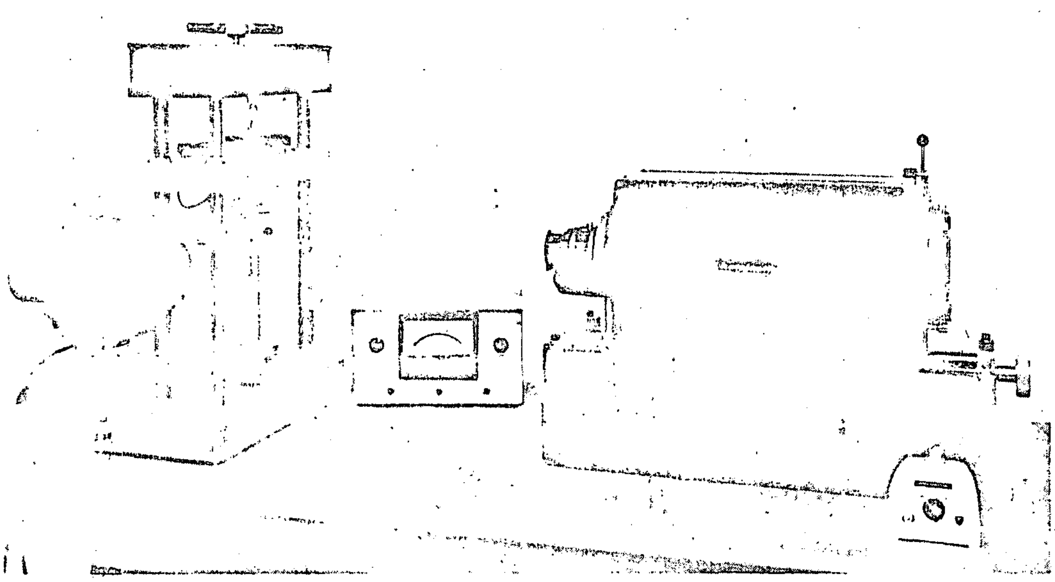

Fig. 2—General view of the moiré instrument (to the right) and a straining frame (to the left)

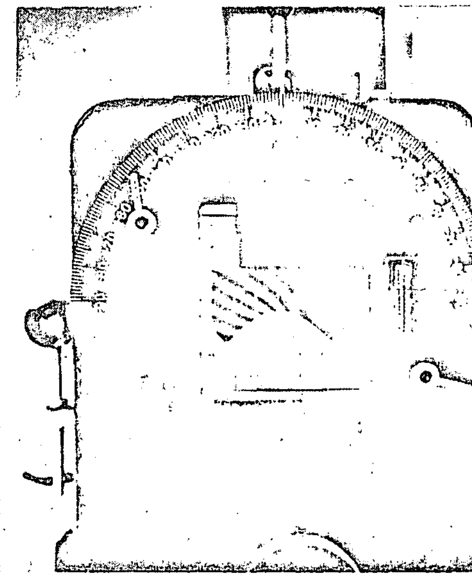

Fig. 3—View of the rear of the moiré instrument where the fringe pattern appears

matched grids (fringes at zero strain) thereby permitting analysis of low strains or measurement over short gage lengths. In addition, photographic film can be used in place of the master in the image plane and, hence, moiré fringes will be produced through double exposure (before and after load application.)

Photographs of the fringes or direct measurement can be made directly from the screen of the instrument (location of the master grid) where the moiré fringes appear. Figures 2 and 3 show the instrument described above.

Limitations of the Transfer-grid Method

Grid Limitations

1. At high temperatures, the epoxy or other adhesive can be destroyed.
2. When applying grids to small radius or complex curvatures, they will usually distort, which will necessitate zero readings. This complicates data reduction.
3. Limited area of a single-transfer pattern.

Instrument Limitations

1. The distance between the instrument and the test part must be rigidly fixed; if not, magnification changes will occur and fringes not related to strain might appear.

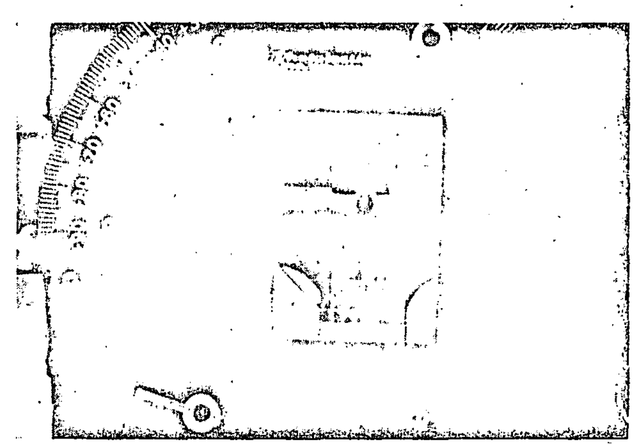

Fig. 4—Moiré pattern visible through a remote observation instrument. Moiré grid located inside the transparent model and master grid of the instrument located at 4 ft from the model

2. Full-field analysis can be accomplished on flat surfaces only. On curved surfaces, measurements are made point by point or line by line.
3. Refocusing of instrument might be required if load-induced warping of the plane containing the grid leads to spurious fringes or out-of-focus areas.
4. A 2000-line-per-inch grid appears as the practical limit for conventional lenses because of

their limited resolution power for large-field observations. Microscope lenses can be used for very high line densities (5 to 10,000 lines per inch); however, then the field of observation becomes very small.

Applications

The main areas where the moiré method of stress analysis can be used uniquely or to more advantage than other methods appear to be:

1. High-temperature applications such as welding, heat treatment, creep.
2. Analysis of interiors of tridimensional models through insertion of grids inside of models and producing moiré fringes with the instrument described above; no contact with grid is required.
3. Strain measurements on soft materials or wherever reinforcement caused by the strain-measuring device is a problem.
4. Long-term measurements wherever stability of the strain-measuring device is a problem.
5. In combination with photoelasticity for two- or three-dimensional problems (stress freezing or not), providing a means of separation of principal strains without resorting to graphical integration, as follows:
   (*a*) Two-dimensional photoelastic model with grid on one of its surfaces. Separate values of principal strains are obtained at any point through the use of moiré or combination of moiré and photoelasticity.
   (*b*) Grid applied inside a three-dimensional photoelastic model. After model "freezing," the slice containing the grid is cut out and analyzed photoelastically and moiré-wise at any desired point. Three principal strains in sign, magnitude and orientation are obtainable without graphical integration.
   (*c*) A slice is cut out from a three-dimensional "frozen" model. A photoelastic analysis is made of the slice. A transfer grid is then applied to the slice and the slice annealed so as to remove from it its birefringence. Because of strain relaxation, the grid is now distorted and can be analyzed. The photoelastic and moiré information are sufficient to obtain the three principal strains as in 5(*b*) above.
6. The method, being very basic, can be used efficiently as a teaching tool in classes of elasticity and stress analysis.
7. An extremely important advantage of the moiré method exists for those problems in which displacements are the desired quantities. *Example:* A simple example will illustrate one of the above-mentioned applications. A section of a rail made of a transparent material was analyzed in its plane directly under a point-acting load (three-dimensional problem.) The model was cut along the plane to be analyzed. A transfer grid was applied to the plane. The model was recemented and a point-like load applied directly above the plane containing the grid. The moiré instrument was then focused on the interior grid and the resulting moiré fringes analyzed without resorting to stress "freezing." Figure 4 shows a portion of the model and the moiré fringes as visible through the instrument.

Conclusion

The technique of grid transfer and moiré–fringe production without master contact appears to be a realistic, economical and practical approach for industrial and laboratory problems. Technicians without special skills can apply grids to any part within minutes and at a reasonable cost.

The future of the method as an industrial tool will depend very much on the level of education of the users, as for any new technique, and upon future developments still needed in high-temperature cements, fringe readout systems for data-reduction simplification, and grids of larger dimensions.

Acknowledgments

Most of the work contained in this paper was inspired by the excellent pioneering work done in this field by P. Dantu of the Laboratoire Central des Ponts et Chaussees, Paris, France. The particular technique of grid transfer, as well as the instrument described in the paper, was developed in a team effort by D. Post, S. S. Redner, M. Wishner, and the author.

References

1. *Theocaris, P. S., "The Moiré Method in Thermal Fields,"* EXPERIMENTAL MECHANICS *4 (8) 223–231 (August 1964).*
2. *Sciammarella, C. A., "Thermal Stresses at High Temperatures in Steel Rings by the Moiré Method,"* EXPERIMENTAL MECHANICS *6 (5) 235–243 (May 1966).*

Homegrown Strain-gage Transducers

Simple compensation procedures can be used to correct errors in strain-gage transducer bridges

by James Dorsey

ABSTRACT—Small errors commonly encountered in experimental stress analysis are often unacceptably large when building strain-gage transducers—even crude ones. Fortunately, the procedures necessary to remove the errors are simple. The steps are discussed in detail and examples given. These compensation techniques can also be useful in strain-measuring applications under certain circumstances. Also discussed briefly is the effect of instrument circuits on transducer performance.

Symbols

- R = resistance
- ΔR = change in resistance
- GF = gage factor
- ε = strain in in./in. (m/m)
- R_B = resistance of transducer strain gages
- V = Wheatstone-bridge supply voltage
- $S.G.$ = strain gage
- V_0 = transducer output
- R_m = Resistance of span-shift compensation resistor
- ΔE = temperature-induced change in spring-element modulus of elasticity
- ΔK = temperature-induced change in gage factor of strain gages
- α_m = temperature coefficient of resistance of span-shift compensation resistor

Introduction

Most strain gages are used in testing to learn about the strain on a surface. But another large quantity is employed on devices called transducers. In the latter applications, users want to measure a physical quantity such as load or pressure and do it by means of an electrical output.

Resistance strain gages are convenient for these devices because they easily convert strains to electrical signals. Although this qualifies them, or the complete devices, to be called transducers, it is more useful for this paper if transducers are defined as devices (a) that use strain gages, and (b) that can be precalibrated before use. Strain sensitivity (or transfer coefficient) of the gages will be learned by actually applying known physical quantities to the device.

The study of transducers is very complex and cannot be completely covered here. Material properties, element (spring) design, case construction, sealing, use of flexures, etc. are all important considerations. But perhaps the least understood area involves compensation techniques needed for initial bridge unbalance and for several errors caused by temperature changes. This paper discusses bridge errors and their corrections, a subject often neglected because cost or time involved is thought to be great. In fact, simple adjustable resistors can be used to quickly and easily achieve good results. In any case, accuracy improvement is often so dramatic that, on a unit-cost basis, nothing else done to improve the transducer can possibly be as effective. As a corollary: failure to make simple corrections for problems caused by temperature changes can result in very large errors (as is also true in experimental stress analysis).

Finally, many of the techniques described find application in experimental stress analysis use of multiple-strain-gage circuits. Bridge compensation has been used both to produce more accurate data and to save installations in which unmatched gages were inadvertently used.

Errors

Unfortunately there are many ways in which the strain gages and their installations can deviate from the ideal. However, most of the serious errors are easily corrected. The four most important are normally considered when transducers will experience temperature excursions or must be interchangeable.

Zero Shift with Temperature Changes

Strain gages respond to temperature. Changes in resistance result from the temperature coefficient of resistance of the grid and the expansion coefficients of the grid and the spring element. Although the temperature coefficient of resistance of most foil strain gages can be adjusted to minimize the changes caused by temperature, zero output cannot be achieved over any appreciable temperature range.

The resulting error is particularly bad because it is, in no way, related to the size of the measurement. In other words, even if the quantity to be measured is zero, a large output can result if temperature changes.

Theoretically, use of a fully active half- or full-bridge will eliminate zero shift by subtraction. In practice, no two strain gages are ever identical and there are variations in installation and in the spring element. (Zero shift will also occur when adjacent bridge arms are mounted on surfaces with different radii.)

Bridge Balance

In general applications, it is convenient to use transducers whose output is zero (or close to zero) when input is zero. Even if the strain gages are well balanced and uniformly installed, compensation for zero shift with

James Dorsey is Vice-President, Engineering, Micro-Measurements Division, Measurements Group, Vishay Intertechnology, Inc., Romulus, MI 48174.

Paper was presented at 1976 SESA Spring Meeting held in Silver Spring, MD on May 9-14.

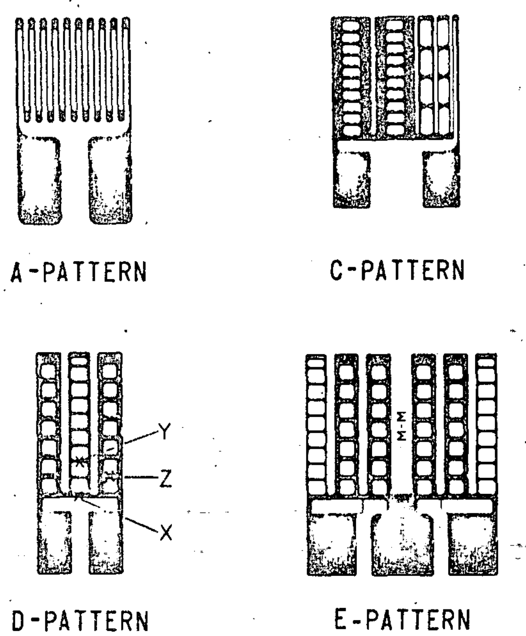

Fig. 1—Bondable resistors

temperature change will often unbalance the bridge zero.

Span Vs. Temperature

Output (span) of an uncompensated transducer will normally change as temperature changes. Differences in span occur with temperature change because both gage factor of the strain gages and modulus of the elasticity of the spring element are functions of temperature.

Normally these two effects combine to cause increasing span as temperature rises.

Span Adjust

The output of a transducer can be set to a specific desired level. Although adjustment of span does not directly affect accuracy, it is usually desirable because it is an advantage to have the transducer/instrument system output displayed in convenient units (e.g., 137 lb—or kilograms—load reads 137 or 1370 counts on the indicator) and also, if transducers are interchanged, output for a given Q would be the same.

Impedance Match

In some applications, it is helpful if the transducer's input or output impedance is within a specified range.

Other Errors

There are many other types of transducer errors. (Creep and nonlinearity are important examples.) Most can be avoided or, to some extent, corrected. However, correction is often difficult and costly and, in any event, the errors are almost always very small.

For these reasons, no attempt will be made to deal here with subjects other than the first five given above.

Compensation Procedures

When compensating strain-gage transducers, it is possible either to calculate the resistors needed or to determine their values experimentally. If more than one transducer of a given type is to be built, it is sometimes possible to use constant values for span and impedance resistors. Step-by-step procedures follow. Where practical to calculate the resistor value rather than determine it experimentally, both techniques are discussed.

For building one (or a small number of transducers), it is often convenient to use compensation resistors that are adjustable. Figure 1 shows four types of bondable resistors that will be used in the examples which follow. The A-pattern represents any fixed resistor. C-pattern is a fixed grid with an added adjustable section. D and E are single and double ladders, respectively. Patterns C, D and E are designed to allow user adjustments of varying amounts. Using a sharpened dental probe or other convenient tool, steps in the ladder-like arms are cut through to lengthen the conducting path and so raise its resistance. Parallel steps may be cut to increase resistance by very small amounts. In Fig. 1 (D-pattern), cutting step X would increase resistance about 2.8 percent of the maximum value. Cutting steps such as Y and Z would increase it only about 0.2 percent and 0.1 percent, respectively. Cutting steps in the C-pattern are designed to be 20 percent, 10 percent and 1 percent of the *uncut* resistance. There are four 20 percent, four 10 percent, and twenty 1 percent steps. However, like the D- and E-patterns, smaller changes can be obtained by cutting from the top or in the middle. The C-pattern is used if the minimum required value will be about half of the fully cut maximum. When it is not known if any resistance will be needed, D- and E-patterns are better because their uncut resistance is very low.

If possible, all temperature-sensitive (copper, Balco®, nickel) compensation resistors (to be described in following sections) should be located on the transducer element where the strain will be low but as close to the strain gages as possible. Doing so will assure the best temperature tracking without danger of fatigue damage. Also, connecting wires *inside* the bridge should be balanced in length and in good thermal contact with the spring element.

Zero Shift with Temperature Change

When gaging the spring element, it is not known if there will be a zero shift with temperature large enough to require compensation or which arm will require the added resistor.

Pattern E resistors are a convenient means to solve the problem because they are very low in uncut resistance

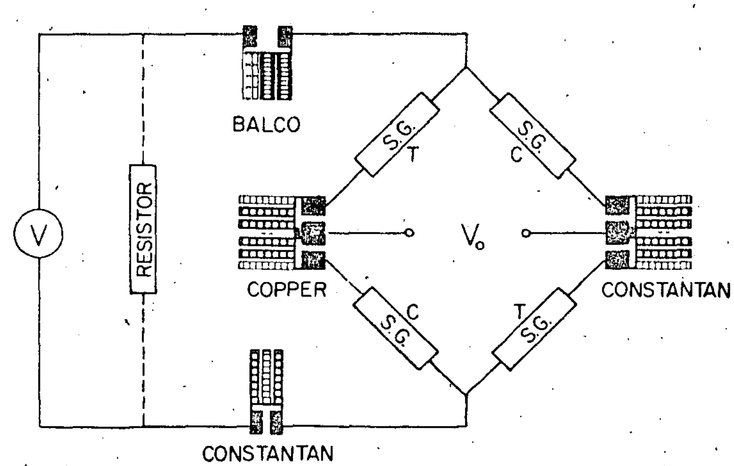

Fig. 2—Bridge circuit with all compensation resistors

TABLE 1—LOAD CELLS AND PRESSURE TRANSDUCERS

	Load Cells		
	General Purpose	Improved Accuracy	High Accuracy
Calibration Inaccuracy	0.5% FS*	0.25% FS	0.1% FS
Temp. Effect on Zero	± 0.005%/°F FS (± 0.009%/°C FS)	± 0.0025%/°F FS (± 0.0045%/°C FS)	± 0.0015%/°F FS (± 0.0027%/°C FS)
Zero-balance Error	± 5% FS	± 2½% FS	± 1% FS
Temp. Effect on Span	± 0.01%/°F OL* (± 0.018%/°C OL)	± 0.005%/°F OL (± 0.009%/°C OL)	± 0.008%/°F OL (± 0.0015%/°C OL)
Nonlinearity	0.25% FS	0.1% FS	0.05% FS
Hysteresis	0.1% FS	0.05% FS	0.02% FS
Non-repeatability	0.1% FS	0.05% FS	0.02% FS
System Inaccuracy†	1% FS	½% FS	0.15% FS
	Pressure Transducers		
Calibration Inaccuracy	0.5% FS	0.25% FS	0.15% FS
Temp. Effect on Zero	± 1%/100°F FS (± 1.8%/100°C FS)	± ½%/100°F FS (± 0.9%/100°C FS)	± ¼%/100°F FS (± 0.45%/100°C FS)
Zero-balance Error	± 8% FS	± 2½% FS	± 1% FS
Temp. Effect on Span	± 1%/100°F OP* (± 1.8%/100°C OP)	± ¾%/100°F OP (± 1.35%/100°C OP)	± ½%/100°F OP (± 0.9%/100°C OP)
Nonlinearity	0.5% FS	0.25% FS	0.1% FS
Hysteresis	0.75% FS	0.25% FS	0.1% FS
Non-repeatability	0.15% FS	0.1% FS	0.05% FS
System Inaccuracy	2%	1%	½%

*FS is 'Full Scale', OL is 'Of Load', OP is 'Of Pressure'.
†Combined effects but not including temperature.

and are designed to be wired in each of two adjacent bridge arms. The copper-foil version can be bonded at the same time as the gages and wired into the bridge at the start. For best performance, the double ladder is most often in a bridge output corner.

Assume that four strain gages (should be same type and lot) are bonded to a spring element and wired in a full-bridge. Output of the bridge will generally not be zero, but is usually close enough so that a reading can be obtained on the transducer-indicator instrument.

If the gages and element are then warmed, output will usually change. (Even in cases where the spring element is part of a large structure such as a bridge or a commercial aircraft, it is usually possible to get readings at two temperatures at different times of the day.)

Theoretically, it is possible to make a very careful measurement of the temperature effect and to calculate the needed compensation resistor. For example: if the bridge output is equivalent to 35μin./in. (μm/m) for a temperature rise of 100°F (55°C) and 350 ohm gages with a gage factor of 2 used:

$$\Delta R = GF \times \epsilon \times R_B \qquad (1)$$

$$\Delta R = 2 \times 35 \times 10^{-6} \times 350 = 0.0245\ \Omega/100°\mathrm{F} =$$

$$0.0245\ \Omega/55°\mathrm{C}$$

Copper wire increases resistance approximately 22 percent/100°F (22 percent/55°C), so a length of wire whose resistance is 0.11 ohms is required to compensate for temperature-induced zero shift of the transducer bridge. [The resistance of a 1.25-in. length of AWG-40 copper wire (0.08-mm diameter × 32 mm long) would be about 0.11 ohms.]

In practice, this calculation is an unproductive exercise. The resistance of copper required is normally extremely small. Selecting such a resistor and soldering it into the bridge arm to achieve compensation is impractical if not all but impossible.

Using a double copper ladder in one corner of the bridge (Fig. 2) assures that the adjustable resistor will be available in the required bridge arm; and also if over-compensation occurs accidentally, it is easy to increase the copper conductive path in the adjacent arm.

When the spring element is gaged and the bridge wired with the double copper ladder in place, it can be put in an oven or otherwise warmed. Bridge-output change will indicate which of the two adjacent arms surrounding the copper ladder needs added temperature sensitivity. By experience and trial and error, the ladder in that arm can be increased in resistance until the temperature-caused zero shift is within acceptable limits.

A word about 'acceptable limits': many of the compensation techniques described can be tuned to as fine a level as is desired. The limits are economic considerations and the fact that compensation is usually not linear. Output can be trimmed to zero at pairs of temperature, such as 77°F and 105°F (25°C and 40°C), but normally is not zero at other temperatures.

Although it is possible to reduce such nonlinearities, the procedure is time-consuming, costly and rarely completely effective. The simple one-resistor compensations discussed here will rotate the curve but not linearize it. Typical magnitudes of correction in Table 1 are chord slope values between temperature points selected by the transducer designer.

Bridge Zero

Bridge zero is adjusted by the same techniques as for zero shift with temperature except a low-temperature coefficient resistor is used. If the initial unbalance is the equivalent of 100 μin./in. in our example, then from eq (1):

$$R = 2 \times 100 \times 10^{-6} \times 350 = 0.07 \text{ ohms}$$

[The resistance of a 1.6-in. length of AWG-40 constantan wire (0.08-mm diameter × 40 mm long) will be approximately 0.07 ohms.] Balance wire can be added after bridge zero is checked or a double ladder can be installed opposite the copper ladder. If the strain gages are made of constantan, then usually an E-pattern resistor made of constantan would be employed, and a Karma-type-alloy resistor would be used for Karma-type gages. The adjustment technique is the same.

The double ladders are connected as shown in Fig. 2.

Span Vs. Temperature

Adjustment of span changes with varying temperature is usually the most difficult compensation to achieve because the quantity to be measured must be applied to the spring element as the temperature is changing.

Nickel temperature sensors have often been used as the compensating element but recently there has been more interest in Balco®, a very stable nickel-iron alloy with a high-temperature coefficient of resistance. Balco has a number of advantages when compared with nickel. It is less expensive, easier to manufacture, and has about 2½ times the resistivity of nickel. Temperature coefficient-of-resistance curves for Balco and nickel are shown in Fig. 3. At temperatures above −100°F (−75°C), the only disadvantage to Balco is a slightly lower temperature coefficient of resistance.

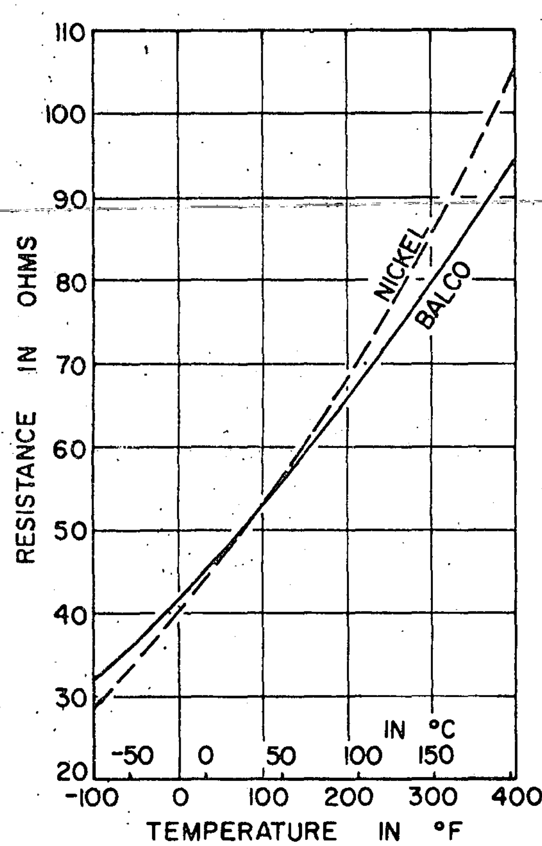

FIG. 3—Temperature vs. resistance for Balco and nickel

If the transducer is put through a temperature cycle and the span change recorded, it is possible to calculate the resistance of the Balco gage required. Or, using approximate values for materials and gage behavior, the following equation will produce a nominal value for this resistor:

$$R_m = \frac{-(\Delta E - \Delta K)R_B}{\alpha_m + (\Delta E - \Delta K)} \tag{2}$$

ΔK (Approximate)

= +0.5%/100°F (+0.9%/100°C) for constantan
= −0.57%/100°F (−1.03%/100°C) for K-alloy - 06 compensation
= −0.83%/100°F (−1.49%/100°C) for K-alloy - 13 compensation

α_m (Approximate)

(for nickel) = +0.31%/°F (+0.56%/°C) OR = 0.0031 Ω/Ω/°F (0.0056 Ω/Ω/°C)
(for Balco) = +0.25%/°F (+0.45%/°C) OR = 0.0025 Ω/Ω/°F (0.0045 Ω/Ω/°C)

Figure 4 is a plot of values obtained with eq (2) and is a good guide to the resistance of the Balco sensors needed. Approximate values for ΔE are also shown for typical transducer element materials. Precise compensation usually does not result from using these resistances because values of R_m from the plots are approximate and will be altered when the calibration resistor is inserted.

A better practice is to pick a value from Fig. 4 and then use a C-pattern resistor that is below the value uncut and above it when fully cut. By successive tests, the value of the resistor can then be adjusted to give best results. It is usually possible to adjust span shift vs. temperature to less than 0.0025 percent of signal/°F (0.0045 percent/°C).

Span Adjust

Span is adjusted by using a temperature-insensitive resistor in series with the voltage supply. A good selection is the D-pattern. By measuring the impedance of the bridge circuit (including the Balco resistor just discussed) and knowing the desired reduction in bridge output, a constantan or Karma D-pattern resistor is easily selected and adjusted by the same method that was used with the Balco.

As with the double ladders within the bridge itself, it is often possible to select suitable span and span vs. temperature adjustable resistors before beginning the gaging and to install them at the same time as the gages.

Impedance Match

If bridge-input impedance match is required, it is usually a fairly high resistance not available in bondable grids. The resistor should be stable with temperature and is installed as shown by the dotted lines in Fig. 2.

Output impedance match is tricky, likely to destroy compensation already achieved, and can only be adjusted to a lower value (by shunting). Since output impedance is

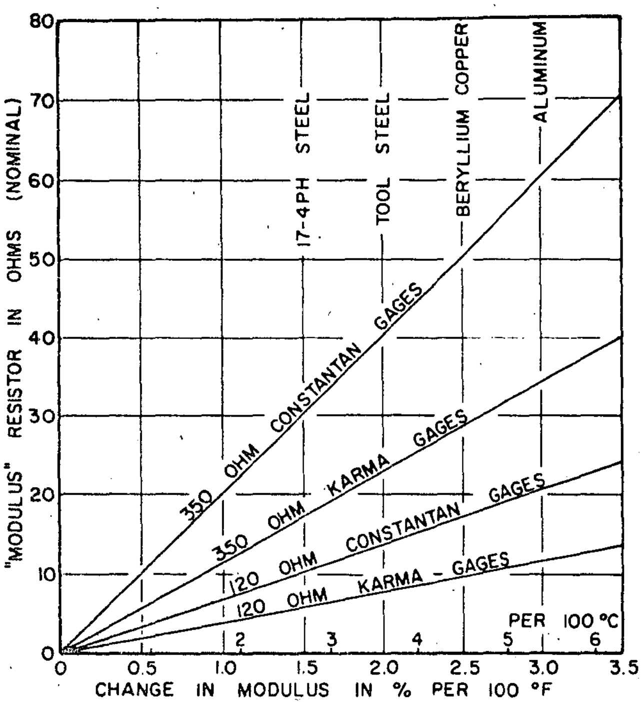

Fig. 4—Calculated-span-shift compensation resistors

close to gage resistance, adjustment is not recommended. Better practice is to use gages with the impedance desired.

General

The completely compensated transducer bridge is shown in Fig. 2. It is actually best to 'split' the Balco and constantan resistors in the voltage circuit so that approximately half of each resistor is in the plus and minus supply arms, respectively. Although two adjustable resistors could be used for each, it is often acceptable and simpler to use a fixed resistor of about the right value in one lead and an adjustable resistor in the other. For example: if Fig. 4 indicates that 28 ohms of Balco is required, a 14-ohm fixed resistor could be put in one lead and a 10- to 24-ohm Balco C-pattern in the other.

When all of the resistors are installed in the beginning, it should not be necessary to repeat the adjustment steps. If, however, tests of the transducer are not satisfactory, a repeat may be needed to 'fine tune' the compensations.

One other problem is sometimes encountered. When the spring element is installed in its case, loads applied by the case itself may change various compensations. Corrections for these difficulties are not recommended because they are complex (usually involving compensation resistor shunts located in a terminal box outside the case). Redesign of the case to avoid trouble is usually possible.

Specifications

Table 1 shows typical specifications for several 'grades' of load and pressure transducers. The compensation techniques above routinely achieve the 'general purpose' specifications. In many applications 'improved accuracy' is not difficult to obtain if there are no adverse effects caused by the case or other environmental protection. 'High accuracy' requires more sophisticated techniques.

In some of the specifications (including system inaccuracy), pressure transducers show worse performance than load cells. There are several reasons, including a greater interaction between the pressure cell diaphragm and its support structure and less freedom of spring-element design in the pressure transducer.

Comments on Instrumentation

Constant Current

The techniques above were discussed for a constant voltage or mV/V device. Constant-current power supplies (or instruments with resistors in series with the voltage supply) will cause little change in zero shift vs. temperature and transducer zero compensations, but completely remove the effect of span adjust and span vs. temperature resistors. (If the current is truly constant, then resistors in series with the power supply do not affect current in the bridge and so compensation does not result from their insertion.)

Transducers can be compensated for constant-current operation by means of shunts rather than series resistors. The procedure is more complex and not recommended for 'homegrown' transducers.

Most transducer manufacturers will provide transducers for use with either-type power supply, often at no difference in cost. Before either buying or building, the type of instrument to be used must be fixed and its operating principles determined. If not done, expensive compensation may either be seriously downgraded or, worse, not work at all.

Instrument Zeroing Circuits

Many instruments used with strain gages and strain-gage transducers have an adjustment that allows the user to balance the reading to zero when the transducer is at zero input. In some cases, these instruments can be set at zero with a fairly large tare input (fixed input of no interest such as the weight of an empty tank).

The zero-balance circuit shown in Fig. 5 is common and, unfortunately, is harmful to the compensation techniques just described. Essentially, the circuit shown shunts two arms of the bridge. For most instruments with this type of balance control, all of the compensations discussed are affected except bridge zero (which it is designed to override). The amount of downgrading depends on the resistors in the instrument but is often enough to put the transducer well outside stated specifications.

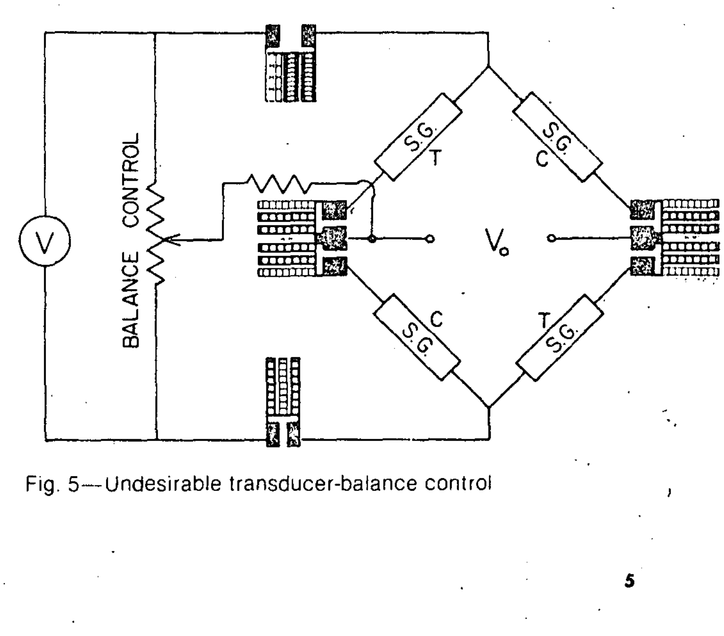

Fig. 5—Undesirable transducer-balance control

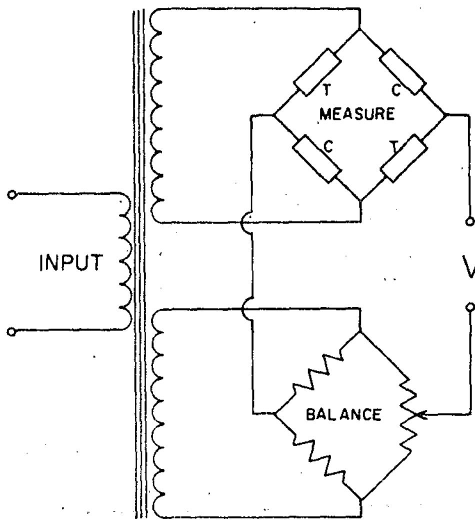

Fig. 6—Recommended transducer circuit

The preferred transducer-instrument circuit is shown in Fig. 6.

Instrument Zero

When building a transducer, it is desirable to know the true instrument zero to assure that the transducer bridge is accurately zeroed. A simple and foolproof method of getting the value is to substitute the circuit shown in Fig. 7 for the complete transducer circuit (gages and compensating resistors). The four resistors in Fig. 7 are all the same and about half the strain-gage resistance. This 'inside out' or star bridge has two important features. The instrument automatically senses zero bridge output and, input and output impedances are about the same as with the transducer in place. (Use of a star bridge is also recommended in strain-gage applications where very small changes in strain are important. Unless the instrument zero is precisely known each time a reading is taken, very large errors can be encountered in these test programs.)

Combining Transducers

If the quantity to be measured requires a combined reading from more than one transducer, special care must be exercised in the circuit used. A typical case would be the use of three or four load cells supporting a tank or a weighing platform. Since the load may be off center, the reading must be either the sum or average of transducers not all seeing the same load.

If inputs and/or outputs of the transducers are paralleled, difficulties are encountered much like those described above under "Instrument Zeroing Circuits"; or worse. The circuit selected for combining transducers must be carefully chosen to prevent interactions. Figure 8 shows a popular arrangement.

General Circuit Considerations

All of the above individual circuit topics relate to some form of problem that occurs because the transducer is built to operate with a relatively 'pure' instrument but often encounters a somewhat less ideal circuit. While some liberties can be taken if a transducer is to be constructed for use only with one particular instrument, this is not the usual case.

It is advisable to investigate the design of instruments to be used with transducers and be sure they will not adversely affect transducer compensation and performance.

Conclusions

In general, building transducers will not be less expensive than buying them. Rather, the decision to build is usually based on one or more of the following:

1. No commercial transducer is available.
2. A portion of a large structure is the required spring element.
3. Many will be used and must be part of an assembly to be manufactured.

Often, readily available commercial transducers will satisfy needs; but in cases where they will not, the techniques needed to compensate for most common strain-gage-bridge errors are straightforward and easy to master. Provided that instrumentation for use with the transducer is wisely selected, quite accurate 'homegrown' transducers are not difficult to construct.

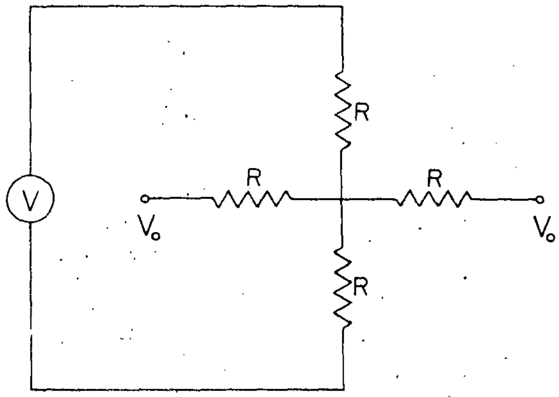

Fig. 7—Star bridge

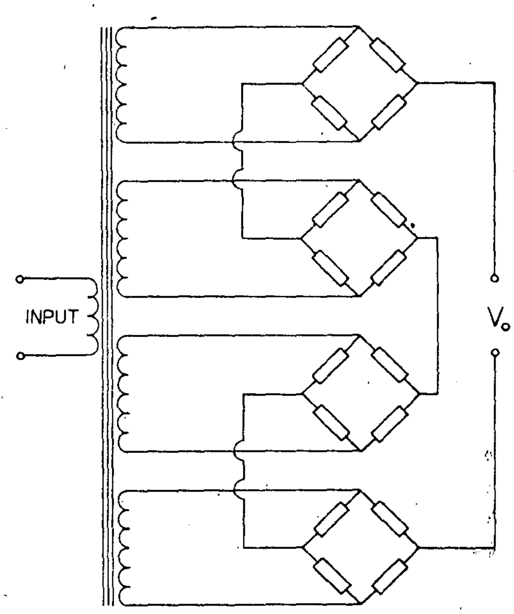

Fig. 8—Circuit for combining transducers

SESSION IV

TRANSDUCER DESIGN

1. Materials

(a) Steels ($E = 30 \times 10^6$ psi)

SAE 4340, 410SS, RDS Tool Steel, Armco 17-4PH SS
Electric furnace or vacuum melt
Hardness: R_c 43 to 48 (BHN 400 to 450)
T.T.S. = 225 to 250 KSI
O.T.S. = 200 to 225 KSI
Y.S. = 175 to 200 KSI (2000 $\mu\varepsilon$ offset)
P.L. = 150 to 175 KSI (20 $\mu\varepsilon$ offset)
E.S. = 85 to 95 KSI ($N = 10^7$ cycles)
K_f = 3.00 (threads)
Elongation = 10 to 15%
Design limits:

$\mu\varepsilon$ (static) = 150,000/30 = 5000 (overloads)
$\mu\varepsilon$ (fatigue) = 90,000/30 = 3000 (reversed cycles)
$\mu\varepsilon$ (threaded) = 3000/3 = 1000 (nominal)

(b) Aluminum Alloys ($E = 10.5 \times 10^6$ psi)

2024 T-81, 2014 T-6, 7075 T-6, X-2020
Hardness: BHN 130 to 140
T.T.S. = 80 to 87 KSI
O.T.S. = 70 to 80 KSI
Y.S. = 50 to 60 KSI (2000 $\mu\varepsilon$ offset)
P.L. = 40 to 50 KSI (20 $\mu\varepsilon$ offset)
E.S. = 20 KSI ($N = 10^7$ cycles)
K_f = 2.00 (threads)
Elongation = 5 to 15%
Design limits:

$\mu\varepsilon$ (static) = 40,000/10.5 = 3800 (overloads)
$\mu\varepsilon$ (fatigue) = 20,000/10.5 = 1900 (reversed cycles)
$\mu\varepsilon$ (threaded) = 1900/2 = 950 (nominal)

(c) Beryllium-Copper ($E = 18.5 \times 10^6$ psi)

Berylco 25 HT
Maximum Hardness (2 hours @ 600°F)
T.T.S. = 200 to 205 KSI
O.T.S. = 200 KSI
Y.S. = 175 KSI (2000 $\mu\varepsilon$ offset)
P.L. = 130 KSI (20 $\mu\varepsilon$ offset)
E.S. = 40 KSI ($N = 10^7$ cycles)
$K_f = 5$ (estimated for threads)
Elongation = 1 to 3%
Design limits:

$\mu\varepsilon$ (static) = 130,000/18.5 = 7000 (overloads)
$\mu\varepsilon$ (fatigue) = 40,000/18.5 = 2150 (reversed cycles)
$\mu\varepsilon$ (threaded) = 2150/5 = 430 (nominal)

2. Design Principles for Spring Element

(a) Integral spring (no bits & pieces)
(b) Maximum strain at gage locations (use flexures)
(c) Uniform strain over grid area of gage
(d) Minimum strain at gage tabs
(e) Gage area consistent with output (MV/V)
(f) Provide adequate heat-sink for power dissipation
(g) Gage area accessible for proper installation
(h) Rated strain consistent with gage endurance
(i) "Caution" with threads:

Preload if possible
Avoid "last-engaged-thread"
Use low nominal stress

(j) Achieve maximum natural frequency:

Maximum overall stiffness
Minimum overall weight

(k) Simple structure - easy to machine - low cost

3. Examples (sketches of good designs)

SESSION IV

TRANSDUCER DESIGN - ELECTRICAL ASPECTS.

1. THE WHEATSTONE BRIDGE (BASIC)

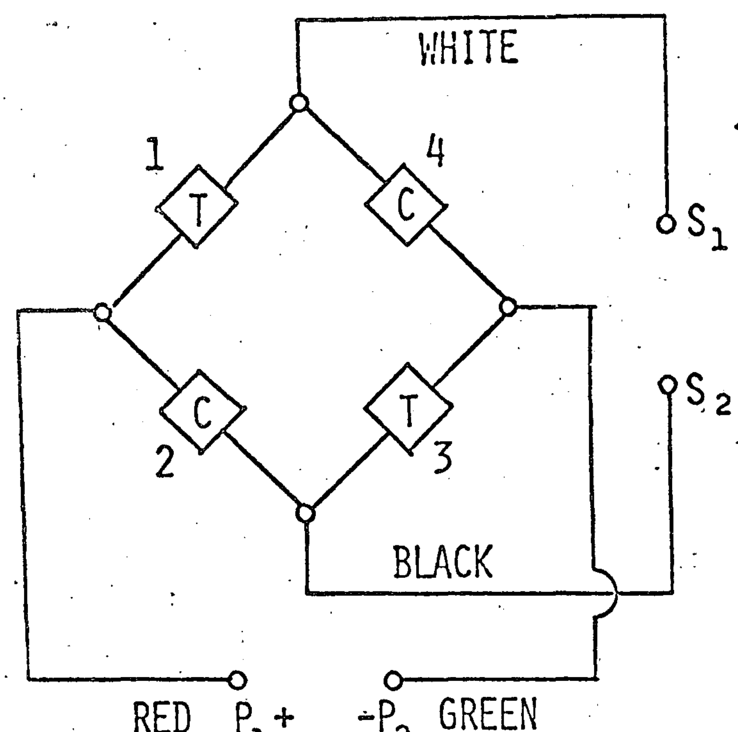

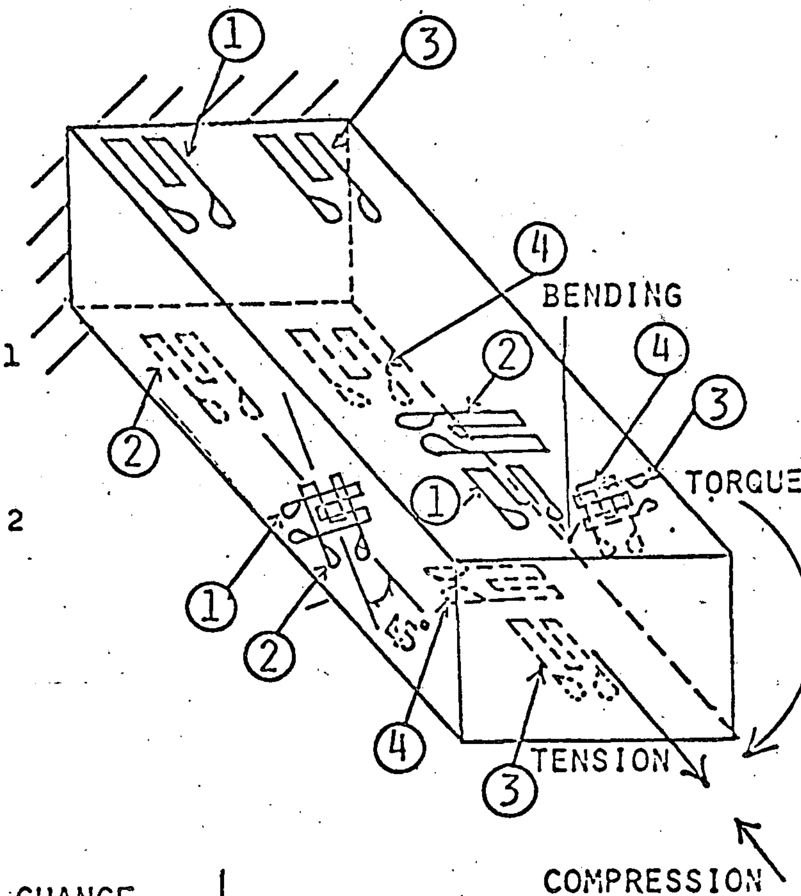

2. ZERO SHIFT DUE TO TEMPERATURE CHANGE

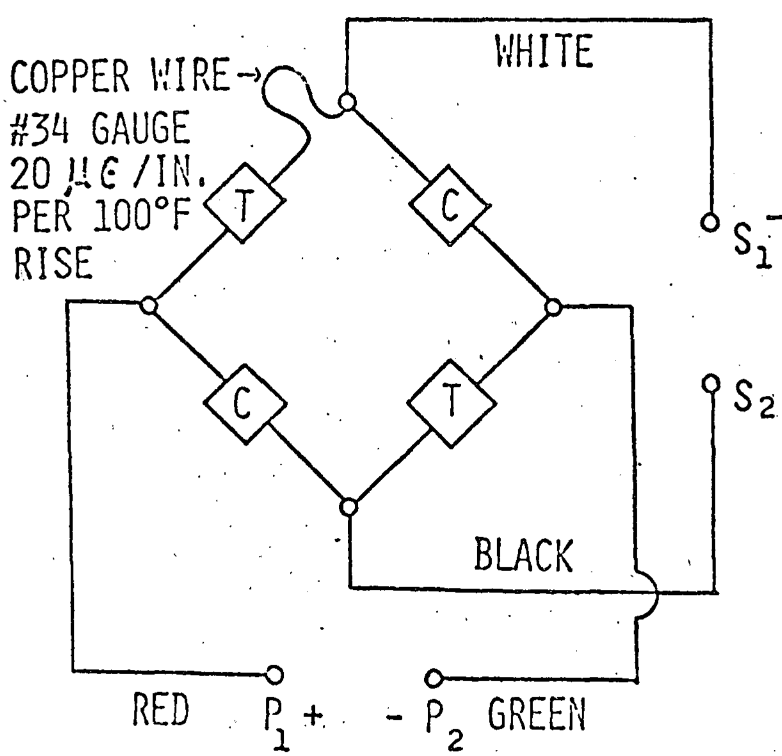

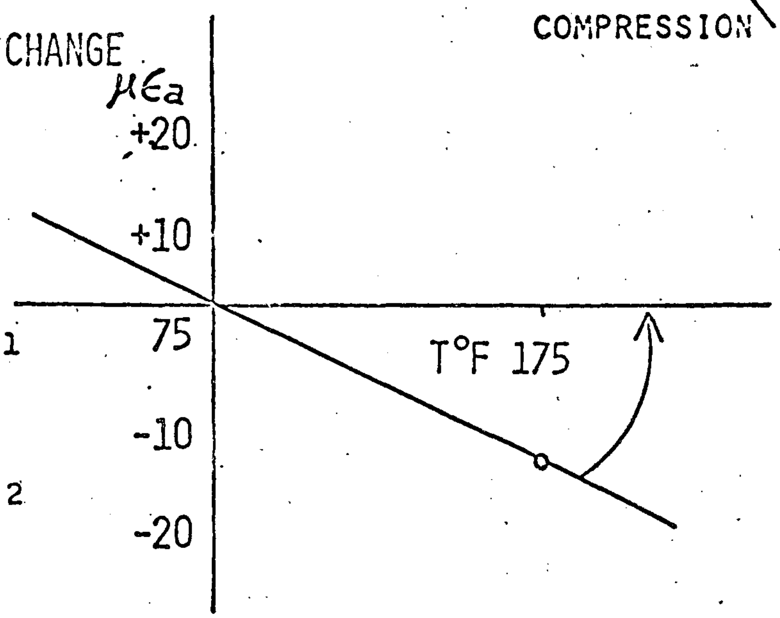

3. SENSITIVITY SHIFT DUE TO TEMPERATURE CHANGE

(A) MODULUS OF ELASTICITY (E) OF TRANSDUCER ELEMENT

TYPICAL VALUES - CHANGE PER 100°F

RDS Tool Steel	1.5%
301 SS	1.4%
17-4PH SS	1.7%
2024 Al.	4 %
6061 Al.	4 %
AZ91 Mag.	6-8 %
HK31 Mag.	2-3 %
8 Mn Ti.	4 %
6 AL4V Ti.	3.6% {full heat treat - 3.7%; full annealed - 3.54%
Inconel X	2.1%
Beryllium Copper	2.5%

(B) GAGE FACTOR OF STRAIN GAGE ALLOY

TYPICAL VALUES - CHANGE PER 100°F

Constantan	+0.5%
K Alloy Compensation	
03	-0.45
06	-0.55
09	-0.72
13	-0.85
Iso Elastic	-0.75

G.F. 2.4 nom.

OPTION B-53

K

06 -1.7%

09 -2.25%

(C) COMBINED EFFECT GAGE & SPECIMEN

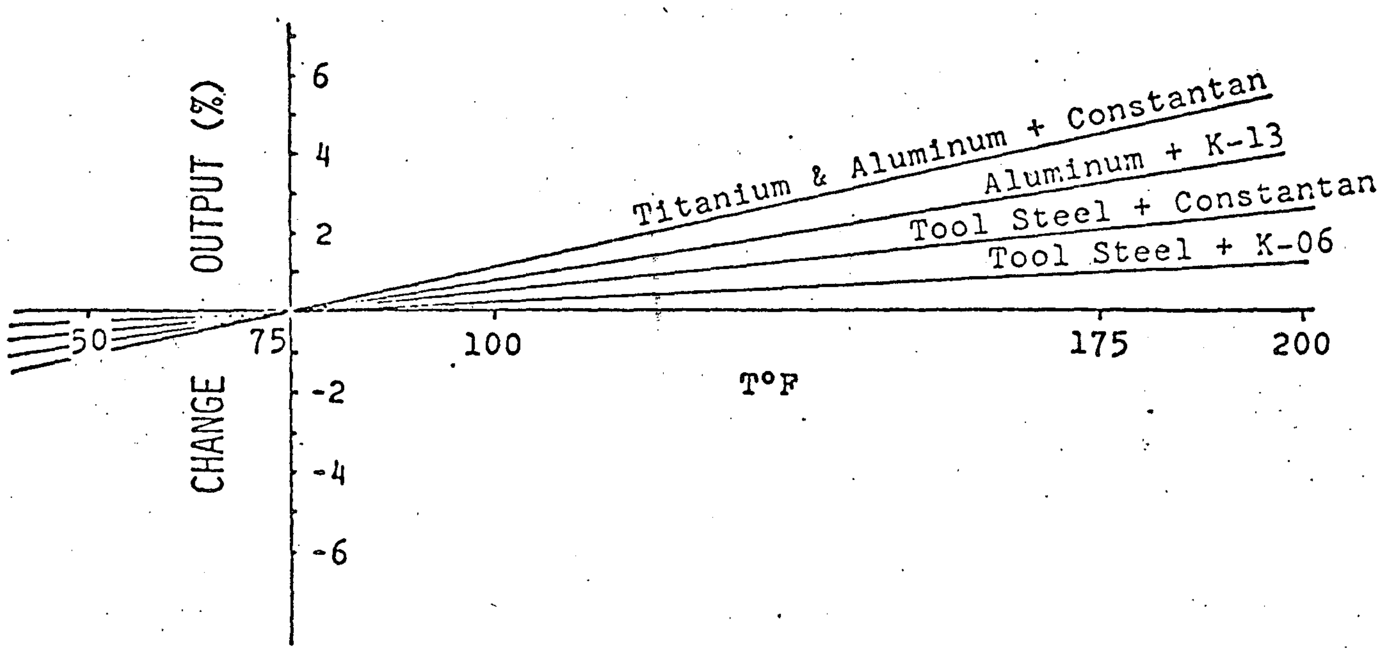

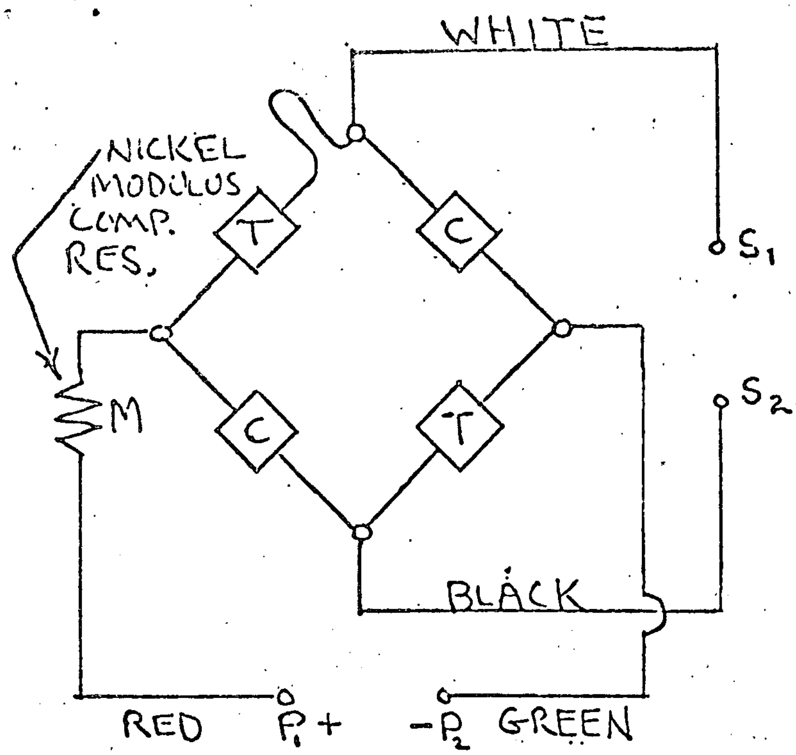

TYPICAL MODULUS RESISTOR VALUE

BRIDGE RESISTANCE CONSTANTAN

	120 OHM M	350 OHM M
Tool Steel and 17-4	7.7	22.5
Aluminum and Titanium	14.3	41.6
Beryllium Cu.	12.0	35.0

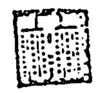

Typical Adjustable
Nickel Resistor
AR Series

4. Bridge Balance

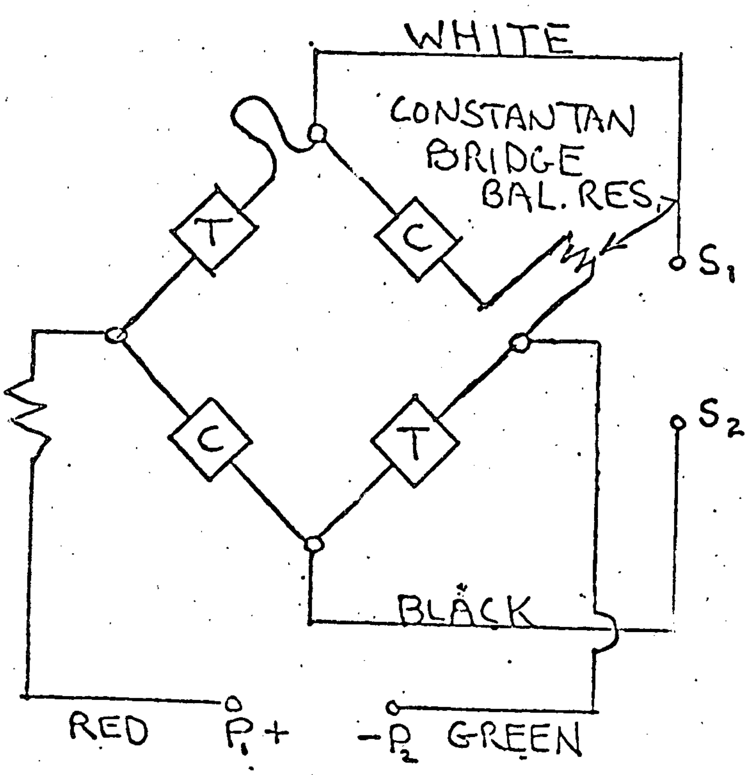

TYPICAL ADJUSTABLE CONSTANTAN BRIDGE

BALANCE RESISTOR

BR SERIES

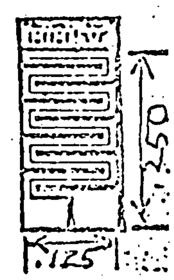

5. BRIDGE CALIBRATION

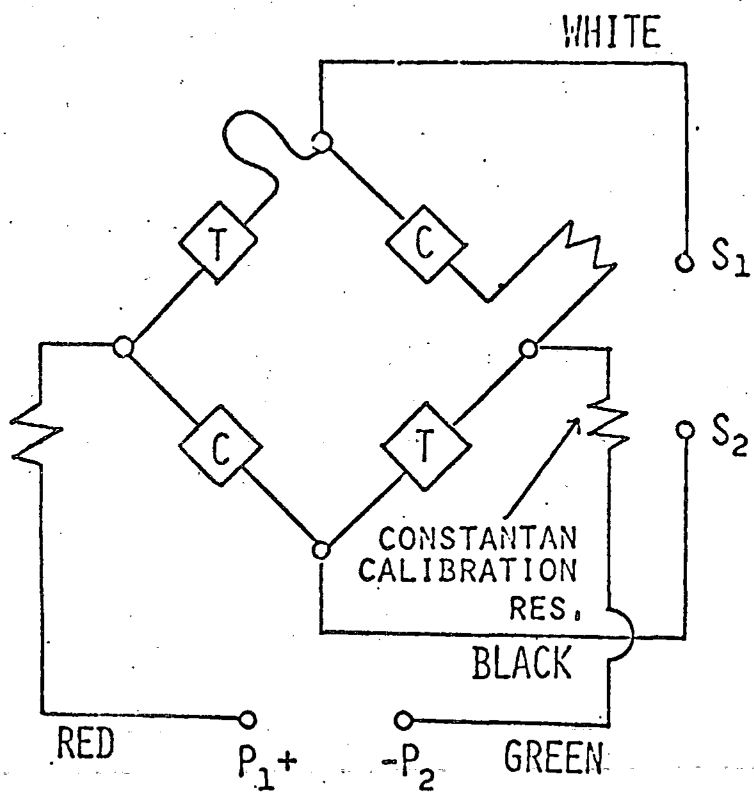

'AR' OR 'BR' SERIES ADJUSTABLE CONSTANTAN RESISTOR MAY BE USED DEPENDING ON VALUE REQUIRED

6. IDEAL COMPENSATION TO MAINTAIN BRIDGE SYMMETRY

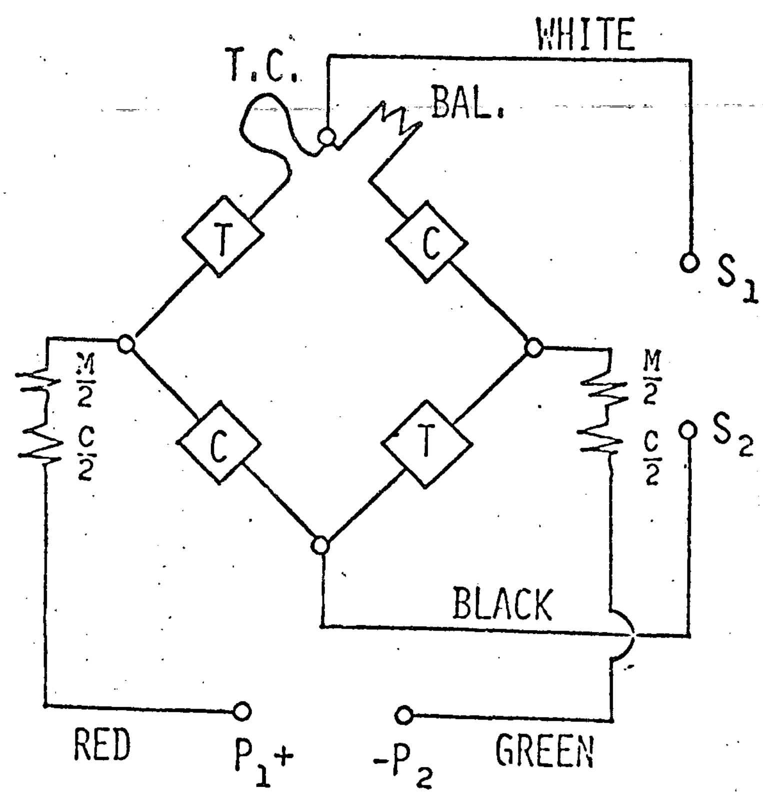

GENERAL INSTRUCTIONS FOR
THE SELECTION AND USE OF
TENS-LAC® BRITTLE LACQUER AND UNDERCOATING

INTRODUCTION TO BRITTLE LACQUER

Brittle Lacquers crack at certain strain levels. These cracks occur perpendicular to the maximum tensile strains and are present at locations where the strain level has exceeded a certain "threshold" value. For Tens-Lac® Brittle Lacquer this threshold is nominally 500 micro-strain ($\mu\varepsilon$). In areas where the threshold is not exceeded, the lacquer will not crack. Since cracks occur where the strain is greatest, stress concentrations can be quickly identified. The cracks also show the direction of maximum strain at a point which allows for accurate alignment of strain gages in order to obtain precise measurements. Test parts are frequently loaded incrementally, and after each load increment, the coating is examined for cracks. Areas where cracks occur can be outlined with a felt-tipped pen, and the applied load noted. The accuracy of brittle lacquer measurements depends on the application of the coating as well as variations in temperature and humidity. If care is taken in the preparation, application, and testing procedure, Tens-Lac® Brittle Lacquer, when properly calibrated, can yield quantitative results accurate to $\pm 100\mu\varepsilon$. Under optimum conditions, accuracy on the order of $\pm 50\mu\varepsilon$ is possible.

SURFACE PREPARATION

It is essential that Tens-Lac® be applied in an oil/water-free environment. The test part must be completely free of oil, dirt, rust, and loose paint. However, a smooth painted film which is not readily softened by the methylene-chloride solvent in Tens-Lac® Brittle Lacquer can be left on the test part. Extremely rough castings, and highly porous surfaces with numerous indentations, can be filled with an eqoxy. Any raised imperfections (e.g., excessive weld splatter scale, should be ground smooth by using a file or rotary grinding wheel. Remove all dirt, grease, etc. using solvents which leave no residue such as Tens-Lac® Brittle Lacquer T-1 solvent.

THE UNDERCOAT

Tens-Lac® Brittle Lacquer Undercoat U-10, which consists of a mixture of aluminum powder and a carrier solvent, is sprayed on the surface of the test part before applying Tens-Lac® Brittle Lacquer. Undercoating with U-10 enhances the visibility of crack patterns. Even if the surface is bright or shiny, U-10 is recommended so as to produce uniform reflectivity. Undercoat also makes it easier to judge the thickness of Tens-Lac® Brittle Lacquer during application.

APPLICATION OF U-10-A UNDERCOAT (AEROSOLS)

One U-10-A aerosol can will cover approximately 8 to 10 square feet. Shake the can vigorously for several minutes to get the aluminum powder in suspension. Periodic shaking of the aerosol can while spraying is also required. Depress the spray head fully while the aerosol is aimed off the part, then move parallel to the surface at a distance of three to six inches (7½ to 15 cm). Do not release the spray head until the aerosol is again beyond the surface of the part. A thin, uniform coating is produced and controlled by the speed of each pass, and the distance from the spray head to the test part. The coating should have a wet appearance immediately after spraying, but will dry to a flat finish in 15 - 30 minutes.

After drying, it is recommended that the surface be brushed gently with a clean tissue or cloth to remove any dust which may adhere to the U-10 undercoat. Undesirable undercoat dust contributes to excessive bubbles in the Tens-Lac® Brittle Lacquer coating.

Spray head clogging is unlikely. If clogging occurs, a 90° rotation of the spray head will usually alleviate the problem. An extra spray head is supplied with each can (found inside the lid). Remove the old spray head and wash out the nozzle hole in the U-10 aerosol can with alcohol. Install the new spray head before the alcohol dries. A lubricant, such as vegetable oil, may be used to ease insertion of the new spray head. If oil is used, be sure to clean out the new spray head by spraying the aerosol for two to five seconds into a waste container. Spray heads for Tens-Lac® Brittle Lacquer and U-10 Undercoat are different and not interchangeable.

APPLICATIONS OF U-10-B UNDERCOAT (BULK SYSTEMS)

The U-10-B is applied to the surface of the test part using a hand held spray gun connected to a remote air supply. The air supply must be completely free of oil and water. It is strongly recommended that separate guns be used when applying Tens-Lac® Brittle Lacquer and Undercoat as this minimizes the possibility of contaminating the Tens-Lac® Brittle Lacquer. Fluid carrying hoses should be Photolastic's type XFH, other hoses can deteriorate when exposed to the methylene-chloride carrier solvent. The canister of the spray gun must be agitated periodically to prevent the aluminum particles from settling.

Spray gun pressure can vary with the type of gun used. Excessive pressure will cause the undercoat to be deposited too dry and dusty. With the pressure properly adjusted, the undercoat should initially appear wet, but not run on a vertical surface. Allow 30 minutes for the undercoat to dry before applying Tens-Lac® Brittle Lacquer.

Immediately after application of the undercoat, clean the spray gun, hoses, and fluid cup, by spraying T-2 solvent followed by T-1 solvent through the system.

SELECTING THE PROPER TENS-LAC® BRITTLE LACQUER

Selecting the proper lacquer is done with the selection chart (see Fig. 1). Your anticipation of the temperature and the relative humidity at the time of testing will determine the proper lacquer.

For example, if the anticipated test temperature will be 70°F (21.1°C) and the relative humidity will be 50%, the proper coating indicated by the selection chart would be TL-500-75. At test conditions of 70°F (21.1°C) and 30% relative humidity, the proper coating could be either TL-500-75 or TL-500-70. The higher number (TL-500-75) would have better sensitivity (lower threshold) while the TL-500-70 would crack at higher strain levels. The lacquer will normally begin to crack when a nominal strain level of 500$\mu\varepsilon$ is reached. However, an increase in temperature or relative humidity will also increase the threshold of the brittle coating causing a loss of sensitivity. At thresholds greater than 700$\mu\varepsilon$, the resultant cracks will not always remain open after removing the load, and it may be necessary to observe the crack patterns on the test part while under load. The threshold of Tens-Lac® Brittle Lacquer can be lowered by decreasing the temperature. However, there is a practical lower threshold limit of 300$\mu\varepsilon$. Below this level Tens-Lac® Brittle Lacquer enters a high state of internal tension and random cracking called "crazing" occurs (see Fig. 2). These random cracks make testing very difficult, and it may be best to respray the part.

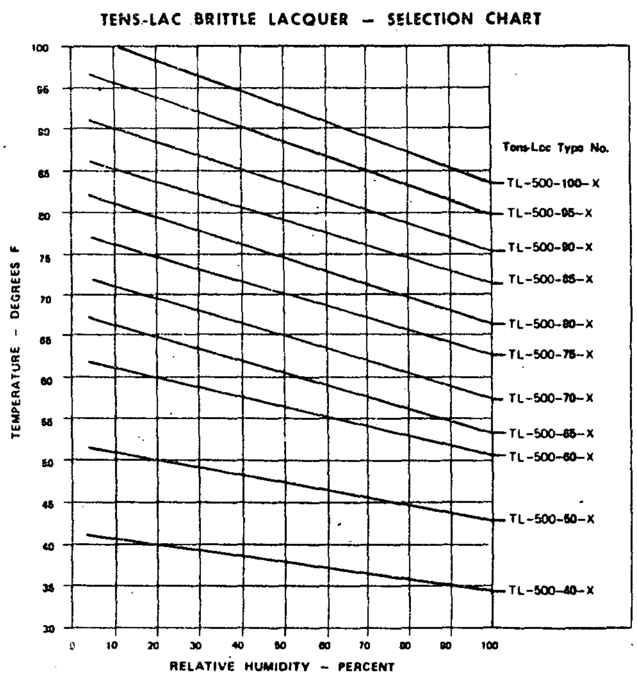

Figure 1

Figure 2

GENERAL SPRAY TECHNIQUES FOR TENS-LAC® BRITTLE LACQUER

The development of good spray techniques is essential in order to obtain perceptable crack patterns. An important point is to avoid producing an excess of bubbles. Spraying too far from the part (depositing dust), or spraying too thick a coat (trapping solvents), can produce too many bubbles. If too many bubbles are present in the coating, the crack patterns will be difficult to detect. Tens-Lac® Brittle Lacquer should be applied in relatively thin, wet layers, allowing approximately two minutes between coats. This method permits the carrier solvents to evaporate. Thin coatings are produced by moving quickly over the part. Wet coatings are produced by decreasing the distance from spray head to the test part.

Sufficient layers of 8 to 12 coats will produce the desired thickness of .003" to .006" (0.08 to 0.15mm). A uniform thickness is seen by noting the variations in color of the coating. Lighter colored areas indicate a thinner coating where more material needs to be added. It is advisable to practice the spraying technique on some calibration bars before doing an actual test. A micrometer can be used to relate the thickness of a coating to the shade of green.

The best lacquer surface is not a flat one, but one that is glossy with an "orange peel" appearance. "Orange peel" surfaces crack in a more repeatable and predictable manner than flat coatings. Spraying in highly humid areas (over 50% R.H.) may produce a "blush" effect caused by water condensing on the cooled surface. Each new coat will dissolve the previous blush. Wait 15 minutes before applying the last coat.

SPRAY TECHNIQUES (AEROSOL)

It is not necessary to shake Tens-Lac® Brittle Lacquer in the aerosol cans. However, if the spray head becomes clogged, an extra nozzle is supplied with each can (found inside the lid). Remove the old nozzle and install the new nozzle following the same procedure as mentioned earlier for the Undercoat U-10 aerosol cans.

Remember, spray heads for Tens-Lac® Brittle Lacquer and U-10 are different and not interchangeable.

The average distance for spraying Tens-Lac® Brittle Lacquer aerosols is about 5 inches (13 cm). The surface temperature of the test part will drop slightly due to evaporation of the solvents and from the propellant in the aerosol can. Thus, the test part needs sufficient time to recover before the next coat is applied (typically 2 min.). This is especially true of thin metal and plastic parts.

SPRAYING TECHNIQUES (BULK SPRAY)*

It is important to have an air supply free of oil and water for any bulk spray system. If a remote feed is used, the fluid hose should be Photolastic's XFH Fluid Hose. Other fluid hoses can contaminate the Tens-Lac® Brittle Lacquer and change its properties. The air pressure needed to spray Tens-Lac® Brittle Lacquer can vary with different guns. If the pressure is too low, the Tens-Lac® Brittle Lacquer may be heavy and run. If the air pressure is too high, the Tens-Lac® Brittle Lacquer may be deposited as dust and the cracks can be difficult to detect. Properly adjusted air pressure should deposit the Tens-Lac® Brittle Lacquer to appear initially wet, but not run on a vertical surface. After spraying, the gun and system components should be thoroughly cleaned by using T-1.

DRYING CONDITIONS FOR TENS-LAC® BRITTLE LACQUER

Parts should be sprayed at ambient conditions, and dried 20-24 hours at 5^{o}F or 10^{o}F (2.8^{o}C to 5.6^{o}C) above the grade of material selected. After drying, the part should be cooled slowly to the environmental test conditions. Rapid cooling will result in "crazing" of the brittle coating. For parts to be tested below 70^{o}F (21.1^{o}C), spray and dry the

*The Photolastic Model TBS-3 System is recommended coating at 70°F (21.1°C) or above for 20-24 hours, and then reduce the temperature slowly to test conditions. Temperature equilibrium must be reached before proceeding with the test.

ALTERNATE DRYING: ELEVATED TEMPERATURE

In some cases, testing requirements dictate that the part be tested in the shortest possible time. Preferably the same day as the Tens-Lac® Brittle Lacquer is applied. For these applications it is suggested that the Tens-Lac® Brittle Lacquer coated part and calibration beams be force dryed at an elevated temperature. Allow ½ to 1 hour of normal drying time at room temperature. Place and cure the coated part and calibration beams in an oven set at 100°F (37.8°C) for several hours (3-5). Cool the coated part and calibration beams to the test temperature. When the coated part and beams are at the test temperature proceed with the calibration of the bars and testing of the coated part. The threshold of the Tens-Lac® Brittle Lacquer might be slightly higher due to the elevated temperature cure.

TESTING CONSIDERATIONS

Always prepare an ample supply of calibration beams (typically four or more). The beams should be sprayed with undercoat and Tens-Lac® Brittle Lacquer in exactly the same manner and at the same time as the test part. During the cure, it is very important that the calibration bars and test part experience identical temperature and humidity conditions. Whenever possible, the bars should be placed directly on the test part during the cure cycle. Further, it is desirable to load the calibration beams over the same length of time that it takes to load the test part. This compensates for creep, or stress relaxation in the Tens-Lac® Brittle Lacquer which can in turn influence the threshold sensitivity.

Cracks are more easily observed when the part is under load and viewed using a portable light source such as a flashlight. Direct the light at an angle of approximately 30 degrees with the coated surface.

It is convenient to outline the crack patterns using a felt tipped pen. The outlines are easier to photograph than the cracks themselves.

For examining the crack patterns during successive loads or incremental loading, reduce the load to zero between each load increment. Zero load should be maintained for twice the duration of the previous load increment before re-loading to the next level.

COMPRESSION TESTING

While brittle coatings are used mainly for locating tensile strains, it is possible to locate areas of compressive strains. This is achieved by loading the test specimen first and then applying and drying Tens-Lac® Brittle Lacquer. After the proper drying time has elasped, the specimen can be unloaded, and the coating will crack showing areas of compression. This occurs when the unloaded compression strains show up as tension strains in the coating. Special calibration procedures are not required.

Another method of measuring compression is to coat and load the specimen in the normal manner, but maintain the load for 3 to 5 hours. During this period the Tens-Lac® Brittle Lacquer relaxes, and when the load is finally removed, the released compression strains appear as tension in the cracked coating. In these instances it is reasonable to calibrate in a like manner. The sprayed calibration beams should be installed in the Tens-Lac® Brittle Lacquer C-220 Calibrator with the sprayed side down. A small clamp, dead weight, etc. will hold the beam in its full deflected position while the lacquer relaxes. The calibration beam should be released at the same time the test part is unloaded.

INSTRUCTIONS FOR TENS-LAC® BRITTLE LACQUER CALIBRATOR C-220

The Calibrator is a convenient, lightweight device for determining the threshold of your Tens-Lac® Brittle Lacquer.

1. Spray a calibration bar on one side except for an area of 1" to 1-½" at one end. Spray it with the same number of coats, at the same time, and same place as the test part is sprayed. Keep the calibration bars with the test part so the bars experience the same cure history as the part. This is very important.

2. At the time of test, put the uncoated end of the bar into the calibrator as shown in Figure 3.

3. Set the strain range selected by turning it until a knob aligns with the strain scale for the range desired. The 300 to 1500 microinches/inch range will be used most often. Even high threshold coatings (above 1500 microinches/inch) should be checked on the 300 to 1500 scale first.

4. Depress the bar until it touches the range selector stop. Important: Place your thumb directly over the stop - not at the end of beam.

5. The first full crack on the bar that is toward the low end of the strain scale (toward you) is the threshold of the lacquer tested. Match this crack with the correct strain scale. Cracks are most easily observed WHILE UNDER LOAD AND by having the light come from behind you as you look at the bar at a shallow angle.

6. Each calibrator has been adjusted and individually calibrated at the factory to produce the correct strain fields in a one-eighth inch thick bar. Therefore do not remove the lacquer from the calibrator bars by sanding or mechanical abrasion. Under the proper ventilation conditions remove the lacquer with Tens-Lac® thinner and the Under-coating with T-2.

Figure 3

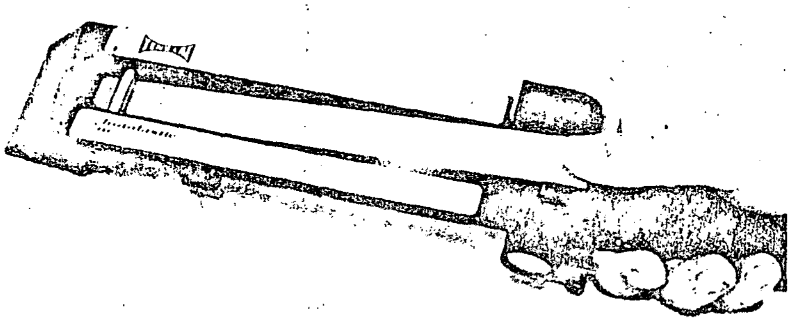

centro de educación continua
división de estudios superiores
facultad de ingeniería, unam

ANALISIS EXPERIMENTAL DE ESFUERZOS

Chapter XXIII

ROSETTE ANALYSIS

DR. LUIS A. FERRER ARGOITE

DR. PORFIRIO BALLESTEROS BAROCIO

ING. ALFREDO OLIVARES PONCE

Outline

1. Reason for Rosette Analysis

2. Stress Fields

   (a) Special Case of Uniaxial Stress
   (b) Special Case of Biaxial Stress
   (c) The General Case

3. Rosette Geometry

   (a) Basic Arrangements Involving 3 Observations of Strain
   (b) Modified Arrangements Involving 4 Observations of Strain

4. Analytical Solutions

   (a) Rectangular Rosette with 3 Observations
   (b) Equiangular or Delta Rosette
   (c) Rectangular Rosette with 4 Observations
   (d) Tee-Delta Rosette

5. Graphical Solutions

   (a) The General Case
   (b) Rectangular Rosette
   (c) Equiangular Rosette
   (c) Nomograph Methods

6. Machine Solutions

7. Corrections for Transverse Sensitivity of SR-4 Gages

   (a) For Rosettes Made Up of Single Component Gages
   (b) For Manufactured Rosettes Containing Three Elements in a Single Unit

8. List of References

9. Laboratory Experiment No, 26 Rosette Analysis

Chapter XXIII ROSETTE ANALYSIS

1. Reason for Rosette Analysis

At any point on a free (unloaded) surface of a solid it is necessary to know three independent quantities in order to specify the state of stress completely. These quantities are the magnitudes of the two principal stresses, σ_1 and σ_2, and their directions, φ or (φ + 90°), with respect to some reference.

For isotropic elastic materials these values can be calculated from strains measured on the surface at the point in question*, and since three independent quantities are to be determined, in general, it will be necessary to make three independent measurements of strain. There are, however, some special situations in which one or two observations of strain will suffice to provide the information necessary for completely establishing the state of stress.

2. Stress Fields

(a) Special Case of Uniaxial Stress (Simple Tension or Compression)

In the case of simple tension or compression, one knows that the directions of the principal stress axes will be parallel and perpendicular to the direction of the applied force, or load, and that the magnitude of the principal stress whose direction is at right angles to the load will be zero.

This means that two of the three quantities are known from the prevailing physical conditions. On this account, it will therefore be necessary to make only a single observation of the strain along the direction of the load in order to determine the one remaining unknown quantity. For an elastic body, the stress may be calculated as follows:

---

* It will be well to draw attention to the fact that, although one refers to the stress condition at a point, the manner of measuring the strain gives the average over a small distance. Therefore, from the practical point of view, the results of a set of rosette observations will approximate the average conditions over a small area. This is not objectionable as long as the length over which the strain is measured is short enough so that there is relatively little change from one end to the other. The gage length will therefore depend upon the strain gradient and may run from small (1/32" or 1/16") values to as much as 6 or 8 inches or even more.

$$\sigma = E \times \epsilon \tag{1}$$

where σ = the stress intensity*
E = the Modulus of Elasticity of the Material
ϵ = the measured strain (+ for tension and - for compression)

(b) Special Case of Biaxial Stress (Principal Stress Directions are Known)

In a few special cases, in which the directions of the principal stress axes (angle ϕ) can be established by auxiliary means such as conditions of symmetry, or through a previous application of Stresscoat, there are only two unknowns, σ_1 and σ_2, the principal stress magnitudes, to be determined. These can be found by measuring the corresponding principal strains, ϵ_1 and ϵ_2, in the directions of the principal stress axes, and calculating the values from equations (2) and (3), which have been developed on the assumption that the material is elastic and isotropic.

$$\sigma_1 = \frac{E}{1 - \mu^2} \times (\epsilon_1 + \mu\epsilon_2) \tag{2}$$

$$\sigma_2 = \frac{E}{1 - \mu^2} \times (\mu\epsilon_1 + \epsilon_2) \tag{3}$$

where σ_1 = the algebraically larger principal stress intensity
σ_2 = the algebraically smaller principal stress intensity
ϵ_1 = the algebraically larger principal strain
ϵ_2 = the algebraically smaller principal strain
E = the Modulus of Elasticity of the Material
μ = Poisson's Ratio

For later use it will be more convenient to express the values of the principal stresses in the form

$$\sigma_1 = E\left\{\frac{A}{1-\mu} + \frac{B}{1+\mu}\right\} \tag{2a}$$

$$\sigma_2 = E\left\{\frac{A}{1-\mu} - \frac{B}{1+\mu}\right\} \tag{3a}$$

---

* If the stress is tension, σ represents σ_1, the algebraically larger principal stress and $\sigma_2 = 0$, whereas if the stress is compression $\sigma_1 = 0$ and σ corresponds to σ_2, the algebraically smaller principal stress.

where $A = \dfrac{\epsilon_1 + \epsilon_2}{2}$ = the hydrostatic component of strain and corresponds to the center of Mohr's Circle

and $B = \dfrac{\epsilon_1 - \epsilon_2}{2}$ = the shear component of strain and corresponds to the radius of Mohr's Circle.

(c) The General Case

In many instances, neither the magnitudes of the principal stresses nor the directions of their axes will be known. This means that for a complete description of the state of stress, at any particular point, three independent quantities must be found. In consequence, it will be necessary to make three measurements of linear strain in different directions, and, from these three observations, to compute the two principal stress magnitudes and the directions of the axes.

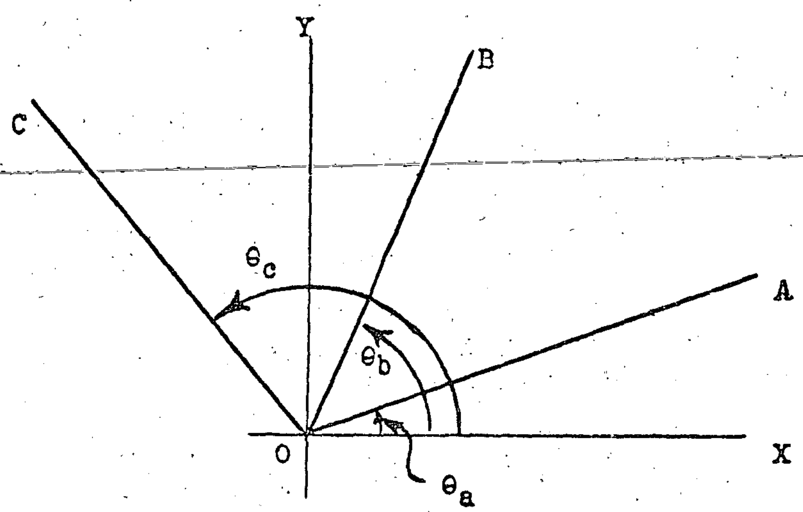

Figure 1

For example, Fig. 1 illustrates a pair of reference axes, OX and OY (90° apart), and three other axes, OA, OB, and OC, making angles θ_a, θ_b, and θ_c, respectively with the reference axis OX. The axes OA, OB, and OC, form what is described as a "Rosette" and, if corresponding linear strains ϵ_a, ϵ_b, and ϵ_c, are measured in their respective directions, one can calculate the linear and shearing strains, ϵ_x, ϵ_y, and γ_{xy}, corresponding to the OX and OY axes of reference.

The values of ϵ_x, ϵ_y, and γ_{xy}, are calculated in terms of the measured strains, ϵ_a, ϵ_b, and ϵ_c, from the simultaneous solution of the equations (4), (5), and (6).

$$\epsilon_a = \epsilon_x \cos^2 \theta_a + \epsilon_y \sin^2 \theta_a + \gamma_{xy} \sin \theta_a \cos \theta_a \quad (4)$$

$$\epsilon_b = \epsilon_x \cos^2 \theta_b + \epsilon_y \sin^2 \theta_b + \gamma_{xy} \sin \theta_b \cos \theta_b \quad (5)$$

$$\epsilon_c = \epsilon_x \cos^2 \theta_c + \epsilon_y \sin^2 \theta_c + \gamma_{xy} \sin \theta_c \cos \theta_c \quad (6)$$

where ϵ_x = Linear strain in the direction of the OX axes
ϵ_y = Linear strain in the direction of the OY axes
γ_{xy} = Shear strain referred to the OX and OY axes

When ϵ_x, ϵ_y, and γ_{xy}, have been determined by the simultaneous solution of equations (4), (5), and (6), the principal strains may be found from the expressions

$$\epsilon_1 = \frac{\epsilon_x + \epsilon_y}{2} + \frac{1}{2}\sqrt{(\epsilon_x - \epsilon_y)^2 + \gamma_{xy}^2} \quad (7)$$

$$= A + B \quad (7a)$$

and

$$\epsilon_2 = \frac{\epsilon_x + \epsilon_y}{2} - \frac{1}{2}\sqrt{(\epsilon_x - \epsilon_y)^2 + \gamma_{xy}^2} \quad (8)$$

$$= A - B \quad (8a)$$

The magnitudes of the principal stresses are then determined from equations (2) and (3) or (2a) and (3a) and the directions from the ratio of the quantities under the radical in (7) or (8) above, since,

$$\tan 2\phi = \frac{\gamma_{xy}}{\epsilon_x - \epsilon_y} \quad (9)$$

where ϕ = the angle of one of the principal axes with respect to the axis of reference. (The distinction between the two principal axes will be considered later.)

3. Rosette Geometry

Theoretically the relative directions of strain measurement (Angles Θ_a, Θ_b, and Θ_c) are of no particular importance, however, from the practical consideration of solving the equations one finds that certain preferred orientations permit of much simpler reduction of the strains into terms of stress.

At the present time there are four generally accepted arrangements of the gage axes for strain rosettes. Basically there are just two arrangements, the rectangular, and equiangular, but each of these has a modification involving a redundant fourth observation of strain.

(a) Basic Arrangements Involving Three Observations of Strain

1. The Rectangular Rosette in which the three gage axes are laid out at 45° and 90° to each other as shown in Fig. 2.

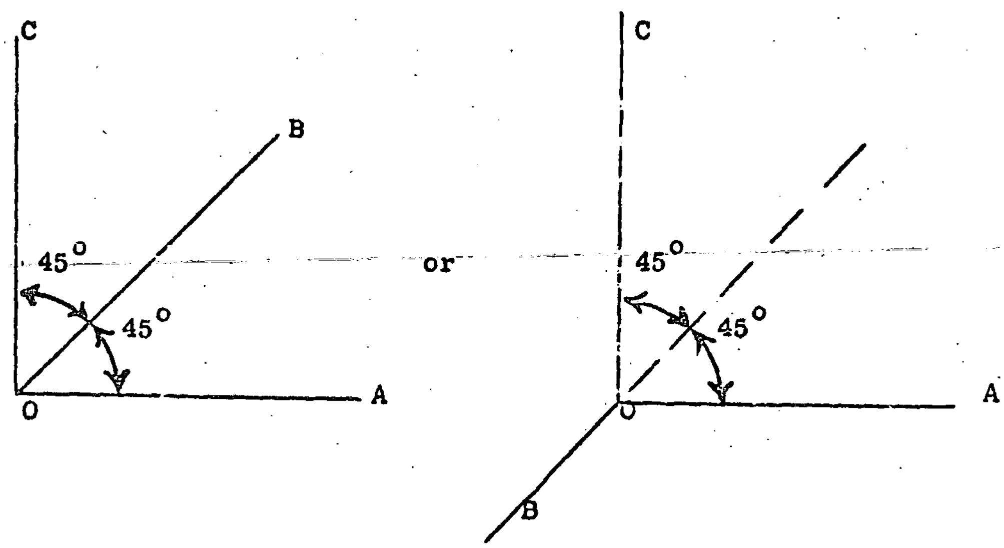

Figure 2

2. The Equiangular or Delta Rosette in which the three gage axes are laid out parallel to the sides of an equilateral triangle. This type of rosette has the most desirable orientations of the directions of strain observation but the equations for computing the stress values are not quite so simple as those of the rectangular rosette, which for this reason, is preferred by many investigators.

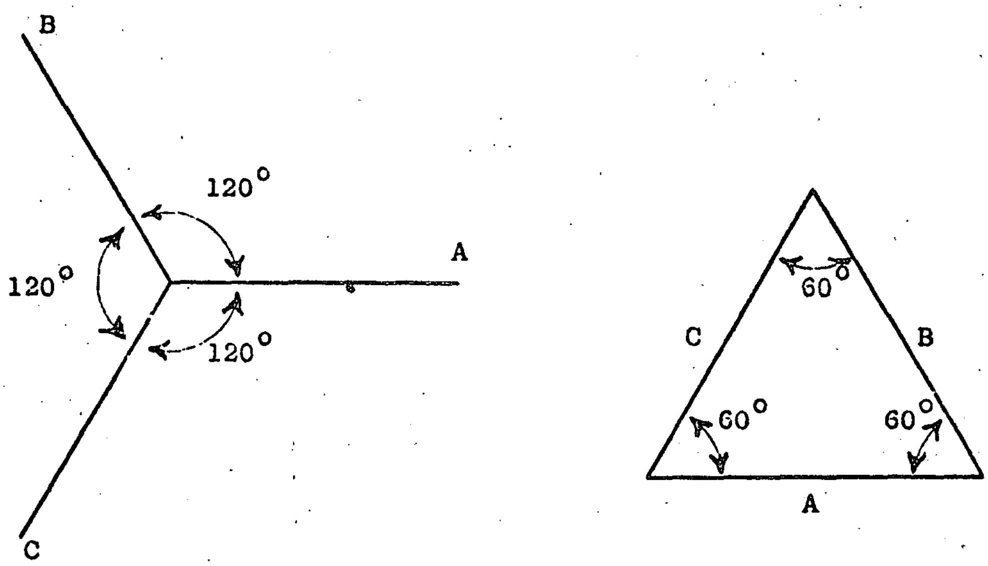

Figure 3

(b) Modified Arrangements Involving Four Observations of Strain

1. The Rectangular or Fan Type Rosette with the four gage axes 45° apart as indicated in Fig. 4. Although the fourth observation is theoretically unnecessary, nevertheless, it provides a convenient means of checking the observations since the sum of the strains in any two directions at right angles should be a constant for a given set of conditions, that is,

$$(\epsilon_a + \epsilon_c) = (\epsilon_b + \epsilon_d)$$

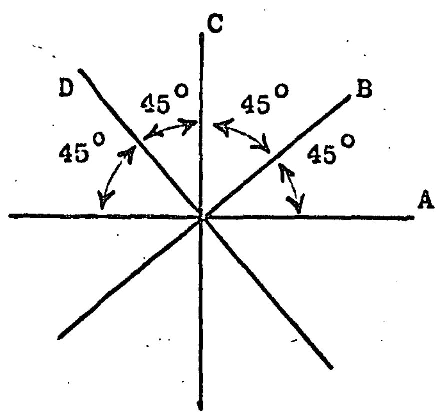

Figure 4

2. The Tee-Delta (T- Δ) Rosette is essentially the same as the equiangular arrangement with the addition of a fourth observation which is made at right angles to the direction of one of the other three. It is claimed that this form of rosette has all the desirable characteristics of the equiangular type plus the advantage of a little more precise determination of the hydrostatic component of strain at the reference point, if this coincides with the intersection of two perpendicular gage axes.

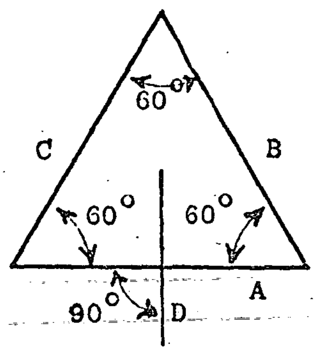

Figure 5

4. Analytical Solutions

(a) The Rectangular Rosette (With Three Observations of Strain)

If the OA axis of the rosette (Fig. 1) is taken as the reference, and considered as coincident with OX, then, for the arrangement of the strain gage axes in the rectangular rosette (Fig. 2),

$$\theta_a = 0 \qquad \theta_b = 45^\circ \qquad \theta_c = 90^\circ$$

and

$$\cos\theta_a = 1 \qquad \cos\theta_b = \frac{1}{\sqrt{2}} \qquad \cos\theta_c = 0$$

$$\sin\theta_a = 0 \qquad \sin\theta_b = \frac{1}{\sqrt{2}} \qquad \sin\theta_c = 1$$

By substituting these particular values of the trigonometric functions into equations (4), (5), and (6), one obtains the relations

$$\epsilon_a = \epsilon_x(1)^2 + \epsilon_y(0)^2 + \gamma_{xy}(0)(1) \tag{10}$$

$$\epsilon_b = \epsilon_x\left(\frac{1}{\sqrt{2}}\right)^2 + \epsilon_y\left(\frac{1}{\sqrt{2}}\right)^2 + \gamma_{xy}\left(\frac{1}{\sqrt{2}}\right)\left(\frac{1}{\sqrt{2}}\right) \tag{11}$$

$$\epsilon_c = \epsilon_x(0)^2 + \epsilon_y(1)^2 + \gamma_{xy}(1)(0) \tag{12}$$

from which it is seen that

$$\epsilon_x = \epsilon_a \qquad (13) \qquad\qquad \epsilon_y = \epsilon_c \qquad (14)$$

and

$$\epsilon_b = \frac{\epsilon_x}{2} + \frac{\epsilon_y}{2} + \frac{\gamma_{xy}}{2}$$
$$= \frac{\epsilon_a}{2} + \frac{\epsilon_c}{2} + \frac{\gamma_{xy}}{2}$$

or

$$\gamma_{xy} = 2\epsilon_b - (\epsilon_a + \epsilon_c) \qquad (15)$$

By substituting (13), (14), and (15), into equations (7) and (8) one obtains the values of the principal strains directly in terms of the observations on the rosette as

$$\epsilon_1 = \frac{\epsilon_a + \epsilon_c}{2} + \frac{1}{2}\sqrt{(\epsilon_a - \epsilon_c)^2 + \left[2\epsilon_b - (\epsilon_a + \epsilon_c)\right]^2} \qquad (16)$$

$$= A + B \qquad (16a)$$

$$\epsilon_2 = \frac{\epsilon_a + \epsilon_c}{2} - \frac{1}{2}\sqrt{(\epsilon_a - \epsilon_c)^2 + \left[2\epsilon_b - (\epsilon_a + \epsilon_c)\right]^2} \qquad (17)$$

$$= A - B \qquad (17a)$$

These values of ϵ_1 and ϵ_2 may now be employed in equations (2) and (3) in order to determine the principal stresses, σ_1 and σ_2. However, in most cases, one does not need to know the numerical values of the principal strains; therefore, a little time and effort can be saved by using equations (2a), (3a), (16a) and (17a) since for this type of rosette

$$A = \frac{\epsilon_a + \epsilon_c}{2} \qquad (18)$$

and

$$B = \frac{1}{2}\sqrt{(\epsilon_a - \epsilon_c)^2 + \left[2\epsilon_b - (\epsilon_a + \epsilon_c)\right]^2} \qquad (19)$$

from which the values of the principal stresses can be expressed directly in terms of the strain observations on the rosette, as follows:

$$\sigma_1 = E\left\{\frac{\epsilon_a + \epsilon_c}{2(1-\mu)} + \frac{1}{2(1+\mu)}\sqrt{(\epsilon_a - \epsilon_c)^2 + \left[2\epsilon_b - (\epsilon_a + \epsilon_c)\right]^2}\right\}, \tag{20}$$

$$\sigma_2 = E\left\{\frac{\epsilon_a + \epsilon_c}{2(1-\mu)} - \frac{1}{2(1+\mu)}\sqrt{(\epsilon_a - \epsilon_c)^2 + \left[2\epsilon_b - (\epsilon_a + \epsilon_c)\right]^2}\right\} \tag{21}$$

Mathematically, equations (20) and (21) are not in the simplest form, but the form given lends itself better to the determination of the directions of the principal stress axes.

Determination of the Directions of the Principal Stress Axes

By substituting equations (13), (14), and (15) into equation (9) one obtains the expression

$$\tan 2\varphi = \frac{2\epsilon_b - (\epsilon_a + \epsilon_c)}{\epsilon_a - \epsilon_c} \tag{22}$$

which yields two values of φ. One value corresponds to each principal stress axis but which of the two axes corresponds to σ_1, the algebraically larger principal stress?

In the literature, no uniform convention has been adopted by the various writers on the subject and in consequence there is an apparent confusion which necessitates the exercise of extreme care in making one's interpretation of the physical significance of the values computed for the angle φ.

Fortunately a check can always be made by sketching Mohr's diagram from which the following rules can be established

Definition:

Let φ_1 = the angle measured (positive in the anti-clockwise direction) from the positive OA axis of the strain rosette to the positive 01 axis which corresponds to the direction of σ_1.

Rules (to be proved later)

1. When $\epsilon_b > \dfrac{\epsilon_a + \epsilon_c}{2}$ φ_1, lies between 0 and +90°

2. When $\epsilon_b < \dfrac{\epsilon_a + \epsilon_c}{2}$ φ_1, lies between 0 and -90°

3. When $\epsilon_b = \dfrac{\epsilon_a + \epsilon_c}{2}$

and (a) $\epsilon_a > \epsilon_c$ $\epsilon_a = \epsilon_1$ and $\varphi_1 = 0$

(b) $\epsilon_a < \epsilon_c$ $\epsilon_a = \epsilon_2$ and $\varphi_1 = \pm 90^\circ$

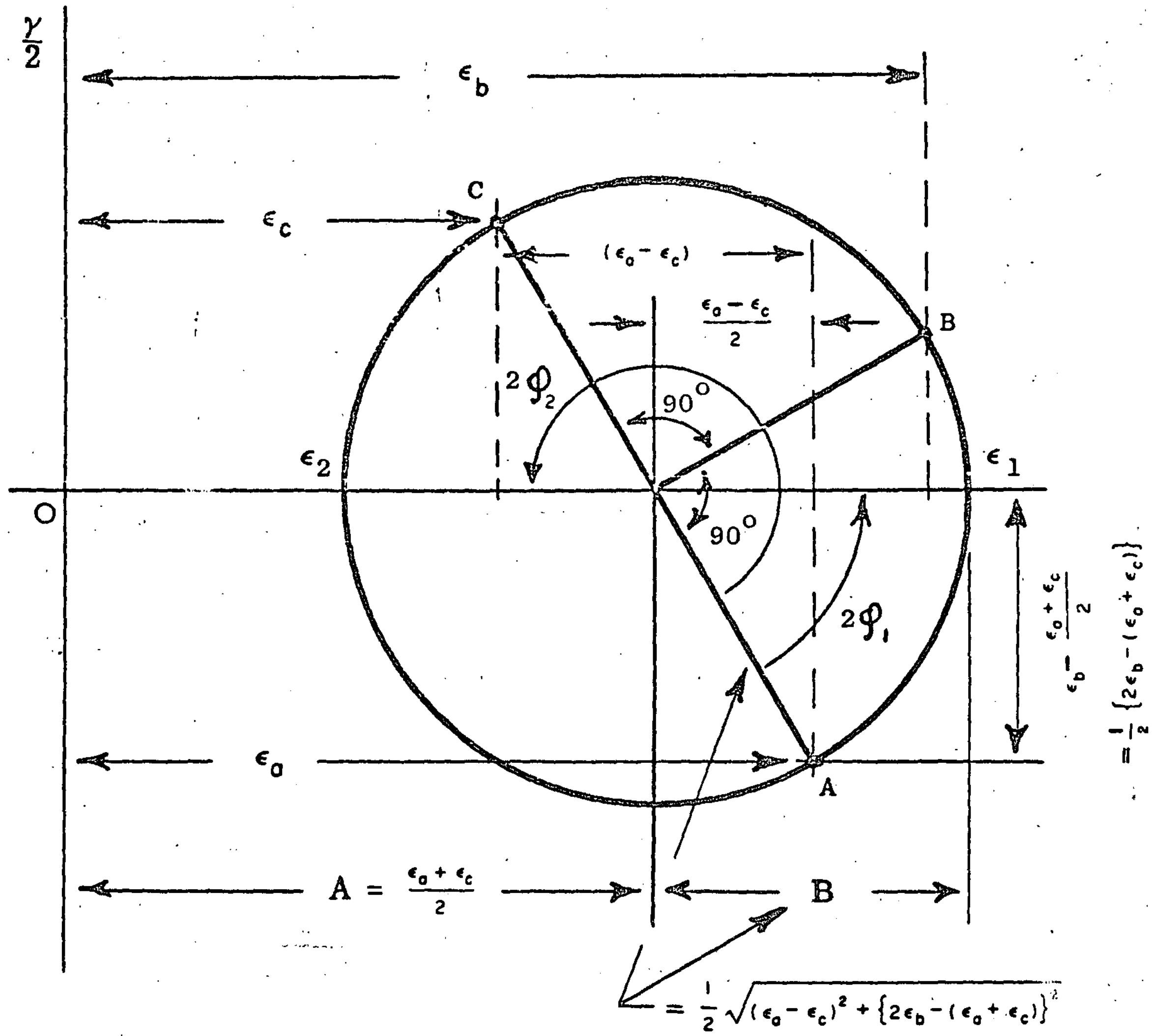

Figure 6

Mohr's Circle for the Rectangular Rosette
(with three observations of strain)

Proof of Rules

An inspection of the diagram, Fig. 6, shows that the strains ϵ_a, ϵ_b, and ϵ_c, are represented by points A, B, and C, on the circumference of the circle and at the ends of the radial lines which are 90^o = (2×45^o) apart taken in the same sequence as the rosette axes which are 45^o apart.

If the point A lies anywhere along the semi-circumference below the abcissa, then the angle $2\phi_1$, will be positive, and have values between 0 and 180^o, so that ϕ_1 will be between 0 and 90^o. If the point A happens to lie on the semi-circumference above the abcissa, then the angle $2\phi_1$ will lie between 0 and -180^o and ϕ_1 will be between 0 and -90^o.

How can one tell whether point A is above or below the abcissa on the Mohr diagram?

A study of Fig. 6 shows that point A will lie below the abcissa whenever point B is to the right of the center of the circle, that is, when $\epsilon_b > \frac{\epsilon_a + \epsilon_c}{2}$. Point A will be above the abcissa when $\epsilon_b < \frac{\epsilon_a + \epsilon_c}{2}$ and will lie on the abcissa when $\epsilon_b = \frac{\epsilon_a + \epsilon_c}{2}$.

Therefore the following rules can be set down:

(a) ϕ_1 will lie between 0 and $+90^o$ when $\epsilon_b > \frac{\epsilon_a + \epsilon_c}{2}$

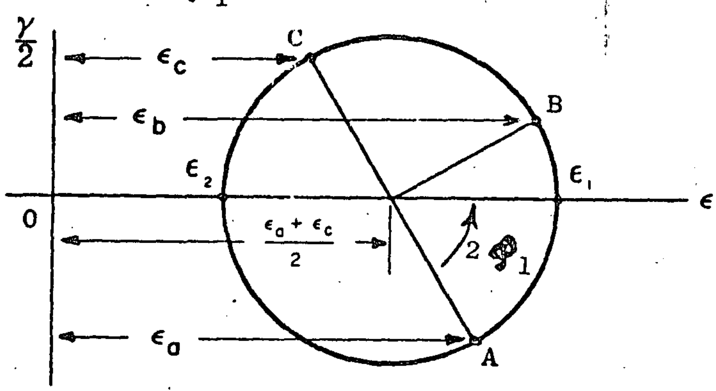

Mohr Diagram for $\epsilon_b > \frac{\epsilon_a + \epsilon_c}{2}$

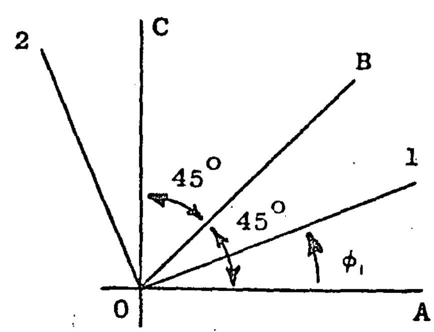

Rosette Diagram

Figure 7

(b) ϕ_1 will lie between 0 and -90^o when $\epsilon_b < \frac{\epsilon_a + \epsilon_c}{2}$

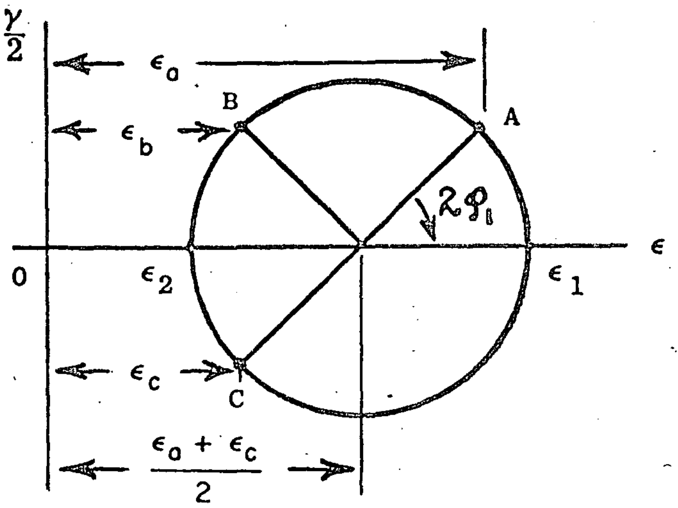

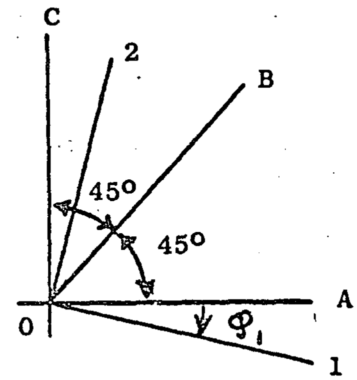

Mohr Diagram $\epsilon_b < \frac{\epsilon_a + \epsilon_c}{2}$

Rosette Diagram

Figure 8

(c) when $\epsilon_b = \frac{\epsilon_a + \epsilon_c}{2}$

$\varphi_1 = 0$ if $\epsilon_a > \epsilon_c$

$\varphi_1 = 90°$ if $\epsilon_a < \epsilon_c$

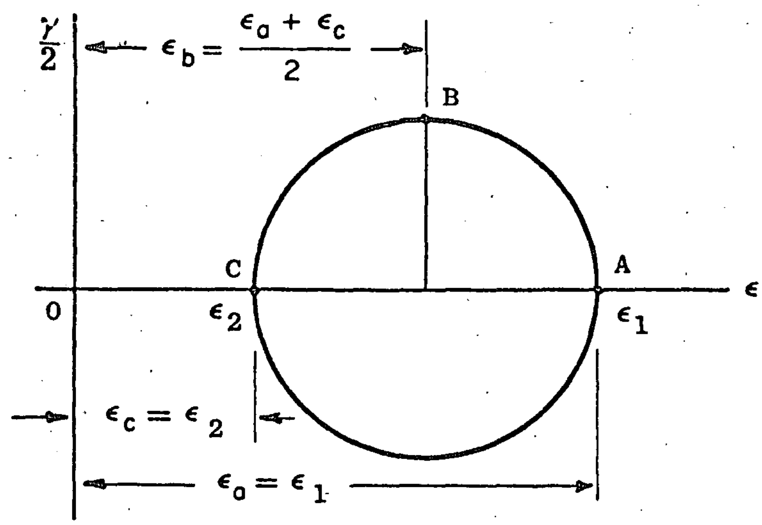

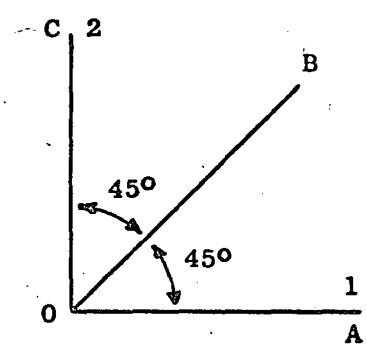

Mohr Diagram

Rosette Diagram

For case in which $\epsilon_b = \frac{\epsilon_a + \epsilon_c}{2}$ and $\epsilon_a > \epsilon_c$

Figure 9 (a)

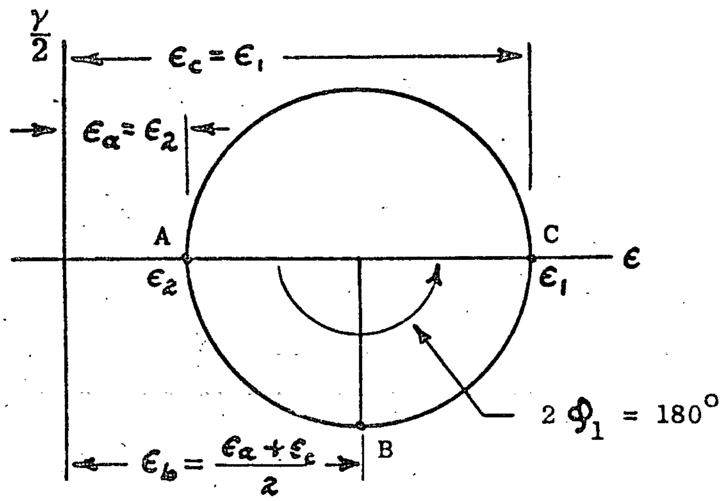

Mohr Diagram

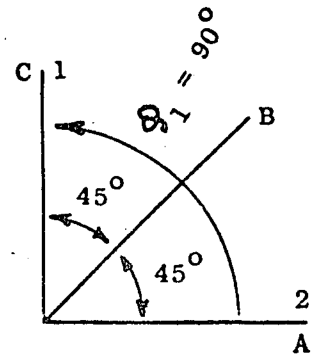

Rosette Diagram

For case in which $\epsilon_b = \dfrac{\epsilon_a + \epsilon_c}{2}$ and $\epsilon_a < \epsilon_c$

Figure 9 (b)

(b) The Equiangular or Delta (Δ) Rosette

Following the previous procedure, in which the OA axis of the rosette is taken coincident with the OX axis of reference, for this arrangement gives

$$\theta_a = 0 \qquad \theta_b = 120^\circ \qquad \theta_c = 240^0$$

and

$$\cos\theta_a = 1 \qquad \cos\theta_b = -1/2 \qquad \cos\theta_c = -1/2$$

$$\sin\theta_a = 0 \qquad \sin\theta_b = \sqrt{3}/2 \qquad \sin\theta_c = -\sqrt{3}/2$$

Upon substitution of these values in equations (4), (5), and (6), there results

$$\epsilon_a = \epsilon_x(1)^2 + \epsilon_y(0)^2 + \gamma_{xy}(0)(1) \qquad (23)$$

$$\epsilon_b = \epsilon_x\left(-\tfrac{1}{2}\right)^2 + \epsilon_y\left(\tfrac{\sqrt{3}}{2}\right)^2 + \gamma_{xy}\left(\tfrac{\sqrt{3}}{2}\right)\left(-\tfrac{1}{2}\right) \qquad (24)$$

$$\epsilon_c = \epsilon_x\left(-\tfrac{1}{2}\right)^2 + \epsilon_y\left(-\tfrac{\sqrt{3}}{2}\right)^2 + \gamma_{xy}\left(-\tfrac{\sqrt{3}}{2}\right)\left(-\tfrac{1}{2}\right) \qquad (25)$$

which reduce to

$$\epsilon_x = \epsilon_a \tag{26}$$

$$\epsilon_b = \frac{\epsilon_x}{4} + \frac{3}{4}\epsilon_y - \frac{\sqrt{3}}{4}\gamma_{xy} \tag{27}$$

$$\epsilon_c = \frac{\epsilon_x}{4} + \frac{3}{4}\epsilon_y + \frac{\sqrt{3}}{4}\gamma_{xy} \tag{28}$$

Adding (27) and (28) gives

$$\epsilon_b + \epsilon_c = \frac{\epsilon_x}{2} + \frac{3}{2}\epsilon_y \tag{29}$$

Introduction of ϵ_a for ϵ_x according to equation (26) above results in

$$\epsilon_b + \epsilon_c = \frac{\epsilon_a}{2} + \frac{3}{2}\epsilon_y$$

from which

$$\epsilon_y = \frac{1}{3}\,(2\epsilon_b + 2\epsilon_c - \epsilon_a) \tag{30}$$

By subtracting equation (27) from (28)

$$\epsilon_c - \epsilon_b = \frac{\sqrt{3}}{2}\gamma_{xy}$$

$$\text{or} \quad \gamma_{xy} = \frac{2}{\sqrt{3}} \times (\epsilon_c - \epsilon_b) \tag{31}$$

We may now proceed to the evaluation of the principal strains in terms of the rosette observations by setting up the expressions for A and B.

$$A = \frac{\epsilon_x + \epsilon_y}{2} = \frac{\epsilon_a + \frac{1}{3}\,(2\epsilon_b + 2\epsilon_c - \epsilon_a)}{2}$$

$$= \frac{\epsilon_a + \epsilon_b + \epsilon_c}{3} \tag{32}$$

$$B = \frac{1}{2}\sqrt{(\epsilon_x - \epsilon_y)^2 + \gamma_{xy}^{\ 2}}$$

$$= \frac{1}{2}\sqrt{\left\{\epsilon_a - \frac{1}{3}(2\epsilon_b + 2\epsilon_c - \epsilon_a)\right\}^2 + \left\{\frac{2}{\sqrt{3}}(\epsilon_c - \epsilon_b)\right\}^2}$$

$$= \sqrt{\left\{\epsilon_a - \frac{1}{3}(\epsilon_a + \epsilon_b + \epsilon_c)\right\}^2 + \left\{\frac{1}{\sqrt{3}}(\epsilon_c - \epsilon_b)\right\}^2} \tag{33}^*$$

* A more concise mathematical form has been given by Mindlin, but the above saves a few steps in the numerical solution.

$$\epsilon_1 = A + B \qquad (7a) \qquad\qquad \epsilon_2 = A - B \qquad (8a)$$

$$\epsilon_1 = \frac{\epsilon_a + \epsilon_b + \epsilon_c}{3} + \sqrt{\left\{\epsilon_a - \frac{1}{3}(\epsilon_a + \epsilon_b + \epsilon_c)\right\}^2 + \left\{\frac{\epsilon_c - \epsilon_b}{\sqrt{3}}\right\}^2} \qquad (34)$$

$$\epsilon_2 = \frac{\epsilon_a + \epsilon_b + \epsilon_c}{3} - \sqrt{\left\{\epsilon_a - \frac{1}{3}(\epsilon_a + \epsilon_b + \epsilon_c)\right\}^2 + \left\{\frac{\epsilon_c - \epsilon_b}{3}\right\}^2} \qquad (35)$$

By substituting the values of A and B, equations (32) and (33), into equations (2a) and (3a), the principal stresses in terms of the equiangular rosette observations are found to be

$$\sigma_1 = E\left[\frac{\epsilon_a + \epsilon_b + \epsilon_c}{3(1-\mu)} + \frac{1}{1+\mu}\sqrt{\left\{\epsilon_a - \frac{1}{3}(\epsilon_a + \epsilon_b + \epsilon_c)\right\}^2 + \left\{\frac{\epsilon_c - \epsilon_b}{\sqrt{3}}\right\}^2}\right] \qquad (36)$$

$$\sigma_2 = E\left[\frac{\epsilon_a + \epsilon_b + \epsilon_c}{3(1-\mu)} - \frac{1}{1+\mu}\sqrt{\left\{\epsilon_a - \frac{1}{3}(\epsilon_a + \epsilon_b + \epsilon_c)\right\}^2 + \left\{\frac{1}{\sqrt{3}}(\epsilon_c - \epsilon_b)\right\}^2}\right] \qquad (37)$$

The angular orientation of the principal stress axes may now be found by taking the ratio of the quantities under the radical in equation (36) or (37). That is equivalent to substituting the values from equations (26), (30), and (31) into equation (9), which will yield

$$\tan 2\phi = \frac{\sqrt{3}\,(\epsilon_c - \epsilon_b)}{2\epsilon_a - \epsilon_b - \epsilon_c} \qquad (38)$$

Since the solution of equation (38) yields two values for the angle ϕ, one must establish some means of determining which of them corresponds to the angle ϕ_1. The following rules, to be proved later, will answer the question,

1. When $\epsilon_c > \epsilon_b$ $\quad \phi_1$ lies between 0 and + 90°
2. When $\epsilon_b > \epsilon_c$ $\quad \phi_1$ lies between 0 and - 90°
3. When $\epsilon_b = \epsilon_c$

   (a) If $\epsilon_a > \epsilon_b = \epsilon_c$ $\qquad \epsilon_a = \epsilon_1$ and $\phi_1 = 0$

   (b) If $\epsilon_a < \epsilon_b = \epsilon_c$ $\qquad \epsilon_a = \epsilon_2$ and $\phi_1 = \pm 90°$

Proof of the Rules

Since the gage axes of the equiangular rosette are inclined at 120^o (or 60^o) relative to each other, the points which represent the corresponding strains on the circumference of Mohr's circle will be located at the vertices of an equilateral triangle ACB as indicated in Fig. 11(c).*

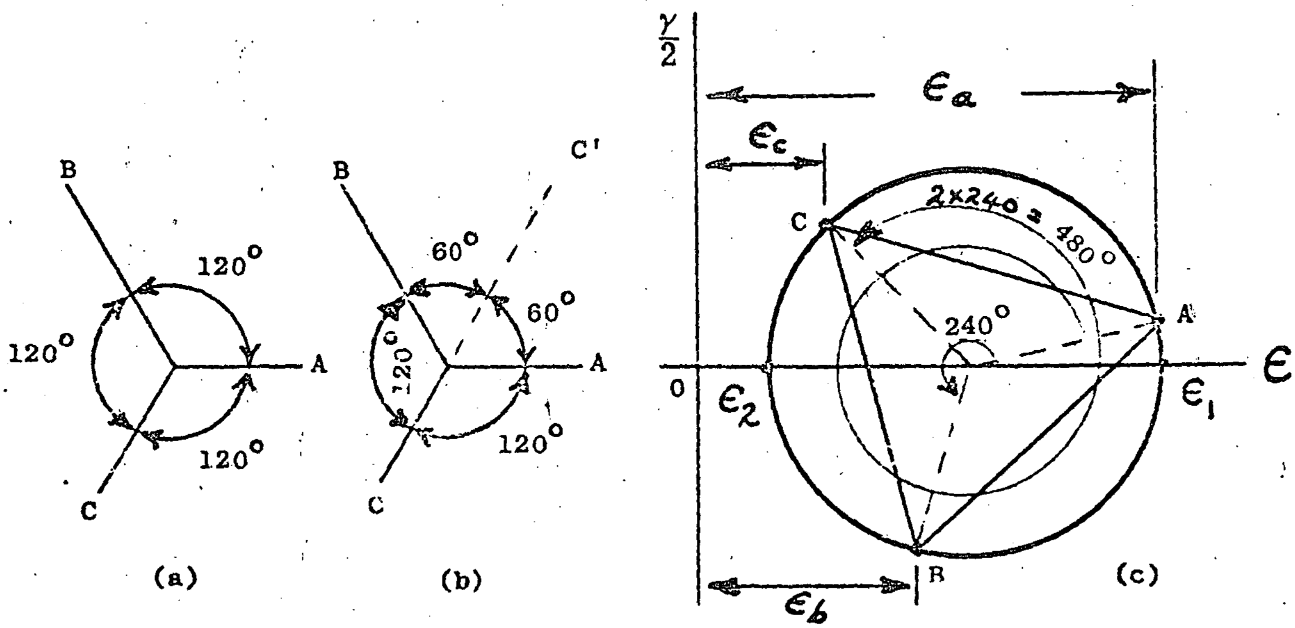

Gage Axes and Mohr Diagram
Equiangular Rosette
Figure 11

A study of the diagram reveals that as the strains ϵ_a, ϵ_b, and ϵ_c, vary, the triangle ACB will rotate about its centroid, which is located at the center of the circle.

*The Reader's attention is drawn particularly to the observation that if one starts at point A and follows around the circumference of Mohr's circle in the anticlockwise direction, the next station reached will be point C. On first thought, this might appear to be an error, since in going around the rosette axes in the same direction, axis B follows axis A as shown in Fig. 11(a). The apparent discrepancy is caused by the fact that the angular displacements are doubled in Mohr's diagram. If one extends the axis OC into the position OC' shown in Fig. 11(b), then the reason for the relative positions of the points A, B, and C on the circumference of Mohr's circle should be clear.

If the point A happens to fall at the extreme left of the circumference of the circle, Fig. 12(a), then, since the centroid of ACB lies on the abcissa, CB is at right angles to OA which means that $\epsilon_c = \epsilon_b$. Also, because A is at the extreme left of the circle $\epsilon_a = \epsilon_2$, the algebraically smaller principal strain. From the diagram it is seen that $2\varphi_1 = \pm 180°$ and therefore $\varphi_1 = \pm 90°$, which substantiates rule 3(b).

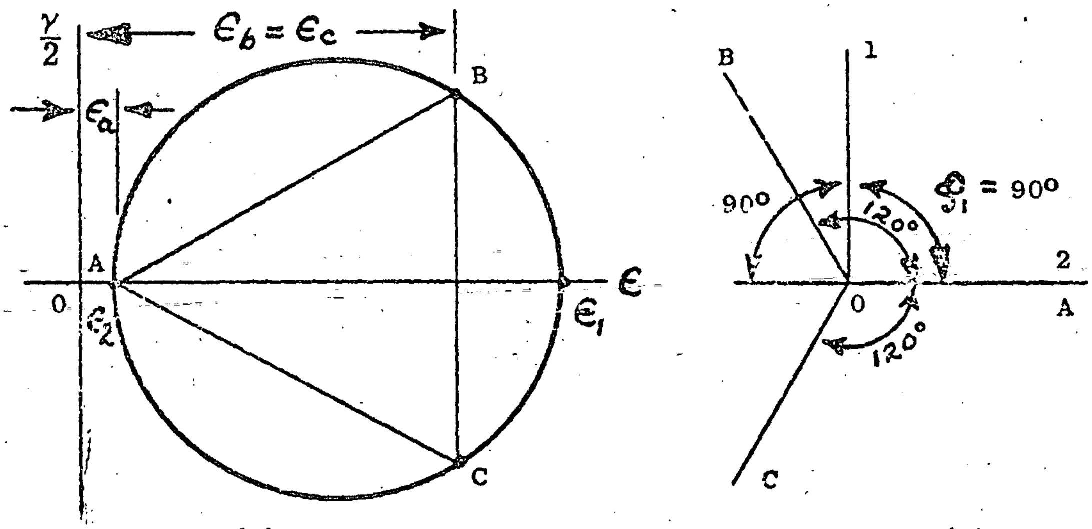

(a) Mohr Diagram

(b) Rosette & Principal Strain Axes

Equiangular Rosette - Special case in which

$\epsilon_b = \epsilon_c > \epsilon_a \quad \epsilon_a = \epsilon_2$ and $\varphi_1 = \pm 90°$

Figure 12

If the relative values of ϵ_a, ϵ_b, and ϵ_c are now changed so that the triangle ACB rotates in an anticlockwise direction from the position in Fig. 12(a), ϵ_b will become smaller than ϵ_c, and point A will move on to the lower half of the circumference of the circle. Under these conditions the angle $2\varphi_1$ will be between 0 and + 180° and φ_1 between 0 and +90° as shown in Fig. 13 and stated in rule 1.

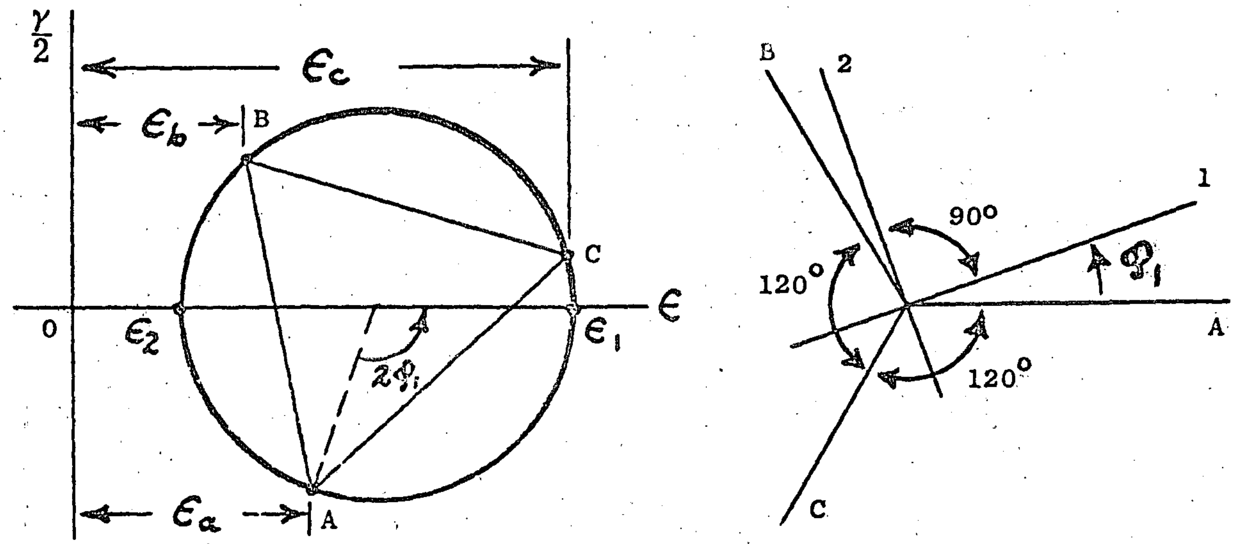

(a) Mohr Diagram (b) Rosette & Principal Strain Axes

Equiangular Rosette - Case in which $\epsilon_c > \epsilon_b$

$0 < 2\varphi_1 < +180^o$ $0 < \varphi_1 < +90^o$

Figure 13

When the trianble ACB has finally rotated through 180^0 the point A will have moved along the entire lower semi-circumference of the circle and taken up the position shown in Figure 14(a), such that $2\varphi_1 = 0$, $\varphi_1 = 0$, $\epsilon_a = \epsilon_1$, and since A is again on the abcissa $\epsilon_c = \epsilon_b$. This time $\epsilon_a > \epsilon_c = \epsilon_b$ and rule 3(a) is satisfied.

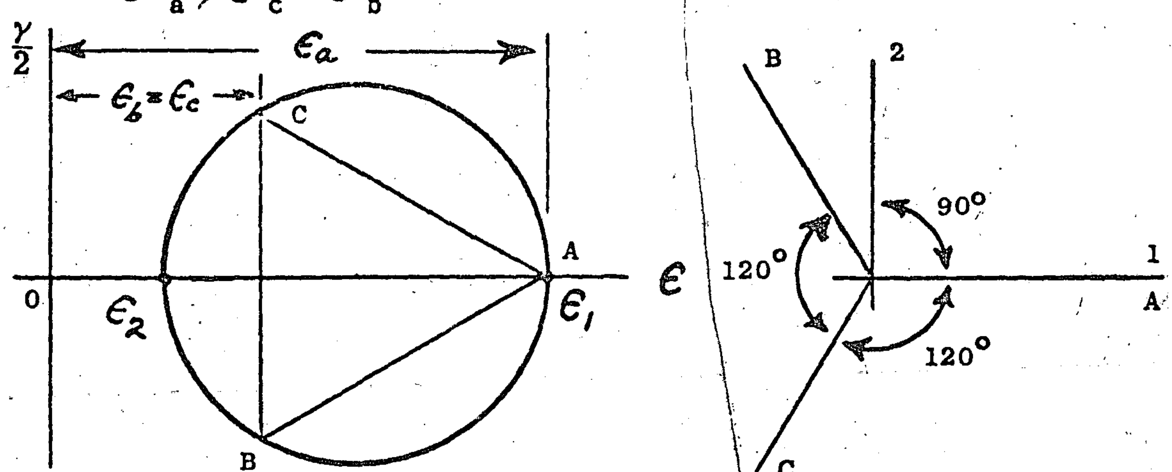

(a) Mohr Diagram (b) Rosette & Principal Strain Axes

Equiangular Rosette - Special case in which

$\epsilon_a > \epsilon_b = \epsilon_c$ $\epsilon_a = \epsilon_1$ $\varphi_1 = 0$

Figure 14

When the strains are further altered so that the continued rotation of the triangle causes the point A to move on to the semi-circumference above the abcissa, then according to definition, $2\phi_1$ becomes negative and will lie between 0 and -180^o, and ϵ_b will be larger than ϵ_c until A returns to the position corresponding to ϵ_2 where equality is again established between ϵ_b and ϵ_c. This establishes rule 2 and is indicated in Fig. 15.

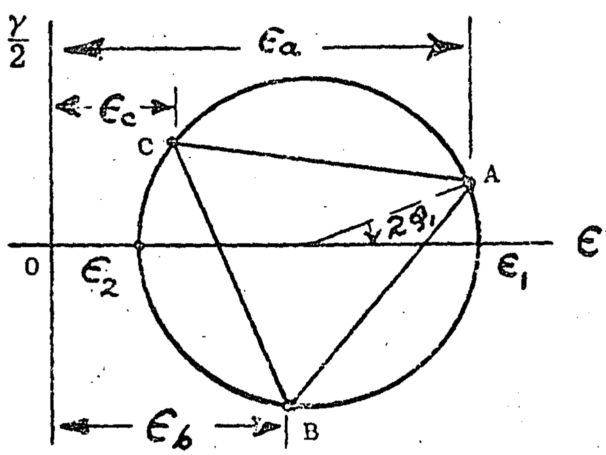

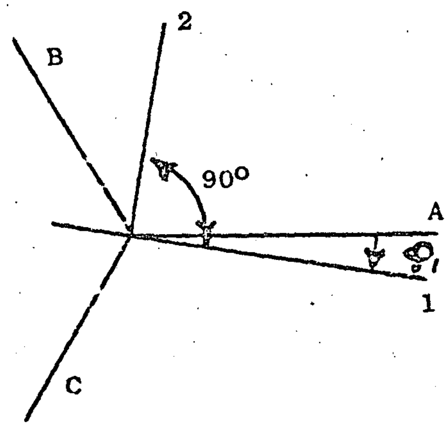

(a) Mohr Diagram (b) Rosette and Principal Strain Axes

Equiangular Rosette - Special Case in which $\epsilon_b > \epsilon_c$

$2\phi_1$ lies between 0 and -180^o

$-90 < \phi_1 < 0$

Figure 15

ROSETTES WITH FOUR STRAIN OBSERVATIONS

(c) The Rectangular Rosette with Four Observations

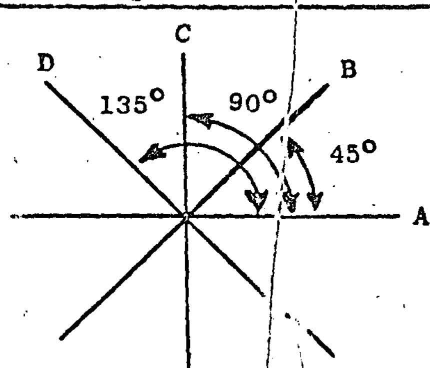

Figure 17

In this rosette arrangement the fourth observation of strain is redundant but it does provide a check since, within the limits of making the strain readings,

$$\epsilon_a + \epsilon_c = \epsilon_b + \epsilon_d \quad (39)$$

In this case, it will be simpler to state the expressions for the principal strains, principal stresses, and the angle ϕ_1 and then to prove them graphically with Mohr's diagram.

Here $$\epsilon_1 = A + B \tag{16a}$$

$$= \frac{\epsilon_a + \epsilon_b + \epsilon_c + \epsilon_d}{4} + \frac{1}{2}\sqrt{(\epsilon_a - \epsilon_c)^2 + (\epsilon_b - \epsilon_d)^2} \tag{40}$$

and $$\epsilon_2 = A - B \tag{17a}$$

$$= \frac{\epsilon_a + \epsilon_b + \epsilon_c + \epsilon_d}{4} - \frac{1}{2}\sqrt{(\epsilon_a - \epsilon_c)^2 + (\epsilon_b - \epsilon_d)^2} \tag{41}$$

From which one sees that

$$A = \frac{\epsilon_a + \epsilon_b + \epsilon_c + \epsilon_d}{4} \tag{42}$$

and

$$B = \frac{1}{2}\sqrt{(\epsilon_a - \epsilon_c)^2 + (\epsilon_b - \epsilon_d)^2} \tag{43}$$

As previously, the direction of the principal axes may be found from the ratio of the quantities under the radical such that

$$\tan 2\phi = \frac{\epsilon_b - \epsilon_d}{\epsilon_a - \epsilon_c} \tag{44}$$

Insertion of the values of A and B into equations (2a) and (3a) produces the expressions for the principal stresses as

$$\sigma_1 = E\left[\frac{\epsilon_a + \epsilon_b + \epsilon_c + \epsilon_d}{4(1-\mu)} + \frac{1}{2(1+\mu)}\sqrt{(\epsilon_a - \epsilon_c)^2 + (\epsilon_b - \epsilon_d)^2}\right] \tag{45}$$

and

$$\sigma_2 = E\left[\frac{\epsilon_a + \epsilon_b + \epsilon_c + \epsilon_d}{4(1-\mu)} - \frac{1}{2(1+\mu)}\sqrt{(\epsilon_a - \epsilon_c)^2 + (\epsilon_b - \epsilon_d)^2}\right] \tag{46}$$

The rules for determining ϕ_1 are as follows:

1. If $\epsilon_b > \epsilon_d$ then $2\phi_1$ lies between 0 and + 180°
   and ϕ_1 lies between 0 and + 90°

2. If $\epsilon_b < \epsilon_d$ then $2\phi_1$ lies between 0 and - 180°
   and ϕ_1 lies between 0 and - 90°

3. If $\epsilon_b = \epsilon_d$ then

   (a) If $\epsilon_a > \epsilon_c$ $\quad \epsilon_1 = \epsilon_a$ and $\phi_1 = 0$

   (b) If $\epsilon_a < \epsilon_c$ $\quad \epsilon_2 = \epsilon_a$ and $\phi_1 = 90^\circ$

The above rules and equations (39) to (46) may be proved by recourse to Fig. 18 which shows Mohr's diagram for this type of rosette. Since the directions of strain measurement in the rosette are inclined successively at 45°, therefore the radial lines to the points A, B, C and D, which represent the strains on Mohr's circle, will be inclined successively at $2 \times 45^\circ = 90^\circ$. Therefore, A, B, C and D will be located at the corners of a square inscribed in the circle.

Since the intersection of the diagonals of the square will coincide with the center of the circle and because the position of the center of square corresponds to the average of the four corners, therefore

$$A = \frac{\epsilon_a + \epsilon_b + \epsilon_c + \epsilon_d}{4} \tag{42}$$

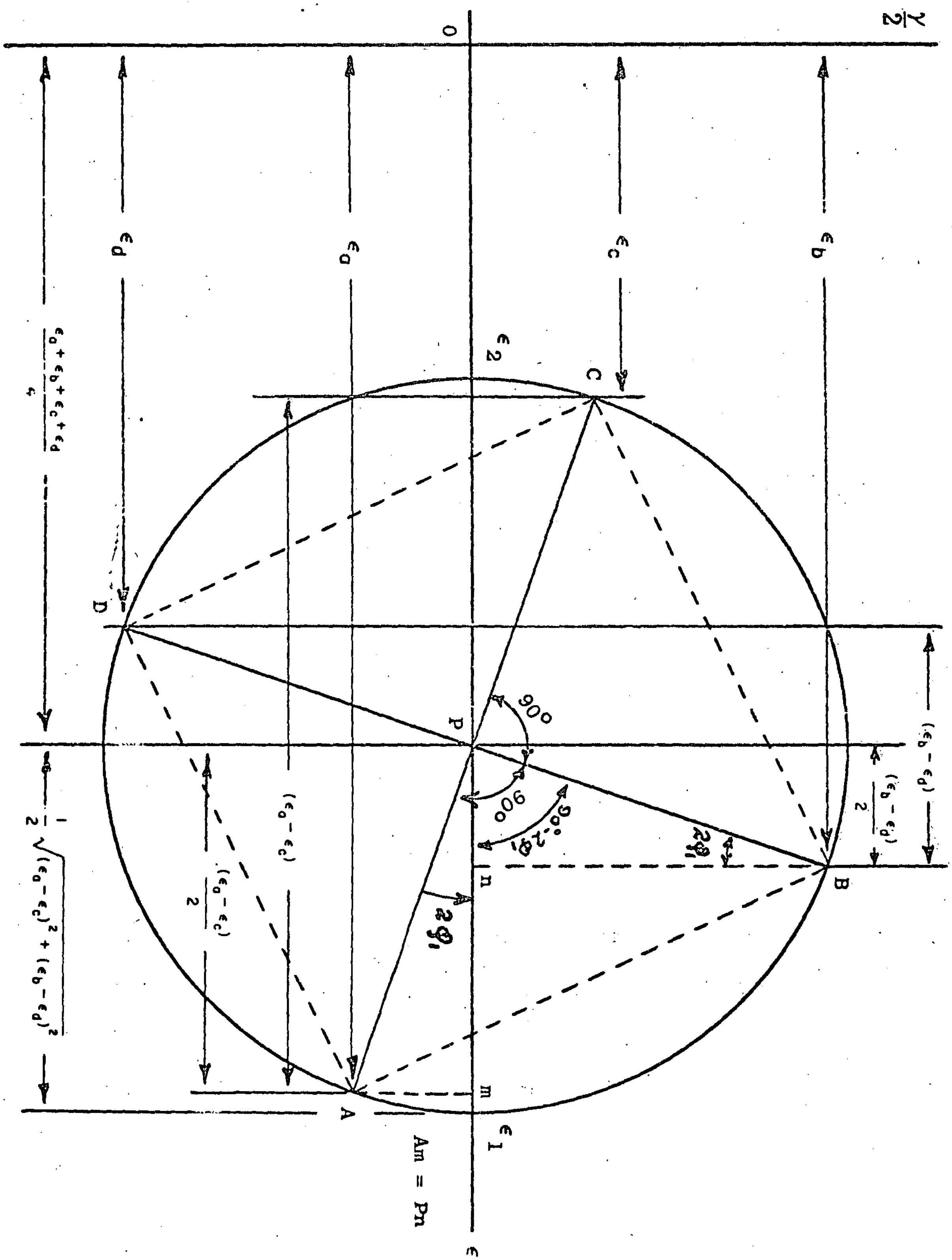

Let us now determine B, the radius of the circle in terms of ϵ_a, ϵ_b, ϵ_c, and ϵ_d, the horizontal distances from the ordinate through 0 to the corners of the square. This will require the following construction. Let P be the center of the circle and drop perpendiculars Am and Bn respectively from A and B on to the abcissa at m and n. Then from the right angled triangles APm and BPn

$$AP = BP \qquad \text{(radius of the circle)}$$

$$\angle PmA = \angle PnB \qquad 90^\circ$$

and since $\angle BPA = 90^\circ$

$$\angle BPn = \angle PAm \qquad (90^\circ - 2\phi_1)$$

Therefore $\triangle^s$ APm and BPn are equal, so that

$$Am = Pn = \frac{\epsilon_b - \epsilon_d}{2}$$

and since $Pm = \dfrac{\epsilon_a - \epsilon_c}{2}$

the hypotenuse = radius of the circle

$$= \sqrt{\left(\frac{\epsilon_a - \epsilon_c}{2}\right)^2 + \left(\frac{\epsilon_b - \epsilon_d}{2}\right)^2}$$

$$= 1/2 \sqrt{(\epsilon_a - \epsilon_c)^2 \ (\epsilon_b - \epsilon_d)^2} = B \qquad (43)$$

also

$$\tan 2\phi_1 = \frac{Am}{Pm} = \frac{\dfrac{\epsilon_b - \epsilon_d}{2}}{\dfrac{\epsilon_a - \epsilon_c}{2}} = \frac{\epsilon_b - \epsilon_d}{\epsilon_a - \epsilon_c} \qquad (44)$$

(d) The T - Δ Rosette

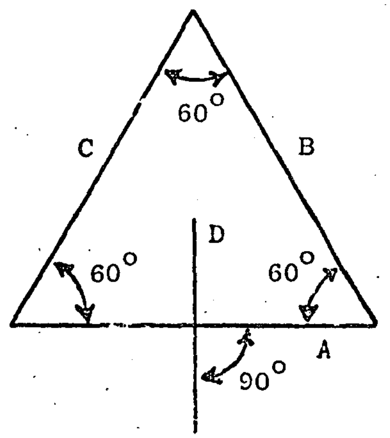

Figure 20

If one considers this rosette arrangement as containing a delta rosette with the addition of a fourth gage whose axis D is at right angles to the axis A, then, although the fourth observation is redundant, a variety of solutions can be obtained utilizing all four strain readings.

Meier* gives a solution based on the method of least squares but its complexity is rather a disadvantage. The following simple solution is therefore presented since its reduction of observed strains into terms of stress will be very much easier.

Since the average of any two strains measured at right angles gives the position of the center of Mohr's circle, therefore, for the T - Δ Rosette the quantity

$$A = \frac{\epsilon_a + \epsilon_d}{2} \tag{45}$$

Also, from the Δ Rosette

$$A = \frac{\epsilon_a + \epsilon_b + \epsilon_c}{3} \tag{32}$$

Therefore for the T - Δ Rosette

$$A = \frac{\epsilon_a + \epsilon_d}{2} = \frac{\epsilon_a + \epsilon_b + \epsilon_c}{3} \tag{46}$$

Furthermore, from the Δ Rosette

$$B = \sqrt{\left\{\epsilon_a - \frac{\epsilon_a + \epsilon_b + \epsilon_c}{3}\right\}^2 + \left\{\frac{1}{\sqrt{3}}(\epsilon_c - \epsilon_b)\right\}^2} \tag{33}$$

---

* Improvements in Rosette Computer, J. H. Meier, SESA Proc. Vol. III, No. 2, p. 1.

so that in the case of the T - Δ Rosette, if one substitutes $\frac{\epsilon_a + \epsilon_d}{2}$ for $\frac{\epsilon_a + \epsilon_b + \epsilon_c}{3}$, then

$$\epsilon_a - \frac{\epsilon_a + \epsilon_b + \epsilon_c}{3} = \epsilon_a - \frac{\epsilon_a + \epsilon_d}{2} = \frac{\epsilon_a - \epsilon_d}{2} \tag{47}$$

and

$$B = \sqrt{\left(\frac{\epsilon_a - \epsilon_d}{2}\right)^2 + \left(\frac{\epsilon_c - \epsilon_b}{\sqrt{3}}\right)^2} \tag{48}$$

Again, from the Rosette since

$$\tan 2\phi = \frac{\frac{1}{\sqrt{3}}(\epsilon_c - \epsilon_b)}{\epsilon_a - \frac{\epsilon a + \epsilon b + \epsilon c}{3}}$$

by substitution of equation (47) in (49) one obtains the ratio of the quantities under the radical of equation (48) such that

$$\tan 2\phi = \frac{\frac{1}{\sqrt{3}}(\epsilon_c - \epsilon_b)}{\frac{1}{2}(\epsilon_a - \epsilon_d)} \tag{50}$$

The rules for assigning the two values of ϕ, given by equation (50), to the correct principal axes will be exactly the same as in the case of the equiangular rosette.

For the T - Δ Rosette one may now express the values of the principal strains as follows,

$$\epsilon_1 = A + B \tag{16a}$$

$$= \frac{\epsilon_a + \epsilon_d}{2} + \sqrt{\left(\frac{\epsilon_a - \epsilon_d}{2}\right)^2 + \left(\frac{\epsilon_c - \epsilon_b}{\sqrt{3}}\right)^2} \tag{51}$$

$$\epsilon_2 = A - B \tag{17a}$$

$$= \frac{\epsilon_a + \epsilon_d}{2} - \sqrt{\left(\frac{\epsilon_a - \epsilon_d}{2}\right)^2 + \left(\frac{\epsilon_c - \epsilon_b}{\sqrt{3}}\right)^2} \tag{52}$$

The principal stresses will be

$$\sigma_1 = E\left\{\frac{A}{1-\mu} + \frac{B}{1+\mu}\right\} \tag{2a}$$

$$= E\left\{\frac{\epsilon_a + \epsilon_d}{2(1-\mu)} + \frac{1}{1+\mu}\sqrt{\left(\frac{\epsilon_a - \epsilon_d}{2}\right)^2 + \left(\frac{\epsilon_c - \epsilon_b}{\sqrt{3}}\right)^2}\right\} \tag{53}$$

and

$$\sigma_2 = E\left\{\frac{A}{1-\mu} - \frac{B}{1+\mu}\right\} \tag{3a}$$

$$= E\left\{\frac{\epsilon_a + \epsilon_d}{2(1-\mu)} - \frac{1}{1+\mu}\sqrt{\left(\frac{\epsilon_a - \epsilon_d}{2}\right)^2 + \left(\frac{\epsilon_c - \epsilon_b}{\sqrt{3}}\right)^2}\right\} \tag{54}$$

SUMMARY

ANALYTICAL EXPRESSIONS FOR SOLVING STRAIN ROSETTES.

	TYPE OF ROSETTE	SPACE DIAGRAM (Arrangement of Rosette Axes)	PRINCIPAL STRESS MAGNITUDES $\sigma_1 = E\left[\frac{A}{1-\mu} + \frac{B}{1+\mu}\right]$ $\sigma_2 = E\left[\frac{A}{1-\mu} - \frac{B}{1+\mu}\right]$	ϕ_1 LIES BETWEEN 0 AND +90° WHEN
3 OBSERVATIONS	RECTANGULAR	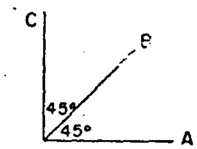	$\sigma_1, \sigma_2 = \frac{E}{1-\mu} \cdot \frac{\epsilon_a + \epsilon_c}{2} \pm \frac{E}{1+\mu} \cdot \frac{1}{2}\sqrt{(\epsilon_a - \epsilon_c)^2 + \left\{2\epsilon_b - (\epsilon_a + \epsilon_c)\right\}^2}$	$\epsilon_b > \frac{\epsilon_a + \epsilon_c}{2}$
3 OBSERVATIONS	EQUIANGULAR OR DELTA	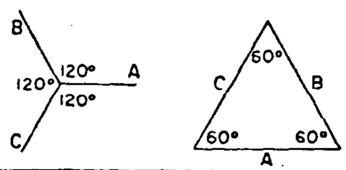	$\sigma_1, \sigma_2 = \frac{E}{1-\mu} \cdot \frac{\epsilon_a + \epsilon_b + \epsilon_c}{3} \pm \frac{E}{1+\mu} \cdot \sqrt{\left(\epsilon_a - \frac{\epsilon_a + \epsilon_b + \epsilon_c}{3}\right)^2 + \left(\frac{\epsilon_c - \epsilon_b}{\sqrt{3}}\right)^2}$	$\epsilon_c > \epsilon_b$
4 OBSERVATIONS	RECTANGULAR	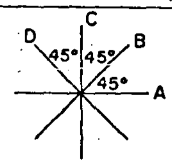	$\sigma_1, \sigma_2 = \frac{E}{1-\mu} \cdot \frac{\epsilon_a + \epsilon_b + \epsilon_c + \epsilon_d}{4} \pm \frac{E}{1+\mu} \cdot \frac{1}{2}\sqrt{(\epsilon_a - \epsilon_c)^2 + (\epsilon_b - \epsilon_d)^2}$ or $= \frac{E}{1-\mu} \cdot \frac{\epsilon_a + \epsilon_c}{2} \pm \frac{E}{1+\mu} \cdot \frac{1}{2}\sqrt{(\epsilon_a - \epsilon_c)^2 + (\epsilon_b - \epsilon_d)^2}$	$\epsilon_b > \epsilon_d$
4 OBSERVATIONS	TEE - DELTA	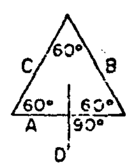	$\sigma_1, \sigma_2 = \frac{E}{1-\mu} \cdot \frac{\epsilon_a + \epsilon_d}{2} \pm \frac{E}{1+\mu} \cdot \sqrt{\left(\frac{\epsilon_a - \epsilon_d}{2}\right)^2 + \left(\frac{\epsilon_c - \epsilon_b}{\sqrt{3}}\right)^2}$	$\epsilon_c > \epsilon_b$

Directions of principal axes are given by equation $\tan 2\phi = \frac{\text{2nd quantity under radical}}{\text{1st quantity under radical}}$, for all of above relations.

5. Graphical Solutions

In addition to the various analytical solutions for the strain rosette equations there are also many graphical (and semi-graphical) procedures for determining the principal stress magnitudes and directions. The choice between analytical and graphical procedures is usually dependent upon personal preference but in the event of two people checking each other it is highly desirable to have one perform the computations analytically and to have the other do the checking by a totally different graphical method, or vice-versa.

For the purpose of these notes, the discussion of graphical methods of solving the rosette equations will be confined to three procedures which have been found convenient and useful. All apply to rosettes with three observations of strain. The first corresponds to the general case, in which the axes of measurement may be inclined to each other in any manner, the second to the rectangular rosette, and the third to the equiangular arrangement.

(a) The General Case

The following method, which has been put forward by McClintock (Special Reference No. 3), applies to the general case in which the rosette axes may have any arbitrarily chosen angles, θ_{ab} and θ_{bc}, between them, as indicated in Figure 21.

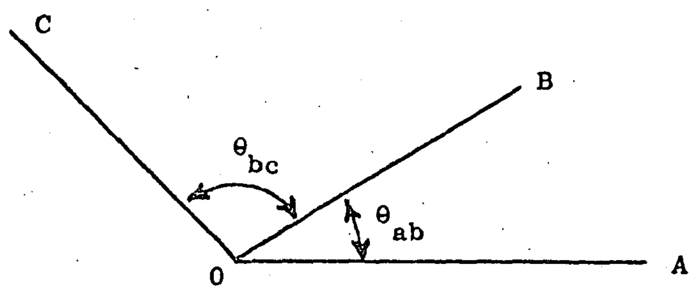

Figure 21

Method of Solution

The object is to establish Mohr's Circle for strain. The procedure is very simple and by some is preferred for the rectangular and equiangular rosettes even though each of these arrangements has methods peculiarly well adapted to itself. The following four steps are employed for finding the strain circle.

1. The rosette axes are rearranged (by extending them if necessary) so that they are:

   (a) Arranged in sequence, in order of ascending or descending strain magnitudes (Algebraic order).

(b) The included angle between the axes of minimum and maximum strain must be less than 180°.

Some examples of this rearrangement are shown in Fig. 22.

Space Diagrams of Physical Layout

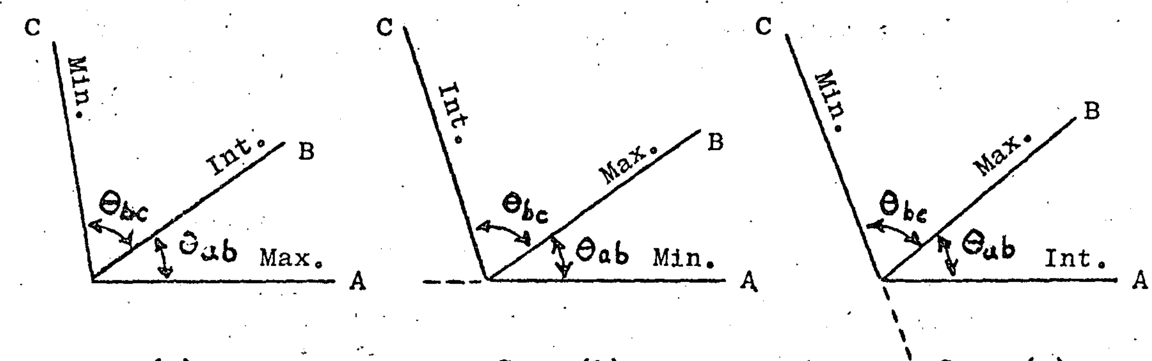

Case (a)

ϵ_a = Maximum
ϵ_b = Intermediate
ϵ_c = Minimum

Case (b)

ϵ_b = Maximum
ϵ_c = Intermediate
ϵ_a = Minimum

Case (c)

ϵ_b = Maximum
ϵ_a = Intermediate
ϵ_c = Minimum

Figure 22 (a)

Rearrangement of Axes in Sequence of Strain Magnitude (Algebraic)

α = Angle between axes of Maximum and Intermediate strain

β = Angle between axes of Intermediate and Minimum strain

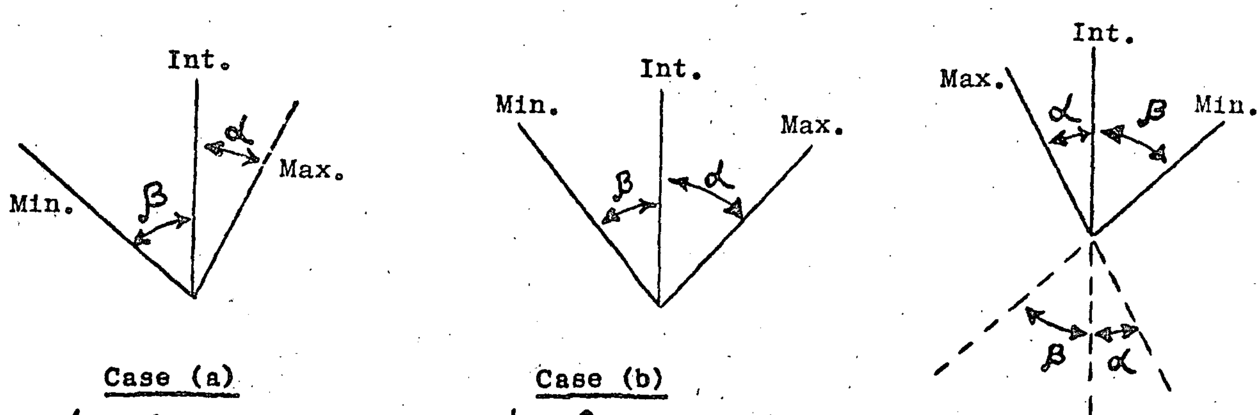

Case (a)

$\alpha = \theta_{ab}$
$\beta = \theta_{bc}$

Case (b)

$\alpha = \theta_{bc}$
$\beta = 180 - (\theta_{ab} + \theta_{bc})$

Case (c)

$\alpha = \theta_{ab}$
$= 180 - (\theta_{ab} + \theta_{bc})$

Note: In Case (c) the axis of max. strain falls to left of intermediate axis

Figure 22(b)

2. Lay out a sheet of paper with a strain scale near one edge and parallel to the direction of the abcissa (which will be established later). Then draw in ordinates at locations corresponding to:

1. Zero strain
2. $\epsilon_a, \epsilon_b, \epsilon_c$.

This is indicated diagramatically in Fig. 23.

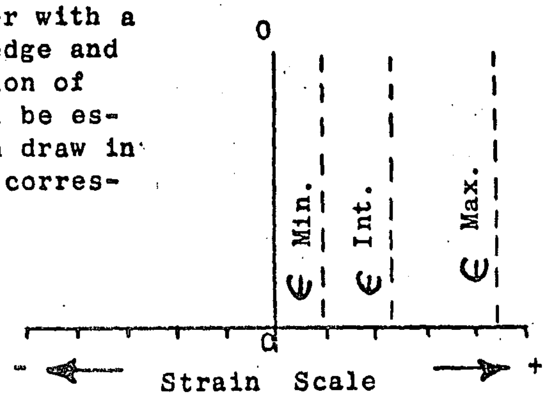

Figure 23

Note: In Fig. 23 the strain values have been indicated as positive but they might all be negative or some positive and negative.

It will also be noted that the measured strains, ϵ_a, ϵ_b, & ϵ_c, may have any relation with one another. In Fig. 23 the values have been plotted in sequence according to magnitude.

3. When the diagram corresponding to Fig. 23 has been drawn, choose any point, D, on the ordinate corresponding to the intermediate strain value.

From point D draw straight lines DE and DF, making angles α and β, respectively, with the ordinate of intermediate strain, to meet the ordinates of $\epsilon_{Max.}$ and $\epsilon_{Min.}$ at E and F respectively.

One will notice that there are two possibilities for drawing the lines DE and DF since the angles α and β can be measured from either the upwards or the downwards direction of the ordinate of intermediate strain.

The following rule governs this choice: If, in the diagram (Fig. 22(b)) showing the strain axes in sequence, the axis of Max. strain falls to the right of the intermediate axis, α and β are measured from the upwards direction, as indicated for Cases (a) & (b). But if the axis of maximum strain is inclined towards the left, as in Case (c), then α and β, should be measured from the downwards direction. This is suggested by the dotted axis extensions indicated for Case (c) in Fig. 22(b) and shown in detail in Fig. 24.

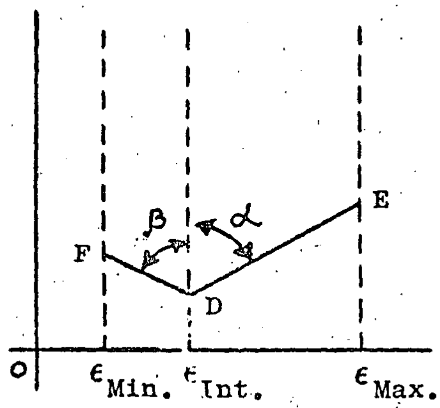

Strain Scale
Corresponds to
Cases (a) & (b)

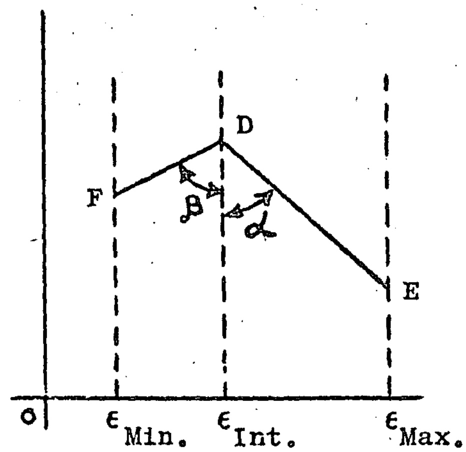

Strain Scale
Corresponds to
Case (c)

Figure 24

4. The final step is now to draw a circle through the points D, E, & F. This will be Mohr's circle for strain. The abcissa, which can now be drawn in, will pass through the center of the circle and the extreme right and left hand positions of the circumference will represent the principal strains ϵ_1 and ϵ_2, as shown in Fig. 25.

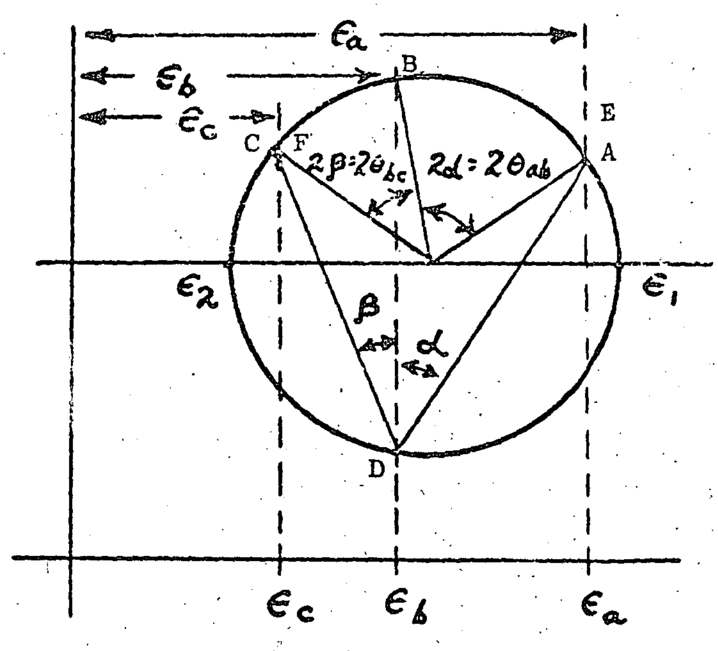

Strain Scale

Figure 25(a)

Mohr's Strain Circle for Case (a)
$\epsilon_a > \epsilon_b > \epsilon_c$

(See also Figs. 25(b) and 25(c))

The points A, B, & C, which represent the strains along the rosette axes, can now be located on the circumference of the circle according to the following two requirements:

1. The magnitudes of the strains ϵ_a, ϵ_b, & ϵ_c.

2. The sequence of order as we go along the circumference of the circle. This must correspond to the sequence in the physical layout of the rosette. For example, if the rosette axes follow the sequence A, B, & C, when one proceeds in the anticlockwise direction, the same order must prevail as one goes around Mohr's circle in the same sense.

Although there are two possible positions for each of points A, B, & C, which will satisfy requirement 1 above, the second requirement eliminates half of them. This means that there is only one arrangement for the points A, B, & C on the circumference of the circle.

Angle of Reference, ϕ_1. As soon as the point A has been located on the circumference of the circle, the radius to this point will establish the angle $2\phi_1$, as shown in Fig. 25. From this we can determine the angle ϕ_1, and locate the axis of ϵ_1, the algebraically larger principal strain, relative to the A axis of the rosette.

Principal Stress Determination. Once the magnitudes of the principal strains, ϵ_1 and ϵ_2, have been determined, then the principal stress values can be computed from equations (2) & (3).

$$\sigma_1 = \frac{E}{1 - \mu^2} \times (\epsilon_1 + \mu \epsilon_2) \tag{2}$$

and

$$\sigma_2 = \frac{E}{1 - \mu^2} \times (\epsilon_2 + \mu \epsilon_1) \tag{3}$$

Or, it may be more convenient to prepare a chart, of the type shown in Fig. 27, from which the values of σ_1 and σ_2 may be read directly.

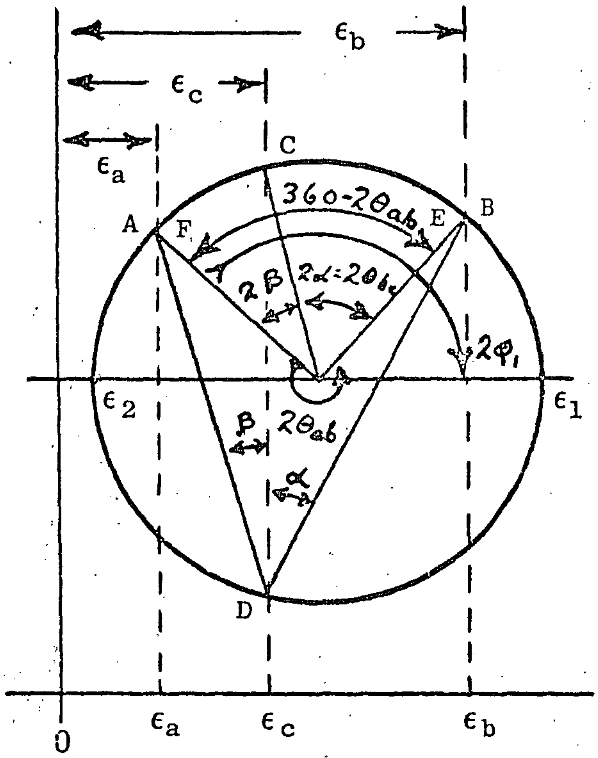

Strain Scale

$$\beta = 180^\circ - (\theta_{ab} + \theta_{bc})$$

$$2\beta = 360^\circ - 2\theta_{ab} - 2\theta_{bc}$$

$$2\alpha = \qquad\qquad + 2\theta_{bc}$$

$$2\beta + 2\alpha = 360 - 2\theta_{ab}$$

Figure 25(b) Mohr's Circle for Strain Case (b) $\epsilon_b > \epsilon_c > \epsilon_a$

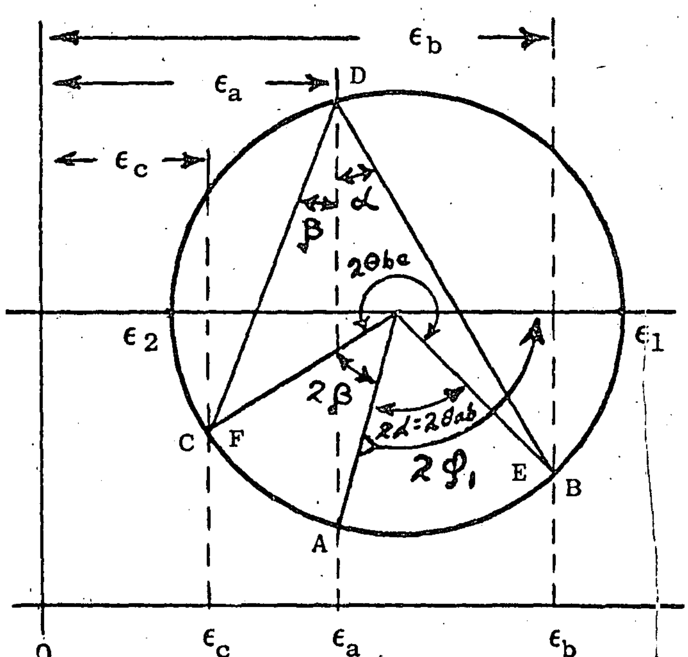

Strain Scale

$$\beta = 180^\circ - (\theta_{ab} + \theta_{bc})$$

$$2\beta = 360^\circ - 2\theta_{ab} - 2\theta_{bc}$$

$$2\alpha = \qquad + 2\theta_{ab}$$

$$2\beta + 2\alpha = 360^\circ - 2\theta_{bc}$$

Figure 25(c) Mohr's Circle for Strain Case (c)

$\epsilon_b > \epsilon_a > \epsilon_c$

(b) The Rectangular Rosette

The method described in the following paragraphs was developed by R. Baumberger* while he was associated with the firm of Ruge-de-Forest. It requires 7 steps which lead directly to the determination of the principal strains and the directions of the principal axes. The calculation of the principal stresses from the principal strains must be carried out as an additional step.

The procedure actually involves a simple means of drawing Mohr's strain circle from which the principal strains and the angle of reference can be read off directly. The use of specially prepared graph paper, with the reference lines printed on it, will eliminate the two initial steps for the person making the graphical calculation so that the complete solution can be achieved in six steps.

The fundamental procedure (without the use of ~~specially~~ prepared graph paper) is as follows:

1. On a piece of paper lay out two perpendicular axes of reference (B-B, and K-K, as shown in Fig. 26-1. Generally it will be well to have the origin of reference (O, the intersection of the axes) about the middle of the paper but for certain special situations it may be more convenient to have it farther to the right or to the left.

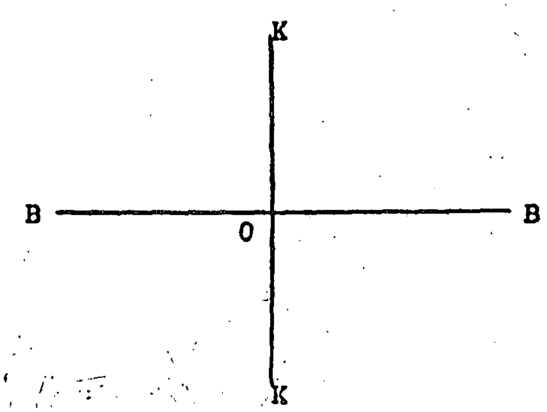

Figure 26-1

2. Parallel to B-B draw two lines, A-A and C-C, such that they are on opposite sides of the abcissa and at equal distances from it. That is, make OR = OT as shown in Fig. 26-2.

* For Baumberger's original note see SESA Proceedings, Vol, 1, No. 1, 1943, pages 145 and 146.

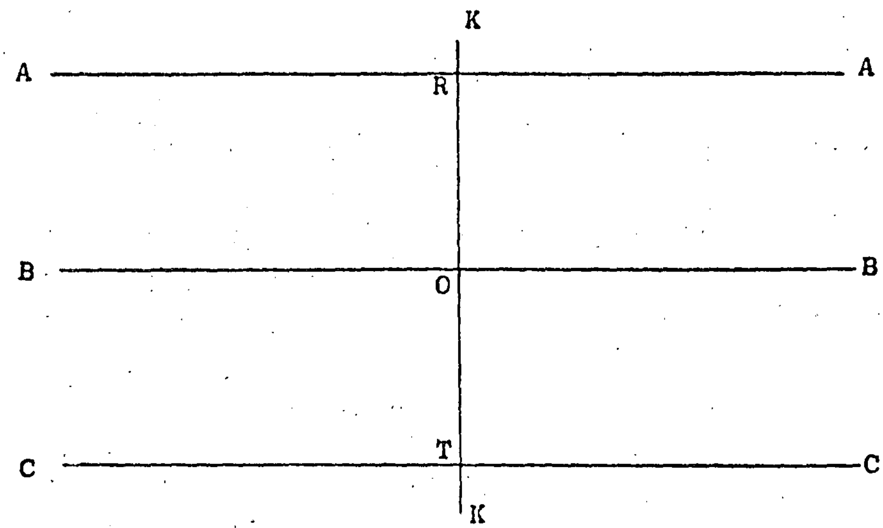

Figure 26-2

3. Let one now define the lines A-A, B-B, and C-C, as:

A-A = Axis of ϵ_a
B-B = Axis of ϵ_b
C-C = Axis of ϵ_c

and proceed to lay off along these lines (using K-K as zero for reference) distances which are respectively proportional to the strains ϵ_a, ϵ_b, and ϵ_c, which have been observed in the directions of the rosette axes, A, B, and C.

Positive (Tensile) strains are represented by distances to the right of K-K and negative (compressive) strains by distances to the left of K-K.

A typical layout for three positive strains is indicated in Fig. 26-3, in which a, b, and c, are points representing strains on the axes of the diagram.

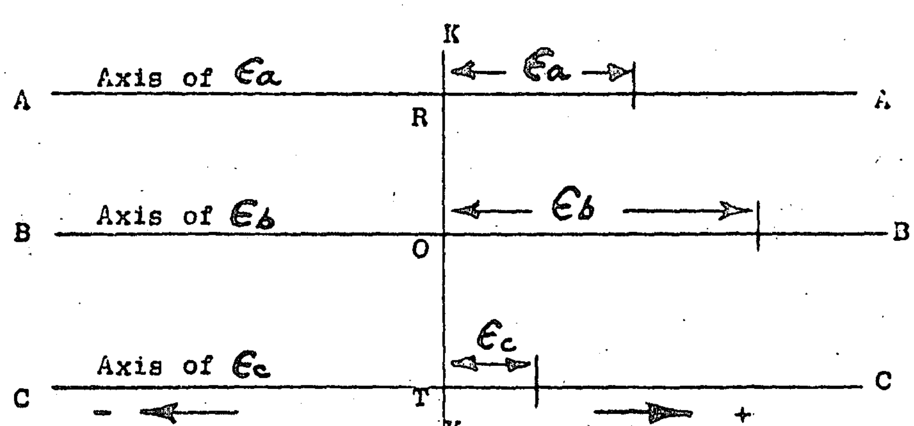

Figure 26-3

4. Now draw a straight line through a and c. The intersection of this line with B-B determines the center of Mohr's strain circle, as indicated by point P in Fig. 26-4.

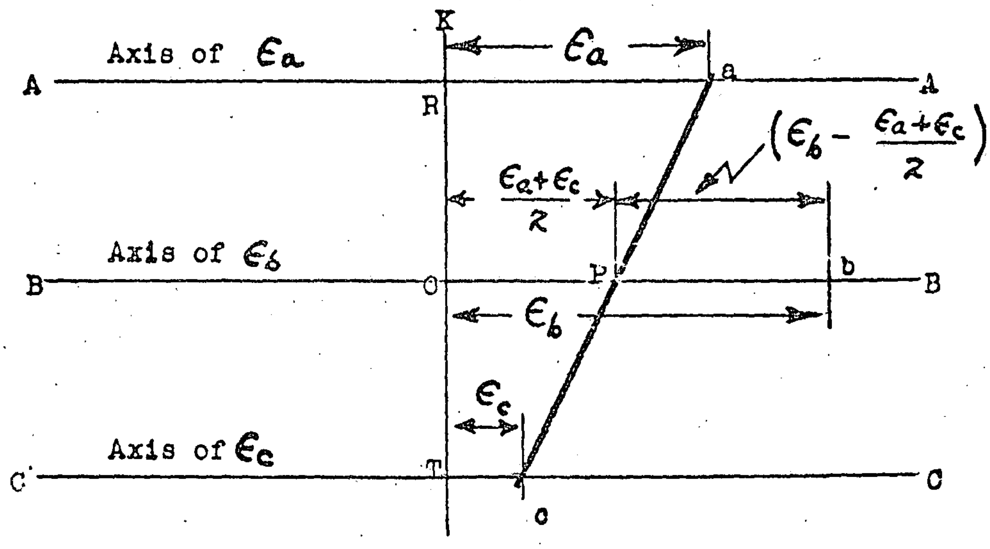

Figure 26-4

5. Through "a" draw a line which will be perpendicular to B-B and which will intersect this axis at m, as shown in Fig. 26-5. The point A, which represents ϵ_a on the circumference of Mohr's circle, must lie somewhere along this line.

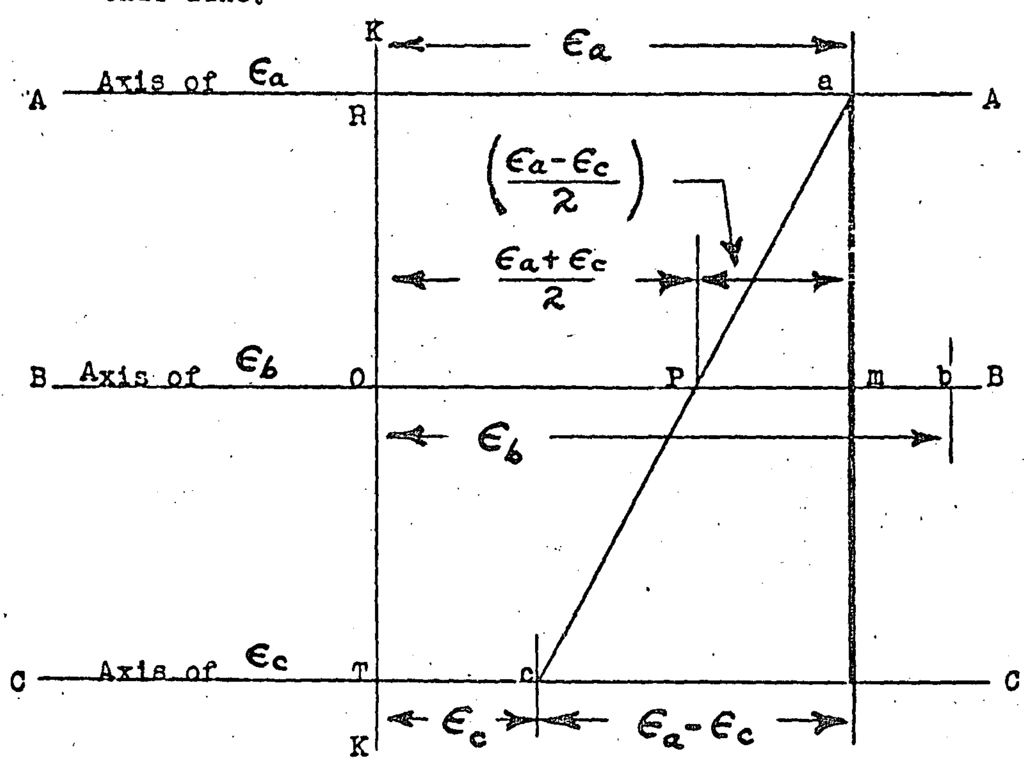

Figure 26-5

6. From the point m, on the line am, lay off a distance MA such that MA = Pb. If b is to the right of P this should lie below the abcissa - as per Fig. 26-6 - but if b is to the left of P than A will be above the axis B-B.

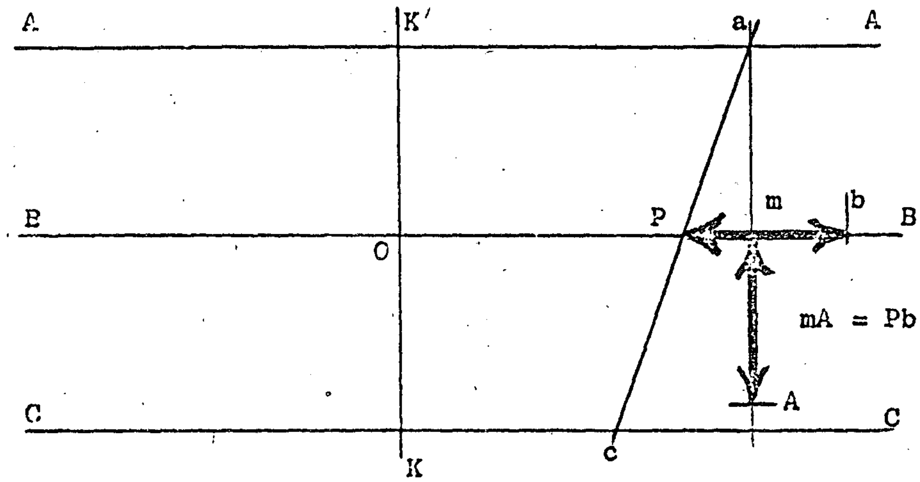

Figure 26-6

7. With center P and radius PA now draw a circle as shown in Fig. 26-7. This is Mohr's circle for strain corresponding to the rectangular rosette observations ϵ_a, ϵ_b, and ϵ_c. The right hand extremity corresponds to ϵ_1, the extreme left to ϵ_2, and the angle $2\varphi_1$, between the radius PA and the abcissa determines the directions of the principal axes relative to the A axis of the rosette.

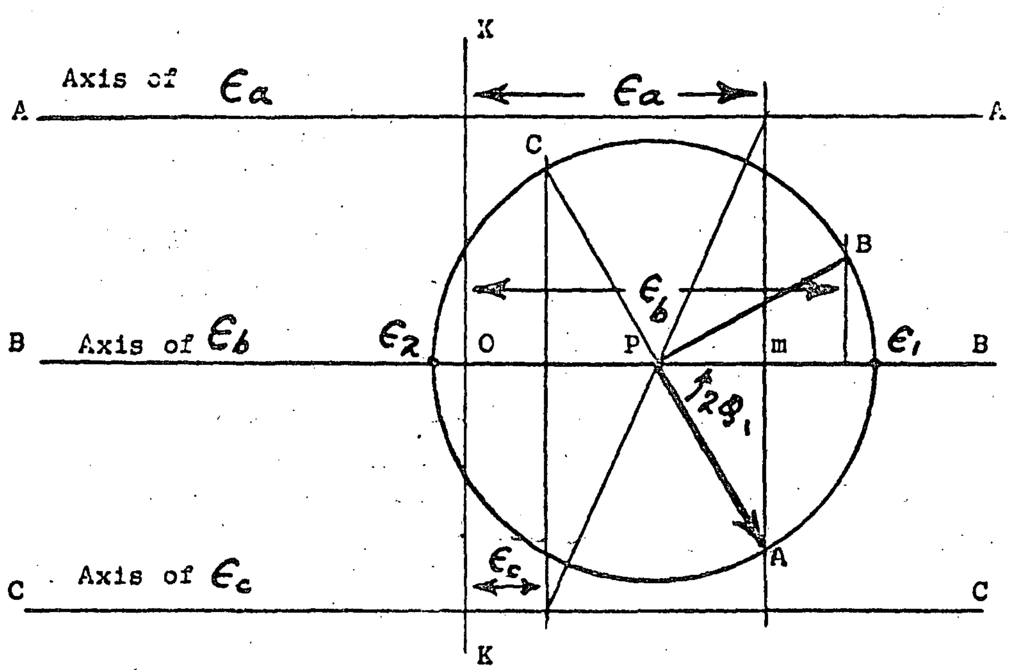

Figure 26-7

8. The principal stresses may now be calculated from the principal strains by means of equations (2) & (3) or read directly from a chart of the type shown in Figure 27.

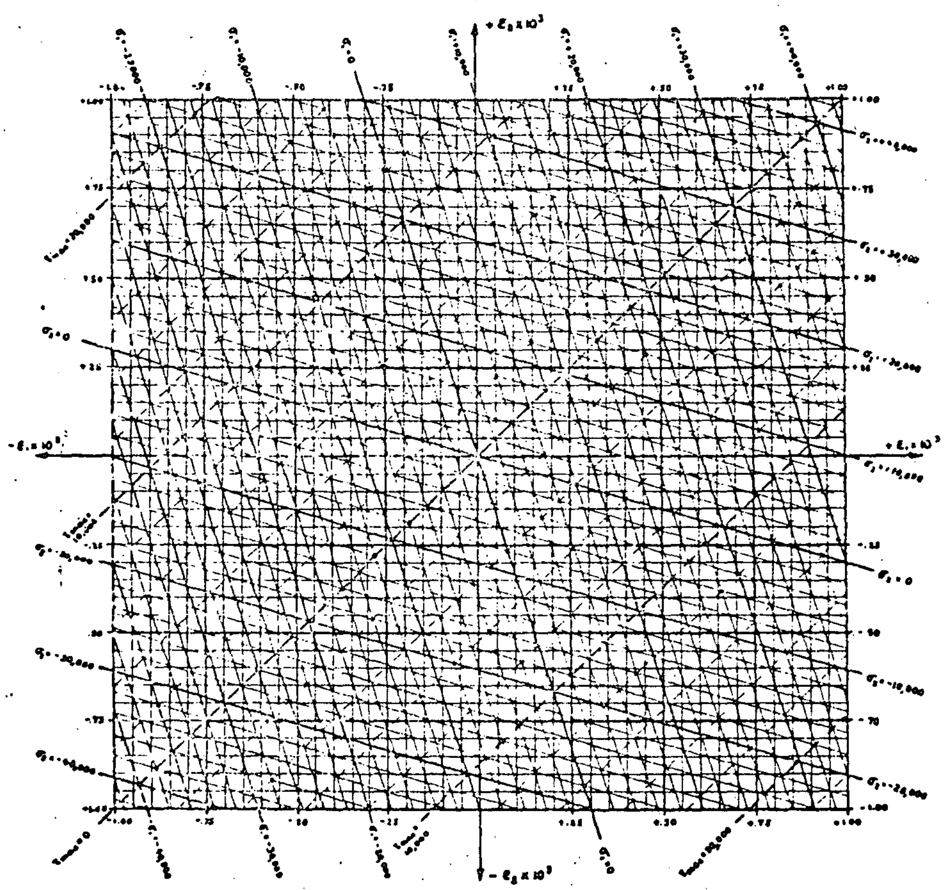

Figure 27

$$\sigma_1 = \frac{E}{1-\mu^2}(\epsilon_1 + \mu\epsilon_2) \qquad \sigma_2 = \frac{E}{1-\mu^2}(\epsilon_2 + \mu\epsilon_1)$$

$$\tau_{max.} = \frac{E}{2(1+\mu)}(\epsilon_1 - \epsilon_2)$$

Conversion Chart from Principal Strains to Principal Stresses and Maximum Shear Stress
(By J. H. Meier)
Chart Based on E = 30,000,000 psi. and μ = .30

Convenience of Specially Prepared Graph Paper

In the event that solutions are required for many sets of rosette observations much time and effort can be saved by employing graph paper upon which the axes of reference have already been printed. This takes care of the first two steps for the person carrying out the computation and permits him to complete the remaining six operations with only a triangle, compass and protractor. If the protractor has a straight edge of sufficient length the triangle will not even be needed.

A preprinted form of typical character is shown in Fig. 28 and in Fig. 29 its application to the solution of a set of observations is indicated.

Proof of Baumberger's Method

Since B-B is midway between A-A and C-C, the point P will fall at a distance from the origin equal to the average of the distances a and c from k-k.

Therefore OP represents $\dfrac{\epsilon_a + \epsilon_c}{2}$

This means that the point P corresponds to the center of Mohr's strain circle for this type of rosette (See equation 18).

One must now establish the radius of Mohr's strain circle. From equation (19) it is seen that the radius of the circle is represented in the expression.

$$\frac{1}{2}\sqrt{(\epsilon_a - \epsilon_c)^2 + \left[2\,\epsilon_b - (\epsilon_a + \epsilon_c)\right]^2} \qquad (19)$$

By taking the factor 1/2 inside the radical, this becomes

$$\sqrt{\left(\frac{\epsilon_a - \epsilon_c}{2}\right)^2 + \left(\epsilon_b - \frac{\epsilon_a + \epsilon_c}{2}\right)^2} \qquad (19a)$$

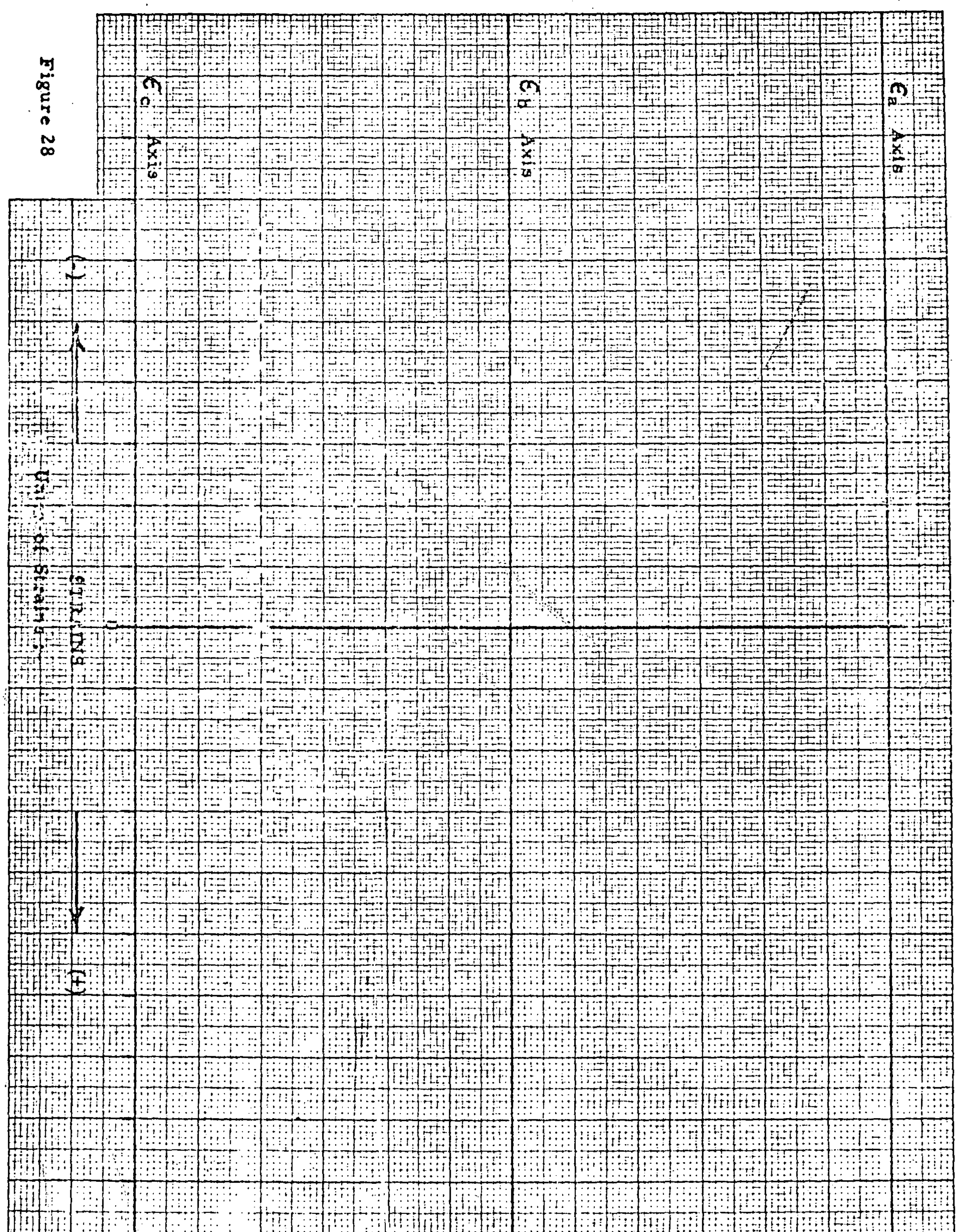
ϵ_c Axis
ϵ_b Axis
ϵ_a Axis
(-)
STRAIN
Units of Strain
(+)

Figure 28

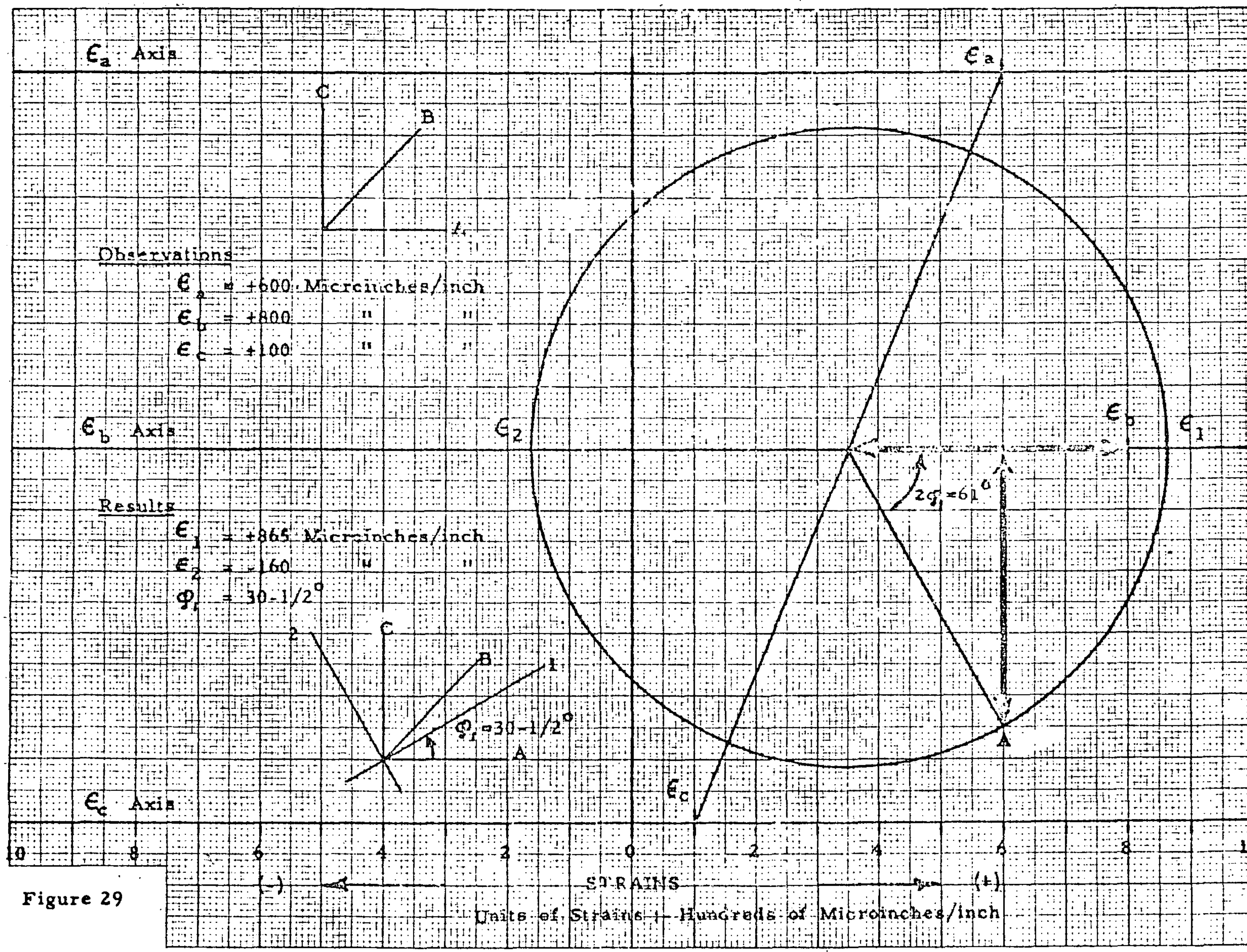
ϵ_a Axis
ϵ_b Axis
ϵ_c Axis
Observations
ϵ_a = +600 Microinches/inch
ϵ_b = +800 " "
ϵ_c = +100 " "
Results
ϵ_1 = +865 Microinches/inch
ϵ_2 = -160 " "
φ_1 = 30-1/2°
φ_1 = 30-1/2°
$2\varphi_1$ = 61°
ϵ_a
ϵ_b
ϵ_c
ϵ_1
ϵ_2
A
B
C
1
2
10 8 6 4 2 0 2 4 6 8 10
(-) STRAINS (+)
Units of Strains — Hundreds of Microinches/inch

Figure 29

Examination of Figs. 26-4 to 26-6 now reveals the following:

1. The horizontal distance between points a and c represents $\epsilon_a - \epsilon_c$, and since P is half way between these points, Pm, the horizontal projection of Pa, represents $\frac{\epsilon_a - \epsilon_c}{2}$ which is the first term under the radical of equation (19a).

2. The distance between points P and b, on the axis of ϵ_b, corresponds to

$$\left(\epsilon_b - \frac{\epsilon_a + \epsilon_c}{2}\right)$$

which is the second quantity under the radical in equation (19a).

3. Now if these distances, which represent the two quantities under the radical of equation (19a), can be made to form the perpendicular sides of a right angled triangle, then the hypotenuse of the triangle will represent equation (19a) which is the radius of the strain circle.

This result is accomplished by erecting mA (=Pb) perpendicular to the axis B-B at the point m, as illustrated in Fig. 26-6.

4. One will also observe that the ratio of the quantities under the radical of equation (19a) gives a measure of the angle of reference, that is,

$$\tan\ 2\phi_1 = \frac{2\epsilon_b - (\epsilon_a + \epsilon_c)}{\epsilon_a - \epsilon_c} \tag{22}$$

$$= \frac{\epsilon_b - \frac{\epsilon_a + \epsilon_c}{2}}{\frac{\epsilon_a - \epsilon_c}{2}} \tag{22a}$$

This means that the inclination of the radius PA (hypotenuse of right angle triangle PmA) with respect to the axis B-B will represent the angle $2\phi_1$, as shown in Fig. 26-7.

(c) The Equiangular or Delta Rosette

A simple and direct method of evaluating the magnitudes and directions of the principal stresses from observations of strains in a delta rosette has been devised by Bossart & Brewer (Special Reference No. 4).

This method possesses the following important characteristics:

1. The values of the principal stresses (rather than principal strains) are determined directly.

2. In its basic form the method is applicable only to those instances in which Poisson's Ratio (μ) = 1/3.

3. By very slight modification the procedure can be extended to cover those cases in which $\mu \neq 1/3$.

   When $\mu = 1/3$ it can be shown that for the delta rosette the following relations exist in regard to the apparent stresses.

(Apparent Stress = Modulus of Elasticity x Observed Strain)

1. The center of Mohr's circle for stress corresponds to the algebraic sum of the half apparent stresses determined in the directions of the three axes of the delta rosette.

2. The radius of Mohr's circle for stress corresponds to the vector sum of the half apparent stresses.

The procedure is as follows:

1. Compute the half apparent stresses from the observed strains -

$$\frac{S_a}{2} = \frac{E \times \epsilon_a}{2} \qquad (55)$$

$$\frac{S_b}{2} = \frac{E \times \epsilon_b}{2} \qquad (56)$$

$$\frac{S_c}{2} = \frac{E \times \epsilon_c}{2} \qquad (57)$$

Where S_a = Apparent stress in direction of the A axis
S_b = Apparent stress in direction of the B axis
S_c = Apparent stress in direction of the C axis

2. Determine the center of Mohr's circle (the hydrostatic component of stress, σ_H) by laying out, in order along the abcissa, arrows proportional in length to the half apparent stresses, as shown in Fig. 30.

   Positive values are drawn to the right and negative values to the left.

3. From point P, the center of Mohr's circle, as determined in item 2, determine the vector sum of the half apparent stresses by laying out another arrow repressing $S_a/2$ along the abcissa (+ to right, - to left) and continuing with arrows representing $S_b/2$ and $S_c/2$ with inclinations and senses as indicated in Fig. 30.

   The tip of the third arrow will fall at point A (which represents σ_a on the Mohr stress circle), the distance PA will be the radius of the circle (sometimes called the shear component of stress and designated by the symbol, σ_s) and the angle measured from PA to the abcissa will be twice the reference angle φ_1.

4. With center P and radius PA draw a circle. This is Mohr's stress circle whose intersections with abcissa determine the principal stress values, σ_1 and σ_2, as shown in the diagram.

Note: Those who are interested in the proof of the method will find it given in the paper entitled "A Graphical Method of Rosette Analysis" by K. J. Bossart & G. A. Brewer, SESA Proceedings, Vol. IV, No. 1, pp. 2 & 3.

Modification for Use When Poisson's Ratio is not 1/3

$$\mu \neq 1/3$$

When Poisson's Ratio is other than 1/3, the procedure indicated above should be followed to the end of item 3. However, OP and PA will now no longer represent the hydrostatic and shear components of stress, σ_H and σ_S, directly.

Fortunately, these quantities, σ_H and σ_S, can be found by multiplying the algebraic and vector sums of the half apparent stresses by the appropriate factors as follows:

$$\sigma_H = (\text{Stress represented by OP}) \times \frac{2}{3\,(1-\mu)} \qquad (58)$$

$$\sigma_S = \text{(Stress represented by PA)} \times \frac{4}{3\,(1+\mu)} \qquad (59)$$

$$\sigma_1 = \sigma_H + \sigma_S \qquad (60)$$

$$\sigma_2 = \sigma_H - \sigma_S \qquad (61)$$

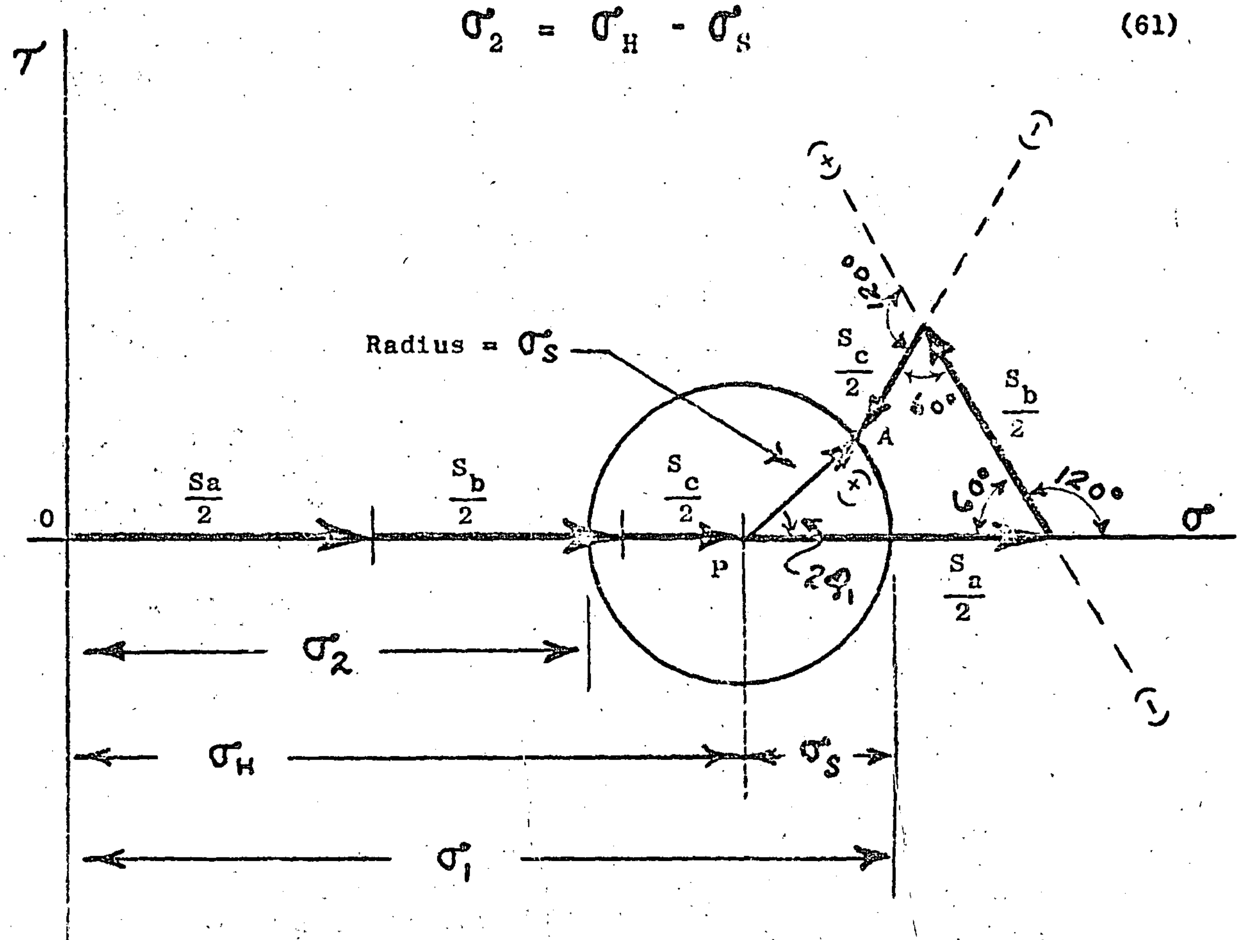

Figure 30

(d) Nomograph Methods

In addition to the above two graphical solutions there are various other graphical and semi-graphical procedures which can be employed for evaluating strain rosette observations. Some of the nomographic charts which have been developed will be found most helpful, particularly those developed by Hewson. See reference No. 4 under graphical methods in attached list of references.

6. Machine Solutions

In situations involving the solution of large numbers of rosette equations the employment of machines may be very advantageous both for economy of time and cost.

Some of the elaborate calculating machines, such as the Differential Analyser, can be used for this purpose if they are available, but except in unusual situations the use of such versatile machines is not warranted, particularly when one considers the cost involved.

A number of special purpose computers (See references at end) have been developed to evaluate rosette data. Some are electronic and others have mechanical and electrical components. The earlier machines depended upon manual introduction of strain data whereas newer devices can be connected directly to strain gages for their input, and to electric typewriters for tabulation of the computed results, provided of course, that the strain observations are not made faster than the typewriters can handle the results.

At the present time it appears as though the ultimate aim would be to develop a combined computer-plotter-tabulator for direct connection to the strain gages. Such an instrument, directly connected to the strain gages, would be capable of receiving the gage signals, computing the results, providing temporary or permanent storage of information, selecting data on the basis of, location of observation, stress level, frequency, or time of event, then tabulating and plotting the results.

For those who are faced with the problem reduction of a fairly sizeable amount of rosette data, but not enough to warrant the purchase of a special computer, attention is drawn to the methods worked out by Bassett, Cromwell, & Wooster, (SESA Proceedings, Vol. III, No. 2, p. 76) for the employment of standard office calculators.

7. Corrections for Transverse Sensitivity of SR-4 Gages

(a) For rosettes made up of single component gages which have been calibrated in a uni-axial stress field on material for which Poisson's Ratio $= \mu_m$.

One will observe that any two dimensional strain distribution may be considered as being made up of hydrostatic component and a pure shear component. Allowance for the lateral effects in SR-4 gages may therefore be made by multiplying

the hydrostatic component by $\left[\dfrac{1 - \mu_m K}{1 + K}\right]$ (62)

and the pure shear component by $\left[\dfrac{1 - \mu_m K}{1 - K}\right]$ (63)

where K = the transverse sensitivity coefficient for the gages in the rosette (assumes that the gages are alike)

and μ_m = Poisson's Ratio of the material upon which calibration was made. (0.285)

Equations (2a) and (3a) which represent the principal stress intensities can therefore be modified to the form given in expressions (64) & (65) if one wishes to take account of the transverse effect, which is usually rather small.

$$\sigma_1 = E\left\{\frac{A}{1-\mu}\left[\frac{1-\mu_m K}{1+K}\right] + \frac{B}{1+\mu}\left[\frac{1-\mu_m K}{1-K}\right]\right\} \tag{64}$$

$$\sigma_2 = E\left\{\frac{A}{1-\mu}\left[\frac{1-\mu_m K}{1+K}\right] - \frac{B}{1+\mu}\left[\frac{1-\mu_m K}{1-K}\right]\right\} \tag{65}$$

(b) For Manufactured Rosettes Consisting of Three or Four Independent Strain Gages Mounted Together on a Common Carrier

In the case of SR-4 rosette gages manufactured as complete units incorporating three or four separate elements, two gage factors, a and b, are furnished with the gages.

The factor a = the axial strain sensitivity factor. This is comparable to the Gage Factor for a single gage, however, due to the method of calibration the numerical value is slightly different.*

The factor b = the auxiliary strain sensitivity factor. By means of this coefficient one can correct the indicated strains to the proper values.

---

* Practical Reduction Formulas for Use on Bonded Wire Strain Gages, R. Baumberger and F. Hines, SESA Proceedings, Vol. II, No. 1, p. 116.

In the literature it has been stated that neglect of the factor b (which is related to the transverse sensitivity coefficient, K) will not introduce an error of more than 3% in the numerically larger principal strain.*

Let ϵ^1_a, ϵ^1_b, ϵ^1_c, and ϵ^1_d, represent the apparent strains in the directions of the rosette axes. They are obtained from the relation

$$\epsilon^1 = \frac{\frac{\Delta R}{R}}{a} \tag{66}$$

The values of the apparent strains are not quite equal to the true values, however, they may be corrected to the true values, ϵ_a, ϵ_b, ϵ_c, and ϵ_d, as follows:

I. Rectangular Rosette with Three Observations

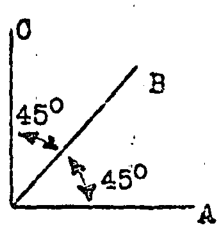

$$\epsilon_a = \epsilon^1_a - \frac{1}{b}\epsilon^1_c \tag{67}$$

$$\epsilon_b = (1 + \tfrac{1}{b})\,\epsilon^1_b - \tfrac{1}{b}(\epsilon^1_a + \epsilon^1_c) \tag{68}$$

$$\epsilon_c = \epsilon^1_c - \tfrac{1}{b}\,\epsilon^1_a \tag{69}$$

from which the principal strains may be calculated as

$$\epsilon_1 \text{ or } \epsilon_2 = (1 - \tfrac{1}{b})\frac{\epsilon^1_a + \epsilon^1_c}{2} \pm (1 + \tfrac{1}{b})\ 1/2\sqrt{(\epsilon^1_a - \epsilon^1_c)^2 + \left[2\epsilon^1_b - (\epsilon^1_a + \epsilon^1_c)\right]^2} \tag{70}$$

and

$$\tan 2\varphi = \frac{2\epsilon^1_b - (\epsilon^1_a + \epsilon^1_c)}{\epsilon^1_a - \epsilon^1_c} \tag{71}$$

II. The Equiangular Rosette

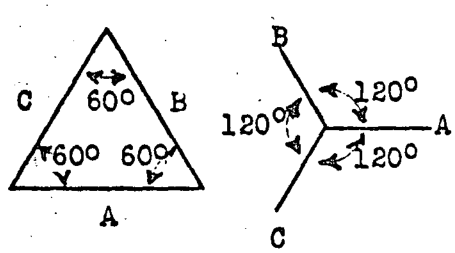

$$\epsilon_a = \epsilon^1_a - \tfrac{1}{b}\ (\epsilon^1_b + \epsilon^1_c) \tag{72}$$

$$\epsilon_b = \epsilon^1_b - \tfrac{1}{b}\ (\epsilon^1_a + \epsilon^1_c) \tag{73}$$

$$\epsilon_c = \epsilon^1_c - \tfrac{1}{b}\ (\epsilon^1_a + \epsilon^1_b) \tag{74}$$

* Practical Reduction Formulas for Use on Bonded Wire Strain Gages, R. Baumberger and F. Hines, SESA Proceedings, Vol. II, No. 1, p. 116.

and the principal strains are

$$\epsilon_1 \text{ or } \epsilon_2 = \left(1 - \frac{2}{b}\right)\frac{\epsilon_a^1 + \epsilon_b^1 + \epsilon_c^1}{3} \pm \left(1 + \frac{1}{b}\right)\sqrt{\left(\epsilon_a^1 - \frac{\epsilon_a^1 + \epsilon_b^1 + \epsilon_c^1}{3}\right)^2 + \left(\frac{\epsilon_c^1 - \epsilon_b^1}{\sqrt{3}}\right)^2} \quad (75)$$

$$\tan 2\phi = \frac{\sqrt{3}\left(\epsilon_c^1 - \epsilon_b^1\right)}{2\epsilon_a^1 - \epsilon_b^1 - \epsilon_c^1} \quad (76)$$

III. Rectangular Rosette with Four Observations

Since this form of rosette is not regularly made as a single unit it will be necessary to make it up from four independent units and to correct the A^1 and B^1 quantities accordingly, or else to make some other special arrangement.

IV. The T - Δ Rosette

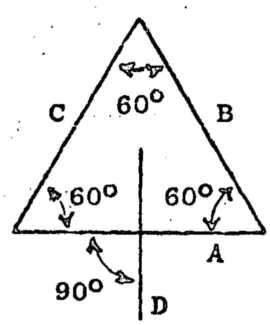

$$\epsilon_a = \epsilon_a^1 - \frac{1}{b}\,\epsilon_d^1 \quad (77)$$

$$\epsilon_b = \left(1 + \frac{1}{b}\right)\epsilon_b^1 - \frac{1}{b}\left(\epsilon_a^1 + \epsilon_d^1\right) \quad (78)$$

$$\epsilon_c = \left(1 + \frac{1}{b}\right)\epsilon_c^1 - \frac{1}{b}\left(\epsilon_a^1 + \epsilon_d^1\right) \quad (79)$$

$$\epsilon_d = \epsilon_d^1 - \frac{1}{b}\,\epsilon_a^1 \quad (80)$$

$$\tan 2\phi = \frac{\frac{1}{\sqrt{3}}\left(\epsilon_c^1 - \epsilon_b^1\right)}{\frac{1}{2}\left(\epsilon_a^1 - \epsilon_d^1\right)} \quad (82)$$

$$\epsilon_1 \text{ or } \epsilon_2 = \left(1 - \frac{1}{b}\right)\frac{\epsilon_a^1 + \epsilon_d^1}{2} \pm \left(1 + \frac{1}{b}\right)\sqrt{\left(\frac{\epsilon_a^1 - \epsilon_d^1}{2}\right)^2 + \left(\frac{\epsilon_c^1 - \epsilon_b^1}{\sqrt{3}}\right)^2} \quad (81)$$

8. List of References

Special References:

1. An Adjunct to the Strain Rosette (and following discussions), W. M. Murray, Proceedings, Society for Experimental Stress Analysis, Vol. 1, No. 1, p. 128.

2. Determination of Principal Stresses from Strains in Four Intersecting Gage Lines 45° Apart, Wm. R. Osgood, Journal of Research of the National Bureau of Standards, Vol. 15, December 1935, p. 579.

3. On Determining Principal Strains from Strain Rosettes with Arbitrary Angles, F. A. McClintock, Letter to the Editor, SESA Proceedings, Volume IX, No. 1, p. 209.

4. A Graphical Method of Rosette Analysis, K. J. Bossart & G. A. Brewer, SESA Proceedings, Vol. IV, No. 1, p. 1.

5. Practical Reduction Formulas for Use on Bonded Wire Strain Gages in Two-Dimensional Stress Fields, R. Baumberger & F. Hines, SESA Proceedings, Vol. II, No. 1, p. 113.

General References:

1. Photoelasticity, Vol. I, M. M. Frocht, Arts. 1.26 - 1.28

2. Handbook of Experimental Stress Analysis - Ch. 9.

Graphical Methods:

1. The Analysis of Strains Indicated by Multiple-Strand Resistance-Type Wire Strain Gages used as Rosettes, Norris F. Dow, National Advisory Committee for Aeronautics, Wartime Report, ARR, January 1943.

2. Charts for Rapid Analysis of 45° Strain Rosette Data, S. S. Manson, NACA Technical Note No. 940, May 1944.

3. The Equilateral Electric Strain Gage Rosette, G. Brewer, Metal Progress, Vol. 51, No. 5, May 1947, p. 758.

4. A Nomographic Solution to the Strain Rosette Equations, T. A. Hewson, SESA Proceedings, Vol. IV, No. 1, p. 9.

5. A Nomographic Rosette Computer, N. Grossman, SESA Proceedings, Vol. IV, No. 1, p. 27.

Graphical Methods: (Continued)

6. The Graphical Solution of 45° Strain-Rosette Data and Determination of Error in the Calculated Stresses due to Errors in Measured Strains, M. E. Duke & E. Wenk, Jr., David Taylor Model Basin, Report No. 600, November 1949. (Navy Department)

7. Resistance Strain Gauges, J. Yarnell, - Chapter 8.

Machine Methods:

1. A Rosette Strain Computer, W. B. Klemperer, NACA Technical Note No. 875, December 1942.

2. An Automatic Electrical Analyser for 45° Strain Rosette Data, S. S. Manson, NACA Technical Note No. 941, May 1944.

3. An Electrical Computer for the Evaluation of Strain Rosette Data, E. E. Hoskins, & R. C. Oleson, SESA Proceedings, Vol. II, No. 1, p. 67.

4. Electronic Computing Apparatus for Rectangular and Equiangular Strain Rosettes, J. H. Meier & W. R. Mehaffey, SESA Proceedings, Vol. II, No. 1, p. 78.

5. Machine Solution of the Strain Rosette Equation, W. M. Murray, SESA Proceedings, Vol. II, No. 1, p. 106.

6. Improvements in Rosette Computer, J. H. Meier, SESA Proceedings, Vol. III, No. 2, p. 1.

7. Improved Techniques and Devices for Stress Analysis with Resistance Wire Gages, W. V. Bassett, H. Cromwell, & W. E. Wooster, SESA Proceedings, Vol. III, No. 2, p. 76.

8. Geometry in the Design of Stress Measurement Circuits; Improved Methods through Simpler Concepts, S. B. Williams, SESA Proceedings, Vol. XVII, No. 2, 1960.

Experiment No. 26 - Strain Gage Rosettes

Object: To illustrate the use of Strain Gage Rosettes for determining the magnitudes of the principal stresses and the directions of their axes under biaxial conditions.

Problem: By strain measurement, to determine the stresses set up in a thin walled cylinder due to an internal pressure of 1500 lbs/sq. in.

Several gage arrangements have been set up with different axes of reference. All arrangements of strain gages should indicate the same results which should agree with theoretical calculations.

Specimen: Steel cylinder closed at both ends

Outside Diameter	4.50"
Wall Thickness	0.14"
Length	30"

Material Properties

Ultimate Strength	60,000	lbs./sq.in.
Yield Strength	35,000	" " "
Modulus of Elasticity	30,000,000	" " "
Poisson's Ratio	0.3	

Strain Gages:

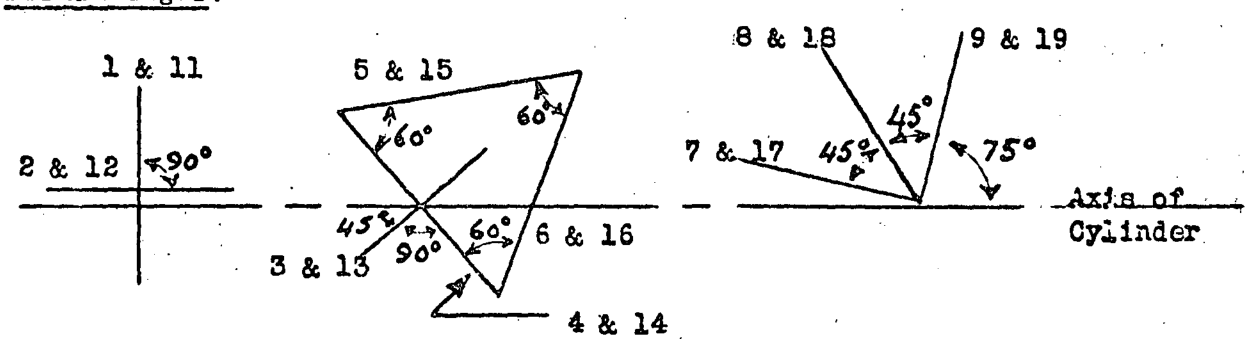

Diagram of Gage Orientation

Gages are mounted in pairs diametrically opposite each other on the cylinder; for example, 1 is opposite 11, 2 is opposite 12, etc.

Resistance of all gages is nominally 120 ohms. Gage Factors are as follows:

Experiment No. 26 - Strain Gage Rosettes (Continued)

	Gage Factor
Axial & Circumferential Gages: 1, 11, 2, 12	2.03
Rectangular Rosettes: 7, 8, 9, 17, 18, 19	2.03
Tee-Delta Rosette: 3, 4, 5, 6; 13, 14, 15, 16	2.01

(Note that the T-Δ Rosette can be used as a Δ Rosette by omitting observations on gages 3 & 13

Equipment:

1 Switching Unit
1 Baldwin Portable Strain Indicator
1 Oil Reservoir & Pump with Pressure Gage

Results Wanted:

1. Determination of the principal stresses, σ_1 & σ_2, and the directions of the corresponding axes from strains measured

   (a) With axial & circumferential gages
   (b) With Rectangular rosettes
   (c) With T-Δ (or Δ) rosettes

2. Comparison with theoretical calculations

Procedure:

1. Take zero readings on all strain gages.

2. Apply pressure to the cylinder in increments of 200 lbs./sq.in. up to a maximum of 1600 lbs./sq.in. and take readings on all gages after each pressure increment.

3. Release pressure to zero and check zero readings on all gages.

   NOTE: Since time is limited it is suggested that you take readings either on a few gages at all pressure levels or all gages at a few pressure levels and refer to the accompaying table (See Page 644) for the remainder of the required observations.

4. Plot pressure vs. indicated strain for each gage. Curves for one rosette can be arranged together on a single graph sheet.

Experiment No. 26 - Strain Gage Rosettes (Continued)

Procedure: (Continued)

5. Average the slopes of plots of item 4 for diametrically opposite gages and determine the strain on each gage for a pressure increment of 1500 lbs./sq.in.

6. Neglecting transverse effects in the strain gages, calculate the magnitudes of the principal stresses and determine the directions of the corresponding axes for each of the three gage arrangements

   (a) by analytical means
   (b) by graphical means

7. Check the results of item 6 by making the necessary theoretical calculations for the hoop stress and the longitudinal stress.

$$\text{Hoop Stress (psi)} = \frac{\text{Pressure (psi)} \times \text{Radius (in)}}{\text{Wall Thickness (in)}}$$

$$\text{Longitudinal Stress} = \frac{1}{2}\ \text{Hoop Stress}$$

8. If the Transverse Sensitivity factor, K, for the axial and circumferential gages is 0.02, and the "b" factor for Rectangular and T-Δ Rosettes is 55, how much error is introduced by neglecting the transverse effects?

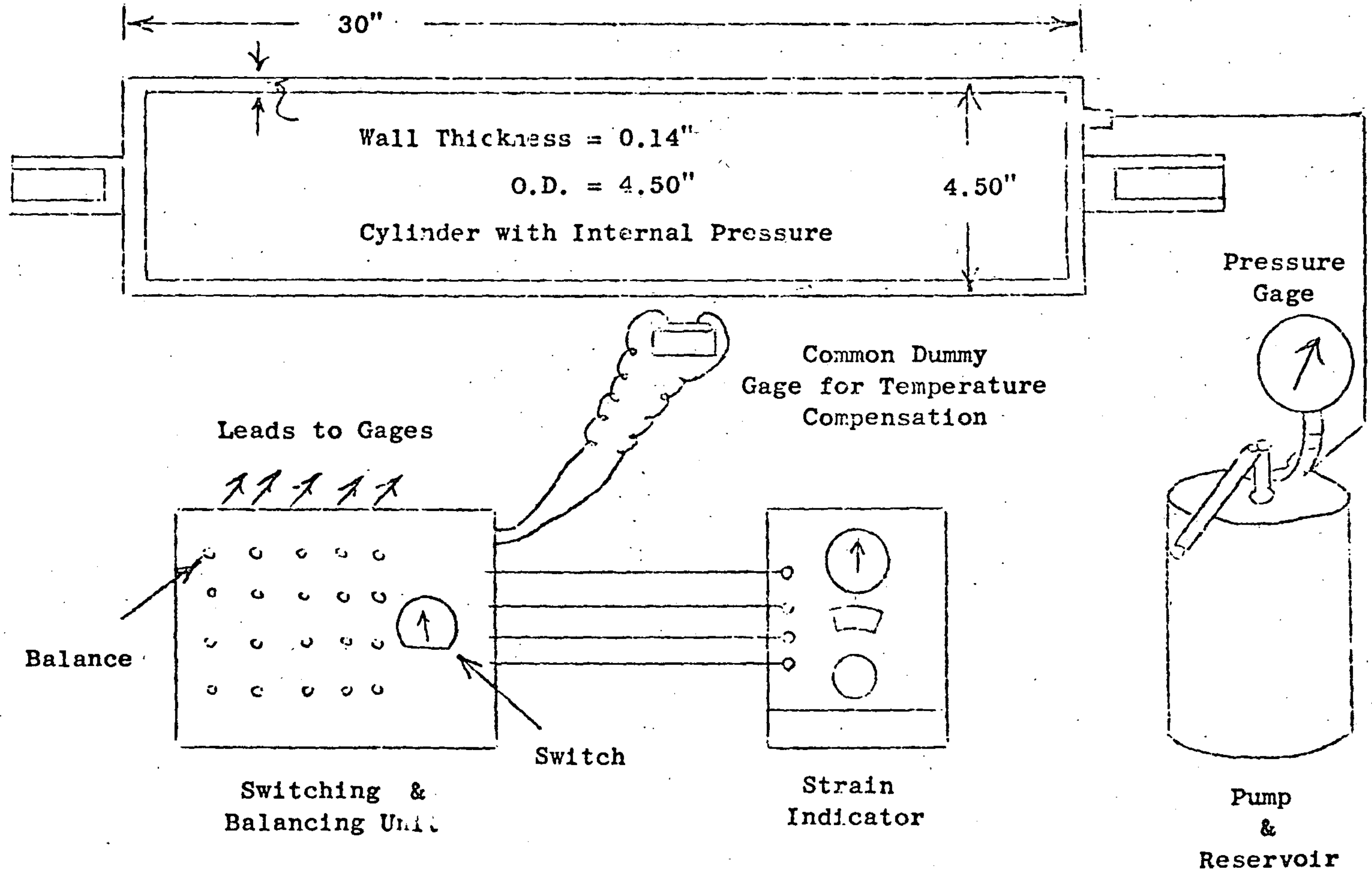

SCHEMATIC DIAGRAM OF APPARATUS

REDUCED DATA for EXPERIMENT No. 26

GAGE NO.	PRESSURE IN P.S.I.								
	0	200	400	600	800	1000	1200	1400	1600
	STRAIN IN MICRO-INCHES PER INCH								
1	0	74	169	260	341	422	492	580	670
2	0	20	50	74	110	118	140	162	189
3	0	49	113	175	232	282	350	398	455
4	0	48	111	170	226	276	340	375	440
5	0	21	52	81	110	133	164	189	219
6	0	75	174	261	350	430	525	602	698
7	0	29	51	80	105	130	160	180	210
8	0	70	149	222	292	360	432	500	575
9	0	81	174	262	349	425	515	593	682
11	0	80	171	260	340	422	510	592	680
12	0	20	49	71	92	115	140	160	183
13	0	50	111	170	214	270	322	379	428
14	0	51	115	170	217	270	329	382	430
15	0	21	52	80	109	130	155	180	202
16	0	75	171	260	330	410	488	560	640
17	0	21	52	82	110	135	160	183	212
18	0	59	155	230	290	360	425	498	562
19	0	71	171	250	312	392	462	540	611

Zero shift after experiment less than 2 μ"/"

Equipment: 20 Station Switching and Balancing Unit Baldwin No. 5009-3
Baldwin Type L-Strain Indicator No. H-80797
Common Zero Setting at each Gage: 0-8-1000

centro de educación continua
división de estudios superiores
facultad de ingeniería, unam

ANALISIS EXPERIMENTAL DE ESFUERZOS

Chapter XXII

SOME EXAMPLES

OF

DYNAMIC STRAIN MEASUREMENT

DR. LUIS FERRER ARGOITE

DR. PORFIRIO BALLESTEROS BAROCIO

ING. ALFREDO OLIVARES PONCE

Outline

1. Introduction

2. Steady State Dynamic Test with Strain Gages - Experiment No. 20

(a) Statement of the Problem
(b) Specifications of System Components
(c) Theoretical Solution
(d) Instruments and Equipment
(e) Design of the Strain Gage System
  Measuring System Input Requirements
  Maximum Strain Gage Sensitivity
  Circuit Design
  Circuit Properties
    Sensitivity - Maximum Output - Non-Linearity
  Amplifier Specifications
  Comparison with Available Amplifier
(f) Calibration
(g) Experimental Procedure

3. Unsteady State Low Frequency Dynamic Measurements - Experiment No. 21

(a) Experimental Procedure
(b) Qualitative Analysis of the Transient Phenomenon
(c) Specifications of System Components
(d) Theoretical Solutions
(e) Instrument Characteristics

4. Transients of Short Duration - Impact - Experiment No. 22

(a) General Remarks
(b) The Problem
(c) Experiment
(d) Information
(e) Calibration of CRO X Axis in Terms of Time
(f) Determination of the Striking Velocity
(g) Triggering the CRO - Internally - Externally
(h) Qualitative Study

1. Introduction

Three experiments have been designed as samples of some of the techniques available for dynamic strain gage studies.

(1) A steady state vibration phenomenon where, with fairly simple equipment, it is possible to obtain good results.

(2) A non-steady state, or transient, vibration problem where the main phenomena occur at frequencies which permit the use of a paper-type recorder without the necessity of resorting to oscillographic-photographic methods.

(3) A transient problem the duration of which is so short, that oscillographic-photographic methods are a necessity.

2. Steady State Dynamic Test with Strain Gages - Experiment No. 20

(a) Statement of the Problem

A freely vibrating beam supported at its nodes is to be investigated. The stress distribution along the upper surface is to be determined at a given amplitude of vibration, by two methods:

(1) Direct strain measurement, to be interpreted in terms of stress, by locating six strain gages along the beam as shown in the diagram.

The amplitude of vibration will be measured with an optical micrometer at the center of the vibrating bar.

(2) Analytically determined values of stress along the beam divided by the amplitude of vibration at the center of the beam can be determined from theoretical considerations.

The two methods are to be compared.

(b) Specification of System Components

Beam:	L	length of beam	37 3/16 inches
	t	thickness of beam	3/4 inch
	b	width of beam	2.00 inches
	ρ	density of beam material (steel)	0.286 lbs/ins^3
	E	Young's modulus of beam material	30×10^6 lbs/ins^2
	d	distance from center of beam to nodes of vibration	$(0.276L) = 10.25$ ins.

σ_e	endurance limit of beam material	23,000 psi
f	natural frequency of beam vibration	$\frac{20.21\ t}{L^2}\sqrt{\frac{E}{\rho}}$ = 112.8 cyc/sec.

(c) Theoretical Solution

A	fundamental constant	1.1532
B	fundamental constant	0.1532
m	fundamental constant	4.7300
a	amplitude of vibration at center of beam in inches	
x	distance along beam from center, in inches	
σ_x	stress at any point x along the beam supported at its nodes of vibration, vibrated at its natural frequency.	

$$\sigma_x = a\ E\ \frac{t}{2}\ \frac{m^2}{L^2}\left[A\cos\frac{mx}{L} + B\cosh\frac{mx}{L}\right]$$

and for this beam:

Value of x (inches)	0	3	6	9	12	15	(18-19/32)
Value of σ_x/a (lbs/ins^3)	238,500	224,500	189,000	134,000	75,400	28,100	0

(d) Instruments and Equipment

Amplitude Measurement Cathetometer, continuous range of 10 cm. 0.01 mm smallest scale division

Strain Gages
Type SR-4 C-1
Resistance R_g = 500 ohms
Gage Factor (GF) = 3.23
Maximum Current Rating 30 milliamperes (continuous)
Location: at 0, 3, 6, 9, 12, 15 inches from center

Vibration Exciter Rayflex Fatigue Machine, description attached.

Available Amplifier

Gain (in linear range) G 26
Linear Range 0.05 volts input maximum

Lower Frequency Cut-Off	f_1 2 cps
Upper Frequency Cut-Off	f_2 7000 cps
Input Impedance	0.5 μF. 1MΩ
Output Impedance	less than 100,000

Measuring Instrument:

DuMont Cathode Ray Oscillograph	Type 208B
Maximum Sensitivity along Y-axis	0.01 rms volts/ins
Useful screen diameter	4 inches
Lower frequency limit	2 cycles/second
Upper frequency limit	100,000 cycles/second
Input impedance	2 MΩ 50 $\mu\mu$ F

Calibration:

Type	Parallel resistance
Calibration resistor	125,000 ohms
Switch	1/60 second period (square wave)

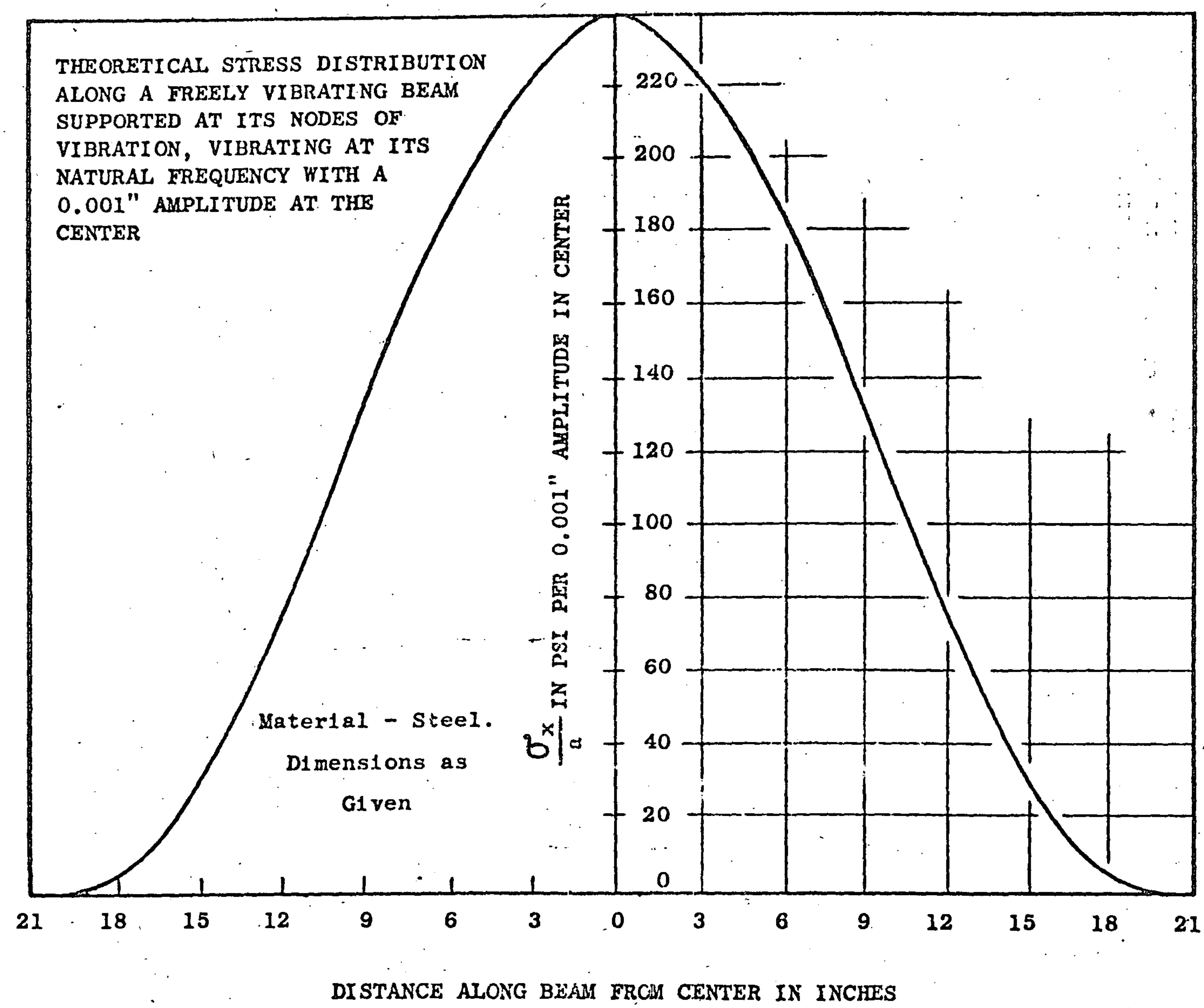
THEORETICAL STRESS DISTRIBUTION ALONG A FREELY VIBRATING BEAM SUPPORTED AT ITS NODES OF VIBRATION, VIBRATING AT ITS NATURAL FREQUENCY WITH A 0.001" AMPLITUDE AT THE CENTER
Material - Steel. Dimensions as Given
$\frac{\sigma_x}{a}$ IN PSI PER 0.001" AMPLITUDE IN CENTER
0
20
40
60
80
100
120
140
160
180
200
220
21
18
15
12
9
6
3
0
3
6
9
12
15
18
21
DISTANCE ALONG BEAM FROM CENTER IN INCHES

DETERMINATION OF YOUNG'S MODULUS

The principle of free vibration lends itself to the accurate determination of Young's Modulus. For this purpose, the natural period of vibration or frequency must be measured to an accuracy of 0.1%. This is readily done as stated above, the measurement being made at low amplitudes of vibration, well below the fatigue limit. From this natural frequency, the dimensions and the weight of the specimen, the modulus may be calculated (see formulae, page 4).

MAGNAFLUX TEST

The Magnaflux test for discontinuities in steel or iron has been found useful in conjunction with fatigue investigations. Incipient failures may be located and studied in relation to surface conditions or local metallurgical factors before the spread of the crack has proceeded beyond a few thousandths of an inch. Coils for Magnaflux testing are supplied with the machine, and a limited license will be granted to customers who are not already licensees of the Magnaflux Corporation.

Reference: Rate of Growth of Fatigue Cracks
Journal of Applied Mechanics, Mar. '36, Vol. 3, No. 1

STROBOSCOPE ATTACHMENT

A stroboscopic device is supplied. This permits "slow motion" observation of the specimen; the growth of the failure crack being readily followed visually.

DETERMINATION OF STRESS

The stress applied to a specimen of uniform section is readily obtained from a knowledge of the maximum deflection at the center of the specimen, its dimensions, and Young's Modulus for the particular material being tested. The maximum deflection or amplitude may be read on a meter mounted on the control panel. This instrument is fitted with an arbitrary scale, the actual amplitude in thousandths of an inch being supplied by a calibration curve.

An optical method of changing the amplitude is also provided.

STRESS CALCULATIONS

Theory: The equation of motion for a uniform free bar vibrating in its first mode is:

$$y = a\left(A \cos m \frac{X}{L} - B \cosh m \frac{X}{L}\right) \cos \omega t$$

where $\omega = 2\pi f = \frac{m^2 K}{L^2} \sqrt{\frac{Eg}{\rho}}$

A, B, and m are fundamental constants.
$A = 1.1532 \quad B = 0.1532 \quad m = 4.7300$

The bending moment may be derived thus:

$$M = EI \frac{\delta^2 y}{\delta x^2} = EIa \frac{m^2}{L^2}\left(A \cos m \frac{X}{L} + B \cosh m \frac{X}{L}\right) \cos \omega t$$

The deflection and bending moment curves are shown in the figure. The deflection is zero at the nodes, where $\frac{X}{L} = 0.2758$ and the bending moment is a maximum at the mid point of the specimen.

The notation is as follows:

- S Maximum Stress (Lbs. In.^{2})
- y Deflection from Mean Position (In.)
- x Distance from Mid-Point of Specimen (In.)
- L Length (In.)
- d Diameter (In.)
- M Bending Moment (In. Lbs.)

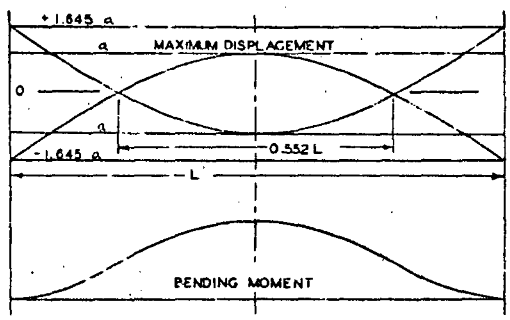

Courtesy of
Baldwin-Lima-Hamilton
Corporation

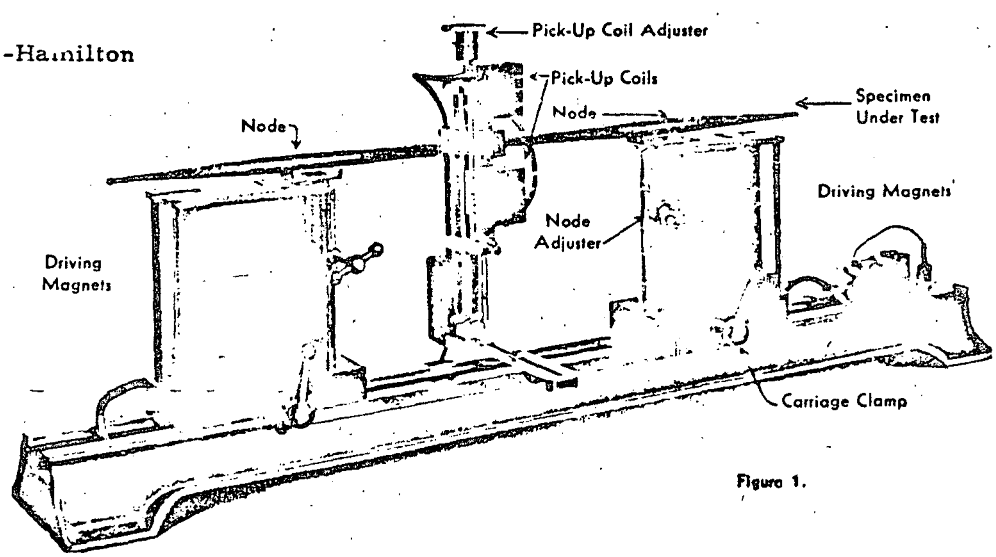

Figure 1.

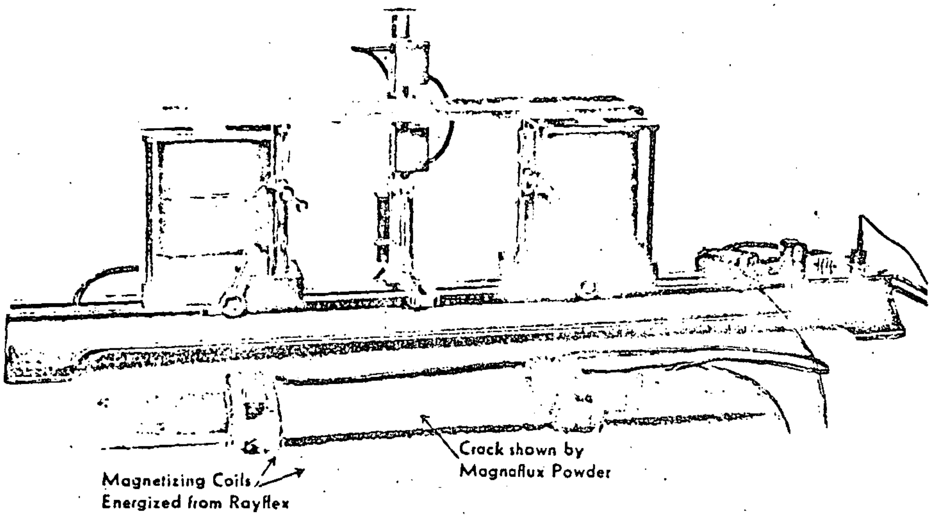

Figure 2

E Young's Modulus (Lbs. In.^{2})
ρ Density (Lbs. In.^{3})
f Frequency of Vibration (Cycles Sec.)
I. Moment of Inertia of Cross Section (In.^{4})
K Radius of Gyration of Cross Section (In.^{4})
t Thickness (In.)
g Acceleration of Gravity (In. sec.^{2})
a Amplitude of Vibration, one-half Total Travel at Mid-Point of Specimen (In.)

PRACTICAL FORMULAE

The following practical formulae are derived from the above equations.

$$\text{Maximum } M = 29.23\,\frac{EIa}{L^2}$$

$$\text{Maximum } S = 14.61\,\frac{Eda}{L^2}$$

$$\text{Distance between nodes} = 0.5516L$$

$$\text{Frequency} = 3.561\,\frac{K}{L^2}\sqrt{\frac{Eg}{\rho}}$$

Round Bars, Any Size:

$$S = 14.61\,\frac{Ead}{L^2}$$

$$E = .003266\,L^4\rho\,\frac{f^2}{d^2}$$

$$f = \frac{17.50d}{L^2}\sqrt{\frac{E}{\rho}}$$

Flat Bars, Any Size:

$$S = 14.61\,\frac{Eat}{L^2}$$

$$E = .002449\,L^4\rho\,\frac{f^2}{t^2}$$

$$f = \frac{20.21t}{L^2}\sqrt{\frac{E}{\rho}}$$

TESTING OF NON-MAGNETIC MATERIALS

Non-magnetic materials may be tested by simply fastening soft iron sleeves to the ends of the specimen. A set of standard sleeves for round specimens will be supplied with the Rayflex. In testing a specimen loaded with these sleeves or armatures, the above standard formulae do not apply directly. Means for calculating stress under these conditions will also be supplied with the Rayflex.

SPECIAL TESTS

The Rayflex is admirably suited to tests on welded sections and, of course, non-uniform sections and threaded couplings may be tested on a comparative basis and in some cases stress can be computed from the theory of elasticity.

MAINTENANCE

Extreme precautions have been taken to make the Rayflex a tool for fatigue testing and not a "gadget" requiring tinkering or service to make it work. The tubes used are available at any standard radio supply house and suitable instructions will be furnished so that any competent radio service man can handle tube replacement and repairs.

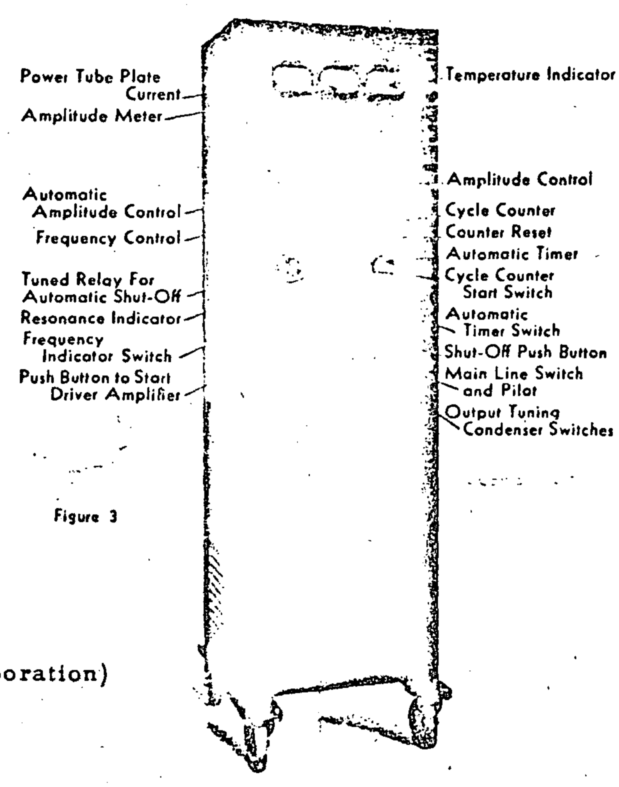

Figure 3

(Courtesy of Baldwin-Lima-Hamilton Corporation)

(e) Design of the Strain Gage System

General

In order to combine most of the preceding chapters into one focal problem, the design of this system will be presented in detail as a sample.

Measuring System Input Requirements

It is usually necessary to start at one end of the measuring system, and unless one has the choice of several measuring instruments, that portion of the system serves as a satisfactory point of departure.

Since the endurance limit of the bar material is about 23,000 psi., and since the bar is not to be destroyed, a maximum operating stress of 20,000 psi., is arbitrarily assigned to the bar. Thus the peak to peak stress variations during the experiment will be in the vicinity of 40,000 psi. For best results, these 40,000 psi are to occupy the full 4 inches of the CRO screen. At maximum sensitivity, the CRO requires 0.010 volts rms at the Y-input terminals per inch deflection on the screen. The minimum input sensitivity to the measuring instrument, in terms of micro-volts per micro-inch-per-inch strain will be:

$$\frac{4\text{(inches on screen)}}{40{,}000\text{ (psi stress)}} \times \frac{0.01\text{ (volts rms)}}{1\text{ (inch on screen)}} \times \frac{\sqrt{2}\text{ (volts peak)}}{1\text{ (volt rms)}}$$

$$\times \frac{30 \times 10^{6}\text{ (psi stress)}}{1\text{ (inch/inch strain)}}$$

$=$ 42.2 micro-volts per micro-inch per inch strain in the bar.

$=$ 1.414 micro-volts per psi stress in the bar.

Corollary

If a strain gage circuit can be designed with this output sensitivity, then an amplifier will not be needed. Can such a circuit be designed?

Maximum Strain Gage Sensitivity

The maximum strain gage sensitivity in terms of S_g in micro-volts per volt output from the circuit per micro-inch per inch strain has been shown to be a property only of the strain gage used and independent of the circuit configuration (so long as it is passive) or of any supply voltages used.

$$S_{g_{max}} = \text{(Gage Resistance)(Gage Factor)(Maximum Current Capacity)}$$

In this case it is assumed that there is no choice in gage type available, but that the gages specified must be used:

$$S_{s_{max}} = 500 \times 3,23 \times \frac{30}{1000} = 48,45 \text{ micro-volts per micro-inch per inch strain.}$$

Corollary

If the output from the actual strain gage circuit to be designed can be made to be:

$$\frac{42,42 \times 100}{48,45} = 87,7\% \text{ of maximum sensitivity}$$

no amplifier will be needed.

Circuit Design

The design chart on page 119 may be used both for a Potentiometric Circuit and for a Wheatstone Bridge, so that at this point a design can be made without as yet specifying the type of circuit to be finally employed.

On the chart draw the horizontal line $E_{max} = \frac{500 \times 30}{1000}$

$$= I_{max} \cdot R_g = 15 \text{ volts}$$

Find the horizontal line $S_r = 87,7\% \text{ of } \frac{S_s}{(GF)} = 13,16$

Now find that value of a for which the line of $E = f(a,V)$ intersecting the $E = 15$ volt line and the line of $S_r = f(a,V)$ intersecting the 13,16 volt line belongs to the same value of V.

For the limited choices available on the graph the solution is:

$$a = 9$$

$$V = 150 \text{ volts}$$

By solving numerically from the corresponding relationships

$$S_r = E \frac{a}{1 + a}$$

$$V = E\,(1 + a)$$

one finds $13,16 = 15\left(\frac{a}{1 + a}\right)$

and $V = 15\,(1 + a)$ or

$a = 7.07$
$V = 121.1$ volts
hence $R_b = 3535\ \Omega$

Corollary

Through proper choice of ballast resistance and supply voltage, a system has been designed which does not need a pre-amplifier between the circuit and the CRO, but which demands operation of the CRO at maximum sensitivity. Furthermore, it turns out that there is no voltage source above 45 volts available so that the "ideal" circuit cannot be used.

Redesign of Circuit

With V = 45 volts, in order to have 30 milliamperes through the gage, the ballast resistor must be $R_b = 1000$ ohms and the sensitivities from page 119 will be, for the value of $a = 2$:

$$S_r = V \frac{a}{(1 + a)} = 45 \times \frac{2}{(1 + 2)^2} = 10 \text{ micro-volts/micro-ohm per ohm}$$

$$S_s = S_r(GF) = 10 \times 3.23 = 32.3 \text{ micro-volts/micro-inch/inch}$$

$$\text{Circuit efficiency} = \frac{a}{1 + a} = 66\ 2/3\%$$

Choice of Type of Circuit

Since the phenomenon does not contain any static stresses, a Wheatstone bridge circuit would unnecessarily complicate matters. The extra resistors and zero-balancing devices would be cumbersome. A Potentiometric circuit is called for in this case. The circuit values:

$V = 45$ volts

$R_b = 1000$

$R_g = 500$

$I = 30$ ma

$a = 2$

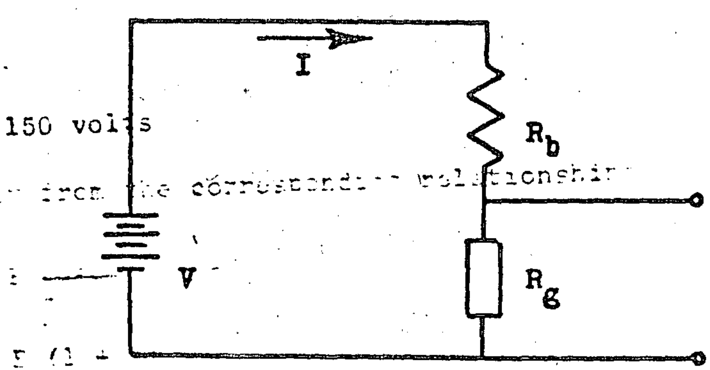

Circuit Properties

Sensitivity

$$S_s = \frac{V}{(GF)} \quad \frac{a}{(1+a)^2} = 32.3 \quad \text{volts}/\mu \text{ inch/inch}$$

Maximum Output at 20,000 psi

$$\Delta E/20{,}000 = \frac{S_s \times \sigma}{E} = \frac{32.3 \times 20{,}000}{30 \times 10^6} = 0.0216 \text{ volts}$$

Non-Linearity at 20,000 psi

$$n \Big|_{20{,}000} = \frac{1}{1 + \frac{a+1}{\Delta R/R}} = \frac{1}{1 + \frac{2+1}{\frac{3.23 \times 20{,}000}{30 \times 10^6}}} = 0.072\%$$

$$= \frac{0.072}{100} \times 0.216 = 15.5 \text{ micro-volts}$$

Measuring Instrument Reading Accuracy

Assuming the four inches on the CRO can be read to 0.05 inches, the equivalent input to the CRO is:

0.05 inches x 0.010 volts/inch x 1.414 volts peak/volt rms = 0.707 mV

Amplifier Specifications

Since an amplifier will be needed, the specifications should be drawn up:

Gain: The minimum gain must be:

$$\frac{42.42 \text{ micro-volts/micro-inch/inch required at CRO input}}{32.30 \text{ micro-volts/micro-inch/inch available circuit output}}$$

$$= 1.31$$

Linear Input Region: The minimum specifications should read:

0.072% deviation from linearity at 21.5 millivolts input in order to mate with the circuit output and linearity. The CRO, however, can be read to only 1-1/2% approximately, such that a revised specification may be:

1-1/2% deviation from linearity at 21.6 millivolts input.

Noise Level: This figure is dictated, either by the circuit nonlinearity, since it does not make sense to have a much lower noise level than the linearity-limit of the system,

(This limit would be 15.5 micro-volts)

or, the limit could be the CRO readability. 0.05 inches on the CRO at maximum sensitivity correspond to 0.707 millivolts input to the CRO which corresponds to $\frac{0.707}{G}$ millivolts input to the amplifier.

This limit would be $\frac{0.707}{G}$ millivolts

The larger limit should prevail in the amplifier chosen.

Frequency Response: The use of the Potentiometric Circuit determines that the amplifier shall have a lower frequency limit.

Signal frequency: 112.8 cycles theoretically
Calibration frequency: 1/60 second square wave.

f_1 to be at least 6 cps., such that the fundamental of the square wave is fairly well in the "flat region."

f_2 to be at least 6000 cps., if it is desired to pass that component in the square wave whose frequency is 100 times the fundamental. This upper limit must be set by some rule of thumb as regards the number of harmonics of the fundamentals to be passed.

Since these frequency limits contain the expected signal frequency and any normal deviation from it, they may stand as specifications for the amplifier needed.

Input Impedance: In order not to interfere with the measurements, the input impedance should be at least 100 times the gage resistance:

Input impedance of amplifier greater than 50,000 ohms.

Output Impedance: In this case the output impedance should be much lower than the CRO input impedance which is 50,000 ohms.

Comparison with Available Amplifier

	Desired	Available	Comment
Gain	1,3	26	ok
Lower frequency	6 cps	1,5 cps	ok
Upper frequency	6000 cps	7000 cps	ok
Input impedance	50,000 ohms	10^6 ohms	ok
Noise level	27,2 u-volts	---	check
Output impedance			check
Linear Input Region	21,6 mv, 1-1/2%	50 mv	no percentage deviation figure given. Should be checked.

The phase characteristics can only be assumed to be satisfactory. A good assumption is that the phase lag is constant between the upper and lower frequency limits.

Conclusion

The amplifier will be used with the circuit as finally designed. If the calibration is performed with the amplifier in the circuit, exact fulfillment of all the characteristics is not really necessary. The effect of too high an amplifier output impedance, for example, would be accounted for in the calibration proceedings.

(f) Calibration

Since it has been decided to operate the bar at no more than 40,000 psi peak-to-peak stress, and since there are 4 inches available on the CRO screen, a convenient calibration figure would seem to be 10,000 psi/inch. The calibration resistor necessary to simulate the application of 40,000 psi stress to the bar beneath one of the gages would be:

$$R_c = \left[\frac{1}{\epsilon\ (GF)} - 1\right] R_g = \left[\frac{30 \times 10^6}{40,000 \times 3.23} - 1\right] 500 = 116,000 \text{ ohms}$$

The only resistor available, however, in that order of magnitude has a resistance of 125,000 ohms, which will give equivalent stress of:

$$= \frac{E}{G.F.} \times \left[\frac{R_g}{R_g + R_c}\right] = \frac{30 \times 10^6}{3.23} \left[\frac{500}{125,500}\right] = 37,100 \text{ psi stress,}$$

Hence, if the total amplitude of the square wave which results from the periodic switching into and out of the circuit of the calibration resistor, is made to occupy 3.71 inches on the CRO screen, the calibration conditions will correspond to 10,000 psi stress per inch deflection on the CRO screen.

It is to be noted that direct calibration in stress is possible only because there is a uni-axial stress field and stress and strain are related directly through Young's Modulus.

(g) Experimental Procedure

Strain Measurement

(1) Calibrate the screen of the CRO using the equivalent strain method and a 125,000 ohm calibrating resistor. The resulting signal will represent a stress of:

$$\sigma = \frac{E}{(GF)} \cdot \frac{R_g}{R_c + R_g} = 37{,}100 \text{ psi}$$

on the CRO screen. If the Y-gain adjustment on the CRO is set such that this signal occupies 3.71 inches on the screen of the CRO along the Y-axis, the calibration constant for the system is a convenient:

10,000 psi stress/inch deflection on the screen

(2) Adjust the Rayflex machine such that the beam vibrating with an approximate stress amplitude of 20,000 psi zero-to peak for the center gage, No. 1. (The maximum stress in the beam of 20,000 psi is then below the endurance limit of the beam material of about 23,000 psi. This condition is desirable since the specimen is not to be destroyed.)

(3) By means of the switching arrangement, read the stress amplitudes for all six gages without changing the Y-axis setting on the CRO control panel. The readings should be taken in as short a period of time as possible so that it may be assumed that the beam is vibrating at a constant amplitude for all readings.

Amplitude Measurement

(1) Focus the Cathetometer on one of the punch marks in the center section of the beam, while the beam is at rest.

(2) As the beam vibrates, this punch mark will appear as a line whose length is to be measured with the Cathetometer.

The length of this line is the double amplitude of vibration of the beam.

(3) The amplitude reading should be performed simultaneously with the direct stress reading such that the results may be compared as having been obtained under the same conditions.

3. Unsteady State Low Frequency Dynamic Measurements - Experiment No. 21

Purpose

To demonstrate the use and limitations of a recorder for the study of vibrations.

(a) Experimental Procedure

A cantilever beam with two pairs of strain gages mounted as shown in the diagram is to be subjected to various conditions.

(1) An original deflection at the free end, which is suddenly released to permit the beam to vibrate freely.

(2) A concentrated load is applied to the free end, which is given an initial deflection and then suddenly released to permit the beam to vibrate freely.

(3) A concentrated load is suddenly applied to the free end, being permitted to fall through zero distance onto the beam.

(4) Taps with the steel hammer at various locations along the beam.

(5) Taps with the steel hammer at a location 0.78L from the clamped end of the beam. (L is the beam length).

Recordings will be made of all five conditions, and these records will be examined for:

Conditions	Experimental Results Desired
1	The frequency of the first mode of vibration and the time constant of decay of this vibration.
2	The frequency of the first mode of vibration and the time constant of decay of this vibration.

3 Verify that this condition of dynamic loading produces an initial deflection (or strain) which is twice the final value.

4 The frequency of the second mode of vibration of the beam. Also ascertain the non-reliability of the recorder for frequencies above about 40 cycles per second, by observing the same phenomenon on the recorder and on the screen of a Cathode Ray Tube.

5 Notice the absence of the second mode of vibration because the beam is excited at the node of vibration of the second mode.

Note that the frequency of vibration remains constant and independent of the amplitude of vibration.

Methods of Calculation of Desired Results

Frequencies

The recordings obtained show periodic pips along a line at the bottom of the record. These pips are 1 second apart and provide a convenient time scale, such that one must merely count the number of cycles of vibration occuring in any given time interval in order to determine the frequency of vibration in cycles per second.

The first, second, and third modes of vibration will be evidenced in the following type of record, and it is possible to distinguish between them as shown:

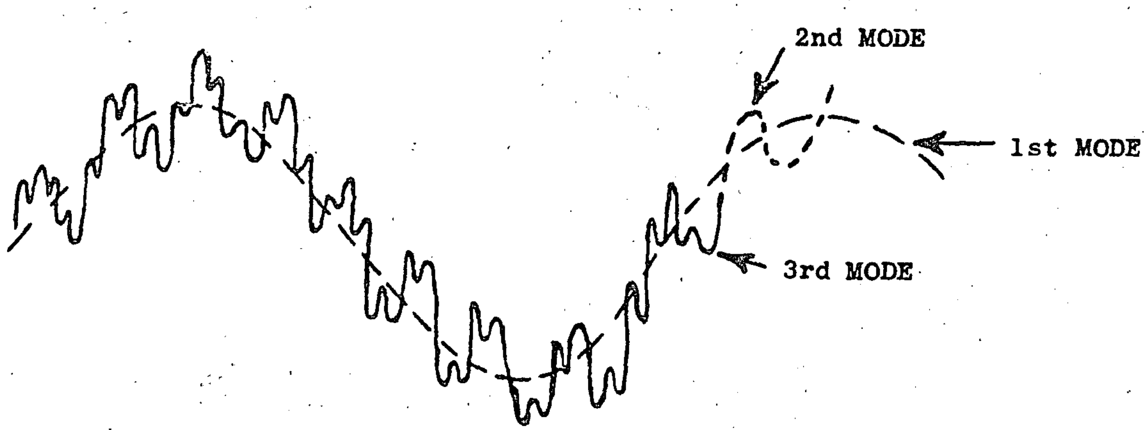

Time Constants

To a very good approximation, the rate of decay of the vibration may be expressed by a function:

Decay Factor: $e^{-t/T}$

where e is the base of the natural logarithm (2.71828),
t is the time in seconds
T is the Time Constant of Decay

at t = 0 the decay factor is 1
at t = T the decay factor is $1/e = 0.3670$
at t = 2T the decay factor is $1/(e^2) = 0.1353$

One may therefore determine T by ascertaining the time in seconds, in which the amplitude of the vibration has decreased to 36.7% of its initial value.

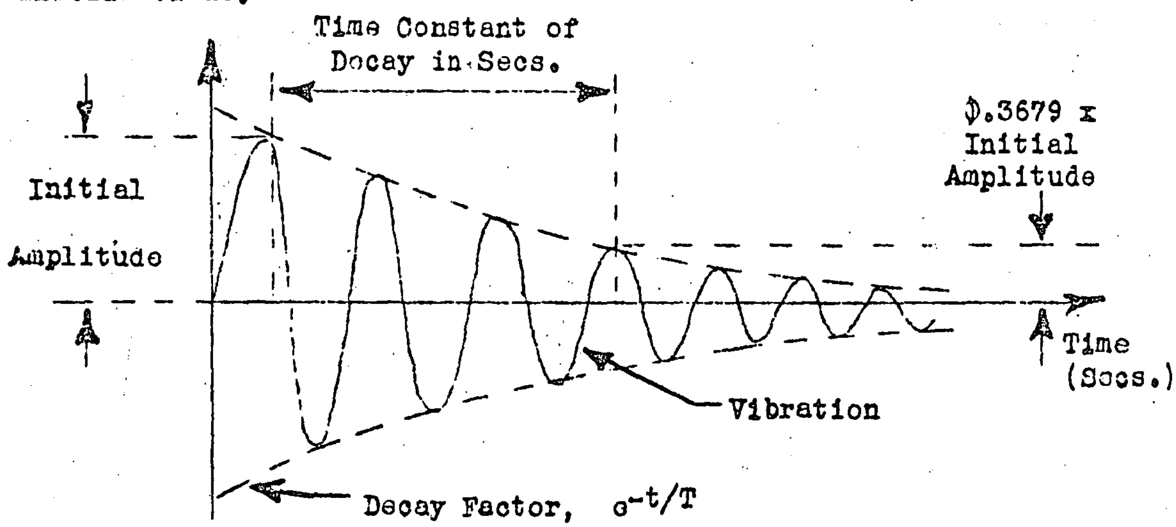

(b) Qualitative Analysis of the Transient Phenomenon

The theoretical analysis of the freely vibrating cantilever beam becomes extremely complicated when the initial transient phenomena are taken into account. Since the initial transient is of short duration, an exceedingly good approximate theory exists as a tool of analysis. A qualitative analysis of the cause of these transients, however, is indicated.

When the beam is released from its static constraint (the initial end deflection), the effective loading on the beam is changed from a concentrated end load to a distributed dynamic load. This change in loading condition is accompanied by a change in shape of the deflection curve.

Since these changes cannot occur in zero time, a transient period of several cycles of vibration is needed before the beam settles down to its normal free vibration for which the theoretical equations are derived.

Furthermore, the initial deflection condition of the beam corresponds to its static deflection curve. This curve may be regarded as a superposition of the deflection curves for all the modes of vibration of the beam in proportion to the intensities with which they exist. Thus, roughly, the static curve may be said to be composed of a positive deflection of 103% of the first mode, plus a negative deflection of 3% of the second mode, adding up to 100% of the static deflection curve.

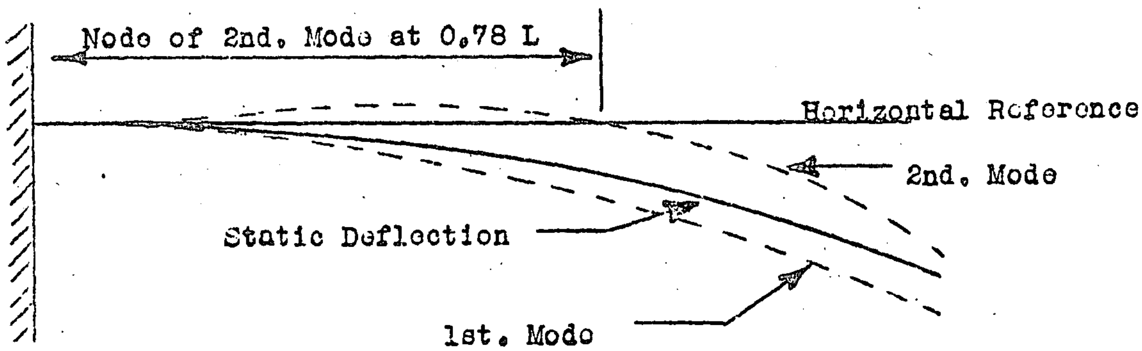

It stands to reason, therefore, that during the initial few cycles of vibration, several modes will be present until all but the first mode have decayed. This decay takes place rapidly because the initial amplitudes of all higher modes of vibration are exceedingly small compared to that of the first mode. A check on this explanation may be obtained by exciting the bar at the node of vibration of the second mode (Condition No. 5). The resulting record should show the absence of the second mode of vibration.

It also becomes apparent that if only the higher modes of vibration are of interest, the beam must be excited at locations where the initial amplitude of the first mode is small, whereas the amplitudes of the higher modes are at their maximum.

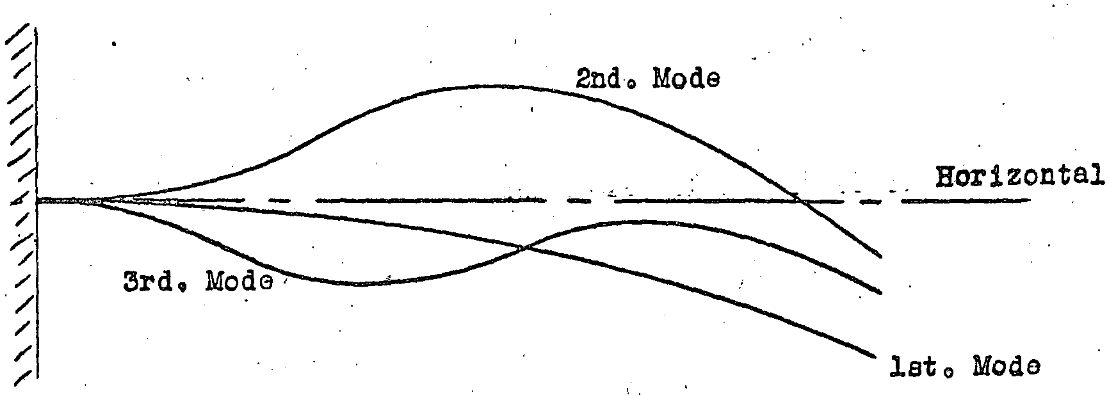

(c) Specifications of System Components

Symbols	Items	Units	Numerical Values
L	Length of the Beam	(ins)	20.45
b	Width of the Beam	(ins)	1
h	Thickness of the Beam	(ins)	0.060
I	Moment of Inertia of Beam Section $b.h.^3/12$	(ins^4)	18×10^{-6}
E	Modulus of Elasticity of the Beam	(lbs/ins^2)	30×10^6
ρ	Density of Beam Material	(lbs/ins^3)	0.283
λ	Weight of Beam per Unit Length	(lbs/ins)	0.017
w	Total Weight of Beam	(lbs)	0.344
g	Gravity Constant	(ins/sec^2)	386.
t	Time	(sec)	
f	Frequency	(cycles/sec)	
d_o	Initial End Deflection of Beam	(ins)	
W	Concentrated End Load Applied to the Beam	(lbs)	0.1
C_i	Constants obtained as solution to ($\cos C_i . \cosh C_i + 1) = 0$ See below		
i	Subscript to Denote Modes of Vibration 1, 2, 3, 4, 5, 6		
	Strain Gage Type		A-7
	Gage Factor		1.93
	Gage Resistance	(ohms)	120.
	Node of Vibration of Second Mode (from Clamped End)		0.78 x L
	Circuit Type	2 active gages	Potentiometric
	Supply Voltage	(volts)	6

(d) Theoretical Solution

(1) Theoretical Solution for Freely Vibrating Cantilever Beam

$$f_i = \frac{C_i}{2\pi L^2} \sqrt{\frac{E.I.g}{\lambda}} \quad \text{cps}$$

where

Mode of Vibration	1	2	3	4	5	6
Value of C_i	3.515	22.04	61.7	120.9	200	298.6
Value of f_i in cps	4.77	28.6	81.8	164.2	272	408

(2) Theoretical Solution (approximate) for the Beam with an End Load W

$$f_1 = \frac{\sqrt{3}}{2\pi L^2} \sqrt{\frac{E.I.g.L}{\frac{33}{140} w + W}} = 3.03 \text{ cps}^{*}$$

(e) Instrument Characteristics

The operating manuals for the Recorder will be available at test location. From them, obtain the recorder characteristics

Type of System

Null Balance, Unbalance or both?
Carrier System or D.C.?
If Carrier System, what type carrier function?
If Carrier System, is it phase-sensitive?

System Characteristics

Sensitivity, maximum and minimum in term of millimeters pen deflection per micro-inch per inch strain in a single gage.

Frequency response, upper and lower limits

Noise level in equivalent strain

Imput impedance

Linear Input Region in terms of strain

Zero shift

Calibration Conditions

Type of System: Equivalent strain, equivalent bridge output, parallel resistance?

Transducer Source Impedance Limits: explanation

Range Extenders: use and manipulation

Zero-Suppression: use and manipulation

Gage Factor Dial: use and interpretation

Circuit

Bridge or Potentiometric

Supply Voltage

Initial Balancing Means Available and Their Range

General Comments Which May be of Interest

Types of Transducers Accommodated

Anything Else Which Seems Appropriate

Note

If all these characteristics are not to be found in the instruction books, then either the manufacturer has published an incomplete set of characteristics, or the user desires information not really necessary. Comment on the availability of the information, its relative importance, and give a short description of the instrument.

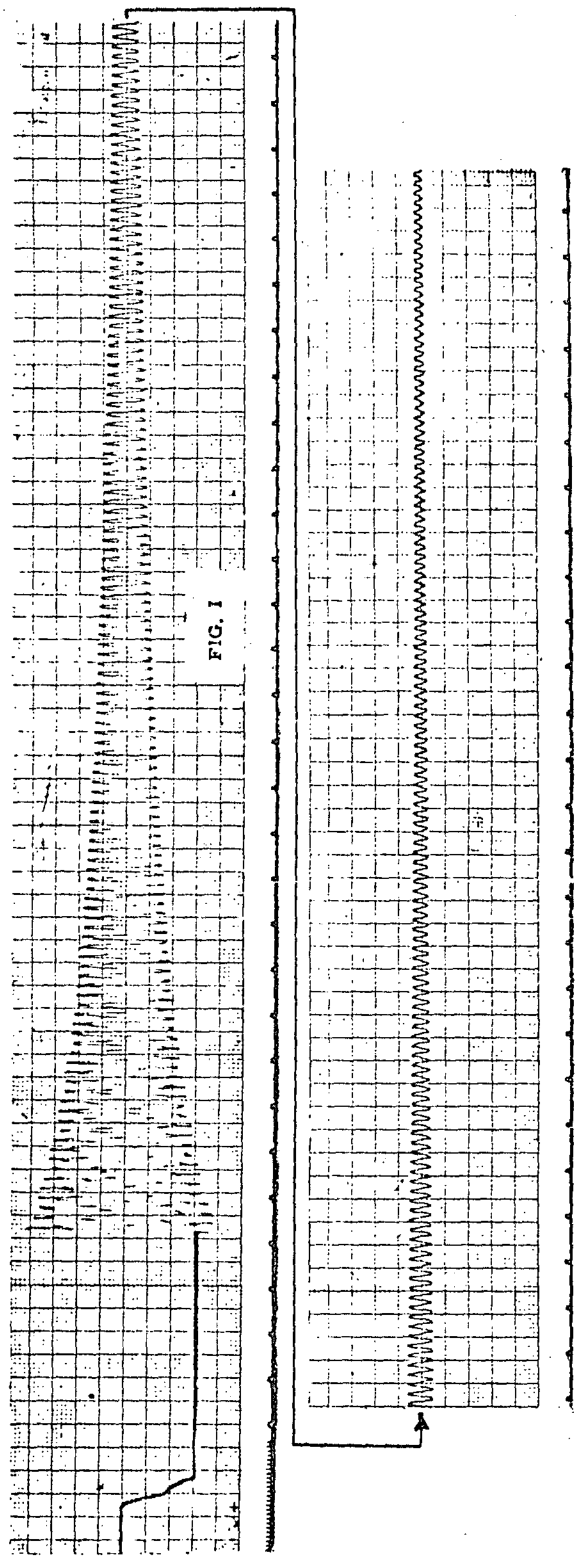

FIG. I

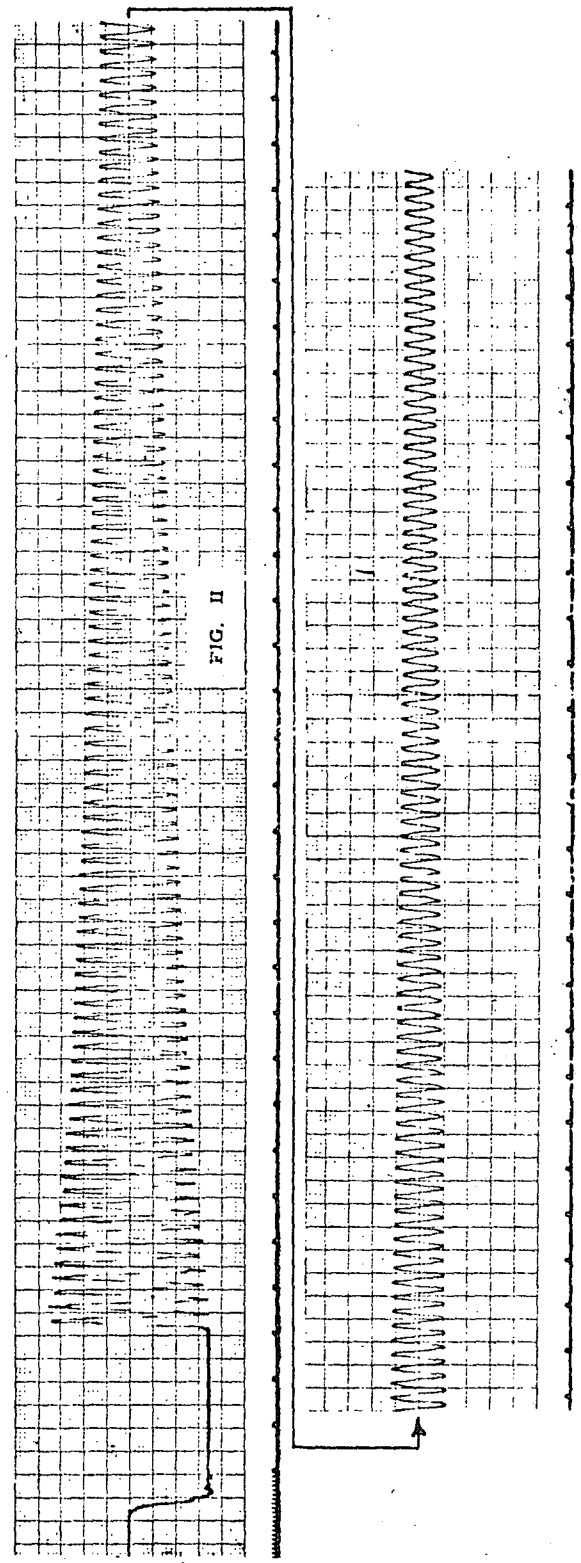

FIG. II

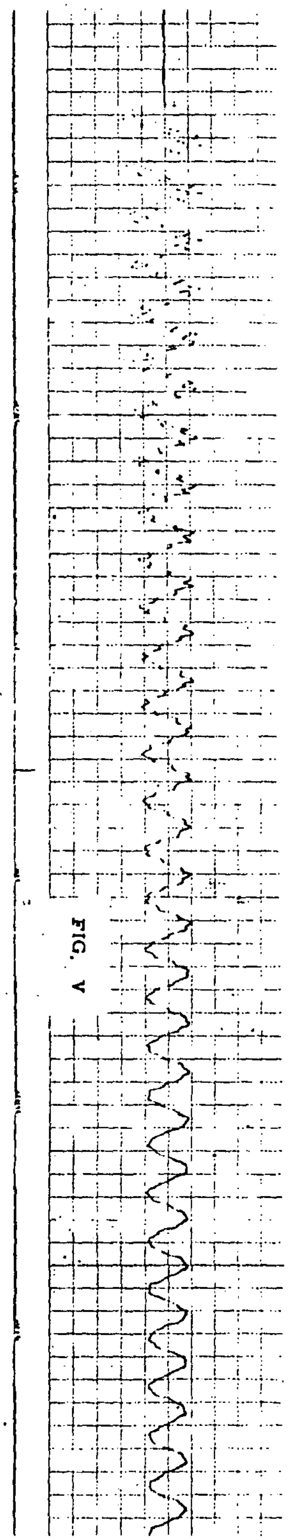

FIG. V

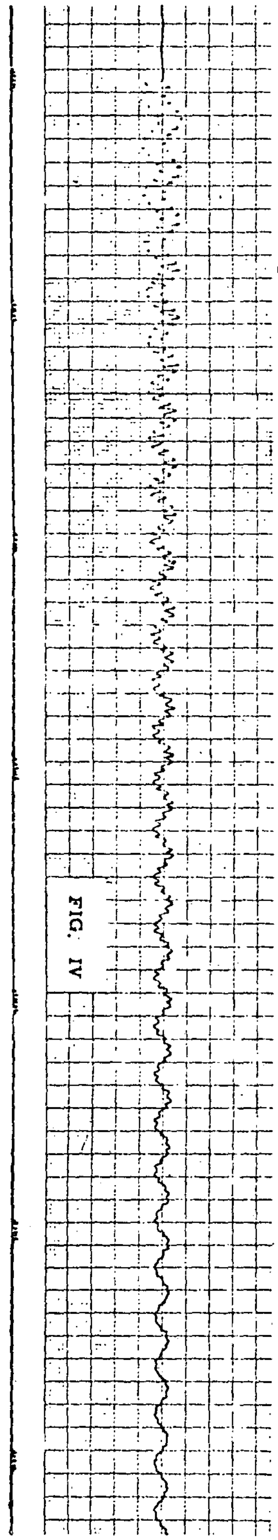

FIG. IV

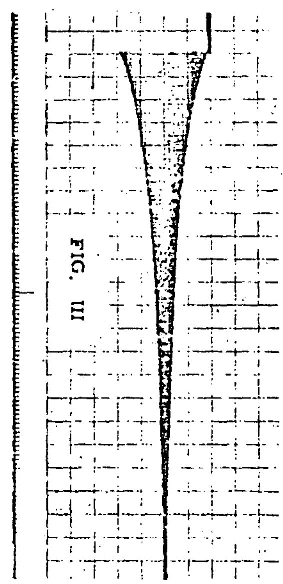

FIG. III

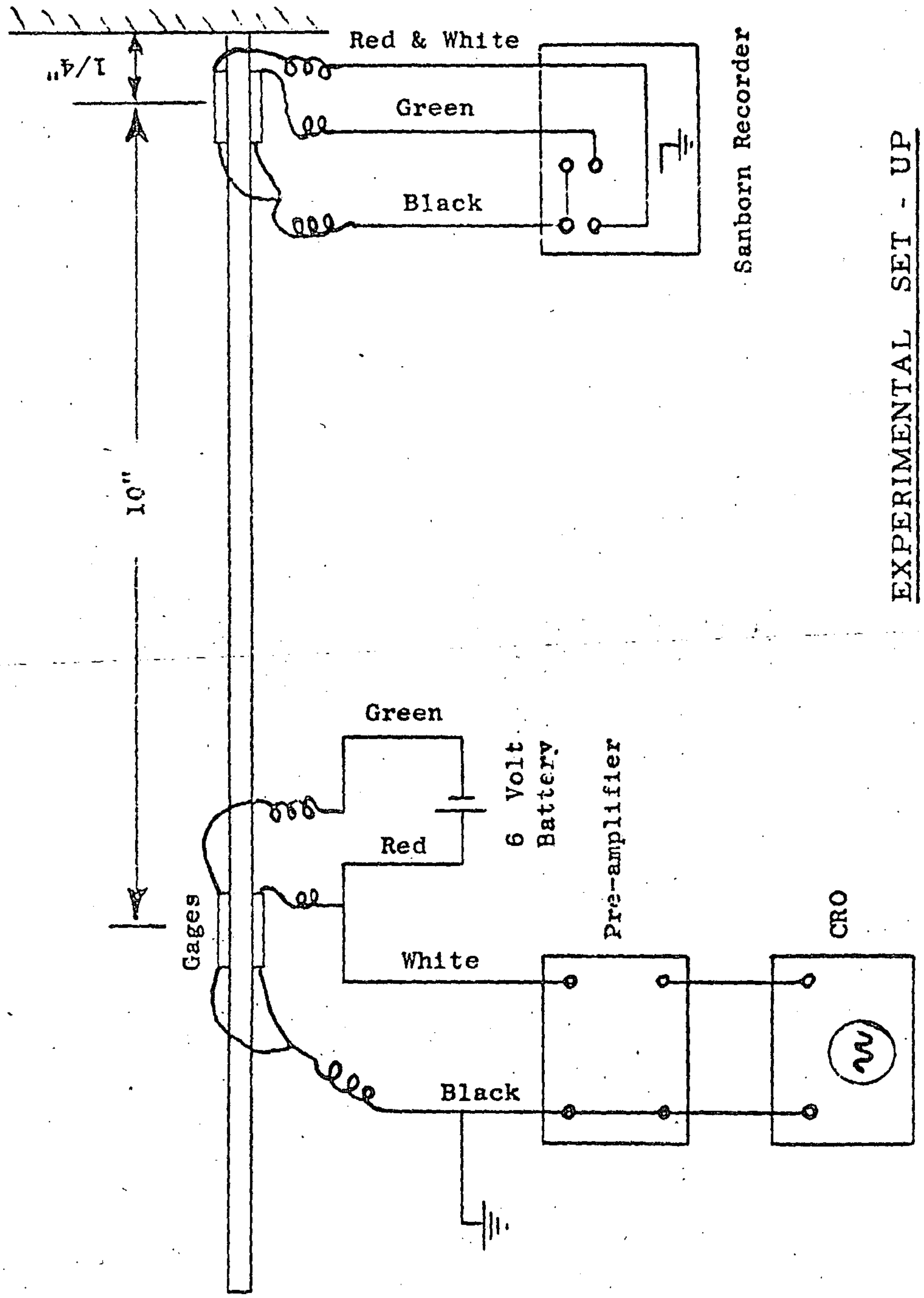

EXPERIMENTAL SET - UP

4. Transients of Short Duration --- Impact - Experiment No. 22

(a) General Remarks

The problem of impact has two major aspects:

(1) When considered as that of maximum and most efficient energy transfer from one struck body to another, such as occurs in pile drivers or air-hammers for example. The problem there is to transfer the energy from the hammer to the pile to the ground without excessive energy dissipation in the pile.

(2) When considered from the point of view of design where it is desired to determine the stress values due to impact, or optimum damping and redesign methods to lower peak stress values.

The proposition is rendered the more difficult since theoretical solutions to impact problems, although frequently available, are complex and difficult to carry to completion; furthermore, experimental methods of investigation must contend with the extremely short periods of time during which the entire phenomenon occurs. Work has been done, and is continuing, employing photoelastic techniques. Other investigators have used the electric resistance strain gage and its fore-runner, the carbon ESS strip for investigations of impact problems. References to some previous work may be found in this section.

(b) The Problem

To determine the amplitudes and the rate of repetition of a stress wave set up by the impact of two freely swinging bars; correlation between some experimentally determined quantities with some physical characteristics of the system.

(c) Experiment

Obtain a photograph of part of the initial wave and two or three subsequent reflections, using the internal trigger mechanism of the CRO.

Calibrate the screen of the CRO in terms of stress or strain along the Y-axis, and time along the X-axis.

Check the time between peaks of successive reflections determined experimentally with theoretical values calculated from the information given.

(d) Information

Test Bar

Length:	24 inches
Diameter:	1.062 inches
Radius at struck end:	very large
Radius at free end:	very large
Material:	steel
Young's Modulus:	30×10^6 psi approx.
Poisson's Ratio:	0.265
Speed of Sound in Medium:	201,800 ins/sec at room temp.
Supports:	at 2 locations by flexible strings.

Striking Bar

Length:	24 inches
Diameter:	0.627 inches
Radius at Striking End:	1.0 inches
Radius at Free End:	very large
Material:	steel
Properties:	exact props. unknown
Supports:	at 2 locations by steel rods on ball bearings as shown
Distance Dropped:	5 to 10 inches
Repeatability of Distance Dropped:	assured by an Ames Dial Gage which determines initial position to 0.001 inches

Transducer

Type:	Electric resistance bonded strain gage
Style:	Baldwin SR-4, C-8
Resistance:	515 $\pm$ 3 ohms
Gage Factor:	3.0 $\pm$ 2%
Location:	Three gages 120° apart-four from struck end of test bar, mounted axially.

Measuring Equipment

"Ellis Strain Gage Unit" used as a 2 stage amplifier
DuMont Cathode Ray Oscilloscope Type 304-H long persistance screen
Polaroid Camera Attachment for CRO.

Characteristic of interest for these instruments may be obtained from the instruction booklets available at the test location.

Strain Gage Circuit

Type:	Potentiometric
Ballast Resistor	7,500 ohm wire-wound precision non-inductive resistors.
Gage Resistance:	3 series gages - 515 ohms ea.
Supply Volgage:	3 series adding 45-volt dry cells.

Strain Calibration

Type:	Apparent strain
Method:	Entire System
Calibration Resistor:	5 Megohms rated. To be accurately measured on a Wheatstone Bridge provided.
Switch	60 cycle buzzer contactor

Time Axis Calibration

Method:	See next few pages.
Type:	Using an oscillator as standard

Velocity Determination of Dropping Bar

Type:	Experimental and/or theoretical
Methods:	See next pages
Phototube:	RCA 934
Series Resistor:	10 Megohm precision resistor
Supply Voltage:	2 series adding 45 v. dry cells
Light Source:	6 - volt automobile headlight No. 1503 with lens system
Width of test strip:	0.75 inches.

(e) Calibration of CRO Screen X-Axis in Terms of Time

Method

One simple method of calibrating the X-axis of the CRO screen in terms of time is to apply a sinusoidal signal of known frequency to the Y-input Terminals of the CRO.

The distance between peaks along the X-axis of the CRO screen corresponds to a time interval of 1/(frequency of input signal) in seconds. The screen may thus be calibrated in terms of second per inch along its X-axis.

It is to be noted that the frequency-adjustment dials on the CRO must not be touched between the experiment itself and the calibration of the screen!

(f) Determination of the Striking Velocity of the Impinging Bar

Theoretical

The striking velocity of the impinging bar is given by: $V = \sqrt{2.g.h}$, where h is the height of drop of the bar and g is gravity acceleration.

Experimental

The experimental method available involves the mounting of a strip of known width near the striking end of the bar. As a bar drops, a photocell arrangement is interrupted by the strip. An oscillographic record of the time of passage of the test strip through the photocell arrangement, coupled with the known width of the strip permits calculation of the velocity of the bar at the photocell location. The photocell must therefore be located such that the test strip passes through it only an instant before impact occurs.

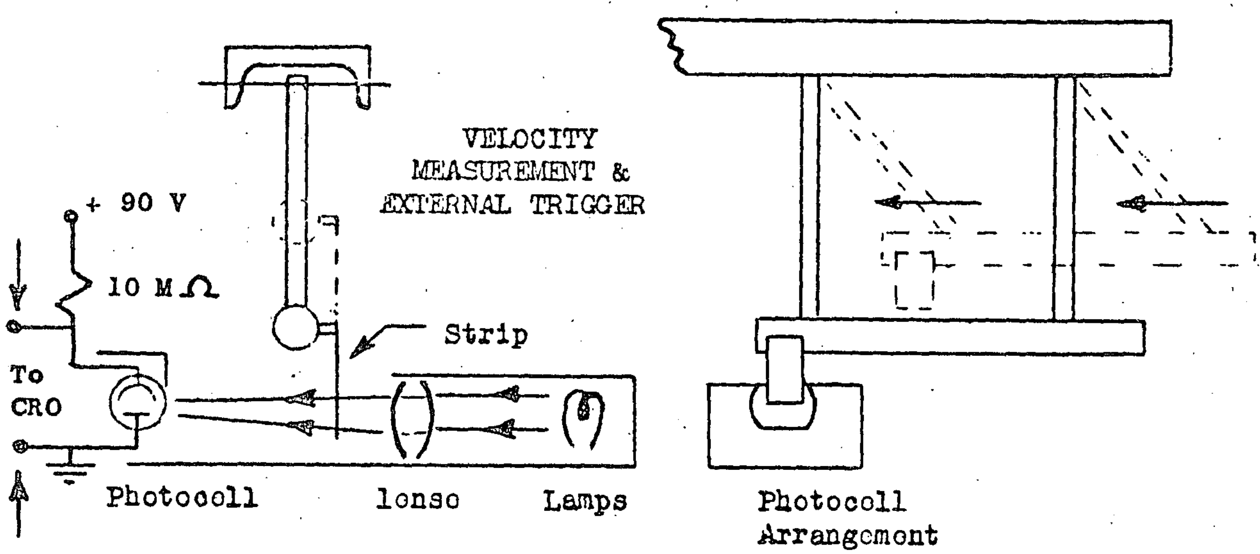

(g) Triggering the CRO

With an open-shutter camera attached to the CRO, it becomes necessary to trigger the CRO beam at an instant such that the part of the wave to be photographed appears on the screen.

Several such triggering devices exist, three of which will be mentioned here:

(1) Internal Trigger Mechanism of the CRO

The DuMont 304-H possesses an internal triggering mechanism which is actuated by the incoming signal to be measured. As soon as that signal reaches a predetermined amplitude (adjustable on the SYNCH control), the beam commences one traverse of the screen, displaying during that time, whatever phenomenon is applied to the input terminals. Since the time of traverse of the beam across the screen is variable (by means of the FREQUENCY controls), this trigger is convenient on occasion. It possesses one drawback, however, and that is the following: there is a time delay between the instant the desired signal arrives at the CRO and the instant the beam commences its traverse of the screen. Usually, this delay of some 30 micro-seconds is not serious. In this case, however, 20 micro-seconds corresponds to almost one-half of the first compressive wave which travels past the gage locations. The photographs on the following pages show this fact. Hence, if it is desired to obtain only the latter half of the first wave, and several of the subsequently reflected waves, this method is quite adequate.

(2) External Triggering Mechanism

If the complete first wave is desired, a mechanism must be found which emits an electrical signal at some short, adjustable time prior to impact. This signal enters the CRO at the EXTERNAL SYNCH binding post and starts the beam on its traverse.

a) One simple method is to use the instant of impact itself to trigger the CRO. Active terminals may be connected one each to each bar. At the moment of impact, the bars make contact, and the resulting electrical signal may be used to trigger the CRO. The duration of that trigger will be the time of contact between the bars. This method, however, does not give an adjustable trigger in terms of time.

b) Another method available here is the photocell arrangement. Instead of using it for velocity measurement, the electrical signal emitted by the photocell circuit may be used to trigger the CRO. By appropriate placement of the photocell, a controllable amount of time elapses between CRO triggering and time of impact. Thus the initial wave may be photographed. The only drawback here is that a second trigger signal is emitted when the beam bounces back from impact.

EXPERIMENTAL
SET - UP

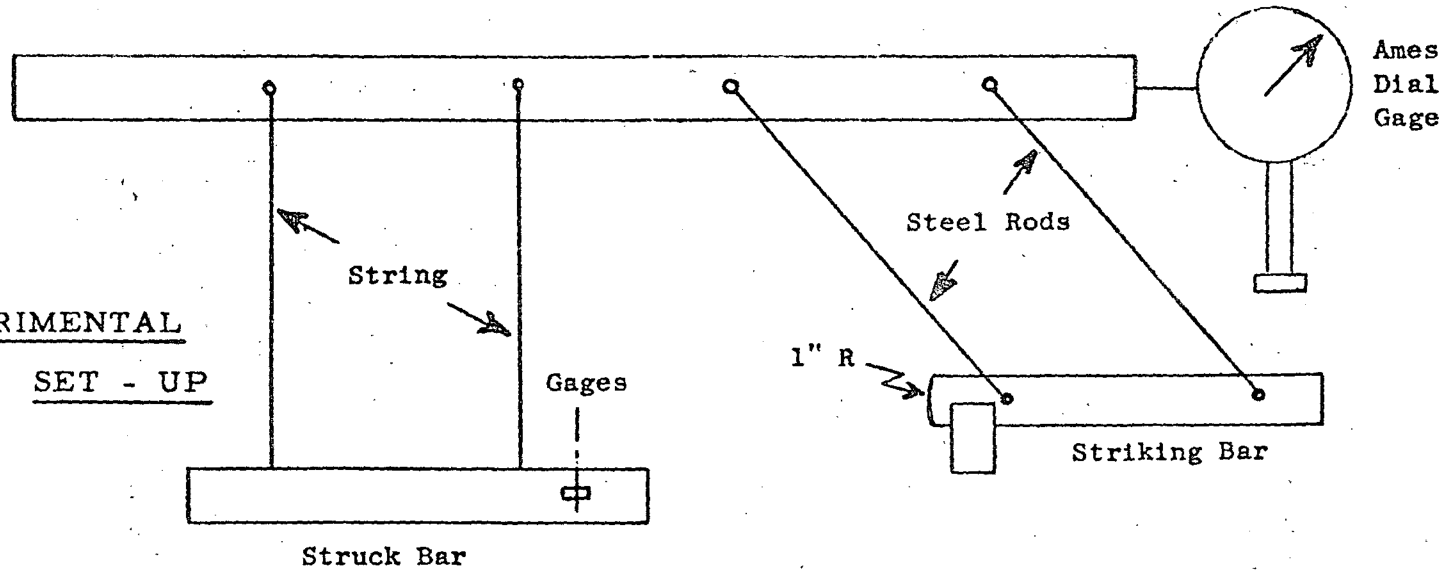

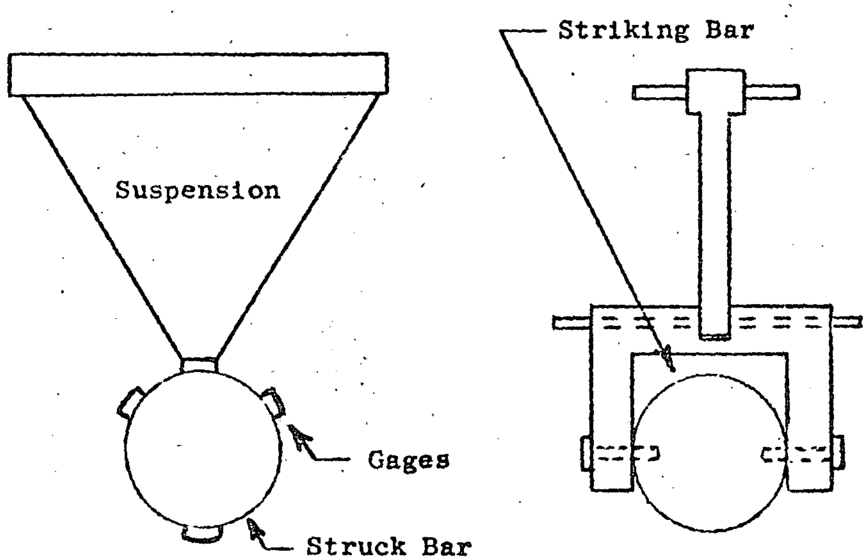

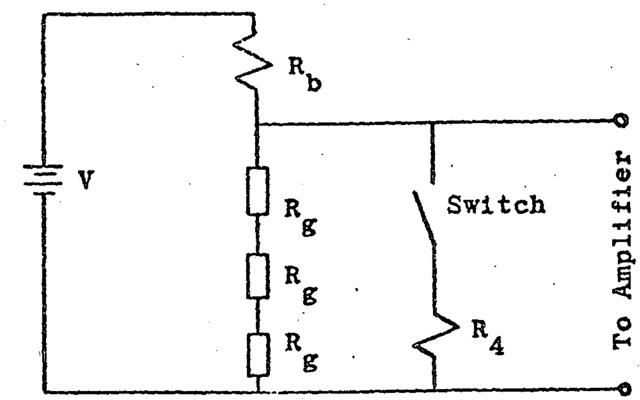

Circuit

(h) Qualitative Study of the Impact Phenomenon

Impact studies are complex even in the simplest theoretical cases. It is possible, however, with some imagination and physical reasoning, to study the phenomena qualitatively.

When impact occurs between two horizontally moving bars, stress waves are set up in both bars at the point of contact. These stress waves travel along the respective bars, much like a worm crawling along the ground. The velocity of propagation of these waves is equal to the velocity of sound in the medium in which they travel.

Referring to the diagrams on the following pages, the sequence of events may roughly be described as follows:

(1) Impact occurs sending compressive stress waves down both bars. When each wave reaches the end of its bar, it is reflected according to the boundary conditions existing at that end in the bar. Since the boundary conditions in this problem are "free-free bars," hence zero-stress at the free ends, the compressive wave arriving at such a termination is reflected as a tensile wave. Hence after the first reflected wave in the struck bar has passed the gage location, zero stress exists beneath the gage, (Refer to Nos. on the following pages). Furthermore, the two bars exhibit slightly different properties, such that the two waves travelling in the bars do not do so at the same velocity, the reflected wave in the struck bar reaching the point of contact slightly before the corresponding wave in the striking bar.

(2) The condition of zero stress prevails in the struck bar after the first wave has been reflected. Since the bars are still in contact, the striking bar, (which is still under a compressive stress at the point of contact because its reflected wave has not yet reached that point), shares some of its stress with the struck bar producing a new compressive wave which travels down the struck bar (See Nos. 2 on the following pages) and a corresponding tensile wave in the striking bar.

(3) The reflected wave from the free end of the striking bar now reaches the point of contact a very short time after the phenomena in No. 2 have occurred. Its arrival leaves the end of the striking bar with a condition of tensile stress, which is shared with the struck bar, setting up a tensile wave (See No. 3) in the struck bar.

SAMPLE RESULTS

STRAIN vs. TIME AT GAGE LOCATION

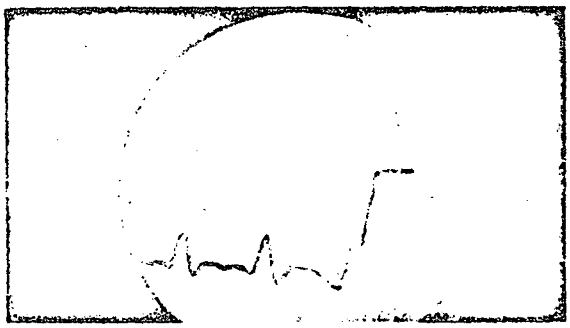

10,000 CPS TIME AXIS CALIBRATION

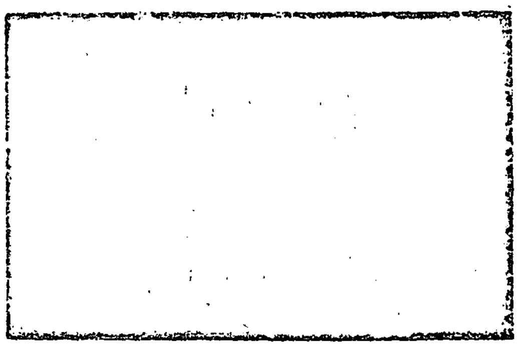

4.97 MEGHOM SHUNT RESISTOR STRAIN CALIBRATION

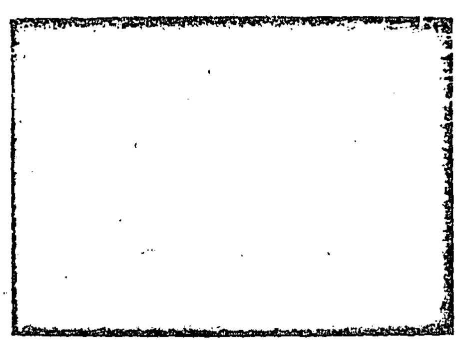

EXPERIMENTAL DATA:

R_b	7,500 ohms
R_g	three 500 ohm gages in series
V	135 volts
h	height of drop: 5.75"

COMPLETE IMPACT PHENOMENA

USING EXTERNAL PHOTOCELL TRIGGER

STRAIN WAVE	TIME BASE
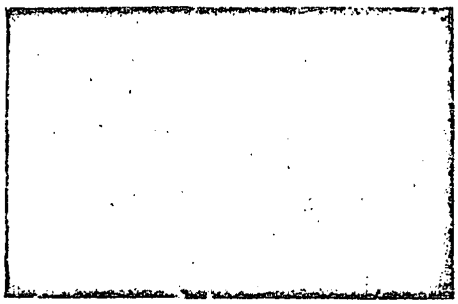	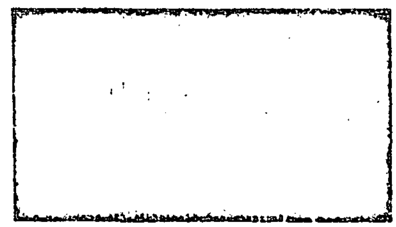 50,000 cycles/sec
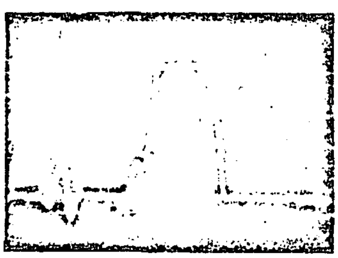	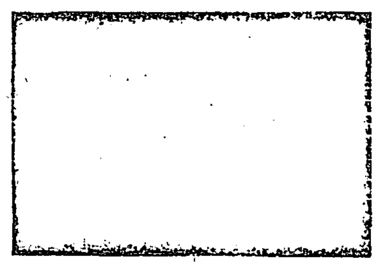 20,000 cycles/sec
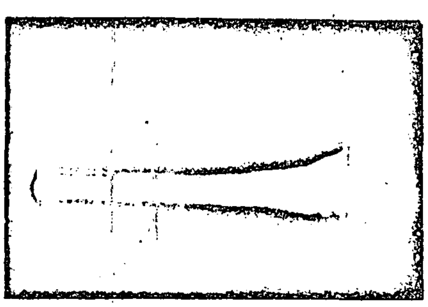	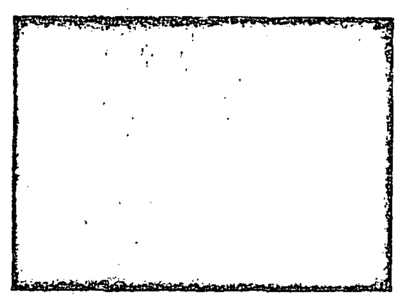 100 cycles/sec

(4) The duration of contact is over as soon as the reflected wave from the free end of the striking bar reaches the point of contact. The bars part company and a new set of boundary conditions must be satisfied: zero stress at the point which was the point of contact. In order to satisfy that new condition, a compression wave (See No. 4) starts from the ex-point-of-contact in the struck bar, leaving behind it a state of zero stress in the bar.

(5) Three separate waves are now left bouncing back and forth in the struck bar. They arose under conditions Nos. 2, 3 and 4, and they have different stress amplitudes and are delayed relative to one another in time. This triplet gives rise to successively smaller pulse shapes which are reflected from the free ends of the bars until they are completely dissipated and the struck bar is again in a condition of rest.

The next page shows these steps in terms of stress along the bar. The page following shows the stress vs. time relationship corresponding to that at the gage location. The actual phenomenon in the bar will not exhibit sharp square edges as a simple theory might predict, and the rounding-off effect is shown. It will be noted that this roughly predicted curve shape corresponds in general to the one actually obtained.

It is to be noted that the distance between successive peaks in the reflected waves after impact, should correspond to the amount of time it takes a wave travelling with the speed of sound in steel to travel twice the total length of the bar.

Further more, the duration of the initial wave is:

$$\frac{2 \times (\text{distance from the gage location to the free end of the bar})}{\text{speed of sound in the bar material}}$$

Thus an experimental check can be made with theoretically calculated values.

STRESS ALONG BARS DURING CONTACT TIME

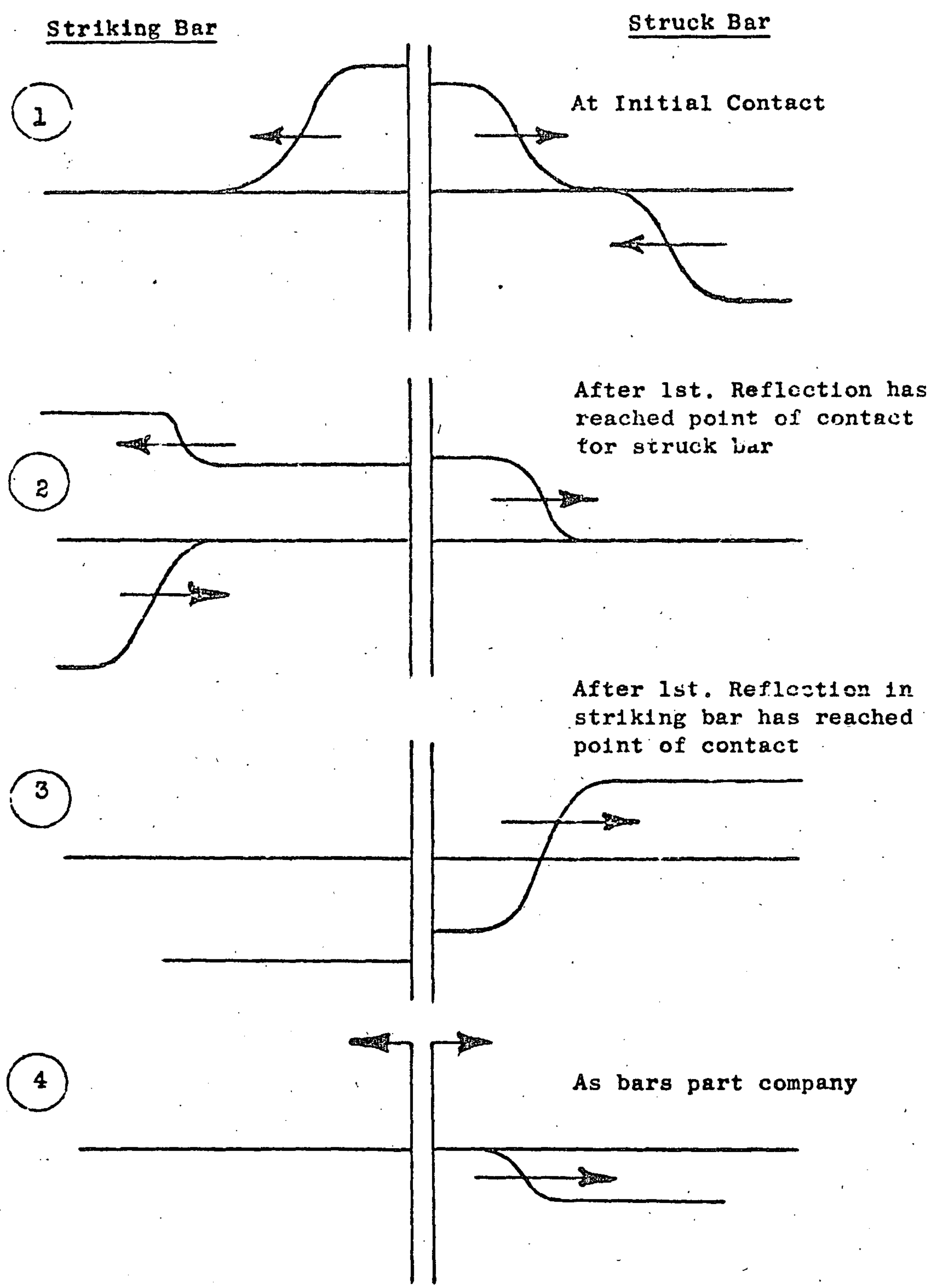

EXPECTED AND ACTUAL STRAIN - TIME PLOTS
AT THE GAGE LOCATION
(Qualitatively)

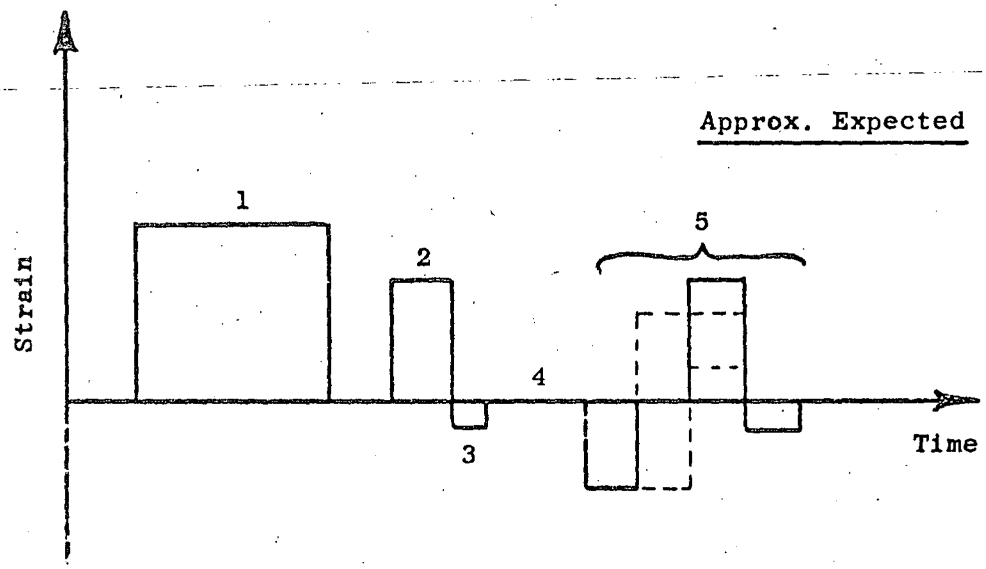

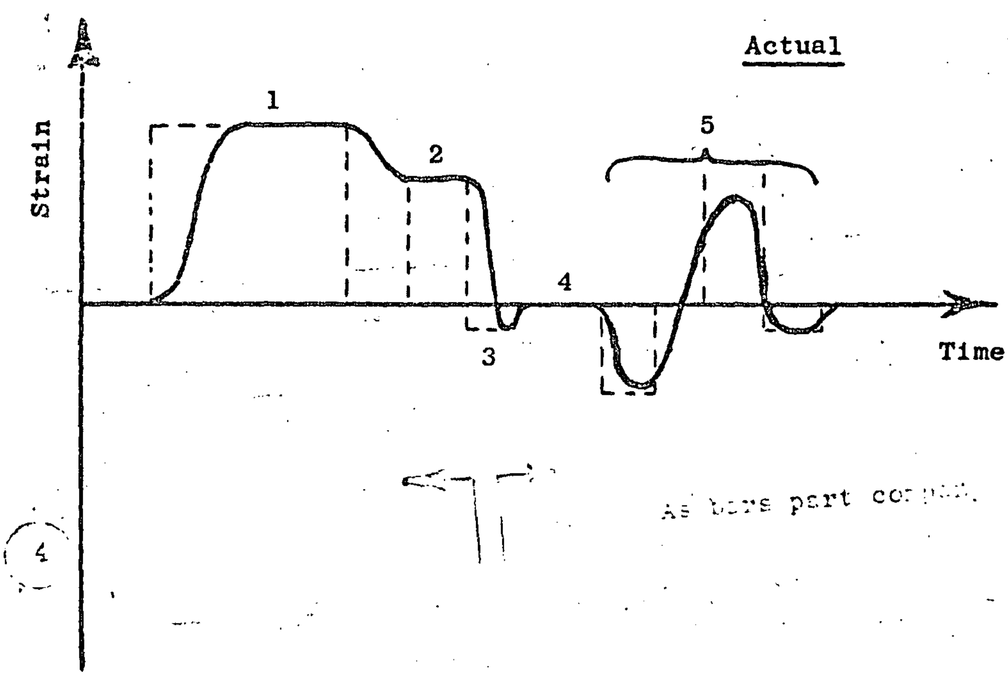

REFERENCES

1. Operation of Equipment:

Instruction books available at test locations

2. Traveling Waves in Impact:

Timoshenko, "Theory of Elasticity," Chapter XII

Timoshenko & Goodier, "Theory of Elasticity," Chapter XV

3. Experimental Investigations of Impact Problems:

R. N. Arnold, "Impact Stresses in a Freely Supported Beam," Proceedings of the Institute of Mechanical Engineers, Vol. 137, 1937, p. 217

D. K. Felbeck, "A Longitudinal Impact Testing Apparatus," Pre-publication report, 1953. (Available at test location)

4. Investigation of High Speed Mechanical Transients:

P. H. McDonald, M. A. Koontz, and H. S. Reichard, Department of Engineering Research North Carolina State College Bulletin No. 63, March, 1957

5. Recorder Survey: Recording Surfaces and Marking Methods:

G. Keinath, National Bureau of Standards Circular No. 601, September 1, 1959. Available from Superintendent of Documents, U. S. Government Printing Office, Washington 25, D. C. (Price 30 cents)

centro de educación continua
división de estudios superiores
facultad de ingeniería, unam

ANALISIS EXPERIMENTAL DE ESFUERZOS

ANALISIS DIMENSIONAL

NOVIEMBRE 1978.

CHAPTER 12

DIMENSIONAL ANALYSIS

12.1. Introduction. This chapter can be developed in an autonomous way without using the methods of analysis introduced in the theory of elasticity. It is also true that, although dimensional analysis will help in a better understanding of some problems in theory of elasticity, the latter can be completely developed without using any of the dimensional-analysis approaches. As a matter of fact, the organized approach to dimensional analysis is very recent, whereas the theory of elasticity is an old science. In stress analysis, the main application of dimensional analysis will be found in the design of models.

A knowledge of dimensional analysis is necessary for the proper design of models and the correct interpretation of the test results obtained from them.

12.2. Dimensions of Physical Quantities. In mechanics, the fundamental dimensions are usually taken as mass, length, and time, denoted, respectively, by M, L, and T. The dimensions of other physical quantities follow from their definitions or from physical laws. For example, the dimension of velocity, LT^{-1}, follows from its definition, quotient of length by time. Acceleration is defined as the quotient of velocity by time and has the dimension LT^{-2}. From Newton's law, force equals the product of mass and acceleration; it follows that force has the dimension MLT^{-2}. The dimensions of various physical quantities commonly encountered in mechanics are given in Table 12.1. Note that strain, angle, and Poisson's ratio are dimensionless.

12.3. Dimensionless Products. Given the five variables, length l, area A, strain ϵ, force F, and modulus of elasticity E, it may be observed that there are an infinite number of products of powers of these five variables. Examples are $\mu_1 = l^2A^3F^2E$, $\mu_2 = A^2\epsilon^{\frac{1}{2}}$, $\mu_3 = Al^{-2}$, $\mu_4 = F^{-1}EA$. Here the exponents may be either an integer or a fraction, and positive, zero, or negative. The dimensions of products of powers are calculated by replacing each variable by its corresponding dimensions and computing the resulting exponents of M, L, and T. Thus we replace l by $[L]$, A by $[L]^2$, ϵ by $[1]$, F by $[MLT^{-2}]$, E by $[ML^{-1}T^{-2}]$ and obtain

$(L^T$

TABLE 12.1. DIMENSIONS OF ENTITIES

Length, l	$[L]$
Area, A	$[L^2]$
Volume, V	$[L^3]$
Time, t	$[T]$
Force, F, P	$[MLT^{-2}]$
Mass, m	$[M]$
Specific weight, γ	$[ML^{-2}T^{-2}]$
Mass density, ρ	$[ML^{-3}]$
Angle, θ, ϕ, etc.	$[1]$
Pressure and stress, p, σ	$[ML^{-1}T^{-2}]$
Velocity, v	$[LT^{-1}]$
Acceleration, a	$[LT^{-2}]$
Angular velocity, ω	$[T^{-1}]$
Angular acceleration, α	$[T^{-2}]$
Energy, work, T, W	$[ML^2T^{-2}]$
Momentum, $\mathfrak{M}$	$[MLT^{-1}]$
Power, P	$[ML^2T^{-3}]$
Moment of a force, M	$[ML^2T^{-2}]$
Moment of inertia of an area, I	$[L^4]$
Moment of inertia of a mass, I	$[ML^2]$
Modulus of elasticity, E	$[ML^{-1}T^{-2}]$
Strain, ϵ	$[1]$
Poisson's ratio, ν	$[1]$

$$\text{Dimension of } \mu_1 = [L]^2[L^2]^3[MLT^{-2}]^2[ML^{-1}T^{-2}] = [M^3L^0T^{-6}]$$

$$\text{Dimension of } \mu_2 = [L^2]^2[1^2]^{\frac{1}{2}} = [L^4]$$

$$\text{Dimension of } \mu_3 = [L^2][L]^{-2} = 1$$

$$\text{Dimension of } \mu_4 = [MLT^{-2}]^{-1}[ML^{-1}T^{-2}][L^2] = 1$$

In general, the dimensions of a product of powers

$$\mu = l^{k_1}A^{k_2}\epsilon^{k_3}F^{k_4}E^{k_5}$$

will be

$$[L]^{k_1}[L^2]^{k_2}[1]^{k_3}[MLT^{-2}]^{k_4}[ML^{-1}T^{-2}]^{k_5}$$

or

$$[M]^{k_4+k_5}[L]^{k_1+2k_2+k_4-k_5}[T]^{-2k_4-2k_5}$$

Products of powers like μ_3 and μ_4, whose exponents of M, L, and T all vanish, are called dimensionless products of powers. Evidently the product μ will be dimensionless if and only if the exponents k_1, k_2, k_3, k_4, and k_5 satisfy all three of the following equations:

$$\begin{aligned} k_4 + k_5 &= 0 \\ k_1 + 2k_2 + k_4 - k_5 &= 0 \\ -2k_4 - 2k_5 &= 0 \end{aligned} \qquad (12.1)$$

There are an infinite number of combinations of the exponents k_1, k_2, k_3, k_4, and k_5 which satisfy the above condition so that the number of dimensionless products of powers which can be formed out of the five variables l, A, ϵ, F, and E is infinite. Examples are $\pi_1 = Al^{-2}$, $\pi_2 = F^{-1}El^2$, $\pi_3 = F^{-1}EA$, $\pi_4 = A^2l^{-4}$, and $\pi_5 = \epsilon^{-1}$. Here π denotes a dimensionless product of powers and has no connection whatsoever with the value 3.1416. In this chapter, μ will denote a product of powers of variables, whether dimensionless or not. The use of π will be reserved to designate a dimensionless product of powers of variables, and the shortened term *dimensionless product* will be used for this.

Forming some products of powers of the dimensionless products, it can be noticed that

$$\pi_3 = \pi_1\pi_2$$
$$\pi_4 = \pi_1^2$$

so that π_3 and π_4 can be expressed as products of powers of π_1 and π_2. This suggests the following definition:

A set of *independent* dimensionless products of given variables is one in which none of these products can be expressed as a product of powers of other dimensionless products in the set. Here again, the exponents of the powers may be integers or fractions, positive, zero, or negative.

For example, π_1 and π_2 form a set of independent dimensionless products, π_2 and π_3 form another set of independent dimensionless products, π_2, π_3, and π_5 form still another set of independent dimensionless products, and many more sets of independent dimensionless products can be formed out of the infinite number of dimensionless products. Evidently if, in a set of dimensionless products, only one of them contains a particular variable, then this dimensionless product will be an independent one. The simplest way to construct a set of independent dimensionless products is therefore to make one variable appear exclusively in one dimensionless product, another variable to appear exclusively in another dimensionless product, etc.

For example, in the set of independent dimensionless products composed of π_1, π_3, and π_5, l appears exclusively in π_1, F appears exclusively in π_3, and ϵ appears exclusively in π_5.

12.4. Matrices and Determinants. Dimensional analysis is based on a theorem demonstrated first by Buckingham and known sometimes as the *π theorem.* To understand this theorem, some knowledge is required of the elementary properties of matrices. These will be given below.

A rectangular array of numbers is called a matrix. If the number of columns equals the number of rows, the matrix is called a square matrix, of order n. If there are n rows and m columns ($n \neq m$), the matrix is said to be of order $n \times m$. Associated with every square matrix of order n is a number called the determinant of order n. The determinants obtained after crossing out certain rows or columns or both from a matrix are called the "determinants of the matrix." Tables 12.2 and 12.3 give an example of a matrix and one of its third-order determinants

TABLE 12.2. EXAMPLE OF A MATRIX

a_1	a_2	a_3	a_4
b_1	b_2	b_3	b_4
c_1	c_2	c_3	c_4

TABLE 12.3. A THIRD-ORDER DETERMINANT OF THE MATRIX OF TABLE 12.2

$$\begin{vmatrix} a_1 & a_3 & a_4 \\ b_1 & b_3 & b_4 \\ c_1 & c_3 & c_4 \end{vmatrix}$$

Determinants can be evaluated by the methods commonly used in algebra. For example, the value of the determinant of Table 12.3 is $a_1b_3c_4 + a_3b_4c_1 + a_4b_1c_3 - a_1b_4c_3 - a_3b_1c_4 - a_4b_3c_1$. It occasionally happens that all determinants above a certain order taken from a matrix have the value zero. The following definition is employed in algebra:

If a matrix contains a nonzero determinant of order r, and if all determinants of order greater than r that the matrix contains have the value zero, the rank of the matrix is said to be r.

12.5. Complete Set of Dimensionless Products. The concept of a complete set of dimensionless products is essential in dimensional analysis. The following is the definition of a complete set of dimensionless products:

A set of dimensionless products of given variables is *complete* if each product in the set is independent of the others in the set, and every dimensionless product of the variables is a product of powers of dimensionless products in the set. In other words, a complete set of dimensionless products is a set of independent dimensionless products with the additional property that every possible dimensionless product of the variables may be expressed as a product of powers of the dimensionless products in the set. For example, π_1 and π_2 have been shown to be independent of each other and form a set of independent dimensionless products. Also, π_3 and π_4 have been shown to be expressible as products of powers of π_1 and π_2. Now if it can be shown furthermore that any dimensionless product $\pi = l^{k_1}A^{k_2}\epsilon^{k_3}F^{k_4}E^{k_5}$ is expressible as a product of powers of π_1 and π_2, then π_1 and π_2 will form a complete set. Similarly π_2 and π_3 will form a complete set if they meet the above conditions for a complete set.

After dealing with the previous example the general case will be discussed next. Let us consider the n variables whose dimensions are given in Table 12.4. The rectangular array of numbers a_i, b_i, giving the

TABLE 12.4. A DIMENSIONAL MATRIX

	x_1	x_2	$\cdots$	x_n
M	a_1	a_2	$\cdots$	a_n
L	b_1	b_2	$\cdots$	b_n
T	c_1	c_2	$\cdots$	c_n

dimensions of the variables $x_1, x_2, \ldots, x_n$ corresponding to the fundamental units in the first column is called the dimensional matrix of these variables. Evidently the product $x_1^{k_1}x_2^{k_2}\cdots x_n^{k_n}$ will be dimensionless if and only if the exponents $k_1, k_2, \ldots, k_n$ satisfy all three of the following equations:

$$\begin{aligned} a_1k_1 + a_2k_2 + \cdots + a_nk_n &= 0 \\ b_1k_1 + b_2k_2 + \cdots + b_nk_n &= 0 \\ c_1k_1 + c_2k_2 + \cdots + c_nk_n &= 0 \end{aligned} \tag{12.2}$$

By the theory of algebra it can be shown† that (1) Eqs. (12.2) possess exactly $n - r$ linearly independent solutions in which r is the rank of the dimensional matrix given in Table 12.4 and (2) any solution $(k_1, k_2, \cdots, k_n)$ is a linear combination of these $n - r$ linearly independent solutions. Since each solution $(k_1, k_2, \cdots, k_n)$ represents a dimensionless product, property (1) is equivalent to stating that these $n - r$ dimensionless products are independent of each other and property (2) is equivalent to stating that all other dimensionless products may be expressed as a product of powers of these $n - r$ dimensionless products. Hence the following important theorem on dimensional analysis:

The number of dimensionless products in a complete set is equal to the total number of variables minus the rank of their dimensional matrix.

It should be pointed out that there is an infinite number of complete sets. By accumulating any $n - r$ independent dimensionless products, a complete set is obtained.

Returning to the example given earlier in this chapter, we have the five variables l, A, ϵ, F, and E. Their dimensions are given in Table 12.5.

TABLE 12.5. THE DIMENSIONAL MATRIX OF THE FIVE VARIABLES l, A, ϵ, F, AND E

	l	A	ϵ	F	E
M	0	0	0	1	1
L	1	2	0	1	−1
T	0	0	0	−2	−2

†See any standard text on theory of equations, for instance, L. W. Griffiths, "Introduction to the Theory of Equations," chap. 7, John Wiley & Sons, Inc., New York, 1947.

It can be shown by evaluation that all determinants of the third order taken from the matrix of Table 12.5 are zero and at least one of the second-order determinants is not zero. Therefore the rank of the dimensional matrix is 2. Hence there are only 5 − 2, or 3, dimensionless products in the complete set. Accordingly, $\pi_1 = Al^{-2}$, $\pi_2 = F^{-1}El^2$, $\pi_3 = \epsilon^{-1}$ constitutes a complete set of dimensionless products of the variables l, A, ϵ, F, and E. It should be noted that any three independent dimensionless products here will form a complete set.

12.6. Dimensional Homogeneity. An equation will be said to be dimensionally homogeneous if the form of the equation does not depend on the units of measurement. For example, the equation of the falling body ($h = \frac{1}{2}gt^2$) is valid whether length is measured in feet, meters, or inches and whether time is measured in hours, years, or seconds, provided g is measured in the same units of length and time as h and t. Therefore, by definition, the equation is dimensionally homogeneous. If the value $g = 32.2$ ft/sec^2 is substituted in the equation, there results $h = 16.1t^2$. This equation applies only if length is measured in feet and time is measured in seconds and is not dimensionally homogeneous.

The application of dimensional analysis to physical problems is based on the hypothesis that the solution of physical problems is always expressible by means of a dimensionally homogeneous equation in terms of specified variables. This hypothesis is justified by the fact that the fundamental equations of mechanics are dimensionally homogeneous and that relationships that may be deduced from these equations are consequently dimensionally homogeneous.

We quote, without proof, a fundamental theorem on dimensional analysis called Buckingham's theorem:†

If an equation is dimensionally homogeneous, it can be reduced to a relationship among a complete set of dimensionless products.

12.7. Elastic Structures Statically Loaded. All the above applies to any physical phenomenon. In the following, an application will be developed to the case of statically loaded elastic structures. The material of the structure can be completely defined by the modulus of elasticity E and Poisson's ratio ν as shown in the chapter on the theory of elasticity. The geometry of the structure can be defined by one length l and the ratios $r_1, r_1', r_1'', \ldots$ of all other lengths to l. The loads can be divided into five categories.

1. Concentrated loads acting on a point can be specified by one of them, P, and the ratios $r_2, r_2', r_2'', \ldots$ of the others to P. P will have the dimension of a force.

†For the proof of this theorem, see Henry L. Langhaar, "Dimensional Analysis and Theory of Models," chap. 4, John Wiley & Sons, Inc., New York, 1951.

2. Loads distributed on a line can be specified by one of them, Q, and the ratios $r_3, r_3', r_3'', \ldots$ of all others to Q. Q will have the dimension of a force per unit length.

3. Loads distributed on a surface can be specified by one of them, R, and the ratios $r_4, r_4', r_4'', \ldots$ of all others to R. R will have the dimension of a force per unit area.

4. Loads distributed in a volume can be specified by one of them, S, and the ratios $r_5, r_5', r_5'', \ldots$ of all others to S. S will have the dimension of a force per unit volume. Body forces such as the dead weight of structures and seismic loads belong to this category.

5. Prescribed boundary displacements can be specified by one of them, U, and the ratios $r_6, r_6', r_6'', \ldots$ of all others to U. U will have the dimension of a length.

The directions of the loads can be specified by $\theta, \theta', \theta'', \ldots$. The formula for the stress at a point whose coordinates are x, y, z, will be

$$\sigma = f_1(x,y,z,E,\nu;l,r_1,r_1',\cdots;P,r_2,r_2',\cdots;Q,r_3,r_3'\cdots;R,r_4,r_4',\cdots; S,r_5,r_5',\cdots;U,r_6,r_6',\cdots;\theta,\theta',\theta'',\cdots) \tag{12.3}$$

assuming isotropy and homogeneity and Hooke's law. The dimensional matrix of the above variables is

TABLE 12.6. DIMENSIONAL MATRIX OF VARIABLES OF ELASTIC STRUCTURES

	σ	x	y	z	E	ν	l	P	Q	R	S	U
M	1	0	0	0	1	0	0	1	1	1	1	0
L	−1	1	1	1	−1	0	1	1	0	−1	−2	1
T	−2	0	0	0	−2	0	0	−2	−2	−2	−2	0

r_1	r_1'	...	r_2	r_2'	...	r_3	r_3'	...	r_4	r_4'	...	r_5	r_5'	...	r_6	r_6'	...	θ	θ'	...
0	0	...	0	0	...	0	0	...	0	0	...	0	0	...	0	0	...	0	0	...
0	0	...	0	0	...	0	0	...	0	0	...	0	0	...	0	0	...	0	0	...
0	0	...	0	0	...	0	0	...	0	0	...	0	0	...	0	0	...	0	0	...

Since all the third-order determinants taken from the above matrix are zero, and at least one of the second-order determinants is not zero, the rank of the matrix is 2. The number of independent dimensionless products necessary to form a complete set of dimensionless products is therefore two less than the number of variables. The following constitutes a complete set of dimensionless products:

$$\frac{\sigma}{E}, \frac{x}{l}, \frac{y}{l}, \frac{z}{l}, \nu, \frac{P}{El^2}, \frac{Q}{El}, \frac{R}{E}, \frac{Sl}{E}, \frac{U}{l}, r_1, r_1', \cdots,$$

$$r_2, r_2', \cdots \quad , r_3', \cdots, r_4, r_4', \cdots, r_5, r_5', \cdots, r_6, r_6', \cdots, \theta, \theta', \cdots$$

By Buckingham's theorem, Eq. (12.3) is reducible to the following form:

$$\frac{\sigma}{E} = f_2\Big(\frac{x}{l}, \frac{y}{l}, \frac{z}{l}, \nu, \frac{P}{El^2}, \frac{Q}{El}, \frac{R}{E}, \frac{Sl}{E}, \frac{U}{l}, r_1, r_1', \cdots; r_2, r_2', \cdots; r_3, r_3', \cdots; r_4, r_4', \cdots; r_5, r_5', \cdots; r_6, r_6', \cdots; \theta, \theta', \cdots\Big) \tag{12.4}$$

In experimental stress analysis, it is often impracticable to perform tests on the real structure or prototype. In such cases, a model of the real structure is built, usually at a reduced scale and often of a different material. Tests are performed on the model, and the stresses and strains in the model are determined. The stresses and strains in the real structure can then be obtained if the relations between the stresses and strains in the model and the prototype are known. This relation can be established by dimensional analysis and will now be shown. Equation (12.4) is applied to both model and prototype. Although the form of the function f_2 is unknown, it is the same for both. If we make a model such that the numerical values of all the dimensionless products x/l, y/l, z/l, ν, . . . at the right-hand side of Eq. (12.4) are equal to those of the prototype, respectively, then the numerical value of σ/E for the model will also be equal to that of the prototype. If the subscript m is used for the model and p for the prototype, then

$$\frac{\sigma_p}{E_p} = \frac{\sigma_m}{E_m}$$

or

$$\sigma_p = \frac{E_p}{E_m}\sigma_m$$

The true stress at any point x, y, z in the prototype would then be equal to the stress at the similarly situated point in the model multiplied by the ratio between the modulus of elasticity of prototype to that of model.

Making x/l, y/l, z/l the same for both model and prototype means that the stress is to be taken at similarly situated points in the model and prototype. Making $r_1, r_1', \ldots$ the same for both model and prototype means geometric similarity for the model and prototype. Making $r_2, r_2', \ldots; r_3, r_3', \ldots; r_4, r_4', \ldots; r_5, r_5', \ldots; r_6, r_6', \ldots; \theta, \theta', \ldots$ the same means similarity of load distribution. If the stresses do depend on ν, then the model material should have the same Poisson's ratio as the prototype. Making P/El^2, Q/El, R/E, Sl/E, U/l th[illegible]me for both means

$$\frac{P_m}{P_p} = \frac{E_m}{E_p}\left(\frac{l_m}{l_p}\right)^2$$

$$\frac{Q_m}{Q_p} = \frac{E_m}{E_p}\frac{l_m}{l_p}$$

$$\frac{R_m}{R_p} = \frac{E_m}{E_p}$$

$$\frac{S_m}{S_p} = \frac{E_m}{E_p}\frac{l_p}{l_m}$$

$$\frac{U_m}{U_p} = \frac{l_m}{l_p}$$

The loads must therefore be scaled down according to these rules.

Similar analyses can be carried out for the displacement w and the strain ϵ at any point x, y, z, of the structure. Thus

$$\frac{w}{l} = f_3\left(\frac{x}{l},\frac{y}{l},\frac{z}{l},\nu,\frac{P}{El^2},\ldots\right)$$

$$\epsilon = f_4\left(\frac{x}{l},\frac{y}{l},\frac{z}{l},\nu,\frac{P}{El^2},\ldots\right)$$

For a model which has all its values of x/l, y/l, z/l, ν, P/El^2, . . . equal to that of the prototype,

$$\frac{w_m}{w_p} = \frac{l_m}{l_p}$$

$$\epsilon_m = \epsilon_p$$

The deformations have not been assumed small. The above applies to all structures made of materials obeying Hooke's law and stressed below its proportional limit. Very flexible steel springs, thin plates transversely loaded to large deflection, and other structures where the stresses, strains, displacements, and redundant reactions are in general not proportional to the loads can therefore also be analyzed by the above procedure.

12.8. Linear Structures. From the theory of elasticity, we know that, for stiff structures where the deformations do not affect the action of the loads, the stresses, strains, displacements, and redundant reactions are always linear functions of the loads. This knowledge makes the following simplification of Eq. (12.4) possible:

$$\begin{aligned}\frac{\sigma}{E} = {} & \frac{P}{El^2}\, g_1\left(\frac{x}{l},\frac{y}{l},\frac{z}{l},\nu,r_1,r_1',\ldots,r_2,r_2',\ldots,\theta,\theta',\ldots\right)\\ & + \frac{Q}{El}\, g_2\left(\frac{x}{l},\frac{y}{l},\frac{z}{l},\nu,r_1,r_1',\ldots,r_2,r_2',\ldots,\theta,\theta',\ldots\right)\\ & + \frac{R}{E}\, g_3\left(\frac{x}{l},\frac{y}{l},\frac{z}{l},\nu,r_1,r_1',\ldots,r_2,r_2',\ldots,\theta,\theta',\ldots\right)\\ & + \frac{Sl}{E}\, g_4\left(\frac{x}{l},\frac{y}{l},\frac{z}{l},\nu,r_1,r_1',\ldots,r_2,r_2',\ldots,\theta,\theta',\ldots\right)\\ & + \frac{U}{l}\, g_5\left(\frac{x}{l},\frac{y}{l},\frac{z}{l},\nu,r_1,r_1',\ldots,r_2,r_2',\ldots,\theta,\theta',\ldots\right)\end{aligned} \tag{12.5}$$

Similar expressions exist for w/l and ϵ. If we make x/l, y/l, z/l, ν, r_1, r_1', . . . , r_2, r_2', . . . , r_3, r_3', . . . , r_4, r_4', . . . , r_5, r_5', . . . , r_6, r_6', . . . , θ, θ', . . . the same for model and prototype, then

$$\frac{\sigma}{E} = C_1\frac{P}{El^2} + C_2\frac{Q}{El} + C_3\frac{R}{E} + C_4\frac{Sl}{E} + C_5\frac{U}{l}$$

where the constants C_1, C_2, . . . , C_5 are independent of the loads P, Q, R, S, U and are the same for model and prototype. By running five separate tests on the model, each test using only one among the five types of loads P, Q, R, S, U, the values of these constants C_1, C_2, . . . , C_5 can be determined for any point whose stress is required.

Similar constants for the strain ϵ and displacement w/l can be determined in the same manner. This reasoning will be applied to two concrete cases in the following examples.

Example 1. Let us consider a thick plate with a hole (Fig. 12.1), under a uniformly distributed load R_p at its two ends. Let the modulus of elasticity and Poisson's ratio of the material of the plate be E_p and ν_p, respectively. The problem is to design a model to study the stress distribution of this thick plate.

By Eq. (12.5), the stresses σ_p in the prototype at any point A_p whose coordinates are x, y, z are given by

$$\frac{\sigma_p}{E_p} = \frac{R_p}{E_p}\, g_3\left(\frac{x}{l},\frac{y}{l},\frac{z}{l},\nu,r_1,r_1',r_1''\right) \tag{12.6}$$

or

$$\sigma_p = R_p g_3\left(\frac{x}{l},\frac{y}{l},\frac{z}{l},\nu,r_1,r_1',r_1''\right)$$

Consider a model which is geometrically similar to the prototype so

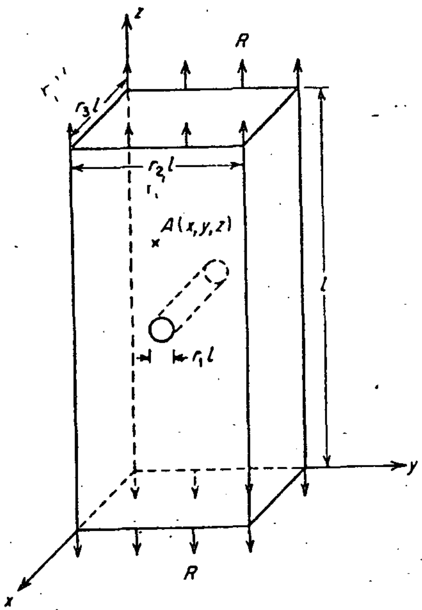

FIG. 12.1. Thick plate with a hole, under a uniformly distributed load.

that r_1, r_1', r_1'' are the same for the model and prototype. Let the model be made of a material having the same Poisson's ratio as that of the prototype. Under a uniformly distributed load R_m, the stresses in the model at a similarly situated point A_m will be given by

$$\sigma_m = R_m g_3\left(\frac{x}{l},\frac{y}{l},\frac{z}{l},\nu,r_1,r_1',r_1''\right) \tag{12.7}$$

where g_3 will have the same value as in Eq. (12.6).

Equation (12.6) is divided by Eq. (12.7) to obtain

$$\frac{\sigma_p}{\sigma_m} = \frac{R_p}{R_m} \tag{12.8}$$

The stresses in the prototype and in the geometrically similar model at similarly situated points are therefore in the same proportion as the intensity of the uniformly distributed load. The materials of the prototype and the model must have the same Poisson's ratio but not necessarily the same modulus of elasticity. The length scale factor of the model does not appear in Eq. (12.8), so that the model can be made one-tenth or five times as large as the prototype and Eq. (12.8) still holds.

If the plate is thin, from the theory of elasticity we have the additional knowledge that the plane-stress solution is applicable. This means that

for this case both the thickness of the plate and Poisson's ratio will not enter the solution for stresses. For such a prototype the model must be geometrically similar to the prototype in the direction of its width and length. It can be a thin plate of any thickness which is small compared with the diameter of the hole, made of any elastic material. The relation between the stresses in the model and the prototype will still be given by Eq. (12.8). Here again, the length scale factor of the model does not enter Eq. (12.8). The model can be half or twice the size of the prototype and Eq. (12.8) always holds.

Example 2. Let us consider a thick cylinder with an eccentric hole, loaded as shown in Fig. 12.2. By Eq. (12.5) the stresses σ_p at any point A_p whose coordinates are x, y, z are given by

$$\frac{\sigma_p}{E_p} = \frac{P_p}{E_p l_p^2}\, g_1\left(\frac{x}{l},\frac{y}{l},\frac{z}{l},\nu,r_1,r_1',r_1''\right) + \frac{R_p}{E_p}\, g_3\left(\frac{x}{l},\frac{y}{l},\frac{z}{l},\nu,r_1,r_1',r_1''\right) \tag{12.9}$$

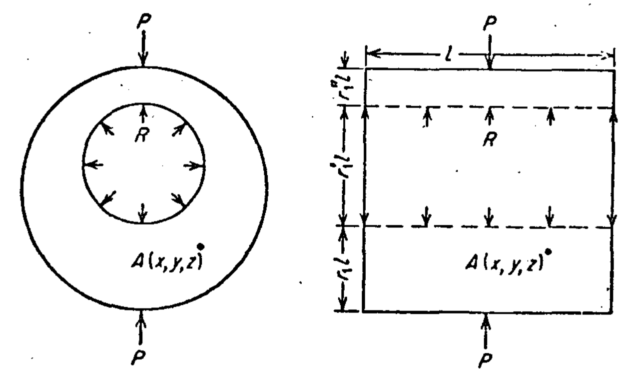

FIG. 12.2. Cylinder under internal pressure and a concentrated diametral load.

Construct a model geometrically similar to the given cylinder, and made of a material whose Poisson's ratio is the same as that of the prototype. Then, at a similarly located point A_m in the model, the stresses under similarly distributed loads P_m and R_m will be

$$\frac{\sigma_m}{E_m} = \frac{P_m}{E_m l_m^2}\, g_1\left(\frac{x}{l},\frac{y}{l},\frac{z}{l},\nu,r_1,r_1',r_1''\right) + \frac{R_m}{E_m}\, g_3\left(\frac{x}{l},\frac{y}{l},\frac{z}{l},\nu,r_1,r_1',r_1''\right) \tag{12.10}$$

where g_1 and g_3 have the same values as in Eq. (12.9).

To get σ_p from the observed σ_m in the model, either one of the two following methods can be used.

Method 1. The principle of superposition will be used. The portion of the stress $(\sigma_p)_1$ due to P_p alone will be determined separately from the portion of the stress $(\sigma_p)_2$ due to R_p alone. Then the true stress σ_p due to P_p and R_p will be obtained as the sum of $(\sigma_p)_1$ and $(\sigma_p)_2$. Two separate tests must therefore be conducted, one employing P_m only on the model, and the other employing R_m only on the model. The values of $(\sigma_p)_1$ and $(\sigma_p)_2$ are obtained from these two tests separately by the method shown in Example 1.

Method 2. The ratio of P/l^2 to R will be made the same in model as in prototype, so that

$$\frac{P_p}{l_p^2} = R_p \frac{P_m}{R_m l_m^2} \tag{12.11}$$

By Eqs. (12.9), (12.11),

$$\begin{aligned}\sigma_p &= \frac{P_p}{l_p^2} g_1 + R_p g_3 \\ &= R_p \frac{P_m}{R_m l_m^2} g_1 + R_p g_3 \\ &= \frac{R_p}{R_m}\left[\frac{P_m}{l_m^2} g_1 + R_m g_3\right]\end{aligned} \tag{12.12}$$

Therefore by Eqs. (12.10) and (12.12),

$$\sigma_p = \frac{R_p}{R_m}\sigma_m \tag{12.13}$$

Given any combination of P_p and R_p, it is sufficient to load the specimen in such a way that Eq. (12.11) is fulfilled, and the stresses in the prototype σ_p can be calculated from the observed stress σ_m in the model. In this method only one test needs to be conducted. But the stresses obtained will be only those corresponding to the given combination of P_p and R_p. To obtain the stresses of a different combination of P_p and R_p, a second test must be performed in a similar manner. After the stresses corresponding to any two different combinations of P_p and R_p are obtained, the stresses due to a load of P_p or R_p alone can be computed by solving two simultaneous equations. The stresses corresponding to any other combinations of P_p and R_p can then be obtained by superposition.

It should be pointed out that no restrictions are imposed on the value of the modulus of elasticity E_m of the material of the model. The stresses are independent of the modulus of elasticity. The strains in the prototype ϵ_p are always calculated from the stresses and will of course depend on E_p.

12.9. Composite Structures. Where the structure is composed of two or more materials whose moduli of elasticity and Poisson's ratios are E, E_1, E_2, . . . ; ν, ν_1, ν_2, . . . respectively, the additional dimensionless products E_1/E, E_2/E, . . . ; ν, ν_1, ν_2, . . . would appear, and these must be the same for model and prototype. Often Poisson's ratio does not affect appreciably the stresses sought and can therefore be omitted. For example, the model of a reinforced-concrete structure may be made of materials having the same ratio of moduli as between steel and concrete but with Poisson's ratios different from steel and concrete.

12.10. Application of the Method to a Specific Stress-analysis Problem. Suppose it is desired to determine experimentally stresses and strains set up by shock waves impinging upon obstructions embedded in a wave-propagating medium. Since full-scale tests are expensive, the possibility of experimentally studying the problem by means of scaled-down models might be considered. For example, the stresses could be determined photoelastically, and a purely optical approach might be used to obtain displacements and hence strains. By means of the methods of dimensional analysis discussed in this chapter, the feasibility of using such experimental methods to study this problem will be investigated. It is cautioned, however, that this discussion should be looked upon as only an example illustrating the use of the methods of this chapter; and while a set of scale laws are derived which must necessarily be adhered to in conducting the experiment, there is no reason to believe that these laws represent a sufficient set of conditions to be met. For a new problem such as this which is gone into for the first time, a simplified approach is useful as a preliminary feasibility study; but it may be found that additional variables over the ones selected have influence on the problem.

The variables involved in specifying the phenomena are contained in some function

$$\sigma = F(x,y,z,E,E_0,\epsilon,\nu,\nu_0,\rho,\rho_0,t;l,r_1,r_1',\ldots;P,r_2,r_2',\ldots; \\ Q,r_3,r_3',\ldots;R,r_4,r_4',\ldots;S,r_5,r_5',\ldots;U,r_6,r_6',\ldots;\theta,\theta',\theta'',\ldots) \tag{12.14}$$

which gives the stress at the point x, y, z. Symbols which appear here and were not present in the previous examples are those arising from the dynamic nature of the problem, viz., mass density ρ and time t. The terms E_0, ν_0, ρ_0 refer to to the obstructions, while E, ϵ, ν, ρ refer to the wave-transmitting medium. The remainder of the variables apply throughout both.

The following simplification and assumptions are made: By the introduction of E and ν it is implicitly assumed that the phenomenon occurs entirely within the elastic range. This is not quite true in the case of many photoelastic materials. In most plastics, for example, the modulus of elasticity E has been found to vary with strain rate. If this effect is very pronounced, the problem becomes much more complicated. It will nevertheless be supposed in this illustrative example that E and ν are constants and that this approximation will lead to sufficiently accurate results.

It will be further assumed that no damping occurs, i.e., that there is no wave attenuation resulting from internal friction, or, as it is often called, "hysteresis damping." Damping is present to some extent in all materials, but in this example it will be neglected.

Isotropy and homogeneity are, of course, also assumed. The terms $S, r_5, r_5', \cdots$ can be excluded if body forces are neglected. In many applications, obstructions can be considered to be acted upon by a plane-strain shock wave (i.e., one for which the strain perpendicular to the direction of its travel is zero). This suggests using for the model wave-transmitting medium a slab of photoelastic material (see Fig. 12.3). Knowing the stress-time shape of the shock wave approaching the obstructions, a simulated stress- (or displacement-) time wave can be applied to one end of the model

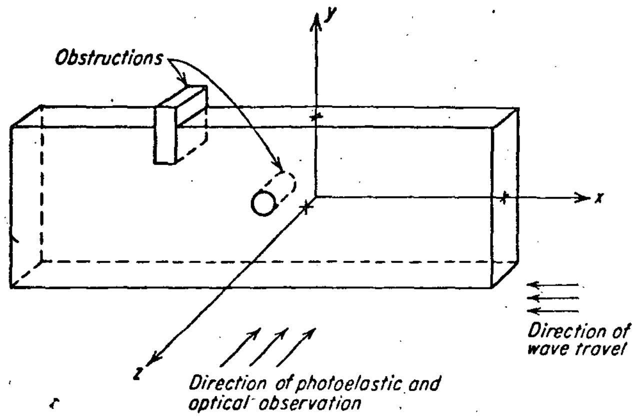

FIG. 12.3. Possible laboratory method for determining stresses around and displacements of obstructions partially or fully embedded in an elastic medium.

medium, and the resulting stresses and displacements around the obstructions can be determined by photoelasticity and optical techniques as schematically indicated in the figure. By so formulating the problem, the variables $P, r_2, r_2', \ldots ; Q, r_3, r_3', \ldots ; R, r_4, r_4', \ldots ; r_6, r_6', \ldots ; \theta, \theta', \theta'', \ldots$ can be omitted in Eq. (12.14), leaving simply the displacement $U = U(t)$, which represents the plane motion of particles in the medium immediately in front of the obstruction. Equation (12.14) thus simplifies to

$$\sigma = F[x,y,z,E,E_0,\epsilon,\nu,\nu_0,\rho,\rho_0;t;l,r_1,r_1',\ldots;U(t)] \tag{12.15}$$

Examination of the dimensional matrix of these variables will show that at least one third-order determinant is not zero†, so that the rank of the

†One nonzero determinant is that corresponding to the three variables σ, ρ, t; that is,

$$\begin{vmatrix} 1 & 1 & 0 \\ -1 & -3 & 0 \\ -2 & 0 & 1 \end{vmatrix} = -2$$

matrix is 3. The number of independent dimensionless products necessary to form a complete set of dimensionless products is therefore three less than the number of variables. One of the ways of writing the complete set is

$$\frac{\sigma}{E\epsilon}, \frac{x}{l}, \frac{y}{l}, \frac{z}{l}, \frac{E_0}{E}, \epsilon, \nu, \nu_0, \frac{\rho l^2}{Et^2}, \frac{\rho_0}{\rho}, r_1, r_1', \ldots, \frac{U}{l\epsilon} \tag{12.16}$$

If the value of each of these groups is made the same for the model and prototype, then, by Buckingham's theorem, the law [Eq. (12.15)] governing the phenomena will hold for both. Making x/l, y/l, z/l, r_1, r_1', . . . equal for both means that the model will be geometrically similar to the prototype and that the stresses occurring in the model will occur in the prototype at geometrically similar locations. Using subscripts m and p to denote model and prototype, respectively, and introducing the scale factors

$$K_\sigma = \frac{\sigma_p}{\sigma_m} \qquad K_E = \frac{E_p}{E_m} \qquad K_\epsilon = \frac{\epsilon_p}{\epsilon_m}$$

the condition of equality between model and prototype of the first dimensionless product can be written

$$K_\sigma = K_E K_\epsilon$$

This can be done for all the dimensionless groups, with the results

$$K_\sigma = K_E K_\epsilon \qquad K_{E_0} = K_E \qquad K_\epsilon = 1 \qquad K_\nu = K_{\nu_0} = 1$$
$$K_\rho K_l^2 = K_E K_t^2 \qquad K_\rho = K_{\rho_0} \qquad K_U = K_l K_\epsilon$$

If the test is kept within the linear range of elasticity, the requirement $K_\epsilon = 1$ need not be met. This is because a deviation from this requirement corresponds only to an equal deviation in K_σ and K_U, which in turn merely implies a higher or lower stress and displacement level.

The requirement that $K_\nu = K_{\nu_0} = 1$ means that Poisson's ratio for both model and prototype obstruction and wave-transmitting medium must be equal. Quite probably it will not be possible to adhere to the requirement, and it must be neglected.

A final simplification: if E_0 is much larger than E (that is, the obstructions can be assumed to be rigid compared with the wave-transmitting medium), E_0 can be dropped from the analysis. The final set of scale-law equations is then

$$K_\sigma = K_E K_\epsilon \tag{12.17a}$$
$$K_\rho K_l^2 = K_E K_t^2 \tag{12.17b}$$
$$K_\rho = K_{\rho_0} \tag{12.17c}$$
$$K_U = K_l K_\epsilon \tag{12.17d}$$
$$K_\epsilon = \text{arbitrary but below elastic limit} \tag{12.17e}$$

There are many possible ways of combining the variables to obtain a complete set of dimensionless products such as given in (12.16); however, the one chosen leads to a form of Eqs. (12.17) which admits a direct physical interpretation. Thus, Eq. (12.17*a*) is representative of the stress-strain relations [see Eqs. (4.17)], and Eq. (12.17*b*) corresponds to the wave equation in mechanics.† The third equation simply states that the ratio of densities of obstruction to wave-propagating medium must be the same for both model and prototype, and Eq. (12.17*d*) expresses the strain-displacement relations of the theory of elasticity [Eqs. (2.11) and (2.13)].

Other scale factors can be derived from those in Eq. (12.17), viz.:

$$\text{Wave-velocity scale factor} = K_l/K_t \tag{12.18a}$$

$$\text{Wave-acceleration scale factor} = K_l/K_t^2 \tag{12.18b}$$

$$\text{Particle velocity scale factor} = K_u/K_t = K_l K_\epsilon/K_t \tag{12.18c}$$

$$\text{Particle acceleration scale factor} = K_u/K_t^2 = K_l K_\epsilon/K_t^2 \tag{12.18d}$$

The basic design equation for setting up the experiment is Eq. (12.17*b*). To illustrate, suppose the values

$$E_p = 55{,}000 \text{ psi}$$

$$\rho_p = 90 \text{ lb/ft}^3$$

are assumed for soil; and

$$E_m = 18 \text{ psi}$$

$$\rho_m = 62 \text{ lb/ft}^3$$

are taken for the chosen photoelastic model material; then by Eq. (12.17*b*)

$$\frac{K_l}{K_t} = \sqrt{\frac{55{,}000/18}{90/62}} \cong 46$$

This means that, for a wave traveling 1,700 fps in the soil, the model wave velocity will be 1,700/46 = 37 fps. The above also establishes the ratio of the scales for length and time. If a convenient length scale is 150, the time scale will be approximately 3. The acceleration scale will correspondingly be, by Eq. (12.18*b*),

$$\frac{K_l}{K_t^2} = \frac{150}{9} = 16.7$$

From Eqs. (12.18*c*), (12.18*d*), particle velocities and accelerations will, on the other hand, be $K_l K_\epsilon/K_t = 46K_\epsilon$ and $K_l K_\epsilon/K_t^2 = 16.7K_\epsilon$, respectively, which indicates that these are proportional to the strain scale factor, whatever its value is chosen to be.

†A simplified form of which is, for example, that the velocity v of a wave propagating in a long slender elastic bar having density ρ and modulus of E is expressed by: $v = \sqrt{E/\rho}$.

12.11. Structural Similarity. If the fundamental equations governing the phenomena are known, the scale-factor laws may be derived directly from these equations without utilizing the methods of dimensional analysis. Thus in the example mentioned in Sec. 12.10 we might expect that the stress-strain relations, the strain-displacement relations, and the wave equations of mechanics are known to apply. By writing these equations in their most general form for both the model and the prototype, and introducing the scale factors, Eqs. (12.17) will result directly.

In order that the reader may understand these concepts, he is advised to pursue the following simple examples which illustrate the use of structural similarity in the derivation of the basic scale-factor laws in each particular problem.

Straight Member under Axial Load. One of the simplest problems which may be solved by the principles of structural similarity is that of a straight tension member under a unidimensional uniformly distributed axial load. Such a member of rectangular cross section is shown in Fig. 12.4. Here

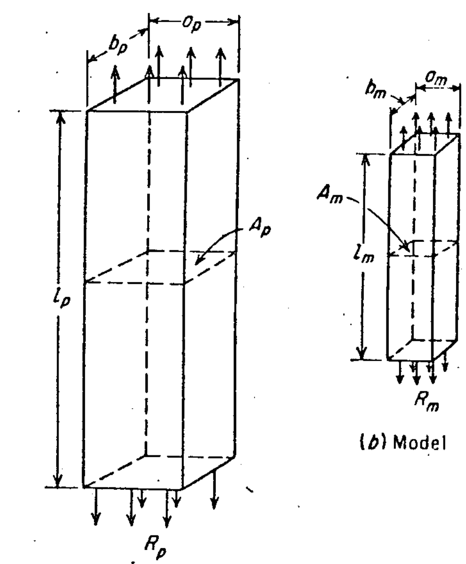

(*a*) Prototype (*b*) Model

FIG. 12.4. Geometric similarity between model and prototype in the case of a straight bar under a unidimensional state of stress.

it may seem that the dimensions of a geometrically similar model are given by $l_m = \lambda l_p$, $a_m = \lambda a_p$, and $b_m = \lambda b_p$, where λ is a given constant factor. The cross-sectional area of the prototype is given by

$$A_p = a_p \times b_p \tag{12.19}$$

The area in the model will be given by

$$A_m = \lambda^2 \times A_p \tag{12.20}$$

Similarly it is seen that

$$V_m = \lambda^3 \times V_p \tag{12.21}$$

where V_m and V_p represent the volumes of the model and prototype respectively.

If the stresses are defined as total force across any cross section divided by cross-sectional area, i.e., $\sigma_p = R_p/A_p$ and $\sigma_m = R_m/A_m$, it may be seen, using Eq. (12.20), that

$$\sigma_m = \frac{R_m}{\lambda^2 A_p} \tag{12.22}$$

If the requirement that the stresses in the model and in the prototype be the same is to be satisfied, it is necessary that the load on the model satisfy the relation

$$R_m = \lambda^2 R_p \tag{12.23}$$

If the requirement that the load on the model and on the prototype be the same is to be satisfied, it is necessary that the stress in the model satisfy the following relation:

$$\sigma_m = \frac{\sigma_p}{\lambda^2} \tag{12.24}$$

At this point it may be observed that the elastic constants E and ν do not influence the scaling laws of either the model stresses or model loads. Assuming that the elastic constants of the mode and the prototype are different, it is necessary that the scale-factor laws for the model strains contain one of these constants, viz., Young's modulus, E. Thus, we have

$$\epsilon_p = \frac{\sigma_p}{E_p} = \frac{R_p}{A_p E_p} \tag{12.25}$$

$$\epsilon_m = \frac{\sigma_m}{E_m} = \frac{R_m}{\lambda^2 A_p E_m} \tag{12.26}$$

From (12.26) it is easily seen that the requirement that the strains in the model and in the prototype be the same implies either that $E_m = E_p$ and $R_m = \lambda^2 R_p$ or that $E_m \neq E_p$ and

$$R_m = \frac{\lambda^2 E_m}{E_p} R_p \tag{12.27}$$

The requirement that the loads on the model and on the prototype be the same implies that

$$\epsilon_m = \frac{E_p}{\lambda^2 E_m} \epsilon_p \tag{12.28}$$

It should be observed from Eq. (12.22) that, regardless of the geometric shape of the cross section, if $A_m = A_p/K$,

$$\sigma_m = K\sigma_p \tag{12.29}$$

provided that the loads are the same. It should also be pointed out that Eqs. (12.25) and (12.26), relating the strains in the model to the strains in the prototype, will be valid regardless of the shape of the cross section. That is, if

$$A_m = \lambda^2 A_p$$

whatever the shape of A_m and A_p, the strains in the model will still be related to the strains in the prototype and Eqs. (12.27) and (12.28) will still be valid. Another important result shown by these considerations is that the modulus of elasticity may be determined from specimens of any cross section.

The total displacement of any specimen is given by

$$\Delta l = l\epsilon \tag{12.30}$$

Thus the total displacements in the model and in the prototype are given respectively as

$$\Delta l_m = l_m \epsilon_m \tag{12.31}$$

$$\Delta l_p = l_p \epsilon_p \tag{12.32}$$

Substituting (12.26) into (12.31), we obtain

$$\Delta l_m = \frac{R_m l_m}{\lambda^2 A_p E_m} \tag{12.33}$$

If $\Delta l_p = \Delta l_m$, then it follows from (12.32) and (12.33) that

$$\frac{R_p}{E_p} = \frac{l_m}{\lambda^2 l_p} \frac{R_m}{E_m} \tag{12.34}$$

Then Eq. (12.34) must be the scale-factor law relating the model loads and modulus of elasticity to the prototype loads and modulus of elasticity when it is desired that displacements in the model and in the prototype be the same. It can be seen from (12.34) that if $E_m = E_p$, then

$$R_m = \lambda^2 R_p l_p / l_m \tag{12.35}$$

If, on the other hand, the loads on the model and prototype are the same. i.e., $R_m = R_p$, then it follows from (12.25), (12.26), (12.31), and (12.32) that the scale-factor law relating the total displacement and modulus of elasticity of the model to the total displacement and modulus of elasticity of the prototype is given by

$$\Delta l_m = \frac{l_m}{l_p} \frac{E_p}{\lambda^2 E_m} \Delta l_p \tag{12.36}$$

Uniformly Loaded, Simply Supported Beam. The second example of interest is the problem of the uniformly loaded, simply supported beam. Figure 12.5 illustrates such a beam. If it were desirable to study the mechanical behavior of such a beam by means of a model, it would be

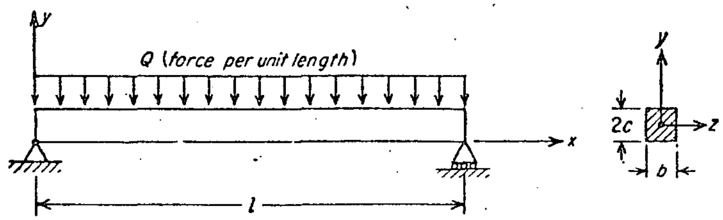

FIG. 12.5. Simply supported beam under uniformly distributed load.

necessary to determine the scale-factor laws relating the deflections and stresses in such a model to the stresses and deflections in the prototype.

The length, depth, and width of the model are assumed to be given respectively as $l_m = \lambda l_p$, $2c_m = 2\lambda c_p$, and $b_m = \lambda b_p$. The coordinate system is defined in Fig. 12.5. If we define a value C as

$$C = \frac{I}{c} \tag{12.37}$$

where I is the moment of inertia of the cross section of any beam and $2c$ is the depth of that beam, then we have from the properties of geometrical similarity that

$$I_m = \lambda^4 I_p \tag{12.38}$$
$$C_m = \lambda^3 C_p \tag{12.39}$$

From elementary strength of materials the deflection at any point on this beam, the elastic moment, and the longitudinal normal stress are given respectively by:

$$y = \frac{Qx}{24EI}(-l^3 + 2lx^2 - x^3) \tag{12.40a}$$

$$M = \frac{Qx}{2}(l - x) \tag{12.40b}$$

$$\sigma = \frac{M}{C} = \frac{Qx}{2C}(l - x) \tag{12.40c}$$

Substituting into Eqs. (12.40) the geometrical dimensions and constants of the prototype and model, we arrive at the relations

$$y_p = \frac{Q_p x_p}{24E_p I_p}(-l_p^3 + 2l_p x_p^2 - x_p^3) \tag{12.41a}$$

$$y_m = \frac{Q_m x_m}{24E_m I_m}(-l_m^3 + 2l_m x_m^2 - x_m^3) \tag{12.41b}$$

$$M_p = \frac{Q_p x_p}{2}(l_p - x_p) \tag{12.41c}$$

$$M_m = \frac{Q_m x_m}{2}(l_m - x_m) \tag{12.41d}$$

$$\sigma_p = \frac{M_p}{C_p} = \frac{Q_p x_p}{2C_p}(l_p - x_p) \tag{12.41e}$$

$$\sigma_m = \frac{M_m}{C_m} = \frac{Q_m x_m}{2C_m}(l_m - x_m) \tag{12.41f}$$

Substituting the geometrical dimensions of the model in terms of the geometrical dimensions of the prototype into Eq. (12.41*b*), (12.41*d*), and (1241*f*) and using the relations (12.41*a*), (12.41*c*), and (12.41*e*), we get

$$y_m = \frac{Q_m}{Q_p} \frac{E_p}{E_m} y_p \tag{12.42a}$$

$$M_m = \frac{Q_m}{Q_p} \lambda^2 M_p \tag{12.42b}$$

$$\sigma_m = \frac{Q_m}{Q_p} \frac{\sigma_p}{\lambda} \tag{12.42c}$$

From Eqs. (12.42) we see that, if $E_m = E_p$ and $Q_m = Q_p$, the deflections of the model and prototype are the same. It should be pointed out at this time that because Q_m and Q_p are defined as loads per unit length, if the length is doubled the total load will be doubled but the deflections will remain the same.

It is observed from Eqs. (12.41) and (12.42) that if $\sigma_m = \sigma_p$, the resulting scale factor laws will be

$$Q_m = \lambda Q_p \tag{12.43a}$$
$$M_m = \lambda^3 M_p \tag{12.43b}$$
$$y_m = \lambda \frac{E_p}{E_m} y_p \tag{12.43c}$$

Cantilever Beam under Concentrated Load. Another example similar to the last one is the problem of the cantilever beam under a concentrated end load. Fig. 12.6 shows such a beam of length l under load P. The maximum deflection y_{max} is found from elementary strength theory considerations to be given by:

$$y_{max} = \frac{Pl^3}{3EI} \tag{12.44}$$

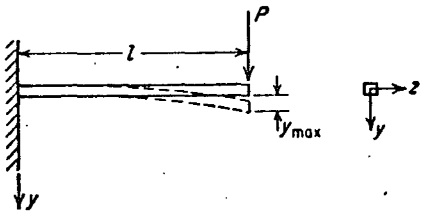

FIG. 12.6. Cantilever beam under concentrated load at the end.

If a model were constructed geometrically similar to the prototype, its length would be given as $l_m = \lambda l_p$ and the moment of inertia I_m would be given as $I_m = \lambda^4 I_p$. As is easily seen, the equations for the maximum deflection in the prototype and model are then given respectively as

$$y_{p\ max} = \frac{P_p l_p^3}{3E_p I_p} \tag{12.45a}$$

$$y_{m\ max} = \frac{P_m l_m^3}{3E_m I_m} \tag{12.45b}$$

By substituting into (12.45b) the geometrical dimensions of the model in terms of those of the prototype, we obtain the scale-factor law for the maximum deflections,

$$y_{m\ max} = \frac{P_m}{P_p}\frac{E_p}{E_m}\frac{(y_{p\ max})}{\lambda} \tag{12.46}$$

From Eq. (12.46) it can be seen that one way to have $y_{m\ max} = y_{p\ max}$ is to make $E_p = E_m$ and $P_m = \lambda P_p$.

Thus if we construct a model whose dimensions are, say, one-half of those of the prototype and which is made of the same material, and load them in a manner such that $P_m = \frac{1}{2}P_p$, we will observe that the bar AB as shown in Fig. 12.7 will remain horizontal after deflection of the two cantilever beams (See Fig. 12.7).

Heavy Beam Simply Supported. The last example is the problem of the simply supported beam under its own weight. Fig. 12.8 illustrates this beam in its undeflected and deflected positions. Although this beam may be considered for structural purposes as a special case of the simply supported beam under a uniform load, it is also of interest to obtain scale-

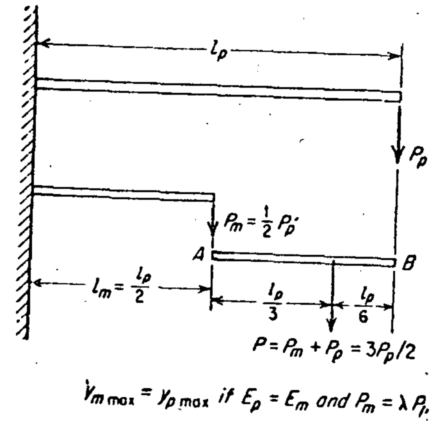

FIG. 12.7. Cantilever beams assembly applying the scaling law $y_{m\ max} = \frac{P_m}{P_p}\frac{E_p}{E_m}\frac{y_{p\ max}}{\lambda}$. The bar AB should remain horizontal if $E_p = E_m$ and $P_m = \lambda P_p$.

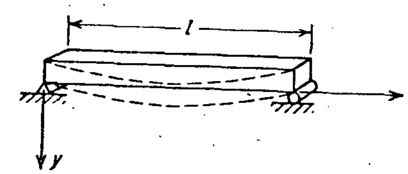

FIG. 12.8. Simply supported beam under its own weight.

factor laws relating the densities and other physical constants of the model to the corresponding quantities in the prototype. Let γ_m and γ_p be the densities of the model and the prototype respectively.

From Eq. (12.43a) and the fact that

$$Q_m = \gamma_m A_m = \gamma_m(\lambda^2 A_p)$$

we conclude that to have $y_m = y_p$, the scale-factor law relating the density of the model to the density of the prototype must be given by

$$\gamma_m = \frac{E_m}{\lambda^2 E_p}\gamma_p \tag{12.47}$$

If $E_m = E_p$, the scale-factor law reduces to

$$\gamma_m = \frac{1}{\lambda^2}\gamma_p \tag{12.47a}$$

If it were desirable to have $\sigma_m = \sigma_p$, then the scale-factor law relating the densities is given by

$$\gamma_m = \frac{1}{\lambda}\gamma_p \tag{12.48}$$

and as a result the relation between the deflections is given by

$$y_m = \lambda \frac{E_p}{E_m} y_p \tag{12.49}$$

If the models were made of the same material, then it is easily seen that the scale-factor laws for the stresses, deflections, and moments would be given respectively by

$$\sigma_m = \lambda \sigma_p \tag{12.50a}$$

$$y_m = \lambda^2 y_p \tag{12.50b}$$

$$M_m = \lambda^4 M_p \tag{12.50c}$$

Use of Two Scale Factors. Sometimes it becomes convenient to have two factors: one (call it λ) for the longitudinal dimensions, and the second (call it η) for transversal dimensions. Thus the dimensions and mechanical constants of a beam might be $l_m = \lambda l_p$, $x_m = \lambda x_p$, $A_m = \eta^2 A_p$, $I_m = \eta^4 I_p$, $C_m = \eta^2 C_p$. In the first example above for the simply supported beam under uniform loading the equation relating the deflections becomes, using these quantities,

$$y_m = \frac{Q_m \lambda^4 x_p}{24 E_m \eta^4 I_p} (-l_p^3 + 2 l_p x_p^2 - x_p^3) \tag{12.51}$$

It is obvious that the equation relating the bending moments is identical to Eq. (12.42b). However, the equation relating the stresses becomes

$$\sigma_m = \frac{Q_m}{Q_p} \frac{\lambda^2}{\eta^3} \sigma_p \tag{12.52}$$

Therefore the scale-factor law relating the loads necessary to make $\sigma_p = \sigma_m$ is given by

$$Q_m = \frac{\eta^3}{\lambda^2} Q_p \tag{12.53}$$

The scale-factor law relating the deflections is then given by

$$y_m = \frac{E_p}{E_m} \frac{\lambda^2}{\eta} y_p \tag{12.54}$$

PART 3

GRID METHODS

centro de educación continua
división de estudios superiores
facultad de ingeniería, unam

ANALISIS EXPERIMENTAL DE ESFUERZOS

METODO DE GRID

DR. LUIS FERRER ARGOTE

NOVIEMBRE, 1978.

CHAPTER 13

GRID METHODS

13.1. Introduction. The first simple idea that comes to mind for the detection of surface strains in a model is to put a grid on its surface and observe the distortions of the grid as the load is put on. For rectangular grids, if the initial and final spacing of the grid lines as well as the change in length of one of the diagonals of the elementary squares are measured, the principal strains and principal directions can be calculated easily by the rosette formula. For other types of grid geometries, for instance, polar grids, similar measurements can be made and the strains determined. There are various methods of putting the grid on the specimen and of measuring the distortion of the grid under load. The methods of putting on the grid will be discussed first.

13.2. Methods of Putting on Grids. *a. Hand Scratching.* For plates made of relatively soft, transparent materials like plastics, grid lines can be hand-scratched on the front face by a sharp razor blade guided by a straightedge. For these thin scratches to show, the light source should come from behind the specimen. The scratches will then appear as thin, dark lines against a light background. Filling the scratches with ink will also increase the contrast. This method is the simplest and the least expensive, but the grid lines cannot be spaced with precision.

Circular scratches can be obtained by using a compass with a sharpened point. The scratches obtained in this way, however, are not so thin as those obtained using razor blades.

b. Machine Scribing. Grid lines can be scratched on the surface of the model by machine scribing. The lines obtained are well defined and evenly spaced.

c. Ink Drawing. For rubber models which cannot take scratches, the grid lines may be drawn in ink by hand. In measuring the spacing between two lines, the centers of these lines must be estimated. Since the error of this estimate increases with increasing thickness of the lines, the accuracy of this method will be higher with thin lines. An alternative is to try to draw relatively thick lines but with sharply defined edges. Measurements are then made from the edges rather than from the center of the lines.

Grid lines can also be drawn in ink on transparent plastics to study

large deformations. An example of ink lines drawn on a Lucite sheet, to study its formability properties, is shown in Fig. 13.1. Using vacuum, a sphere was produced in the center of the sheet, and the amount of permanent strain introduced was determined by comparing the grid on the spherical part to the grid on the undeformed sheet.

d. Rubber Threads. For soft porous materials, thin rubber threads of about 0.008 in. in diameter can be firmly glued on the specimen by latex. The threads have a very low modulus of elasticity so that their effect on the rigidity of the specimen is negligible. Because threads are manufactured by the extrusion process, they have uniform thickness and straight sides.

e. Photogrid. A fine grid can be printed on the surface of the model by photographic means. The surface is first cleaned and lightly roughened by rubbing with fine pumice. It is then coated with a thin layer of high-contrast light-sensitive emulsion. Many types of emulsions are satisfactory for this work, for instance, those used by Brewer and Glasco† or by Miller.‡ Generally four or five thin layers are sprayed at about 1-min intervals to allow the layers to dry. The model should be kept out of the light between sprayings and under subdued light during sprayings. Provision should often be made for fume removal. After drying, a master negative is placed in close contact with the model. Exposure to an intensive light source is made. To secure maximum clarity of the lines, a vacuum printing frame is preferred. The development of the exposed emulsion then follows the procedure set down for the particular emulsion used.

To make the master negative, a plate glass is first coated with wax. A fine grid is ruled on the plate glass. These lines are etched and filled with lead sulfide. The master negative is then obtained from the master grid by contact printing. In this way master negatives of 100 lines per inch with a maximum of ±1 per cent deviation from the nominal spacing of 0.01 in. may be obtained. This deviation becomes negligible only for large strains involving 50 per cent or more elongation or shortening. For such cases, measurements need be made only on the spacings under maximum load, and no measurements are made on the initial spacings under zero load, because the nominal spacing can be taken as the initial spacings.

An example of a photogrid on an aluminum sheet is shown on Fig. 13.2.

f. Embedded Rubber Threads. The grid method can also be used in conjunction with soft transparent plastics. For this application the grid network is constructed of thin rubber threads which are fastened to

†G. A. Brewer, and R. B. Glassco, Determination of Strain Distribution by the Photogrid Process, *J. Aeronaut. Sci.*, vol. 9, no. 1, pp. 1–7, November, 1941.

‡J. A. Miller, Improved Photogrid Techniques for Determination of Strain over Short Gage Lengths, *Proc. Soc. Exptl. Stress Anal.*, vol. 10, no. 1, pp. 29–34, 1952.

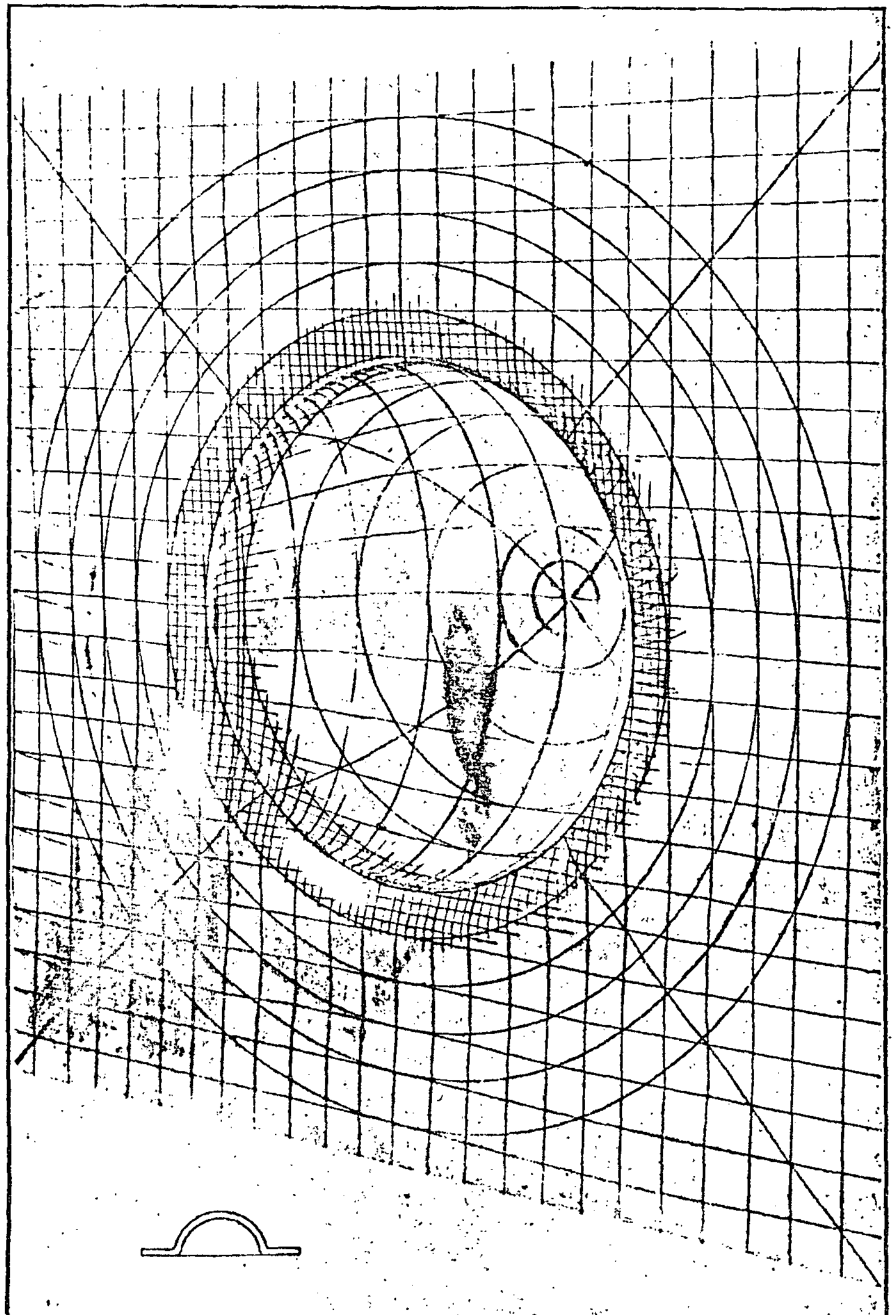

FIG. 13.1. Grid lines drawn in ink used to study formability properties of transparent plastics. The sketch shows a central cross section.

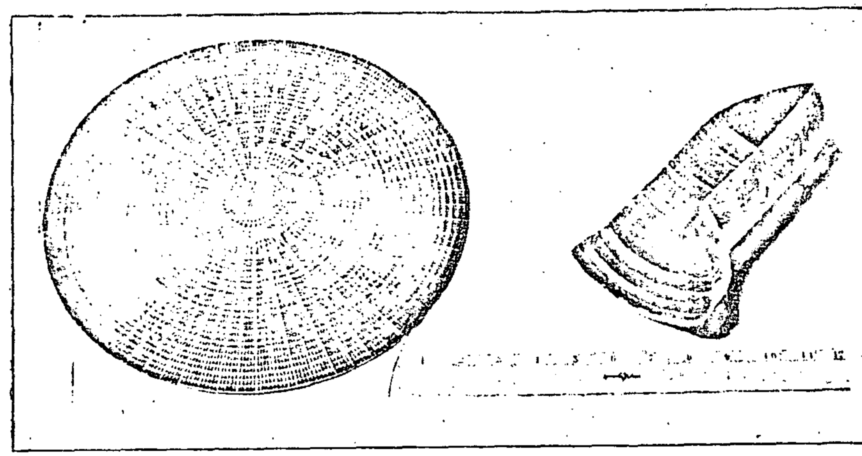

FIG. 13.2 Photogrid applied to the surface of an aluminum Alclad 24-S0 sheet. The photograph at right shows the distortion produced by forming. (Brewer and Glassco.)

the edges of a mold. The soft plastic is then cast around the network. The properties and the manufacturing details of a typical soft material used can be found elsewhere.† In this manner, the grid can be located at any desired position in the model. In cases where the grid is cemented to the surface of the model, the light transmitted through the model is distorted somewhat, since the latex emulsion builds up around the threads, and the light rays are refracted by this uneven surface. When the grid is embedded in the model this difficulty is not encountered. Fig. 13.3*a* shows a photograph of a mold with the rubber thread grid in place prior to pouring. As can be seen from this photograph, the grid can be placed at any desired distance from the surface of the model, and the grid lines can be easily spaced at intervals as close as $\frac{1}{16}$ in. Fig. 13.3*b* shows a cured sheet of the plastic with the embedded grid in place. Fig. 13.3*c* shows a typical model machined from a sheet of the material. Sheets of the material can be cast in any desired size and thickness.

This method can be used in three-dimensional, dynamic, and plastic deformation studies.

13.3. Methods of Measurement of Grids. There are two common methods for the measurement of the distortions of the grid lines.

1. For strains that remain after the load is removed, a micrometer microscope can be used to measure the spacings of the grid lines directly on the specimen both before and after the loading, or only after the loading if the original spacing is accurately known. For elastic strains the dis-

†A. J. Durelli and W. F. Riley, Developments in the Grid Method of Experimental Stress Analysis, *Proc. Soc. Exptl. Stress Anal.*, vol. 14, no. 2, pp. 91-100, 1957.

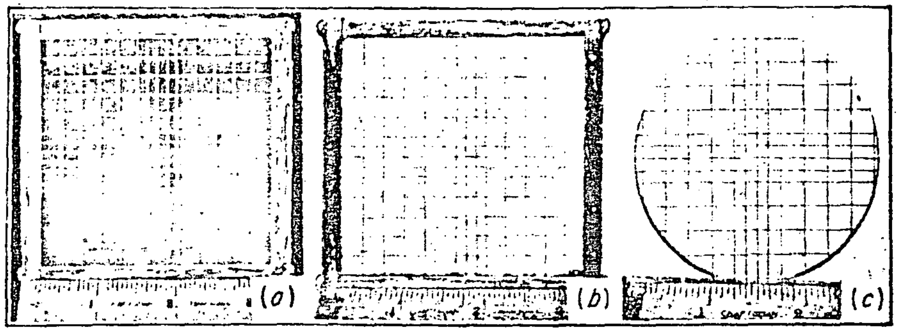

FIG. 13.3. A series of photographs showing various stages in the preparation of a photoelastic model with an embedded grid. (*a*) A mold with the rubber thread grid in place prior to casting. (*b*) A sheet of cured plastic with the embedded grid. (*c*) A model machined from the sheet.

tortions of the grid will be gone after the load is removed so that this method cannot be used. If the strains at only a few points are needed, measurements directly on the specimen can be made by the microscope while the load is on. Where a large number of measurements is to be made, these measurements become difficult to conduct and the method given below may be used.

2. Two pictures of the specimens are taken, one at zero load and the other at maximum load. These will furnish a permanent record of the distortion of the grid, which can later be examined at ease. Measurements on the spacings of grid lines are made on these two pictures instead of on the specimen. Two important sources of error in this method must be carefully guarded against. First, photographic paper usually shrinks with time. Measurements on the same print on different days often show discrepancies of the order of the strains due to the stresses. Glass plates, though more expensive, are therefore preferred. Second, often owing to slack motions in loading mechanisms, the specimen may move a little during the loading process. Since the camera is usually unaffected by the loading, there will be a relative motion between specimen and camera caused by the loading. The component of this relative motion in the plane of the specimen does not change the distance between the specimen and camera so that the size of the image formed on the plate will not be changed. But the component in the direction of the camera will change the size of the image and often cause a serious error in the computed strain. For instance, let P_1Q_1 represent an object placed at a distance d from the center of the lens (Fig. 13.4). Let $P'Q_1'$ be its image formed on the photographic plate at a distance d' away from the center of the lens. Let the object be displaced to its new position P_2Q_2 without

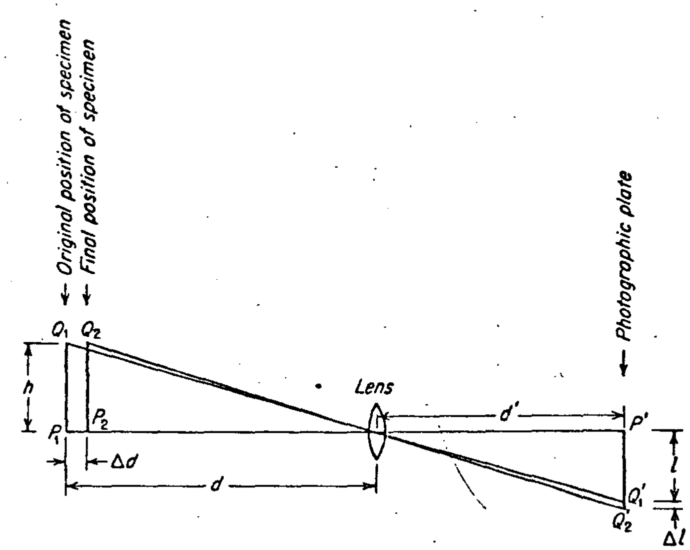

FIG. 13.4. Error introduced in photographic strain measurements due to movement of specimen.

changing its length. Then the new image will be represented by $P'Q_2'$. Using the properties of similar triangles, we have

$$\frac{l}{d'} = \frac{h}{d} \tag{13.1}$$

$$\frac{l + \Delta l}{d'} = \frac{h}{d - \Delta d} \tag{13.2}$$

Taking the difference of the above two equations, we have

$$\frac{\Delta l}{d'} = \frac{h}{d}\frac{\Delta d}{d - \Delta d} \tag{13.3}$$

By Eqs. (13.1) and (13.3) we obtain the apparent strain ϵ_{ap} due to the movement of the specimen,

$$\epsilon_{ap} = \frac{\Delta l}{l} = \frac{\Delta d}{d - \Delta d} \tag{13.4}$$

At each point in the specimen this apparent strain is the same in all directions; hence it is a hydrostatic strain. In general, the amount of displacement in the direction of the camera may be different at different points so that this hydrostatic strain may vary from point to point in the specimen and is not necessarily homogeneous. An idea of the magnitude of the error involved in experiments using flexible loading mechanisms having slack motions can be obtained from this numerical example. Let $d = 10$ in. and $\Delta d = 0.01$ in.; then, by Eq. (13.4), $\epsilon_{ap} = 0.001$, which may be larger than the strains caused by the loading. Such small movements of the specimen will not throw the image out of focus so that the presence of the error cannot be detected through inspection of the image to check whether it becomes blurred or not. Since the slack motion of most loading mechanisms will have taken place by the time a small load is on, it is advisable to use a fraction of the maximum load, say, one-fifth, as the initial load, to take two pictures, one at this load and one at the maximum load, and to measure the change of strain due to the increase of load. Where portions of the specimen have zero or known strains under load, these can be used to compute the motion of the specimen. Usually the hydrostatic apparent strain does not vary appreciably from point to point so that it can be taken as the same for all points and a single correction applied to all the measured strains.

13.4. Determination of Stress Concentrations by Fischer's Method. Suppose we have a number of points $A_0, A_1, \ldots, A_n$ on a straight line parallel to the X axis (Fig. 13.5). Let $X_0, X_1, \ldots, X_n$ be the X coordinates of these points before the body undergoes deformation. After deformation,

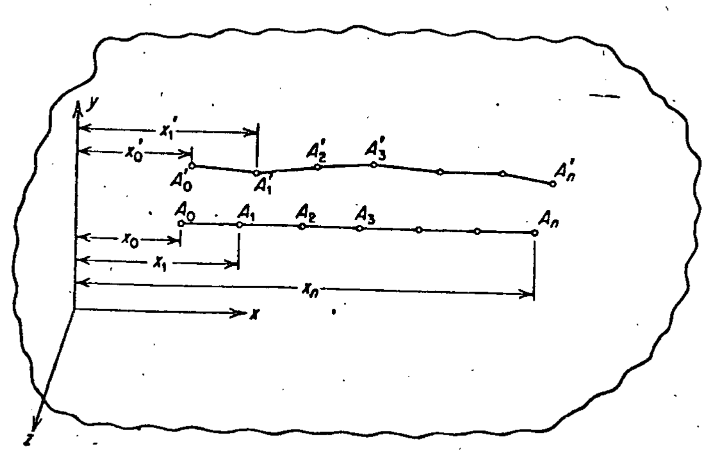

FIG. 13.5. Fischer's method of determination of stress concentrations. After deformation, A_0A_n is displaced to $A_0'A_n'$.

suppose these points move to their new positions $A_0', A_1', \ldots, A_n'$. Let $X_0', X_1', \ldots, X_n'$ be the X coordinates of these new positions. By definition, the displacements in the X direction, denoted by u, are $X_0' - X_0$, $X_1' - X_1, \ldots, X_n' - X_n$ for the points $A_0, A_1, \ldots, A_n$, respectively. If we plot these displacements against the X coordinates of the undeformed positions

of the points, we obtain a number of points $a_0, a_1, \ldots, a_n$ (Fig. 13.6). If we pass a smooth curve through these points, then the slope of the curve, du/dx, will give the strain in the X direction, ϵ_x. This method of plotting the ux curve and obtaining ϵ_x from its slope was due to Fischer.† It has several advantages over the usual method of calculating the strains. (1) A point which deviates excessively from the smooth curve can be

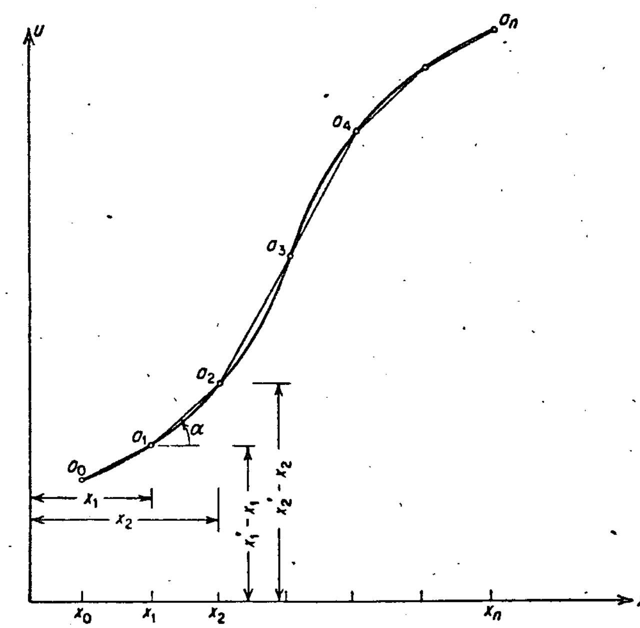

FIG. 13.6. Fischer's method of determination of stress concentrations. The slope of the curve at each point gives the strain at that point.

discovered immediately from a glance at this ux curve. Measurements on this point can be carefully checked again to detect a probable mistake, or, if that is not possible, the point is discarded. (2) In the usual method, the average strain in the interval A_1A_2 is computed by the formula $\epsilon_x = \Delta l/l$ or

$$\epsilon_x = \frac{(x_2' - x_1') - (x_2 - x_1)}{x_2 - x_1}$$

This corresponds to the slope tan α of the chord a_1a_2 in Fig. 13.6. Similarly the average strain in the interval A_0A_1 is given by the usual method as the slope of the chord a_0a_1. The strain ϵ_x at A_1 is then taken as the mean

†G. Fischer, "Versuche uber die Wirkung von Kerben an elastische beanspruchten Biegestaben," dissertation T. H. Aachen, 1932, VDI Verlag G.m.b.h., Düsseldorf, 1932.

slope of the chords a_0a_1 and a_1a_2. This mean is close to the slope of the tangent at a_1, so that here the accuracy of the usual method, though not so good as Fischer's method, is almost as good. At or near a stress concentration (for instance, A_3), however, the average of the two slopes of the chords a_2a_3 and a_3a_4 is much lower than the slope of the tangent through a_3. The ordinary method therefore misses the peak strain, whereas Fischer's method does not. For the determination of stress concentration, Fischer's method is therefore always preferred.

13.5. Determination of the Distribution of Stresses in a Plate with a Circular Hole, under Unidimensional Load by the Rubber-model Method. The problem of the hole in a plate under tension was investigated by the rubber-model method. A rubber sheet 36 in. in length, 12 in. in width, and $\frac{1}{4}$ in. in thickness was used (Fig. 13.7). A circular hole 1 in. in diameter was drilled in its center, and a constant deformation was applied to the sheet by means of a turnbuckle. When the sheet was hung vertically, it was found that the dead weight of the loading jig and rubber sheet produced enough strains to distort the circular hole. To avoid this, the sheet was therefore placed in a horizontal position. To avoid friction, the sheet was supported on ball bearings, as shown in Fig. 13.8. On the rubber sheet, a fine grid was drawn with India ink (Fig. 13.9). Both polar and cartesian-coordinate systems were used. The distance between lines varied from 1/32 to $\frac{1}{2}$ in.

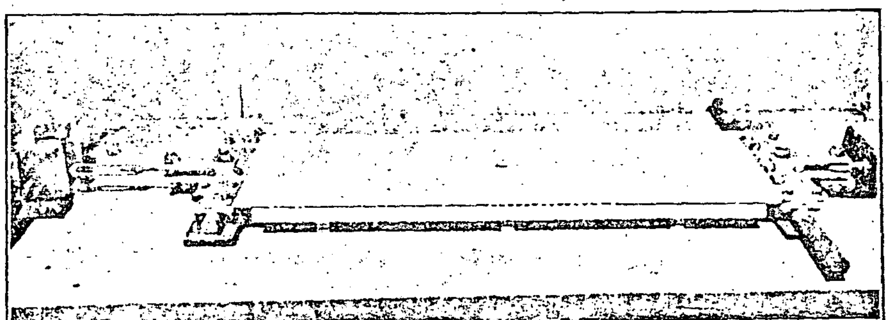

FIG. 13.7. Test setup for rubber sheet (36 by 12 by $\frac{1}{4}$ in. with a 1-in. hole stretched in its plane). The grid is drawn with India ink. The sheet rests on ball bearings to decrease friction.

Photographs of the sheet were taken for a small initial load and for increasing amounts of load. The camera setup is shown in Fig. 13.10. The photograph of the grid at about 10 per cent longitudinal deformation is shown in Fig. 13.11. Photographic plates and not films were used.

The first obvious feature of the photographs is that the drawn circles become ellipses after deformation. The circle on the longitudinal axis

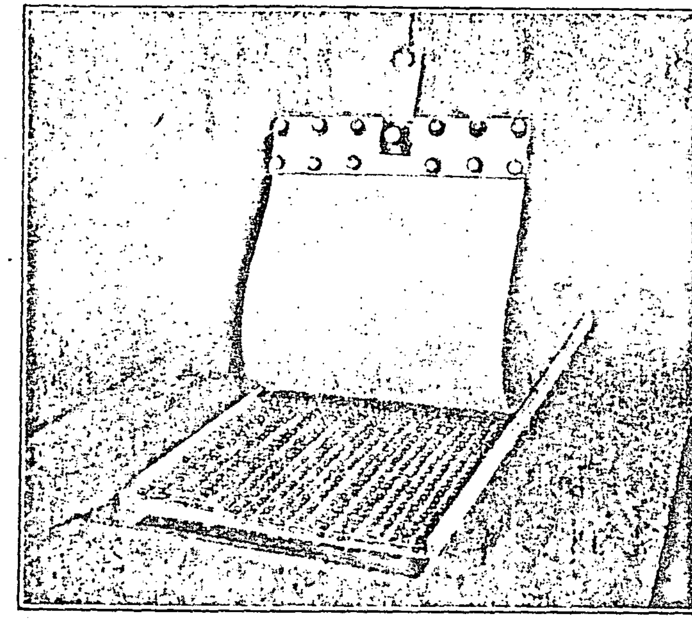

FIG. 13.8. Ball bearings used to support the rubber sheet loaded horizontally.

of the sheet away from the hole and the two ends elongates longitudinally and contracts transversely. With the micrometer microscope, it is easy to measure on the two photographic plates the lengths of the longitudinal and transversal diameter before and after deformation. Dividing the change in length by the original length, the two principal strains are obtained. The ratio between them is Poisson's ratio, since the transversal stress is negligible there.

It is also obvious that, although the directions of the axes of the ellipse on the longitudinal axis of the plate remain longitudinal and transversal, the axes of the other ellipses shifted. The directions of these axes are the directions of the principal strains and stresses.

Superimposing the original circle on the deformed ellipse, as shown in Fig. 13.11, the strains in all directions become apparent. These strains are proportional to the distance between the circle and ellipse. (The circles should be small for this to be true.)

The hole in the plate becomes elliptical; its axes coincide with the axis of the plate. In the polar-coordinate system radial lines diverge prominently at the boundary near the transversal axis and converge at the boundary near the longitudinal axis, making it easy to understand the two fundamental facts produced by the hole:

1. There is an extra elongation at the boundary on the transversal axis (stress-concentration phenomenon).

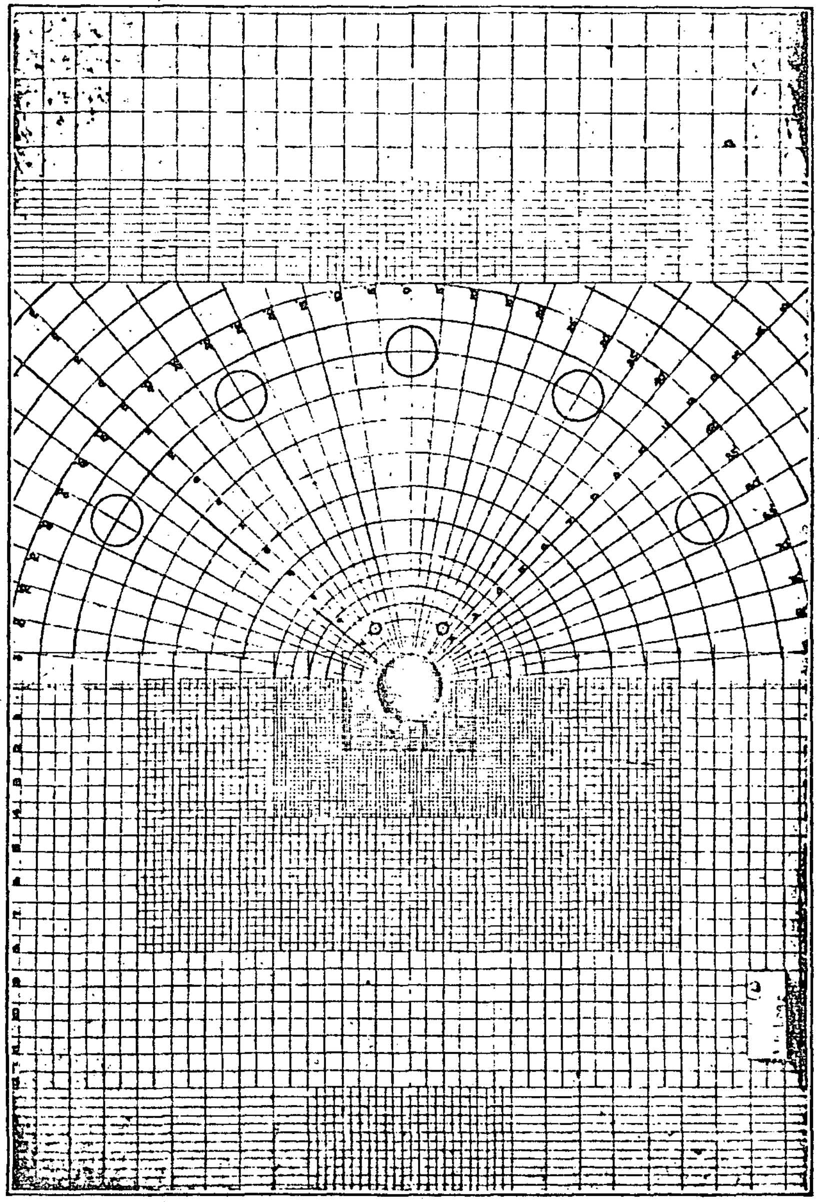

FIG. 13.9. Grid system used in the rubber-sheet test.

2. There is a contraction at the boundary on the longitudinal axis. Since at free boundaries the state of stress is unidimensional, this contraction demonstrates the existence of a compressive stress.

The longitudinal and transversal strains on the transversal axis through

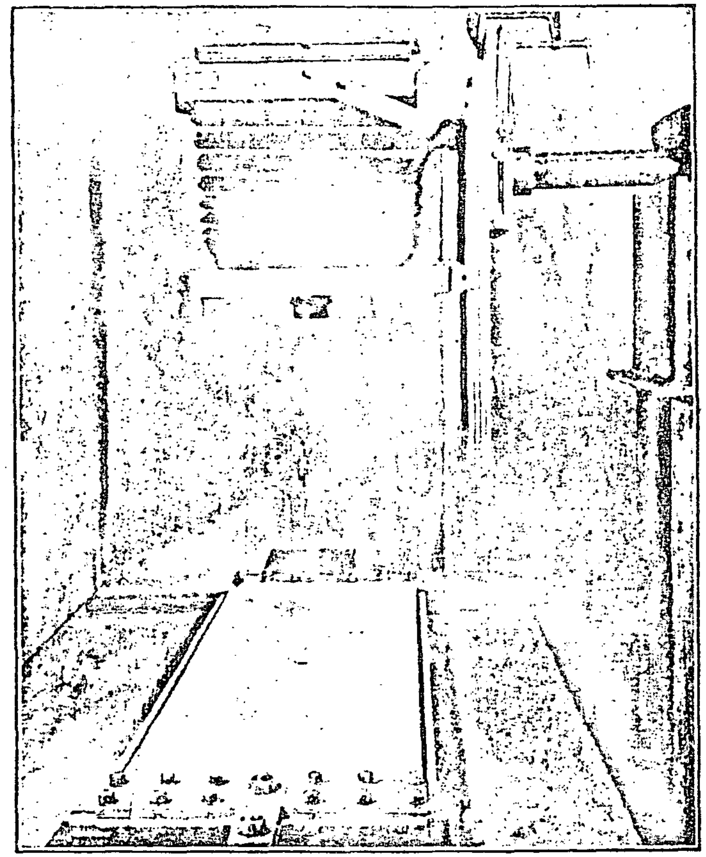

FIG. 13.10. Camera arrangement in the rubber-sheet test.

the center of the hole are obtained by micrometer-microscope measurements on the two photographs, one at a small initial load and the other at about 10 per cent longitudinal deformation. Fischer's method was used. The uniform longitudinal strain at the portion of the plate midway between the hole and the clamped ends is also measured. These measured strains are translated into stresses by the stress-strain relations. The ratios of the stresses on the transversal axis to the stress in the uniform field are computed, plotted, and compared with Howland's theoretical values (Fig. 13.12). The agreement is fair. It was found that the stress-strain relationship for the particular rubber used (Hevea natural rubber 28.5%, fillers 56.3%, vulcanizer 8.6%, sulfur 3.1%, oils 3.5%) is practically straight for strains not larger than 10 per cent. The modulus of elasticity was therefore assumed to be constant. Its value did not enter the final result because only the stress ratios, not stresses, were calculated. Poisson's ratio of the rubber was assumed to be 0.32 in the computations. A point ($r = 2.12a$; $\theta = 28°17'$) was arbitrarily selected for th[illegible] termina-

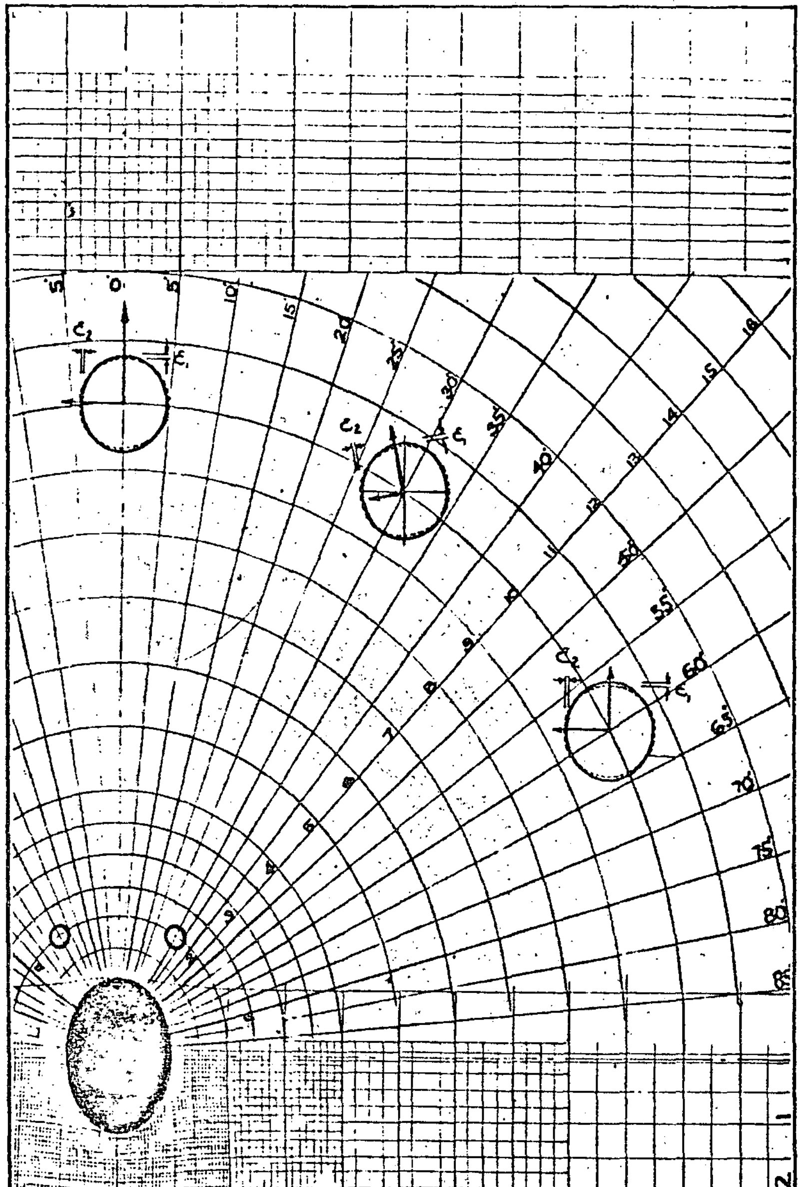

FIG. 13.11. Rubber sheet under about 10 per cent elongation.

tion of stresses from measured strains. Three strains were measured (longitudinally, transversally, and at 45°), and the principal stresses and principal directions were calculated by the rosette formula and the stress-strain relations (Fig. 13.13). Here also, the check with values obtained by Kirsch's formula is fair.

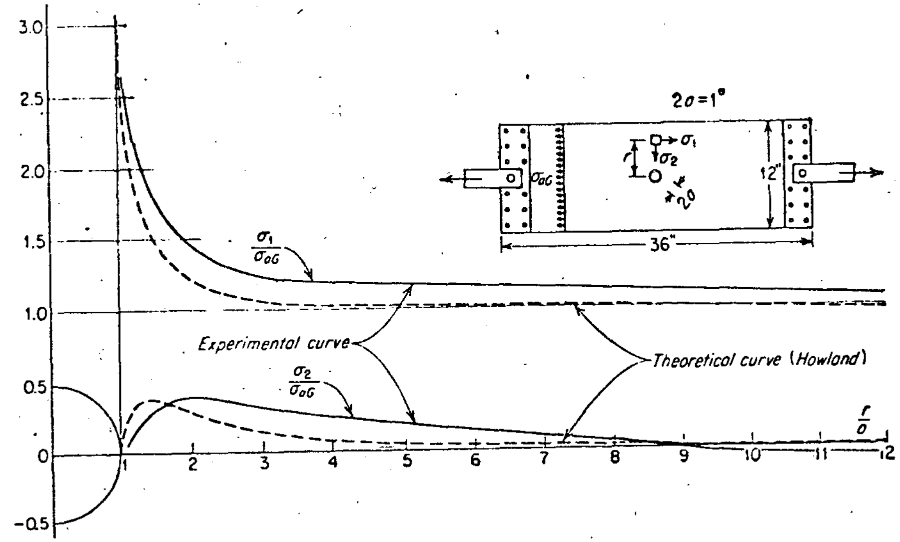

FIG. 13.12. Distribution of stress on the transversal axis of a plate with a circular hole, under a unidimensional uniformly distributed load. (Comparison of theory and rubber-model measurements.) Poisson's ratio of rubber is taken as 0.32.

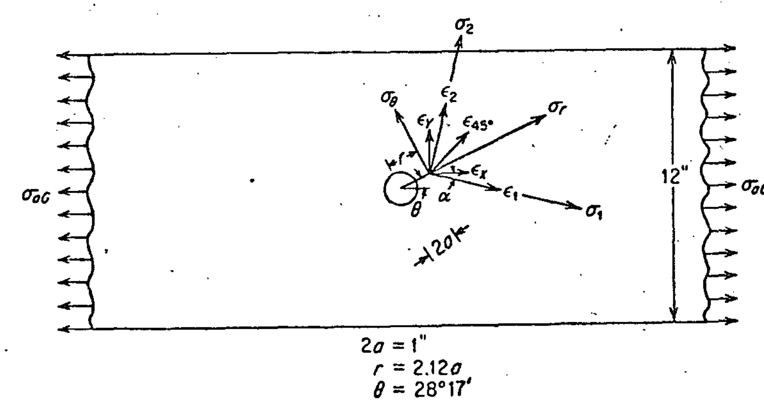

	Theoretical value (Kirsch)	Experimental value
σ_1	$0.924\sigma_{aG}$	$0.938\sigma_{aG}$
σ_2	$-0.168\sigma_{aG}$	$-0.190\sigma_{aG}$
α	12°20′	13°10′

FIG. 13.13. Theoretical and experimental determination of stress and strain at any point on a plate with a circular hole, under unidimensional uniformly distributed load.

13.6. Determination of the Stress-Strain Relations of a Rubberlike Material. The rubber-thread method was used to determine the stress-strain relations of a rocket propellant. The thread used has a diameter of 0.008 in., and was glued on the specimen by latex. A series of motion pictures were taken on the specimen as it was loaded to failure.

Measurements were made on these pictures by means of a comparator and the stress-strain curve plotted. Owing to the large deformations involved, true stress and natural strain were used. Figure 13.14 shows pictures of the specimen before loading, during loading, and after failure. The straight rubber threads become wavy under loading. This strongly indicates that the material is not homogeneous.

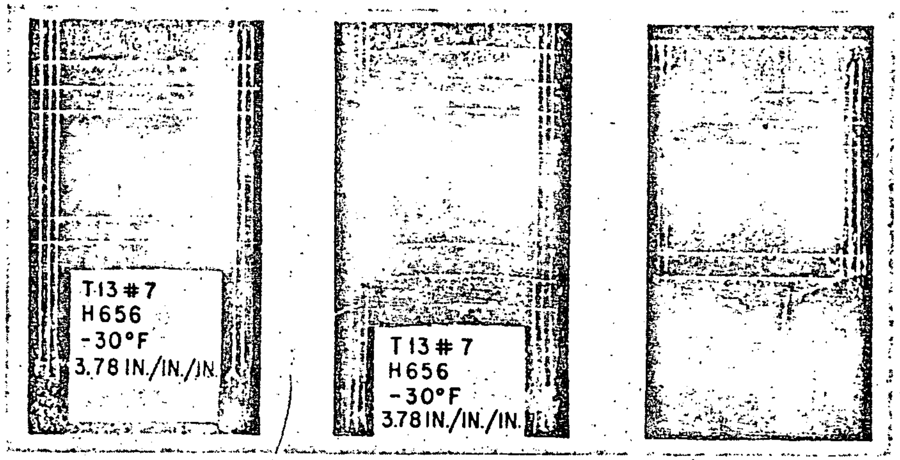

FIG. 13.14. Rubber-thread grid cemented to a rubberlike-material, tensile specimen. The photograph at the left shows the unloaded specimen. The photograph at the right shows the specimen after failure. The photograph in the middle shows nonhomogeneous strain produced by heterogeneity in the material.

13.7. Grids for Point Location. Sometimes in experimental stress analysis, in particular in connection with photoelasticity and the brittle-coating method, it is found convenient to have a grid on the specimen to help in the location of points. When the specimens are of complicated shape, this is often a necessity. The grids are then used, not to measure strains, but to allow a precise location of the points where strains or stresses are determined, and they often coincide with a coördinated system, either cartesian or polar. For photoelastic applications these grids are often scribed on the surface of the plastic specimen. For brittle-coating applications the grids are usually drawn with Dykem Steel Blue. An example of grids on brittle-coating specimens is shown in Figs. 17.2 and 17.3 of the chapter on applications of brittle coating. An example of grids on photoela[illegible] specimens is shown in Fig. 13.15.

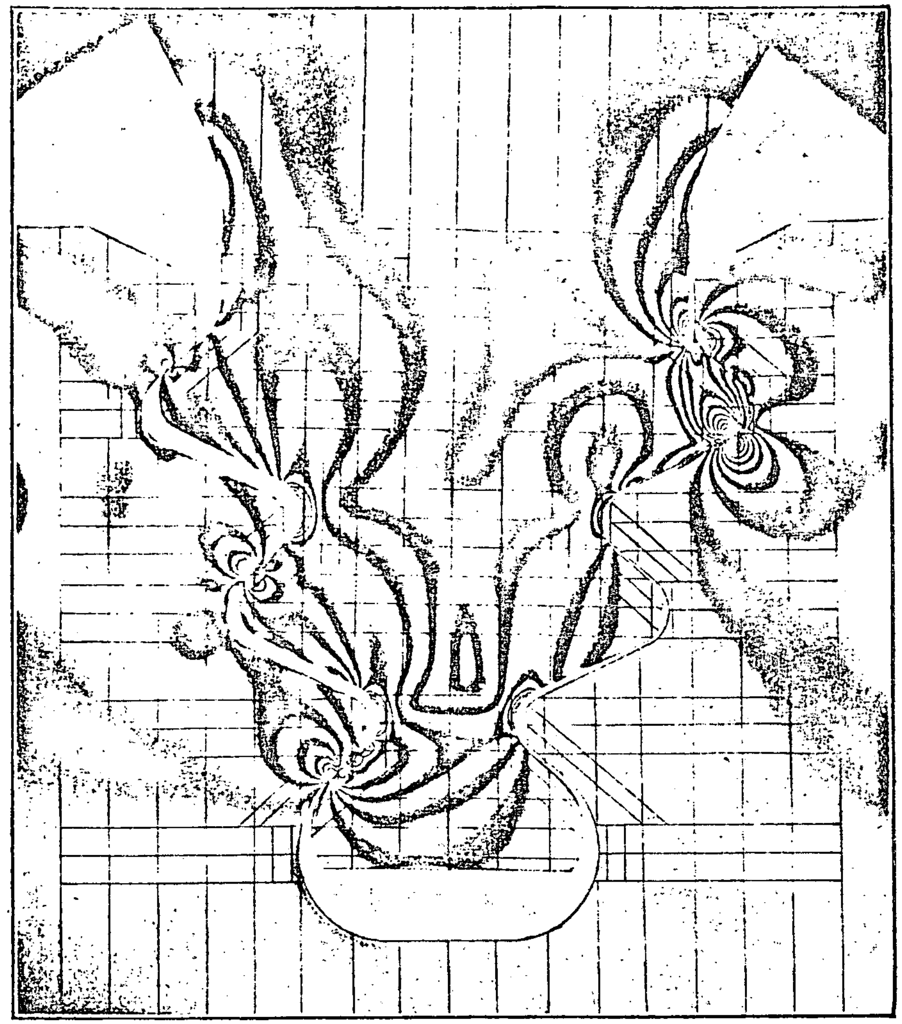

FIG. 13.15. Grid scribed on a photoelastic specimen to allow a precise location of the points where stresses are determined. The grid lines were scratched on a plastic model by means of a sharp-point steel scriber.

13.8. Determination of the Distribution of Strains in a Disk under Diametral Compression. To use the embedded-rubber-thread technique, a sheet of plastic was molded about a grid of rubber threads, and then cured for two days. A disk was then machined from the sheet and placed in a loading frame. Since the plastic had photoelastic properties the disk and loading frame were placed in a field of circularly polarized light. Fringe patterns and the grid network were photographed simultaneously. These data are illustrated in Fig. 13.16, which shows (*a*) a light-field photograph before the load was applied, (*b*) a loaded photograph o[illegible] distor-

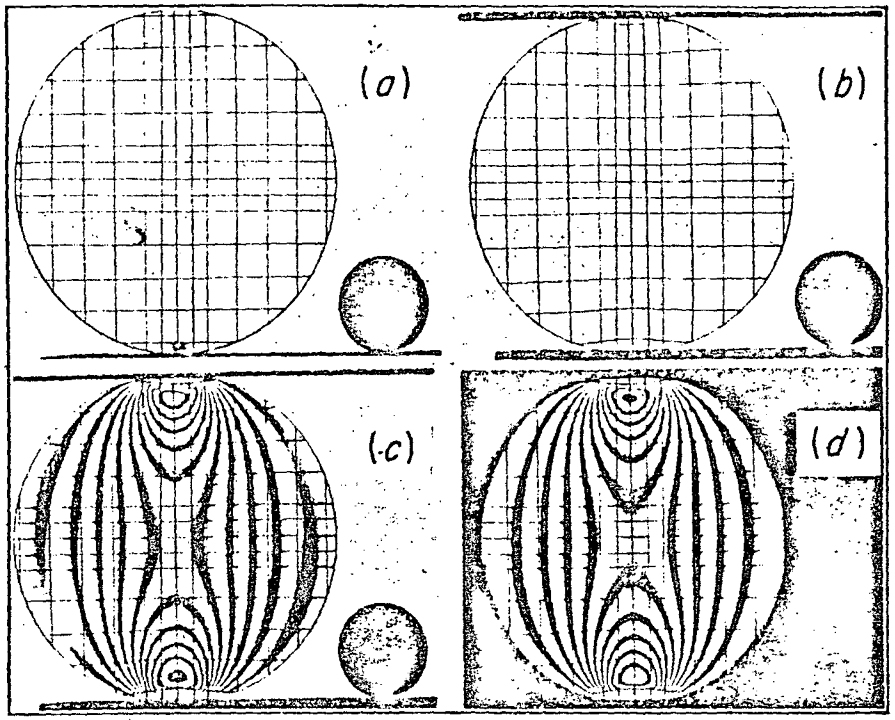

FIG. 13.16. A series of photographs showing complete photoelastic and grid displacement data. (a) A light-field photograph before the load was applied. The fringe at the point of support is due to the dead weight of the disk. (b) A photograph of the grid displacements after the load was applied with the polariscope elements removed. (c) A photograph of the light-field isochromatics and grid displacements. (d) A photograph of the dark-field isochromatics and grid displacements. The black circles in (a), (b), and (c) are a reference sphere used to compensate for film shrinkage. Data obtained from the grids are sufficient to solve the elastic problem.

tions only, (c) light-field isochromatics and grid distortions, and (d) dark-field isochromatics and grid distortions. Only Figs. 13.16a and b are needed for the grid analysis. These two photographs give all values of strain and by use of E and ν all values of stress. However Figs. 13.16c and d will be used for comparison.

An enlarged view of the isochromatic pattern and the grid distortions in the neighborhood of the load are shown in Fig. 13.17.

A fixed reference should always be placed in the field of the photographs to compensate for possible errors which could be introduced by film shrinkage. In this study a small sphere was used, as seen in Fig. 13.16.

The photographs of the disk were taken on a diffused-light polariscope, and both a measuring microscope and an optical comparator were used to make the grid measurements. It is believed that the optical measurements of grid displacements are accurate to $\pm$ 0.0002 in.

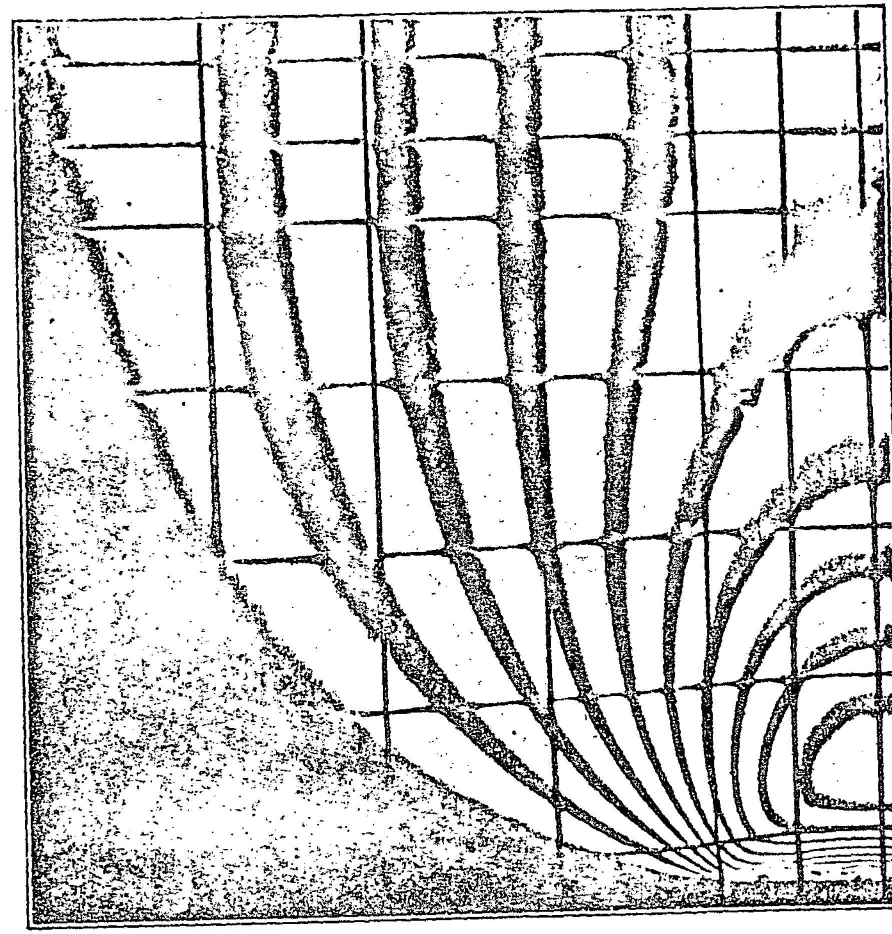

FIG. 13.17. An enlarged view of the photoelastic isochromatics and grid displacements in the neighborhood of the point of application of the load.

In order to compare the photoelastic results with the strain measurements determined from the grid displacements, the following relationship was derived. From the plane-stress equations in Exercise 6.3,

$$\epsilon_1 = \frac{1}{E}(\sigma_1 - \nu\sigma_2) \qquad \epsilon_2 = \frac{1}{E}(\sigma_2 - \nu\sigma_1)$$

The difference in principal strain is then found to be

$$\epsilon_1 - \epsilon_2 = \frac{1+\nu}{E}(\sigma_1 - \sigma_2)$$

The ratio of principal stress difference to principal strain difference is thus a constant.

$$\frac{\sigma_1 - \sigma_2}{\epsilon_1 - \epsilon_2} = \frac{E}{1+\nu}$$

The difference in principal stress was computed for the horizontal and vertical diameters of the disk using the photoelastic isochromatics and the fringe value for the material of 0.54 psi in./fringe. The two principal strains were determined for the two diameters from the grid displacements by Fischer's method. The strain difference was then computed and plotted. The results of these calculations are presented in the form of the curves shown in Figs. 13.18 and 13.19. A comparison between the photoelastic and grid network results is shown in Tables 13.1 and 13.2.

TABLE 13.1. HORIZONTAL DIAMETER

Position	$\sigma_1 - \sigma_2$ psi	$\epsilon_1 - \epsilon_2$	$\dfrac{\sigma_1 - \sigma_2}{\epsilon_1 - \epsilon_2}$ psi
0.1D	3.26	0.0053	612†
0.2D	7.80	0.0183	426
0.3D	13.40	0.0320	419
0.4D	18.55	0.0433	427
0.5D	20.55	0.0490	419

TABLE 13.2. VERTICAL DIAMETER

Position	$\sigma_1 - \sigma_2$ psi	$\epsilon_1 - \epsilon_2$	$\dfrac{\sigma_1 - \sigma_2}{\epsilon_1 - \epsilon_2}$ psi
0.1D	39.70	0.090	441
0.2D	29.80	0.069	429
0.3D	24.60	0.058	424
0.4D	21.60	0.052	415
0.5D	20.55	0.049	419

†Not used for the statistical measures.

From the data of Tables 13.1 and 13.2, statistical measures of the quantity $\dfrac{\sigma_1 - \sigma_2}{\epsilon_1 - \epsilon_2}$ were calculated as indicated below:

a. Mean = 424.3
b. Standard deviation = 7.76
c. Coefficient of variation = 1.83

The results presented in Tables 13.1 and 13.2 show that the strain measurements correlate very well with the photoelastic results. Except in the region of very low strains near the boundary of the disk and in the region of high strain gradient near the point of application of the load,

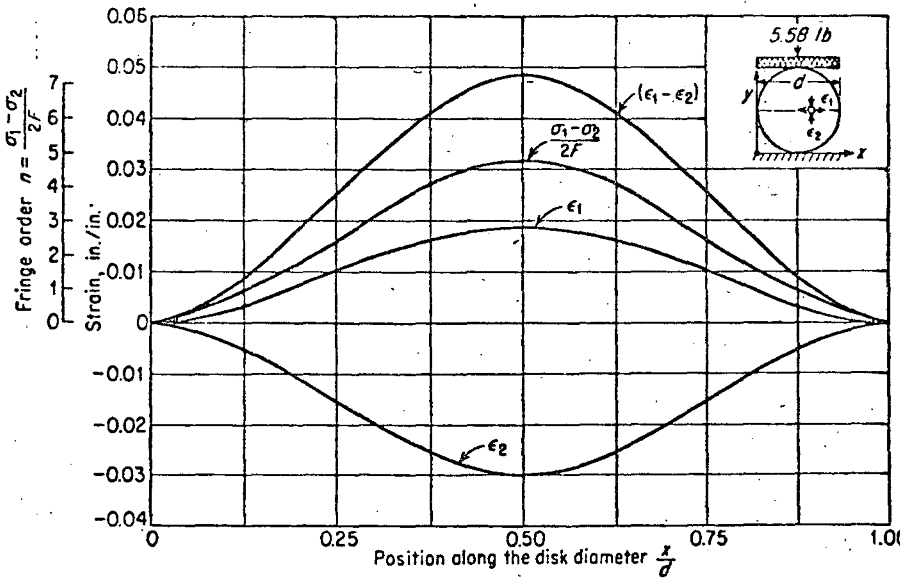

FIG. 13.18. Photoelastic and grid measurement results for the horizontal diameter of the disk.

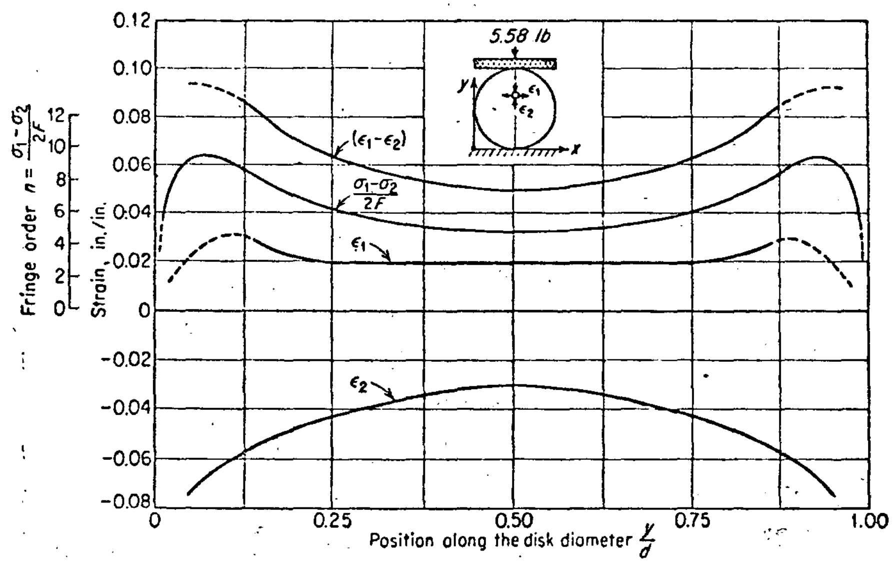

FIG. 13.19. Photoelastic and grid measurement results for the vertical diameter of the disk.

the coefficient of variation is less than 2.00. The value of $E/(1 + \nu)$ computed independently was found to be 420. This compar- favorably with the mean of the disk results, 424.3.

In addition to the comparisons of Tables 13.1 and 13.2, a static equilibrium check was conducted by determining the distributions of σ_y across the horizontal diameter from the measured strains and the elastic constants of the material. The total normal force across the diameter checked to within 2.5 per cent of the applied load.

The usefulness of the method is limited to cases in which large deformations of the plastic do not produce appreciable changes in the boundary conditions. It is obvious in Fig. 13.17 that the distribution of stress at the zone of contact is very different from the corresponding distribution produced by a load concentrated at a point. This limitation is also encountered in other methods of stress analysis such as the "freezing" technique in three-dimensional photoelasticity.

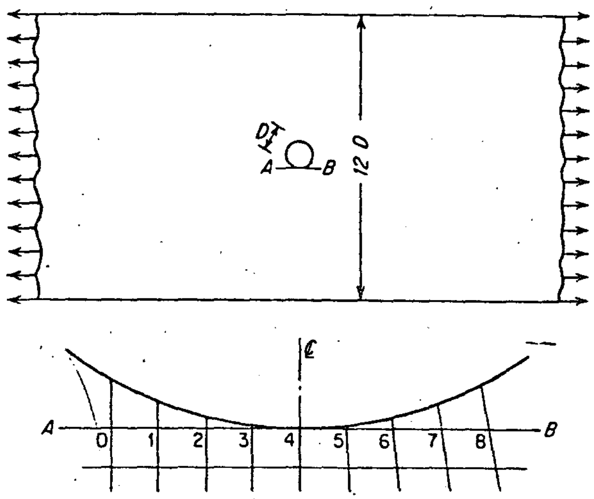

Points on the longitudinal grid line tangent to the hole	Distance measured from point O, in.	
	Plate not loaded	Plate loaded
0	0	0
1	0.018	0.027
2	0.034	0.053
3	0.057	0.089
4	0.073	0.116
5	0.098	0.158
6	0.111	0.181
7	0.136	0.222
8	0.162	0.261

Fig. 13.20. Use of Fischer's method to determine the stress concentration at the boundary of a hole.

EXERCISE

Determine the average strains in the eight intervals on the line AB (Fig. 13.20). From these average strains compute the strains at the seven interior points 1, 2, . . . , 7. Determine the strains at these seven interior points again by Fischer's method, and calculate the per cent difference between the results obtained from these two methods. Determine the strains a third time using Fischer's method; however, in addition, take advantage of the symmetry in respect to the transversal axis.

BIBLIOGRAFIA

1. "A Review of the Photoelastic Method of Stress Analysis, Part I" by R.D.Mindlin. Jl. Of App. Physics, Vol. 10, No. 4, Apr. 1939.

   A special issue on phtoelasticity, includes several other articles. Obtainable from American Institute of Physics, 57 E. 55th St., New York, N.Y.

2. "A Review of the Photoelastic Method of Stress Analysis, Part II" Jl. of App. Physics, Vol. 10, No. 5, May 1939.

   Contains complete bibliography from 1930-1939 on Photoelasticity.

3. "Photoelasticity" Vol. 1 by M.M. Frocht J. Wiley & Sons, 1941.

4. "Photoelasticity" Vol. 11 by M.M. Frocht J. Wiley & Sons, 1948.

5. "Treatise on Photoelasticity" Coker and Filon, Cambridge University Press, 1931.
   Contains complete bibliography up to 1930.

6. "Strength of Materials" Part II by S. Timoshenko, D. Van Nostrand, 1941.

7. "Two-and Three - Dimensional Cases of Stress Concentration and Comparison with Fatigue Tests" J l. of App. Mechanics, Vol. 3, 1936, A15-22. by R.E. Peterson and A. M. Wahl.

8. "Theory of Elasticity" p. 182, by S. Timoshenko, Mc Graw-Hill, 1934.

9. "Prevention of the Failure of Metals under Repeated Stress, Battelle Memorial Institute, J. Wiley & Sons, 1941.

10. "The Numerical Solution of LaPlace's Equation" by Shortley & Weller, Jl. App. Physics 9, 334-348 (1938.).

11. "A membrane analogy supplementing Photoelasticity. Mc Givern & Supper, Jl. Franklin Inst., 217, 491-504 (1934).

12. "The Fundamentals of Three-Dimensional Photoelasticisty" by M. Hetenyi, Jl. Appl. Mechanics, 5, A149-A155 (1938).

13. "Brittle Coatings for Quantative Strain Measurements", A.V.DeForest, Greer Ellis, F.B. Stern, Jl. App. Mechanics, Vol. 9, No. 4, Dec. 1942.

14. "Practical Strain Analysis by Use of Brittle Coatings by Greer Ellis, Proc. Soc. of Exp. Stress Analysis, Vol. 1, No. 1, 1943.

    Also several articles on wire resistance strain gages.

15. "Photoelastic Analysis of Three Dimensional Stress System using Scattered Light" R. Weller and J. Bussey, Tech. Note No. 737, NACA.

16. Handbook of Experimental Stress Analysis" M. Hetenyi, Editor, J. Wiley, 1950.

17. Introduction to the Theoretical and Experimental Analisis of Stress and Strain". A.J. Durelli, E.A. Phillips and C.H. TSAO Mc Graw-Hill Book Co.

18. "Introduction to Photomechanics" A.J. Durelli, W.F. Riley Prentice-Hall Inc. N.Y.

19. "Applied Stress Analysis" A.J. Durelli. Prentice-Hall Inc. N.Y. (Edición en Español 1968).

20. "Moire Analysis of Strain. A.J. Durelli and V.J. Parks. Prentice -Hall, Inc. N.J.

21 "Strain Gages Techniques", Murray, W.M. and Stein, P.K. SESA

22. "The Strain Gage Primer" C.C. Perry and H.R. Lissner. Mc. Graw-Hill, N.Y.

23. " Photoelastic Coatings. Felix Sandman and Salomon Redner, James W. Dally. S.E.S.A.

24. " Photoelasticity" Encyclopedia of Polymer Science and Technology Vol. 9, S.S. Redner John Wiley and Sons, N.Y.

25. "Experimental Stress Analysis "J.W. Dally and W.F. Riley Mc. Graw Hill, N.Y.

26. "Experimental Stress Analysis . Holister G.S. Cambridge University Press, London.

27. " Manual on Experimental Stress Analysis " W.H. Tuppeny Jr. and A.S. Kobayashi S.E.S.A.

DIRECTORIO DE ASISTENTES AL CURSO ANALISIS EXPERIMENTAL DE ESFUERZOS
(DEL 27 DE NOVIEMBRE AL 8 DE DICIEMBRE DE 1978)

NOMBRE Y DIRECCION	EMPRESA Y DIRECCION
1. ING. FELIPE ALMEIDA GALINA Unidad Juan de Dios Batiz 21-B-304 Col. Zacatenco México 14, D. F. Tel: 5-86-38-21	LABORATORIO DE ESTRUCTURAS I.P.N. Unidad Profesional de Zacatenco México 14, D. F. Tel: 5-86-01-44
2. ING. HEBER BADA PULIDO Leoncavallo No. 156-18 Col. Vallejo México 14, D. F. Tel: 5-86-01-44	LABORATORIO DE ESTRUCTURAS I.P.N. Unidad Profesional de Zacatenco México 14, D. F. Tel: 5-86-01-44
3. JOSE ANTONIO CASTILLA CORONA Planta XIA No. 55 Casa 15 Col. Electra Edo. de México Tel: 3-97-46-10	COMISION FEDERAL DE ELECTRICIDAD Río Ródano No. 14 Col. Cuauhtémoc México 5, D. F. Tel: 5-53-71-33 Ext. 2530
4. ING. FRUCTUOSO CASTILLO ROMERO Av. Industria Militar s/n Lomas de Sotelo México, D. F. Tel: 5-89-29-85	DEPARTAMENTO DE LA INDUSTRIA MILITAR Av. Industria Militar s/n Lomas de Sotelo México, D. F. Tel: 5-89-29-85
5. ELOY CRUZ GOMEZ Medicina 32 Capilco México 20, D. F. Tel: 5-48-32-18	DESFI-UNAM Ciudad Universitaria México 20, D. F.
6. ING. ROBERTO CHAVEZ JIMENEZ Av. Central 296 Col. Educación México 21, D. F. Tel: 5-44-24-63	SISTEMA DE TRANSPORTE COLECTIVO "METRO" Av. Hangares Col. Federal México, D. F. Tel: 5-71-56-00 Ext. 815
7. J. CARLOS DOURIET Benito Juárez No. 787 Ote. Culiacán, Sin. Tel: 2-11-27	ESCUELA DE INGENIERIA CIVIL-U.A.S. Ciudad Universitaria Culiacán, Sin.
8. ING. GABRIEL GALLO ORTIZ Cali No. 337 Valle Dorado Edo. de México Tel: 3-79-69-16	LABORATORIO DE ESTRUCTURAS-I.P.N. Unidad Profesional de Zacatenco México 14, D. F. Tel: 5-86-01-44

DIRECTORIO DE ASISTENTES AL CURSO ANALISIS EXPERIMENTAL DE ESFUERZOS
(DEL 27 DE NOVIEMBRE AL 8 DE DICIEMBRE DE 1978)

NOMBRE Y DIRECCION	EMPRESA Y DIRECCION
9. LOURDES LOBERA MAYA Colina de Lajas No. 4 Boulevares Cd. Satélite Edo. de México Tel: 5-62-47-82	LABORATORIO DE ESTRUCTURAS I.P.N. Unidad Profesional de Zacatenco México 14, D. F. Tel: 5-86-01-44
10. ING. RUBEN M. MARTINEZ CASILLAS Ed. 39-D-401 Unidad Lindavista Vallejo México 14, D. F. Tel: 5-67-59-32	LABORATORIO DE ESTRUCTURAS I.P.N. Unidad Profesional de Zacatenco México 14, D. F. Tel: 5-86-01-44
11. BASILIA QUIÑONES DE ESCALANTE Calle 10 No. 1279 Culiacán, Sin. Tel: 3-32-75	ESCUELA DE INGENIERIA CIVIL- U.A.S. Ciudad Universitaria Culiacán, Sin. Tel: 2-49-70
12. ING. RAMON RAMIREZ URIBE Av. 523-162 Unidad Aragón México 14, D. F. Tel: 5-89-65-33	DEPARTAMENTO DE LA INDUSTRIA MILITAR Av. Industria Militar s/n Tecamachalco México 10, D. F. Tel: 5-89-65-33
13. FIS. HORACIO NOVELO RETANA Oriente 229-B No. 121 Col. A. Oriental México 9, D. F.	SECRETARIA DE AGRICULTURA Y RECURSOS HIDRAULICOS Sierra Gorda No. 23 Lomas de Chapultepec Tel: 5-20-73-07
14. SALVADOR VALLE VALLE Privada de Mendoza No. 27 Col. Huipulco México 22, D. F. Tel: 5-73-13-39	DESFI-UNAM Ciudad Universitaria México 20, D. F.
15. ING. ARMANDO WONG RAMOS Calle 7 Edif. 57-B Departamento 203 Lomas de Sotelo México 10, D. F. Tel: 5-57-70-42	SECRETARIA DE AGRICULTURA Y RECURSOS HIDRAULICOS Sierra Gorda No. 23 Lomas de Chapultepec México 10, D. F. Tel: 5-20-73-07
16. ALFREDO ZATARAIN TISNADO Av. Universidad 1900 Edif. 50-403 Col. Oxtopulco México 20, D. F.	DESFI-UNAM Ciudad Universitaria México 20, D. F.